Chalcone derivatives in cancer research and tissue engineering

Ciupa, Alexander

Award date:
2013

Awarding institution:
University of Bath

Chalcone Derivatives in Cancer Research and Tissue Engineering

Alexander Ciupa
A thesis submitted for the degree of Doctor of Philosophy
University of Bath
Department of Pharmacy and Pharmacology
February 2013

This research has been carried out under the supervision of Dr Lorenzo Caggiano and Dr Paul De Bank

Signed.....

Date.....

Abstract

The chalcone motif is a privileged structure present in an extensive range of biologically active molecules. The chalcone structure can also serve as a versatile starting material for more complex molecules in medicinal chemistry.

Eleutherobin, isolated from the Australian coral *Eleutherobia* and sarcodictyin, isolated from the Mediterranean coral *Sarcodictyon roseum* are natural products displaying nanomolar cytotoxicity against a range of cancer cell lines including Taxol®-resistant cell lines. Both natural products act as microtubule stabilising agents and will be valuable additions to the clinic, however their limited availability and lengthy total syntheses prevent further development. The urocanic ester side chain present in eleutherobin and sarcodictyin was identified as being critical for biological activity. We discuss the design, synthesis and biological evaluation of fourteen chalcone analogues based on this urocanic motif with the lead chalcone displaying promising antiproliferative activity in a range of cancer cell lines.

Combretastatin A-4 is a promising microtubule destabiliser under clinical development. The *Z* configuration is vital for biological activity, however it can isomerise to the inactive *E* configuration. We report a library of twenty pyrazolines synthesised from chalcones as "*Z* restricted" combretastatin analogues with the lead pyrazoline displaying potent antiproliferative activity in cancer cell lines due to the disruption of tubulin.

Tissue engineering is a diverse interdisciplinary field that applies engineering principles to the biological sciences with the aim of maintaining or replacing tissue function. Recent developments have revealed metal chelation to be a valuable tool to control the architecture of tissue engineering scaffolds. We report a library of ten novel pyrazolines and their potential as metal chelators. Maltol is a well established Fe^{3+} chelator with a low toxicity profile. We report a novel maltol hydrazide which can be attached to the cell surface which upon addition of Fe^{3+} results in cellular aggregation due to metal chelation. Further studies revealed that this process can be applied to form heterocellular aggregates composed of two different cancer types with valuable applications in tissue engineering and cancer research.

Acknowledgements

Firstly I would like to thank my two supervisors Lorenzo and Paul for all their help and support over the last three years in this very interdisciplinary project. Both Lorenzo and Paul have provided the freedom to generate my own ideas and drive my own project while giving valuable advice and guidance along the way.

I owe a huge thanks to Dr Pauline Wood for her help and support with the cell work particularly taking the time to teach me the MTS assays which have been the core of this project. I have always viewed Pauline as my unofficial third supervisor, her knowledge and experience has been invaluable during this project and the majority of this work would not have been possible without her.

I also owe a big thanks to Prof Mike Threadgill for providing access to the MTS reagents and Prof Steve Husbands for use of his chiral HPLC column without which none of the enantiomer work would be possible.

During the last three years I have received countless help and assistance from my three favourite Post-Docs Amit, Liz and Jo, thank you for letting me borrow reagents and helping me during this PhD.

My time here in Bath would not have been the same without my fellow PhD students Ben, Natalie, Gemma, Helen, Kim, Elvis, Katerina, Nour and Chris who have made my time here so memorable.

Finally a big thanks to Jasmine and my family for their help and support over the last few years and the University of Bath for funding my studentship.

Publications

Simple pyrazoline and pyrazole "turn on" fluorescent sensors selective for Cd^{2+} and Zn^{2+}. **Ciupa A**, Mahon MF, De Bank PA and Caggiano L, *Org. Biomol*. *Chem*., **2012**, *10,* 8753-8757.

Design, synthesis and antiproliferative activity of urocanic-chalcone hybrid derivatives. **Ciupa A**, Griffiths NJ, Light SK, Wood PJ and Caggiano L, *Med. Chem. Comm.,* **2011**, *2,* 1011-1015.

Two further manuscripts are in preparation.

Oral Presentations

Departmental Research Afternoon,
University of Bath,
26th January 2012.

Poster Presentations

6th BMCS Postgraduate Symposium in Biological and Medicinal Chemistry,
University of Cambridge,
14th December 2012.

Cancer Research at Bath (CR@B) Symposium Event,
University of Bath,
28th March 2012 & 14th November 2012.

Contents

1. Aims and Objectives

2. Chapter 2: Urocanic-Chalcone Hybrids

3. Chapter 3: Pyrazoline Combretastatin A-4 Analogues

List of Figures

List of Schemes

List of Tables

List of Abbreviations

Å	Angstroms
Aq.	Aqueous
Ar	Aryl
Bn	Benzyl
Bz	Benzoyl
Bu	Butyl
conc.	Concentrated
DMF	Dimethylformamide
ED_{90}	Concentration required to induce 90% tubulin polymerisation
ee	Enantiomeric excess
equiv.	Equivalents
ESI	Electrospray ionisation
Et	Ethyl
g	Grams
GI_{50}	Concentration required to inhibit cell growth by 50%
h	Hours
HPLC	High performance liquid chromatography
HRMS	High resolution mass spectroscopy
Hz	Hertz
IC_{50}	Concentration required to inhibit cell proliferation by 50%
IR	Infrared
J	Coupling constant
M	Moles per litre
MA	Microtubule assembly
Me	Methyl
MeCN	Acetonitrile
MeOH	Methanol
min.	Minutes

mol	Moles
Mp	Melting point
MS	Mass spectroscopy
m/z	Mass to charge ratio
NCI	National Cancer Institute
NMR	Nuclear magnetic resonance
OD	Optical density
Pd/C	Palladium on activated carbon
PE	Petroleum ether, fraction boiling point 40-60 ^{o}C
Ph	Phenyl
ppm	Parts per million
R_f	Retention factor
rt	Room temperature
t_R	Retention time
SAR	Structure-activity relationship
THF	Tetrahydrofuran
TLC	Thin layer chromatography
UV	Ultraviolet

List of Cell lines

786-0	Renal Carcinoma
A498	Renal Carcinoma
A549/ATCC	Non-Small Cell Lung Carcinoma
ACHN	Renal Carcinoma
BT-549	Breast Carcinoma
CAKI-1	Renal Carcinoma
CCRF-CEM	Leukaemia
COLO 205	Colon Carcinoma
DU-145	Prostate Carcinoma
EKVX	Non-Small Cell Lung Carcinoma

HCC-2998	Colon Carcinoma
HCT-15	Colon Carcinoma
HCT-116	Colon Carcinoma
HeLa	Cervical Carcinoma
HOP-62	Non-Small Cell Lung Carcinoma
HT29	Colon Carcinoma
HS-578T	Breast Carcinoma
IGROV	Ovarian Carcinoma
K562	Leukaemia
KM12	Colon Carcinoma
LOX IMVI	Melanoma
LnCaP	Prostate Carcinoma
M14	Melanoma
MALME-3M	Melanoma
MCF-7	Breast Carcinoma
MDA-MB-231	Breast Carcinoma
MDA-MB-435	Melanoma
NCI/ADR-RES	Multidrug Resistant Ovarian Carcinoma
NCI-H226	Non-Small Cell Lung Carcinoma
NCI-H23	Non-Small Cell Lung Carcinoma
NCI-H322M	Non-Small Cell Lung Carcinoma
NCI-H460	Non-Small Cell Lung Carcinoma
NCI-H522	Non-Small Cell Lung Carcinoma
OVCAR-3	Ovarian Carcinoma Sensitive to Microtubule Binding Agents
OVCAR-4	Ovarian Carcinoma
OVCAR-5	Ovarian Carcinoma
OVCAR-8	Ovarian Carcinoma
PC-3	Prostate
RXF 393	Renal Carcinoma
RPMI-8226	Leukaemia
SF-268	Glioblastoma
SF-539	Glioblastoma

SK-MEL-2	Melanoma
SK-MEL-5	Melanoma
SK-MEL-28	Melanoma
SK-OV-3	Ovarian Carcinoma
SK-OV-3-3TR	Taxol® Resistant Ovarian Carcinoma
SN12C	Renal Carcinoma
SR	Leukaemia
SW-620	Colon Carcinoma
T-47D	Breast Carcinoma
TK-10	Renal Carcinoma
U251	Glioblastoma
UACC-257	Melanoma
UACC-62	Melanoma
UO-31	Renal Carcinoma

Chapter 1: Introduction to Cancer Research

1.1 Cancer Research

Cancer is one of the most feared diseases in the modern world with an estimated 12.7 million cases in 2008 resulting in 7.6 million deaths worldwide.[1] Cancer is characterised by uncontrolled cellular proliferation involving most, if not all, of the hallmarks of cancer as proposed by Hannah and Weinberg (Figure 1A).[2,3] With over 100 different types of cancer, arising from multiple cell types, research into the molecular biology and treatment of cancer is one of the most extensively studied fields in modern science.

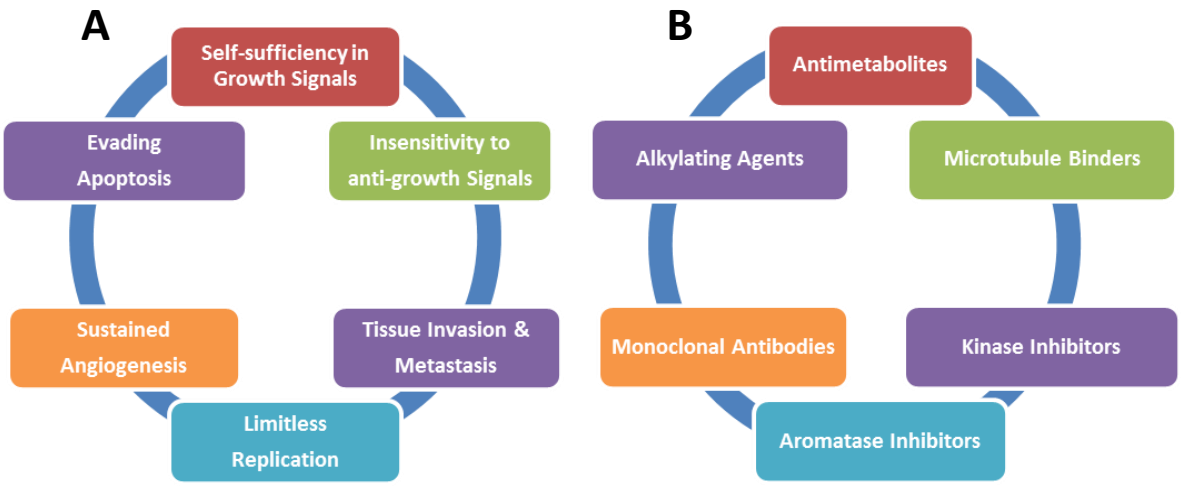

Figure 1: A) The hallmarks of cancer,[2,3] B) common chemotherapy approaches.

There are three traditional approaches to treating cancer: surgery, radiotherapy and chemotherapy of which chemotherapy (Figure 1B) is the most commonly employed both in initial cancer treatment and in preventing reoccurrence in the future.[4] The majority of agents target the increased cellular proliferation of cancer cells with alkylating agents,[5] antimetabolites[6] and microtubule binding agents[7] commonly used in combination to target multiple cellular pathways. The continued development of new therapies is of paramount importance with the microtubule binders set to continue to play a critical role in combination chemotherapy in the near future.

1.2 Targeting Microtubules

Microtubules are highly dynamic biological polymers performing key cellular functions including maintaining cell shape, cell signalling, transport of materials within the cell and provide the scaffold for cell division and mitosis to occur.[7,8] Microtubule assembly is highly regulated and critically involved in coordinating newly synthesised chromosomes during mitosis (Figure 2).[8]

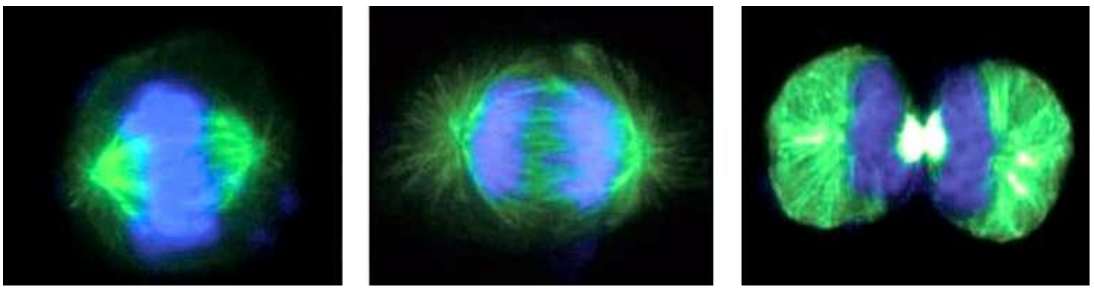

Figure 2: The role of microtubules in mitosis, microtubules (green) and chromosomes (blue).[8]

A microtubule is a hollow tubular structure composed of α-β tubulin heterodimers comprising one α and one β tubulin unit bound in a head to tail arrangement (Figure 3A). Heterodimers assemble into a microtubule nucleus (**B**) acting as a nucleation site for additional heterodimers forming a microtubule (**C**).[7] Microtubule formation is completely reversible enabling microtubules to expand and contract on demand to perform the functions required by the cell.

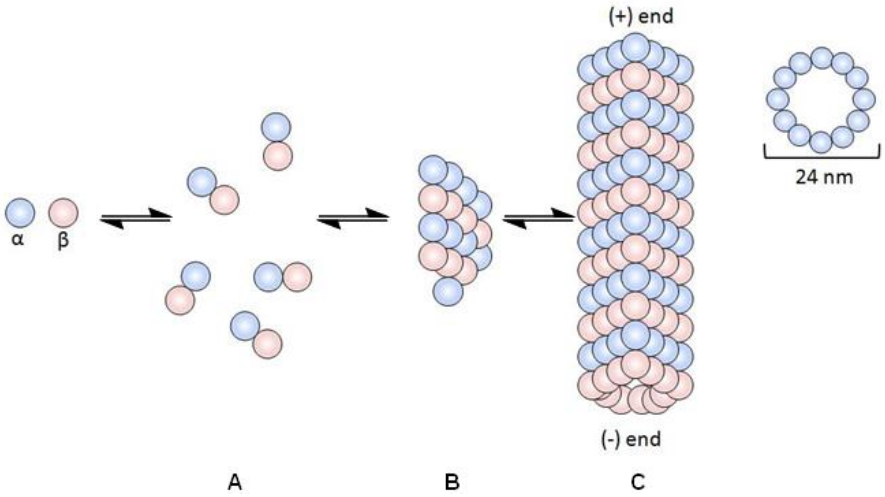

Figure 3: The three stages of microtubule formation, (A) heterodimer, (B) microtubule nucleus and (C) microtubule, all stages are fully reversible.

1.3 Tubulin Binding Sites

The critical role of microtubules in cellular processes inspired the search for novel compounds which interact with microtubule assembly providing valuable tools to inhibit cellular proliferation. There are three recognised binding sites in which agents can interact with tubulin and include the i) vinca and ii) taxane site located on β tubulin and the iii) colchicine site located at the interface between α and β tubulin (Figure 4).[7,9]

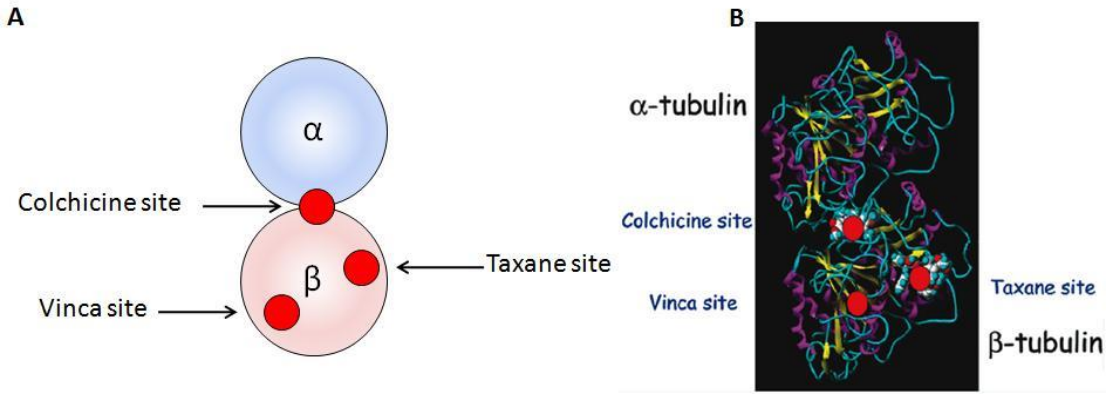

Figure 4: The three binding sites on tubulin are vinca, taxane and colchicine sites B) A crystal strucuture of a-β tubulin dimer with the binding sites labelled in red adapted from Fojo *et al*.[9]

A diverse range of natural and synthetic compounds interact with tubulin and either disrupt the formation of microtubules, classed as microtubule destabilisers or interact with tubulin within a fully formed microtubule and prevent its disassembly classed as microtubule stabilisers.[10] Due to their distinct mode of action, microtubule binding drugs are commonly used alongside other cytotoxic drugs in combination chemotherapy for a range of different cancers and are set to continue to play a pivotal role in the future.

1.4 Microtubule Stabilisers

Microtubule stabilisers commonly bind to the taxane site on β tubulin within a formed microtubule resulting in a subtle conformation change preventing the α-β tubulin heterodimers from disassociating from the formed microtubule.[11] The success of this class of compounds is exemplified by the taxane natural product Paciltaxel (Taxol®) **(1)** isolated from the Pacific yew tree (*Taxus brevifolia)* (Figure 5) approved in 1992 for breast and ovarian cancers and later for use in lung cancers.[12] However despite the success of Taxol®, the poor water solubility and emergence of drug resistance are major limitations and have inspired the search for improved agents to overcome these complications.[13]

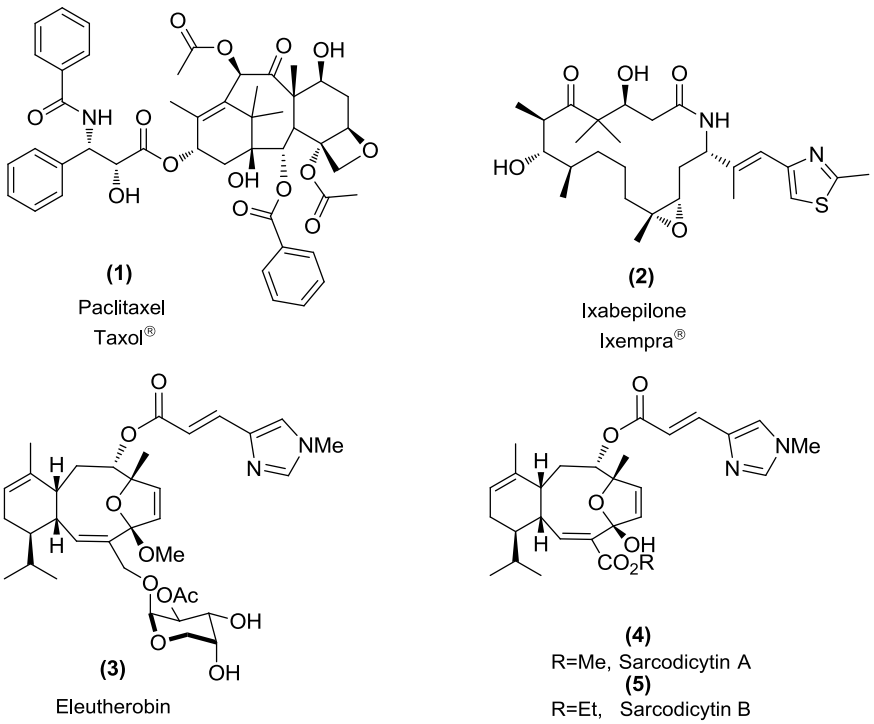

Figure 5: Microtubule stabilisers.

Ixempra® **(2)** is derived from the gram negative bacteria (*Sorangium Cellulosum*) and binds to the taxane site on tubulin and was approved by the FDA in 2007 for use in metastatic breast cancer and in Taxol®-resistant cancers.[14] Ixempra® **(2)** demonstrates the importance of developing the next generation of drugs with improved biological profiles to replace existing treatments in the clinic.

Two further additions to this library are eleutherobin **(3)** isolated in 1993 from the Australian coral *Eleutherobia*[15,16] and sarcodictyin A **(4)** and B **(5)** isolated in 1987 from the Mediterranean coral *Sarcodictyon roseum.*[17] Eleutherobin **(3)** and sarcodictyin **(4,5)** were shown to be microtubule stabilisers which bind to the taxane binding site with potent antiproliferative activities exemplified by eleutherobin **(3)** displaying IC_{50} values of 11 nM and 14 nM in a colon (HCT116) and ovarian (A2780) cell lines respectively.[18] The most promising property of these natural products are their activities in Taxol®-resistant cell lines suggesting they may be valuable additions to the clinic.[18,19] One major problem limiting the further development of these compounds is the limited availability from natural sources and the complex total syntheses currently available (>35 steps).[20-25]

1.5 Sarcodictyin SAR Study

An extensive structure activity relationship (SAR) study by Nicolaou *et al.*[26] highlighted the importance of the urocanic ester side chain (Figure 6) inspiring the design of simplified structurally related analogues in an attempt to pursue the clinically potential of these natural products.

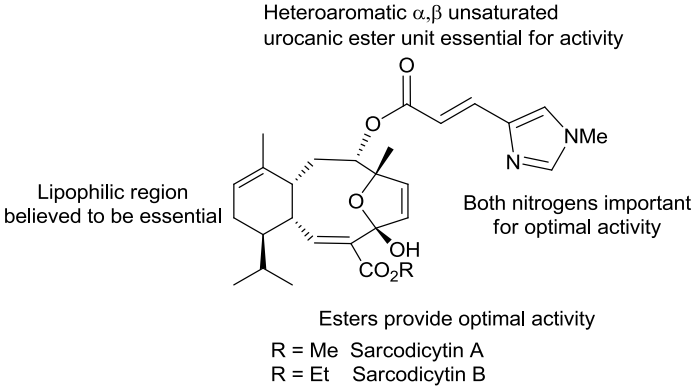

Figure 6: Nicolaou *et al.* SAR study.[26]

Numerous research groups incorporated the urocanic ester side chain into simplified analogues in attempts to confer the nanomolar activity of the sarcodictyins, however they met with limited success. Gennari *et al.* reported an analogue **(6)** synthesised in 21 steps from carvone displaying low micromolar activity in human ovarian (A2780) and two colon cancer cell lines (HCT116 and HT29 Figure 7).[27]

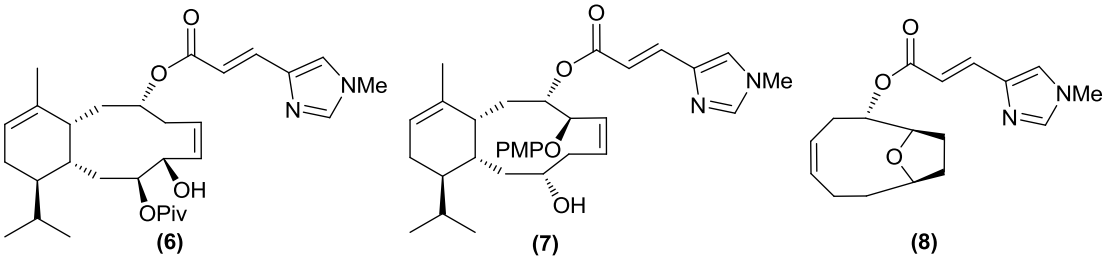

(6)
ED_{90}: 2.0 μM
IC_{50} (A2780): 4.0 μM
IC_{50} (HCT116): 4.0 μM
IC_{50} (HT29): 5.0 μM

(7)
ED_{90}: 0.5 μM
IC_{50} (A2780): 1.9 μM
IC_{50} (HCT116): 0.9 μM
IC_{50} (K562): 2.3 μM

(8)
ED_{90}: 6.0 μM

Figure 7: Simplified sarcodictyin analogues.[27-29]

The simplified analogue **(6)** was confirmed as a tubulin stabiliser with an ED_{90} value of 2.0 μM (concentration required to induce 90% tubulin polymerisation). Gennari *et al.* suggested that the failure to confer the potent tubulin stabilisation properties of **(6)** to antiproliferative activity *in vitro* may be due to esterase mediated hydrolysis of the urocanic ester side chain previously identified as vital for biological activity.[27] Gennari *et al.* also reported a further analogue **(7)** synthesised in 22 steps from carvone with improved tubulin stabilising and antiproliferative activities.[28] Analogue **(7)** displayed an ED_{90} value of 0.5 μM however the antiproliferative activities *in vitro* remained in the low micromolar range. This inability to translate tubulin stabilisation properties to potent antiproliferative activities within cancer cell lines highlights the potential weakness of the ester linkage. Holmes *et al.* reported a much simplified analogue **(8)** synthesised in 9 steps from 2-deoxy-D-ribose which had an ED_{90} value of 6.0 μM however no IC_{50} values were reported.[29]

To pursue the clinical potential of simplified eleutherobin **(3)** and sarcodictyin **(4,5)** analogues we envisaged replacing the ester linkage with an isostere less susceptible to hydrolysis. We wished to simplify the synthesis of simplified eleutherobin **(3)** and sarcodictyin **(4,5)** analogues (<3 steps) overcoming the long syntheses previously reported (>20 steps) enabling rapid screening for useful biological activities, as outlined in the aims and objectives section.

1.6 Microtubule Destabilisers

Compounds can interact with tubulin resulting in depolymerisation of microtubules (Figure 8) and are classified as microtubule destabilisers. This class of compounds are structurally diverse and have been reported to interact at the vinca or colchicine binding site preventing the assembly of α-β tubulin heterodimers.[30] The most notable examples of this class of compounds are the vinca alkaloids vincristine **(9)** and vinblastine **(10)** (Figure 8). These compounds were isolated from the Madagascar periwinkle (*Catharanthus roseus*) and have been in clinical use for leukaemia and lymphoma since the 1950s.[31]

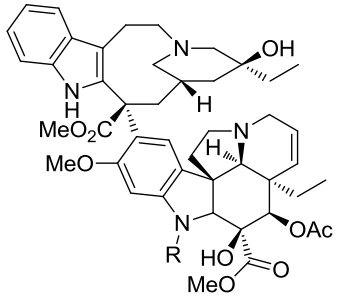

(9)
R = CHO, Vincristine, Velban®
(10)
R = Me, Vinblastine, Oncovin®

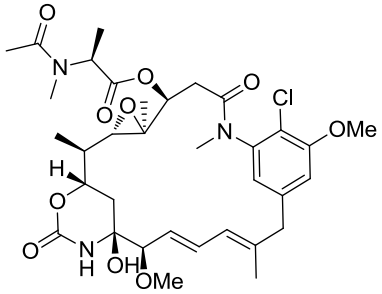

(11)
Maytansine

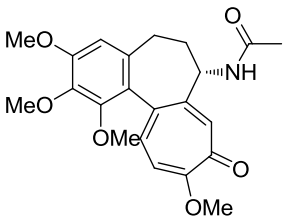

(12)
Colchicine

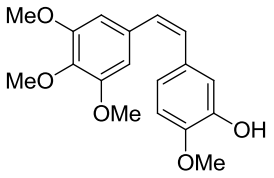

(CA4, 13)
Combretastatin A-4

Figure 8: Microtubule destabilisers.

The emergence of drug resistance to the vinca alkaloids has inspired the search for novel alternatives which overcome this problem. The natural products maytansine **(11)**, derived from the staff vine plant (*Maytenus*)[32] and colchicine **(12)**, derived from the meadow saffron plant (*Colchicum autumnale*)[31] (Figure 8), display very potent microtubule destabilising properties. A major complication with colchicine (**12**) and maytansine (**11**) is severe toxicity limiting the clinical progression of these natural products.[31]

1.7 The Combretastatins

Combretastatins are a group of phenolic stilbenes derived from the South African Willow tree (*Combretum Caffrum)* displaying lower toxicity than colchicine and maytansine, while still retaining excellent microtubule destabilising properties. Combretastatin A-4 (**CA4**, **13**) shows the most promise by reversibly binding at the colchicine site on β tubulin preventing its association with α tubulin.[33] The destabilising effect on microtubule dynamics results in potent antiproliferative activity across multiple cancer cell lines including multidrug resistant cell lines. One of the most promising properties of **CA4** is its ability to disrupt tumour vasculature without disrupting normal vasculature.[34] **CA4** is poorly water soluble therefore a range of analogues have been developed and evaluated in clinical trials with Zybrestat® currently being studied in a phase III trial for thyroid cancer (Figure 9 and table 1).[35]

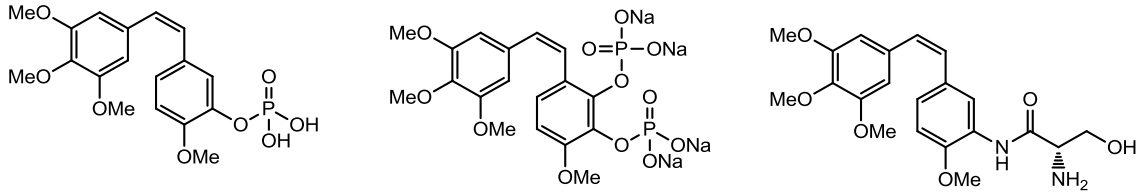

(14) Zybrestat®

(15) Oxi4503

(16) Ombrabulin

Figure 9: Various CA4 analogues are available.

Drug	Sponsor	Clinical Development		
		Phase I	**Phase II**	**Phase III**
Zybrestat® **(14)**	OXiGENE	Completed in solid tumours	Completed in lung cancer	Ongoing in thyroid cancer
Oxi4503 **(15)**	OXiGENE	Completed in solid tumours	Ongoing in liver cancer	-
Ombrabulin **(16)**	Sanofi-Aventis	Completed in solid tumours	Ongoing in lung and ovarian cancer	-

Table 1: Combretastatin prodrugs are under clinical evaluation in multiple cancer types as of 2009.[35]

1.8 Combretastatin SAR Study

Combretastatin A-4 **(CA4, 13)** inspired extensive research into its SAR in attempts to develop second generation **CA4** analogues with improved biological properties. The 3,4,5-trimethoxy aryl A ring is a major structural feature present in **CA4** and in a number of natural products with microtubule disruption properties (Figure 10).[36]

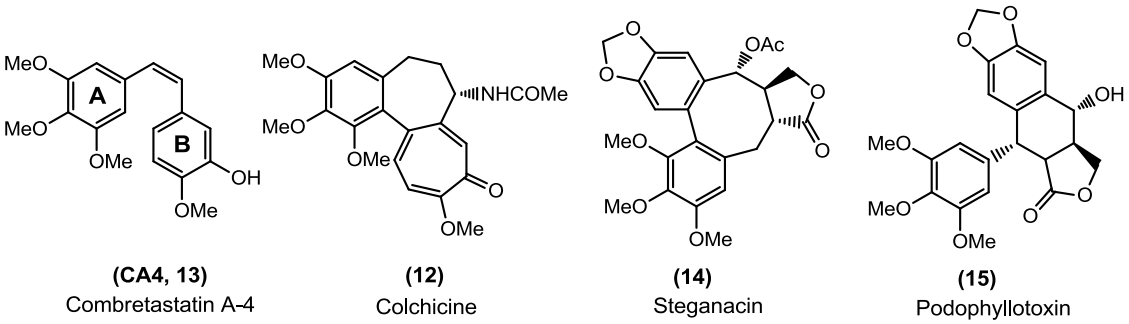

Figure 10: The 3,4,5-trimethoxy aryl unit present in a number of natural products.[36]

McGown *et al.* synthesised and screened 52 **CA4** analogues to confirm the importance of this motif. Replacing the methoxy groups in **CA4** for ethyloxy groups in analogue **(16)** or methyl groups in analogue **(17)** resulted in a twenty fold decrease in antiproliferative activity in the human leukaemia K562 cell line (Figure 11).[37] Interestingly while analogue **(17)** displayed a twenty fold loss of activity in K562 compared to **CA4**, it was a more potent inhibitor of microtubule assembly (MA). Fluorine was also investigated in analogue **(18)** however it displayed a hundred fold loss in antiproliferative activity. This SAR study suggested that the 3,4,5-trimethoxy aryl was the preferential unit for antiproliferative activity.

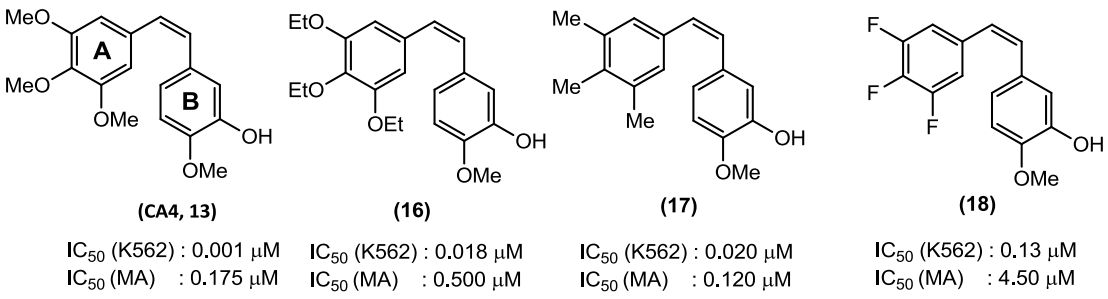

Figure 11: CA4 SAR study highlighting the importance of the 3,4,5- trimethoxy aryl unit.

A recent study by Ley *et al.* challenged this SAR study by reporting a 3,5 dibromo **CA4** analogue **(19)** with comparable activity to **CA4** in human epithelial cervical (HeLa) and ovarian (SK-OV-3) cancer cell lines but improved activity in a Taxol®-resistant ovarian cell line (SK-OV-3-3TR) (Figure 12).[38]

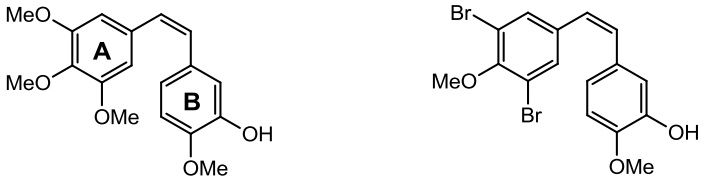

(CA4, 13)

IC_{50} (HeLa) : 1.4 nM
IC_{50} (SK-OV-3) : 1.2 nM
IC_{50} (SK-OV-3-3TR): 3.1 nM

(19)

IC_{50} (HeLa) : 6.7 nM
IC_{50} (SK-OV-3) : 1.7 nM
IC_{50} (SK-OV-3-3TR): 1.1 nM

Figure 12: Bromination of the A ring can confer addition Taxol®-resistant properties.[38]

Ley *et al.* suggest that a halogen bonding interaction may be operating between the tubulin protein and 3,5 dibromo analogue **(19)** resulting in this biological activity. This demonstrates that substituting the A ring of **CA4** with bromine may confer additional useful properties such as activity in Taxol®-resistant cell lines.[38] McGown *et al.* reported that when the 4-OMe in the B ring in **CA4** is replaced with 4-H in analogue **(20)** there is a 100 fold loss in activity. Replacing the 3-OH in **CA4** with 3-F in analogue **(21)** resulted in a 10 fold loss of activity in K562, despite more potent microtubule assembly (MA) IC_{50} than **CA4** (Figure 13).[37]

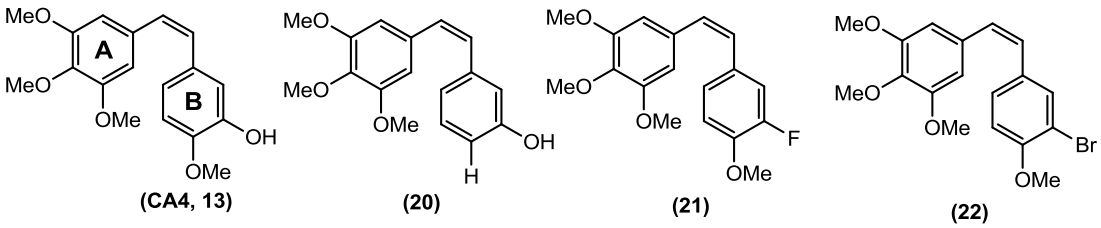

(CA4, 13)

IC_{50} (K562): 0.001 μM
IC_{50} (MA): 0.175 μM

(20)

IC_{50} (K562): 0.14 μM
IC_{50} (MA): >10 μM

(21)

IC_{50} (K562): 0.010 μM
IC_{50} (MA): 0.085 μM

(22)

IC_{50} (K562): 0.001 μM
IC_{50} (MA): 0.400 μM

Figure 13: The B ring can be substituted however 3-OH, 4-OMe is the preferred configuration.

Replacing the 3-OH in **CA4** with a 3-Br in analogue **(22)** retained comparable activity as **CA4** in K562 but with a higher MA IC_{50} demonstrating the ability to disrupt microtubule assembly does not always correlate with antiproliferative activity *in vitro*. The *cis* (*Z*) orientation of the double bond in **CA4** is vital for biological activity however it can isomerise to the thermodynamically more stable *trans* (*E*) configuration **(23)** during storage and *in vivo* resulting in a loss in activity (Scheme 1).[39]

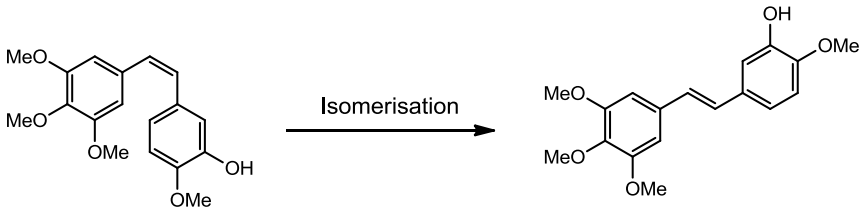

(CA4, 13) **(23)**

IC_{50} (NCI-H460): 1.90 nM
IC_{50} (DU-145): 2.50 nM

IC_{50} (NCI-H460): 120 nM
IC_{50} (DU-145): 117 nM

Scheme 1: Isomerisation of the active *Z* figuration to the less active *E* configuration.[39]

Numerous studies have investigated replacing the double bond of **CA4** with heterocycle isosteres which retain the *Z* figuration required for potent antiproliferative activity.[40-45] This strategy enables the introduction of additional function groups to overcome the poor water solubility of **CA4** previously reported. A diverse range of different heterocyclic **CA4** analogues have been reported including pyrrole[40] **(24)**, furan[41] **(25)** and 1,2,3-triazole[42] **(26)** which retain nanomolar antiproliferative activities (Figure 14). One particularly interesting example is thiazole[43] **(27)** with an IC_{50} value of 0.03 nM in the HeLa cell line (human human cervical carcinoma) (Figure 14). In contrast **CA4** displayed an IC_{50} value of 1.4 nM in HeLa. This 46 fold increase in antiproliferative activity in the HeLa cell line for thiazole **(27)** confirms that heterocyclic **CA4** analogues are a valid method of overcoming the problems experienced with **CA4**.

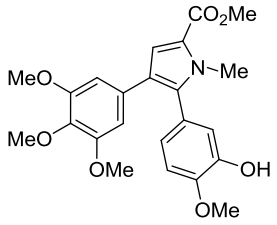

(24)

IC_{50} (CA46): 31 nM[40]

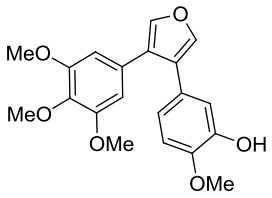

(25)

IC_{50} (SH-SY5Y): 2.9 nM[41]

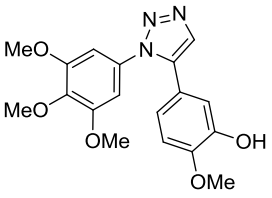

(26)

IC_{50} (SHSY-5Y): 4.7 nM[42]

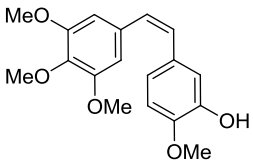

(**CA4, 13)**

IC_{50} (HeLa): 1.4 nM

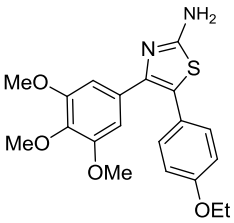

(27)

IC_{50} (HeLa): 0.03 nM[43]

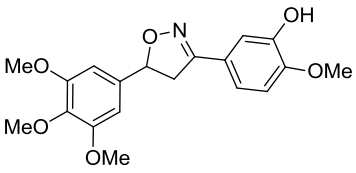

(28)

IC_{50} (HL60):1500 nM[44]

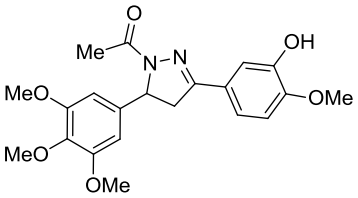

(29)

IC_{50} (NCI-H460): 210 nM[45]

Figure 14: Recent *Z* restricted combretastatin A-4 analogues.[40-45]

The design, synthesis and biological evaluation of novel combretastatin A-4 analogues derived from chalcones is reported in chapter 3.

1.9 Chalcones as Tubulin Binding Agents

Chalcones (1,3-diarylprop-2-en-1-ones) consist of two aromatic rings connected by an enone and are privileged structures present in an extensive range of biologically active molecules (Scheme 2). Chalcones exhibit various activities including anti-inflammatory, anti-infective, anti-oxidative, anti-malarial and anti-cancer properties.[46] The versatility of the chalcone structure and the ease of its synthesis provide a valuable opportunity to develop novel molecules in the field of medicinal chemistry.

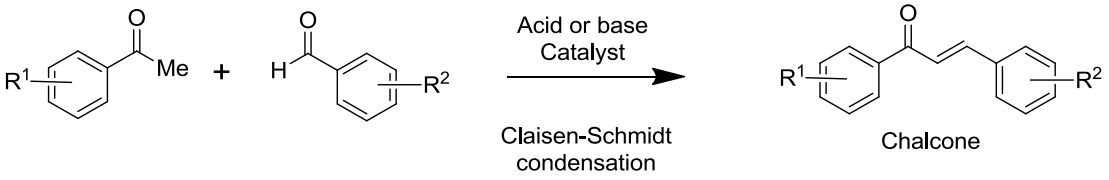

Scheme 2: Chalcone synthesis.

Chalcones have been reported to display a range of microtubule binding properties including nanomolar and picomolar IC_{50} values in various cancer cell lines (Figure 15).[47-50]

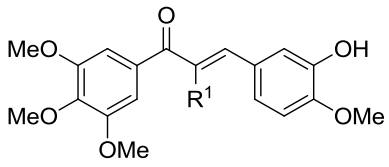

(30)

R^1 = H IC_{50} (K562): 4.3 nM[47]

(31)

R^1 = Me IC_{50} (K562): 0.21 nM[47]

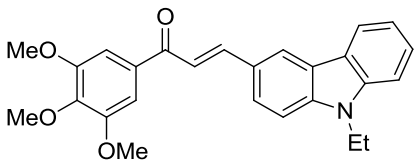

(32)

Microtubule inhibitor

IC_{50} (Tubulin): 9-12 μM[48]

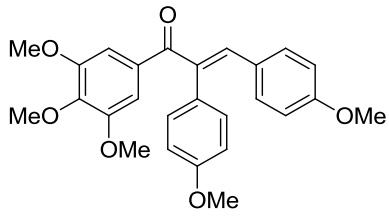

(33)

Microtubule inhibitor

IC_{50} (Tubulin): 2.5 μM[49]

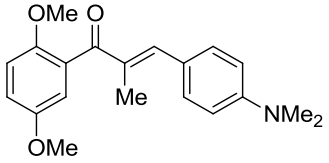

(34)

Microtubule inhibitor

IC_{50} (Tubulin): 10 μM[50]

Figure 15: Previously reported chalcones with microtubule binding properties.[47-50]

1.10 Chalcones as Starting Materials for Pyrazolines

Chalcones, while interesting in themselves, can also serve as versatile starting materials for more complex molecules in medicinal chemistry. The vast range of commercially available substituted acetophenone and benzaldehydes in addition to the modular design and flexibility enables large compound libraries to be generated using simple and robust chemical synthesis. The pyrazoline motif is a particularly useful scaffold in medicinal chemistry enabling the arrangement of pharmacophores in a three dimensional arrangement and has been used to generate a variety of compounds that display antiproliferative activity in cancer cell lines (Figure 16).[51-54]

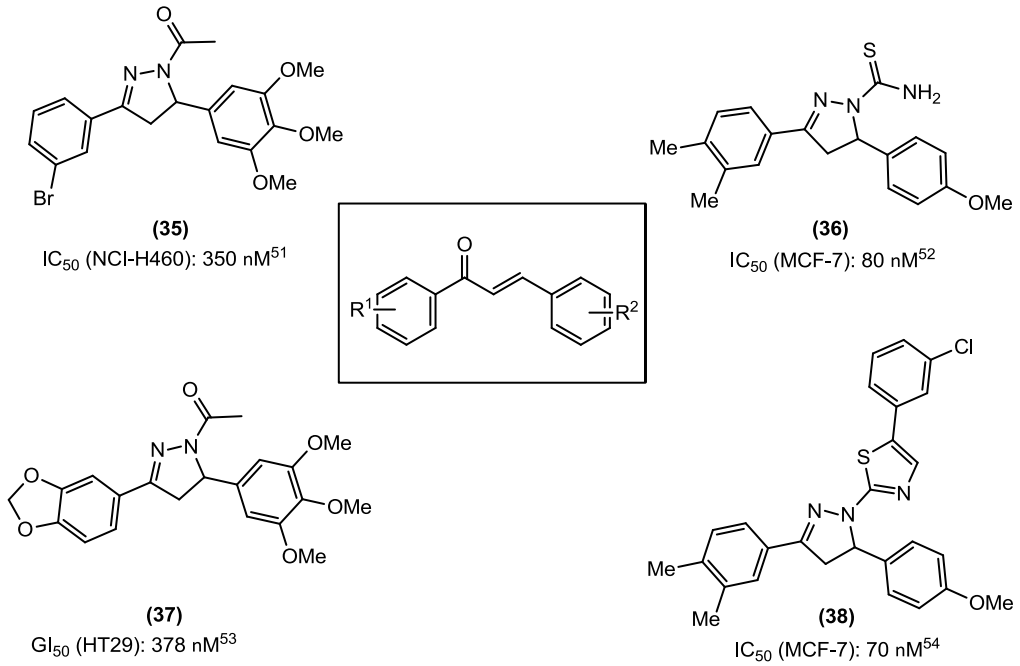

Figure 16: Chalcones as starting materials for pyrazolines.[51-54]

The design, synthesis and investigation of novel pyrazolines are the subjects for discussion in chapters 3 and 5.

1.11 National Cancer Institute (NCI) 60 Cell Line Panel

The National Cancer Institute (NCI) developed the 60 cell line panel in the late 1980s as a rapid screening tool for academic and industrial laboratories to submit novel natural or synthetic compounds to assess anti-cancer activity across 60 different cancer cell lines from eight different cancer types without charge.[55] To date, the NCI has screened over 50,000 novel compounds and has been involved in the development of many clinically used drugs including Taxol® and will continue to play a significant role in the future. A flow chart of the screening service available at the NCI is presented in Figure 17.

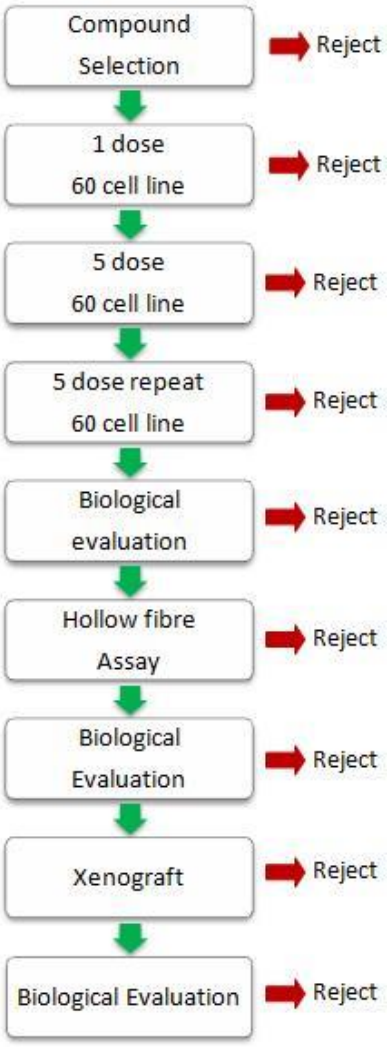

Figure 17: Flow chart of the screening services available at the NCI.

To enter the NCI 60 cell panel suppliers provide the molecular structure of the compound including a short description of potential anti-cancer properties, typically including some initial IC_{50} values in cancer cell lines. The NCI assesses the novelty of the compound to ensure it or a related analogue has not been previously screened and if the compound satisfies these requirements then the NCI will accept the sample. The compound is initially screened in all 60 cell lines at a single high dose (10^{-5}M) and only compounds which meet NCI predetermined levels of growth inhibition are selected for further screening at 5 doses. Growth inhibition is reported as a GI_{50} which is the concentration that inhibits cell growth by 50% with potent GI_{50} values in well characterised cell lines of particular interest. For example, NCI/ADR-RES is a multidrug resistant ovarian cell line and OVCAR-3 is an ovarian line which is particularly sensitive to tubulin binders.[56] Compounds with promising activity are screened a second time to ensure reliability and consistency after which the compound is assessed by the biological evaluation committee to determine if it should progress to an *in vivo* hollow fibre assay. If the compound performs well *in vivo* the NCI will sponsor the clinical development of the compound. This is exemplified by the success of bortezomib which entered the single dose screen in July 1995 and after 8 years of development at the NCI was FDA approved in 2003 for use in myeloma.[55]

1.12 COMPARE Algorithm

To fully capitalise on the vast database at the NCI, the COMPARE algorithm was developed in which the biological profile of a submitted compound is compared against the entire NCI library to identify compounds with similar activities across the 60 cell lines.[56] Generally compounds with similar activities across 60 cell lines have similar modes of action therefore COMPARE can be used to predict the mode of action of a novel compound.[38] Halichondrin B, a natural product from the *Halichondria okada* marine sponge, was submitted to the NCI with an unknown mode of action. COMPARE analysis demonstrated a high correlation with microtubule binders, this was further investigated and Halichondrin B was experimentally confirmed to be a potent microtubule destabiliser.[56]

1.13 Identifying Novel Tubulin Binders

Tubulin binders display characteristic hallmarks which can identify a compound as a tubulin binder and classify it as a microtubule stabiliser or destabiliser. These three hallmarks were used throughout our investigations and are discussed below.

1.14 Cell Cycle Analysis

Tubulin binding compounds typically cause cell cycle arrest in the G2/M phase of the cell cycle which can be easily determined using cell cycle analysis. This technique relies on measuring the DNA content of a cell using propidium iodide; a DNA intercalator which becomes fluorescent when bound to DNA. As the cell progresses through the cell cycle the DNA content increases therefore the extent of fluorescence is a direct indication of the amount of DNA within the cell and indicates progression within the cell cycle (Figure 18A). A healthy cell population without the presence of a tubulin binder will give a histogram as shown in figure 18B where the majority of cells as in the G1 phase. The presence of a tubulin binder, for example **CA4** as shown in figure 18C increases the cell population arresting in the G2/M phase of the cell cycle.[57]

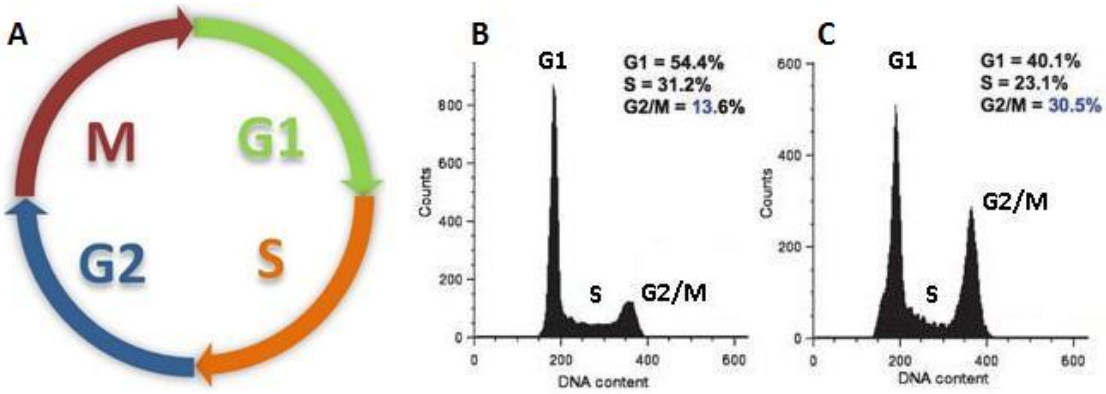

Figure 18: Cell cycle analysis to determine the location of cells in the cell cycle (A), histograms for SK-1OV-3 (ovarian carcinoma) without (B) and in the presence of 5 nM of CA4 (C).[38]

G2/M cell cycle arrest is a characteristic feature of tubulin binders however it cannot classify a compound as a stabiliser or destabiliser.

1.15 *In Vitro* Tubulin Polymerisation Assay

This assay is based on the method reported by Shelanski *et al.*[58] in which the polymerisation of tubulin into microtubules scatters light (measured as an optical density, OD) and provides an indication as to the extent of microtubule polymerisation. The presence of a tubulin stabiliser will promote microtubule polymerisation increasing the OD whereas the presence of a tubulin destabiliser will disrupt polymerisation lowering the OD compared to control (Figure 19).

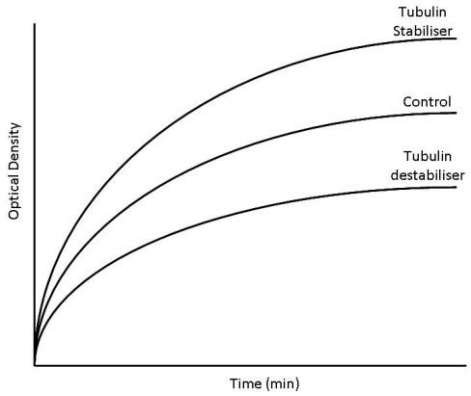

Figure 19: Idealised *in vitro* tubulin polymerisation curves for tubulin binders.

1.16 Confocal Microscopy

This technique involves fluorescently labelling microtubules, enabling direct visualisation of the effect a compound has on microtubule assembly (Figure 19). The presence of a microtubule stabiliser is typical of the results shown in figure 20B whereas figure 20C is typical of a microtubule destabiliser such as vincristine.[59]

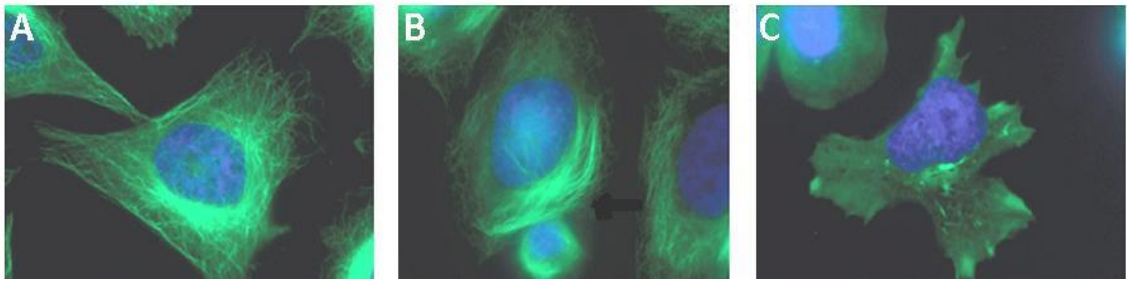

Figure 20: Typical confocal microscopy results of HeLa cells without drug (A), with Taxol® (B) and with vincristine (C), microtubules (green) and chromosomes (blue).[59]

1.17 Urocanic-Chalcone Hybrids

Design, synthesise and investigate the antiproliferative properties of structurally related urocanic-chalcone hybrids containing the urocanic pharmacophore of which hybrid **(51)** is predicted to be the most active (Figure 21).

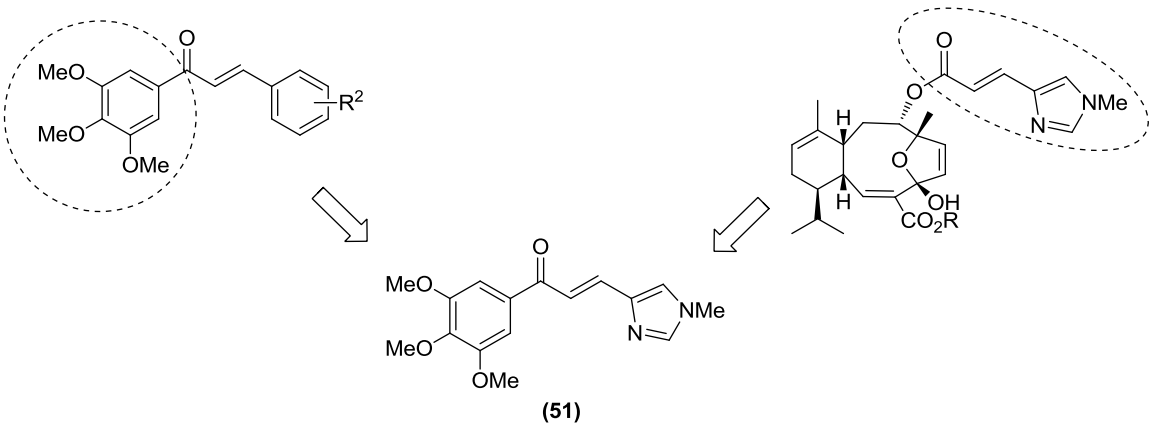

Figure 21: Proposed urocanic-chalcone hybrids.

A range of different substituted acetophenone and aldehydes will be used to produce structurally related analogues enabling a simple SAR study (Figure 22).

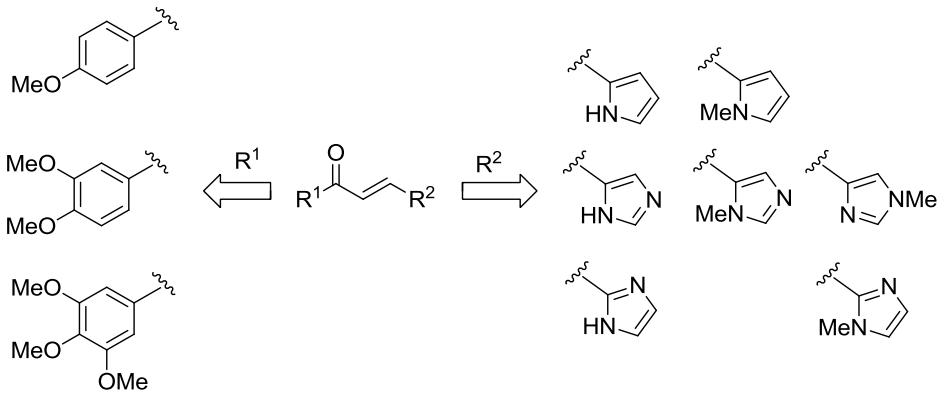

Figure 22: Urocanic-chalcone library design.

Each hybrid will be screened for antiproliferative activity in three cancer cell lines and one non cancer cell line to determine selectivity. The most promising compounds will be submitted to the NCI for 60 cell line analysis, and COMPARE analysis to determine the mode of action which will be confirmed experimentally.

1.18 Pyrazoline Combretastatin A-4 Analogues

Design, synthesis and investigation of the antiproliferative properties of **CA4** analogues, of which **(68)** is predicted to be the most active (Scheme 3).

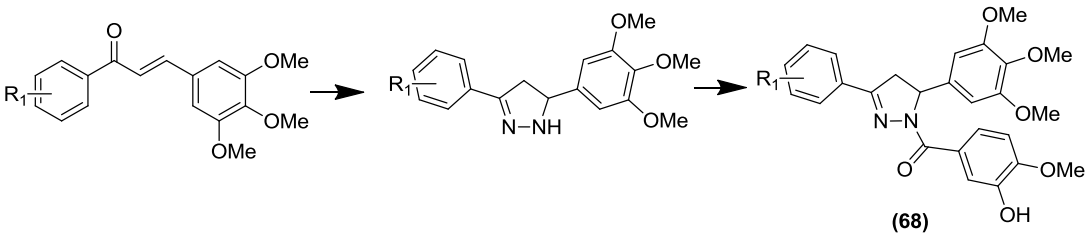

Scheme 3: Pyrazoline CA4 analogues.

A range of analogues with different R^1 and R^2 groups will be used to produce structurally related compounds enabling a SAR study (Figure 23).

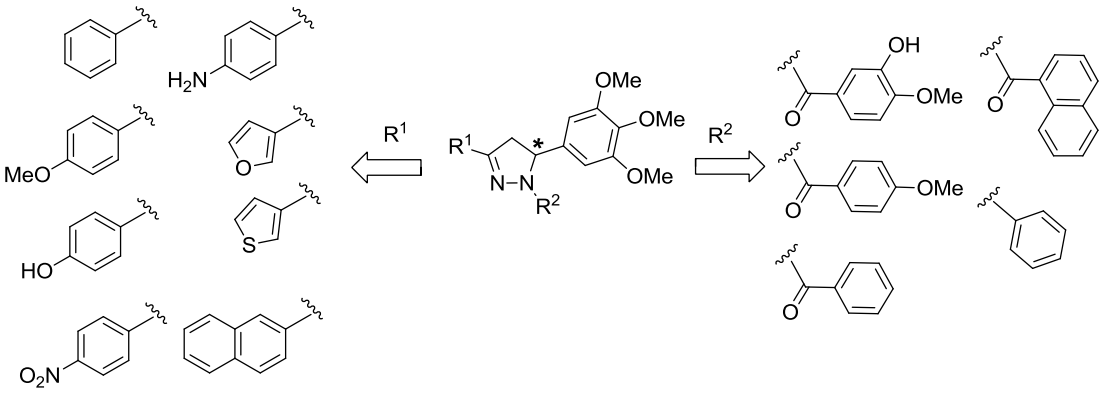

Figure 23: Pyrazoline CA4 library design.

Each analogue along with its corresponding chalcone will be screened for antiproliferative activity and the most promising analogues screened in a non cancer cell line to determine selectivity towards cancer. Due to the presence of a stereogenic centre at position five of the pyrazoline ring (* in figure 23), the most promising analogues will be enantiomerically enriched to determine the effect of stereochemistry on biological activity. The most promising compounds will be submitted to the NCI for 60 cell line analysis, and COMPARE analysis to determine the mode of action which will be investigated experimentally.

Chapter 2: Urocanic-Chalcone Hybrids

2.1 Overview

The natural products eleutherobin **(3)**[15,16] and sarcodictyin **(4,5)**[17] are potent microtubule stabilisers displaying nanomolar antiproliferative activities in Taxol®-resistant cancer cell lines (Figure 24).

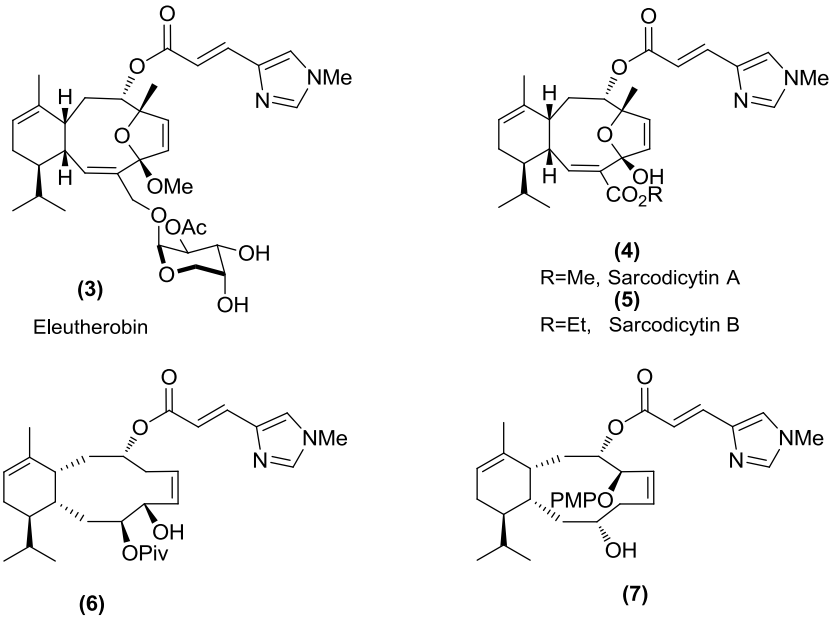

Figure 24: Urocanic ester chain side in the natural products and simplified analogues.[15-17, 27-28]

Nicolaou *et al.* reported the importance of the urocanic ester side chain for biological activity[26] inspiring the design of simplified analogues containing this key pharmacophore. Gennari *et al.* reported two simplified analogues **(6,7)**[27,28] containing the urocanic ester side chain which retained microtubule stabilising properties but only micromolar antiproliferative activities in cancer cell lines (Figure 24). Gennari *et al.* proposed that hydrolysis of the ester side chain was responsible for the loss in antiproliferative activity *in vitro*. The chalcone motif is a privileged structure present in a diverse range of range of biologically active molecules including microtubule binders. Herein we report the design and synthesis of fourteen urocanic-chalcones analogues and their antiproliferative activities in three cancer and one non cancerous cell line. Mechanistic studies are also reported to identify the mode of action of this class of compounds.

2.2 Chemical Synthesis

Chalcones are commonly prepared using a Claisen-Schmidt condensation reaction between an acetophenone, benzylaldehyde and a base in a protic solvent with the general reaction mechanism outlined below (Scheme 4).

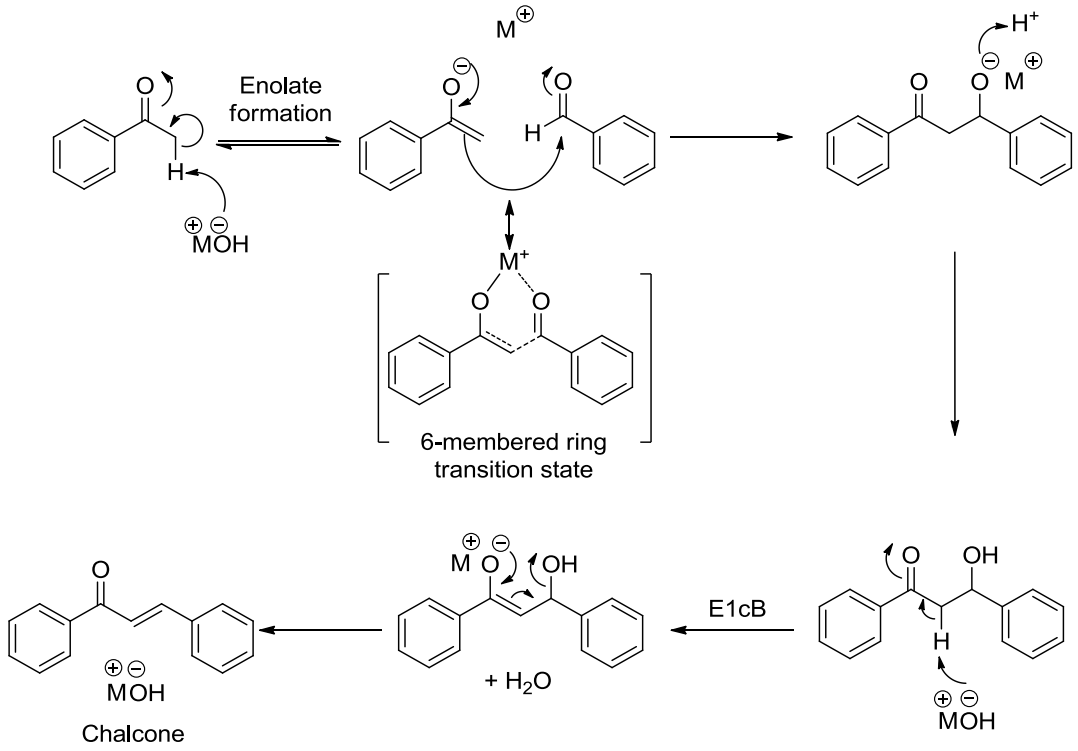

Scheme 4: Claisen-Schmidt condensation mechanism.

A solvent free method was adapted from a literature procedure of similar substrates,[60] in which an acetophenone and ketone are ground together in a mortar and pestle in the presence of excess NaOH for five minutes to afford chalcones (**43-45**) in high yield (Scheme 5).

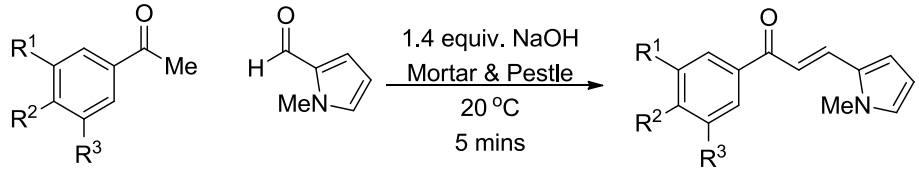

(43) R^1 = H, R^2 = OMe, R^3 = H, 63%
(44) R^1 = OMe, R^2 = OMe, R^3 = H, 79%
(45) R^1 = OMe, R^2 = OMe, R^3 = OMe, 63%

(43-45)

Scheme 5: Method A.[60]

The method above was found to be only applicable for this carboxaldehyde as all other attempts at synthesising the remaining chalcones via this route gave complete recovery of starting materials. One possible explanation for this observation is that the carboxaldehyde is a liquid at room temperature whereas all other carboxaldehydes were solid. An alternative method using LiOH[61] was optimised affording chalcones **(40-42)** in yields up to 74% (Scheme 6).

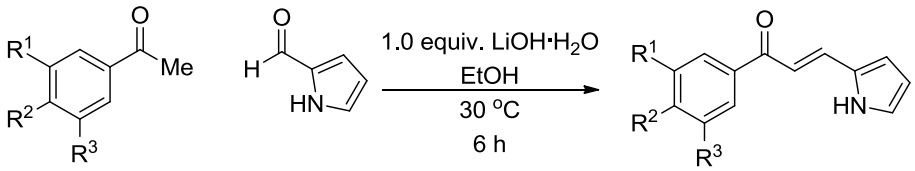

(40) R^1 = H, R^2 = OMe, R^3 = H, 43%
(41) R^1 = OMe, R^2 = OMe, R^3 = H, 53%
(42) R^1 = OMe, R^2 = OMe, R^3 = OMe, 74%

(40-42)

Scheme 6: Method B to afford chalcones (40-42).[61]

The reaction conditions above were not effective with the imidazole analogues so a third method was investigated for chalcones **(46-48)** by adapting a literature procedure involving the Lewis acid $BF_3{\cdot}OEt_2$ (Scheme 7).[62]

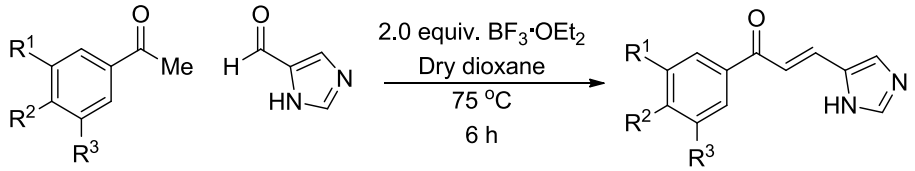

(46) R^1 = H, R^2 = OMe, R^3 = H, 53%
(47) R^1 = OMe, R^2 = OMe, R^3 = H, 74%
(48) R^1 = OMe, R^2 = OMe, R^3 = OMe, 74%

(46-48)

Scheme 7: Method C to afford chalcones (46-48).[62]

Using one equivalent of $BF_3{\cdot}OEt_2$ as reported[62] failed to afford the desired chalcone resulting in complete recovery of starting materials. Increasing the $BF_3{\cdot}OEt_2$ to two equivalents was required to afford the desired chalcone in yields up to 74%. It is believed that the first equivalent of BF_3 coordinates to the basic nitrogen in the imidazole preventing enolate formation. A second equivalent is required to enable enolate formation allowing the reaction to proceed. It was found that BF_3 remained

coordinated to the chalcone product and required an additional step during purification to dissociate the BF_3 from the final chalcone. The addition of 2M NaOH and gentle heating during the work up procedure successfully disrupted BF_3 coordination affording chalcones (**46-48**) in good yield (Scheme 7).

To investigate the effect of the enone group, the saturated derivative **(49)** was synthesised using a standard hydrogenation procedure (Scheme 8).

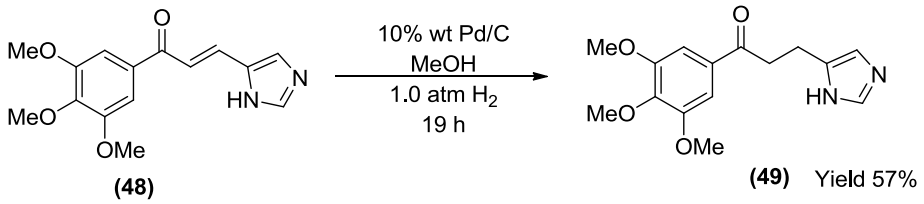

Scheme 8: Method D to afford chalcone (49).

Methylation of the imidazole ring in chalcone **(48)** was attempted using caesium carbonate and methyl iodide to afford both isomers **(50)** and **(51)** in a single step (Scheme 9). ^{1}H NMR indicated a 1:1 ratio of chalcones **(50)** and **(51)** however it was difficult to separate each isomer by column chromatography.

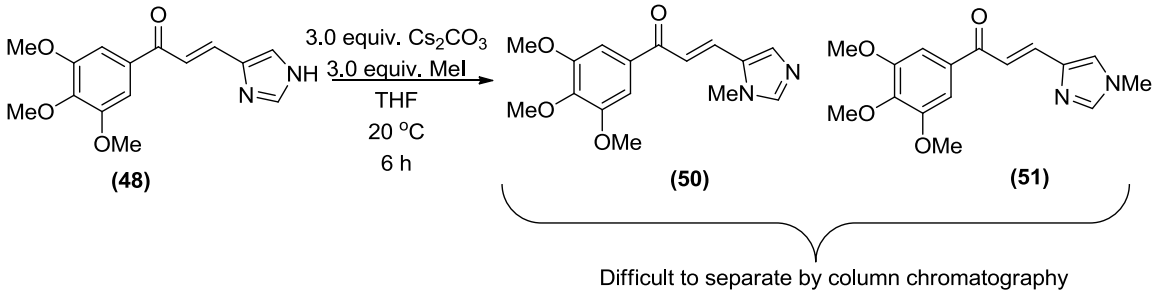

Scheme 9: Method E to afford chalcones (50,51) in a 1:1 ratio.

The distal methylated carboxaldehyde was not commercially available, therefore an existing literature procedure[63] was adapted using NaH and MeI in DMF at 0^{o}C resulting in selective distal methylation (Scheme 10). Crude ^{1}H NMR revealed the presence of **(51)** and **(50)** in a ratio of 75:25 (**51**:**50**) which could be separated by column chromatography using a dichloromethane and isopropanol solvent system to afford **(51**) in >95% purity.

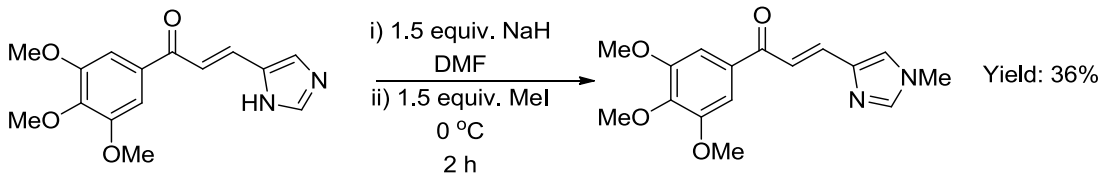

(48) **(51)**

Scheme 10: Method F to afford chalcone (51) selectively.[63]

Chalcone **(50)** was synthesised directly from the commercially available distal methylated carboxaldehyde using method C (Scheme 11) in 54% yield avoiding the purification difficulties experienced with methylation of chalcone **(48)** using method C.

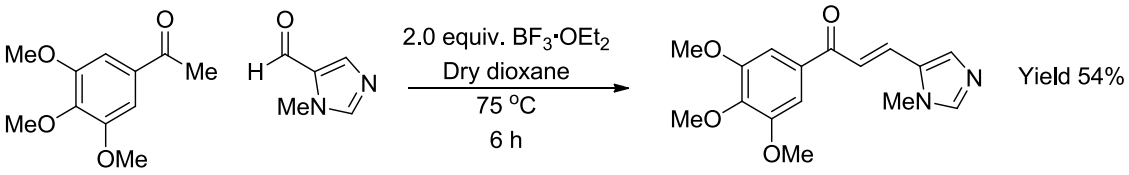

(50)

Scheme 11: Method C to afford chalcone (50).

Chalcone **(52)** was synthesised from imidazole-2-carboxaldehyde using method C in 38% (Scheme 12). Chalcone **(52)** contains a symmetrical imidazole ring which upon methylation using method E afforded a single methylated product chalcone **(53)**, due to symmetry in 54% yield (Scheme 12).

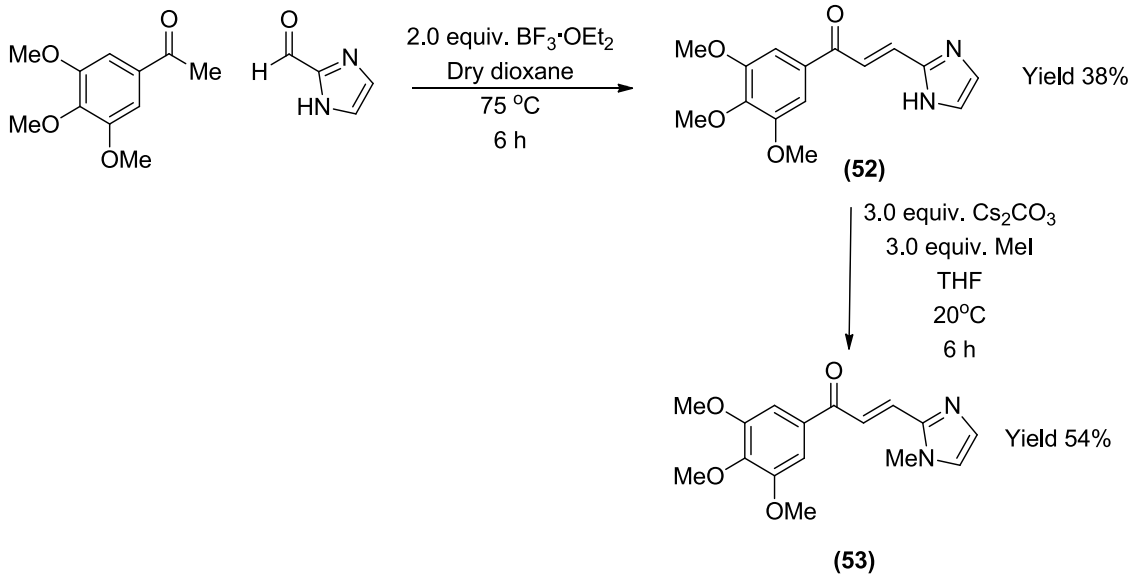

Scheme 12: Method C to give chalcone (52) which upon methylation afforded chalcone (53).

The successful synthesis of this library of compounds via one or two step procedures enables the antiproliferative properties in various cancer and non cancer cell lines to be explored using the MTS cell proliferation assay. All chalcones were confirmed to be ≥95% pure by HPLC at two wavelengths prior to submission to biological evaluation.

2.3 Biological Evaluation

The antiproliferative activity of each analogue was investigated in three cancer cells, HT29 a human colon carcinoma, MDA-MB-231 a human breast carcinoma and LNCaP, an androgen-dependent human prostate cancer. The antiproliferative activity in a non cancerous human skin fibroblast cell line FEK-4 was also investigated to determine selectivity. All activities are reported as an average IC_{50} (concentration required to inhibit 50% cell proliferation) of at least three independent experiments ± standard deviation, except where indicated (Table 2).

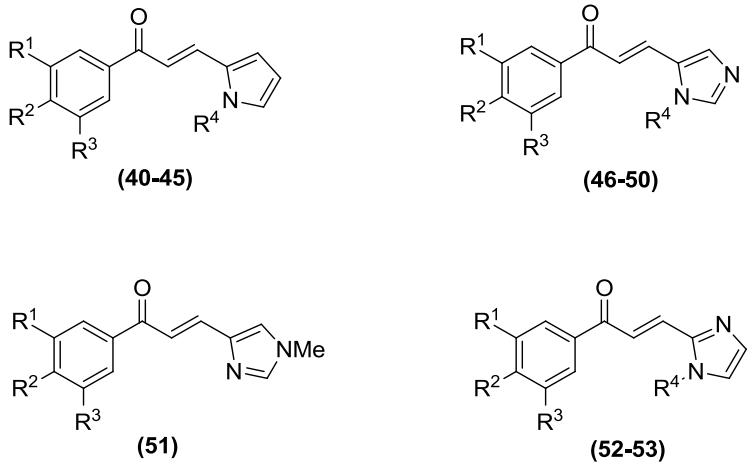

Figure 25: Chalcone structures.

						IC_{50} (μM)			
cpm	**R^1**	**R^2**	**R^3**	**R^4**	**Yield %**	**HT29**	**MDA-MB-231**	**LNCaP**	**FEK-4**
40	H	OMe	H	H	43	>500	>500	>500	>500
41	OMe	OMe	H	H	53	86.0 ± 2.6	102.4 ± 3.0	104.6 ± 7.9	135.1 ± 30.4
42	OMe	OMe	OMe	H	74	43.0 ± 6.5	49.9 ± 9.6	59.9 ± 7.5	156.1 ± 30.7
43	H	OMe	H	Me	63	61.8 ± 2.3	53.5 ± 4.6	75.5 ± 5.3	188.2 ± 74.9
44	OMe	OMe	H	Me	79	60.4 ± 10.7	42.8 ± 9.1	56.3 ± 10.1	161.7 ± 39.3
45	OMe	OMe	OMe	Me	83	12.5 ± 3.9	18.0 ± 6.3	69.5 ± 8.9	117.5 ± 20.1
46	H	OMe	H	H	53	23.6 ± 4.0	17.6 ± 3.8	33.5 ± 7.8	92.0 ± 11.2[a]
47	OMe	OMe	H	H	74	37.9 ± 8.6	18.2 ± 1.7	46.2 ± 5.5	84.2 ± 15.5
48	OMe	OMe	OMe	H	74	19.5 ± 0.4	22.9 ± 3.0	48.1 ± 6.2	53.2 ± 6.1
49	OMe	OMe	OMe	H	57	>500	223.4 ± 16.8	367.7 ± 111	>500[b]
50	OMe	OMe	OMe	Me	54	15.9 ± 1.5	16.9 ± 1.2	30.6 ± 6.8	49.9 ± 1.5
51	OMe	OMe	OMe	Me	36	2.9 ± 1.0	4.8 ± 1.8	48.4 ± 11.0	85.0 ± 21.1
52	OMe	OMe	OMe	H	38	5.0 ± 0.4	4.9 ± 0.8	17.1 ± 2.8	28.6 ± 8.7
53	OMe	OMe	OMe	Me	54	4.2 ± 0.5	4.9 ± 0.2	11.0 ± 2.9	17.5 ± 1.9
(Dox)	-	-	-	-	-	0.164	0.120	0.154	n.d

Table 2: MTS Assays, IC_{50} is the concentration that inhibits 50% cell proliferation, values are the mean from three independent experiments ± standard deviation, except [a] two and [b] one experiment, (DOX) doxorubicin was used as a positive control compounds, ≥95% pure by HPLC.

The addition of methoxy groups significantly increased the antiproliferative activity of the pyrrole series of hybrids across all cancer cell lines highlighting the importance of the 3,4,5 trimethoxy unit pharmacophore (Figure 26).

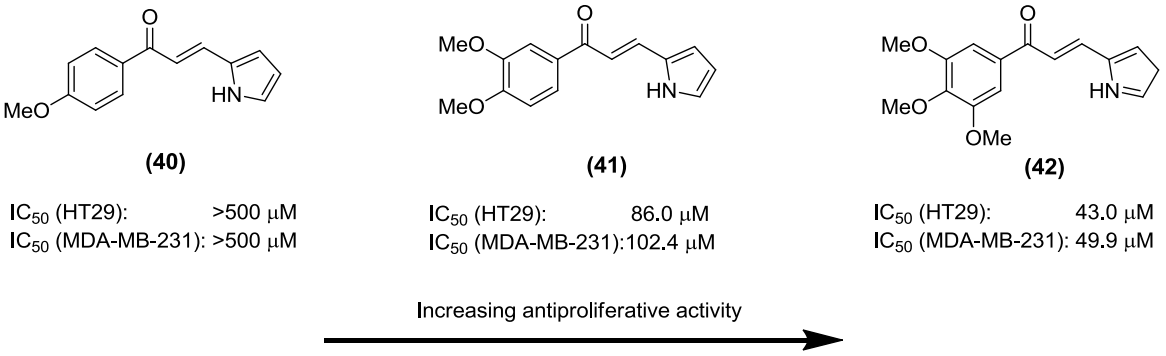

Figure 26: The importance of the 3,4,5 trimethoxy pharmacophore.

Nitrogen methylation increased antiproliferative activity, however the site of methylation was important, with proximal methylation in chalcone **(50)** giving only a minor increase, whereas distal methylation **(51)** was significantly more active (Figure 27).

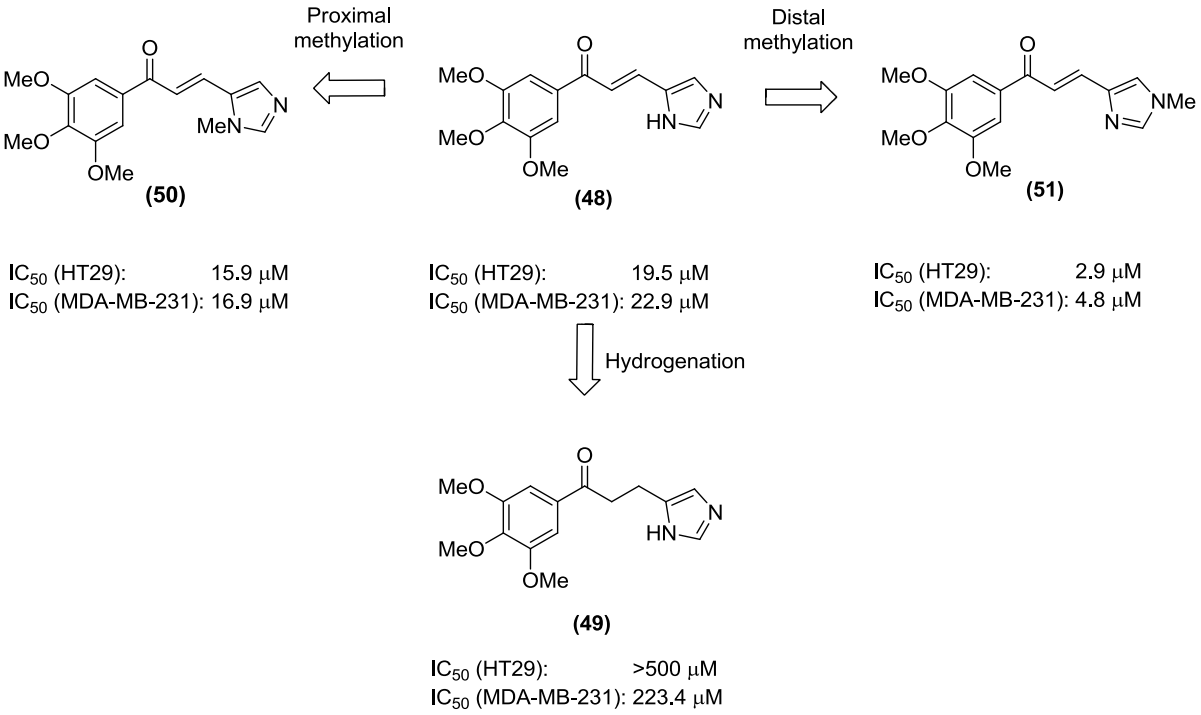

Figure 27: Distal methylation of chalcone (48) to afford chalcone (51) increased antiproliferative activity.

Removal of the *E* double bond in chalcone **(48)** to afford chalcone **(49)** resulted in a dramatic loss in activity, highlighting the importance of the enone

(Figure 27). The 5-substituted imidazole analogue **(48)** displayed improved antiproliferative activities compared to the 2-pyrrole derivative **(42)** (Figure 28). The 2-substituted imidazole analogue **(52)** displayed three fold higher antiproliferative activity than chalcone **(48)** (Figure 28).

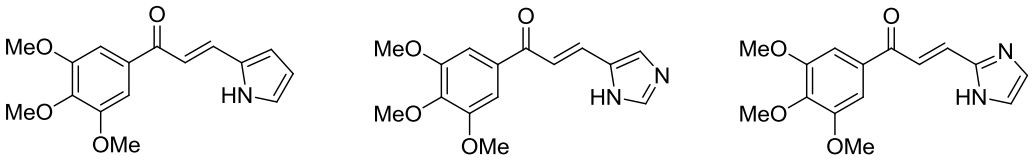

(42)

IC_{50} (HT29): 43.0 μM
IC_{50} (MDA-MB-231): 49.9 μM

(48)

IC_{50} (HT29): 12.5 μM
IC_{50} (MDA-MB-231): 18.0 μM

(52)

IC_{50} (HT29): 5.0 μM
IC_{50} (MDA-MB-231): 4.9 μM

Figure 28: Chalcone (52) containing 2-imidazole ring more potent that chalcone (48) containing a 4-imidazole ring.

All chalcones were selective towards the cancer cells compared against the non cancerous FEK-4 human skin fibroblast cells. The extent of selectivity varied widely with the most active chalcone **(53)** being the least selective whereas the chalcone which closely resembles the natural products **(51)** displayed the most selectivity (Figure 29).

(53)

IC_{50} (HT29): 4.2 μM
IC_{50} (MDA-MB-231): 4.9 μM
IC_{50} (LNCaP): 11.0 μM

IC_{50} (FEK-4): 17.5 μM

(51)

IC_{50} (HT29): 2.9 μM
IC_{50} (MDA-MB-231): 4.8 μM
IC_{50} (LNCaP): 48.4 μM

IC_{50} (FEK-4): 85.0 μM

Figure 29: Chalcone selectivity varied widely.

In summary chalcone **(51)** which most closely resembles the natural products eleutherobin and sarcodictyin displayed low micromolar activity in HT29 and MDA-MB-231 and good selectivity towards cancer cell lines.

2.4 NCI 60 Cell Line Screen

Six of the most promising chalcones **(45, 48, 50, 51, 52, 53)** were accepted for screening at the NCI at the single (10^{-5}) dose (see appendix A) of which only chalcone **(51)** was selected for further screening at the 5 dose level. Chalcone **(51)** displayed low micromolar GI_{50} values across multiple cancer cell lines including the multidrug resistant cell line NCI/ADR-RES (GI_{50} 2.96 μM) (Table 3). Chalcone **(51)** also displayed the most promising results in the colon panel with GI_{50} values of 3.52-4.84 μM in six of the seven colon cell lines, however, it was not selected for further screening.

Panel	Cell Line	GI_{50} (μM)	Panel	Cell Line	GI_{50} (μM)
Leukemia	CCRF-CEM	7.44	**Melanoma**	LOX IMVI	6.70
	HL-60(TB)	6.31		MALME-3M	8.51
	MOLT-4	17.3		M14	3.27
	RPMI-8226	7.63		MDA-MB-435	1.45
	SR	1.47		SK-MEL-2	6.28
				SK-MEL-28	9.55
				SK-MEL-5	3.93
				UACC-257	36.2
				UACC-62	3.95
Non-Small Cell Lung	A549/ATCC	6.74	**Ovarian**	IGROV1	8.28
	EKVX	47.9		OVCAR-3	5.10
	HOP-62	7.07		OVCAR-4	26.5
	NCI-H226	9.32		OVCAR-5	11.4
	NCI-H23	7.37		OVCAR-8	18.9
	NCI-H322M	12.3		NCI/ADR-RES	2.96
	NCI-H460	3.66		SK-OV-3	7.79
	NCI-H522	5.74			
Colon	COLO 205	4.15	**Renal**	786-0	8.30
	HCC-2998	9.89		A498	19.0
	HCT-116	3.86		ACHN	16.5
	HCT-15	4.84		CAKI-1	7.35
	HT29	3.52		RXF 393	6.99
	KM12	3.63		SN12C	9.34
	SW-620	3.53		TK-10	60.4
				UO-31	14.5
CNS	SF-268	10.3	**Breast**	MCF7	3.10
	SF-539	10.5		MDA-MB-231	8.20
	SNB-19	7.86		HS 578T	48.1
	SNB-75	2.02		BT-549	8.22
	U251	5.39		T-47D	6.30
				MDA-MB-468	2.65
Prostate	PC-3	59.7			
	DU-145	9.70			

Table 3: NCI 60 cell line screen, GI_{50} is the concentration required to inhibit growth by 50%.

2.5 COMPARE Analysis

A COMPARE analysis of chalcone **(51)** was performed to correlate the biological profile of this hybrid against all previously screened compounds in the NCI database to predict the possible mode of action of chalcone **(51)** (Table 4).

Rank	Correlation (%)	Compound	Target
1	49	Rhizoxin	Microtubule destabiliser
2	46	Tetraplatin	Alkylation of DNA
3	41	Cyanomorpholino-ADR	Alkylation of DNA
4	40	Taxol®	Microtubule stabiliser
5	40	Methotrexate	Antimetabolite

Table 4: COMPARE analysis results.

The highest correlation was with the potent microtubule destabiliser rhizoxin which acts as a microtubule destabiliser binding to the vinca alkaloid binding site on β tubulin. The second and third highest correlations were with tetraplatin and cyanomorpholino-ADR two compounds which are known alkylators of DNA which do not interact with tubulin. The fourth highest correlation was the microtubule stabiliser Taxol® followed by the antimetabolite methotrexate. This analysis suggested that chalcone **(51)** may be a possible microtubule binder, although alternative mechanisms of action may be responsible for the activity observed. In order to investigate further, mechanistic studies including cell cycle analysis and *in vitro* tubulin polymerisation assays were performed and are now discussed.

2.6 Cell Cycle Analysis

To confirm microtubule binding was responsible for the biological activity of chalcone **(51)**, cell cycle analysis was performed on HT29 cells which were exposed to 5.0 µM and 25 µM of chalcone **(51)** over 24 hours. The histograms obtained were then compared to untreated cells and cells treated with 100 nM of the potent microtubule destabiliser colchicine (Figure 30).

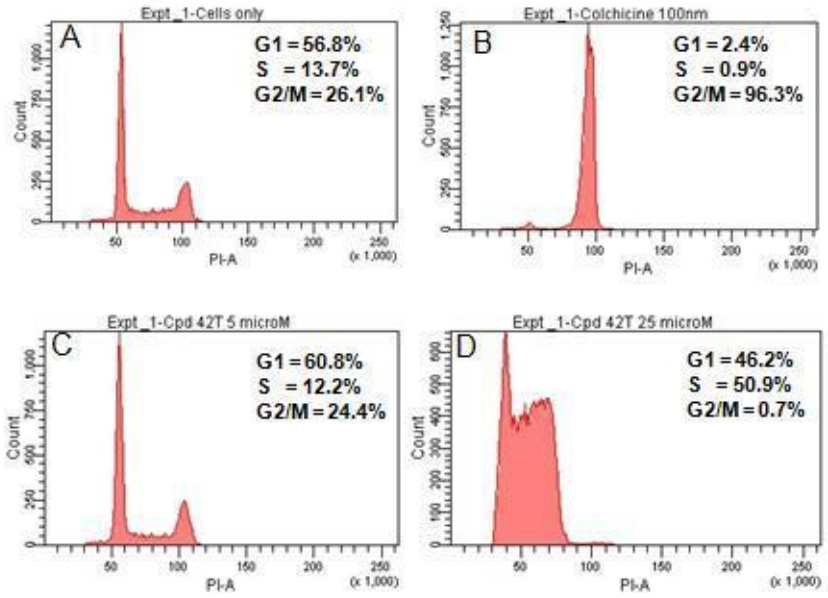

Figure 30: Cell cycle analysis, A) HT29 cells only, B) + 100 nM colchicine C) + 5.0 µM chalcone (51), D) + 25 µM chalcone (51).

The untreated HT29 cells displayed a histogram in which the majority of the cell population (57%) resided in the G1 phase of the cell cycle (Figure 30A). In the presence of the positive control colchicine (B) the majority of the cell population (96%) resided in the G2/M phase of the cell cycle. The presence of 5.0 µM chalcone **(51)** (C) resulted in a histogram similar to the untreated cells (A) suggesting that chalcone **(51)** was not disrupting microtubules at this concentration. This is interesting as despite chalcone **(51)** having an IC_{50} value of 2.9 µM in HT29 the histogram is very similar to untreated cells (A). Increasing the concentration of chalcone **(51)** to 25 µM (D) resulted in the majority of the cell population (51%) now residing in the S phase of the cell cycle. The absence of the characteristic G2/M peak

for chalcone **(51)** at 5.0 and 25 µM, suggests that chalcone **(51)** is not a microtubule binder.

2.7 *In Vitro* Tubulin Polymerisation Assay

An *in vitro* tubulin polymerisation assay was also performed to investigate if chalcone **(51)** displayed microtubule binding properties and is shown in figure 31. The control curve is tubulin only, showing the steady increase in optical density over the first 40 minutes as tubulin naturally polymerises into microtubules. The presence of 5.0 µM of the positive control Taxol® (orange dots) resulted in a rapid increase in tubulin polymerisation over the first 10 minutes after which the microtubules retain in their fully formed state. The presence of 20 µM chalcone **(51)** resulted in a curve almost identical to the control curve suggesting that chalcone **(51)** is neither stabilising nor destabilising tubulin polymerisation at this concentration.

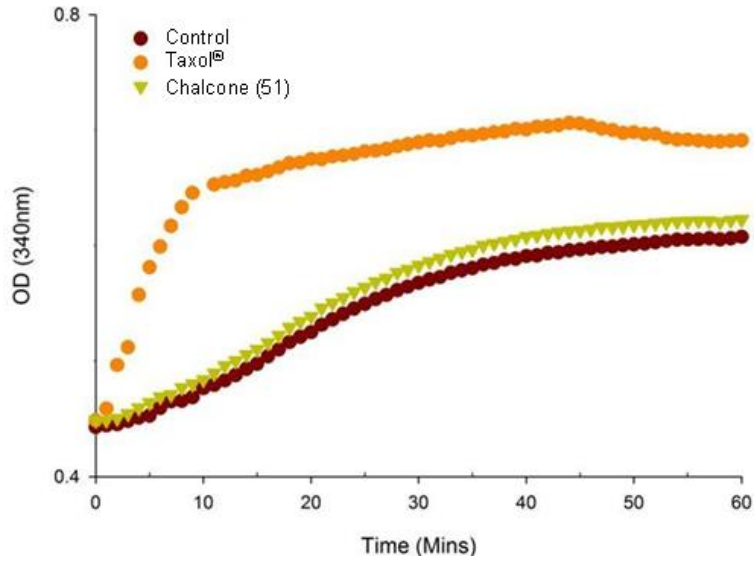

Figure 31: *In vitro* tubulin polymerisation assay, Taxol and chalcone (51) concentration 5.0 µM.

In summary, further mechanistic studies including cell cycle analysis and *in vitro* tubulin polymerisation assay suggest that chalcone **(51)** is not a tubulin binder and is exerting its biological action through a currently unknown mechanism.

2.8 Conclusions

Fourteen urocanic-chalcone analogues were synthesised using simple one or two step procedures and screened for antiproliferative activity in multiple cancer cell lines. A simple SAR study confirmed the importance of key structural units consistent with the proposed hypothesis (Figure 32) enabling the design of a second library with improved biological properties.

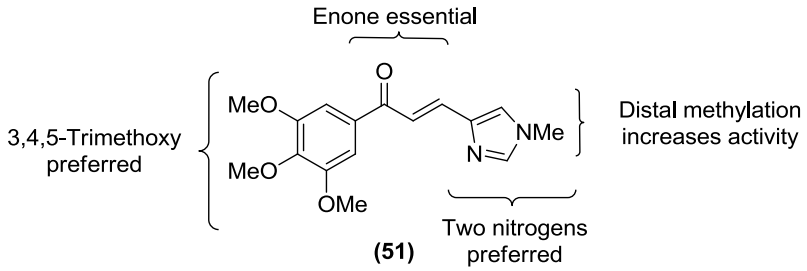

Figure 32: Important structural requirements for antiproliferative activity.

Chalcone **(51)** which most closely resembles the urocanic ester side chain in the natural products eleutherobin **(3)** and sarcodictyin **(4,5)** displayed low micromolar GI_{50} values across multiple cancer cell lines in the NCI 60 cell line panel including the multidrug resistant cell line NCI/ADR-RES (GI_{50}: 2.96 µM). Of great interest is that this chalcone was also one of the most selective towards cancer cell lines.

Further investigations into the mode of action of chalcone **(51)** suggest that it does not interact with tubulin. The importance of the enone for antiproliferative activity suggests this chalcone **(51)** may be acting at a Michael acceptor and interacting with intracellular nucleophiles during the S phase of the cell cycle (Scheme 13). Further investigations are required to confirm this mode of action.

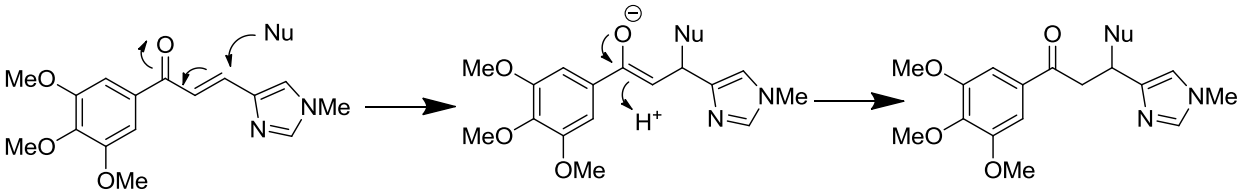

Scheme 13: Chalcone (51) may be acting as an intracellular Michael acceptor.

2.9 Future Work

2.10 Determination of Mode of Action of Chalcone (51)

One vital avenue for future work is to identify the mode of action of the lead chalcone **(51)**. Cell cycle analysis suggested chalcone **(51)** was disrupting cellular proliferation in the synthesis phase of the cell cycle possibly via Michael addition. Honda *et al.* recently reported using ^{1}H NMR and UV/Vis spectroscopy to identify a series of monocyclic cyanoenones as potent Michael acceptors in the presence of the model nucleophile dithiothreitol.[64] A similar study could be conducted with chalcone **(51)** in the presence of increasing concentrations of dithiothreitol. The gradual disappearance of protons H^a and H^b from chalcone **(51)** alongside the formation of new peaks for H^c and H^d upon dithiothreitol addition would suggest chalcone **(51)** was acting as a Michael acceptor (Scheme 14).

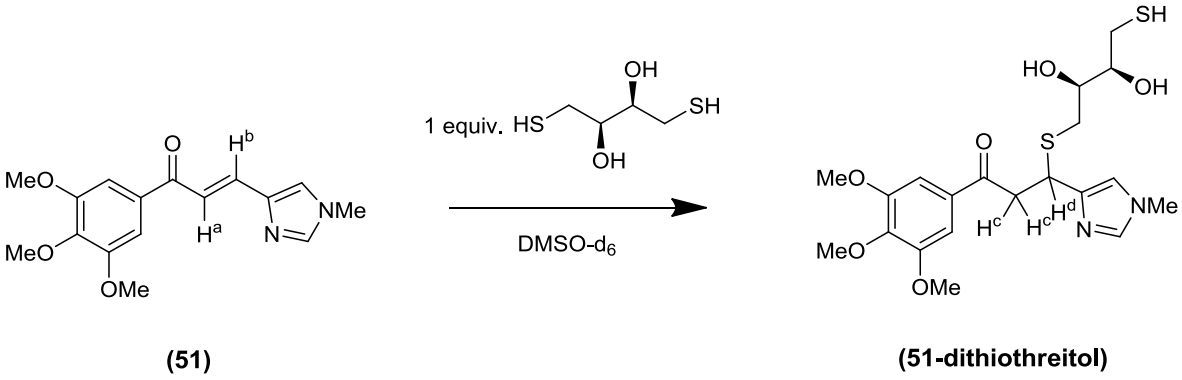

Scheme 14: Proposed ^{1}H NMR study with dithiothreitol.

Honda *et al.* also observed spectra changes upon addition of dithiothreitol to the monocyclic cyanoenones using UV/Vis spectroscopy.[64] The disruption of the enone in chalcone **(51)** upon Michael addition of dithiothreitol would result in changes in the UV/Vis spectrum which could also be used to confirm that chalcone **(51)** is a Michael acceptor. Performing the above experiment with glutathione a nucleophile present in multiple cell lines would also be a valuable experiment to perform.

2.11 Prenylation of Chalcone (51)

The prenyl group is present in a range of biologically active compounds including chalcone isobavachalcone **(54)** with an IC_{50} value of 6.2 μM in NB-39, a neuroblastoma cell line[65] and chalcone xanthohumol **(55)** with an IC_{50} value of 3.5 μM in MCF-7, a human breast carcinoma cell line[66] (Figure 33). Prenylation is thought to increase the affinity between a compound and its target protein and has been reported to increase the growth inhibition profiles of bis-prenylated chalcone **(57)** compared with mono-prenylated chalcone **(56)**[67] (Figure 33).

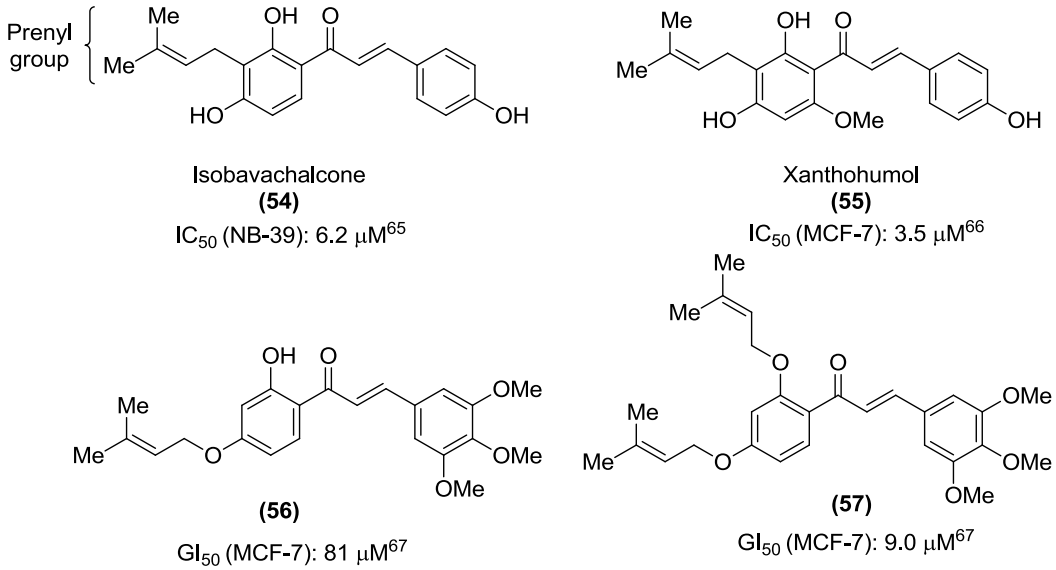

Figure 33: The prenyl group in biologically active chalcones.[65-67]

Caggiano *et al.*[68] reported a novel single step procedure involving $Bi(OTf)_3$ and isoprene which could be applied to chalcone **(51)** to generate both the mono- and bis-prenylated chalcones **(51A)** and **(51B)** respectively (Scheme 15). Exploring the antiproliferative activity of chalcones **(51A)** and **(51B**) compared to chalcone **(51)** is of interest and worthy of investigation.

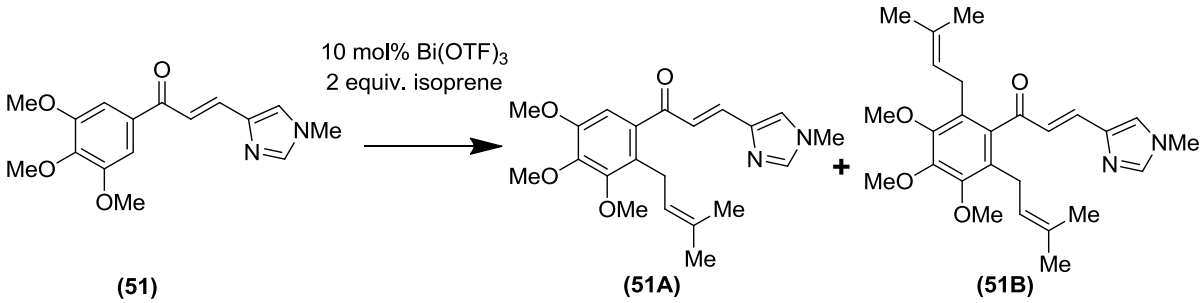

Scheme 15: Prenylation of chalcone (51) to generate chalcones (51A) and (51B).

Chapter 3: Pyrazoline Combretastatin A-4 Analogues

3.1 Overview

Combretastatin A-4 **(CA4, 13)**[33] is a promising microtubule destabiliser with potent antiproliferative activity across multiple cancer cell lines including multidrug resistant cell lines (Figure 34). Combretastatin A-4 **(CA4, 13)** is poorly water soluble and susceptible to isomerisation to the less biologically active *E* configuration.[39] As highlighted in chapter 1, numerous studies have reported heterocyclic combretastatin A-4 **(CA4, 13)** analogues with potent nanomolar antiproliferative activities without the limitations of combretastatin A-4 **(CA4, 13)**.[40-45] The pyrazoline motif is easily accessible from chalcone starting materials and provides an opportunity to develop novel heterocyclic **CA4** analogues (Figure 34).

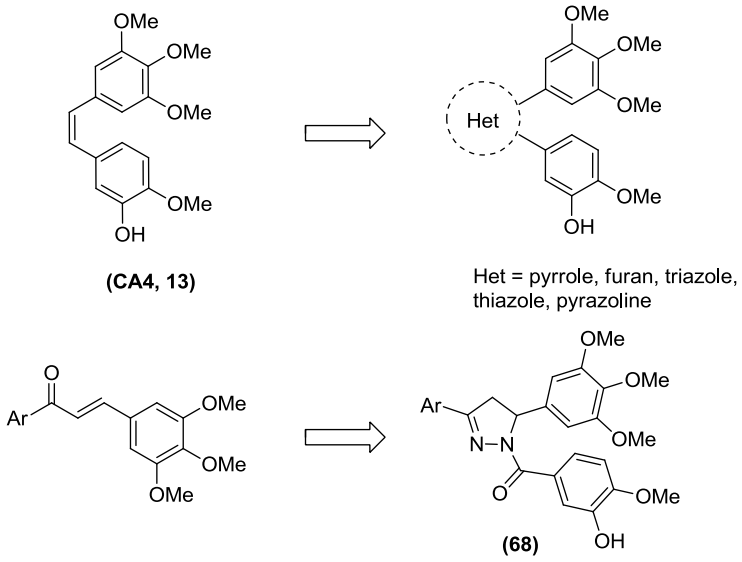

Figure 34: Combretastatin (CA4)[33] and proposed lead pyrazoline (68), Ar = C_6H_4.

Herein we now report the design, synthesis and evaluation of pyrazoline **CA4** analogues derived from chalcones of which pyrazoline **(68)** is predicted to be the most potent due to structural similarity to **CA4**. All pyrazolines and their corresponding chalcone starting materials will be evaluated for antiproliferative activities and the most potent pyrazolines will be submitted to the NCI for screening in the 60 cell line panel. Mechanistic studies including cell cycle analysis, *in vitro* tubulin polymerisation assays and confocal microscopy will be performed to determine the mode of action of the lead pyrazoline.

3.2 Chemical Synthesis

A simple and efficient synthesis of the pyrazoline scaffold was established in three steps from the commercially available starting materials in high yield (Scheme 16). The chalcone precursors were synthesized in good to excellent yield giving the *E* isomer exclusively as identified by characteristic ^{3}J coupling of *ca* 15Hz. Chalcones have been reported to display a range of biological activities[46-50] therefore all chalcone precursors were screened for antiproliferative activity in human colon carcinoma (HT29) and human breast carcinoma (MDA-MB-231) cell lines.

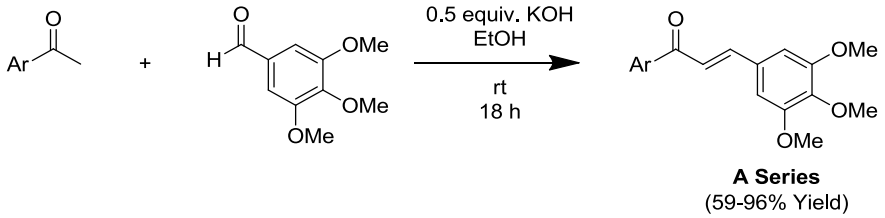

Scheme 16: Chalcone synthesis.

			IC_{50} (μM)	
cpm	**Ar**	**Yield (%)**	**HT29**	**MDA-MB-231**
58	C_6H_5	96	3.7 ± 0.5	5.3 ± 0.2
59	4-OMe-C_6H_4	78	3.9 ± 0.7	10.1 ± 1.8
60	4-OBn-C_6H_4	80	9.9 ± 1.0	>100
61	4-OH-C_6H_4	44	4.2 ± 0.6	13.3 ± 1.6
62	4-NO_2-C_6H_4	76	6.5 ± 1.3	12.4 ± 2.0
63	4-NH_2-C_6H_4	59	14.9 ± 1.7	31.6 ± 6.6
64	Pyridin-2-yl	85	9.6 ± 0.9	9.7 ± 4.3
65	Furan-2-yl	80	9.6 ± 0.8	10.3 ± 1.0
66	Thiophen-2-yl	93	4.9 ± 1.1	5.5 ± 1.0
67	Naphthalen-2-yl	70	8.7 ± 1.2	10.6 ± 2.3
Colchicine	-	-	0.007 ± 0.001	0.008 ± 0.001

Table 5: MTS Assays, IC_{50} is the concentration that inhibits 50% cell proliferation, values are the mean from three independent experiments ± standard deviation, colchicine was used as a positive control, compounds ≥95% pure by HPLC and elemental analysis.

The unsubstituted phenyl-derived chalcone **(58)** displayed the most promising antiproliferative activity, whilst the 4-OMe **(59)**, 4-OBn **(60)** and 4-OH **(61)** substituted analogues retained similar activity in HT29. Surprisingly the 4-OBn substituted analogue **(60)** displayed poor activity (>100 μM) in MDA-MB-231 yet displayed good

antiproliferative activity (9.9 μM) in HT29. Analogues with an electron withdrawing 4-NO_2 group **(62)** and electron donating 4-NH_2 group **(63)** were well tolerated at this position. Substitution of the phenyl ring in analogue **(58)** for a heterocycle such as pyridin-2-yl **(64)** or furan-2-yl **(65)** slightly reduced activity except for the thiophen-2-yl analogue **(66)** which displayed comparable activity to the parent pyrazoline **(58)** in both cancer cell lines.

3.3 Pyrazoline Formation

2-Pyrazolines are commonly prepared by heating a chalcone and hydrazine in ethanol for between 1 -2 hours. The mechanism is believed to proceed through 1,2 addition of hydrazine affording a hydrazone which upon intramolecular conjugate addition results in cyclisation to the pyrazoline ring (Scheme 17).[69,70] Tautomerisation affords the more stabilised 2-pyrazoline in which the double bond is localised on the benzylic position.

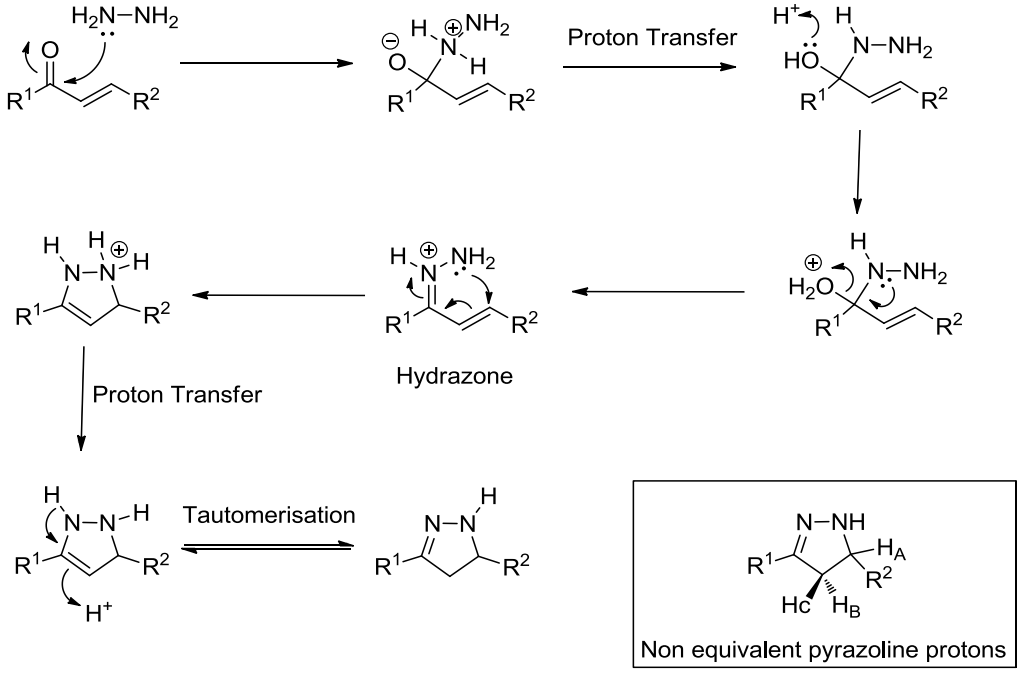

Scheme 17: Pyrazoline synthesis.[69,70]

Formation of the 2-pyrazoline ring is confirmed via the three non equivalent protons (H_A, H_B and H_C) on the pyrazoline ring, resulting in three sets of doublet of doublet peaks in the ^{1}H NMR spectrum.

3.4 Chemical Synthesis of Pyrazolines

The chalcones (A series) shown in Scheme 16 were treated with hydrazine hydrate to afford the corresponding pyrazoline derivatives (B series). The B series were unstable and rapidly decomposed within a few days of isolation so were immediately treated with the desired acid chloride to afford the final pyrazoline derivatives (C series) (Scheme 18). The C series was found to be stable to decomposition and were purified, fully characterised and screened for antiproliferative activity in human colon carcinoma (HT29) and human breast carcinoma (MDA-MB-231) cell lines.

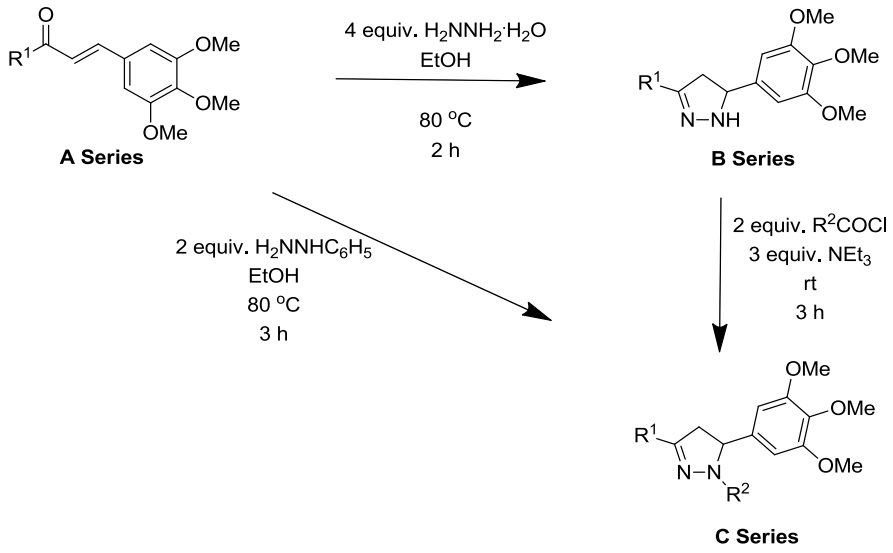

Scheme 18: Pyrazoline synthesis and biological evaluation.

To investigate the possibility of synthesising the C series of pyrazolines directly from the chalcone, chalcone **(58)** was treated with phenyl hydrazine to afford pyrazoline **(75)** directly in 60% yield. All compounds were determined to be ≥95% pure by HPLC at two different wavelengths and elemental analysis prior to biological evaluation.

3.5 Biological Evaluation

All C series pyrazolines displayed similar or improved antiproliferative activities across both cancer cell lines compared to the corresponding A series chalcones demonstrating that chalcones are useful starting materials for more biologically active compounds (Table 6).

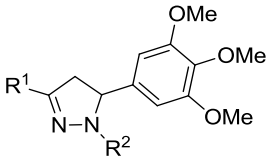

C Series

C Series				IC_{50} (μM)	
cpm	**R^1**	**R^2**	**Yield (%)**	**HT29**	**MDA-MB-231**
68	C_6H_5	3-OBn,4-OMe-C_6H_3-CO	54	>100	>100
69	C_6H_5	3-OH,4-OMe-C_6H_3CO	81	1.8 ± 0.1	0.51 ± 0.07
70	C_6H_5	4-OMe-C_6H_3-CO	68	1.4 ± 0.1	0.82 ± 0.05
71	C_6H_5	C_6H_5-CO	84	0.17 ± 0.04	0.17 ± 0.02
71 (-)[b]	C_6H_5	C_6H_5-CO	-	0.19 ± 0.03	0.10 ± 0.02
71 (+)[b]	C_6H_5	C_6H_5-CO	-	45.0 ± 7.8	99.6 ± 6.3
72	C_6H_5	1-napthyl-CO	84	1.1 ± 0.1	0.9 ± 0.1
73	C_6H_5	C_6H_5	58	40.5 ± 3.5	63.7 ± 13.7
74	4-OMe-C_6H_4	C_6H_5-CO	61	0.75 ± 0.17	0.5 ± 0.03[a]
74 (-)[b]	4-OMe-C_6H_4	C_6H_5-CO	-	0.84 ± 0.12	0.56 ± 0.12
74(+)[b]	4-OMe-C_6H_4	C_6H_5-CO	-	45.4 ± 7.8	56.5± 5.0[a]
75	4-OH-C_6H_4	C_6H_5-CO	72	0.66 ± 0.06	0.25 ± 0.05
76	4-NO_2-C_6H_4	C_6H_5-CO	60	7.9 ± 0.6	19.6 ± 3.6
77	4-NH_2-C_6H_4	C_6H_5-CO	95	0.35 ± 0.03	0.36 ± 0.02
78	Pyridin-2-yl	C_6H_5-CO	72	1.3 ± 0.4	0.24 ± 0.04
78 (-)[b]	Pyridin-2-yl	C_6H_5-CO	-	0.49 ± 0.07	0.33 ± 0.01
78 (+)[b]	Pyridin-2-yl	C_6H_5-CO	-	13.0 ± 1.06	82.0 ± 18.9
79	Furan-2-yl	C_6H_5-CO	65	4.00 ± 0.27	2.18 ± 0.25
80	Thiophen-2-yl	C_6H_5-CO	61	1.19 ± 0.18	0.85 ± 0.02
81	Naphthalen-2-yl	C_6H_5-CO	58	10.1 ± 1.4	1.1 ± 0.2

Table 6: MTS Assays, IC_{50} is the concentration that inhibits 50% cell proliferation, values are the mean from three independent experiments ± standard deviation, except [a] two experiments, compounds ≥95% pure by HPLC and CHN analysis, [b] determined by chiral HPLC to be ≥95% ee.

Pyrazoline **(69)** containing the 3-OH, 4-OMe arrangement present in **CA4** displayed modest antiproliferative activity in HT29 and good activity in MDA-MB-231 (Table 6). Protection of the 3-OH to 3-OBn in pyrazoline **(68)** abolished activity

whereas removal of the 3-OH in pyrazoline **(70)** retained similar activity as pyrazoline **(69)**. Interestingly, the removal of the 4-OMe group in pyrazoline **(71)** significantly increased activity with low nanomolar activity in both HT29 and MDA-MB-231 cell lines (Figure 35).

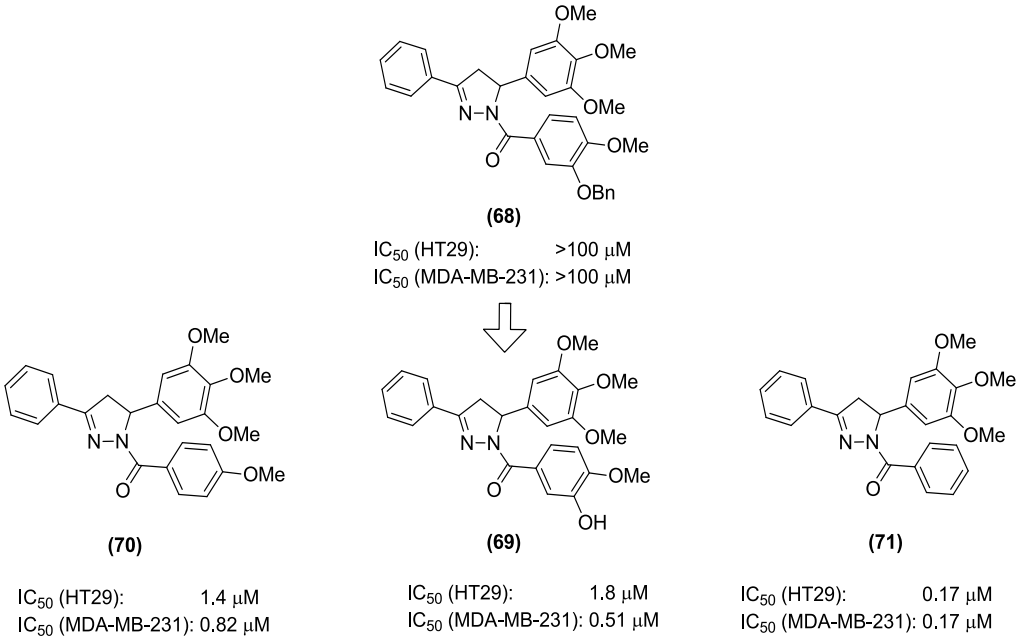

Figure 35: Unsubstituted benzoyl ring preferred.

Increasing the steric bulk of R^1 and R^2 was investigated in pyrazoline **(72)** and **(81)** respectively however both pyrazolines displayed reduced activity (Figure 44). Pyrazoline **(73)** without a carbonyl group displayed poor activity suggesting this is vital for antiproliferative activity (Figure 36).

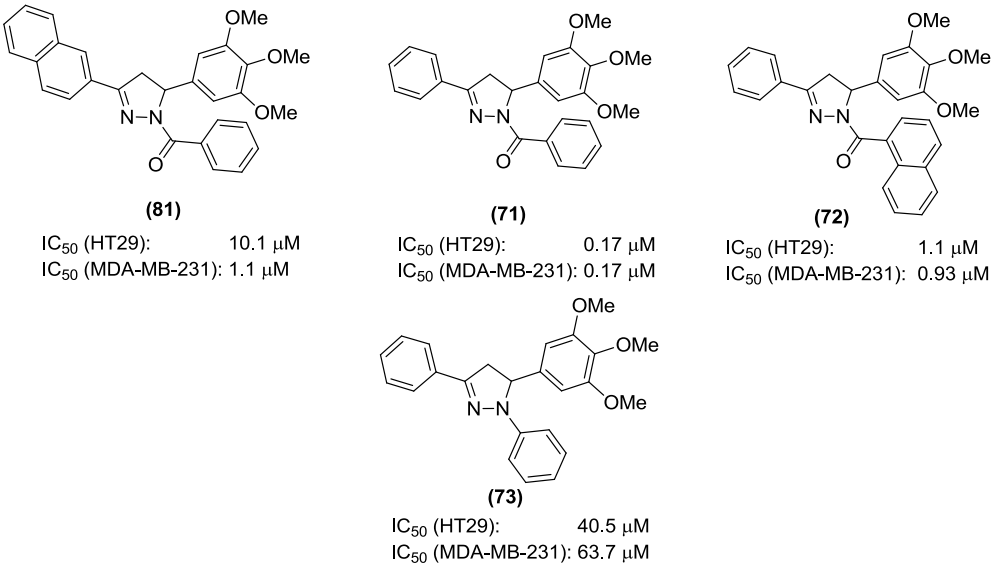

Figure 36: Effect of steric bulk on antiproliferative activity.

Substitution at the 4 position was investigated with pyrazolines **(74)**, **(75)** and **(77),** all displaying good antiproliferative activities (Figure 37).

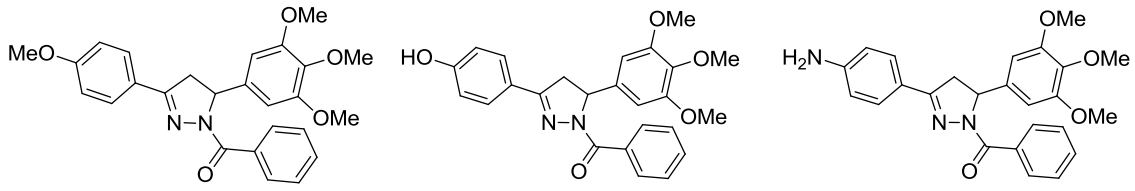

(74)
IC_{50} (HT29): 0.75 μM
IC_{50} (MDA-MB-231): 0.50 μM

(75)
IC_{50} (HT29): 0.66 μM
IC_{50} (MDA-MB-231): 0.25 μM

(77)
IC_{50} (HT29): 0.35 μM
IC_{50} (MDA-MB-231): 0.36 μM

Figure 37: Substitution tolerated at 4 position.

Replacing the phenyl ring for a pyridin-2-yl in pyrazoline **(78)** resulted in diminished activity in HT29 compared to pyrazoline **(71)**, but surprisingly retained activity in MDA-MB-231. The furan-2-yl pyrazoline **(79)** and thiophen-2-yl pyrazoline **(80)** were investigated with both displaying micromolar activity with a slight preference for the thiophen-2-yl over furan-2-yl (Figure 38).

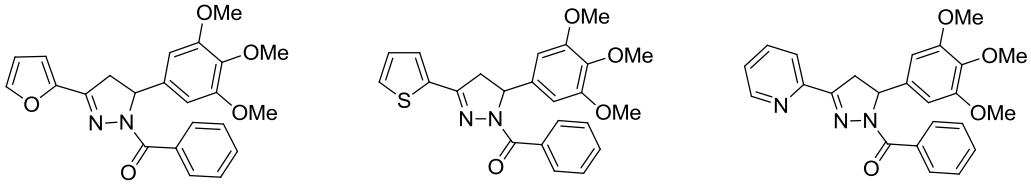

(79)
IC_{50} (HT29): 4.00 μM
IC_{50} (MDA-MB-231): 2.2 μM

(80)
IC_{50} (HT29): 1.2 μM
IC_{50} (MDA-MB-231): 0.85 μM

(78)
IC_{50} (HT29): 1.3 μM
IC_{50} (MDA-MB-231): 0.24 μM

Antiproliferative activity

Figure 38: Heterocycles detrimental to activity.

Due to the presence of a stereogenic centre at position five of the pyrazoline ring, three of the most promising compounds **(71, 74** and **78)** were selected for semipreparatory chiral HPLC to separate the enantiomers and determine the effect of stereochemistry on antiproliferative activity.

3.6 Enantiomerically Pure Pyrazoline Combretastatin Analogues

Pyrazolines **(71)**, **(74)** and **(78)** were selected for semipreparatory chiral HPLC using a vancomycin based stationary phase, a mobile phase of 1:1 MeCN:H_2O and a flow rate of 10 mL/min. The first eluting component was identified as the (+) enantiomer and the later eluting component was identified as the (-) enantiomer using polarimetry (Figure 39).

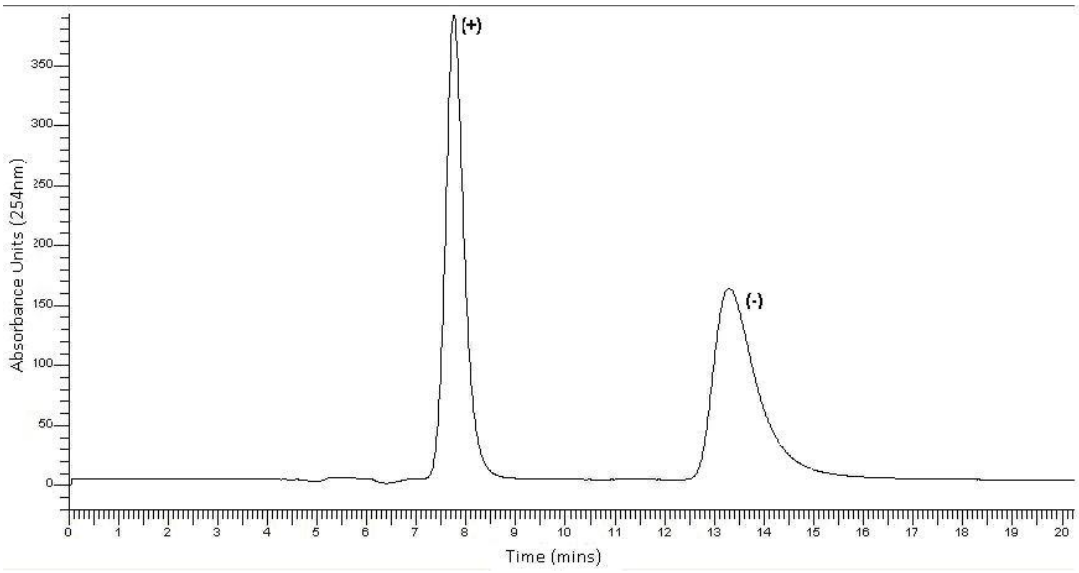

Figure 39: Separation of pyrazoline (71+/-) enantiomers using semipreparatory chiral HPLC.

All enantiomers were confirmed to be ≥95 ee (enantiomeric excess) by chiral HPLC analysis prior to biological evaluation. The (-) enantiomer was found to be the most active component in all cases and displayed similar or better antiproliferative activity compared to the racemic mixture (Figure 40 and Table 6).

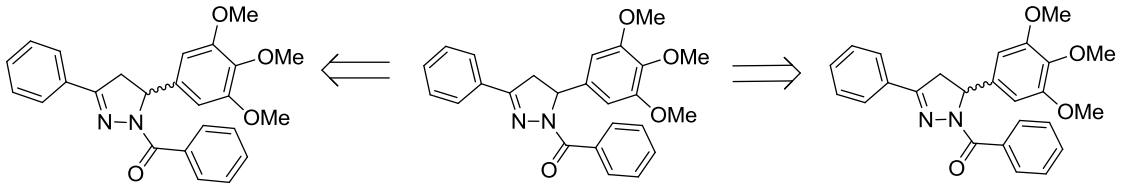

(71-)	(71+/-)	(71+)
IC_{50} (HT29): 0.19 μM IC_{50} (MDA-MB-231): 0.10 μM	IC_{50} (HT29): 0.17 μM IC_{50} (MDA-MB-231): 0.17 μM	IC_{50} (HT29): 45.0 μM IC_{50} (MDA-MB-231): 99.6 μM
IC_{50} (FEK-4): 0.28 μM	IC_{50} (FEK-4): 0.24 μM	IC_{50} (FEK-4): 157.7 μM

Figure 40: Enantiomerically pure pyrazoline combretastatin analogues.

Selectivity was determined using the FEK-4 cell line with pyrazolines **(71-)** and **(71+/-)** displaying similar IC_{50} values in FEK-4 as in HT29 and MDA-MB-231. The poor selectively for HT29 and MDA-MB-231 cell lines is an interesting observation compared to chalcone **(51)** reported previously in chapter 2 (Figure 29). Chalcone **(51)** displayed low micromolar IC_{50} values in multiple cancer cell lines but good selectively with an IC_{50} of 85 μM in FEK-4. In constrast pyrazoline **(71-)** displayed low nanomolar IC_{50} values in both cancer cell lines and FEK-4. One potential solution to this problem to increase selectively for cancer cell lines over non cancer cell lines involves modifying the pyrazoline structure via prodrug strategies, potential options are discussed in the future work section.

3.7 NCI 60 Cell Line Screen

Pyrazolines **(71+/-)**, **(71-)** and **71(+)** were submitted to the NCI for 60 cell line analysis and were selected for both the single dose and five dose screens. A summary of the five dose data is below (Table 7) (see appendix A for full data sets).

		GI_{50} (μM)					GI_{50} (μM)		
Panel	**Cell Line**	**71+/-**	**71-**	**71+**	**Panel**	**Cell Line**	**71+/-**	**71-**	**71+**
Leukemia	CCRF-CEM	0.269	0.274	3.98	Melanoma	LOX IMVI	0.537	0.078	5.12
	HL-60(TB)	0.284	0.101	2.32		MALME-3M	0.587	10.3	5.57
	K-562	0.099	0.039	2.15		M14	0.238	0.065	2.38
	MOLT-4	0.517	0.372	4.84		MDA-MB-435	0.037	0.025	0.59
	RPMI-8226	0.284	0.387	4.08		SK-MEL-2	0.512	0.037	2.43
	SR	0.044	0.026	0.297		SK-MEL-28	0.155	0.066	3.69
						SK-MEL-5	0.118	0.047	2.51
						UACC-257	25.8	0.093	3.76
						UACC-62	0.057	0.076	4.78
Non-Small Cell Lung	A549/ATCC	0.177	0.083	3.82	Ovarian	IGROV1	0.394	0.205	6.91
	EKVX	24.2	3.14	6.56		OVCAR-3	0.386	0.025	2.10
	HOP-62	0.296	0.077	3.88		OVCAR-4	0.472	0.933	4.76
	NCI-H226	0.249	0.056	3.25		OVCAR-5	0.510	0.585	5.43
	NCI-H23	0.514	0.121	3.06		OVCAR-8	0.632	0.222	4.16
	NCI-H322M	0.971	3.44	7.25		NCI/ADR-RES	0.086	0.035	1.62
	NCI-H460	0.320	0.044	3.25		SK-OV-3	0.191	0.039	2.77
	NCI-H522	0.201	0.025	1.48					
Colon	COLO 205	0.227	0.059	3.53	Renal	786-0	0.391	0.073	4.68
	HCC-2998	0.282	0.135	3.22		A498	0.540	0.037	1.09
	HCT-116	0.326	0.056	4.28		ACHN	1.15	1.38	9.59
	HCT-15	0.371	0.117	4.33		CAKI-1	2.38	0.055	4.22
	HT29	0.314	0.044	2.74		RXF 393	0.188	0.048	1.94
	KM12	0.339	0.037	2.77		SN12C	0.514	0.770	6.74
	SW-620	0.335	0.051	2.97		TK-10	29.0	0.497	6.89
						UO-31	0.98	3.85	10.2
CNS	SF-268	0.862	0.318	7.23	Breast	MCF7	0.054	0.036	2.51
	SF-539	0.288	0.048	2.58		MDA-MB-231	0.898	1.36	9.86
	SNB-19	0.383	0.059	3.66		HS 578T	18.6	0.060	2.47
	SNB-75	0.053	0.180	1.95		BT-549	0.983	0.091	13.7
	U251	0.426	0.065	3.16		T-47D	21.3	15.0	8.90
						MDA-MB-468	0.207	0.057	2.21
Prostate	PC-3	0.566	0.070	3.74					
	DU-145	0.477	0.077	2.49					

Table 7: NCI 60 cell line screen for pyrazolines (71+/-, 71- and 71+), GI_{50} is the concentration required to inhibit growth by 50%.

Pyrazoline **(71-)** displayed potent growth inhibition across the melanoma panel with GI_{50} values <80 nM in six of the eight cell lines, it also displayed GI_{50} values of 25 nM in a lung cancer cell line (NCI-H522) and an ovarian cell cancer line (OVCAR-3) which is particularly sensitive to tubulin binding agents.[56] Of great interest is that pyrazoline **(71-)** also displayed a GI_{50} value of 35 nM in the multidrug resistance NCI/ADR-RES cell line, suggesting that this compound may be useful in treating drug resistant cancers. Pyrazoline **(71-)** is currently under evaluation at the biological evaluation committee to determine if it should progress to *in vivo* screening. The GI_{50} value for pyrazoline **(71+)** show that this enantiomer is much less active.

3.8 COMPARE Analysis

A COMPARE analysis was performed using the NCI GI_{50} values to predict the likely mode of action of the lead compounds pyrazoline **(71+/-)** and **(71-)** (Table 8). Pyrazoline **(71+/-)** showed good correlation with maytansine and vinblastine. Pyrazoline **(71-)** displaying strong correlation with maytansine, vinblastine and vincristine suggesting that the disruption of tubulin polymerization was responsible for the biological activity of these compounds. Pyrazoline **(71+)** showed good correlation with non tubulin disrupting agents suggesting that it is not a tubulin disruptor.

Pyrazoline	Rank	Correlation %	Compound	Target
(71+/-)				
	1	49	maytansine	Microtubule
	2	46	trimetrexate	dihydrofolate reductase
	3	46	vinblastine sulphate	Microtubule
(71-)				
	1	62	maytansine	Microtubule
	2	58	vinblastine sulphate	Microtubule
	3	57	vincristine sulfate	Microtubule
(71+)				
	1	62	neocarzinostatin	
	2	62	CCNU	DNA
	3	60	didemnin B	DNA

Table 8: COMPARE analysis for pyrazoline (71+/-, 71- and 71+).

3.9 Cell Cycle Analysis

Tubulin disruptors are known to cause arrest in the G2/M phase of the cell cycle therefore cell cycle analysis was performed. Using 100 nM pyrazoline **(71-)** resulted in 65% of the cell population arresting in G2/M which increased to 93% at a concentration of 500 nM providing further evidence that pyrazoline **(71-)** is a tubulin binder (Figure 41).

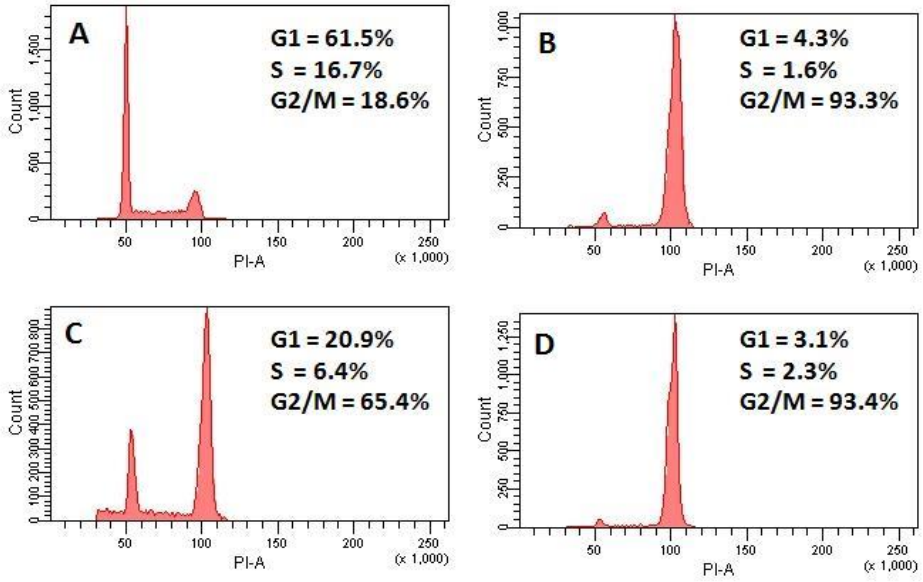

Figure 41: Cell cycle analysis, A) HT29 cells only, B) + 100 nM colchicine C) + 100 nM pyrazoline (71-), D) + 500 nM pyrazoline (71-), results are representative of three independent experiments.

The promising cell cycle analysis results above, combined with the COMPARE analysis suggest that pyrazoline **(71-)** was exerting its biological mode of action via microtubule binding. To provide further evidence that tubulin binding was responsible for the activity of pyrazoline **(71-)** and to classify it as a microtubule stabiliser or destabiliser, an *in vitro* tubulin polymerization assays were performed.

3.10 *In Vitro* Tubulin Polymerisation Assay

The control experiment showed the steady increase in optical density (OD) observed over time as tubulin naturally polymerises into microtubules whereas the presence of 5.0 µM of the tubulin stabiliser Taxol® resulted in rapid microtubule formation within the first 20 minutes (Figure 42). The addition of 5.0 µM pyrazoline **(71-)** reduced the OD reading compared to the control experiment. This suggests that the polymerization of tubulin to microtubules is being disrupted, similar to maytansine and vinblastine, and not acting as a tubulin stabiliser like Taxol®.

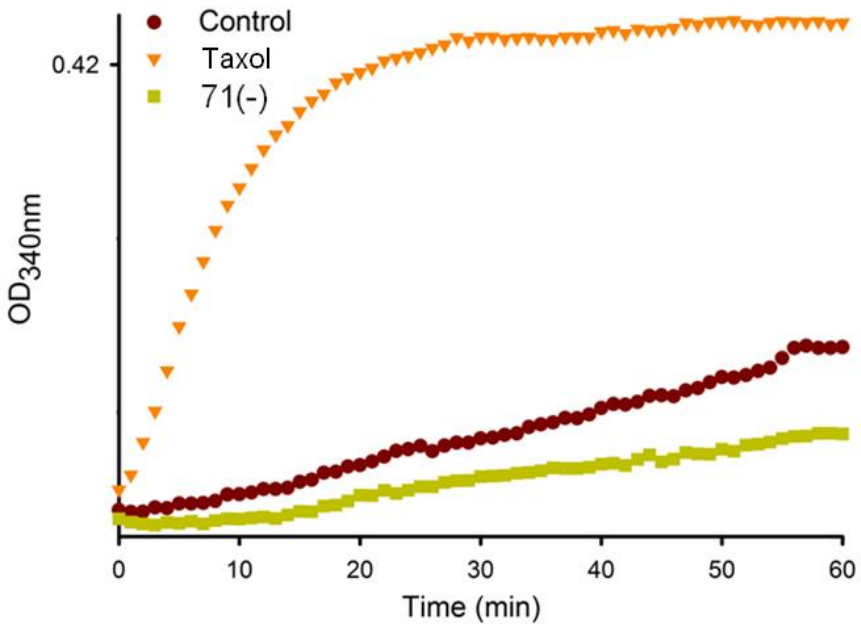

Figure 42: *In vitro* tubulin polymerisation assay for 5.0 µM pyrazoline (71-) and 5.0 µM Taxol.

This assay was repeated a second time giving results identical to the assay above confirming the cell cycle analysis results and enabling classification of pyrazoline **(71-)** as a microtubule destabiliser.

3.11 Confocal Microscopy

Additional evidence of the microtubule disrupting properties of pyrazoline **(71-)** was obtained using the technique of confocal microscopy (Figure 43).

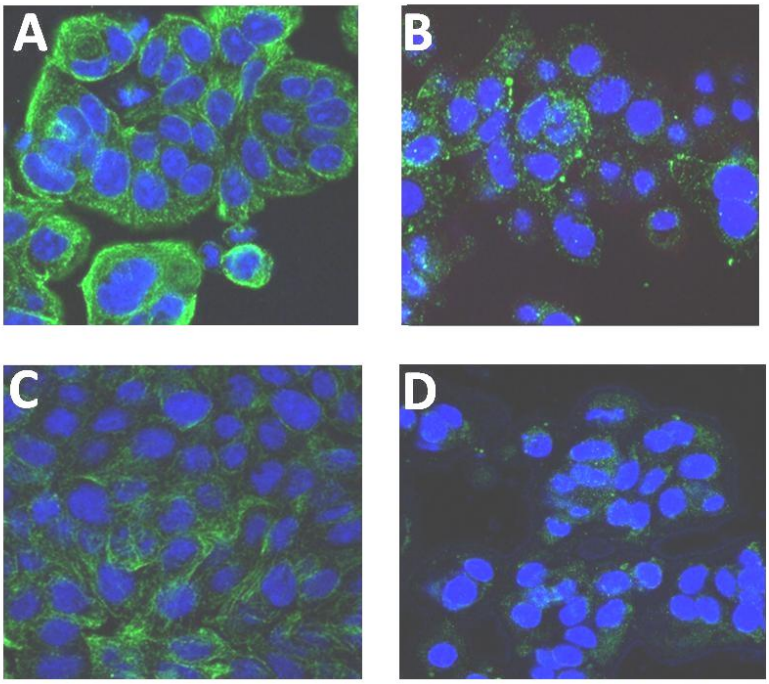

Figure 43: Confocal microscopy A) HT29 cells only, B) + 100 nM colchicine, C) + 100 nM pyrazoline (71-), D) + 500 nM pyrazoline (71-).

In Panel A (Figure 43A) the microtubule network (green) is clearly visible as a green cloud which encompasses the chromosomes (blue) within the dividing cells. In the presence of the positive control colchicine, the microtubule network is dramatically reduced providing visual evidence that colchicine is disrupting microtubule formation (B). The addition of 100 nM of pyrazoline **(71-)**, the same concentration which resulted in 65% of the cell population residing in G2/M in the cell cycle analysis, the microtubule network is still present but reduced in volume (C). Increasing the concentration to 500 nM, a concentration resulting in 93% of the cell population residing in G2/M, severely reduced microtubule volume. This study provides direct visual evidence that pyrazoline **(71-)** was disrupting microtubule formation providing further support with the results of the COMPARE and cell cycle analyses along with the *in vitro* tubulin polymerisation assays.

3.12 Determination of Absolute Stereochemistry

A commonly used method for assigning the absolute stereochemistry of crystalline solids is to obtain an X-ray crystal structure and assign the absolute stereochemistry as *R* or *S* using the Cahn-Ingold-Prelog priory rules (Figure 44).[71]

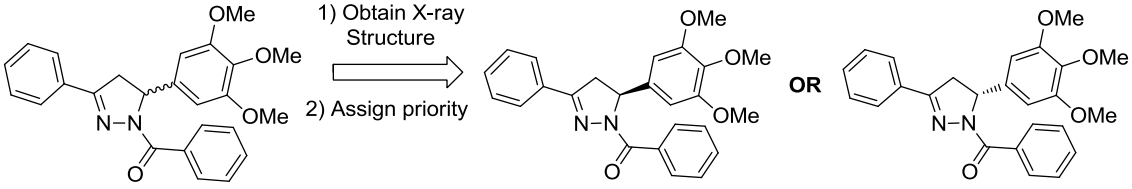

(71-) ***S*** ***R***

Figure 44: Assignment of absolute stereochemistry.

Pyrazoline **(71-)** was screened in a number of different solvents in order to produce crystals of sufficient size and quality for a X-ray structure determination (Table 9). Although crystals were obtained in many cases, they were not of suitable quality for x-ray crystallography. Compounds containing the nitro (NO_2) group are often highly crystalline, therefore the nitro pyrazoline **(76)** was also submitted to this solvent screen but also failed to yield suitable crystals.

Cpm	EtOH	MeOH	MeCN	THF	EtOAc	$CHCl_3$	EtOH	Toluene	IPA	CH_2Cl_2
71(-) **76**	**X**	**X**	**X**	**X**	**X**	**X**	**X**	**X**	**X**	**X**

Table 9: Solvent screen.

A literature search revealed very few examples of enatiomerically pure pyrazolines with defined absolute stereochemistry (Figure 45).[72,73] The examples found suggest that pyrazoline **(71-)** may have an *S* configuration based on the optical rotation, however further experiments are required in order to confirm this.

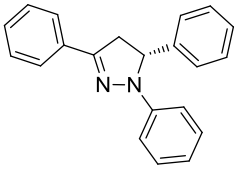

(82)

(+) Enantiomer[72]
R Stereochemistry

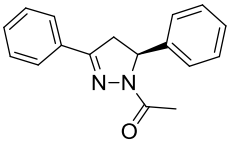

(83)

(-) Enantiomer[73]
S Stereochemistry

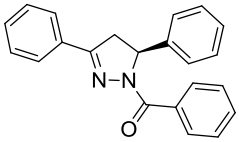

(84)

(-) Enantiomer[73]
S Stereochemistry

Figure 45: Defined absolute stereochemistry of pyrazolines in the literature.[72,73]

3.13 Pyrazole Combretastatin Analogue

To overcome the problem with determining the absolute stereochemistry of pyrazoline **(71-)** and remove the issues arising from it, oxidation of pyrazoline **(71)** to pyrazole **(85)** lacking a stereogenic centre was attempted (Figure 19).

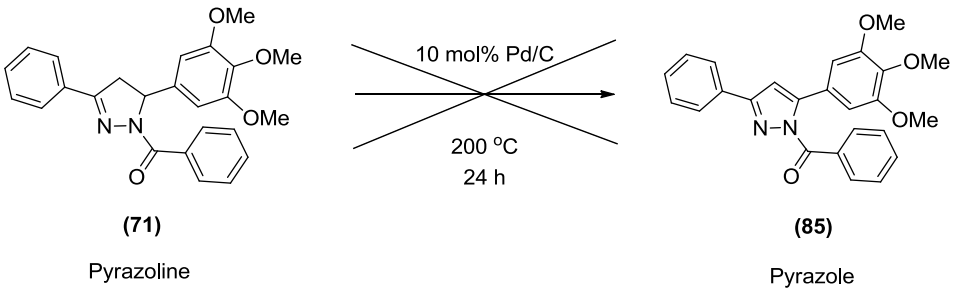

(71)

Pyrazoline

(85)

Pyrazole

Scheme 19: Removal of stereogenic centre by oxidation of pyrazoline (71) to pyrazole (85).[103]

Several attempts at this oxidation were attempted however none were successful despite similar compounds in the literature.[103] It was predicted that the benzoyl ring was responsible for the difficulty therefore an alternative was investigated in which the NH pyrazoline was initially oxidised followed by addition of benzoyl chloride (Scheme 20).

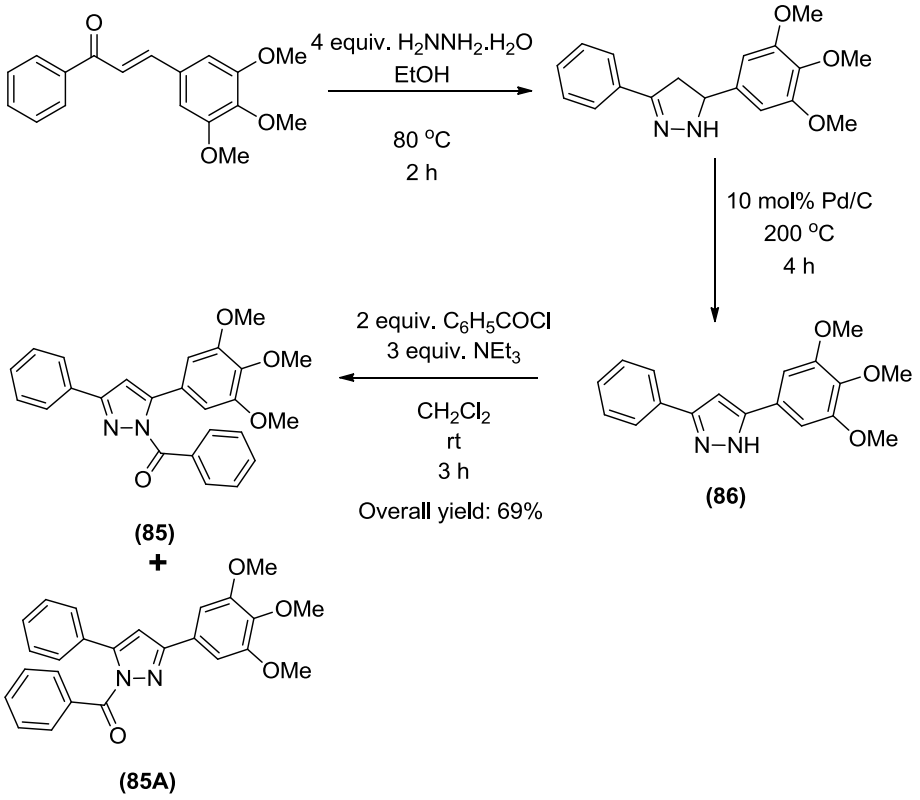

Scheme 20: An alternative synthesis of pyrazole (85) and its regioisomer (85A).

This reaction was successful however a mixture was obtained of the desired pyrazole **(85)** and the corresponding regioisomer **(85A)** in a ratio of 61:39 **(85:85A)** determined by ^{1}H NMR due to tautomerisation of the NH pyrazole (Scheme 21).

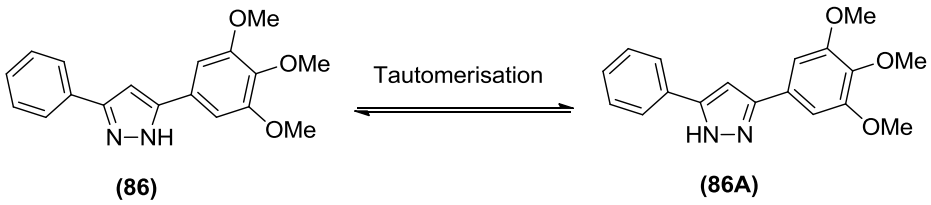

Scheme 21: Tautomersation of the NH pyrazole.

Separation of regioisomers **(85** and **85A)** was attempted using silica gel column chromatography however without success. Molecular modelling with MOPAC indicated that the stereogenic centre present in pyrazoline **(71-*S*)** induces a curved conformation with a dihedral angle of 123^o and bond distance of 4.9 Å between the A and B rings (Figure 55). A similar result was obtained with pyrazoline **(71-*R*)** (data not

shown). In contrast pyrazole **(85)** contains a flat aromatic pyrazole ring which forces the A and B rings to have a dihedral angle of 179° without significantly changing the bond length (Figure 46). In addition, the orientation of the C ring in pyrazole **(85)** is significantly altered which may influence activity.

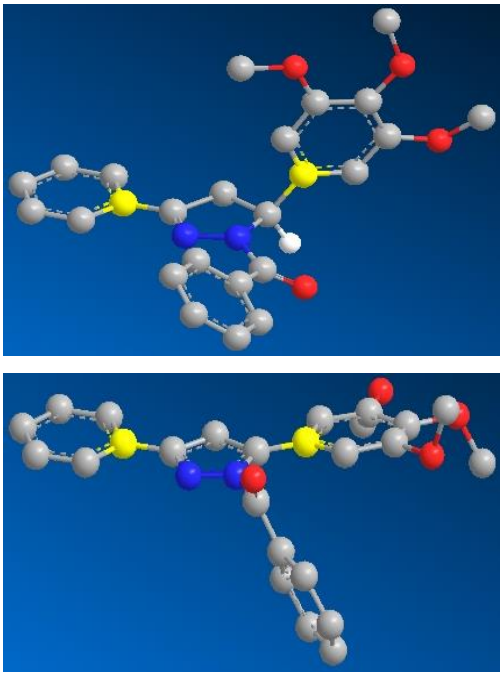

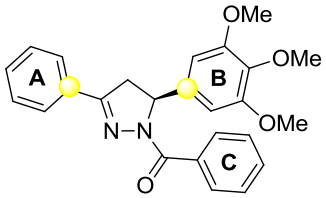

(71-*S*)

Bond distance : 4.9 Å
Dihedral angle : 123°

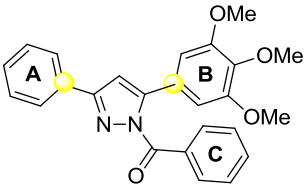

(85)

Bond distance : 4.8 Å
Dihedral angle : 179°

Figure 46: Molecular models of pyrazoline (71-*S*) and pyrazole (85).

To investigate how this structural change influenced antiproliferative activity, regioisomers **(85** and **85A)** were submitted for biological evaluation. Pyrazole mixture **(85** and **85A)** displayed over a hundred fold loss in antiproliferative activity compared to the parent pyrazoline confirming the importance of the curved shape in pyrazoline **(71)** for biological activity (Figure 47).

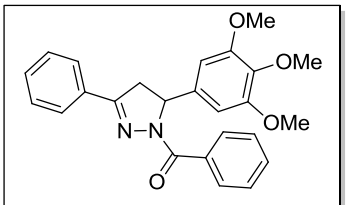

(71+/-)

IC_{50} (HT29): 0.17 μM
IC_{50} (MDA-MB-231): 0.17 μM

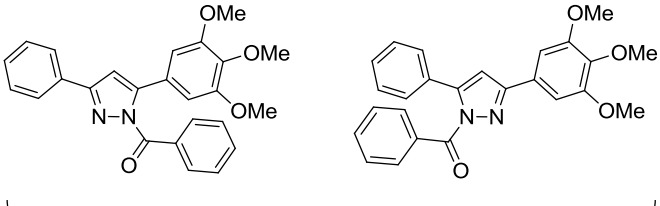

(85) Ratio of 69:31 **(85A)**

IC_{50} (HT29): 26.1 μM
IC_{50} (MDA-MB-231): 17.6 μM

Figure 47: Pyrazoline (85) and its regioisomer (85A) display a hundred fold less antiproliferative activity compared to pyrazoline (71).

3.14 Prodrug Strategies

Prodrugs are a useful technique of increasing the activity of a drug by incorporating a structural unit which can be biologically converted *in vitro* generating the active drug within the cell.[75,76] The SAR study revealed substitution at the 4 position of the A ring with OH **(75)** and NH_2 **(77)** displayed similar levels of activity to the unsubstituted pyrazoline **(71)** in HT29 and MDA-MB-231. This suggests these two analogues may be candidates for prodrug strategies (Scheme 22). In order to investigate further the ester **(86)** and amide pyrazoline **(87)** were generated in high yield and submitted to biological evaluation to determine if the parent OH (**75**) and NH_2 (**77**) analogues could be generated within the cell (Scheme 22).

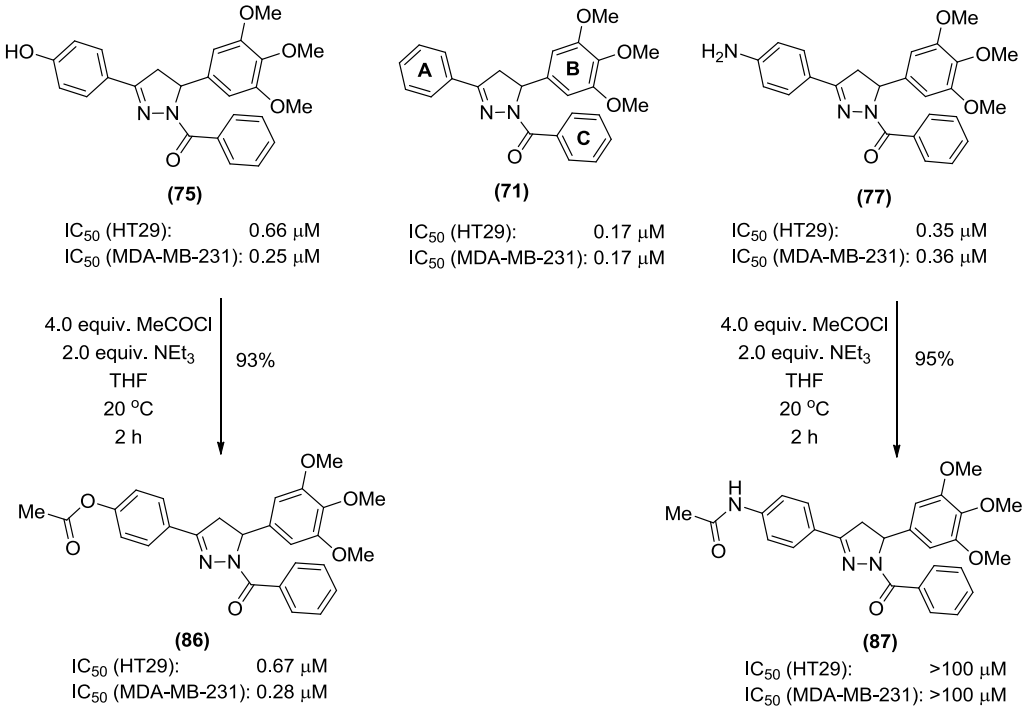

Scheme 22: Prodrug synthesis and biological evaluation.

The ester **(86)** displayed comparable antiproliferative activity as the parent OH pyrazoline **(75)**, whereas the amide **(87)** displayed poor antiproliferative activity. To confirm that the antiproliferative activity of ester **(86)** was due to ester hydrolysis within the cell generating the parent OH pyrazoline intracellularly and not due to hydrolysis in the culture medium, a mass spectroscopy study was conducted. This study involved incubating the ester **(86)** and amide **(87)** pyrazolines in culture media

only (without cells) for 72 h, the time course of the MTS assay. Aliquots of the culture media were extracted at 0 h, 24 h, and 72 h time points and the presence and quantity of prodrug and corresponding parent pyrazoline calculated by comparing the relative signal intensities of the sodium adduct at each time point. The mass spectroscopy data obtained suggested that the activity observed for the ester pyrazoline **(86)** was due to hydrolysis in the culture media generating the active patent pyrazoline **(75)** which then elicited the antiproliferative activity observed (Table 10).

	Incubation Time			
cpm	0 h	24 h	48 h	72 h
Ester **(86)**	100%	47%	27%	20%
Amide **(87)**	100%	100%	100%	100%

Table 10: Prodrug stability studies.

This suggests that simple ester groups may not be suitable for future prodrug strategies. In contrast, the amide pyrazoline **(87)** was fully stable over the 72 h time period without any detection of the parent NH_2 pyrazoline **(77)** in the mass spectra. The poor biological activity of the amide suggests the amide unit was fully stable to intracellular amidases which were unable to hydrolyse the amide **(87)** to the active parent NH_2 pyrazoline **(77)** within the cell.

3.15 Conclusions

A library of fourteen pyrazoline combretastatin A-4 analogues, along with the ten chalcone precursors, were synthesised and screened for antiproliferative activity in two cancer line lines. Pyrazoline **(69)** was predicted to be the most active due to structural similarity to **CA4** however analogue **(71)**, lacking the 3-OH and 4-OMe substituted benzoyl ring, was the most active compound in the library (Figure 48).

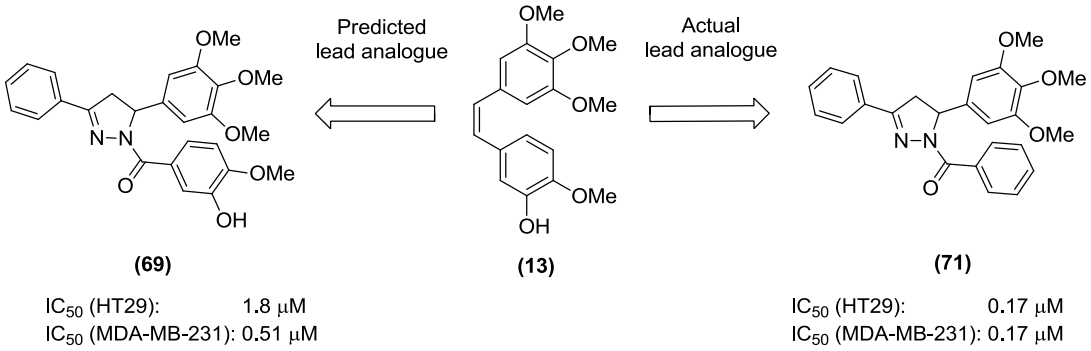

Figure 48: Predicted lead pyrazoline vs actual lead pyrazoline.

An SAR study revealed that a single aryl ring was preferred at A, with minor substitutions at the *para* position tolerated. A 3,4,5-trimethoxy aryl unit at B was critical for activity, a single aryl ring at position C was preferred and the ketone linking ring C to the pyrazoline ring was essential for antiproliferative activity (Figure 49).

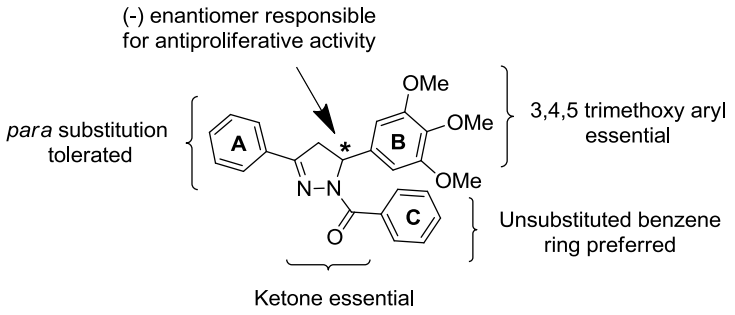

Figure 49: Pyrazoline SAR study.

Six enantiomerically pure pyrazolines were obtained using semipreparatory chiral HPLC and in all cases the (-) enantiomer was the active enantiomer and was the component responsible for the antiproliferative activity observed in the racemates. Pyrazoline **(71-)** displayed excellent nanomolar GI_{50} values across multiple cancer cell lines in the NCI 60 cell panel including the multidrug resistant NCI/ADR-RES (GI_{50} 35

nM) cell line (Figure 50). Pyrazoline **(71-)** displayed modest selectivity towards cancer cell lines and is currently under evaluation at the NCI biological evaluation committee to determine if it should progress to *in vivo* screening.

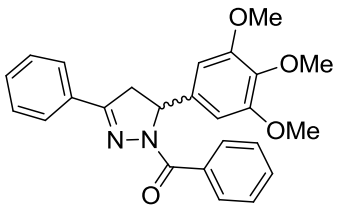

(71-)

GI_{50} (NCI-H522):	25 nM
GI_{50} (MDA-MB-435):	25 nM
GI_{50} (OVCAR-3):	25 nM
GI_{50} (MCF-7):	36 nM
GI_{50} (KM12):	37 nM
IC_{50} (FEK-4):	284 nM

Figure 50: Pyrazoline (71-) displayed excellent growth inhibition activity across multiple cancer cell lines and modest selectivity in FEK-4 human skin fibroblasts.

COMPARE analysis demonstrated a high correlation with microtubule binders suggesting pyrazoline **(71-)** had a similar mode of action. Cell cycle analysis, *in vitro* tubulin polymerisation and confocal microscopy analysis provided further evidence to suggest that pyrazoline **(71-)** is a microtubule destabiliser. The simple molecular structure, combined with its simple three step synthesis from commercially available materials enables the design of a second library of pyrazoline **(71-)** analogues.

Attempts to obtain suitable crystals for an X-ray crystal structure of pyrazoline **(71-)** to assign the absolute stereochemistry were unfortunately unsuccessful. Attempts to generate the corresponding pyrazole **(85)** resulted in a mixture of the desired product and its regioisomer **(85A)**. Biological evaluation of this mixture indicated a hundred fold loss in antiproliferative activity confirming the importance of the stereogenic centre.

To investigate the potential of applying prodrug strategies to this series of compounds, the *para* substituted OH pyrazoline **(75)** and NH_2 pyrazoline **(87)** were aceylated to give ester **(86)** and amide pyrazolines **(87)** respectively. Biological evaluation indicated that amide **(87)** failed to confer the antiproliferative activity of the parent NH_2 pyrazoline *in vitro* (Scheme 23). In contrast ester **(86)** conferred equal antiproliferative activity as the parent OH pyrazoline *in vitro*. To investigate if the activity observed was due to esterase hydrolysis intracellularly and not due to hydrolysis in the culture media, a mass spectroscopy (MS) study was performed. This

MS study indicated that ester **(86)** was rapidly hydrolysing in culture medium within 24 hours to generating the active OH pyrazoline **(75)**. After 72 hours only 20% of the original ester **(86)** remained suggesting that the ester is not suitable for future prodrug strategies (Scheme 23).

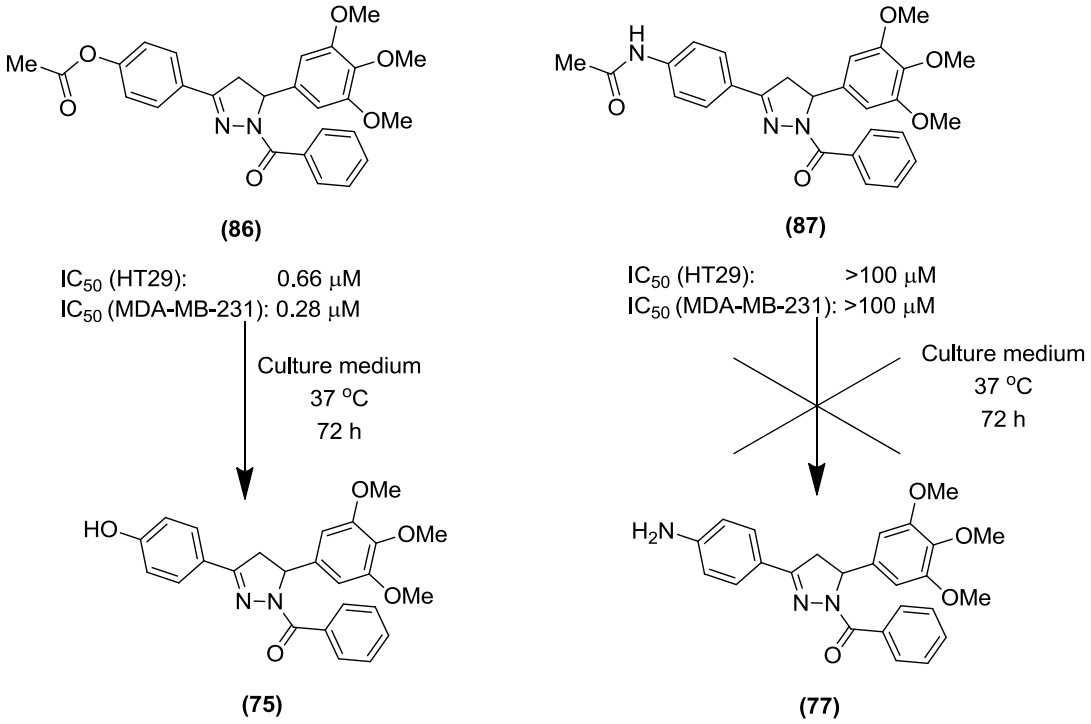

Scheme 23: Prodrug summary.

A MS study was conducted with amide **(87)** which indicated that this compound was stable over the 72 hour period. Unfortunately, while the amide **(87)** was fully stable in culture medium after a 72 hour period, the poor antiproliferative activity observed *in vitro* suggests that this amide was too stable for future prodrug strategies.

3.16 Future Work

3.17 Enantioselective Synthesis of Pyrazoline (71-)

One vital avenue for future work is the development of an enatioselective synthesis of pyrazoline **(71-)** enabling gram quantities of this potent nanomolar compound to be produced in high enantiomeric excess (ee). Fortunately Briere *et al.* reported a two step enatioselective synthesis of pyrazolines via the corresponding chalcone using quininium based catalysts.[73] Briere *et al.* successfully synthesised unsubstituted pyrazoline **(84-)** in 99% yield with 99% ee (Figure 51). This procedure was also used to synthesise the **(+)** enantiomer in high ee by selecting a quininum based catalyst with inverted stereochemistry. This procedure should be applied to pyrazoline **(71)** enabling access to both enantiomers in high yield and high ee (Figure 51).

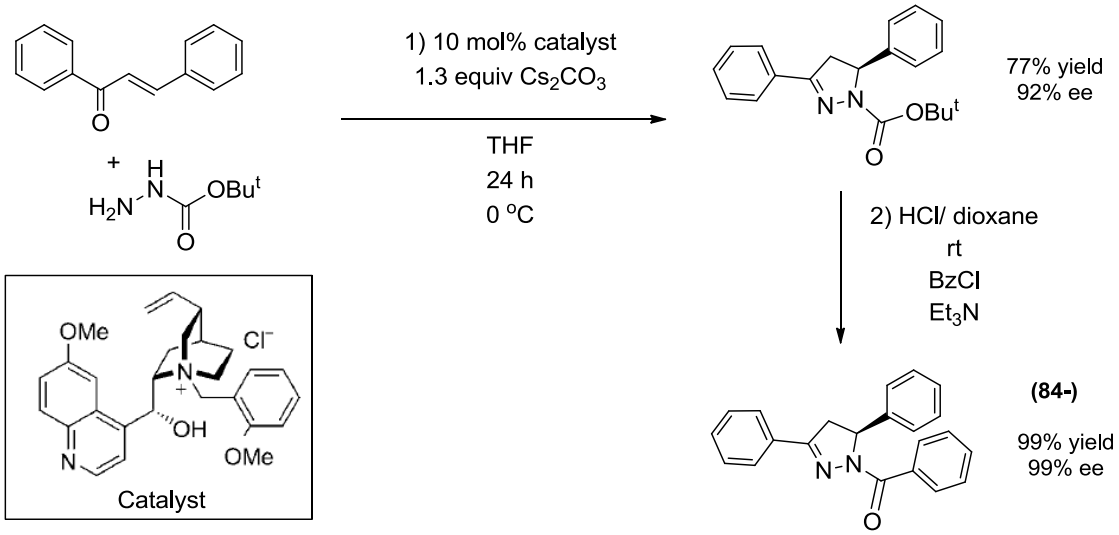

Figure 51: Enantioselective synthesis of (84-).[73]

Synthesising **(71-)** on a gram scale in two steps would be a significant advancement from the time consuming and limited scale semipreparatory chiral HPLC currently in use. Access to larger quantities of **(71-)** would also greatly assist in the determination of absolute stereochemistry of this potent microtubule destabiliser.

3.18 Determination Pyrazoline (71-) Absolute Stereochemistry

The ability to synthesise **71(-)** on a larger scale enables a much wider range of recrystallisation solvents and conditions to be investigated to obtain crystals of sufficient size and quality for an X-ray structure determination enabling assignment of (**71-)** as *R* or *S*. A range of different chiral acids could also be investigated to determine if forming a diastereomeric mixture improves recrystalisation facilitating an X-ray structure determination. The use of Moshers acid[74] and ^{1}H NMR spectroscopy could also be use to assign absolute stereochemistry.

3.19 Determination of Tubulin Binding Site of Pyrazoline (71-)

Cell cycle analysis, *in vitro* tubulin polymerisation assays and confocal microscopy suggest that **(71-)** is a microtubule destabiliser, however a key question remaining is where is **(71-)** binding to tubulin. The majority of microtubule destabilisers containing a 3,4,5-trimethyloxyl unit bind to the colchicine binding site on β tubulin therefore it is predicted that **(71-)** is also binding at the colchicine binding site. This hypothesis can be investigated using a [^{3}H]colchicine competition assay.[75] In this assay tubulin is exposed to radioactive [^{3}H]colchicine which binds to the colchicine binding site on β tubulin. Excess [^{3}H]colchicine is then removed and **(71-)** added which if it binds at or near the colchicine binding site, will compete with [^{3}H]colchicine resulting in an increase in radioactivity. The assignment of the tubulin binding site, alongside with an X-ray crystal structure of **(71-)** enables molecular modelling and *in silico* docking experiments facilitating the rational design of a second generation of analogues with improved tubulin binding properties.

3.20 3,5 Dibromo Analogue of Pyrazoline (71-)

Ley *et al.*[38] demonstrated that **CA4** analogue **(19)** retained nanomolar activity in cancer cell lines while also conferring activity in Taxol®-resistant cell lines (Figure 64). A similar approach could be applied to our lead pyrazoline **(71)** generating the dibromo analogue **(71B)** with potential improved biological properties (Figure 52).

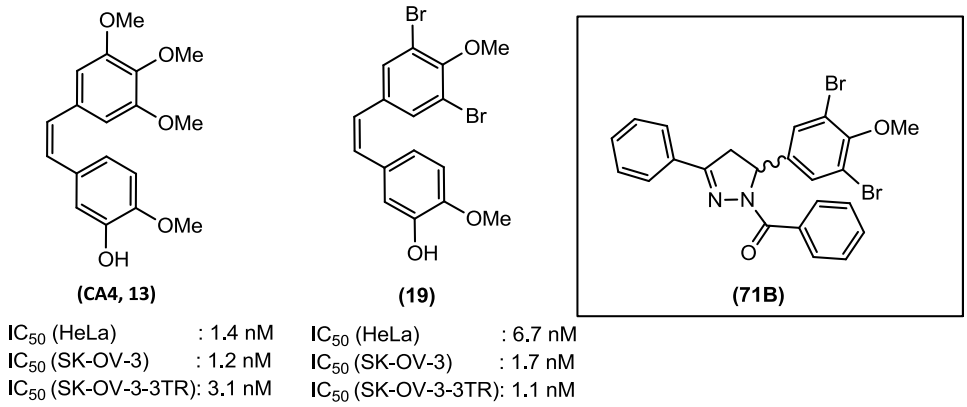

Figure 52: 3,5 Dibromo analogue of (71B).

3.21 Prodrug Analogues

A second generation of pyrazoline prodrugs with improved water solubility via a range of salt derivatives could be developed (Scheme 24). Zybrestat® **(14)** the phosphate prodrug of **CA4** currently in phase III clinical trials demonstrates that the phenolic group in pyrazoline **(75)** could be converted to the phosphate prodrug (**75B**).

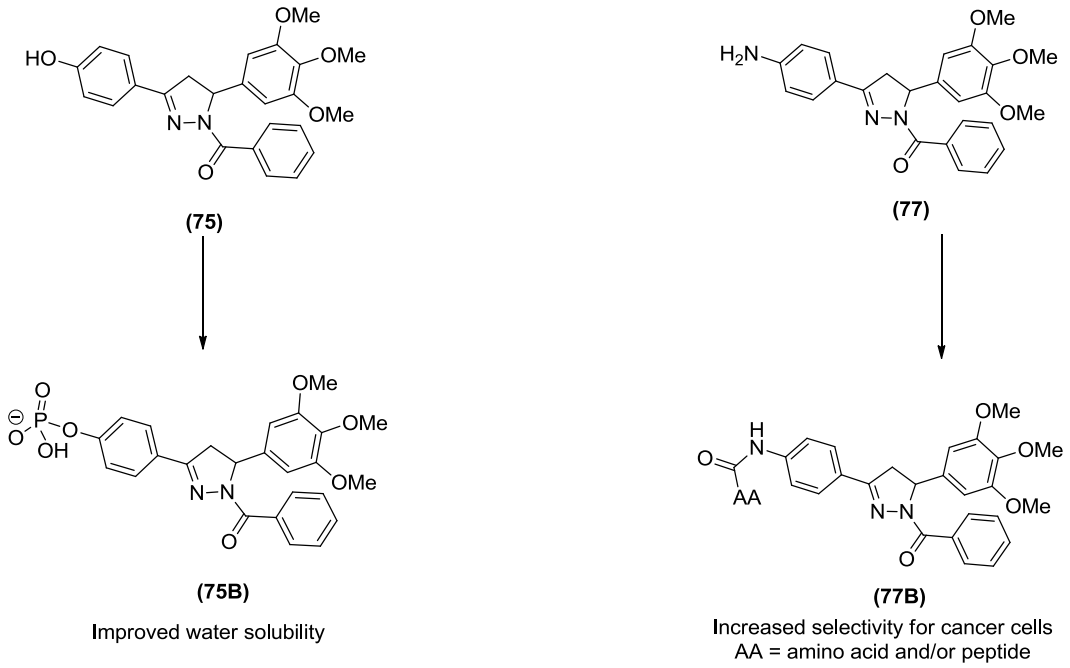

Scheme 24: Future prodrug approaches.

Pyrazoline **(71)** demonstrated modest selectivity towards cancer cells therefore a further avenue worth exploring is increasing this selectivity by modifying

pyrazoline **(71)** to increase uptake in cancer cells. PEPT1, an oligopeptide transporter over expressed in the intestine is involved in conveying amino acids (AA) and di or tri peptides into the cell fuelling cell division.[76] Numerous prodrugs have been reported which are designed to be taken up by PEPT1 including the anticancer drugs floxuridine[77] and gemcitabine.[78] Pyrazoline **(71)** displayed excellent nanomolar activity (GI_{50} 277-371 nM) across all seven colon line lines in the NCI screen suggesting that it may be suitable for PEPT1 prodrug strategies.

Chapter 4: Introduction to Tissue Engineering

4.1 Tissue Engineering

Tissue engineering is a diverse interdisciplinary field that applies engineering principles to the biological sciences with the aim of maintaining, repairing or replacing tissue function.[79,80] Three dimensional (3D) polymeric scaffolds are commonly used in tissue engineering to provide a framework for cells to attach and proliferate. A scaffold must meet strict criteria (Figure 53A) to be of clinical use with numerous natural and synthetic materials available (53B).[81]

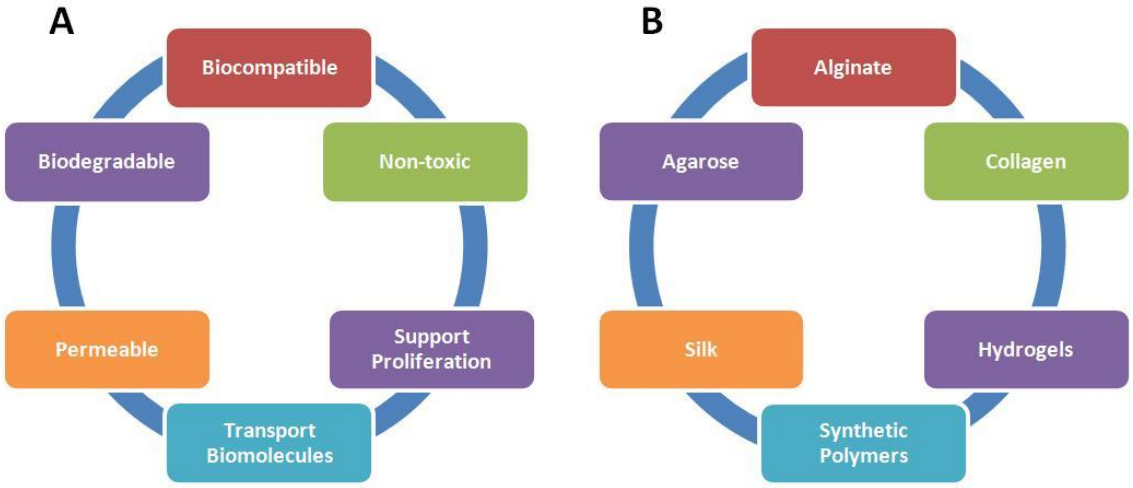

Figure 53: A) Cellular scaffold criteria[81] B) materials for cellular scaffolds.[81]

Since its conception in the late 1980s, tissue engineering has grown into a multibillion dollar industry with the global tissue engineering industry estimated to have a value of 4.7 billion dollars in 2007.[82] Current success stories include tissue-engineered bladders in 2006,[83] a trachea in 2008[84] and urethras in 2011 (Figure 54).[85] The continued development of more sophisticated cellular scaffolds will enable more complex tissues to be produced in the near future.

Figure 54: Success stories, tissue-engineered A) bladder,[83] B) trachea[84] and C) urethra.[85]

4.2 Metal Triggered Collagen Scaffolds

A key challenge in current scaffold design involves controlling the architecture and porosity of a scaffold while enabling the scaffold to be removed when no longer required. Chmielewski *et al.* recently reported a method of modifying collagen with the well known metal chelator dipyridine (dipy). In the presence of various transition metals (Zn^{2+}, Cu^{2+}, Ni^{2+} and Ru^{2+}) the modified collagen strands assembled into a 3D-metal collagen network (Figure 55).[86]

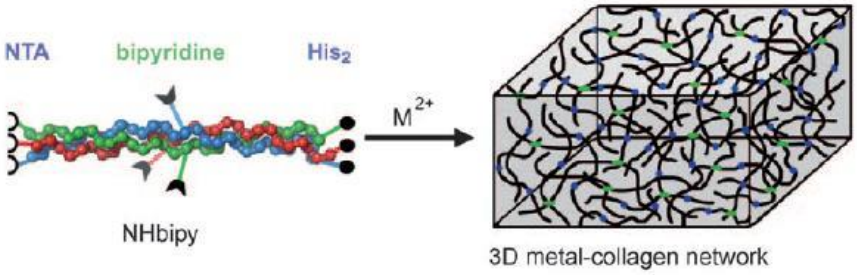

Figure 55: A) Bipyridine modified collagen, adapted from Chmielewski *et al.*[86]

Chmielewski *et al.* successfully encapsulated HeLa cells, a human cervical carcinoma cell line, into the scaffold and confirmed the cells retained high viability and proliferated within the scaffold. Further studies demonstrated that the incorporation of two different metals during assembly resulted in scaffolds with different architectures and porosities (Figure 56). This is particularly interesting as it allows control of the interior of the scaffold by simply modifying the transition metal ratio.

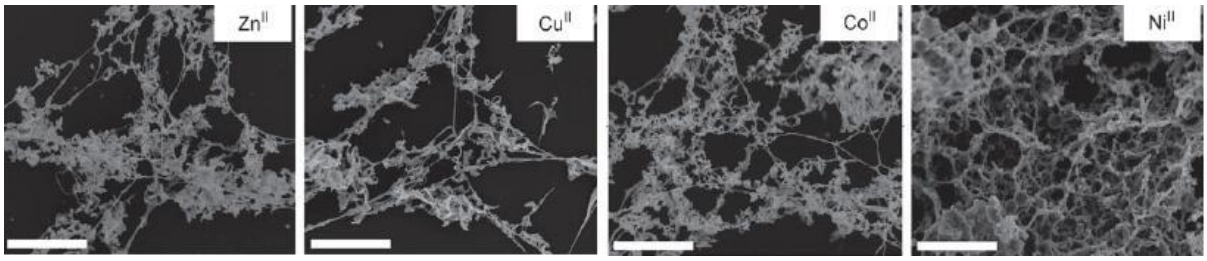

Figure 56: A) Scaffold architecture in the presence of Ru^{2+} and the above transition metals, adapted from Chmielewski *et al.*[86]

The addition of the potent metal chelator EDTA (ethylenediaminetetraacetic acid) disrupts the scaffold as the EDTA sequesters the transition metals from the bipy (Figure 57). This is a useful property as the scaffold can be easily removed once the encapsulated cells have achieved the desired population.

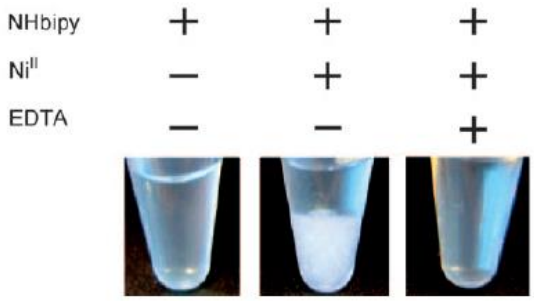

Figure 57: Scaffold formation is reversible, adapted from Chmielewski *et al*.[86]

Chmielewski *et al.* recently modified this technique to produce metal triggered collagen particles which assemble in the presence of various transition metals (Figure 58).[87]

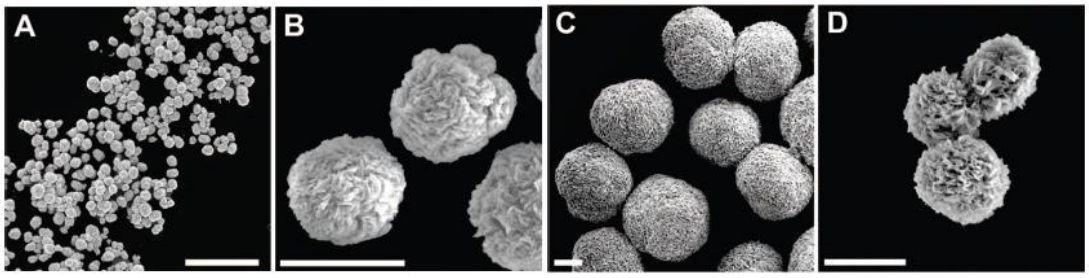

Figure 58: Metal triggered particle formation, A) +400 µM $CuCl_2$ scale bar = 100 µm, B) +400 µM $CuCl_2$ scale bar 5 µm, C) +400 µM $ZnCl_2$ scale bar = 5 µm, D) + 400 µM $CoCl_2$ scale bar 5 µm, adapted from Chmielewski *et al*.[87]

These recent developments validate metal chelation as a useful tool to assemble and control the architecture of tissue engineering scaffolds. The diverse range of metal chelators available, along with the range of transition metals and the potential to use combinations of transition metals, provide a valuable opportunity to advance current cellular scaffolds.

4.3 Modifying the Cell Surface

Cell-cell contact is critically involved in a diverse range of applications including cellular communication and proliferation.[88] The cell surface is a highly complex environment composed of lipids, proteins and carbohydrates which enable the cell to interact with surrounding cells and its environment. The ability to modify the cell surface to introduce additional functionality provides a valuable opportunity to increase cell-cell and cell-scaffold interactions. Bertozzi *et al.* reported a mild procedure for the introduction of non-native functional groups such as aldehydes on the cell surface.[89] Treatment of cells with sodium periodate ($NaIO_4$) oxidatively cleaves the vicinal diol on sialic acid residues in the cell surface to generate the corresponding aldehyde which remained on the cell surface for over 24 hours (Scheme 25).

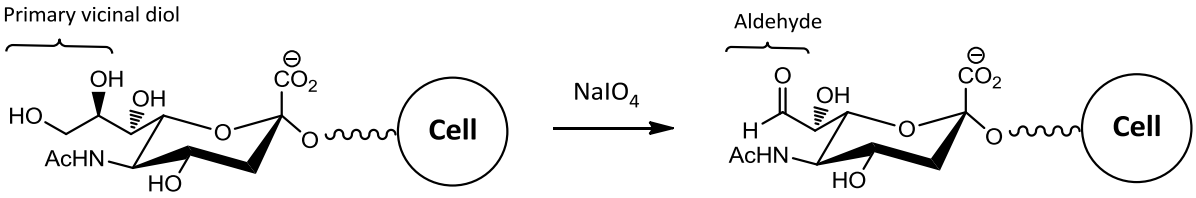

Scheme 25: Generation of non-native aldehydes on the cell surface.[89]

Further studies confirmed that this process was non-toxic to the cells enabling the chemical ligation of compatible molecules onto the cell surface.

4.4 Multicellular Aggregation

Shakesheff *et al.* demonstrated that the non-native aldehydes were versatile functional groups for the attachment of biotin hydrazides via the formation of a hydrazone bond (Scheme 26).[90,91]

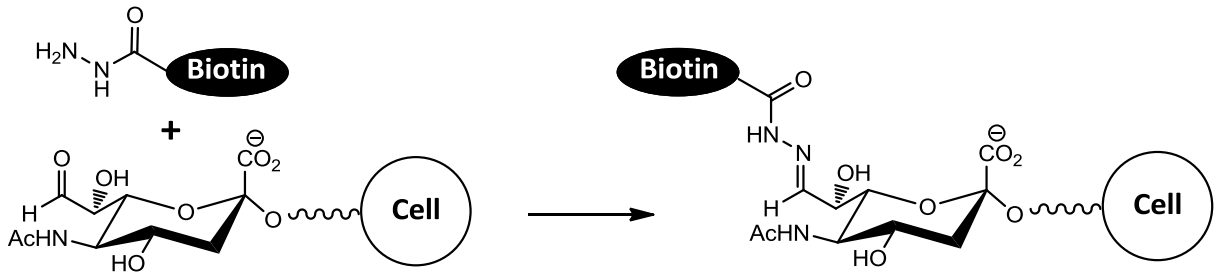

Scheme 26: Attachment of biotin hydrazide via hydrazone bond formation, adapted from Shakesheff *et al.*[90]

Shakesheff *et al.* proposed that upon addition of avidin, a tetrameric protein with four biotin binding sites, the biotinylated cells above would crosslink together forming a multicellular aggregate (Figure 59A).[90,91]

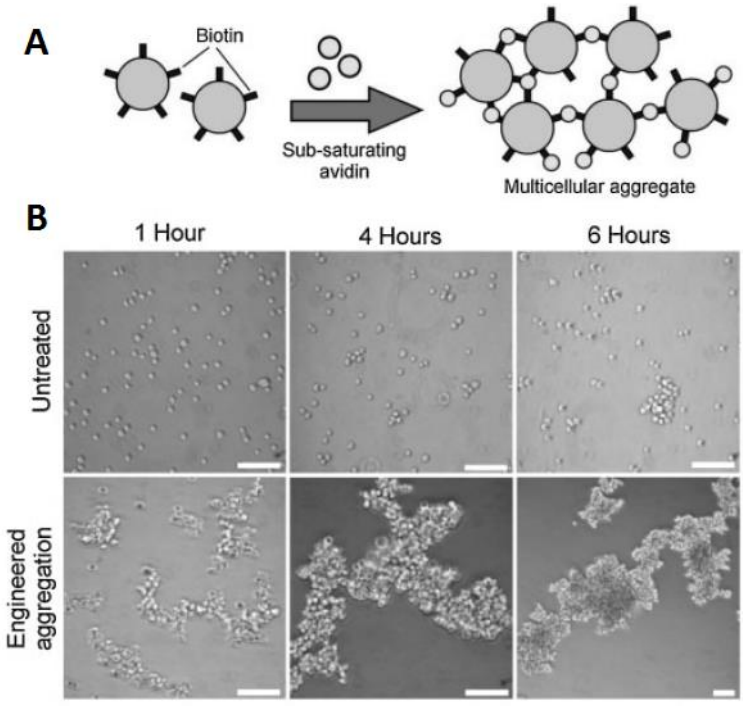

Figure 59: A) Schematic representation of aggregation process, B) phase contrast images of engineered aggregation of L6 cells compared to untreated cells, scale bar = 100 µm, adapted from Shakesheff *et al.*[91]

After one hour of gentle agitation in the presence of 10 µg/mL avidin the biotin engineered cells formed multicellular aggregates in contrast to the untreated cells which retained in a single cell suspension (Figure 59B). Continued agitation for four hours increased the aggregate size compared to the untreated cells confirming

that modifying the cell surface was responsible for the aggregation observed. Shakesheff *et al.* proposed that as sialic acid residues are conserved across different cell lines, this process could be applied to heterocellular aggregates composed of two different cell types.[91] This theory was confirmed for 3T3 fibroblasts (green) and L6 myoblasts (red) which were aggregated together to form a randomly arranged heterocellular aggregate (Figure 60A). A layered aggregate with a 3T3 fibroblast (green) core and L6 myoblast (red) shell was also generated using this method (B).

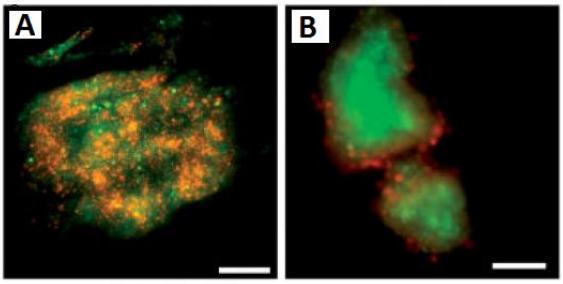

Figure 60: Heterocellular aggregates in A) random aggregate B) layered aggregate, 3T3 fibroblasts (green) and L6 myoblasts (red), scale bar = 100 µm, adapted from Shakesheff *et al.*[91]

Sakai *et al.* expanded this approach by demonstrating that heterocellular aggregates formed via surface modification could under go self-organisation *in vitro*. They report that aggregates of biotinylated Hep G2 cells, (a human hepatoma cell line green) and avidin expressing MS1 cells (a mouse pancreatic cell line red) self-organise over the course of 18 hours, shown in Figure 61.

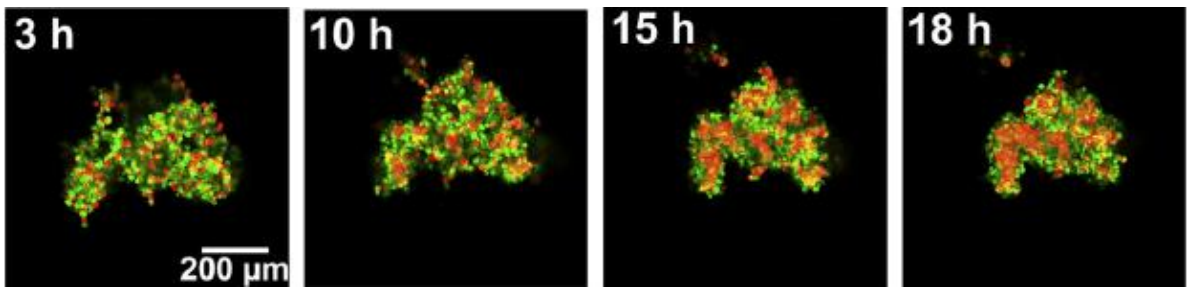

Figure 61: Time-lapse images of heterocellular aggregates composed of Hep G2 (green) and MS1 (red) cells over a 18 hour period, adapted from Sakai *et al.*[92]

This result is particularly interesting as it demonstrates that MS1 cells (red) within the aggregate migrate towards other MS1 cells. Sakai *et al.* also investigated the formation of heterocellular aggregates composed of three different cell types Hep

G2 (green), MS1 (red) and NIH3T3 cells (a mouse fibroblast cell line magenta) and allowed them to self-organise over a 24 hour period (Figure 62). Interestingly the MS1 cells (red) and NIH3T3 (magenta) cells organised around each other whereas the Hep G2 cells (green) preferred to aggregate with each other forming a central core (Figure 62).

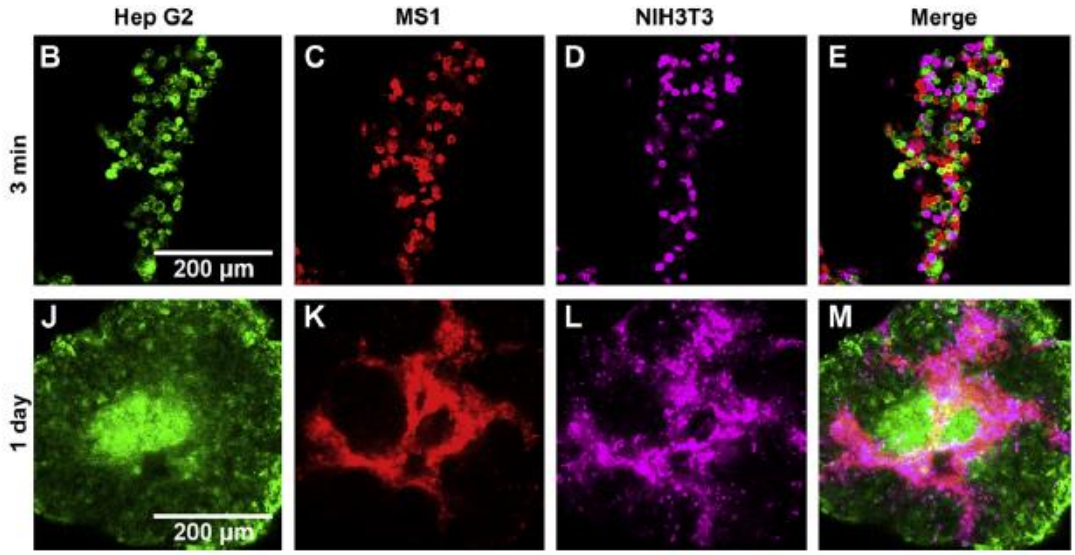

Figure 62: Remodelling of heterocellular aggregate composed of Hep G2 (green), MS1 (red) and NIH3T3 (magenta) cells, adapted from Sakai *et al.*[92]

These pioneering experiments confirm the versatility of cell surface modification as a method of forming multicellular aggregates which can self-organise to form complex architectures *in vitro*. One significant disadvantage of this technique is the cost of the regents required, for example biotin hydrazide 10 mg = £60 and avidin 10 mg = £117. The high cost of the reagents limits this technique to small scale experiments and prevents its wider application on an industrial scale. The development of more cost effective reagents and methods should be investigated to ensure this technique becomes more widescale.

4.5 Pyrazolines as Novel Metal Chelators

As discussed in chapters 2 and 3, chalcones have previously been shown to be interesting compounds themselves and as valuable starting materials for pyrazolines with potent antiproliferative activities reported (Figure 16 and 48). The pyrazoline structure also serves as a useful scaffold for the design of novel metal chelators with a variety of transition metals (Figure 63).

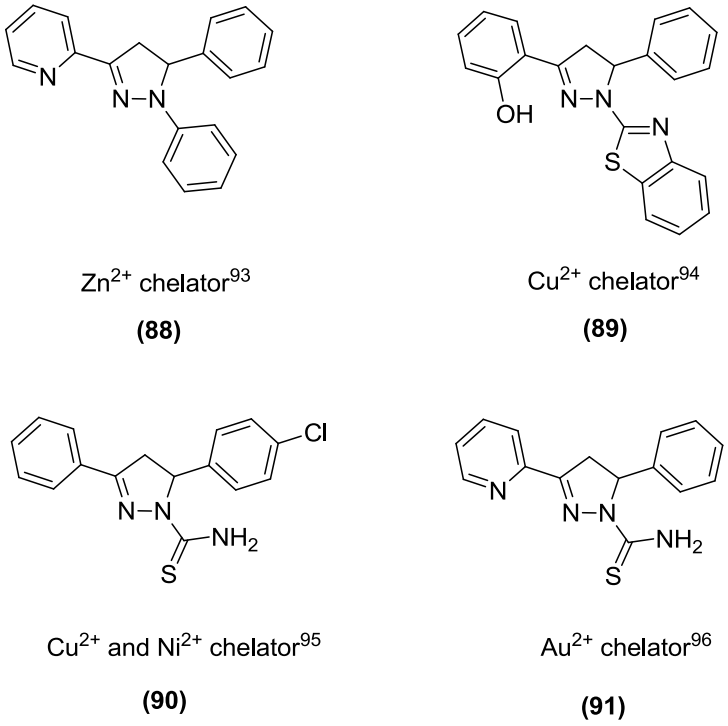

Zn^{2+} chelator[93] **(88)**

Cu^{2+} chelator[94] **(89)**

Cu^{2+} and Ni^{2+} chelator[95] **(90)**

Au^{2+} chelator[96] **(91)**

Figure 63: Recent pyrazoline metal chelators.[93-96]

The modular design of the pyrazoline scaffold, combined with a variety of chalcone starting materials, enables a diverse range of pyrazolines to be designed to chelate specific transition metals, as shown in Figure 63.[93-96]

4.6 Maltol Derivatives as Metal Chelators

Maltol (3-hydroxyl-2-methyl-4-pyrone, **92**) is a FDA approved food additive present in a variety of products including beer, bread and tobacco due to its malty favour and low toxicity profiles.[97,98] Maltol **(92)** is a well established Fe^{3+} chelator and its structurally related analogue deferiprone **(93)** is FDA approved for use in iron overload disease and beta thalassemia (Figure 65).[99] Two further maltol analogues are malten **(94)**, which has antiproliferative activities in cancer cell lines,[100] and derivative **(95)** which displays antimalarial activity (Figure 64).[101]

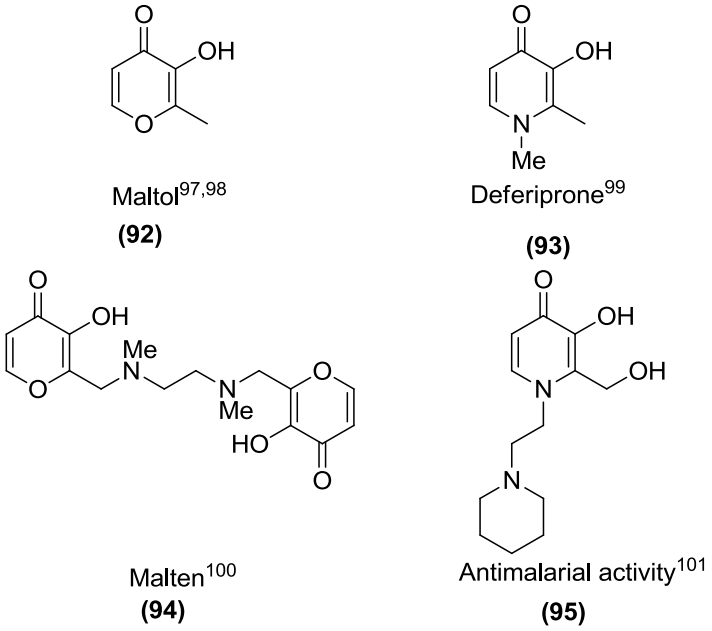

Figure 64: Maltol derivatives.[97-101]

Maltol **(92)** is available on an industrial scale and is cheap and readily available enabling its chemistry to be thoroughly investigated. The versatility of maltol is due to the ability to displace the oxygen atom in the pyrone ring for a variety of functional groups while retaining the Fe^{3+} chelation site (Figure 65).

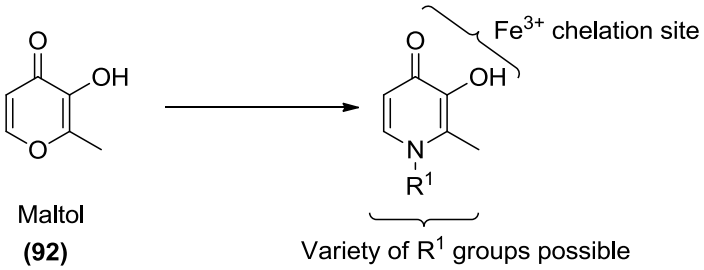

Figure 65: Insertion of various R^1 groups onto the maltol motif.

4.7 Pyrazoline Metal Chelators in Tissue Engineering

One potential avenue for development of pyrazoline metal chelators is in tissue engineering by incorporating pyrazolines onto the cell surface (Figure 66). Pyrazolines could be attached onto the cell surface by incorporating a hydrazide on the R^1 functional group and attaching it to cells using the methods reported by Bertozzi *et al.*[89] It is proposed that upon addition of transition metals to a solution of pyrazoline modified cells, multicellular aggregation would occur in a similar process observed by Shakesheff *et al.* (Figure 66A).[90,91]

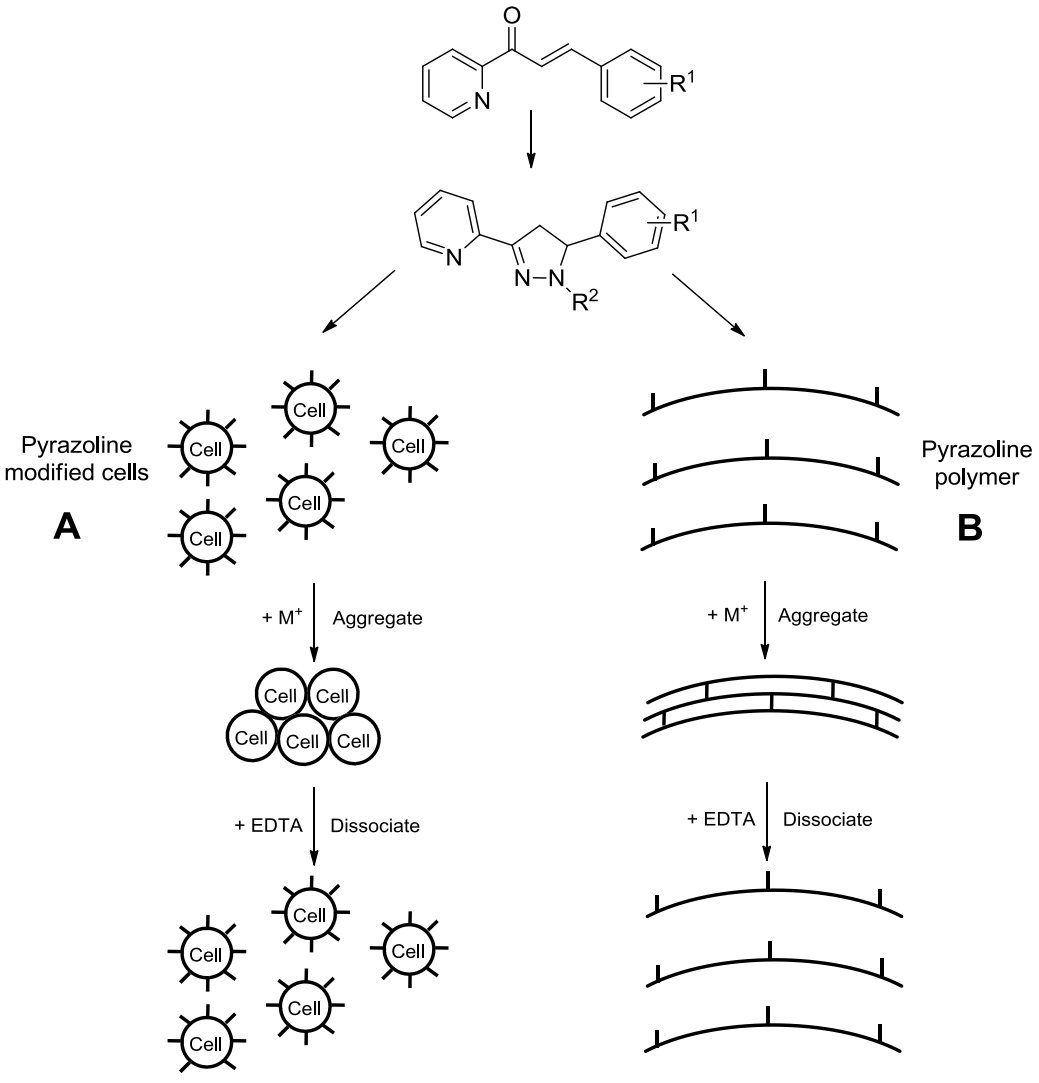

Figure 66: Proposed pyrazoline scaffold and pyrazoline modified cells, M^+ = transition metals.

If successful, the cheap and commercial availability of chalcone starting materials, combined with the ability to fine tune metal chelation by altering the R^2 groups will provide a valuable alternative to the current biotin and avidin method. The pyrazoline motif could also be incorporated directly into tissue engineering scaffolds in a similar approach to Chmielewski *et al.*[86] A suitable chemical handle, for example amine or carboxylic acid group, could be incorporated into the R^1 group of the chalcone facilitating attachment of the pyrazoline to a polymer backbone (Figure 66B). Upon addition of transition metals to a pyrazoline polymer solution metal chelation triggered cross-linking would occur generating a 3D network. The ability to alter the coordination site of the pyrazoline by altering the R^2 group enables different metals to be chelated providing an opportunity to control scaffold porosity and architecture (Figure 66).

4.8 Maltol Derivatives in Tissue Engineering

The ability to functionalise the maltol **(92)** motif provides an opportunity to investigate the use of maltol derivatives in tissue engineering. The maltol motif could be attached to the cell surface via a hydrazide functional group enabling the generation of maltol modified cells that aggregate in the presence of Fe^{3+} cations (Figure 67A). The high specificity of maltol towards Fe^{3+} will ensure that additional biologically relevant metals (Na^+, K^+, Mg^{2+} and Ca^{2+}) present in culture medium do not interfere with Fe^{3+} chelation. Furthermore, the low toxicity profile of maltol should ensure that the cells retain high viability and good proliferation. The maltol motif could also be attached to a polymer backbone via the activated ester enabling the generation of a Fe^{3+} triggered tissue engineering scaffold (Figure 67B).

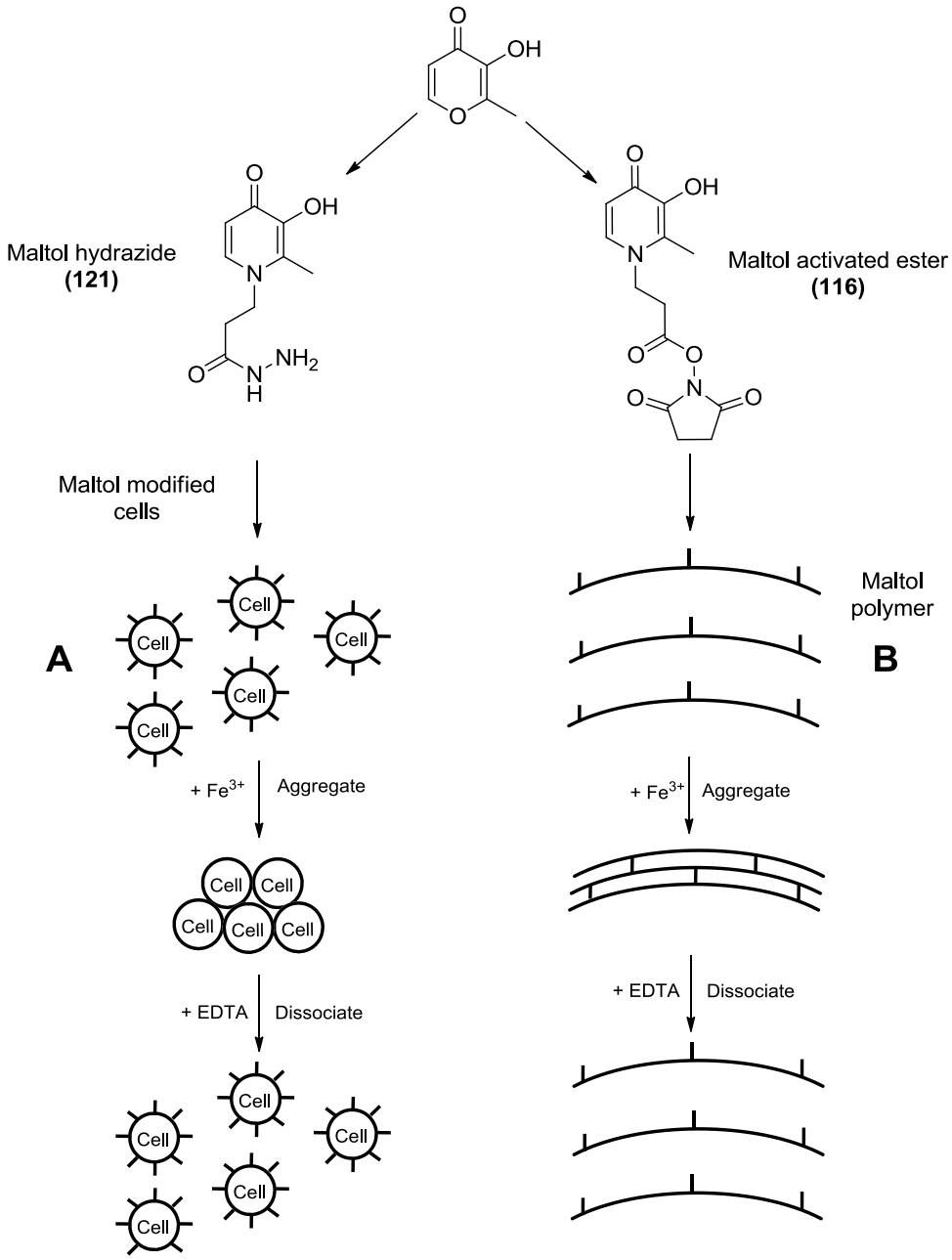

Figure 67: Proposed maltol modified cells and maltol scaffold.

Chapter 5: Pyrazoline Based Metal Chelators

5.1 Overview

Chapter 5: Pyrazoline Based Metal Chelators

Design, synthesis and investigation of the metal chelation properties of a range of substituted pyrazolines derived from chalcones (Figure 68).

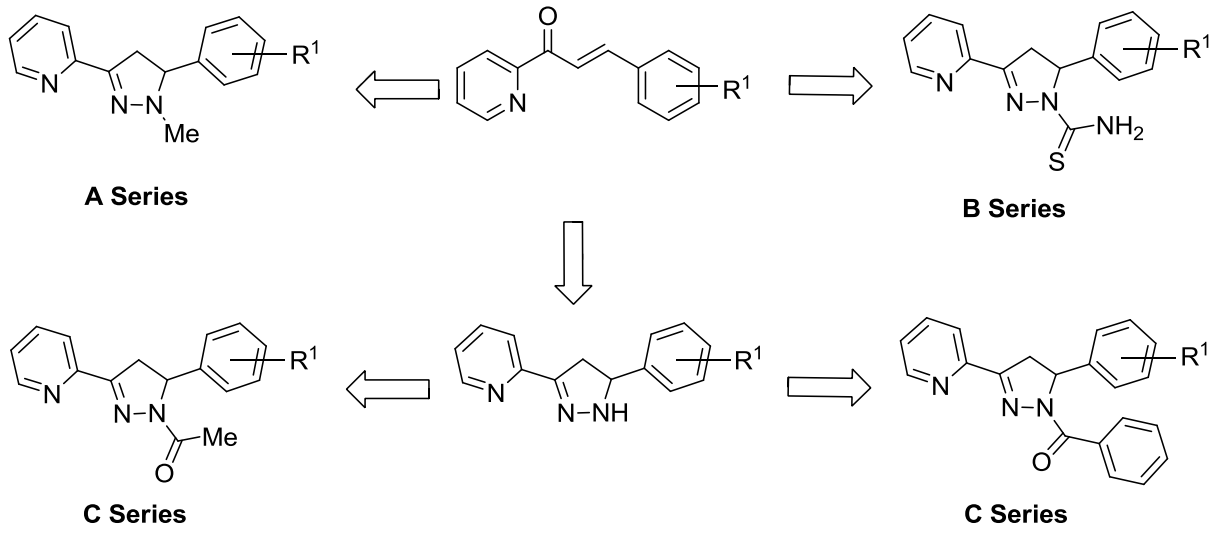

Figure 68: Pyrazoline metal chelator library design.

Pyrazolines will be screened for the ability to chelate a range of metals using the techniques of UV/Vis and ^{1}H NMR spectroscopy. Pyrazolines have previously been reported as fluorescence sensors[93] for Zn^{2+} therefore fluorescence spectroscopy will be to investigate potential useful sensor applications. To be useful for tissue engineering purposes they must be non-toxic and able to chelate metals in the presence of competing biological metals including Na^{+}, K^{+} and Ca^{2+} present in culture media. To confirm this MTS proliferation assays along with a range of competition assays will be performed.

5.2 Chemical Synthesis

A simple and robust procedure using cheap commercially available starting materials was developed. Chalcone **(96)** was synthesised in excellent yield using a previously reported procedure,[102] in which 2-acetylpyridine and benzaldehyde were added to 10% NaOH(aq) and left at 4 ^{o}C. After 24 hours the solid precipitate was collected, washed and dried to afford chalcone **(96)** in 97% without the need for further purification (Scheme 27).

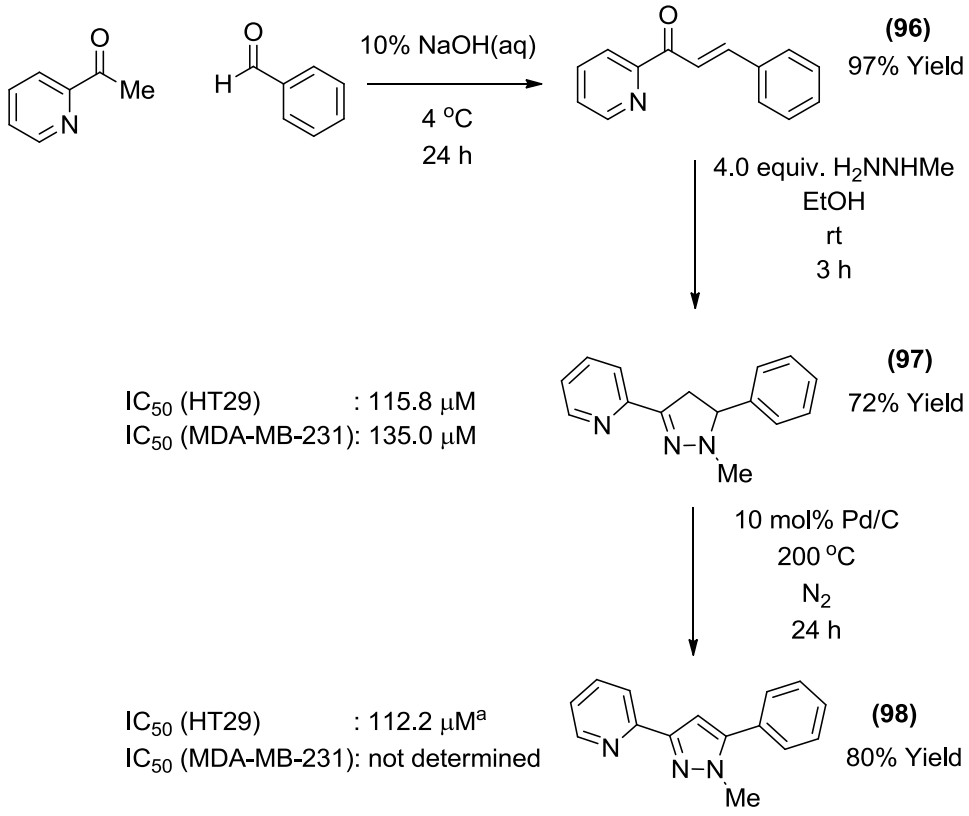

Scheme 27: Chemical synthesis of pyrazoline (97) and pyrazole (98) and MTS assays, values are the mean from three independent experiments except [a] from a single experiment.

Conversion of chalcone **(96)** to pyrazoline **(97)** was achieved in good yield by the addition of methylhydrazine at room temperature (Scheme 27). With pyrazoline **(97)** in hand a literature procedure[103] was used to oxidise the pyrazoline to the pyrazole **(98)** in 80% yield. The MTS assay was used to confirm that both compounds displayed poor antiproliferative activities (ie not toxic) and therefore both were suitable for tissue engineering purposes (Scheme 27).

5.3 Reaction Mechanism

The reaction of chalcone **(96)** with methylhydrazine is believed to proceed through a similar reaction mechanism as seen discussed previously with hydrazine (Scheme 17).[69,70] The non symmetrical arrangement in methylhydrazine could result in two possible products, pyrazoline **(97)** and the isomer pyrazoline **(97A)**. In methylhydrazine the lone pair of electrons on nitrogen 2 are less sterically hindered by the methyl group than nitrogen 1 and therefore more available for 1,2 nucleophilic attack on the carbonyl group in chalcone **(96)** (Scheme 28). 1,2 nucleophilic attack by nitrogen 1 would generate pyrazoline **(97A)** which was not observed.

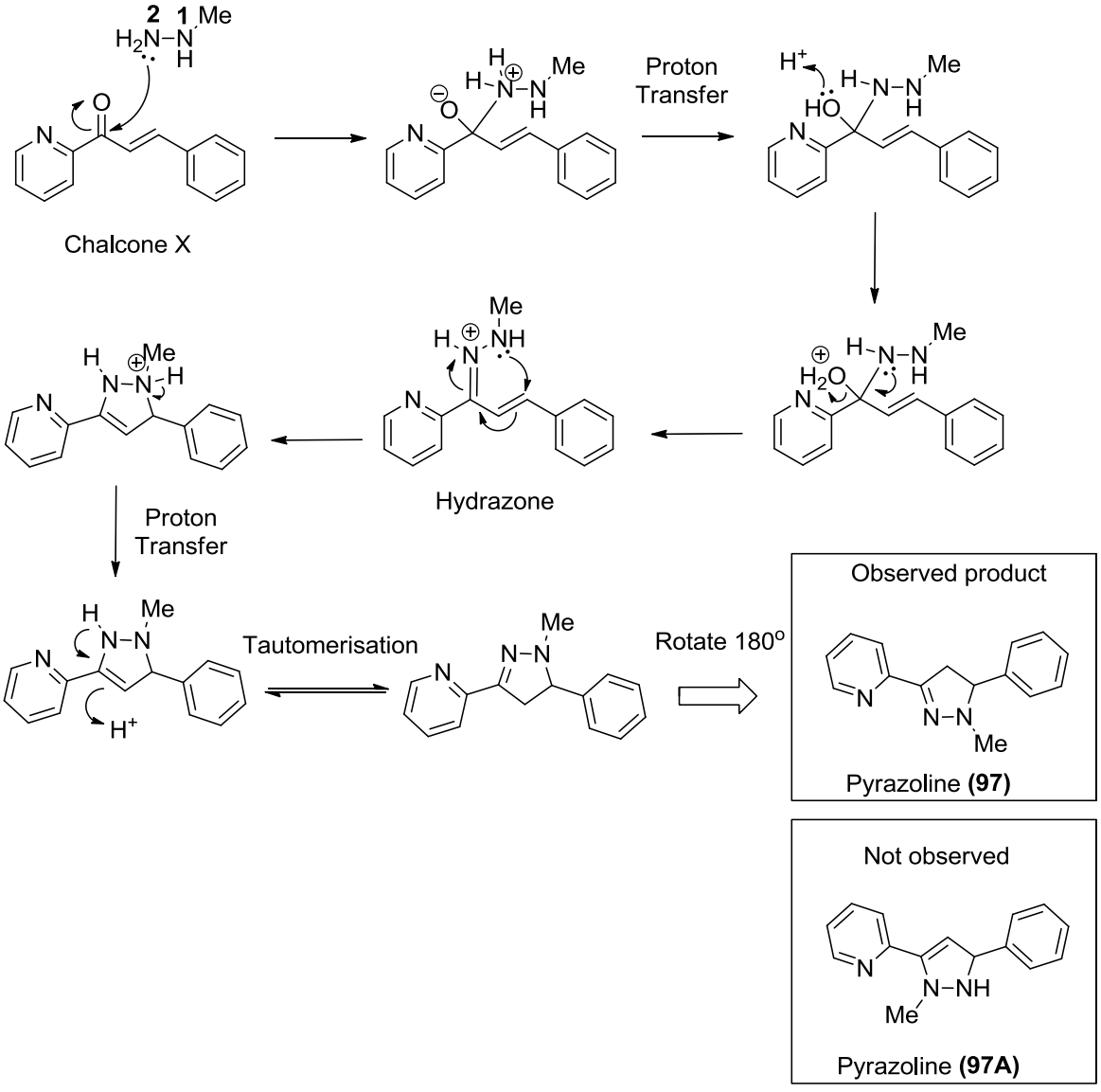

Scheme 28: Proposed reaction mechanism for the synthesis of pyrazoline (97).

5.4 UV/Vis Spectroscopy

UV/Vis spectroscopy is a rapid method of determining chelation properties by monitoring changes in the absorbance spectra in the absence and presence of metal cations. Pyrazoline **(97)** and pyrazole **(98)** were screened against a variety of metals, a summary of the results is below (Table 11).

	Li^{+}	Na^{+}	Mg^{2+}	K^{+}	Ca^{2+}	Mn^{2+}	Fe^{3+}	Co^{2+}	Cu^{2+}	Ni^{2+}	Cu^{2+}	Zn^{2+}	Ru^{3+}	Cd^{2+}	Hg^{2+}
(97)	X	X	X	X	X	✓	✓	✓	✓	✓	✓	✓	✓	✓	✓
(98)	X	X	X	X	X	✓	✓	✓	✓	✓	✓	✓	✓	✓	✓

Table 11: Pyrazoline (97) and pyrazole (98) UV/Vis metal screen, cross indicates no change whereas tick indicates changes in absorbance spectra upon addition of cation.

Pyrazoline **(97)** and pyrazole **(98)** produced negligible changes in absorbance spectra in the presence of Group 1 & 2 metals, however spectral changes were observed upon addition of a variety of transition metals. The addition of Zn^{2+} and Cd^{2+} to pyrazoline **(97)** is representative of the results obtained and shows the formation of a new absorbance band at 360 nm (ε = 8650 M^{-1} cm^{-1}) and 350 nm (ε = 7650 M^{-1} cm^{-1}) upon addition of Zn^{2+} and Cd^{2+} respectively (Figure 69).

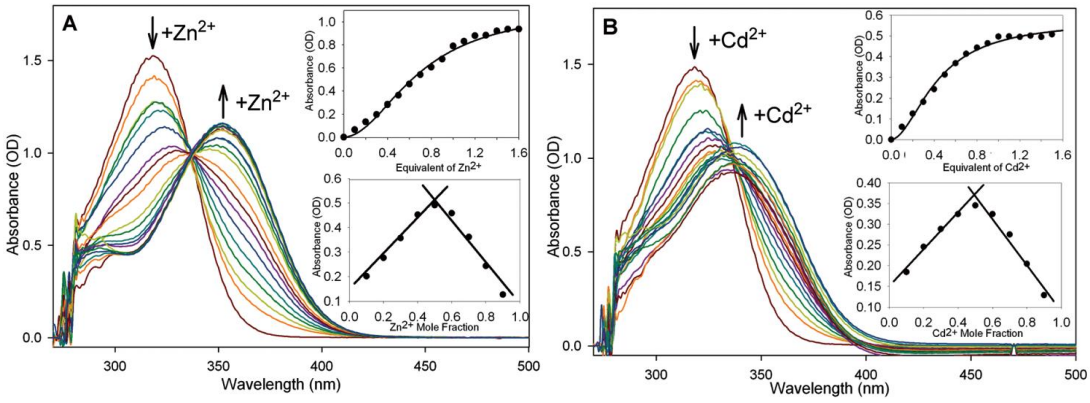

Figure 69: Pyrazoline (97) absorbance spectra (MeCN, 500 µM) with the addition of 0–1.5 equiv. in 0.1 increments of Zn^{2+} (A) and Cd^{2+} (B), Insets at λem = 370 nm, Lower inset Job plot.

Interestingly these new bands increased linearly in absorbance up to 1.0 equivalent of cation after which further addition produced negligible changes in absorbance suggesting a 1:1 stoichiometry between ligand and cation. Job plot analysis indicated a mole fraction of 0.5 of Zn^{2+} and Cd^{2+} achieved the highest absorbance, again suggesting that pyrazoline **(97)** and pyrazole **(98)** formed a 1:1 complex with these cations. This result is consistent with similar pyrazolines found in the literature.[104] An X-ray structure determination was sought to visually confirm that pyrazoline **(97)** was chelating Zn^{2+} in a 1:1 ratio and to provide information on bond lengths and angles.

5.5 X-Ray Crystal Structure

Attempts to obtain an X-ray structure of pyrazoline **(97)** chelated to Zn^{2+} using a previously reported method,[104] actually resulted in crystals of pyrazole **(98)** chelated to Zn^{2+} (Scheme 29). It is presumed that under the reaction conditions or during the recrystallisation process an aerobic oxidation occurred oxidising the pyrazoline ring to the corresponding pyrazole.

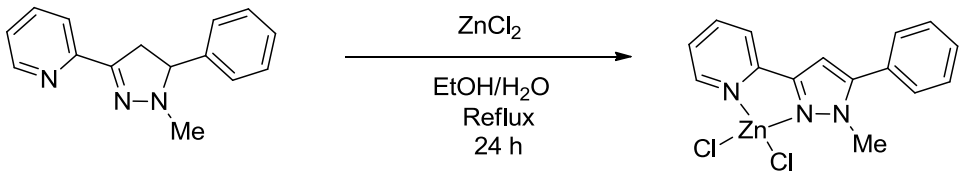

(99)

Scheme 29: Synthesis of Zn^{2+} complex.

The crystal structure confirmed the pyrazole **(98)** was chelating Zn^{2+} with a 1:1 stoichiometry (Figure 70) reinforcing the previous studies.

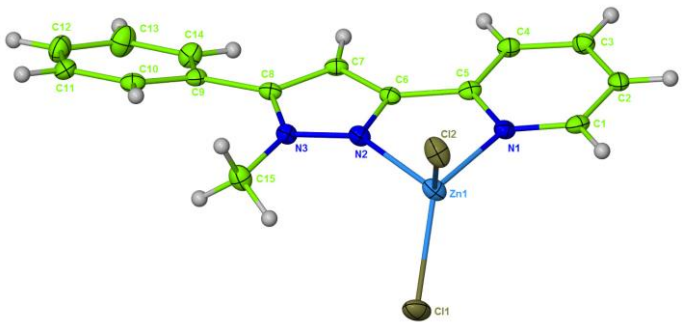

Figure 70: An X-ray structure of the pyrazole Zn^{2+} complex, ellipsoids represented at 30% probability.

5.6 ^{1}H NMR Spectroscopy

Cd^{2+} has a d^{10} electronic configuration and is therefore diamagnetic enabling ^{1}H NMR studies to investigate how chelation influenced the ^{1}H chemical shifts of the pyrazole **(98)** protons. In the absence of Cd^{2+} the pyrazole protons are distinct peaks in the aromatic region (i), however upon addition of Cd^{2+} the peaks begin to broaden and move downfield to higher chemical shifts (ii to iv in Figure 71).

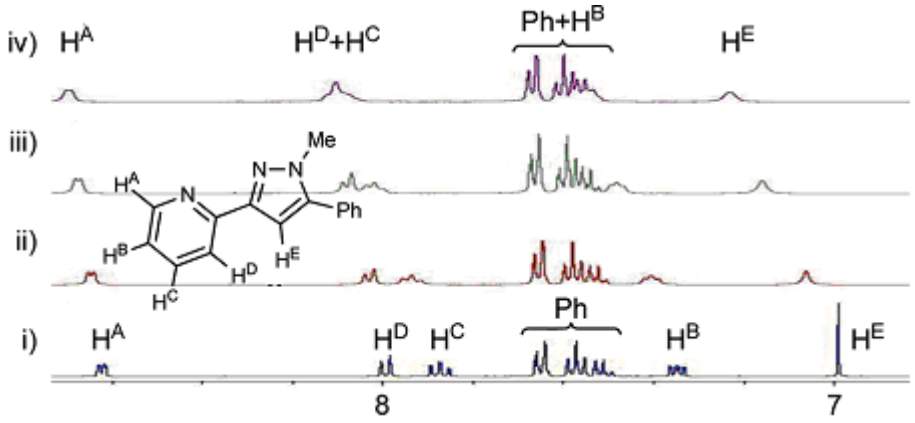

Figure 71: ^{1}H NMR study of pyrazole (98) (DMSO-d_6, 63 mM) with (i) 0.0, (ii) 0.9, (iii) 2.0 and (iv) 3.0 equiv. Cd^{2+}.

A similar effect was observed with Zn^{2+} and for pyrazoline **(97)** in the presence of Zn^{2+} and Cd^{2+} (data not shown). The broadening and increasing in chemical shift of aromatic protons is indicative of chelation and has been reported for a variety of fluorescence sensors in the literature.[105-107]

5.7 Fluorescence Spectroscopy

We investigated the potential use of pyrazoline **(97)** and pyrazole **(98)** as Zn^{2+} fluorescence sensors as structurally similar pyrazolines have been reported in the literature.[93,104,113] In the presence of various Group 1 and 2 metals no significant increase in fluorescence was observed as was expected from the UV/Vis spectroscopy studies (Figure 72A).

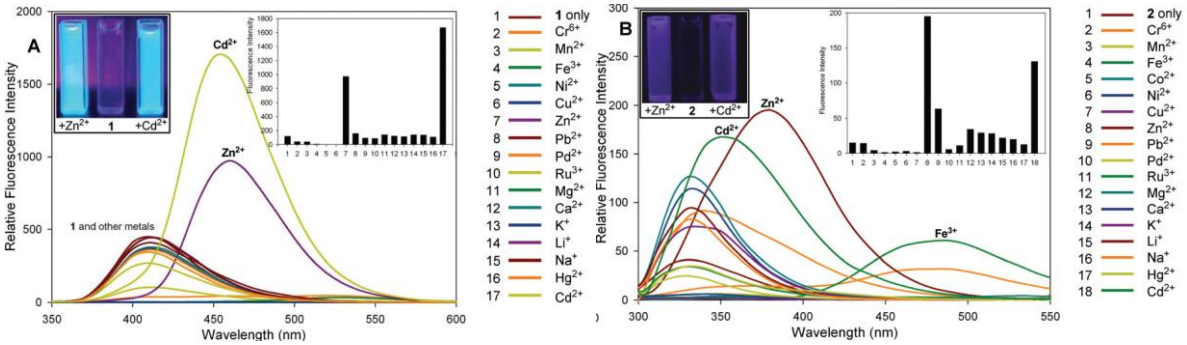

Figure 72: Fluorescence spectra of pyrazoline (97) (A, λex = 320 nm) and pyrazole (98) (B, λex = 285 nm, MeCN, 20 μM) upon addition of 5 equiv. of metal.

In the presence of a variety of transition metals there was little change in fluorescence intensity of pyrazoline **(97)**, except in the presence of Zn^{2+} and Cd^{2+} (Figure 72A). The addition of Zn^{2+} resulted in an eight fold increase in fluorescence at 460 nm, whereas the addition of Cd^{2+} resulted in a fourteen fold increase also at 460 nm suggesting that this pyrazoline may be a useful fluorescence sensor for Cd^{2+}. This is of interest as the UV/Vis studies demonstrated that although pyrazoline **(97)** chelated a variety of transition metals, only Zn^{2+} and Cd^{2+} resulted in an increase in fluorescence. One major challenge in current Zn^{2+} sensor research is the ability to distinguish Zn^{2+} from Cd^{2+} due to the similar chemical properties of both cations[108-109] and pyrazoline **(97)** suffers from this difficulty. Pyrazole **(98)** was also screened against a variety of cations with addition of Zn^{2+} resulting in a modest increase in fluorescence at 380 nm whereas the Cd^{2+} resulted in an increase at 350 nm (72B). This difference in wavelength of 30 nm, albeit small, enables pyrazole **(85)** to distinguish Zn^{2+} from Cd^{2+}, fulfilling a major requirement of a Zn^{2+} sensor. This initial metal screen suggests that pyrazoline **(97)** may be a useful Cd^{2+} fluorescence sensor whereas oxidation to pyrazole **(98)**

generated a sensor more suitable for the detection of Zn^{2+}. Titration studies were performed to further investigate the potential of pyrazoline **(97)** to act as fluorescence sensors for Cd^{2+} and Zn^{2+}. Job plot analysis was in agreement with the previous UV/Vis studies confirming a 1:1 stoichiometry (Figure 73). The increased fluorescence intensity observed with pyrazoline **(97)** with Cd^{2+} confirmed it is more sensitive towards Cd^{2+} than Zn^{2+}.

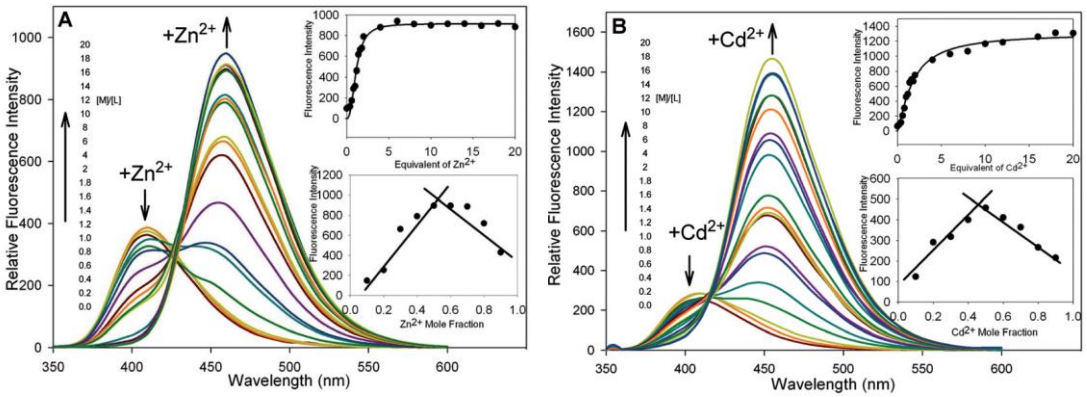

Figure 73: Fluorescence spectra of pyrazoline (97) (MeCN, 20 µM, λex = 320 nm) upon addition of 0–20 equiv. Zn^{2+} (A) and Cd^{2+} (B), lower inset Job plot.

Titration studies were also performed on pyrazole **(98)** alongside Job plot analysis which was consistent with previous studies giving a 1:1 stoichiometry (Figure 74). The increased fluorescence intensity observed with pyrazole **(98)** in the presence of Zn^{2+} suggests it is more suited as a Zn^{2+} fluorescence sensor.

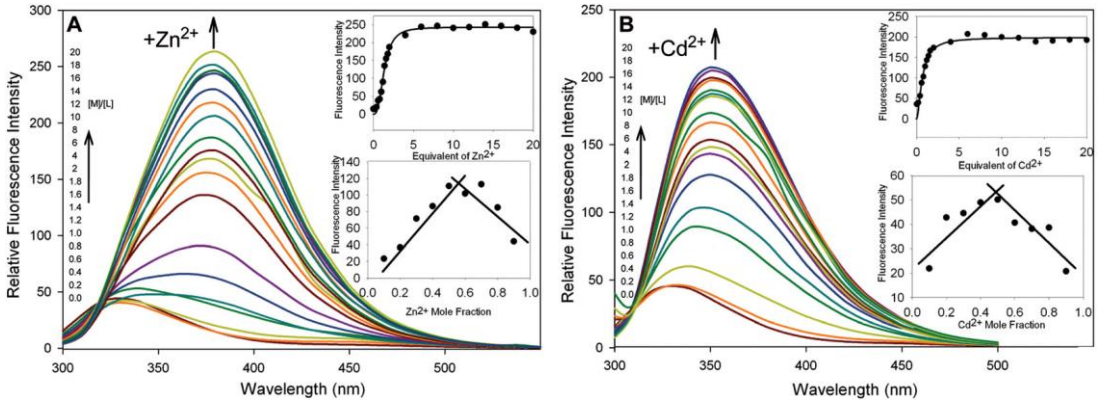

Figure 74: Fluorescence spectra of pyrazole (98) (MeCN, 20 µM, λex = 285 nm) upon addition of 0-20 equiv. Zn^{2+} (A) and Cd^{2+} (B), lower inset Job plot.

Detection limits were calculated using a literature method[110] to determine the sensitivity of each compound towards Zn^{2+} and Cd^{2+} (Table 12). As expected from the fluorescence studies, pyrazoline **(97)** was more sensitive towards Cd^{2+} with a detection limit of 0.12 µM compared with a detection limit of 0.20 µM for Zn^{2+}. In contrast pyrazole **(98)** was more sensitive towards Zn^{2+} than Cd^{2+} with detection limits of 0.24 and 0.34 µM respectively.

	Detection Limit (µM)	
Compound	Zn^{2+}	Cd^{2+}
Pyrazoline **(97)**	0.20	0.12
Pyrazole **(98)**	0.24	0.34

Table 12: Detection limits for pyrazoline (97) and pyrazole (98).

5.8 Competition Assays

In order for these ligands to be useful for tissue engineering purposes they must chelate Zn^{2+} in the presence of competing cations present in biological systems, for example culture media containing Na^{+}, K^{+} , Mg^{2+} and Ca^{2+}. Zn^{2+} was selected as the most suitable metal for chelation as Zn^{2+} is non toxic and is the second most abundant transition metal in the human body whereas Cd^{2+} is highly toxic and linked to a range of diseases including cancer. A competition assay[106,111] involves measuring the fluorescence of the ligand with the competing cation (white bar), and in the presence of the competing cation and Zn^{2+} after a 3 minute equilibrium time (black bar) (Figure 75).

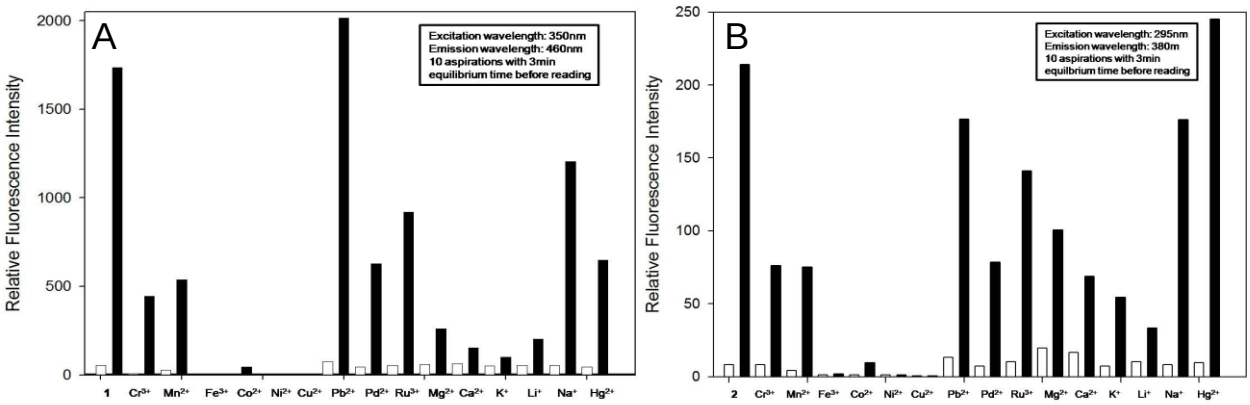

Figure 75: Competition assay, the white bar represents ligand (MeCN, 20 µM), and 5 equiv. of the cation, the black bar is the same plus 5 equiv. Zn^{2+} after equilibrating for 3 minutes.

The competition assay for pyrazoline **(97)** indicated that paramagnetic Fe^{3+}, Co^{2+} and Ni^{2+} cations resulted in fluorescence quenching as observed in previous studies (Figure 75A).[105,112] The presence of Pb^{2+}, Ru^{3+} and Na^{+} resulted in a minor decrease in fluorescence intensity (75A). Unfortunately in the presence of biologically relevant metals present in culture media resulted in major decreases in fluorescence intensity suggesting these cations are competing with Zn^{2+} chelation. This indicated that pyrazoline **(97)** would not be a suitable Zn^{2+} chelator for tissue engineering purposes. A similar assay was performed for pyrazole **(98)** (75B), fluorescence quenching with the paramagnetic metals was also observed along with competition from biologically relevant metals demonstrating that pyrazole **(98)** is also unsuitable for tissue engineering purposes. The presence of additional chelation sites via the R^1 group may be a possible solution to overcome this problem by increasing Zn^{2+} chelation. R^1 groups with larger steric bulk may also prevent competing cations from accessing the chelation site and prevent displacement of the bound Zn^{2+} (Scheme 30). This can be achieved using the chemistry previously reported in chapter 3 and will be investigated further with the B and C pyrazoline series.

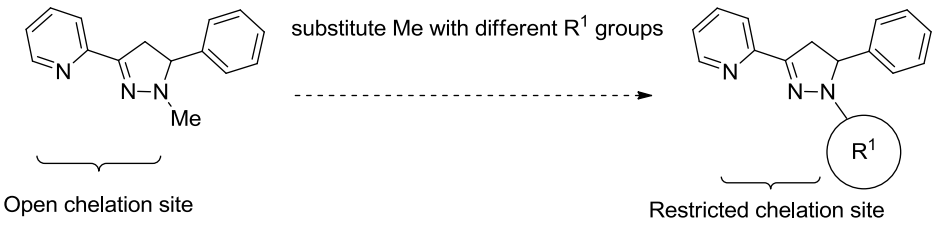

Scheme 30: Restricting the chelation site by increasing the R^1 group.

5.9 B & C Pyrazoline Series Synthesis

A range of additional R^1 groups was investigated including thiocarbamide group in the B series and acetyl and benzoyl R^1 substituents in the C series. All pyrazolines were synthesised from the corresponding chalcones using the procedures previously reported in chapter 4. The chalcone precursors were synthesized under Claisen-Schmidt conditions in excellent yield (85-97%) affording the thermodynamically stable *E* isomer as identified by characteristic ^3J coupling of ca 15 Hz (Scheme 31).

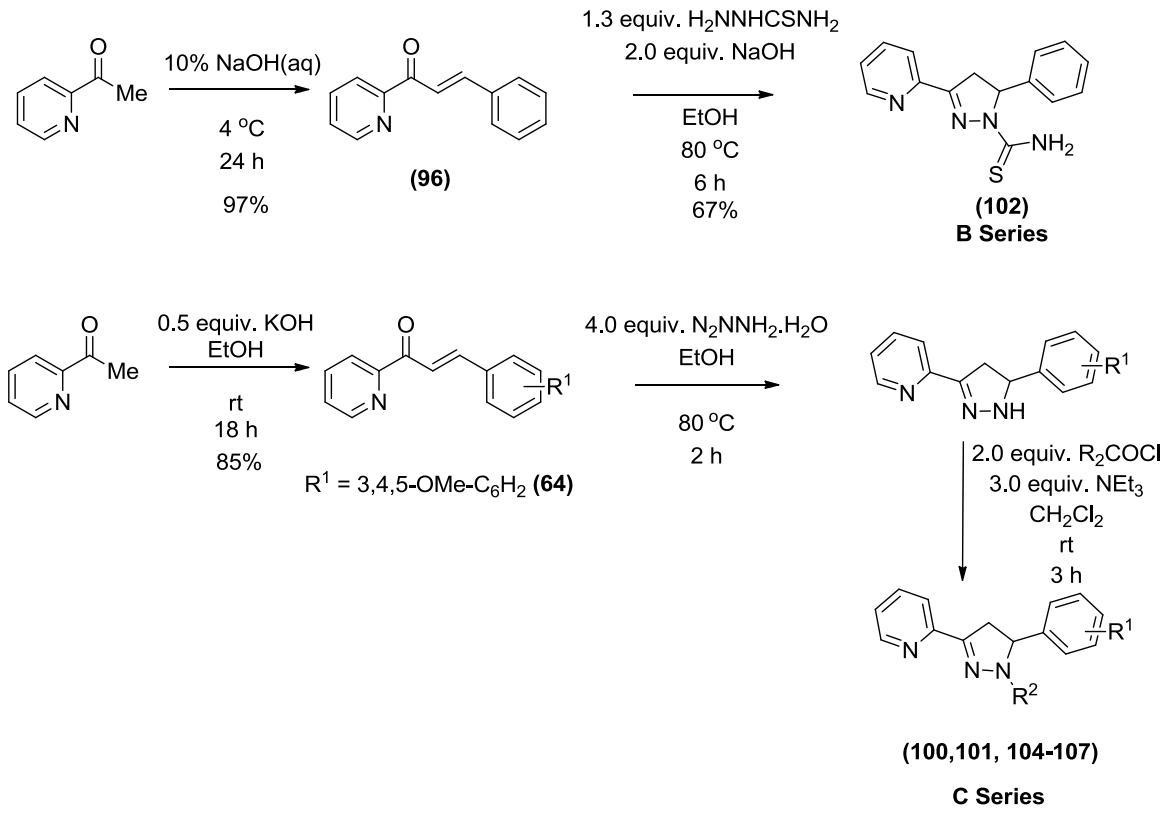

Scheme 31: Synthesis of B and C pyrazolines series.

Chalcone **(96)** was treated with thiosemicarbazide to synthesise the B series whereas treatment with hydrazine followed by the desired acid chloride gave the C series of pyrazolines. All pyrazolines were fully characterised and confirmed to be >95% pure by HPLC before analysis.

5.10 UV/Vis Spectroscopy and MTS antiproliferative Assays

All pyrazolines were screened for Fe^{3+} chelation properties using UV/Vis spectroscopy however no changes in the absorbance spectra were observed. Pyrazoline **(105)** displayed excellent antiproliferative activities, therefore all pyrazolines were screened in HT29 and MDA-MB-231 (Table 13) to investigate potential therapeutic applications.

					IC_{50} (μM)	
cpm	**R^1**	**R^2**	**Yield**	**Fe^{3+} chelator**	**HT29**	**MDA-MB-231**
100	C_6H_5	COMe	72	**X**	161.3 ± 21.9	294.1 ± 71.1
101	C_6H_5	$COCF_3$	65	**X**	>500	>500
102	C_6H_5	$CSNH_2$	67	**X**	350.2 ± 42.0	140.5 ± 42.0
103	C_6H_5	CSNHMe	89	**X**	25.6 ± 4.0	20.7 ± 0.79
104	C_6H_5	C_6H_5-CO	76	**X**	>500	>500[a]
105	C_6H_5	3,4,5-OMe-C_6H_2-CO	75	**X**	2.5 ± 0.39	0.69 ± 0.11
106	3,4,5-OMe-C_6H_2	3,4,5-OMe-C_6H_2-CO	84	**X**	22.5 ± 2.5	11.4 ± 0.75
107	3,4,5-OMe-C_6H_2	COMe	80	**X**	>500	52.5 ± 6.5
108	3,4,5-OMe-C_6H_2	C_6H_5	34	**X**	26.2 ± 3.4	4.36 ± 0.8

Table 13: MTS Assays, IC_{50} is the concentration that inhibits 50% cell proliferation, values are the mean from three independent experiments ± standard deviation, except a from a single experiment, compounds ≥95% pure by HPLC, cross indicated no change in absorbance spectra on addition of Fe^{3+}.

5.11 SAR Study

This library displayed a broad spectrum of activity from inactive unsubstituted pyrazoline **(104)** to active 3,4,5-trimethoxy aryl pyrazoline **(105)** demonstrating the importance of the 3,4,5-trimethoxy aryl pharmacophore (Figure 76).

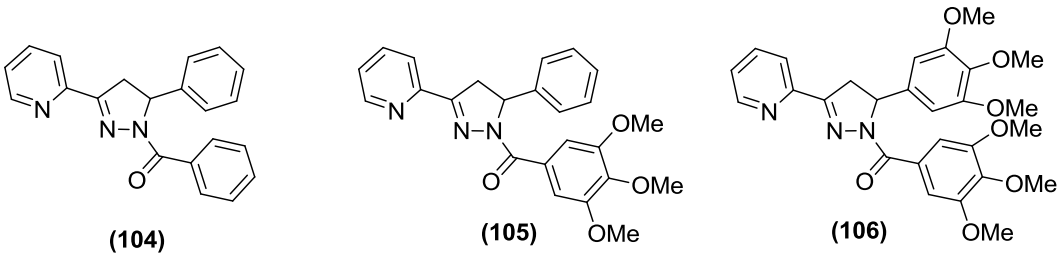

IC_{50} (HT29): >500 μM	IC_{50} (HT29): 2.5 μM	IC_{50} (HT29): 22.5 μM
IC_{50} (MDA-MB-231): >500 μM	IC_{50} (MDA-MB-231): 0.69 μM	IC_{50} (MDA-MB-231): 11.4 μM

Figure 76: The importance of the 3,4,5-trimethoxy aryl group.

The addition of a second 3,4,5-trimethoxy aryl ring in pyrazoline **(106)** was detrimental to activity suggesting that only a single 3,4,5-trimethoxy aryl ring is preferred for antiproliferative activity. Suitable crystals of pyrazoline **(105)** for an x-ray structure were obtained and the results are displayed in Figure 77.

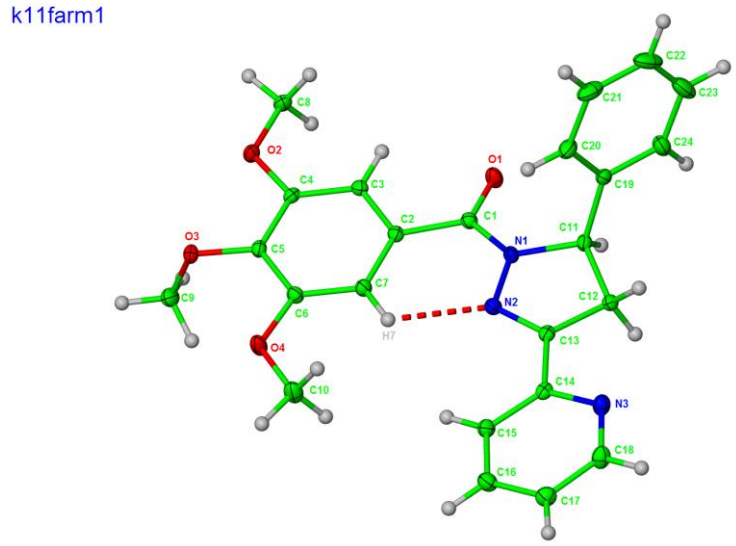

Figure 77: X-ray structure determination of pyrazoline (105), ellipsoids represented at 30% probability.

An interesting SAR observation was the increase in activity observed when pyrazoline **(102)** was mono methylated to give pyrazoline **(103)** with low micromolar IC_{50} values in HT29 and MDA-MB-231 (Figure 78).

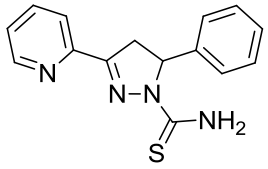

(102)

IC_{50} (HT29): 350.2 μM
IC_{50} (MDA-MB-231): 140.5 μM

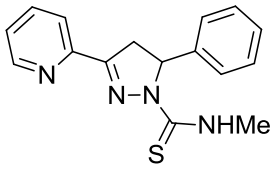

(103)

IC_{50} (HT29): 25.6 μM
IC_{50} (MDA-MB-231): 20.7 μM

Figure 78: Methylation of pyrazoline (102) significantly increased antiproliferative activity.

An X-ray structure of pyrazoline **(102)** was obtained which indicated the formation of an intramolecular hydrogen bond between the thiosemicarbazide amino group and the basic pyrazoline nitrogen atom restricting free rotation in the solid state (Figure 79).

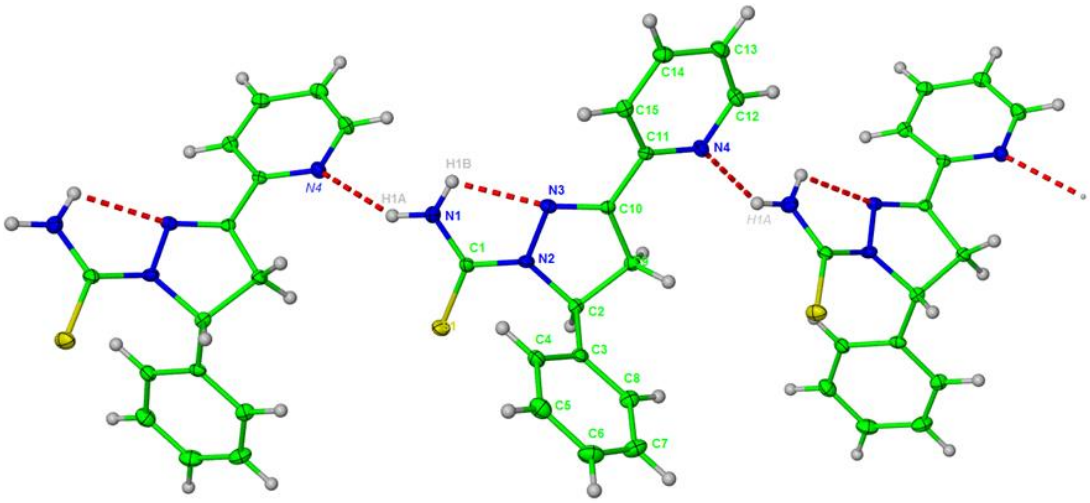

Figure 79: X-ray structure determination of pyrazoline (102), ellipsoids represented at 30% probability.

Mono methylation of pyrazoline **(102)** to generate pyrazoline **(103)** could be easily achieved under mild conditions (Scheme 32) resulting in an increase in biological activity. Interestingly, under these reaction conditions the only product obtained was the mono methylated product **(103)** with no sign of the dimethylated product **(109)**.

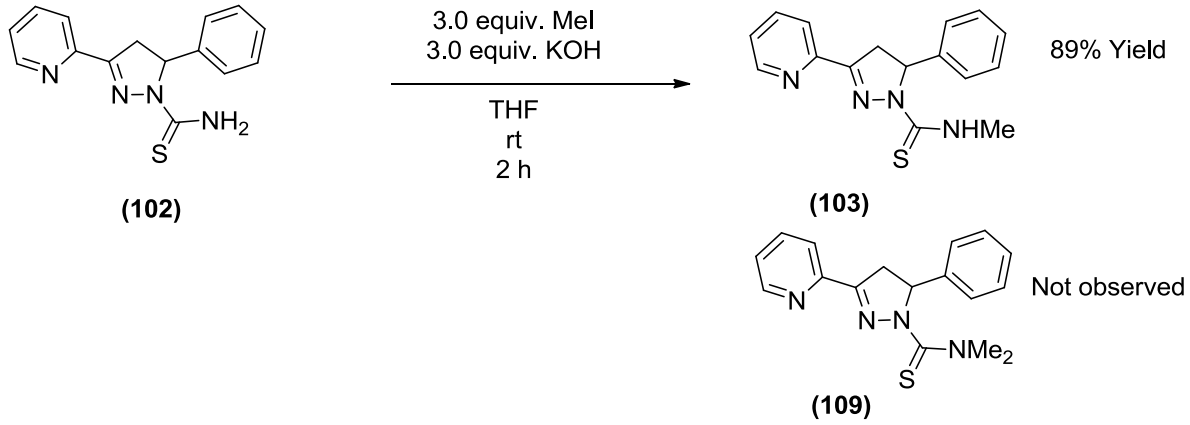

(102) **(103)** **(109)**

Scheme 32: Mild methylation conditions gives single methylated product (103) only.

Pyrazoline **(103)** retained an amino hydrogen suitable for forming intramolecular hydrogen bonds resisting rotation around the thiosemicarbazide unit. In order to overcome this problem more vigorous reaction conditions were attempted (Scheme 33) using the stronger base NaH however without success.

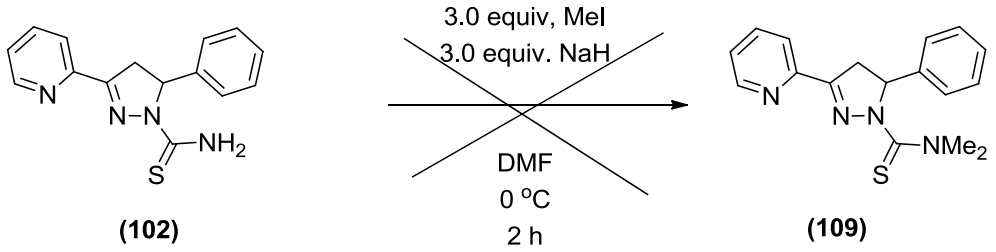

(102) **(109)**

Scheme 33: Harsh methylation conditions.

An alternative method of generating dimethylated pyrazoline **(109)** was to synthesise it directly from chalcone **(96)** using dimethyl-3-thiosemicarbazide. Surprisingly submitting this dimethylated thiocarbazide to identical reaction conditions used to generate pyrazoline **(102)** failed to give the desired product (Scheme 34).

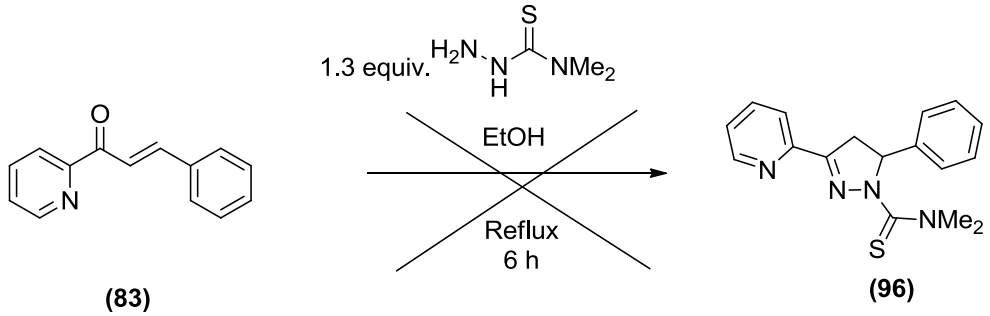

(83) **(96)**

Scheme 34: Dimethyl-3-thiosemicarbazide reaction.

5.12 NCI 60 Cell Line Screen

Pyrazoline **(105)** was the most active compound in the C series of compounds and was submitted for screening at the NCI at the single (10^{-5}) dose (see appendix A) and was selected for screening at the five dose level. Pyrazoline **(105)** displayed promising GI_{50} values across the NCI 60 cell line screen including nanomolar activity (0.277-0.848 µM) in six of the seven colon cancer cell lines including the multidrug resistant ovarian cell line NCI/ADR-RES 0.519 µM (Table 14). Of the five ovarian cell lines, the greatest activity was observed with OVCAR-3, a cell line sensitive to tubulin disruptors suggesting that pyrazoline **(105)** may also be a tubulin binder.

Panel	Cell Line	GI_{50} (µM)	Panel	Cell Line	GI_{50} (µM)
Leukemia	CCRF-CEM	2.08	**Melanoma**	LOX IMVI	1.13
	HL-60(TB)	0.747		MALME-3M	>100
	MOLT-4	4.46		M14	0.801
	RPMI-8226	66.3		MDA-MB-435	0.273
	SR	0.415		SK-MEL-2	0.699
				SK-MEL-28	1.51
				SK-MEL-5	0.432
				UACC-257	>100
				UACC-62	0.541
Non-Small Cell Lung	A549/ATCC	0.957	**Ovarian**	IGROV1	7.13
	EKVX	>100		OVCAR-3	0.719
	HOP-62	1.82		OVCAR-4	5.95
	NCI-H226	1.33		OVCAR-5	4.01
	NCI-H23	3.45		OVCAR-8	3.28
	NCI-H322M	>100		NCI/ADR-RES	0.519
	NCI-H460	0.505		SK-OV-3	0.762
	NCI-H522	0.688			
Colon	COLO 205	0.585	**Renal**	786-0	1.54
	HCC-2998	2.32		A498	0.943
	HCT-116	0.586		ACHN	4.29
	HCT-15	0.848		CAKI-1	0.493
	HT29	0.431		RXF 393	1.03
	KM12	0.711		SN12C	3.53
	SW-620	0.567		TK-10	>100
				UO-31	5.01
CNS	SF-268	33.4	**Breast**	MCF7	0.324
	SF-539	1.06		MDA-MB-231	0.989
	SNB-19	1.89		HS 578T	9.18
	SNB-75	0.277		BT-549	5.13
	U251	0.868		MDA-MB-468	0.417
Prostate	PC-3	>100			
	DU-145	4.26			

Table 14: NCI screen for pyrazoline (105).

5.13 Cell Cycle Analysis

To investigate the mode of action of pyrazoline **(105)** as a microtubule binding agent, cell cycle analysis was performed on HT29 cells (Figure 80). Panel A contained the typical histogram for untreated HT29 cells with the majority of the cell population (60.2%) resided in the G1 phase of the cell cycle, whereas the presence of 100 nM colchicine resulted in the majority of the cells (88.8%) residing in the G2/M phase. The presence of 100 nM pyrazoline **(105)** resulted in the formation of the distinct G2/M peak of over half of the cell population in this phase of the cell cycle. Increasing the concentration of pyrazoline **(105)** to 500 nM resulted in over 94% of the cells residing in the G2/M phase, providing further evidence that pyrazoline **(105)** is a microtubule disruptor.

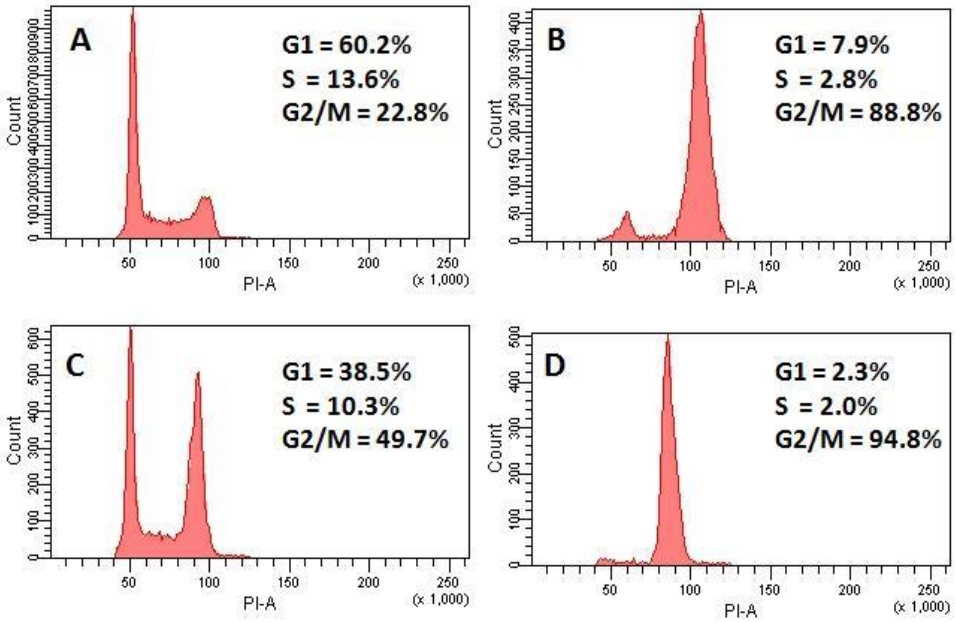

Figure 80: Cell cycle analysis, A) Untreated HT29 cells, B) + 100 nM colchicine, C) + 1.0 µM pyrazoline (105), D) + 5.0 µM pyrazoline (105), results are representative of three independent experiments.

In order to investigate further into the mode of action of pyrazoline **(105)** and to classify it as a microtubule stabiliser or destabiliser an *in vitro* tubulin polymerisation assay was performed.

5.14 *In Vitro* Tubulin Polymerisation Assay

The control shows the increase in optical density (OD) as tubulin naturally polymerises over the course of 60 minutes whereas in the presence of the 5.0 µM of the microtubule stabiliser Taxol® polymerisation is rapidly achieved within the first 10 minutes (Figure 80). The curve for pyrazoline **(105)** indicated that at a concentration of 20.0 µM this compound was disrupting microtubule formation compared to control, suggesting that this is responsible for the mode of action of pyrazoline **(105)** (Figure 81).

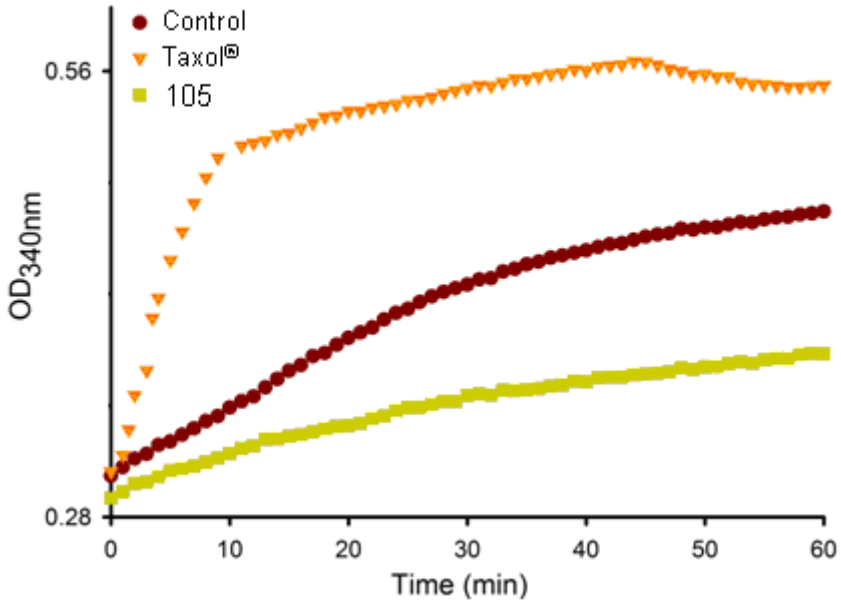

Figure 81: *In vitro* tubulin polymerisation assay for 20.0 µM pyrazoline (105).

In order to provide further evidence that pyrazoline **(105)** was disrupting microtubule formation, a confocal microscopy study was performed to visually confirm the disruption of microtubules *in vitro*.

5.15 Confocal Microscopy

The microtubule network in untreated HT29 cells is shown in panel A (Figure 82A) the microtubule network is visible as a green cloud surrounding the cells with the chromosomes (blue) in the middle. The addition of 100 nM of colchicine as a positive control resulted in an irregular and reduced microtubule network (panel B).

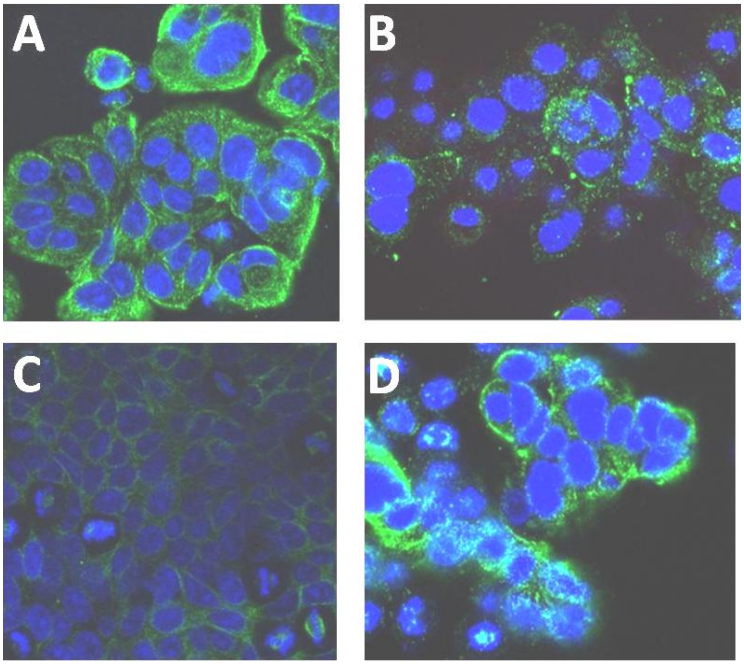

Figure 82: Confocal microscopy A) HT29 cells only, B) + 100 nM Colchicine, C) + 1.0 µM pyrazoline (105), D) + 5.0 µM pyrazoline (105).

Upon addition of 100 nM of pyrazoline **(105)**, the same concentration that resulted in 50% of the cell population residing in the G2/M phase, the microtubule network is reduced slightly in size. Increasing the concentration of pyrazoline **(105)** to 500 nM, the concentration that resulted in 95% of the cell population residing in G2/M resulted in an irregular and reduced microtubule network (Panel D). This study confirmed that pyrazoline **(105)** was disrupting microtubule formation reinforcing the results of the cell cycle and *in vitro* tubulin polymerisation assays.

5.16 Conclusions

A collection of ten pyrazolines was synthesised and screened for metal chelation properties and antiproliferative activities in HT29 and MDA-MB-231 cancer cell lines. Pyrazoline **(97)** chelated a variety of transition metals and was a "turn on" fluorescence sensor with emission of fluorescence at 460 nm in the presence of Zn^{2+} and Cd^{2+} (Figure 83).

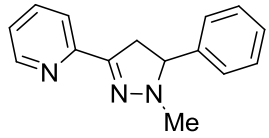

(97)

Zn^{2+} λ_{em} 460 nm
Cd^{2+} λ_{em} 460 nm

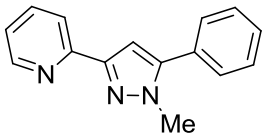

(98)

Zn^{2+} λ_{em} 380 nm
Cd^{2+} λ_{em} 350 nm

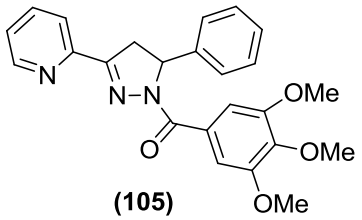

(105)

IC_{50} (MDA-MB-231): 0.69 μM
Microtubule destabiliser

Figure 83: Pyrazoline (97) and pyrazole (98) were "turn on" fluorescence sensors, pyrazoline (105) was a microtubule destabiliser.

Oxidation of pyrazoline **(97)** could be achieved in high yield to afford pyrazole **(98)** which was also a "turn on" fluorescence sensor for Zn^{2+} and Cd^{2+} and could distinguished between Zn^{2+} and Cd^{2+} with fluorescence emission at different wavelengths. Further studies including Job plots and an X-ray crystal structure demonstrated that both pyrazoline **(97)** and pyrazole **(98)** chelated Zn^{2+} and Cd^{2+} with a 1:1 stoichiometry. Competition assays indicated that the presence of additional metal cations including Group 1 & 2 metals disrupted fluorescence restricting the potential use of these sensors in biological environments. In order to overcome this, a range of more sterically crowded chelation sites were investigated including acetyl, benzoyl and thiosemicarbazide units. The presence of large substituents prevented chelation, however pyrazoline **(105)** was discovered to display promising antiproliferative activity. Pyrazoline **(105)** was submitted to the NCI and displayed nanomolar GI_{50} values in six of the seven colon cancer cell lines. Further investigations revealed that pyrazoline **(105)** was a microtubule destabiliser in a similar manner as pyrazoline **(71)** discussed previously in chapter 3.

5.17 Future Work

5.17 Aqueous Zn^{2+} Fluorescent Sensors

Zhao *et al.*[113] recently reported a novel pyrazoline based turn on fluorescent sensor which could detect Zn^{2+} in aqueous solutions and in the presence of a range of competing cations including the biological metals Na^{+}, K^{+}, Ca^{2+} and Mg^{2+} present in culture media (Figure 84). Further studies by Zhao *et al.*[113] indicated that pyrazoline **(110)** chelated Zn^{2+} with a 1:1 stoichiometry and with a detection limit of 0.12 μM which is comparable with pyrazoline **(97)** reported previously.

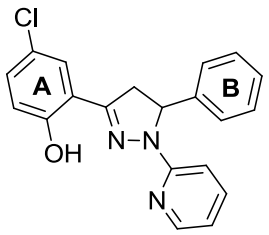

(110)
Aqueous fluoresence sensor
1:1 complex with Zn^{2+}
Detection limit 0.12 μM

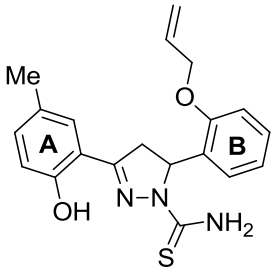

(111)
Aqueous fluoresence sensor
1:1 complex with Zn^{2+}
Detection limit 0.61 μM

Figure 84: Recently reported aqueous fluorescence sensors for Zn^{2+}.[113,114]

Miao *et al.*[114] recently reported the structurally similar pyrazoline **(111)** with thiosemicarbazide substitution which is also a "turn on" fluorescence sensor for Zn^{2+} in aqueous solutions (Figure 84). Pyrazoline **(111)** was confirmed to chelate Zn^{2+} with a 1:1 stoichiometry and retained Zn^{2+} in the present of the biologically relevant metals Na^{+}, K^{+}, Ca^{2+} and Mg^{2+}. The common feature present in these two sensors is the A ring with a single hydroxyl substituent at the ortho position. This may be a key feature required to prevent competition from competing cations while conferring good water solubility. The attachment of a suitable chemical handle onto the B ring would able pyrazoline **(110)** to be investigated as a suitable Zn^{2+} chelator in culture media and could be used as proposed in the aims and objectives (Figure 85).

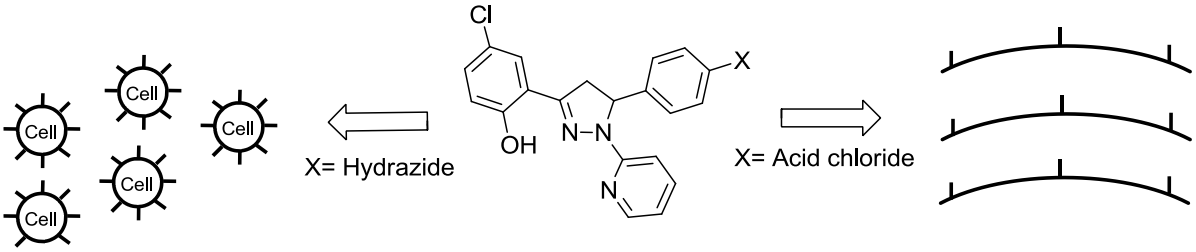

(110A)

Figure 85: Proposed modification of the aqueous fluorescence Zn^{2+} sensors for attachment to the cell surface and polymer backbone for use in tissue engineering.

Chapter 6: Maltol Derivatives in Tissue Engineering

6.1 Overview

Design, synthesis and investigation of maltol derivatives, compounds of interest include a maltol dimer **(111)**, a maltol trimer **(112)** and a maltol hydrazide **(113)** shown in Figure 86.

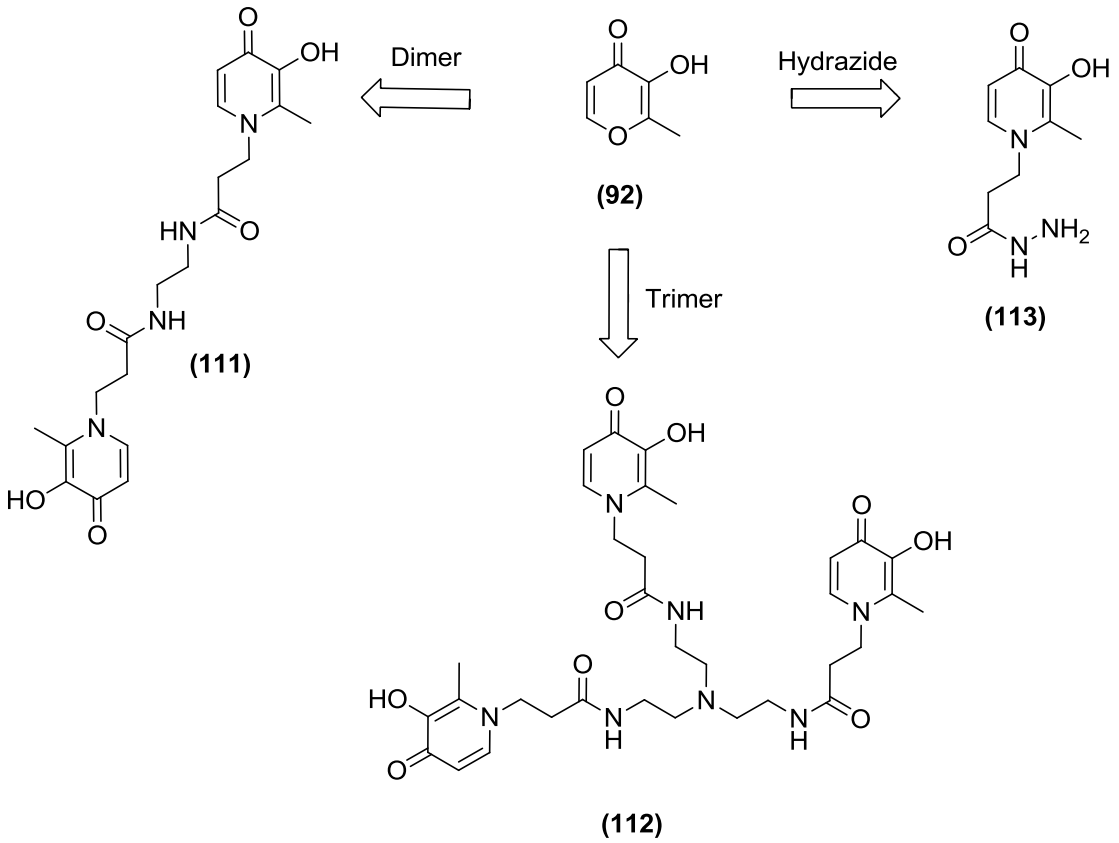

Figure 86: Synthesis of maltol dimer (111), trimer (112) and hydrazide (113) from the industrial produced feedstock maltol (92).

Maltol hydrazide **(113)** was used to form multicellular aggregates in the presence of Fe^{3+} and the dimer and trimer derivatives were used as model systems for future maltol based polymers which assemble upon addition of Fe^{3+}.

6.2 Maltol Dimer and Trimer Synthesis

To investigate the potential of developing a maltol based polymer which assembles in the presence of Fe^{3+} a maltol dimer and trimer were synthesised to act as model systems for more complex polymers (Scheme 35). Maltol **(92)** is highly water soluble therefore it was benzylated using a literature procedure[115] to afford benzylated maltol **(114)** which was soluble in organic solvents enabling further functionalisation (Scheme 35). Treatment with excess β-alanine gave the maltol carboxylic acid **(115)** in 78% yield following a literature procedure.[115] With maltol carboxylic acid **(115)** in hand, a literature procedure[115] was adapted to afford the maltol activated ester **(116)** in 70% which was a versatile intermediate for further amide coupling reactions.

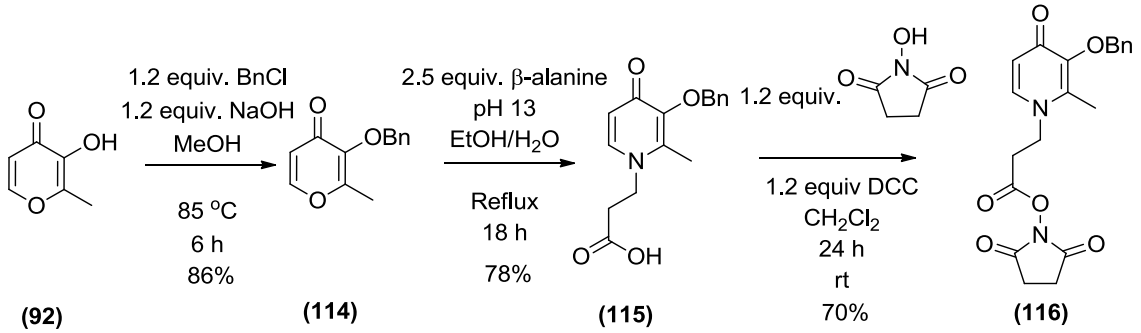

Scheme 35: Synthesis of maltol activated ester (116) from maltol (92).

An excess of maltol activated ester **(116)** with 0.4 equiv. ethylenediamine gave the benzylated maltol dimer **(117)** in 65% yield (Scheme 36).

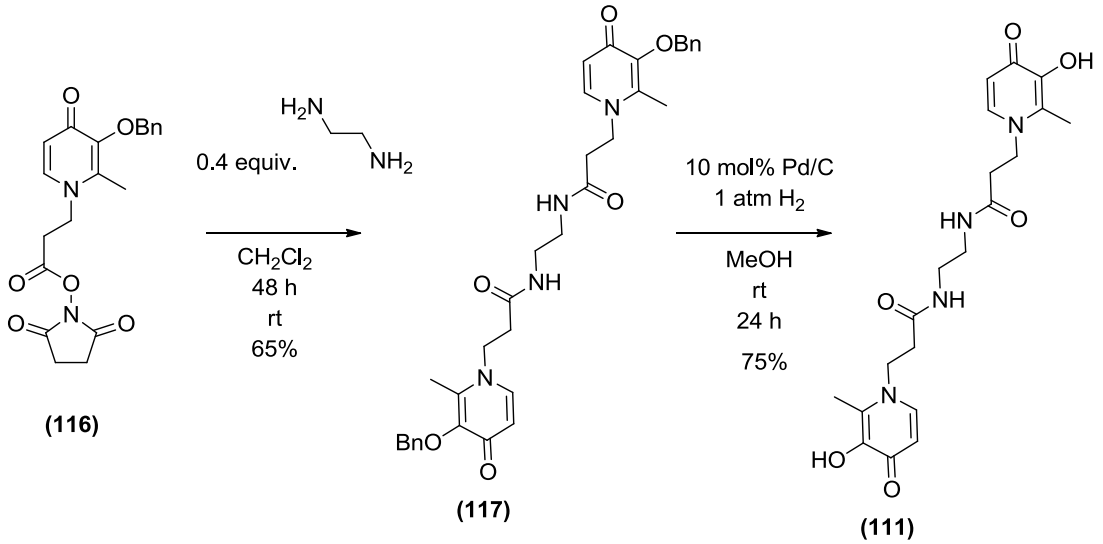

Scheme 36: Synthesis of benzylated maltol dimer (117) from maltol activated ester (116).

The removal of the benzyl group was achieved under standard hydrogenation conditions to give the desired deprotected maltol dimer **(111)** in 75% yield (Scheme 36). The benzylated maltol trimer **(118)** was synthesised from tris(2-aminoethyl)amine in 62% yield.

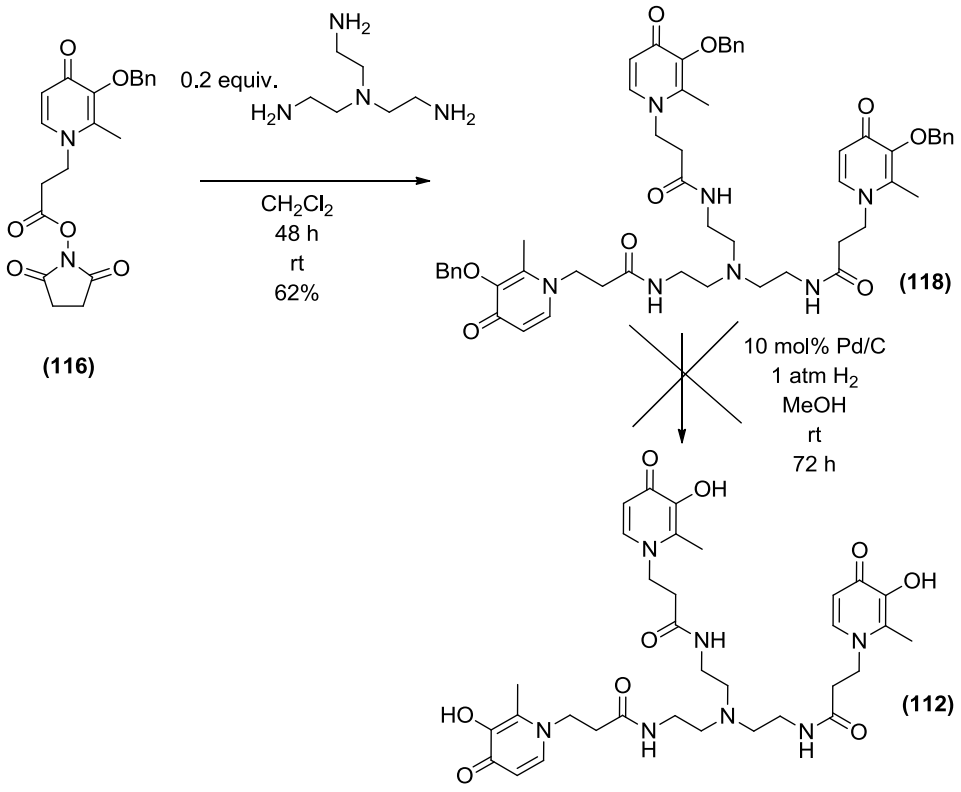

Scheme 37: Synthesis of benzylated maltol trimer (118) from maltol activated ester (116).

An identical procedure was applied to the benzylated maltol trimer **(118)** in an attempt to generate the deprotected maltol trimer **(112)**, however, after 24 h ^{1}H NMR indicated only partial removal of the benzyl groups (Scheme 37). The reaction was resubmitted and the reaction continued for a further 48 h, however full removal of all three benzyl groups was still not achieved. One possible explanation for the failure to fully remove the benzyl protection groups was due to the large steric bulk of the benzylated maltol trimer **(118)** preventing adsorption onto the Pd/C catalyst. The difficulty experienced with the removal of the benzyl protection group in the benzylated maltol trimer **(118)** poses a significant challenge when expanding from a trimer to polymer with several benzyl protection groups. Unfortunately due to time constraints and the success of alternative strategies, further optimisation of reaction conditions was not pursued.

6.3 Maltol Hydrazide (121) Synthesis

A synthetic procedure for the maltol hydrazide **(121)** was developed by conversion of the maltol carboxylic acid **(115)** synthesised previously (Scheme 35) to the maltol methyl ester **(119)** in 99% yield (Scheme 38). Reaction of the maltol methyl ester **(119)** with hydrazine afforded the benzylated maltol hydrazide **(120)** in 62% yield which was deprotected under standard conditions to give the desired maltol hydrazide product **(121)** in 84% yield (Scheme 38).

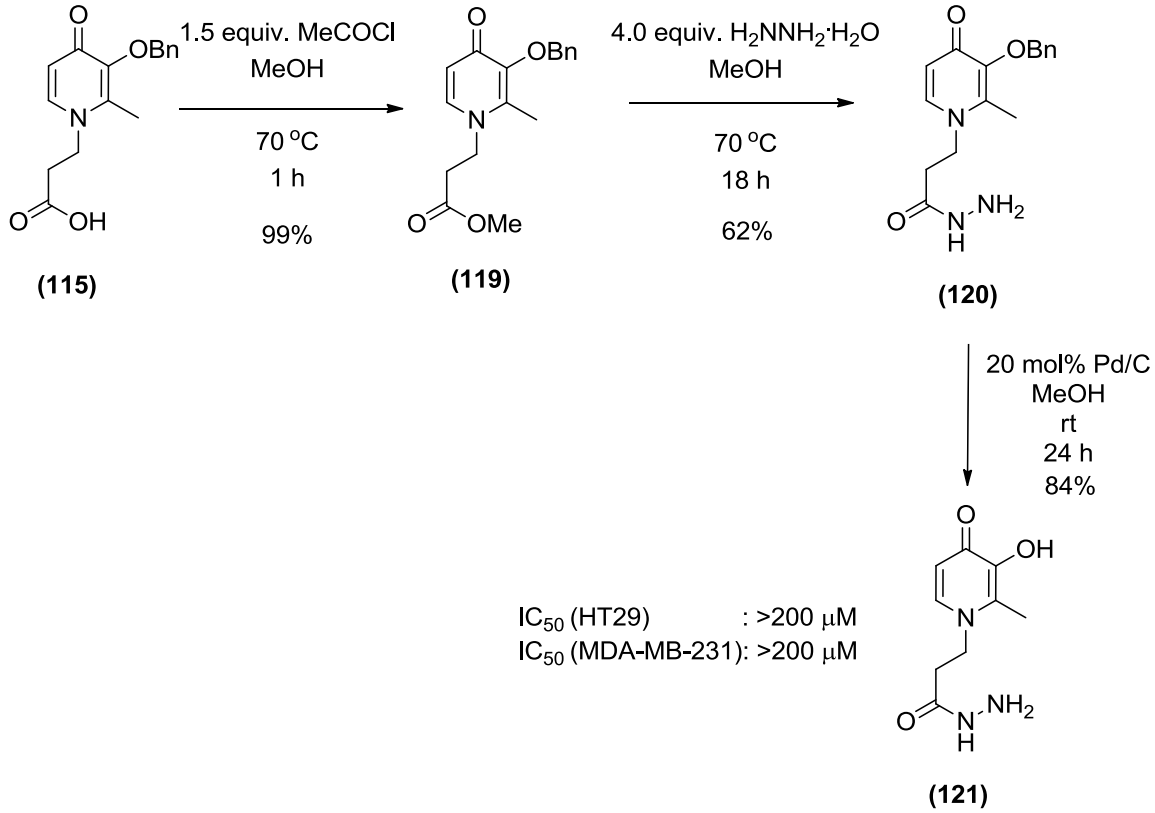

(115) **(119)** **(120)** **(121)**

Scheme 38: Maltol hydrazide (121) synthesis.

The MTS assays confirmed that maltol hydrazide **(121)** was non-toxic in the cell lines examined, with a high IC_{50} value of >200 μM in HT29 and MDA-MB-231 cancer cells suggesting it was suitable for further cell based studies at a concentration of 200 μM or below.

6.4 Fe^{3+} Triggered Homocellular Aggregation

Following the procedure reported by Bertozzi *et al.*[89] HT29 cells were exposed to mild oxidation conditions (1 mM $NaIO_4$, 10 minutes, 4 ^oC) to generate non-native aldehydes on the cell surface (Figure 87). The HT29 cells were exposed to maltol hydrazide **(121)** (200 µM, 60 mins, 20 ^oC) resulting in hydrazone bond formation chemically attaching the maltol unit to the cell surface. The maltol modified HT29 cells were then treated with $FeCl_3$ in PBS (phosphate buffered saline) (50 µM, 20 ^oC) and with gentle rocking agitation, pleasingly resulted in multicellular aggregation within 10 minutes (Figure 87).

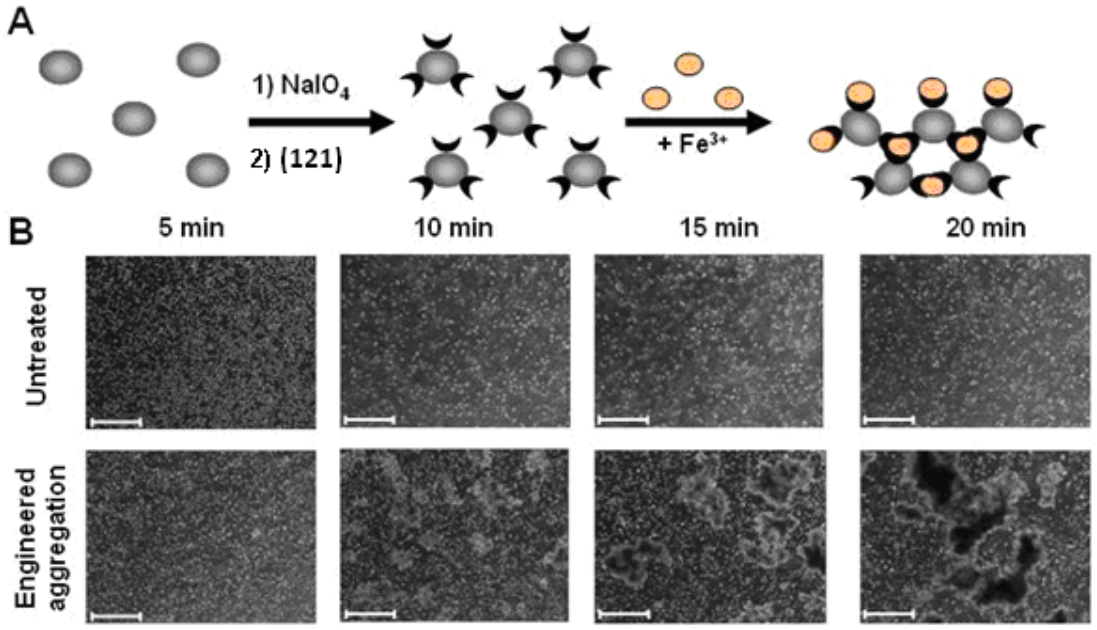

Figure 87: A) Generation of non-native aldehydes on the cell surface followed by attachment of the maltol unit which upon Fe^{3+} chelation form multicellular aggregates, B) representative phase contrast images of the aggregation process in serum free medium, scale bars = 400 µm, results are representative of three independent experiments.

After 20 minutes agitation large cellular aggregates had formed which were visible to the naked eye. Similar results were obtained in PBS medium, however performing the experiment in complete culture medium (containing 10% serum) resulted in no cellular aggregation. It is believed that the proteins in the serum was sequestering the Fe^{3+} and preventing aggregation. As a result of this all further experiments were performed in serum free culture medium. After 1 hour of agitation,

the aggregates were treated with EDTA (1 mM) and further agitated for one hour at room temperature in an attempt to reverse the aggregation process to generate a single cell suspension. Unfortunately, the presence of EDTA failed to dissociate the aggregates suggesting that native cell-cell interactions were now present and cells retained in their aggregated state.

6.5 Optimisation of Aggregation Conditions

A variety of Fe^{3+} concentrations were examined in order to optimise the aggregation process (Figure 88). An Fe^{3+} concentration between 5.0 and 20.0 µM failed to aggregate the cells, increasing the concentration to 50 µM resulted in large aggregate sizes compared to untreated HT29 cells (Figure 88A). Further increases in Fe^{3+} concentration resulted in smaller aggregate sizes, possibly due to Fe^{3+} saturation on the cell surface. The effect on agitation time was also investigated with 20 minutes giving good sized aggregates, extending agitation beyond this gave larger sized aggregates due to the association of different aggregates (Figure 88B).

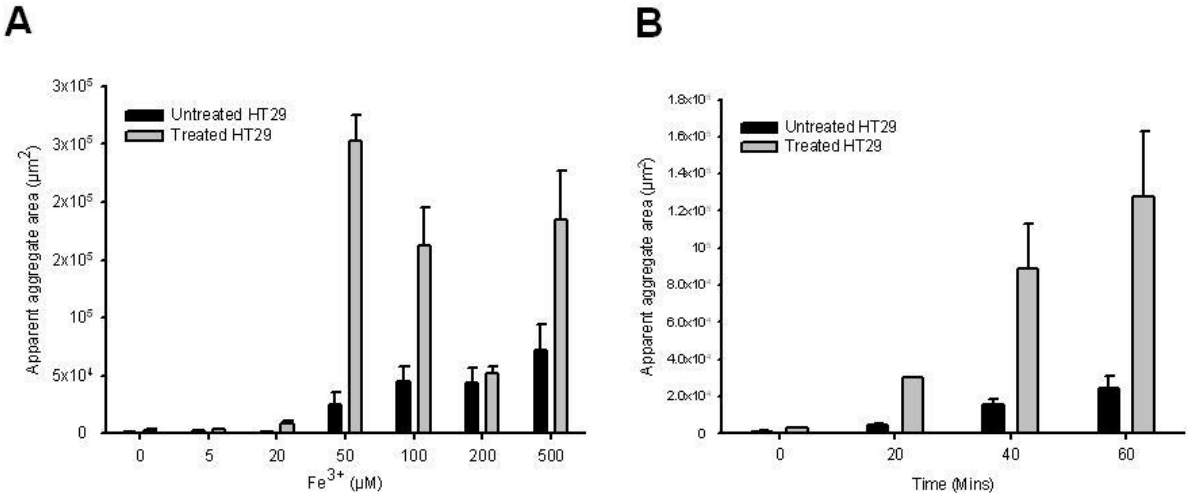

Figure 88: A) The effect of Fe^{3+} concentration on mean apparent area for untreated HT29 and treated cells after 20 min agitation, B) the effect of agitation time on mean apparent area for untreated and maltol engineered HT29 cells after addition of 50 µM Fe^{3+}. Data are shown as mean ± standard deviation, results are representative of three experiments.

6.6 MTS Antiproliferative Assays

To confirm that modifying the cell surface with the maltol motif was not detrimental to cellular proliferation, MTS antiproliferative assays were performed after 24 h, 48 h and 72 h (Figure 87). After 24 h incubation the O.D reading for the untreated cells (1), oxidised cells (2) and maltol cells (3) were all comparable both in the absence and presence of 50 µM Fe^{3+} (Figure 89). After 48 h slightly higher O.D readings were observed indicating that all cell types were actively proliferating. After 72 h the O.D reading remained above 0.7, demonstrating that this process is not having a detrimental effect cellular proliferation. Interestingly after 72 h the maltol cells in the presence of Fe^{3+} had a higher O.D than maltol cells without Fe^{3+}, suggesting that aggregate formation was actually increasing the rate of cellular proliferation. This may be the result of increased cell to cell contact and intracellular signalling.

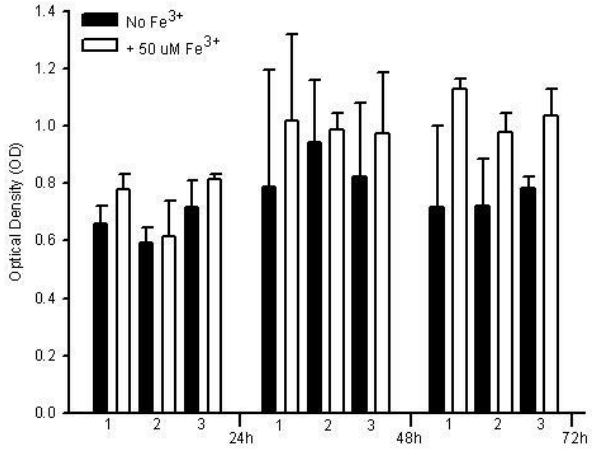

Figure 89: MTS assays on 1) untreated cells, 2) oxidised cells and 3) maltol engineered HT29 cells in the absence (black bar) and presence of 50 µM Fe^{3+} (white bar) after 24 h, 48 h and 72 h incubation. Each bar is the average of three independent experiments ± standard deviation.

6.7 Selectivity for Fe^{3+}

Maltol **(92)** displays excellent selectivity for Fe^{3+} but has been reported to chelate a variety of other transition metals including Ru^{3+}, Cu^{2+} and Zn^{2+}.[97,98] To investigate the influence of different transition metals on the aggregation process a range of specificity assays were performed (Figure 90). In the presence of 50 µM Fe^{3+} the multicellular aggregates formed whereas in the presence of 50 µM Ru^{3+}, Cu^{2+} and Zn^{2+}

no aggregation was observed (Figure 90), confirming that aggregation occurs selectively in the presence of Fe^{3+}.

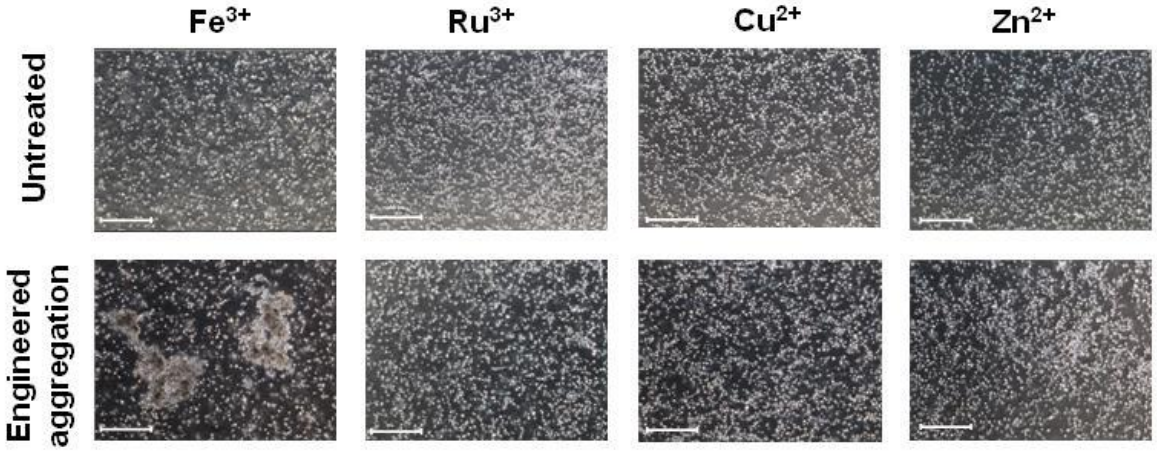

Figure 90: Phase contrast images of untreated and maltol engineered HT29 cells in the presence of 50 µM of transition metals after 20 mins agitation time, scale bars = 400 µm, results are representative of three independent experiments.

6.8 Fe^{3+} Triggered Heterocellular Aggregation

To demonstrate this can be applied to aggregate two different cell types together, HT29 and MDA-MB-231 cells were fluorescently labelled green and red respectively using CellTracker™ and modified to have maltol on the surface. Upon addition of 50 µM Fe^{3+} the two different cell types began to aggregate together resulting in the formation of heterocellular aggregates (Figure 91).

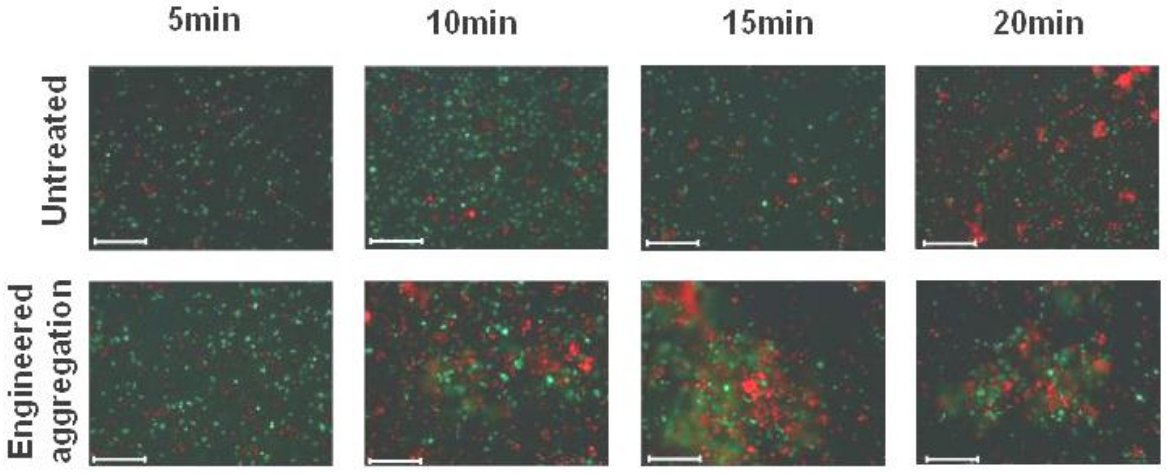

Figure 91: Fluorescence images of HT29 cells (Green) and MDA-MB-231 cells (Red) in the presence of 50 µM Fe^{3+}, scale bars = 400 µm, results are representative of three independent experiments.

Three aggregates are displayed at X 10 magnification clearly showing that the HT29 (green) and MDA-MB-231 (red) cells are randomly arranged within the aggregate giving areas of yellow (ie combination of red and green) (Figure 92).

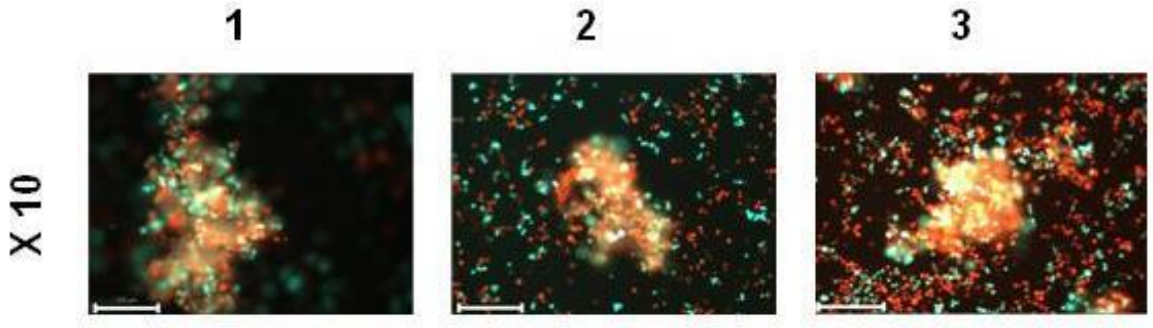

Figure 92: Fluorescence images of three aggregates at X 10 magnification, HT29 cells (Green) and MDA-MB-231 cells (Red) in the presence of 50 µM Fe^{3+}, scale bars = 200 µm.

This result is particularly pleasing as it demonstrates that modifying the cell surface and attachment of the maltol unit is not just limited to HT29 cells and can be applied to other cell types. This process can be applied to replicate the heteroceullar aggregates reported from Shakesheff *et al.*[91] and Sakai *et al.*[92] but using a Fe^{3+} chelation system instead of a biotin and avidin system. To investigate possible self-organisation as reported by Sakai *et al.*[92] the heterocellular aggregates were incubated for several days, however no self-organisation was observed.

In summary, maltol hydrazide **(121)** can be attached to HT29 and MDA-MB-231 cells which have been treated to express non-native aldehydes on the cell surface. Addition of Fe^{3+} to the cell medium resulted in rapid multicellular aggregation within 20 minutes of gentle agitation but only in PBS and serum free culture medium, the presence of serum in the culture medium prevented aggregation. MTS assays confirmed that this process was non-toxic and even slightly increased the proliferation of the aggregated cells compared to untreated cells. The process is Fe^{3+} specific with no sign of aggregation in the presence of Ru^{3+}, Cu^{2+} or Zn^{2+} after 20 minutes agitation. This process can also be applied to generate heterocellular aggregates in which two different cell types are assembled together within 20 minutes. The ability to synthesise the maltol hydrazide **(121)** in high yield in five steps from cheap commercially available starting materials suggests that it could be useful alternative to previously reported reagents.

6.9 Conclusions

Conversion of maltol **(92)** into the maltol activated ester **(116)** enabled synthesis of the benzylated maltol dimer **(117)** and trimer **(118)** in 65% and 62% yield respectively. Removal of both benzyl groups in the maltol dimer **(111)** was achieved within 24 h however complete removal of the benzyl groups in the trimer was not observed, limiting the potential to develop a maltol based polymer via this route.

Maltol hydrazide **(121)** was synthesised in five steps from the industrially available feedstock maltol **(92)** and was confirmed to be non-toxic with an IC_{50} value >200 μM in HT29 and MDA-MB-231 cells. Maltol hydrazide **(121)** was chemically attached to HT29 cells via the procedure reported by Bertozzi *et al.*[89] and upon addition of 50 μM Fe^{3+} these cells aggregated together within 20 minutes with gentle agitation. Further studies demonstrated that this process was specific for Fe^{3+} and could be applied to generate heterocellular aggregates composed of HT29 and MDA-MB-231 cells (Figure 93).

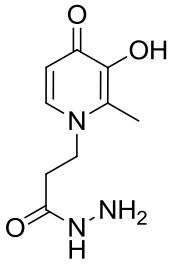

(121)

- 5 step synthesis from maltol **(92)**
- Non-Toxic to HT29 & MDA-MB-231
- Can be attached to cell surface
- Forms multicellular aggregates
- Fe^{3+} specific

Figure 93: Maltol hydrazide (121).

6.10 Future work

6.11 *In Vitro* 3D MTS Assay

Solid tumours *in vivo* are disorganised 3D collections of multiple cancer cells forming cell-cell contacts and intracellular signalling driving cell differentiation and proliferation.[1,2] Solid tumours suffer from poor drug uptake, drug concentration gradients and with up to 60% of solid tumours containing hypoxic regions, all of these features can impact upon a drug response *in vivo*.[116] Current 2D cell culture systems, for example the MTS assay while rapid and efficient, fail to fully replicate this complex interplay *in vitro*. 3D cell culture screening could be the solution by providing a critical bridge between initial 2D cell culture screening and *in vivo* animal models (Figure 94).[116,117] This additional screening step would ensure only drug candidates which retain predetermined levels of activity against 3D cell cultures enter *in vivo* animal models. This would reduce the number of animals required for a drug discovery programme saving time, money and reducing the ethical implications of using large numbers of animal models.

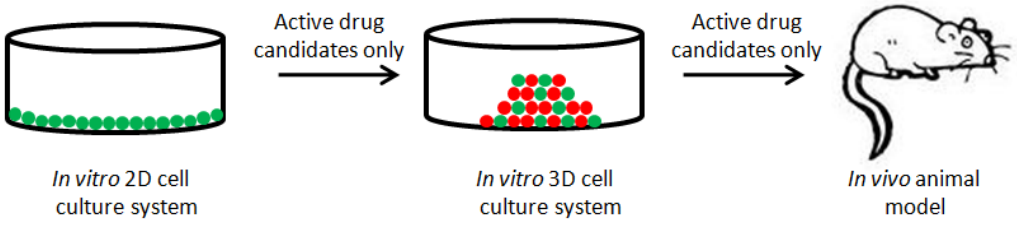

Figure 94: Bridging the gap between 2D cell culture drug screening and animal models.

Numerous methods to generate 3D cell culture systems have been reported,[118,119] however the maltol hydrazide **(121)** aggregation method has the added potential of forming heterocellular aggregates of specific sizes depending on aggregation conditions within twenty minutes. This method is more rapid and cost-effective that the biotin and avidin methods reported by Shakesheff *et al.*[86] and Sakai *et al.*[92] allowing its application on a larger more industrial scale.

6.12 Thiomaltol Hydrazide (123)

One problem encountered with the maltol hydrazide **(121)** cellular aggregation method was sequestration of Fe^{3+} in complete culture media (containing 10% serum) preventing cellular aggregation. This problem was resolved when serum free culture media was used, however for long term cell culture complete culture media is the preferred option. An alternative to overcome this is thiomaltol **(122)** (Scheme 39) which has been reported to chelate a variety of metals[120-122] including Zn^{2+}, Cu^{2+}, Mo^{6+}, Ni^{2+} and Co^{2+} which may be less susceptible to sequestration by the serum in complete culture media. Cohen *et al.* reported a one-pot procedure to synthesis thiomaltol **(122)** from maltol **(92)** in 70% using phosphorus pentasulfide (P_4S_{10}) and hexamethyldisiloxane (HMDO).[123] This approach could be applied to synthesis thiomaltol hydrazide **(123)** directly from maltol hydrazide **(121)** in a single step (Method 1, scheme 39) or via thiomaltol **(122)** (Method 2).

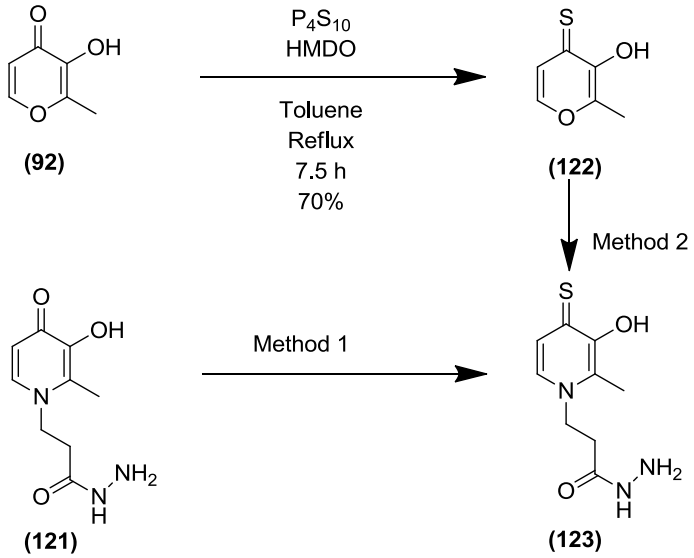

Scheme 39: Thiomaltol (122) and thiomaltol hydrazide (123).

Thiomaltol hydrazide **(123)** could be attached to the cell surface using the methods of Bertozzi *et al.*[89] and then screened against a variety of metals to determine if aggregation occurs in complete culture media. A combination of different metals could also be investigated to determine if cellular aggregates with different morphologies could be formed in a similar manner reported by Chmielewski *et al.*[86]

7.0 Final Conclusions

The chalcone motif is present in an extensive range of biologically active molecules with various activities reported.[46-50] We reported fourteen novel urocanic-chalcone hybrids combining the urocanic side chain pharmacophore in eleutherobin **(3)** and sarcodictyin **(4,5)** and the 3,4,5-trimethoxy aryl pharmacophore present in combretastatin **(CA4)** (Chapter 2). Combining pharmacophores from natural products via the chalcone motif enabled access to novel compounds with promising antiproliferative activities, published in 2011 (*Med. Chem. Comm.,* **2011**, *2,* 1011-1015).[124]

While interesting in themselves, chalcones also serve as valuable starting materials for more complex molecules in medicinal chemistry.[51-54] Twenty pyrazoline based **(CA4)** analogues were synthesised in two steps in good to excellent yield from chalcones (Chapter 3). Pyrazoline **(71-)** displayed nanomolar antiproliferative activities and was classified as a microtubule destabiliser confirming that chalcones are useful intermediates for more potent molecules (*Med. Chem. Comm.,* **2013**, *submitted*).

The pyrazoline motif was modified to generate non-toxic pyridine based pyrazolines as potential metal chelators for use in tissue engineering. Pyrazoline **(97)** was a potential "Turn on" fluorescent sensor for Cd^{2+} which upon oxidation to the corresponding pyrazole **(98)**, could distinguish Cd^{2+} from Zn^{2+} (Chapter 5). This observation provides valuable insight for future pyrazoline sensors and was published in 2012 (*Org. Biomol. Chem.*, **2012**, *10,* 8753-8757).[125] Further studies suggested that they were not suitable for tissue engineering purposes therefore an alternative strategy using the well established Fe^{3+} chelator maltol was developed.

Maltol hydrazide **(121)** was synthesised and attached to the cell surface of HT29 cells which upon addition of Fe^{3+} ions resulted in cellular aggregation due to metal chelation (Chapter 6). This process was applied to generate heterocellular aggregates composed of different cell types with valuable applications for cancer research and tissue engineering (*Chem. Commun.,* **2013**, *Manuscript in preparation*).

Chapter 8: References

1. J. Ferlay, H.R. Shin, F. Bray, D. Forman, C. Mathers and D.M. Parkin, *Int. J. Cancer*, 2010, **137**, 2893-2917.

2. D. Hanahan and R.A. Weinberg, *Cell*, 2000, **100**, 57-70.

3. D. Hanahan and R.A. Weinberg, *Cell*, 2011, **144**, 646-674.

4. B.A. Chabner and T.G. Roberts, *Nat. Rev. Cancer*, 2005, **5**, 65-72.

5. A.D. Huitema, K.D. Smits, R.A. Mathot, J.H. Schellens, S. Rodenhuis and J.H. Beijnen, *Anticancer Drugs*, 2000, **11**, 515-533.

6. G.J. Peters, C.L. Van der Wilt, C.J. Van Moorsel, J.R. Kroep, A.M. Bergman and S.P. Ackland, *Pharmacol. Ther*., 2000, **87**, 227-253.

7. M.A. Jordan and L. Wilson, *Nat. Rev. Cancer*, 2004, **4**, 253-65.

8. M. Kavallaris, *Nat. Rev. Cancer*, 2010, **10**, 194-204.

9. T. Fojo, *The Role of Microtubules in Cell Biology, Neurobiology and Oncology*, Humana Press, 2008, p. 359.

10. S. Nobili, D. Lippi, E. Witort, M. Donnini, L. Bausi, E. Mini and S. Capaccioli, *Pharmacol. Res*., 2009, **59**, 365-378.

11. Y. Zhao, W.S. Fang and K. Pors, *Expert Opin. Ther. Pat*., 2009, **19**, 607-622 and A. E. Prota, K. Bargsten, D. Zurwerra, J. J. Field, J. Fernado Diaz, K-H. Altmann and M. O. Steinmetz, *Science*, 2013, **339**, 587-590.

12. C. Ferlini, D. Gallo and G. Scambia, *Expert Opin. Investig. Drugs*, 2008, **17**, 335-347.

13. G.A. Orr, P. Verdier-Pinard, H. McDaid and S.B. Horwitz, *Oncogene*, 2003, **20**, 7280-7295.

14. R.H. Alvarez, V. Valero and G.N. Hortobagyi, *Ann. Med*., 2011, **43**, 477-486.

15. W. H. Fenical, P. R. Jensen and T. Lindel, 1995, US Patent 5473057.

16. T. Lindel, P.R. Jensen, W. Fenical, B.H. Long, A.M. Casazza, J. Carboni and C.R. Fairchild, *J. Am. Chem. Soc*., 1997, **119**, 8744-8745.

17. M. D'Ambrosio, A. Guerriero and F. Pietra, *Helv. Chim. Acta*, 1987, **70**, 2019-2027.

18. B.H. Long, J.M. Carboni, A.J. Wasserman, L.A. Cornell, A.M. Casazza, P.R. Jensen, T. Lindel, W. Fenical and C.R. Fairchild, *Cancer Res*., 1998, **58**, 1111-1115.

19. E. Hamel, D.L. Sackett, D. Vourloumis and K.C. Nicolaou, *Biochemistry*, 1999, **38**, 5490-5498.

20. K.C. Nicolaou, F. van Delft, T. Ohshima, D. Vourloumis, J. Xu, S. Hosokawa, J. Pfefferkorn, S. Kim and T.Li, *Angew. Chem., Int. Ed. Engl*., 1997, **36**, 2520-2524.

21. K.C. Nicolaou, T. Ohshima, S. Hosokawa, F.L. van Delft, D. Vourloumis, J.Y. Xu, J. Pfefferkorn and S. Kim*, J. Am. Chem. Soc*., 1998, **120**, 8674-8680.

22. X.T. Chen, C.E. Gutteridge, S.K. Bhattacharya, B. Zhou, T.R.R. Pettus, T. Hascall and S.J. Danishefsky, *Angew. Chem., Int. Ed*., 1998, **37**, 185-187.

23. X.T. Chen, B. Zhou, S.K. Bhattacharya, C.E. Gutteridge, T.R.R. Pettus and S.J. Danishefsky, *Angew. Chem., Int. Ed*., 1998, **37**, 789-792.

24. D. Castoldi, L. Caggiano, L. Panigada, O. Sharon, A.M. Costa and C. Gennari, *Angew. Chem., Int. Ed*., 2005, **44**, 588-591

25. D. Castoldi, L. Caggiano, L. Panigada, O. Sharon, A.M. Costa and C. Gennari, *Chem. Eur. J*., 2006, **12**, 51-62.

26. K.C. Nicolaou, J. Pfefferkorn, J. Xu, N. Winssinger, T. Ohshima, S. Kim, S. Hosokawa, D. Vourloumis, F. van Delft and T. Li, *Chem. Pharm. Bull*., 1999, **47**, 1199-1213.

27. R. Beumer, P. Bayon, P. Bugada, S. Ducki, N. Mongelli, F.R. Sirtori, J. Telser and C. Gennari, *Tetrahedron*, 2003, **59**, 8803-8820.

28. D. Castoldi, L. Caggiano, P. Bayon, A.M. Costa, P. Cappella, O. Sharon and C. Gennari, *Tetrahedron*, 2005**, 61**, 2123-2139.

29. G.C.H. Chiang, A.D. Bond, A. Ayscough, G. Pain, S. Ducki and A.B. Holmes, *Chem. Commun*., 2005, 1860-1862.

30. S.M. Chen, L.H. Meng and J. Ding, *Expert Opin. Investig. Drugs*, 2010, 19, 329-343.

31. A.L. Risinger, F.J. Giles and S.L. Mooberry, *Cancer Treat. Rev*., 2009, **35**, 255-261.

32. E. Hamel, *Pharmacol. Ther*., 1992, **55**, 31-51.

33. G.R. Pettit, S.B. Singh, E. Hamel, C.M. Lin, D.S. Alberts and D. Garcia-Kendall, *Experientia.*, 1989, **15**, 209-211.

34. G.M. Tozer, C. Kanthou and B.C. Baguley, *Nat. Rev. Cancer*, 2005, **5**, 423-425.

35. D.W. Siemann, D.J. Chaplin and P.A. Walicke, *Expert Opin. Investig. Drugs*, 2009, **18**, 189-197.

36. R.O. Carlson, *Expert Opin. Investig. Drugs*, 2008, **17**, 707-722.

37. K. Gaukroger, J.A. Hadfield, N.J. Lawrence, S. Nolan and A.T. McGown, *Org. Biomol. Chem.*, 2003, **7**, 3033-3037.

38. T.M. Beale, R.M. Myers, J.W. Shearman, D.S. Charnock-Jones, J.D. Brenton, F.V. Gergely and S.V. Ley, *Med. Chem. Commun*., 2010, **1**, 202-208.

39. G.R. Pettit, N. Melody, A. Thornhill, J.C. Knight, T.L. Groy and C.L. Herald, *J. Nat. Prod.*, 2009, **72**, 1637-1642.

40. M.G. Banwell, E. Hamel, D.C. Hockless, P. Verdier-Pinard, A.C. Willis and D.J. Wong, *Bioorg. Med. Chem.*, 2006, **1**, 4627-4638.

41. T. Pirali, S. Busacca, L. Beltrami, D. Imovilli, F. Pagliai, G. Miglio, A. Massarotti, L. Vertotta, G.C. Tron, G. Sorba and A.A. Genazzani, *J. Med. Chem*., 2006, **49**, 5372-5376.

42. L. Cafici, T. Pirali, F. Condorelli, E.D. Grosso, A. Massarotti, G. Sorba, P.L. Canonico, G.C. Tron and A.A. Genazzani, *J. Comb. Chem*., 2008, **10**, 732-740.

43. R. Romagnoli, P.G. Baraldi, A. Brancale, A. Ricci, E. Hamel, R. Bortolozzi, G. Basso and G. Viola, *J. Med. Chem*., 2011, **54**, 5144-5153.

44. D. Simoni, G. Grisolia, G. Giannini, M. Roberi, R. Rondanin, L. Paccagli, R. Barcuchello, M. Rossi, R. Romagnoli, R.P. Invidiata, S. Grimaudo, M.K. Jung, E. Hamel, N. Gebbia, L. Crosta, V. Abbadessa, A. Di Cristina, L. Dusonchet, M. Meli and M. Tolomeo, *J. Med. Chem*., 2005, **48**, 723-736.

45. C. Congiu, V. Onnis, L. Vesci, M. Castonia and C. Pisano, *Bioorg. Med. Chem.*, 2010, **18**, 6238-6248.

46. D. I. Batovska and I. T. Todorova, *Curr. Clin. Pharmacol*., 2010, **5**, 1-29.

47. S. Ducki, D. Rennison, M. Woo, A. Kendall, J.M.D. Chabert, A.T. McGown and N.J. Lawrence, *Bioorg. Med. Chem,* 2009, **17**, 7698-7710.

48. T. Caulfield, M.P. Cherrier, C. Combeau and P. Mailliet, Patent EP1253141A1.

49. D.J. Kerr, E. Hamel, M.K. Jung and B.L. Flynn, *Bioorg. Med. Chem.*, 2007, **15**, 3290-3298.

50. S. Ducki, G. Mackenzie, N.J. Lawrence and J.P. Snyder, *J. Med. Chem*., 2005, **48**, 457-465.

51. C. Congiu, V. Onnis, L. Vesci, M. Castorina and C. Pisano, *Bioorg. Med. Chem.,* 2010, **18**, 6238-6248.

52. P.C. Lv, H.Q. Li, J. Sun, Y. Zhou and H.L. Zhu, *Bioorg. Med. Chem.*, 2010, **18**, 4606-4614.

53. S.A.F. Rostom, M.H. Badr, H.A. Abd El Razik, H.M.A. Ashour and A.E. Wahag, *Arch. Pharm. Chem. Life. Sci.,* 2011, **344**, 572-587.

54. P.C. Lv, D.D. Li, Q.S. Li, X. Lu, Z.P. Xiao and H.L. Zhu, *Bioorg. Med. Chem. Lett.,* 2011, **21**, 5374-5377.

55. G. Caponigro and W.R. Sellers, *Nat. Rev. Drug Discov*., 2011, **10**, 179-187.

56. R.H. Shoemaker, *Nat. Rev. Cancer*., 2006, **6**, 813-823.

57. W.S. Yang, K. Shimada, D. Delva, M. Patel, E. Ode, R. Skouta and B.R. Stockwell, *ACS. Med. Chem. Lett*., 2012, **12**, 35-38.

58. M.L. Shelanski, F. Gaskin and C.R Cantor, *Proc. Nat. Acad. Sci. USA*., 1973, **70**, 765-768.

59. M.V.R. Reddy, B. Akula, S.C. Cosenza, C.M. Lee, M.R. Mallireddigari, V.R. Pallela, C.V. Subbaiah, A. Udofa and E.P. Reddy, *J. Med. Chem*., 2012, **55**, 5174-5187.

60. N.M. Rateb and H.F. Zohdi, *Synth. Commun.*, 2009, **39**, 2789-2794.

61. S. Bhagat, R. Sharma, D.M. Sawant, L. Sharma and A. K. Chakraborti, *J. Mol. Catal. A: Chem.*, 2006, **244**, 20-24.

62. T. Narender and K. Papi Reddy, *Tetrahedron Lett*., 2007, **48**, 3177-3180.

63. N. Lauth-de Viguerie, N. Sergueeva, M. Damiot, H. Mawlawi, M. Riviere and A. Lattes, *Heterocycles*, 1994, **37**, 1561-1576.

64. S. Zheng, Y.R. Laxmi, E. David, A.T. Dinkova-Kostova, K.H. Shiavoni, T. Ren, T. Zheng, I. Trevino, R. Bumeister, I. Ojima, W.C. Wigley, J.B. Bliska, D.F. Mierke and T. Honda, *J. Med. Chem*., 2012, **55**, 4837-4846.

65. R. Nishimura, K. Tabata, M. Arakawa, Y. Ito, Y. Kimura, T. Akihisa, H. Nagai, A. Sakuma, H. Kohno and T. Suzuki, *Bio. Pharm. Bull*., 2007, **30**, 1878-1883.

66. C.L. Miranda, J.F. Stevens, A. Helmrich, M.C. Henderson, R.J. Rodriguez, Y.H. Yang, M.L. Deinzer, D. W. Barnes and D.R. Buhler, *Food. Chem. Toxicol*., 1999, **37**, 271-285.

67. N.P. Reddy, P. Aparoy, T.C.M. Reddy, C. Achari, P.R. Sridhar and P. Reddanna, *Bioorg. Med. Chem*., 2010, **18**, 5807-5815.

68. K.E. Judd and L. Caggiano, *Org. Biomol. Chem.*, 2011, **9**, 5201-5210.

69. A. Leavai, *J. Heterocyclic Chem*., 2002, **39**, 1-13.

70. Z.-L. Gong, L.-W. Zheng, B.-X. Zhao, D.-Z. Yang, H.-S. Lv, W.-Y. Liu and S. Lian, *J. Photochem. Photobiol., A*, 2010, **209**, 49–55.

71. R.S. Cahn, C. Ingold and V. Prelog, *Angew. Chem. Int. Ed. Engl*., 1966, **5**, 385-415.

72. N. Vanthuyne, C. Roussel, J.V. Naubron, N. Jagerovic, P.M. Lazaro, I. Alkorta and J. Elguero, *Tetrahedron Asymm*., 2011, **22**, 1120-1124.

73. O. Mahe, I. Dez, V. Levacher and J.F. Briere, *Angew. Chem. Int. Ed*., 2010, **49**, 7072-7075.

74. J.A. Dale, D.L. Dull and H.S. Mosher, *J. Org. Chem*., 1969, **34**, 2543-2549.

75. S.K. Tahir, P. Kovar, S.H. Rosenberg and S.C. Ng, *Biotechniques*, 2000, **29**, 156-160.

76. A. Dahan, M. Khamis, R. Agbaria and R. Karaman, *Expert Opin. Drug Deliv*., 2012, **9**, 1001-1013.

77. C.P. Landowski, B.S. Vig, X. Song and G.L. Amidon, *Mol. Cancer. Ther.*, 2005, **4**, 659-667.

78. X. Song, P.L. Lorenzi, C.P. Landowski, B.S. Vig, J.M. Hilfinger and G.L. Amidon, *Mol. Pharm*., 2005, **2**, 157-167.

79. R. Langer and J.P. Vacanti, *Science*, 1993, **260**, 920-926

80. H. Naderi, M.M. Matin and A.R. Bahrami, *J. Biomater. Appl*., 2011, **26**, 383-417.

81. T. Garg, O. Singh, S. Arora and R. Murthy, *Crit. Rev. Ther. Carrier Sys*., 2012, **29**, 1-63.

82. M.J. Lysaght, A. Jaklenec and E. Deweerd, *Tiss. Eng. Part. A*., 2008, **14**, 305-315.

83. A. Atala, S.B. Bauer, S. Soker, J.J. Yoo and A.B. Retik, *Lancet*, 2006, **15**, 1241-1246.

84. P. Macchiarini, P. Jungebluth, T. Go, M.A. Asnaghi, L.E. Rees, T.A. Cogan, A. Dodson, J. Martorell, S. Bellini, P.P. Parnigotta, S.C. Dickinson, A.P. Hollander, S. Mantero, M.T. Conconi and M.A. Birchall, *Lancet*, 2008, **13**, 2023-2030.

85. A. Raya-Rivera, D.R. Esquiliano, J.J. Yoo, E. Lopez-Bayghen, S. Soker and A. Atala*, Lancet*, 2011, **2**, 1175-1185.

86. M.M. Pires, D.E. Przbyla and J. Chmielewski, *Angew. Chem. Int. Ed*. 2009, **48**, 7813-7817.

87. M.M Pires and Chmielewski, *J. Am. Chem. Soc*., 2009, **25**, 2706-2712.

88. M.P. Lutolf and J.A. Hubbell, *Nat. Biotechnol*., 2005, **23**, 47-55.

89. G.A. Lemieux and C.R. Bertozzi, *Trends. Biotechnol*., 1998, **16**, 506-513 and K. E. Norgard, H. H. Powell, M. Kriegler, A. Varki and N. M. Varki, *Proc. Natl. Acad. Sci. U.S.A*., 1993, **90**, 1068-1072.

90. P.A. De Bank, B. Kellam, D.A. Kendall and K.M. Shakesheff, *Biotechnol. Bioeng.*, 2003, **30**, 800-808.

91. P.A. De Bank, Q. Hou, R.M. Warner, I.V. Wood, B.E. Ali, S. Macneil, D.A. Kendall, B. Kellam, K.M. Shakesheff and L.D. Buttery, *Biotechnol. Bioeng*., 2007, **15**, 1617-1625.

92. N. Kojima, S. Takeuchi and Y. Sakai, *Biomaterials*, 2011, **32**, 6059-6067.

93. P. Wang, N. Onozawa-Komatsuzaki, Y. Himeda, H. Sugihara, H. Arakawa and K. Kasuga, *Tetrahedron Lett.*, 2001, **42**, 9199-9201.

94. S. Hu, S. Zhang, Y. Hu, Q. Tao and A. Wu, *Dyes Pigm*ent, 2013, **96**, 509-515.

95. I. Ali, W.A. Wani, A. Khan, A. Hague, A. Ahmad, K. Saleem and N. Manzoor, *Microb. Pathog*., 2012, **53**, 66-73.

96. S. Wang, W. Shao, H. Li, C. Liu, K. Wang and J. Zhang, *Eur. J. Med. Chem*., 2011, **46**, 1914-1918.

97. L.E. Scott and C. Orvig, *Chem. Rev*., 2009, **109**, 4885-4910.

98. K.H. Thompson, C.A. Berta and C. Orvig, *Chem. Soc. Rev*., 2006, **35**, 545-556.

99. T. Zhou, Y. Ma, X. Kong and R.C. Hider, *Dalton Trans*., 2012, **41**, 6371-6389.

100. S. Amatori, I. Bagaloni, E. Macedi, M. Formica, L. Giorgi, V. Fusi and M. Fanelli, *Br. J. Cancer*, 2010, **13**, 239-248.

101. L.S. Dehkordi, Z.D. Liu and R.C. Hider, *Eur. J. Med. Chem*., 2008, **43**, 1035-1047.

102. E.B. Mubofu and J.B.F.N. Engberts, *J. Phys. Org. Chem*.,2004, **17**, 180-186.

103. J. McNulty and I.W.J. Still, *J. Chem. Soc., Perkin Trans. 1*, 1994, 1329- 1337.

104. M. Barceló-Oliver, A. Terrón, A. García-Raso, I. Turel and M. Morell, *Acta Crystallogr., Sect. E: Struct. Rep. Online*, 2010, **66**, m899–m900.

105. Z. Li, L. Zhang, L. Wang, Y. Guo, L. Cai, M. Yu and L. Wei, *Chem. Commun*., 2011, **47**, 5798–5800.

106. Z. Xu, K.-H. Baek, H. N. Kim, J. Cui, X. Qian, D.R. Spring, I. Shin and J. Yoon*, J. Am. Chem. Soc.*, 2010, **132**, 601–610.

107. Z. Xu, X. Liu, J. Pan and D.R. Spring, *Chem. Commun*., 2012, **48**, 4764–4766.

108. Z. Xu, J. Yoon and D.R. Spring, *Chem. Soc. Rev*., 2010, **39**, 1996–2006.

109. M.D. Pluth, E. Tomat and S.J. Lippard*, Annu. Rev. Biochem*, 2011, **80**, 333–355.

110. B.P. Joshi, J. Park, W.I. Lee and K.-H. Lee, *Talanta*, 2009, **78**, 903–909.

111. L. Xue, C. Liu and H. Jiang, *Org. Lett*., 2009, **11**, 1655–1658.

112. H. Chen, W. Gao, M. Zhu, H. Gao, J. Xue and Y. Li, *Chem. Commun*., 2010, **46**, 8389–8391.

113. Z.L. Gong and B.X. Zhao, *Sens. Actuators, B*, 2011**, 159**, 148-153.

114. Z. Zheng, F-W. Wang, S-W. Wang, S-Q. Wang, F. Ge, B-X. Zhao and J-Y. Ming, *Org. Biomol. Chem*., 2012, **10**, 8640-8644.

115. P.S. Dobbin, R.C. Hider, A.D. Hall, P.D. Taylor, P. Sarpong, J.B. Porter, G. Xiao and D.V.D. Helm, *J. Med. Chem*., 1993, **36**, 2448-2458.

116. S. Breslin and L. O'Driscoll, *Drug Discov. Today*, 2013, **18**, 240-249.

117. G. Mehta, A.Y. Hsiao, M. Ingram, G.D. Luker and S. Takayama, *J. Controlled Release*, 2012, **164**, 192-204.

118. F. Hirschhaeuser, H. Menne, C. Dittfeld, J. West, W. Mueller-Klieser and L.A. Kunz-Schughart, *Biotechnol. J.*, 2010, **148**, 3-15.

119. R.Z. Lin and H.Y. Chang, *Biotechnol. J*., 2008, **3**, 1172-1184.

120. S. Chaves, R. Jelic, C. Mendoca, M. Carrasco, Y. Yoshikawa, H. Sakurai and M.A. Santos, *Metallomics*, 2010, **2**, 220-227.

121. J.A. Lewis, B.L. Tran, D.T. Puerta, E.M. Rumberger, D.N. Hendrickson and S.M. Cohen, *Dalton Trans*., 2005, 2588-2596.

122. S. Chaves, M. Gil, S. Canario, R. Jelic, M. Joao Romao, J. Trincao, E. Herdtweck, J. Sousa, C. Diniz, P. Fresco and M.A. Santos, *Dalton Trans*., 2008, 1773-1782.

123. J.A. Lewis, D.T. Puerta and S.M. Cohen, *Inorg. Chem*., 2003, **42**, 7455-7459.

124. A. Ciupa, N.J. Griffiths, S.K. Light, P.J. Wood and L. Caggiano, *Med. Chem. Comm*, 2011, **2**, 1011-1015.

125. A. Ciupa, M.F. Mahon, P.A. De Bank and L. Caggiano, *Org. Biomol. Chem*., 2012, **10**, 8753-8757.

9. Experimental and MTS Assays

General Experimental

Chemicals, solvents and reagents used are commercially available and were used without further purification. PE refers to petroleum ether, bp 40-60 °C. TLCs were carried out on Merck Aluminium backed TLC plates Silica Gel 60 F254 and viewed using UV light of wavelength 254 nm and then stained with potassium permanganate. Merck Silica Gel (0.040-0.063 mm) was used for column chromatography. Compounds were loaded as an oil, CH_2Cl_2 solution or dry loaded by adsorption onto silica. Melting points were obtained using a Reichert-Jung heated-stage microscope. Infrared spectra were recorded on a Perkin-Elmer Spectrum RXI FT-IR system and all values are recorded in cm^{-1}.

NMR spectra were obtained on Varian Mercury VX (400 MHz) or Bruker Avance III (500 or 400 MHz) spectrometers. The chemical shifts are recorded in parts per million (ppm) with reference to tetramethylsilane. The coupling constants *J* are quoted to the nearest 0.5 Hz and are not corrected. The multiplicities are assigned as a singlet (s), doublet (d), triplet (t), doublet of doublets (dd), quartet (q) and multiplet (m). Mass spectra and high resolution mass spectra were obtained on a micrOTOF^{TM} from Bruker Daltonics (Bremen, Germany) coupled with an electrospray source (ESI-TOF) using an autosampler in an Agilent 1100 LC system. Data was processed using external calibration with the Bruker Daltonics software, DataAnalysis^{TM} as part of the overall hardware control software, Compass 1.1^{TM}.

X-ray Crystallography: Single crystals were analysed at 150(2) K using graphite monochromated Mo(Kα) radiation and a Nonius Kappa CCD diffractometer. The structures were solved using SHELXS-97 and refined using SHELXL-97. UV/Vis spectroscopy studies were performed on a BMG labtech Fluostar plate reader with NUNC 96 well flat bottom plates at room temperature. Fluorescence studies were performed on a Hitachi F-2000 fluorescence spectrophotometer with a 150 W xenon lamp using a cuvette with 1 cm path length. Polarimeter was performed on an AA-10 series Optical Activity Ltd polarimeter with a 1 mL flow cell with a path length of 10 cm^3. Data processing and analysis was using performed using SigmaPlot 8.

MTS Cell Proliferation Assay

Human cancer cell lines HT29, MDA-MB-231 and LNCaP were supplied by Cancer Research UK. They were maintained in DMEM with high glucose (4.5 g/L) and $_L$-glutamine, supplemented with penicillin 100 U/mL, streptomycin 100 µg/mL and foetal bovine serum at 10% for HT29 and MDA-MB-231, and 20% for LNCaP. FEK-4 primary human skin fibroblasts were a gift from Prof. Rex M. Tyrrell (University of Bath) and were maintained in MEM supplemented with $_L$-glutamine, supplemented with penicillin 100 U/mL, streptomycin 100 µg/mL and 15% foetal bovine serum. All reagents supplied by Invitrogen.

1. Cells were maintained in 75 cm^2 tissue culture flasks (Nunc) with a weekly 1:10 split.

2: For the MTS assay, seed densities of 500, 1000, 1500 and 2000 cells per well in 50 µL were used for HT29, MDA-MB-231, FEK-4 and LNCaP cell lines respectively. The seed densities had been determined previously to give an acceptable optical density value after 3 days incubation.

3: Plates were incubated at 37 ^oC, in humidified 5% CO_2 in air for 2-4 h.

4: Test agents were prepared at 100 × final concentration in DMSO (Sigma), diluted 1 in 50 in culture medium and 50 µL added to the appropriate wells, to give a final volume of 100 µL.

5: Quadruplicate samples were run as follows:
Culture medium only (background)
Cells only
Cells + 1% DMSO
Cells + test compound

6: Plates were incubated at 37 ^oC, in humidified 5% CO_2 in air.

This exposure time appears to be adequate to demonstrate anti-proliferative activity, and is routinely used by other workers.

7: The MTS reagent was added, 20 µL per well. This is Promega Cell Titer® Aqueous One Solution Cell Proliferation Assay.

8: Plates were incubated at 37 ^{o}C, in humidified 5% CO_2 in air, for colour development.

9: Optical density readings at 490 nm were taken at 1-4 h, because the culture medium gives a high OD_{490nm} this was subtracted from all other OD_{490nm}.

10: Means and standard deviations were calculated from background corrected OD_{490nm} values.

11: IC_{50} values were calculated using the pharmacology function in SigmaPlot 8 (SPSS Inc). Each assay was repeated on three separate occasions.

Note: This assay is based upon the development of a coloured metabolite from viable cells. Therefore the inhibition of colour development by an active agent does not distinguish between inhibition of cell metabolism *ie* cytostasis and reduction in cell number *ie* cytotoxicity. Nevertheless, this assay provides a very quick and easy first approach for screening test compounds.

Cell Cycle Analysis

Following the procedure reported,[38] except using HT29 cells:

1. Cells were subcultured into a T25 flask (5×10^5 cells, 3 mL media) and grown for 24 h.

2. Fresh media containing required concentration of drug/control was added (3 mL) and the cells were incubated with drug for a further 24 h.

3. The supernatant media was collected, and combined with a PBS wash (5 mL). Trypsin (1 mL) was added and cells incubated for 5 min.

4. The trypsin was neutralised with media (2 mL) and this was combined with the supernatant and a further PBS wash (5 mL). The cell suspension was centrifuged (1000 rpm, 6 min), the supernatant was removed, and the cell pellet was resuspended in PBS (5 mL).

5. This was centrifuged (1000 rpm, 6 min), and the supernatant was removed. The cell pellet was resuspended in PBS (0.5 mL), and this suspension was carefully added to ice cold 70% ethanol solution (4.5 mL).The cells were fixed for a minimum of 2 h, before centrifuging (1000 rpm, 5 min).

6. The supernatant was removed and the cells resuspended in PBS (5 mL). The cells were washed *via* two centrifuging and resuspension cycles, and were finally resuspended in 1 mL of a solution of DNase-free RNase A (20 μg/mL) and propidium iodide (20 μg/mL) in 0.1% (v/v) Triton X-100 in PBS.

7. Cells were incubated at rt for 30 min in the dark. Cell fluorescence was determined using a FACSCalibur (BDBiosciences), gating for mononuclear cells.

Cytoskeleton BK004P *In Vitro* Tubulin Polymerisation Assay Kit

Following the manufacturer instructions (Cat # BK004P)[58]:

1. One 4 mg tube of tubulin (HTS03) was resuspended with 1 ml of cold G-PEM buffer (990 µl general tubulin buffer with 10 µl GTP stock) to give a final protein concentration of 4 mg/mL. The tube was placed on ice for 3 min until complete resuspension of the protein was observed.

2. A 96 well half area plate was prewarmed to 37 ^{o}C by placing in an incubator for 30 mins prior.

3. Pipette 10 µL of compound of interest at 10x strength in G-PEM buffer into two wells of the prewarmed 96 well half area plate and 10 µL of general tubulin buffer only into two of the control wells and incubate the plate for 2 min at 37 ^{o}C.

4. Remove the 96 well half area plate and pipette 100 µL of tubulin into the required wells and immediately place the plate into the spectrophotometer prewarmed to 37 ^{o}C and start recording using optical density reading at 340 nm at one reading per minute for one hour.

5. The optical density of each compound was plotted against time to obtain the tubulin polymerisation assay curves.

Confocal Microscopy

Following the procedure reported,[38] except using HT29 cells:

1. HT29 cells were subcultured in each well of a six well plate containing a glass coverslip and incubated at 37 ^{o}C for 24 h.

2. When the cells were approximately 50% confluent, the coverslips were removed and placed into a well of a new 6 well plate containing 450 µL medium. Drug solution in medium (50 µL, 10× concentrations to give appropriate 1× final concentrations) was then added along with a blank (50 µL of medium) and plates incubated for 24 h.

3. After 24 h the media was aspirated, the coverslips washed with PBS (500 µL per well) followed by fixation in freshly diluted 3% formaldehyde solution in PBS (500 µL) followed by incubation at 37 °C for 10 min.

4. After aspiration cells were permeabilised with PBS-T (0.1% Triton in PBS, 500 µL) for 5 min, and then incubated at 37 °C with blocking solution (10% bovine serum albumin (BSA) in PBS (500 µL)) for 5 min.

5. This was removed and DM1A primary mouse antibody (1 in 200 in blocking solution, 500 µL) was added and incubated at 37 °C for 2 h.

6. The primary antibody solution was removed and the cells were washed 3 times (5 min at 37 °C) with PBS-T (500 µL). The appropriate Alexa Fluor® 546-coupled secondary antibody was then added as a solution in BSA in PBS (1 in 200 in blocking solution, 500 µL) and the plate returned to the incubator for a further 2 h ensuring minimal light exposure.

7. Cells washed 3 times (5 min at 37 °C) with PBS-T (500 µL), with a final wash in water (500 µL). The coverslips inverted onto microscope slides with mounting medium containing DAPPI stain (30 µL) and allowed to dry at rt overnight and then stored at 4 °C until they were viewed using a confocal microscope.

HPLC – System 1

Analytical RP-HPLC was performed on a Dionex HPLC system equipped with a Dionex Acclaim 3 µm C-18 (150 × 4.6 mm) column with a flow rate of 1 mL/min. with detection at 214 nm and 254 nm shown. Mobile phase A was 0.1% TFA in H_2O and mobile phase B was 0.1% TFA in MeCN. The gradient was *T* = 0 min., *B* = 5%; *T* = 10 min., *B* = 95%; *T* = 15 min., *B* = 95%; *T* = 15.1 min., *B* = 5%; *T* = 18.1 min., *B* = 5%.

HPLC – System 2

Analytical RP-HPLC was performed on a JASCO HPLC system equipped with a phenomenex Max-RP 80A 4 µm C-18 (150 × 4.6 mm) column with a flow rate of 1.0 mL/min. with detection at 274 nm and 254 nm shown. Mobile phase A was

50% H_2O and mobile phase B was 50% MeCN.

HPLC – System 3

Semipreparative HPLC was performed on a JASCO HPLC system equipped with a Astec semipreparative Chirobiotic V2 column with a flow rate of 10 mL/min. with detection at 254 nm shown. Mobile phase A was 50% H_2O and mobile phase B was 50% MeCN.

HPLC – System 4

Enantiomeric excess determined using a JASCO HPLC system equipped with a Astec analytical Chirobiotic V2 column with a flow rate of 1.0 mL/min. with detection at 254 nm shown. Mobile phase A was 50% H_2O and mobile phase B was 50% MeCN.

1.1 Method A

Following the procedure previously reported,[61] except using 1.0 equivalent $LiOH{\cdot}H_2O$, $LiOH{\cdot}H_2O$ (2.5 mmol) was added to rapidly stirred solution of acetophenone (2.5 mmol) in EtOH (2.0 mL) at 30 ^oC open to the atmosphere for 10 min resulting in a rapid colour change from colourless to yellow. The aldehyde (2.5 mmol) was then added and stirring continued for 6 h resulting in a gradual colour change from yellow to orange. After 6 h the solvent was removed under reduced pressure and distilled water (5 mL) added followed by 1.5M HCl(aq) (5 mL) to the remaining residue. The product was extracted with EtOAc (3 × 20 mL), the organic layers were combined and washed with saturated brine solution (20 mL). The organic fraction was dried (Na_2SO_4), filtered and solvent removed under reduced pressure to give a yellow solid. The solid was purified by column chromatography with silica gel using PE:EtOAc 6:4 to afford the desired chalcone.

(*E*)-1-(4-methoxyphenyl)-3-(1*H*-pyrrol-2-yl)prop-2-en-1-one (40)

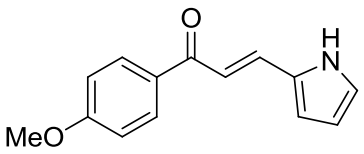

(40)

Following Method A on a 5.0 mmol scale, chalcone **(40)** was obtained as a yellow solid (0.49 g, 43%).

R_f [PE-EtOAc 4:6] 0.85; **Mp** 170-172 ^oC (EtOAc/heptane); **IR** ν_{max}(film)/cm^{-1} 3050, 1649 and 1594; **^{1}H NMR** δ_H (400 MHz; $CDCl_3$) 3.87 (3 H, s, OCH_3), 6.31-6.33 (1 H, m, pyrrole CH), 6.65-6.70 (1 H, m, pyrrole CH), 6.95 (2 H, d, *J* 9.0 Hz, Ar CH), 6.94-6.96 (1 H, m, pyrrole CH), 7.16 (1 H, d, *J* 15.0 Hz, COC*H*=CH), 7.73 (1 H, d, *J* 15.0 Hz, COCH=C*H*), 7.99 (2 H, d, *J* 8.5 Hz, Ar CH) and 8.95 (1 H, br s, pyrrole NH); **^{13}C NMR** δ_C (100 MHz; $CDCl_3$) 55.46 (OCH_3), 111.4 (pyrrole CH), 113.8 (pyrrole CH), 114.7 (Ar CH), 115.7 (pyrrole CH), 122.3 (Ar CH), 129.5 (Cq), 130.5 (HC=CH), 131.6 (Cq), 133.8 (HC=CH), 163.2 (Cq) and 188.7 (C=O); **MS** m/z (ES^+) Found 228.1025 (MH^+) and 250.0846 (MNa^+),

$C_{14}H_{14}NO_2$ (MH^+) requires 228.1025 and $C_{14}H_{13}NO_2Na$ (MNa^+) requires 250.0844; **HPLC** (analytical, system 1) t_R = 9.1 min.

(*E*)-1-(3,4-dimethoxyphenyl)-3-(1*H*-pyrrol-2-yl)prop-2-en-1-one (41)

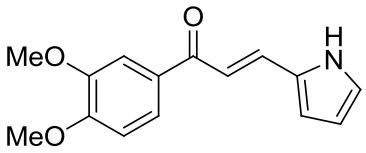

(41)

Following Method A, chalcone **(41)** was obtained as a yellow solid (0.34 g, 53%).

R_f [PE-EtOAc 4:6] 0.63; **Mp** 80-81 ^oC (EtOAc/heptane); **IR** ν_{max}(film)/cm^{-1} 3458, 1651 and 1584; **^{1}H NMR** δ_H (400 MHz; $CDCl_3$) 3.91 (3 H, s, OCH_3), 3.92 (3 H, s, OCH_3), 6.31-6.33 (1 H, m, pyrrole CH), 6.69-6.71 (1 H, m, pyrrole CH), 6.85 (1 H, d, *J* 8.0, Ar CH), 6.95-6.98 (1 H, m, pyrrole CH), 7.21 (1 H, d, *J* 15.5 Hz, COC*H*=CH), 7.59 (1 H, d, *J* 1.5 Hz, Ar CH), 7.61 (1 H, dd, *J* 8.5 and 1.5 Hz, Ar CH), 7.75 (1 H, d, *J* 15.5 Hz, COCH=C*H*) and 9.25 (1 H, br s, pyrrole NH); **^{13}C NMR** δ_C (100 MHz; $CDCl_3$) 56.0 (OCH_3), 110.1 (pyrrole CH), 111.0 (pyrrole CH), 111.4 (pyrrole CH), 115.0 (Ar CH), 115.4 (Ar CH), 122.6 (Ar CH), 122.9 (HC=CH), 129.5 (Cq), 131.8 (Cq), 134.0 (HC=CH), 149.2 (Cq), 153.0 (Cq) and 188.7 (C=O); **MS** m/z (ES^+) Found 258.1135 (MH^+) and 280.0949 (MNa^+), $C_{15}H_{16}NO_3$ (MH^+) requires 258.1130 and $C_{15}H_{15}NO_3Na$ (MNa^+) requires 280.0950; **HPLC** (analytical, system 1) t_R = 8.7 min.

(*E*)-3-(1*H*-pyrrol-2-yl)-1-(3,4,5-trimethoxyphenyl)prop-2-en-1-one (42)

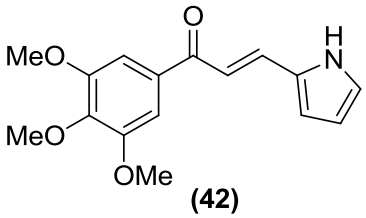

(42)

Following **Method A,** chalcone **(42)** was obtained as a yellow solid (0.53 g, 74%).

R_f [PE-EtOAc 4:6] 0.73; **Mp** 104-106 ^{o}C (EtOAc/heptane); **IR** ν_{max}(film)/cm^{-1} 3457, 1654 and 1575; **^{1}H NMR** δ_H (400 MHz; DMSO) 3.76 (3 H, s, OCH_3), 3.90 (6 H, s, OCH_3), 6.22-6.24 (1 H, m, pyrrole CH), 6.74-6.75 (1 H, m, pyrrole CH), 7.15-7.16 (1 H, m, pyrrole CH), 7.35 (2 H, s, Ar CH), 7.54 (1 H, d, *J* 15.0 Hz, COC*H*=CH), 7.62 (1 H, d, *J* 15.0 Hz, COCH=C*H*) and 11.71 (1 H, br s, pyrrole NH); **^{13}C NMR** δ_C (100 MHz; DMSO) 56.1 (OCH_3), 60.2 (OCH_3), 105.7 (Ar CH), 110.6 (pyrrole CH), 114.4 (pyrrole CH), 116.4 (pyrrole CH), 124.1 (HC=CH) 129.2 (Cq), 133.7 (Cq), 134.1 (HC=CH), 141.5 (Cq), 152.9 (Cq) and 187.1 (C=O); **MS** m/z (ES$^+$) Found 288.1241 (MH^+) and 310.1061 (MNa^+), $C_{16}H_{18}NO_4$ (MH^+) requires 288.1236 and $C_{16}H_{17}NO_4Na$ (MNa^+) requires 310.1055; **HPLC** (analytical, system 1) t_R = 9.0 min.

Method B

Following the procedure previously reported,[60] acetophenone (5.0 mmol), the aldehyde (5.0 mmol) and NaOH (7.0 mmol) was added to a porcelain mortar and ground using a porcelain pestle at rt (20 ^{o}C) for 5 mins resulting in the formation of a viscous yellow paste. The paste was then purified by column chromatography with silica gel using PE:EtOAc 6:4 solvent system to afford the desired chalcone.

(*E*)-1-(4-methoxyphenyl)-3-(1-methyl-1*H*-pyrrol-2-yl)prop-2-en-1-one (43)

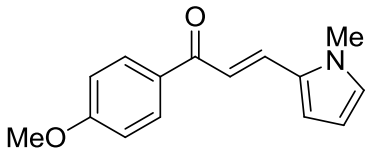

(43)

Following **Method B**, chalcone **(43)** was obtained as a yellow solid (0.76 g, 63%).

R_f [PE-EtOAc 4:6] 0.64; **Mp** 101-103 ^{o}C (EtOAc/heptane); **IR** ν_{max}(film)/cm^{-1} 1654 and 1575; **^{1}H NMR** δ_H (400 MHz; $CDCl_3$) 3.74 (3 H, s, pyrrole CH_3), 3.87 (3 H, s, OCH_3), 6.20-6.22 (1 H, m, pyrrole CH), 6.79-6.80 (1 H, m, pyrrole CH), 6.82-6.83 (1 H, m, pyrrole CH), 6.96 (2 H, d, *J* 9.0 Hz, Ar CH), 7.31 (1 H, d, *J* 15.0 Hz, COC*H*=CH), 7.79 (1 H, d, *J* 15.0 Hz, COCH=C*H*) and 8.02 (2 H, d, *J* 9.0 Hz, Ar CH); **^{13}C NMR** δ_C (100 MHz; $CDCl_3$) 34.3 (pyrrole CH_3), 55.4 (OCH_3), 109.5 (pyrrole CH), 111.9 (pyrrole CH), 113.7 (Ar CH), 116.5 (pyrrole CH), 127.4 (HC=CH), 130.3 (Cq), 130.4 (Ar CH), 131.4 (HC=CH), 131.5 (Cq), 163.0 (Cq) and 188.2 (C=O); **MS** m/z (ES$^+$) Found 242.1191 (MH$^+$) and 264.1007 (MNa$^+$), $C_{15}H_{16}NO_2$ (MH$^+$) requires 242.1181 and $C_{15}H_{15}NO_2Na$ (MNa$^+$) requires 264.1001; **HPLC** (analytical, system 1) t_R = 9.6 min.

(*E*)-1-(3,4-dimethoxyphenyl)-3-(1-methyl-1*H*-pyrrol-2-yl)prop-2-en-1-one (44)

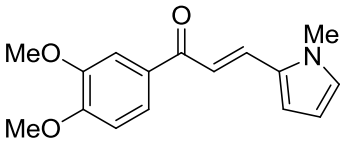

(44)

Following **Method B**, chalcone **(44)** was obtained as a yellow solid (1.07 g, 79%).

R_f [PE-EtOAc 4:6] 0.59; **Mp** 126-126 ^{o}C (EtOAc/heptane); **IR** ν_{max}(film)/cm^{-1} 1647, 1597 and 1573; **^{1}H NMR** δ_H (400 MHz; $CDCl_3$) 3.75 (3 H, s, pyrrole CH_3), 3.94 (3 H, s, OCH_3), 3.95 (3 H, s, OCH_3), 6.19-6.21 (1 H, m, pyrrole CH), 6.78-6.79 (1 H, m, pyrrole CH), 6.82-6.83 (1 H, m, pyrrole CH), 6.90 (1 H, d, *J* 8.5 Hz, Ar CH), 7.30 (1 H, d, *J* 15.5 Hz, COC*H*=CH), 7.61 (1 H, d, *J* 2.0 Hz, Ar CH), 7.64 (1 H, dd, *J* 8.0 and 2.0 Hz, Ar CH) and 7.79 (1 H, d, *J* 15.0 Hz, COCH=C*H*); **^{13}C NMR** δ_C (100 MHz; $CDCl_3$) 34.3 (pyrrole CH_3), 55.9 (OCH_3), 56.0 (OCH_3), 109.6 (pyrrole CH), 109.9 (pyrrole CH), 110.6 (pyrrole CH), 111.9 (Ar CH), 116.3 (Ar CH), 122.4 (HC=CH), 127.5 (Ar CH) 130.3 (HC=CH), 131.4 (Cq), 131.7 (Cq), 149.0 (Cq), 152.8 (Cq) and 188.0 (C=O); **MS** m/z (ES$^+$) Found 272.1273 (MH^+) and 294.1094 (MNa^+), $C_{16}H_{18}NO_3$ (MH^+) requires 272.1287 and $C_{16}H_{17}NO_3Na$ (MNa^+) requires 294.1106; **HPLC** (analytical, system 1) t_R = 9.1 min.

(*E*)-3-(1-methyl-1*H*-pyrrol-2-yl)-1-(3,4,5-trimethoxyphenyl)prop-2-en-1-one (45)

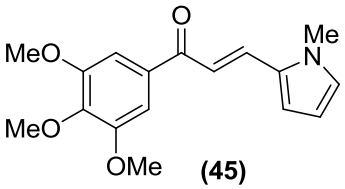

(45)

Following **Method B**, chalcone **(45)** was obtained as an orange oil (1.25 g, 83%).

R_f [PE-EtOAc 4:6] 0.67; **IR** ν_{max}(film)/cm^{-1} 1647 and 1568; **^{1}H NMR** δ_H (400 MHz; $CDCl_3$) 3.77 (3 H, s, pyrrole CH_3), 3.92 (3 H, s, OCH_3), 3.94 (6 H, s, OCH_3), 6.21-6.24 (1 H, m, pyrrole CH), 6.81-6.83 (1 H, m, pyrrole CH), 6.85-6.87 (1 H, m, pyrrole CH), 7.21 (1 H, d, *J* 15.0 Hz, COC*H*=CH), 7.26 (2 H, s, Ar CH) and 7.80 (1 H, d, *J* 15.0 Hz, COCH=C*H*); **^{13}C NMR** δ_C (100 MHz; $CDCl_3$) 34.3 (pyrrole CH_3), 56.3 (OCH_3), 56.3 (OCH_3), 105.7 (Ar CH), 109.7 (pyrrole CH), 112.2 (pyrrole CH), 116.4 (pyrrole CH), 127.8 (HC=CH), 130.2 (Cq), 132.1 (HC=CH), 134.1 (Cq), 153.0 (Cq), 153.0 (Cq) and 188.7 (C=O); **MS** m/z (ES^+) Found 302.1371 (MH^+) and 324.1192 (MNa^+), $C_{17}H_{20}NO_4$ (MH^+) requires 302.1392 and $C_{17}H_{19}NO_4Na$ (MNa^+) requires 324.1212; **HPLC** (analytical, system 1) t_R = 4.7 min.

Method C

Following the procedure previously reported,[62] except using 2.0 equivalents of $BF_3{\cdot}OEt_2$, $BF_3{\cdot}OEt_2$ (5.0 mmol) was added dropwise under dry conditions to a rapidly stirred solution of acetophenone (2.5 mmol) and aldehyde (2.5 mmol) in dry dioxane (2.0 mL) under N_2 at 25 ^oC. The solution was heated to 75 ^oC for 6 h and the reaction followed by TLC. The reaction was cooled and quenched by addition of EtOAc (100 mL) and distilled water (100 mL) and the aqueous fractions extracted with EtOAc (3 × 50 mL). 2M NaOH (50 mL) was added to the aqueous layer and gently heated at 50 ^oC with magnetic stirring for 30 min, resulting in a slight colour change and formation of a black precipitate. The aqueous layer was extracted with EtOAc (3 × 50 mL) and the organic layers were combined and washed with saturated brine solution (50 mL) and dried using Na_2SO_4. The solvent was filtered and removed under reduced pressure to produce a yellow/orange solid/oil which was purified by column chromatography with silica gel using CH_2Cl_2:MeOH 9:1 solvent system to afford the desired chalcone.

(*E*)-3-(1*H*-imidazol-4-yl)-1-(4-methoxyphenyl)prop-2-en-1-one (46)

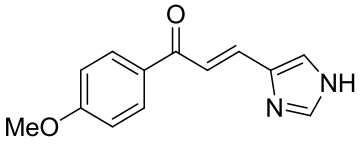

(46)

Following **Method C**, chalcone **(46)** was obtained as an orange solid (0.30 g, 53%).

R_f [CH_2Cl_2:MeOH 9:1] 0.19; **Mp** 173-175 ^oC (EtOAc/heptane); **IR** ν_{max}(film)/cm^{-1} 3458, 1660 and 1604; **^{1}H NMR** δ_H (400 MHz; DMSO) 3.85 (3 H, s, OCH_3), 7.08 (2 H, d, *J* 9.0 Hz, Ar CH), 7.63 (1 H, d, *J* 15.0 Hz, COC*H*=CH), 7.67 (1 H, d, *J* 15.5 Hz, COCH=C*H*), 7.64 (1 H, s, Im CH), 7.85 (1 H, s, Im CH), 8.03 (2 H, d, *J* 9.0 Hz, Ar CH) and 12.56 (1 H, br s, Im NH); **^{13}C NMR** δ_C (100 MHz; DMSO) 55.5 (OCH_3), 114.0, 117.8, 130.4 (Ar CH, Im CH and HC=CH), 130.8 (Cq), 162.8 (Cq), 162.9 (Cq) and 187.2 (C=O); **MS** m/z (ES^+) Found 229.0978 (MH^+), $C_{13}H_{13}N_2O_2$ (MH^+) requires 229.0977; **HPLC** (analytical, system 1) t_R = 6.0 min.

(*E*)-1-(3,4-dimethoxyphenyl)-3-(1*H*-imidazol-4-yl)prop-2-en-1-one (47)

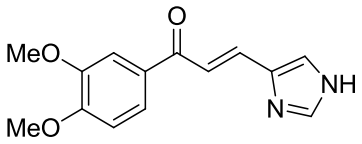

(47)

Following **Method C**, chalcone **(47)** was obtained as a pale yellow solid (0.48 g, 74%).

R_f [CH_2Cl_2:MeOH 9:1] 0.17; **Mp** 170-171 ^oC (THF/heptane); **IR** ν_{max}(film)/cm^{-1} 3457, 1659 and 1605; **^{1}H NMR** δ_H (400 MHz; DMSO) 3.85 (3 H, s, OCH_3), 3.86 (3 H, s, OCH_3), 7.10 (1 H, d, *J* 8.5 Hz, Ar CH), 7.54 (1 H, d, *J* 2.0 Hz, Ar CH), 7.64 (1 H, d, *J* 15.0 Hz, COC*H*=CH), 7.64 (1 H, s, Im CH), 7.68 (1 H, d, *J* 15.5 Hz, COCH=C*H*), 7.73 (1 H, dd, *J* 8.5 and 2.0 Hz, Ar CH), 7.86 (1 H, s, Im CH) and 12.30 (1 H, br s, Im NH); **^{13}C NMR** δ_C (100 MHz; DMSO) 55.5 (OCH_3), 55.7 (OCH_3), 110.5 (Ar CH), 110.9 (Ar CH), 117.7 (Im CH), 122.6 (Ar CH), 130.9 (Cq), 135.0 (HC=CH) 135.6 (HC=CH). 138.0 (Im CH) 148.8 (Cq), 152.9 (Cq) and 187.2 (C=O); **MS** m/z (ES^+) Found 259.1082 (MH^+) and 281.0897 (MNa^+), $C_{14}H_{15}N_2O_3$ (MH^+) requires 259.1083 and $C_{14}H_{14}N_2O_3Na$ (MNa^+) requires 281.0902; **HPLC** (analytical, system 1) t_R = 5.6 min.

(*E*)-3-(1*H*-imidazol-4-yl)-1-(3,4,5-trimethoxyphenyl)prop-2-en-1-one (48)

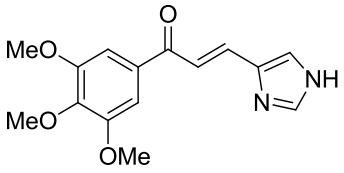

(48)

Following **Method C**, chalcone **(48)** was obtained as an orange solid (0.53 g, 74%).

R_f [CH_2Cl_2:MeOH 9:1] 0.19; **Mp** 174-176 ^oC (EtOAc/heptane); **IR** ν_{max}(film)/ cm^{-1} 3456, 1661 and 1581; **^{1}H NMR** δ_H (400 MHz; $CDCl_3$) 3.85 (6 H, s, OCH_3), 3.89 (3 H, s, OCH_3), 7.26 (2 H, Ar CH), 7.38 (1 H, s, Im CH), 7.69 (1 H, d, *J* 15.5 Hz, COC*H*=CH), 7.77 (1 H, s, Im CH), 7.77 (1 H, d, *J* 15.0 Hz, COCH=C*H*) and 8.17 (1 H, br s, Im NH); **^{13}C NMR** δ_C (100 MHz; $CDCl_3$) 56.2 (OCH_3), 60.9 (OCH_3), 105.9 (Ar CH), 119.3 (Im CH), 123.4 (Im CH), 133.4 (Cq), 134.6 (HC=CH), 135.9 (Cq), 137.2 (HC=CH), 142.3 (Cq), 153.0 (Cq) and 189.1 (C=O); **MS** m/z (ES^+) Found 289.1183 (MH^+), $C_{15}H_{17}N_2O_4$ (MH^+) requires 289.1188; **HPLC** (analytical, system 1) t_R = 5.9 min.

Method D

Chalcone **(48)** (100 mg, 0.347 mmol) was added to a stirred solution of 10wt% Pd/C (20 mg) in MeOH (4 mL) under 1.0 atm of H_2 and stirring continued at 25 ^{o}C for 19 h. The reaction was then quenched with EtOAc (50 mL) and washed through celite with distilled water, the organic layer was extracted with EtOAc (3 × 50 mL) and the organic layers were combined and washed with saturated brine solution (50 mL). The organic fraction was dried (Na_2SO_4), filtered and solvent removed under reduced pressure to give the product **(49)** as a pale yellow oil (57 mg, 57%) without the need for further purification.

3-(1*H*-imidazol-5-yl)-1-(3,4,5-trimethoxyphenyl)propan-1-one (49)

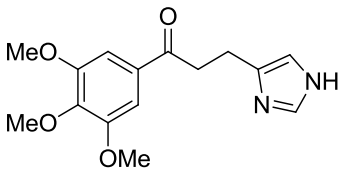

(49)

R_f [CH_2Cl_2:MeOH 9:1] 0.41; **IR** ν_{max}(film)/cm^{-1} 3454, 1678, 1586 and 1505; **^{1}H NMR** δ_H (400 MHz; $CDCl_3$) 3.05 (2 H, t, *J* 7.0 Hz, CH_2), 3.35 (2 H, t, *J* 7.0 Hz, CH_2), 3.89 (6 H, s, OCH_3), 3.90 (3 H, s, OCH_3), 6.85 (1 H, s, Im CH), 7.21 (2 H, s, Ar CH), 7.45 (1 H, br s, Im NH) and 7.65 (1 H, s, Im CH); **^{13}C NMR** δ_C (100 MHz; $CDCl_3$) 20.5 (CH_2), 38.2 (CH_2), 56.3 (OCH_3), 60.9 (OCH_3), 105.5 (Ar CH), 118.2 (Im CH), 131.9 (Cq), 134.2 (Im CH), 135.1 (Cq), 142.7 (Cq), 153.0 (Cq) and 198.7 (C=O); **MS** m/z (ES$^+$) Found 291.1350 (MH^+) and 313.1162 (MNa^+), $C_{15}H_{19}N_2O_4$ (MH^+) requires 291.1345 and (MNa^+) $C_{15}H_{18}N_2O_4Na$ requires 313.1164; **HPLC** (analytical, system 1) t_R = 5.7 min.

Method E

(*E*)-3-(1-methyl-1*H*-imidazol-4-yl)-1-(3,4,5-trimethoxyphenyl)prop-2-en-1-one (51)

Following the procedure reported,[63] except cooled to 0 ^{o}C, NaH (60% dispersion in mineral oil, 1.5 mmol) was added to a stirred solution of chalcone (1.0 mmol) in DMF (5.0 mL) at 0 ^{o}C followed by dropwise addition of MeI (1.5 mmol) and the reaction was kept at 0 ^{o}C and followed by TLC until the disappearance of the chalcone starting material. The reaction was quenched with the addition of EtOAc (50 mL) and H_2O (50 mL), the organic layer separated and the aqueous fraction extracted with EtOAc (2 × 50 mL). The organic fractions were combined and washed with saturated brine solution (20 mL). The organic fraction was dried (Na_2SO_4), filtered and solvent removed under reduced pressure. Crude ^{1}H NMR revealed the presence of chalcone **(50)**, in addition to the product chalcone **(51)** in a ratio of 25:75 **(50:51)**. The mixture was purified by column chromatography with silica gel using CH_2Cl_2:IPA solvent system increasing from 0% to 12% IPA in 1% increments of 200 mL to afford the desired chalcone **(51)** as an orange oil (0.11g, 36%).

(*E*)-3-(1-methyl-1*H*-imidazol-4-yl)-1-(3,4,5-trimethoxyphenyl)prop-2-en-1-one (51)

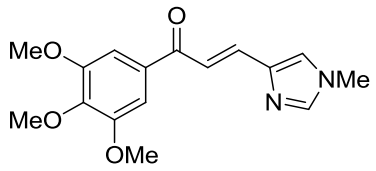

(51)

R_f [CH_2Cl_2:MeOH 9:1] 0.38; **IR** ν_{max}(film)/cm^{-1} 1659, 1603 and 1580; **^{1}H NMR** δ_H (400 MHz; $CDCl_3$) 3.71 (3 H, s, Im CH_3), 3.90 (3 H, s, OCH_3), 3.92 (6 H, s, OCH_3), 7.15 (1 H, s, Im CH), 7.33 (2 H, s, Ar CH), 7.49 (1 H, s, Im CH) and 7.70 (2 H, s, COCH=C*H*); The peak at δ_H 7.70 ppm can vary depending on the concentarion of the sample and can appear as two doublets; **^{1}H NMR – Diluted** δ_H (400 MHz; $CDCl_3$) 3.73 (3 H, s, Im CH_3), 3.92 (3 H, s, OCH_3), 3.94 (6 H, s, OCH_3), 7.17 (1 H, s, Im CH), 7.34 (2 H, s, Ar CH), 7.50 (1 H, s, Im CH), 7.69 (1 H, d, *J* 15.0 Hz, COC*H*=CH) and 7.74 (1 H, d, *J* 15.0 Hz, COCH=C*H*); **^{13}C NMR** δ_C (100 MHz; $CDCl_3$) 33.8 (Im CH_3), 56.4 (OCH_3), 60.9 (OCH_3), 106.0 (Ar CH),

119.6 (Im CH) 124.1 (Im CH), 133.6 (Cq), 135.1 (HC=CH), 138.0 (Cq), 139.1 (HC=CH), 142.3 (Cq), 153.1 (Cq) and 188.9 (C=O); **MS** m/z (ES^+) Found 303.1354 (MH^+) and 325.1166 (MNa^+), $C_{16}H_{19}N_2O_4$ (MH^+) requires 303.1345 and $C_{16}H_{18}N_2O_4Na$ (MNa^+) requires 325.1164; **HPLC** (analytical, system 1) t_R = 5.9 min.

(*E*)-3-(1-methyl-1*H*-imidazol-5-yl)-1-(3,4,5-trimethoxyphenyl)prop-2-en-1-one (50)

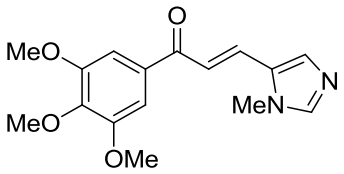

(50)

Following **Method E**, chalcone (**50)** was obtained as an orange oil (0.41 g, 54%).

R_f [CH_2Cl_2:MeOH 9:1] 0.38; **IR** ν_{max}(film)/cm^{-1} 1657, 1591 and 1579; **^{1}H NMR** δ_H (400 MHz; $CDCl_3$) 3.78 (3 H, s, Im CH_3), 3.94 (3 H, s, OCH_3), 3.95 (6 H, s, OCH_3), 7.25 (2 H, s, Ar CH), 7.37 (1 H, d, *J* 15.5 Hz, COC*H*=CH), 7.57 (1 H, s, Im CH), 7.65 (1 H, s, Im CH) and 7.69 (1 H, d, *J* 15.0 Hz, COCH=C*H*); **^{13}C NMR** δ_C (100 MHz; $CDCl_3$) 32.1 (Im CH_3), 56.4 (OCH_3), 61.0 (OCH_3), 105.9 (Ar CH), 119.6 (Im CH), 129.1 (Im CH), 129.6 (Cq), 132.3 (HC=CH), 133.3 (Cq), 141.1 (HC=CH), 142.6 (Cq), 153.1 (Cq) and 188.2 (C=O); **MS** m/z (ES^+) Found 303.1337 (MH^+) and 325.1150 (MNa^+), $C_{16}H_{19}N_2O_4$ (MH^+) requires 303.1345 and $C_{16}H_{18}N_2O_4Na$ (MNa^+) requires 325.1164; **HPLC** (analytical, system 1) t_R = 5.9 min.

(E)-3-(1*H*-imidazol-2-yl)-1-(3,4,5-trimethoxyphenyl)prop-2-en-1-one

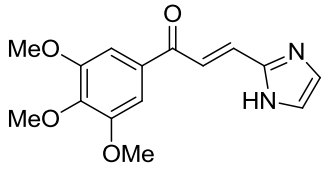

(52)

Following **Method C**, except on a 5.0 mmol scale, chalcone **(52)** was obtained as an yellow solid (0.55 g, 38%).

R_f [CH_2Cl_2:MeOH 9:1] 0.46; **Mp** 198-201 ^oC (EtOAc/heptane); **IR** ν_{max}(film)/cm^{-1} 3439, 1661, 1607 and 1582; **^{1}H NMR** δ_H (400 MHz; $CDCl_3$) 3.89 (6 H, s, OCH_3), 3.93 (3 H, s, OCH_3), 7.26-7.30 (4 H, m, Ar CH and Im CH), 7.75 (1 H, d, *J* 15.0 Hz, COC*H*=CH) and 7.86 (1 H, d, *J* 15.0 Hz, COCH=C*H*); **^{13}C NMR** δ_c (100MHz; $CDCl_3$) 56.3 (OCH_3), 61.0 (OCH_3), 106.1 (Ar CH and Im CH), 122.4 (HC=CH), 131.0 (HC=CH), 132.8 (Cq), 142.8 (Cq), 143.8 (Cq), 153.2 (Cq) and 188.7 (C=O); **MS** m/z (ES^+) Found 289.1184 (MH^+) and 311.0998 (MNa^+), $C_{15}H_{17}N_2O_4$ (MH^+) requires 289.1188 and $C_{15}H_{16}N_2O_4Na$ (MNa^+) requires 311.1008; **HPLC** (analytical, system 1) t_R = 6.0 min.

Method F

Chalcone **(52)** (1.4 mmol) was added to a rapidly stirred solution of 3.0 equivalents of Cs_2CO_3 (4.2 mmol) in THF (30 mL) at 30 ^oC open to the atmosphere for 15 min. followed by dropwise addition of 3.0 equivalents of MeI (4.2 mmol) and stirring continued for 6 h. The reaction was then cooled and quenched by addition of CH_2Cl_2 (50 mL) and distilled water (50 mL) and the organic layer extracted with CH_2Cl_2 (3 × 50 mL), the organic layers were combined and washed with saturated brine solution (50 mL). The organic fraction was dried (Na_2SO_4), filtered and solvent removed under reduced pressure to give a pale yellow oil. The oil was purified by column chromatography with silica using CH_2Cl_2:MeOH 9:1 solvent system to afford the product chalcone **(53)** as a yellow solid (0.23 g, 54%).

(*E*)-3-(1-methyl-1*H*-imidazol-2-yl)-1-(3,4,5-trimethoxyphenyl)prop-2-en-1-one (53)

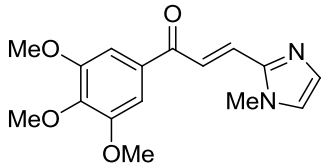

(53)

R_f [CH_2Cl_2:MeOH 9:1] 0.47; **Mp** 100-102 ^oC (EtOAc/heptane); **IR** ν_{max}(film)/cm^{-1} 1658, 1605 and 1580; **^{1}H NMR** δ_H (400 MHz; $CDCl_3$) 3.81 (3 H, s, Im CH_3), 3.93 (3 H, s, OCH_3), 3.94 (6 H, s, OCH_3), 7.03 (1 H, s, Im CH), 7.21 (1 H, s, Im CH), 7.36 (2 H, s, Ar CH), 7.68 (1 H, d, *J* 15.0 Hz, COC*H*=CH) and 8.06 (1 H, d, *J* 15.0 Hz, COCH=C*H*); **^{13}C NMR** δ_C (100

MHz; $CDCl_3$) 33.0 (Im CH_3), 56.4 (OCH_3), 60.9 (OCH_3), 106.0 (Ar CH), 123.9 (HC=CH), 127.2 (Im CH), 130.3 (HC=CH), 131.4 (Im CH), 133.0 (Cq), 142.7 (Cq), 143.7 (Cq), 153.2 (Cq) and 188.1 (C=O); **MS** m/z (ES^+) Found 303.1360 (MH^+) and 325.1172 (MNa^+), $C_{16}H_{19}N_2O_4$ (MH^+) requires 303.1345 and $C_{16}H_{18}N_2O_4Na$ (MNa^+) requires 325.1164; **HPLC** (analytical, system 1) t_R = 5.9 min.

Method G

0.5 equivalent KOH was added to a rapidly stirred solution of the required acetophenone (5.0 mmol) and 3,4,5-trimethoxybenzaldehyde (6.0 mmol) in 20 mL EtOH and allowed to stir at rt (20 ^oC). After 24 h the solvent was removed under reduced pressure and the resulting solid purified by column chromatography with silica gel using PE:EtOAc 6:4 to afford the desired chalcone.

(*E*)-1-phenyl-3-(3,4,5-trimethoxyphenyl)prop-2-en-1-one (58)

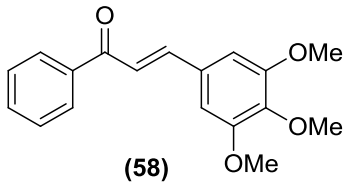

(58)

Following Method G, chalcone **(58)** was obtained as a yellow solid (1.43 g, 96%).

R_f [PE-EtOAc 4:6] 0.65; **Mp** 137-138 ^oC (MeOH); **IR** ν_{max}(film)/cm^{-1} 1662, 1609, 1580, 1508 and 1132; **^{1}H NMR** δ_H (500 MHz; $CDCl_3$) 3.91 (3 H, s, OCH_3), 3.94 (6 H, s, OCH_3), 6.87 (2 H, s, Ar CH), 7.41 (1 H, d, *J* 16.0 Hz, COC*H*=CH), 7.50-7.58 (2 H, m, Ph CH), 7.59-7.61 (1 H, m, Ph CH), 7.72 (1H, d, *J* 15.5 Hz, Ph COCH=C*H*) and 8.02 (2 H, d, *J* 7.0 Hz, Ph CH); **^{13}C NMR** δ_C (125 MHz; $CDCl_3$) 56.2 (OCH_3), 61.0 (OCH_3), 105.7 (CH), 121.5 (CH), 128.5 (CH), 128.6 (CH), 130.4 (Cq), 132.7 (CH), 138.3 (Cq), 140.5 (Cq), 145.0 (CH), 153.5 (Cq) and 190.6 (Cq); **MS** m/z (ES^+) Found 299.1253 (MH^+) and 321.1113 (MNa^+), $C_{18}H_{19}O_4$ (MH^+) requires 299.1283 and $C_{18}H_{18}O_4Na$ (MNa^+) requires 321.1103; **Elemental Analysis** Found C (72.49%) H (6.11%) N (0.00%) requires C (72.47%) H (6.08%) N (0.00%); **HPLC** (analytical, system 2) t_R = 9.0 min.

(*E*)-1-(4-methoxyphenyl)-3-(3,4,5-trimethoxyphenyl)prop-2-en-1-one (59)

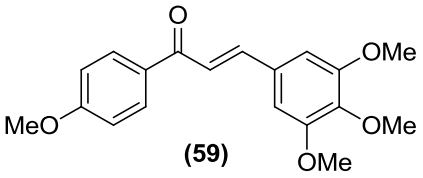

(59)

Following Method G, chalcone **(59)** was obtained as a yellow solid (1.28 g, 78%).

R_f [PE-EtOAc 4:6] 0.44; **Mp** 135-138 ^{o}C (EtOAc); **IR** ν_{max}(film)/cm^{-1} 1605, 1505, 1327 and 1128; **^{1}H NMR** δ_H (500 MHz; $CDCl_3$) 3.89 (3 H, s, OCH_3), 3.90 (3 H, s, OCH_3), 3.92 (6 H, s, OCH_3), 6.86 (2 H, s, Ar CH), 6.99 (2 H, d, *J* 9.0 Hz, Ar CH), 7.42 (1 H, d, *J* 15.5 Hz, COC*H*=CH), 7.71 (1 H, d, *J* 15.5 Hz, COCH=C*H*) and 8.04 (2 H, d, *J* 9.0 Hz, Ar CH); **^{13}C NMR** δ_C (125 MHz; $CDCl_3$) 55.5 (OCH_3), 56.2 (OCH_3), 60.9 (OCH_3), 105.6 (CH), 113.8 (CH), 121.2 (CH), 130.6 (CH), 130.8 (CH), 131.1 (Cq), 140.3 (Cq), 144.1 (Cq), 153.5 (Cq), 163.4 (Cq) and 188.7 (Cq); **MS** m/z (ES$^+$) Found 329.1400 (MH^+) and 351.1209 (MNa^+), $C_{19}H_{21}O_5$ (MH^+) requires 329.1389 and $C_{19}H_{20}O_5Na$ (MH^+) requires 351.1208; **Elemental Analysis** Found C (69.58%) H (6.22%) N (0.00%) requires C (69.50%) H (6.14%) N (0.00%); **HPLC** (analytical, system 2) t_R = 5.2 min.

(*E*)-1-(4-(benzyloxy)phenyl)-3-(3,4,5-trimethoxyphenyl)prop-2-en-1-one (60)

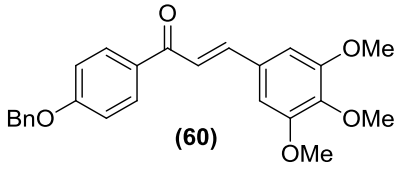

(60)

Following Method G, chalcone **(60)** was obtained as a pale yellow solid (1.61 g, 80%).

R_f [PE-EtOAc 4:6] 0.53; **Mp** 139-140 ^{o}C; **IR** ν_{max}(film)/cm^{-1} 1603, 1419, 1243 and 702; **^{1}H NMR** δ_H (500 MHz; $CDCl_3$) 3.85 (3 H, s, OCH_3), 3.90 (6 H, s, OCH_3), 5.14 (2 H, s, CH_2), 6.86 (2 H, s, Ar CH), 7.05 (2 H, d, *J* 8.5 Hz, Ar CH), 7.34-7.44 (6 H, m, Ph CH and COC*H*=CH), 7.71 (1 H, d, *J* 15.5 Hz, COCH=C*H*) and 8.03 (2 H, d, *J* 8.5 Hz, Ar CH); **^{13}C NMR** δ_c (125 MHz; $CDCl_3$) 56.2 (OCH_3), 60.9 (OCH_3), 70.1 (CH_2), 105.5 (CH), 114.6 (CH), 121.1 (CH), 127.4 (CH), 128.2 (CH), 128.6 (CH), 130.5 (Cq), 130.7 (CH), 131.3 (Cq), 136.1 (Cq), 140.2 (Cq), 144.1 (CH), 153.4 (Cq), 162.5 (Cq) and 188.6 (Cq); **MS** m/z (ES$^+$) Found 427.1572 (MNa^+), $C_{25}H_{24}O_5Na$ (MNa^+) requires 427.1521; **Elemental Analysis**

Found C (74.13%) H (6.09%) N (0.00%) requires C (74.24%) H (5.98%) N (0.00%); **HPLC** (analytical, system 2) t_R = 5.6 min.

(*E*)-1-(4-hydroxyphenyl)-3-(3,4,5-trimethoxyphenyl)prop-2-en-1-one (61)

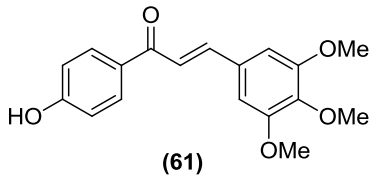

(61)

Following Method G, except using 2 equivalents of KOH and a reaction time of 72 h, chalcone **(61)** was obtained as a yellow solid (0.685 g, 44%).

R_f [CH_2Cl_2-MeOH 9:1] 0.45; **Mp** 240-244 ^oC (MeOH); **IR** ν_{max}(film)/cm^{-1} 3650, 1431, 1240 and 1037; **^{1}H NMR** δ_H (500 MHz; DMSO) 3.71 (3 H, s, OCH_3), 3.86 (6 H, s, OCH_3), 6.90 (2 H, d, *J* 8.5 Hz, Ar CH), 7.20 (2 H, s, Ar CH), 7.63 (1 H, d, *J* 15.5 Hz, COC*H*=CH), 7.86 (1 H, d, *J* 15.5 Hz, COCH=C*H*), 8.08 (2 H, d, *J* 9.0 Hz, Ar CH) and 10.26-10.60 (1H, br s, OH); **^{13}C NMR** δ_C (125 MHz; DMSO) 56.1 (OCH_3), 60.1 (OCH_3), 106.3 (CH), 115.4 (CH), 121.3 (CH), 129.1 (Cq), 130.5 (Cq), 131.2 (CH), 139.5 (Cq), 143.2 (CH), 153.1 (Cq), 162.3 (Cq) and 187.0 (Cq); **MS** m/z (ES^+) Found 315.1249 (MH^+) and 337.1057 (MNa^+), $C_{18}H_{19}O_5$ (MH^+) requires 315.1232 and $C_{18}H_{18}O_5Na$ (MNa^+) requires 337.1052; **Elemental Analysis** Found C (68.64%) H (5.84%) N (0.00%) requires C (68.78%) H (5.37%) N (0.00%).

Method H

1-(4-nitrophenyl)ethanone (5.0 mmol) and 3,4,5-trimethoxybenzaldehyde (5.0 mmol) in EtOH (20 mL) were stirred on ice for 10 min, followed by the slow addition of 0.2 equivalent NaOH in 10 mL H_2O. Stirring was continued on ice for 2 h after which the solution was poured onto ice and the solid filtered and dried to give a yellow solid. The solid was purified by column chromatography with silica gel using PE:EtOAc 6:4 to afford the desired chalcone as a yellow solid (1.31g, 76%).

(*E*)-1-(4-nitrophenyl)-3-(3,4,5-trimethoxyphenyl)prop-2-en-1-one (62)

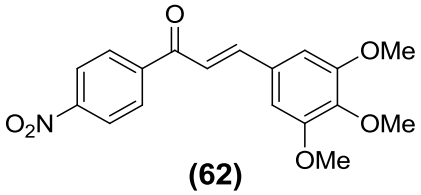

(62)

R_f [CH_2Cl_2-MeOH 9:1] 0.93; **Mp** 172-174 ^oC (MeOH); **IR** ν_{max}(film)/cm^{-1} 1605, 1505, 1327 and 1128; **^{1}H NMR** δ_H (500 MHz; $CDCl_3$) 3.92 (3 H, s, OCH_3), 3.93 (6 H, s, OCH_3), 6.87 (2 H, s, Ar CH), 7.35 (1 H, d, *J* 16.0 Hz, COC*H*=CH), 7.75 (1 H, d, *J* 15.5 Hz, COCH=C*H*), 8.14 (2 H, d, *J* 8.5 Hz, Ar CH) and 8.36 (2 H, d, *J* 9.0 Hz, Ar CH); **^{13}C NMR** δ_C (125 MHz; $CDCl_3$) 56.3 (OCH_3), 61.0 (OCH_3), 106.0 (CH), 120.6 (CH), 123.9 (CH), 129.4 (CH), 129.7 (Cq), 141.1 (Cq), 143.2 (CH), 147.0 (Cq), 150.0 (Cq), 153.6 (Cq) and 189.1 (Cq); **MS** m/z (ES^+) Found 366.0965 (MNa^+), $C_{18}H_{17}NO_6Na$ (MNa^+) requires 366.0953; **Elemental Analysis** Found C (62.91%) H (4.93%) N (4.16%) requires C (62.97%) H (4.99%) N (4.08%); **HPLC** (analytical, system 2) t_R = 14.2 min.

Method I

2.0 equivalents of KOH was added to a rapidly stirred solution of 1-(4-aminophenyl)ethanone (5.0 mmol) and 3,4,5-trimethoxybenzaldehyde (5.0 mmol) in EtOH (20 mL) at rt (20 ^oC). After 18 h the reaction mixuture was poured onto ice and the solid collected and purified by column chromatography with silica gel using PE:EtOAc 6:4 to afford the desired chalcone as a yellow solid (0.93g, 59%).

(*E*)-1-(4-aminophenyl)-3-(3,4,5-trimethoxyphenyl)prop-2-en-1-one (63)

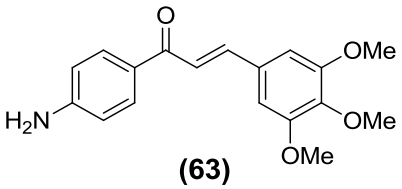

(63)

R_f [CH_2Cl_2-MeOH 9:1] 0.73; **Mp** 159-160 ^oC; **IR** ν_{max}(film)/cm^{-1} 3694, 3513, 1621 and 1282; **^{1}H NMR** δ_H (500 MHz; $CDCl_3$) 3.89 (3 H, s, OCH_3), 3.92 (6 H, s, OCH_3), 4.16 (2 H, s, NH_2), 6.71 (2 H, d, *J* 8.5 Hz, Ar CH), 6.86 (2 H, s, Ar CH), 7.41 (1 H, d, *J* 15.5 Hz, COC*H*=CH), 7.69 (1 H, d, *J* 16.0 Hz, COCH=C*H*) and 7.93 (2 H, d, *J* 8.5 Hz, Ar CH); **^{13}C NMR** δ_C (125 MHz; $CDCl_3$) 56.2 (OCH_3), 61.0 (OCH_3), 105.5 (CH), 113.9 (CH), 121.4 (CH), 128.6 (Cq), 130.8 (Cq), 131.1 CH), 140.0 (Cq), 143.3 (CH), 151.0 (Cq), 153.4 (Cq) and 188.0 (Cq); **MS** m/z (ES^+) Found 314.1394 (MH^+) and 336.1227 (MNa^+), $C_{18}H_{20}N_1O_4$ (MH^+) requires 314.1392 and $C_{18}H_{19}N_1O_4Na$ (MNa^+) requires 336.1212; **Elemental Analysis** Found C (68.83%) H (6.14%) N (4.47%) requires C (68.99%) H (6.11%) N (4.47%); **HPLC** (analytical, system 2) t_R = 5.9 min.

(*E*)-1-(pyridin-2-yl)-3-(3,4,5-trimethoxyphenyl)prop-2-en-1-one (64)

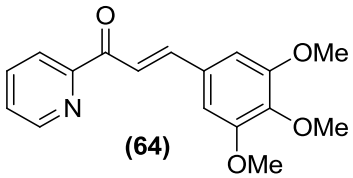

(64)

Following Method G, except using 10.0 mmol 1-(pyridin-2-yl)ethanone and 12.0 mmol 3,4,5-trimethoxybenzaldehyde, chalcone **(64)** was obtained as a yellow solid (2.54 g, 85%).

R_f [PE-EtOAc 4:6] 0.77; **Mp** 155-156 ^oC (MeOH); **IR** ν_{max}(film)/cm^{-1} 1605, 1217 and 791; **^{1}H NMR** δ_H (500 MHz; $CDCl_3$) 3.89 (3 H, s, OCH_3), 3.92 (6 H, s, OCH_3), 6.94 (2 H, s, Ar CH), 7.45 (1 H, dd, *J* 8.0, 5.0 and 1.0 Hz, py CH), 7.86 (1 H, d, *J* 16.0 Hz, COC*H*=CH), 8.16

(1 H, d, *J* 16.0 Hz, COCH=C*H*), 8.18-8.19 (1 H, m, py CH) and 8.73-8.74 (1 H, m, py CH); **^{13}C NMR** δ_C (125 MHz; $CDCl_3$) 56.2 (OCH_3), 60.9 (OCH_3), 106.0 (CH), 119.9 (CH), 122.9 (CH), 126.8 (CH), 130.6 (Cq), 137.0 (CH), 140.5 (Cq), 145.0 (CH), 148.7 (CH), 153.4 (Cq), 154.2 (Cq) and 189.2 (Cq); **MS** m/z (ES^+) Found 322.1074 (MNa^+), $C_{17}H_{17}NO_4Na$ (MNa^+) requires 322.1055; **Elemental Analysis** Found C (68.35%) H (5.79%) N (4.72%) requires C (68.21%) H (5.72%) N (4.68%); **HPLC** (analytical, system 2) t_R = 5.4 min.

(*E*)-1-(furan-2-yl)-3-(3,4,5-trimethoxyphenyl)prop-2-en-1-one (65)

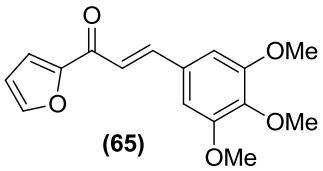

(65)

Following Method G, chalcone **(65)** was obtained as a dark orange solid (1.18 g, 80%).

R_f [PE-EtOAc 4:6] 0.74; **Mp** 150-152 ^oC (EtOAc); **IR** ν_{max}(film)/cm^{-1} 1655, 1579, 1508, 1461 and 1130; **^{1}H NMR** δ_H (500 MHz; $CDCl_3$) 3.90 (3 H, s, OCH_3), 3.92 (6 H, s, OCH_3), 6.60 (1 H, dd, *J* 3.5 and 1.5 Hz, furan CH), 6.88 (2 H, s, Ar CH), 7.34 (1 H, d, *J* 15.5 Hz, COC*H*=CH), 7.34 (1 H, dd, *J* 3.5 and 0.5 Hz, furan CH) 7.66 (1 H, dd, *J* 1.5 and 0.5 Hz, furan CH) and 7.80 (1 H, d, *J* 16.0 Hz, COCH=C*H*); **^{13}C NMR** δ_C (125 MHz; $CDCl_3$) 56.2 (OCH_3), 61.0 (OCH_3), 105.8 (CH), 112.6 (CH), 117.4 (CH), 120.4 (CH), 130.2 (Cq), 140.5 (Cq),144.1 (CH) 146.4 (CH), 153.5 (Cq), 153.7 (Cq) and 177.9 (Cq); **MS** m/z (ES^+) Found 289.1139 (MH^+) and 311.0938 (MNa^+), $C_{16}H_{17}O_5$ (MH^+) requires 289.1076 and $C_{16}H_{16}O_5Na$ (MNa^+) requires 311.0895; **Elemental Analysis** Found C (66.78%) H (5.71%) N (0.00%) requires C (66.66%) H (5.59%) N (0.00%).

(*E*)-1-(thiophen-2-yl)-3-(3,4,5-trimethoxyphenyl)prop-2-en-1-one (66)

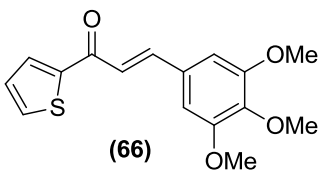

(66)

Following Method G, chalcone **(66)** was obtained as a dark orange solid (1.41 g, 93%).

R_f [PE-EtOAc 4:6] 0.86; **Mp** 153-156 ^{o}C (EtOAc); **IR** ν_{max}(film)/cm^{-1} 1655, 1584, 1504 and 1130; **^{1}H NMR** δ_H (500 MHz; $CDCl_3$) 3.90 (3 H, s, OCH_3), 3.93 (6 H, s, OCH_3), 6.87 (2H, s, Ar CH), 7.19 (1 H, dd, *J* 5.0 and 3.5 Hz, thiophene CH), 7.30 (1 H, d, *J* 15.5 Hz, COC*H*=CH), 7.69 (1 H, dd, *J* 5.0 and 1.0 Hz, thiophene CH), 7.77 (1 H, d, *J* 15.5 Hz, COCH=C*H*) and 7.88 (1 H, dd, *J* 3.5 and 1.0 Hz, thiophene CH); **^{13}C NMR** δ_C (125 MHz; $CDCl_3$) 56.2 (OCH_3), 61.0 (OCH_3), 105.7 (CH), 120.9 (CH), 128.2 (CH), 130.2 (Cq), 131.7 (CH), 133.8 (CH), 140.5 (Cq), 144.2 (CH), 145.5 (Cq), 153.5 (Cq) and 181.9 (Cq); **MS** m/z (ES$^+$) Found 305.0935 (MH$^+$) and 327.0763 (MNa$^+$), $C_{16}H_{17}O_4S$ (MH$^+$) requires 305.0848 and $C_{17}H_{18}N_4SNa$ (MNa$^+$) requires 327.0667; **Elemental Analysis** Found C (63.03%) H (5.20%) N (0.00%) requires C (63.14%) H (5.30%) N (0.00%).

(*E*)-1-(naphthalen-2-yl)-3-(3,4,5-trimethoxyphenyl)prop-2-en-1-one (67)

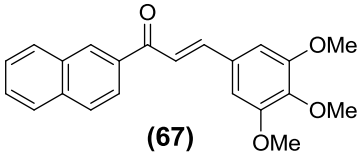

(67)

Following Method G, chalcone **(67)** was obtained as a dark orange solid (1.22 g, 70%).

R_f [PE-EtOAc 4:6] 0.89; **Mp** 115-116 ^{o}C (MeOH); **IR** ν_{max}(film)/cm^{-1} 1655, 1579, 1508 and 1125; **^{1}H NMR** δ_H (500 MHz; $CDCl_3$) 3.92 (3 H, s, OCH_3), 3.95 (6 H, s, OCH_3), 6.91 (2 H, s, CH), 7.55 (1 H, d, *J* 16.0 Hz, COC*H*=CH), 7.56-7.62 (3 H, m, CH), 7.79 (1 H, d, *J* 16.0 Hz, COCH=C*H*), 7.91 (1 H, d, *J* 8.0 Hz, Ar CH), 7.95 (1 H, d, *J* 8.5 Hz, Ar CH), 8.01 (1 H, d, *J* 7.5 Hz, Ar CH) and 8.53 (1 H, s, Ar CH); **^{13}C NMR** δ_C (125 MHz; $CDCl_3$) 56.3 (OCH_3), 61.0 (OCH_3), 105.8 (CH), 121.6 (CH), 124.5 (CH), 126.8 (CH), 127.8 (CH), 128.3 (CH), 128.6 (CH), 129.5 (CH), 129.8 (CH), 130.4 (Cq), 132.6 (Cq), 135.4 (Cq), 135.6 (Cq), 140.5 (Cq), 145.0 (CH), 153.5 (Cq) and 190.4 (Cq); **MS** m/z (ES$^+$) Found 371.1259 (MNa$^+$), $C_{22}H_{20}O_4Na$ (MNa$^+$) requires 371.1300; **Elemental Analysis** Found C (75.93%) H (5.83%) N (0.00%) requires C (75.84%) H (5.79%) N (0.00%); **HPLC** (analytical, system 2) t_R = 14.3 min.

Method J

Hydrazine monohydrate (8.0 mmol) was added to a rapidly stirred solution of chalcone **(58)** (2.0 mmol) in EtOH (20 mL) and heated to 80 ^{o}C for 2 h. The solvent was removed under reduced pressure and the resulting brown oil was dissolved in CH_2Cl_2 (20 mL) and 3-(benzyloxy)-4-methoxybenzoyl chloride (4.0 mmol) added dropwise followed by NEt_3 (6.0 mmol) and the solution stirred at rt for 3 h. The solvent was then removed under reduced pressure and the solid was purified by column chromatography with silica gel using PE:EtOAc 6:4 to afford the desired pyrazoline **(68)** as a white solid (0.60g, 54%).

(3-(benzyloxy)-4-methoxyphenyl)(3-phenyl-5-(3,4,5-trimethoxyphenyl)-4,5-dihydro-1H-pyrazol-1-yl)methanone (68)

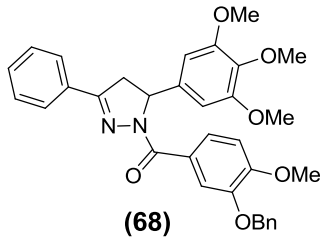

(68)

R_f [PE-EtOAc 4:6] 0.53; **Mp** 75-78 ^{o}C; **IR** ν_{max}(film)/cm^{-1} 1627, 1598, 1437 and 1125; **^{1}H NMR** δ_H (500 MHz; $CDCl_3$) 3.17 (1 H, dd, *J* 17.5 and 5.5 Hz, pyrazoline CH), 3.75 (1 H, dd, *J* 17.5 and 12.0 Hz, pyrazoline CH), 3.79 (3 H, s, OCH_3), 3.80 (6 H, s, OCH_3), 3.96 (3 H, s, OCH_3), 5.20 (2 H, s, Bn CH_2), 5.72 (1 H, dd, *J* 11.5 and 5.0 Hz, pyrazoline CH), 6.49 (2 H, s, Ar CH), 6.97 (1 H, d, *J* 8.5 Hz, Ar CH), 7.26-7.35 (4 H, m, Ar CH), 7.40-7.45 (5 H, m, Ar CH), 7.72-7.77 (3 H, m, Ar CH) and 7.87 (1 H, d, *J* 8.5 Hz, Ar CH); **^{13}C NMR** δ_C (125 MHz; $CDCl_3$) 41.5 (CH_2), 56.0 (OCH_3), 56.0 (OCH_3), 60.7 (OCH_3), 61.8 (CH), 70.9 (CH_2), 102.1 (CH), 110.2 (CH), 115.8 (CH), 124.8 (CH), 126.1 (CH), 126.7 (CH), 127.3 (CH), 127.9 (CH), 128.5 (CH), 128.8 (CH), 130.4 (CH), 131.3 (Cq), 136.8 (Cq), 137.1 (Cq), 137.8 (Cq), 147.3 (Cq), 152.1 (Cq), 153.6 (Cq), 154.6 (Cq) and 165.5 (Cq);

MS m/z (ES^+) Found 553.2318 (MH^+) and 575.2170 (MNa^+), $C_{33}H_{33}N_2O_6$ (MH^+) requires 553.2339 and $C_{33}H_{32}N_2O_6Na$ (MNa^+) requires 575.2158; **Elemental Analysis** Found C (71.65%) H (5.76%) N (5.05%) requires C (71.72%) H (5.84%) N (5.07%); **HPLC** (analytical, system 2) t_R = 16.7 min.

Method K

Pyrazoline **(68)** (0.4 mmol) was added to a stirred solution of 10wt% Pd/C (22 mg) in EtOAc (5 mL) under 1 atm of H_2 and stirring continued at rt for 18 h. The solution was filtered through filter paper and the solvent removed under reduced pressure to a solid which was recrystallised from EtOAc to give pyrazoline **(69)** as a grey solid (0.15g, 81%).

(3-hydroxy-4-methoxyphenyl)(3-phenyl-5-(3,4,5-trimethoxyphenyl)-4,5-dihydro-1*H*-pyrazol-1-yl)methanone (69)

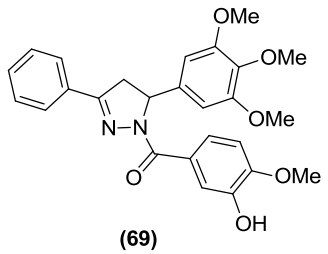

(69)

R_f [PE-EtOAc 4:6] 0.29; **Mp** 218-220 ^oC (EtOAc); **IR** ν_{max}(film)/cm^{-1} 3546, 1631, 1589, 1423 and 1130; **^{1}H NMR** δ_H (500 MHz; $CDCl_3$) 3.17 (1 H, dd, *J* 17.5 and 5.0 Hz, pyrazoline CH), 3.75 (1 H, dd, *J* 18.0 and 12.0 Hz, pyrazoline CH), 3.79 (3 H, s, OCH_3), 3.81 (6 H, s, OCH_3), 3.95 (3 H, s, OCH_3), 5.74 (1 H, dd, *J* 12.0 and 5.0 Hz, pyrazoline CH), 5.79 (1 H, s, OH), 6.51 (2 H, s, Ar CH), 6.91 (2 H, d, *J* 8.5 Hz, Ar CH), 7.40-7.43 (3 H, m, Ar CH) and 7.67-7.76 (4 H, m, Ar CH); **^{13}C NMR** δ_C (125 MHz; $CDCl_3$) 41.5 (CH_2), 56.0 (OCH_3), 61.0 (OCH_3), 61.6 (OCH_3), 102.1 (CH), 109.5 (CH), 116.8 (CH), 123.3 (CH), 126.6 (CH), 126.7 (CH), 127.0 (CH), 127.3 (CH), 130.4 (Cq), 131.2 (Cq), 137.1 (Cq), 137.8 (Cq), 144.6 (Cq), 149.0 (Cq), 153.6 (Cq), 154.5 (Cq) and 165.6 (Cq); **MS** m/z (ES^+) Found 463.1847 (MH^+) and 485.1696 (MNa^+), $C_{26}H_{27}N_2O_6$ (MH^+) requires 463.1869

and $C_{26}H_{26}N_2O_6Na$ (MNa^+) requires 485.1689; **Elemental Analysis** Found C (67.55%) H (5.56%) N (5.94%) requires C (67.52%) H (5.67%) N (6.06%); **HPLC** (analytical, system 2) t_R = 5.9 min.

(4-methoxyphenyl)(3-phenyl-5-(3,4,5-trimethoxyphenyl)-4,5-dihydro-1*H*-pyrazol-1-yl)methanone (70)

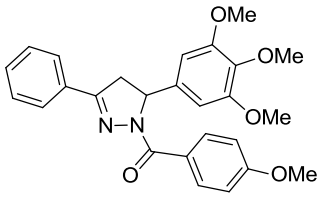

(70)

Following Method J, except using 5.0 mmol chalcone **(58)** and 10.0 mmol 4-methoxybenzoyl chloride, pyrazoline **(70)** was obtained as a white solid (1.51 g, 68%).

R_f [PE-EtOAc 4:6] 0.62; **Mp** 141-143 ^oC (Et_2O); **IR** ν_{max}(film)/cm^{-1} 1627, 1593, 1428 and 1130; **^{1}H NMR** δ_H (500 MHz; $CDCl_3$) 3.19 (1 H, dd, *J* 17.5 and 5.0 Hz, pyrazoline CH), 3.77 (1 H, dd, *J* 18.0 and 12.0 Hz, pyrazoline CH), 3.80 (3 H, s, OCH_3), 3.82 (6 H, s, OCH_3), 3.88 (3 H, s, OCH_3), 5.75 (1 H, dd, *J* 12.0 and 5.0 Hz, pyrazoline CH), 6.52 (2 H, s, Ar CH_2), 6.97 (2 H, d, *J* 9.0 Hz, Ar CH), 7.41-7.43 (3 H, m, Ar CH), 7.72-7.74 (2 H, m, Ar CH) and 8.11 (2 H, d, *J* 9.0 Hz, Ar CH); **^{13}C NMR** δ_C (125 MHz; $CDCl_3$) 41.6 (CH_2), 55.3 (OCH_3), 56.0 (OCH_3), 60.7 (OCH_3), 61.6 (CH), 102.2 (CH), 113.0 (CH), 126.3 (Cq), 126.7 (CH), 128.7 (CH), 130.4 (CH), 131.3 (Cq), 132.3 (CH), 137.2 (Cq), 137.8 (Cq), 153.6 (Cq), 154.4 (Cq), 161.8 (Cq) and 165.8 (Cq); **MS** m/z (ES^+) Found 447.1944 (MH^+) and 469.1746 (MNa^+), $C_{26}H_{27}N_2O_5$ (MH^+) requires 447.1919 and $C_{26}H_{26}N_2O_5Na$ (MNa^+) requires 469.1739; **Elemental Analysis** Found C (70.03%) H (5.76%) N (6.18%) requires C (69.94%) H (5.87%) N (6.27%); **HPLC** (analytical, system 2) t_R = 12.1 min.

Phenyl(3-phenyl-5-(3,4,5-trimethoxyphenyl)-4,5-dihydro-1*H*-pyrazol-1-yl)methanone (71)

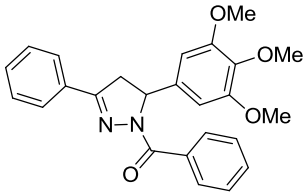

(71)

Following Method J, except using 1.0 mmol chalcone **(58)** and 2.0 mmol benzoyl chloride, pyrazoline **(71)** was obtained as a white solid (0.35 g, 84%).

R_f [PE-EtOAc 4:6] 0.73; **Mp** 124-126 ^{o}C (Et_2O); **IR** ν_{max}(film)/cm^{-1} 1630, 1591, 1424, 1231 and 1132; **^{1}H NMR** δ_H (500 MHz; $CDCl_3$) 3.21 (1 H, dd, *J* 17.5 and 5.0 Hz, pyrazoline CH), 3.78 (1 H, dd, *J* 17.5 and 11.5 Hz, pyrazoline CH), 3.81 (3 H, s, OCH_3), 3.82 (6 H, s, OCH_3), 5.76 (1 H, dd, *J* 11.5 and 5.0 Hz, pyrazoline CH), 6.53 (2 H, s, Ar CH), 7.39-7.52 (6 H, m, Ar CH), 7.71 (2 H, d, *J* 8.0 Hz, Ar CH) and 8.03 (2 H, d, *J* 7.5 Hz, Ar CH); **^{13}C NMR** δ_C (125 MHz; $CDCl_3$) 41.8 (CH_2), 56.1 (OCH_3), 60.7 (OCH_3), 61.4 (CH), 102.3 (CH), 126.8 (CH), 127.7 (CH), 128.7 (CH), 130.0 (CH), 130.5 (CH), 131.0 (CH), 131.3 (Cq), 133.8 (Cq), 137.4 (Cq), 137.6 (Cq), 153.7 (Cq), 154.8 (Cq) and 166.6 (Cq); **MS** m/z (ES^+) Found 417.1873 (MH^+) and 439.1663 (MNa^+), $C_{25}H_{25}N_2O_4$ (MH^+) requires 417.1814 and $C_{25}H_{24}N_2O_4Na$ (MNa^+) requires 439.1633; **Elemental Analysis** Found C (71.96%) H (5.71%) N (6.62%) requires C (72.1%) H (5.81%) N (6.73%); **HPLC** (analytical, system 2) t_R = 9.3 min.

(71+) HPLC (semipreparative, system 3); NMR data consistent with above; **α_D^{20}** +70 (0.001, EtOAc); **HPLC** (analytical, system 4) t_R = 12.3 min, 97% ee.

(71-) HPLC (semipreparative, system 3); NMR data consistent with above; **α_D^{20}** -70 (0.001, EtOAc); **HPLC** (analytical, system 4) t_R = 22.0 min, 98% ee.

Naphthalen-1-yl(3-phenyl-5-(3,4,5-trimethoxyphenyl)-4,5-dihydro-1*H*-pyrazol-1-yl)methanone (72)

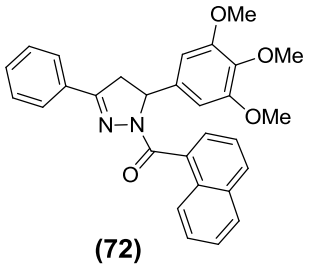

(72)

Following Method J, except using 1.0 mmol chalcone **(58)** and 2.0 mmol 1-naphthoyl chloride, pyrazoline **(72)** was obtained as a white solid (0.39 g, 84%).

R_f [PE-EtOAc 4:6] 0.63; **Mp** 138-141 ^{o}C (Et_2O); **IR** ν_{max}(film)/cm^{-1} 1641, 1598, 1428 and 1130; **^{1}H NMR** δ_H (500 MHz; $CDCl_3$) 3.26 (1 H, dd, *J* 17.5 and 4.5 Hz, pyrazoline CH), 3.83-3.94 (10 H, m, OCH_3 and pyrazoline CH), 5.88 (1 H, dd, *J* 11.5 and 4.5 Hz, pyrazoline CH), 6.63 (2 H, s, Ar CH), 7.29-7.37 (3 H, m, Ar CH), 7.44-7.56 (5 H, m, Ar CH), 7.69 (1 H, d, *J* 7.0 Hz, Ar CH), 7.90 (1 H, d, *J* 8.0 Hz, Ar CH), 7.95 (1 H, *J* 8.0 Hz, Ar CH) and 8.03 (1 H, *J* 8.0 Hz, Ar CH); **^{13}C NMR** δ_C (125 MHz; $CDCl_3$) 42.3 (CH_2), 56.1 (OCH_3), 60.8 (OCH_3), 60.8 (CH), 102.1 (CH), 124.5 (CH), 125.5 (CH), 126.0 (CH), 126.3 (CH), 126.5 (CH), 126.7 (CH), 128.3 (CH), 128.6 (CH), 129.9 (CH), 130.4 (CH), 130.5 (Cq), 131.0 (Cq), 133.3 (Cq), 133.4 (Cq), 137.3 (Cq), 137.5 (Cq), 153.8 (Cq), 154.8 (Cq) and 167.4 (Cq); **MS** m/z (ES^+) Found 467.2001 (MH^+) and 489.1818 (MNa^+), $C_{29}H_{27}N_2O_4$ (MH^+) requires 467.1970 and $C_{29}H_{26}N_2O_4Na$ (MNa^+) requires 489.1790; **Elemental Analysis** Found C (74.70%) H (5.64%) N (5.84%) requires C (74.66%) H (5.62%) N (6.00%); **HPLC** (analytical, system 2) t_R = 11.2 min.

Method L

Phenyl hydrazine (6.0 mmol) was added to a rapidly stirred solution of chalcone **(58)** (3.0 mmol) in EtOH (20 mL) and heated to 80 ^{o}C for 3 h. The solvent was then removed under reduced pressure and the solid was purified by column chromatography with silica gel using PE:EtOAc 6:4 to afford the desired pyrazoline **(73)** as a yellow solid (0.67g, 58%).

1,3-diphenyl-5-(3,4,5-trimethoxyphenyl)-4,5-dihydro-1*H*-pyrazole (73)

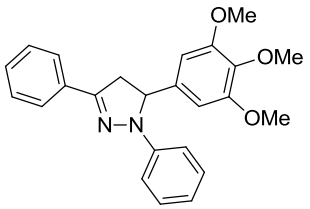

(73)

R_f [PE-EtOAc 4:6] 0.87; **Mp** 173-174 ^{o}C; **IR** ν_{max}(film)/cm^{-1} 1593, 1504 and 1125; ^{1}**H NMR** δ_H (500 MHz; DMSO) 3.15 (1 H, dd, *J* 17.5 and 7.0 Hz, pyrazoline CH), 3.63 (3 H, s, OCH_3), 3.70 (6 H, s, OCH_3), 3.90 (1 H, dd, *J* 17.5 and 12.0 Hz, pyrazoline CH), 5.34 (1 H, dd, *J* 12.0 and 7.5 Hz, pyrazoline CH), 6.63 (2 H, s, Ar CH), 6.75 (1 H, t, *J* 7.0 Hz, Ar CH), 7.05 (2 H, d, *J* 8.0 Hz, Ar CH), 7.18 (2 H, t, *J* 7.5 Hz, Ar CH), 7.37-7.44 (3 H, m, Ar CH) and 7.75 (2 H, d, *J* 8.0 Hz, Ar CH); **^{13}C NMR** δ_C (125 MHz; DMSO) 43.1 (CH_2), 55.8 (OCH_3), 59.9 (OCH_3), 63.9 (CH), 102.9 (CH), 113.1 (CH), 118.8 (CH), 125.7 (CH), 128.6 (CH), 128.7 (CH), 128.8 (CH), 132.2 (Cq), 136.5 (Cq), 138.4 (Cq), 144.8 (Cq), 147.5 (Cq) and 153.3 (Cq); **MS** m/z (ES$^+$) Found 411.1747 (MNa^+), $C_{24}H_{24}N_2O_3Na$ (MNa^+) requires 411.1685; **Elemental Analysis** Found C (74.29%) H (6.21%) N (7.16%) requires C (74.21%) H (6.23%) N (7.21%); **HPLC** (analytical, system 2) t_R = 14.3 min.

(3-(4-methoxyphenyl)-5-(3,4,5-trimethoxyphenyl)-4,5-dihydro-1*H*-pyrazol-1-yl)(phenyl)methanone (74)

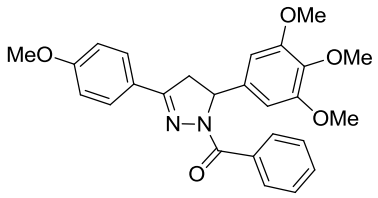

(74)

Following Method J, except using 1.0 mmol chalcone **(59),** pyrazoline **(74)** was obtained as a white solid (0.27 g, 61%).

R_f [PE-EtOAc 4:6] 0.55; **Mp** 126-128^{o}C (EtOAc); **IR** ν_{max}(film)/cm^{-1} 1630, 1598, 1452 and 1420; **^{1}H NMR** δ_H (500 MHz; $CDCl_3$) 3.18 (1 H, dd, *J* 17.5 and 5.0 Hz, pyrazoline CH), 3.75 (1 H, dd, *J* 17.5 and 11.5 Hz, pyrazoline CH), 3.81 (3 H, s, OCH_3), 3.82 (3 H, s, OCH_3), 3.84 (3 H, s, OCH_3), 5.74 (1 H, dd, *J* 11.5 and 4.5 Hz, pyrazoline CH), 6.53 (2 H, s, Ar CH), 6.92 (2 H, d, *J* 7.0 Hz, Ar CH), 7.44-7.51 (3 H, m, Ar CH), 7.65 (2 H, d, *J* 8.5 Hz, Ar CH) and 8.03 (2 H, d, *J* 7.0 Hz, Ar CH); **^{13}C NMR** δ_C (125 MHz; $CDCl_3$) 41.8 (CH_2), 55.4 (OCH_3), 56.1 (OCH_3), 60.7 (OCH_3), 61.3 (CH), 102.4 (CH), 114.2 (CH), 123.9 (Cq), 127.7 (CH), 128.4 (CH), 130.0 (CH), 130.9 (CH), 134.5 (Cq), 137.3 (Cq), 137.7 (Cq), 153.6 (Cq), 154.6 (Cq), 161.4 (Cq) and 166.3 (Cq); **MS** m/z (ES$^+$) Found 447.1997 (MH^+) and 469.1819 (MNa^+), $C_{26}H_{26}N_2O_5$ (MH^+) requires 447.1920 and $C_{26}H_{26}N_2O_5Na$ (MNa^+) requires 469.1739; **Elemental Analysis** Found C (69.83%) H (5.95%) N (6.17%) requires C (69.94%) H (5.87%) N (6.27%); **HPLC** (analytical, system 2) t_R = 18.1 min.

(74+) HPLC (semipreparative, system 3); NMR data consistent with above; α_D^{20} +70 (0.001, EtOAc); **HPLC** (analytical, system 4) t_R = 8.5 min, 99% ee.

(74-) HPLC (semipreparative, system 3); NMR data consistent with above; α_D^{20} -70 (0.001, EtOAc); **HPLC** (analytical, system 4) t_R = 15.6 min, 98% ee.

(3-(4-(benzyloxy)phenyl)-5-(3,4,5-trimethoxyphenyl)-4,5-dihydro-1*H*-pyrazol-1-yl)(phenyl)methanone (75A)

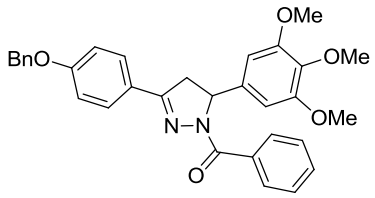

(75A)

Following Method J, except using 1.8 mmol chalcone **(60)**, pyrazoline **(75A)** was obtained as a pale yellow solid (0.75 g, 80%).

R_f [PE-EtOAc 4:6] 0.65; **Mp** 75-77 ^{o}C; **IR** ν_{max}(film)/cm^{-1} 1230, 1660 and 710; **^{1}H NMR** δ_H (500 MHz; $CDCl_3$) 3.17 (1 H, dd, *J* 17.5 and 5.0 Hz, pyrazoline CH), 3.74 (1 H, dd, *J* 17.5 and 11.5 Hz, pyrazoline CH), 3.78 (3 H, s, OCH_3), 3.82 (6 H, s, OCH_3), 5.11 (2 H, s, Bn CH_2), 5.73 (1 H, dd, *J* 11.5 and 4.5 Hz, pyrazoline CH), 6.52 (2 H, s, Ar CH), 6.98 (2 H, d, *J* 8.5 Hz, Ar CH), 7.32-7.51 (8 H, m, Ar CH), 7.65 (2 H, d, *J* 8.5 Hz, Ar CH) and 8.02 (2 H, d, *J* 7.0 Hz, Ar CH); **^{13}C NMR** δ_C (125 MHz; $CDCl_3$) 41.8 (CH_2), 56.1 (OCH_3), 60.7 (OCH_3), 61.3 (CH), 70.1 (CH_2), 102.3 (CH), 115.1 (CH), 124.1 (Cq), 127.4 (CH), 127.7 (CH), 128.2 (CH), 128.4 (CH), 128.7 (CH), 130.0 (CH), 130.9 (CH), 134.4 (Cq), 136.4 (Cq), 137.3 (Cq), 137.7 (Cq), 153.7 (Cq), 154.5 (Cq), 160.6 (Cq) and 166.3 (Cq); **MS** m/z (ES^+) Found 545.2201 (MNa^+), $C_{32}H_{30}N_2O_5Na$ (MNa^+) requires 545.2052.

Method M

Pyrazoline **(75A)** (1.0 mmol) was added to a stirred solution of 10wt% Pd/C (52 mg) in EtOAc (10 mL) under 1 atm of H_2 and stirring continued at rt for 20 h. The solution was filtered through filter paper and the solvent removed under reduced pressure affording an oil which was purified by column chromatography with silica gel using PE:EtOAc 6:4 to afford the desired pyrazoline **(75)** as a white solid (0.31g, 72%).

(3-(4-hydroxyphenyl)-5-(3,4,5-trimethoxyphenyl)-4,5-dihydro-1*H*-pyrazol-1-yl)(phenyl)methanone (75)

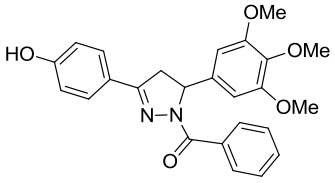

(75)

R_f [PE-EtOAc 4:6] 0.39; **Mp** 186-187 ^oC; **IR** ν_{max}(film)/cm^{-1} 3695, 1199 and 685; **^{1}H NMR** δ_H (500 MHz; DMSO) 3.15 (1 H, dd, *J* 18.0 and 5.0 Hz, pyrazoline CH), 3.63 (3 H, s, OCH_3), 3.74 (6 H, s, OCH_3), 3.82 (1 H, dd, *J* 18.0 and 12.0 Hz, pyrazoline CH), 5.67 (1 H, dd, *J* 11.5 and 5.0 Hz, pyrazoline CH), 6.57 (2 H, s, Ar CH), 6.81 (2 H, d, *J* 9.0 Hz, Ar CH), 7.47-7.55 (5 H, m, Ar CH), 7.86 (2 H, d, *J* 7.5 Hz, Ar CH) and 9.97 (1 H, s, OH); **^{13}C NMR** δ_C (125 MHz; DMSO) 41.7 (CH_2), 55.8 (OCH_3), 59.9 (OCH_3), 60.5 (CH), 102.5 (CH), 115.6 (CH), 121.9 (Cq), 127.8 (CH), 128.6 (CH), 129.3 (CH), 130.6 (CH), 135.0 (Cq), 136.5 (Cq), 138.2 (Cq), 153.1 (Cq), 155.4 (Cq), 159.6 (Cq) and 165.3 (Cq); **MS** m/z (ES^+) Found 433.1789 (MH^+) and 455.1650 (MNa^+), $C_{25}H_{25}N_2O_5$ requires 433.1763 and $C_{25}H_{24}N_2O_5Na$ (MNa^+) requires 455.1583; **Elemental Analysis** Found C (69.49%) H (5.67%) N (6.62%) requires C (69.43%) H (5.59%) N (6.48%); **HPLC** (analytical, system 2) t_R = 9.9 min.

(3-(4-nitrophenyl)-5-(3,4,5-trimethoxyphenyl)-4,5-dihydro-1*H*-pyrazol-1-yl)(phenyl)methanone (76)

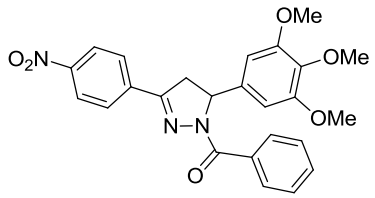

(76)

Following Method J, except using 2.0 mmol chalcone **(62)**, pyrazoline **(76)** was obtained as a yellow solid (0.55 g, 60%).

R_f [PE-EtOAc 4:6] 0.61; **Mp** 197-199 ^{o}C; **IR** ν_{max}(film)/cm^{-1} 1645, 1593, 1428 and 1125; **^{1}H NMR** δ_H (500 MHz; $CDCl_3$) 3.25 (1 H, dd, *J* 18.0 and 5.5 Hz, pyrazoline CH), 3.79-3.85 (10 H, m, OCH_3 and pyrazoline CH), 5.82 (1 H, dd, *J* 12.0 and 5.5 Hz, pyrazoline CH), 6.52 (2 H, s, Ar CH), 7.47-7.56 (3 H, m, Ar CH), 7.85 (2 H, d, *J* 9.0 Hz, Ar CH), 7.99 (2 H, d, *J* 7.0 Hz, Ar CH) and 8.27 (2 H, d, *J* 7.0 Hz, Ar CH); **^{13}C NMR** δ_C (125 MHz; $CDCl_3$) 41.5 (CH_2), 56.1 (OCH_3), 60.8 (OCH_3), 62.0 (CH), 102.3 (CH), 124.0 (CH), 127.4 (CH), 127.9 (CH), 129.9 (CH), 131.4 (CH), 133.8 (Cq), 136.9 (Cq), 137.2 (Cq), 137.6 (Cq), 148.5 (Cq), 152.3 (Cq), 153.8 (Cq) and 166.9 (Cq); **MS** m/z (ES$^+$) Found 484.1571 (MNa$^+$), $C_{25}H_{23}N_3O_6Na$ (MNa$^+$) requires 484.1485; **Elemental Analysis** Found C (65.02%) H (5.07%) N (9.10%) requires C (65.07%) H (5.02%) N (9.11%); **HPLC** (analytical, system 2) t_R = 9.1 min.

Method N

Pyrazoline **(76)** (0.2 mmol) was added to a stirred solution of 10wt% Pd/C (9.0 mg) in EtOAc (10 mL) under 1 atm of H_2 and stirring continued at 40 ^{o}C for 18 h. The solution was filtered through filter paper and the solvent removed under reduced pressure affording a residue which was recrystallised from Et_2O to afford the desired pyrazoline **(77)** as yellow crystals (82 mg, 95%).

(3-(4-aminophenyl)-5-(3,4,5-trimethoxyphenyl)-4,5-dihydro-1*H*-pyrazol-1-yl)(phenyl)methanone (77)

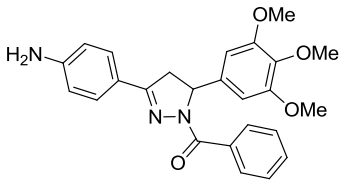

(77)

R_f [PE-EtOAc 4:6] 0.48; **Mp** 104-106 ^{o}C; **IR** ν_{max}(film)/cm^{-1} 1589, 1532, 1504 and 1130; **^{1}H NMR** δ_H (500 MHz; $CDCl_3$) 3.14 (1 H, dd, *J* 17.5 and 4.5 Hz, pyrazoline CH), 3.71 (1 H, dd, *J* 17.5 and 11.5 Hz, pyrazoline CH), 3.80 (3 H, s, OCH_3), 3.82 (6 H, s, OCH_3), 3.95 (2 H, s, NH_2), 5.71 (1 H, dd, *J* 11.5 and 4.0 Hz, pyrazoline CH), 6.53 (2 H, s, Ar CH), 6.66 (2 H, d, *J* 8.5 Hz, Ar CH), 7.43-7.53 (5 H, m, Ar CH) and 8.04 (2 H, d, *J* 6.5 Hz, Ar CH); **^{13}C NMR** δ_C (125 MHz; $CDCl_3$) 41.8 (CH_2), 56.1 (OCH_3), 60.7 (OCH_3), 61.2 (CH), 102.3 (CH), 114.6 (CH), 121.3 (Cq), 127.6 (CH), 128.4 (CH), 130.0 (CH), 130.8 (CH), 134.1 (Cq), 137.2 (Cq), 137.9 (Cq), 148.7 (Cq), 153.6 (Cq), 155.0 (Cq) and 166.5 (Cq); **MS** m/z (ES$^+$) Found 454.1863 (MNa$^+$), $C_{25}H_{25}N_3O_4Na$ (MNa$^+$) requires 454.1743; **Elemental Analysis** Found C (69.52%) H (5.91%) N (9.80%) requires C (69.59%) H (5.84%) N (9.74%); **HPLC** (analytical, system 2) t_R = 3.9 min.

Phenyl(3-(pyridin-2-yl)-5-(3,4,5-trimethoxyphenyl)-4,5-dihydro-1*H*-pyrazol-1-yl)methanone (78)

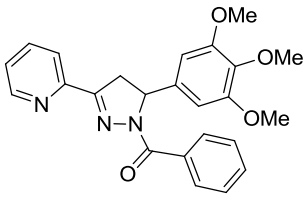

(78)

Following Method J, except using 1.0 mmol chalcone **(64)**, pyrazoline **(78)** was obtained as a white solid (0.30 g, 72%).

R_f [PE-EtOAc 4:6] 0.45; **Mp** 189-191 ^{o}C (EtOAc); **IR** ν_{max}(film)/cm^{-1} 1641, 1598, 1414 and 1338; **^{1}H NMR** δ_H (500 MHz; $CDCl_3$) 3.43 (1 H, dd, *J* 18.5 and 5.0 Hz, pyrazoline CH), 3.80 (3 H, s, OCH_3), 3.82 (6 H, s, OCH_3), 3.89 (1 H, dd, *J* 18.5 and 11.5 Hz, pyrazoline CH), 5.78 (1 H, dd, *J* 12.0 and 5.0 Hz, pyrazoline CH), 6.53 (2 H, s, Ar CH), 7.28-7.44 (1 H, m, Ar CH), 7.47-7.53 (3 H, m, Ar CH and py CH), 7.70-7.73 (1 H, m, py CH), 7.99-8.03 (3 H, m, py CH and Ar CH) and 8.59-8.60 (1 H, m, py CH); **^{13}C NMR** δ_C (125 MHz; $CDCl_3$) 41.6 (CH_2), 56.1 (CH), 60.7 (OCH_3), 61.6 (OCH_3), 102.5 (CH), 121.4 (CH), 124.4 (CH), 127.7 (CH), 129.9 (CH), 131.1 (CH), 134.2 (Cq), 136.2 (CH),137.3 (Cq), 137.4 (Cq), 149.4 (CH), 150.6 (Cq), 153.6 (Cq), 156.4 (Cq) and 166.9 (Cq); **MS** m/z (ES$^+$) Found 418.1834 (MH^+) and 440.1581 (MNa^+), $C_{24}H_{24}N_4O_4$ (MH^+) requires 418.1767 and $C_{24}H_{23}N_4O_4Na$ (MNa^+) requires 440.1586; **Elemental Analysis** Found C (68.96%) H (5.49%) N (10.08%) requires C (69.05%) H (5.55%) N (10.07%); **HPLC** (analytical, system 2) t_R = 8.2 min.

(78+) HPLC (semipreparative, system 3); NMR data consistent with above; **α_D^{20}** +70 (0.001, EtOAc); **HPLC** (analytical, system 4) t_R = 8.0 min, 98% ee.

(78-) HPLC (semipreparative, system 3); NMR data consistent with above; **α_D^{20}** -70 (0.001, EtOAc); **HPLC** (analytical, system 4) t_R = 13.1 min, 96% ee.

(3-(furan-2-yl)-5-(3,4,5-trimethoxyphenyl)-4,5-dihydro-1*H*-pyrazol-1-yl)(phenyl)methanone (79)

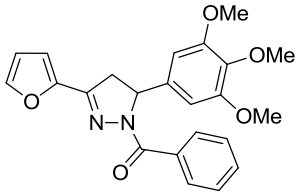

(79)

Following Method J, except using 1.25 mmol chalcone **(65)**, pyrazoline **(79)** was obtained as a white solid (0.33 g, 65%).

R_f [PE-EtOAc 4:6] 0.70; **Mp** 126-130°C (Et_2O); **IR** ν_{max}(film)/cm^{-1} 1631, 1428 and 1130; **^{1}H NMR** δ_H (500 MHz; DMSO) 3.10 (1 H, dd, *J* 18.0 and 5.5 Hz, pyrazoline CH), 3.63 (3 H, s, OCH_3), 3.74 (6 H, s, OCH_3), 3.81 (1 H, dd, *J* 18.0 and 12.0 Hz, pyrazoline CH), 5.68 (1 H, dd, *J* 12.0 and 5.5 Hz, pyrazoline CH), 6.57 (2 H, s, Ar CH), 6.64 (1 H, dd, *J* 3.5 and 1.5 Hz, furan CH), 6.97 (1 H, dd, *J* 3.5 and 0.5 Hz, furan CH), 7.47-7.52 (3 H, m, Ar CH), 7.81 (2 H, d, *J* 7.0 Hz, Ar CH) and 7.86 (1 H, dd, *J* 1.5 and 0.5 Hz, furan CH); **^{13}C NMR** δ_C (125 MHz; DMSO) 41.5 (CH_2), 55.9 (OCH_3), 60.1 (OCH_3), 102.5 (CH), 112.2 (CH), 114.5 (CH), 127.4 (CH), 127.9 (CH), 128.5 (CH), 129.1 (CH), 130.7 (CH), 134.8 (Cq), 136.6 (Cq), 137.7 (Cq), 145.7 (CH), 146.0 (Cq), 146.6 (Cq), 153.1 (Cq) and 165.8 (Cq); **MS** m/z (ES^+) Found 407.1646 (MH^+) and 429.1452 (MNa^+), $C_{23}H_{23}N_2O_5$ (MH^+) requires 407.1607 and $C_{23}H_{22}N_2O_5Na$ (MNa^+) requires 429.1426; **Elemental Analysis** Found C (68.03%) H (5.39%) N (6.73%) requires C (67.97%) H (5.46%) N (6.89%); **HPLC** (analytical, system 2) t_R = 9.8 min.

Phenyl(3-(thiophen-2-yl)-5-(3,4,5-trimethoxyphenyl)-4,5-dihydro-1*H*-pyrazol-1-yl)methanone (80)

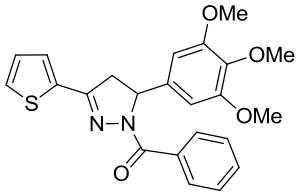

(80)

Following Method J, except using 5.0 mmol chalcone **(66)**, pyrazoline **(80)** was obtained as a white solid (1.28 g, 61%).

R_f [PE-EtOAc 4:6] 0.67; **Mp** 122-124 ^{o}C (Et_2O); **IR** ν_{max}(film)/cm^{-1} 1630, 1509, 1452 and 1132; **^{1}H NMR** δ_H (500 MHz; $CDCl_3$) 3.19 (1 H, dd, *J* 17.5 and 5.5 Hz, pyrazoline CH), 3.76-3.83 (10 H, m, OCH_3 and pyrazoline CH), 5.75 (1 H, dd, *J* 11.5 and 5.0 Hz, pyrazoline CH), 6.52 (2 H, s, Ar CH), 7.07 (1 H, dd, *J* 5.0 and 4.0 Hz, thiophene CH), 7.25 (1 H, dd, *J* 4.0 and 1.0 Hz, thiophene CH), 7.42 (1 H, dd *J* 5.0 and 1.0, thiophene CH), 7.44-7.51 (3 H, m, Ar CH) and 8.02 (2 H, d, *J* 7.0 Hz, Ar CH); **^{13}C NMR** δ_C (125 MHz; $CDCl_3$) 42.4 (CH_2), 56.1 (CH), 60.7 (OCH_3), 61.6 (OCH_3), 102.3 (CH), 127.6 (CH), 127.7 (CH), 128.8 (CH), 128.9 (CH), 130.1 (CH), 131.1 (CH), 134.8 (Cq), 134.9 (Cq), 137.3 (Cq), 137.4 (Cq), 150.3 (Cq), 153.7 (Cq) and 166.2 (Cq); **MS** m/z (ES^+) Found 423.1454 (MH^+) and 445.1278 (MNa^+), $C_{23}H_{23}N_2O_4S$ (MH^+) requires 423.1379 and $C_{23}H_{22}N_2O_4SNa$ (MNa^+) requires 445.1198; **Elemental Analysis** Found C (65.48%) H (4.99%) N (6.59%) requires C (65.38%) H (5.25%) N (6.63%); **HPLC** (analytical, system 2) t_R = 15.0 min.

(3-(naphthalen-2-yl)-5-(3,4,5-trimethoxyphenyl)-4,5-dihydro-1*H*-pyrazol-1-yl)(phenyl)methanone (81)

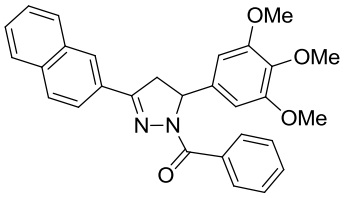

(81)

Following Method J, except using 2.0 mmol chalcone **(67)**, pyrazoline **(81)** was obtained as a white solid (0.54, 58%).

R_f [PE-EtOAc 4:6] 0.76; **Mp** 188-189 ^{o}C; **IR** ν_{max}(film)/cm^{-1} 1655, 1231 and 692; **^{1}H NMR** δ_H (500 MHz; $CDCl_3$) 3.36 (1 H, dd, *J* 17.5 and 5.0 Hz, pyrazoline CH), 3.81 (3 H, s, OCH_3), 3.83 (6 H, s, OCH_3), 3.90 (1 H, dd, *J* 17.5 and 11.5 Hz, pyrazoline CH), 5.81 (1 H, dd *J* 11.5 and 5.0 Hz, pyrazoline CH), 6.57 (2 H, s, Ar CH), 7.48-7.55 (5 H, m, Ar CH) and 7.83-7.94 (7 H, m, Ar CH); **^{13}C NMR** δ_C (125 MHz; $CDCl_3$) 41.7 (CH_2), 56.1 (OCH_3), 60.8 (OCH_3) 61.6 (CH),77.2 (CH), 102.4 (CH), 123.4 (CH), 126.8 (CH), 127.4 (CH), 127.8 (CH), 127.9 (CH), 128.4 (CH), 128.5 (CH), 128.9 (Cq), 130.1 (CH), 131.1 (CH), 132.9 (Cq), 134.2 (Cq), 134.3 (Cq), 137.4 (Cq), 137.6 (Cq), 153.7 (Cq), 154.8 (Cq) and 166.6 (Cq); **MS** m/z (ES^+) Found 489.1886 (MNa^+), $C_{29}H_{26}N_2O_4Na$ (MNa^+) requires 489.1790; **Elemental Analysis** Found C (74.72%) H (5.59%) N (6.04%) requires C (74.66%) H (5.62%) N (6.00%); **HPLC** (analytical, system 2) t_R = 17.0 min.

Method O

To a stirred solution of chalcone **(58)** (0.6 g, 2 mmol) in EtOH (10 mL) at rt was added hydrazine hydrate (0.26 g, 8 mmol) and the solution heated to 80 ^{o}C for 3 h. The solvent was then removed under reduced pressure to afford an orange residue which was ground together with 10mol% Pd/C (0.2 g) and heated at 200 ^{o}C for 2 h under nitrogen. The flask was then allowed to cool to rt and the residue the dissolved in EtOAc (50 mL) and filtered through celite. The solvent was then removed under reduced pressure and the pale brown solid obtained was dissolved in EtOAc (10 mL) followed by dropwise addition of benzoyl chloride (0.84 g, 6 mmol) and NEt_3 (0.6 g, 6 mmol) and the solution allowed to stir at 50 ^{o}C for 18 h. After 18 h the solvent was

removed under reduced pressure to afford a mixture of 69:31 **(85:85A)** as a white solid (0.57 g, 69%).

Phenyl(3-phenyl-5-(3,4,5-trimethoxyphenyl)-1*H*-pyrazol-1-yl)methanone & phenyl(5-phenyl-3-(3,4,5-trimethoxyphenyl)-1*H*-pyrazol-1-yl)methanone (85 and 85A)

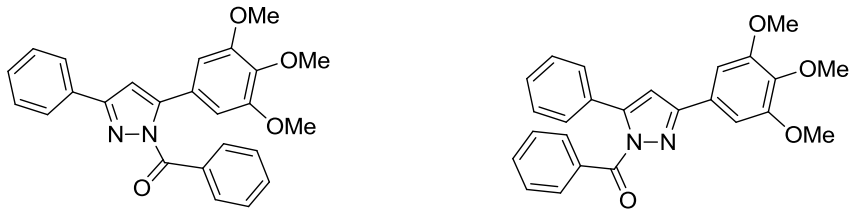

(85) Ratio 69:31 **(85:85A)** **(85A)**

IR ν_{max}(film)/cm^{-1} 1708, 1580, 1427 and 1326; **^{1}H NMR** δ_H (500 MHz; $CDCl_3$); 3.87 (6 H, s, (85) CH_3), 3.89-3.91 (10 H, m, (85 and 85A) CH_3), 6.71 (2 H, s, (85) Ar CH), 6.83 (0.6 H, s, pyrazole (85A) CH), 6.86 (1 H, s, pyrazole (85) CH), 7.09 (1.2 H, s, (85A) CH), 7.39-7.45 (5 H, m, (85A) CH), 7.48-7.53 (5 H, m, 85 CH), 7.61-7.65 (2 H, m, CH), 7.87 (2 H, d, *J* 7.0, (85) CH), 8. 11-8.13 (3.5 H, t, *J* 7.0, CH); **^{13}C NMR** δ_C (125 MHz; $CDCl_3$); 56.2 (CH_3), 56.3 (CH_3), 60.9 (CH_3), 61.0 (CH_3), 103.6 (CH), 106.1 (CH), 108.8 (CH), 108.9 (CH), 126.2 (Cq), 126.3 (Cq), 127.4 (Cq), 128.0 (CH), 128.0 (CH), 128.3 (CH), 128.5 (CH), 128.8 (CH), 128.8 (CH), 129.1 (CH), 130.7 (Cq), 131.7 (CH), 131.9 (CH), 132.0 (CH), 132.4 (Cq), 132.5 (Cq), 133.2 (CH), 138.6 (Cq), 139.1 (Cq), 148.5 (Cq), 148.7 (Cq), 153.0 (Cq), 153.4 (Cq), 153.5 (Cq), 153.5 (Cq), 167.4 (Cq); **MS** m/z (ES^+) Found 415.1703 (MH^+), $C_{25}H_{23}N_2O_4$ (MH^+) requires 415.1658.

Method P

To a solution of pyrazoline **(75)** (50 mg, 0.12 mmol) in THF (10 mL) was added acetyl chloride (36 mg, 0.46 mmol) followed by NEt_3 (23 mg, 0.23 mmol) and the solution allowed to stir at rt for 2 h. After 2 h the solvent was removed under reduced

pressure to afford a white solid which was recrysalised from Et_2O to give pyrazoline **(86)** as a white solid (51 mg, 93%)

4-(1-benzoyl-5-(3,4,5-trimethoxyphenyl)-4,5-dihydro-1*H*-pyrazol-3-yl)phenyl acetate (86)

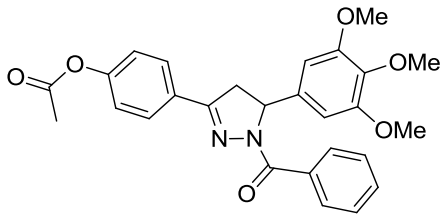

(86)

Mp 158-160 ^{o}C (Et_2O); **IR** ν_{max}(film)/cm^{-1} 1660, 1625, 1452; **^{1}H NMR** δ_H (500 MHz; $CDCl_3$) 2.32 (3 H, s, CH_3), 3.19 (1 H, dd, *J* 17.5 and 5.0 Hz, pyrazoline CH), 3.77 (1 H, dd, *J* 18.0 and 12.0 Hz, pyrazoline CH), 3.80 (3 H, s, OCH_3), 3.82 (6 H, s, OCH_3), 5.76 (1 H, dd, *J* 12.0 and 5.0 Hz, pyrazoline CH), 6.52 (2 H, s, Ar CH), 7.14 (2 H, d, *J* 8.5 Hz, Ar CH), 7.44-7.52 (3 H, m, Ar CH), 7.73 (2 H, d, *J* 8.5 Hz, Ar CH) and 8.00 (2 H, d, *J* 7.0 Hz, Ar CH); **^{13}C NMR** δ_C (125 MHz; $CDCl_3$) 21.1 (CH_3), 41.8 (CH_2), 56.1 (CH_3), 60.7 (CH_3), 61.6 (CH), 102.3 (CH), 122.0 (CH), 127.7 (CH), 128.0 (CH), 129.0 (Cq), 130.0 (CH), 131.0 (CH), 134.3 (Cq), 137.4 (Cq), 137.5 (Cq), 152.2 (Cq), 153.7 (Cq), 153.8 (Cq), 166.5 (Cq) and 169.1 (Cq); **MS** m/z (ES$^+$) Found 475.1908 (MH$^+$), $C_{27}H_{27}N_2O_4$ requires 475.1869 (MH$^+$).

Method Q

To a solution of pyrazoline **(77)** (20 mg, 0.046 mmol) in THF (5 mL) was added acetyl chloride (14 mg, 0.09 mmol) and the solution stirred at rt for 2.5 h. After 2.5 h the solvent was removed under reduced pressure to afford a yellow solid which was recrystallised from EtOAc to give pyrazoline **(87)** as a yellow solid (21 mg, 95%).

***N*-(4-(1-benzoyl-5-(3,4,5-trimethoxyphenyl)-4,5-dihydro-1*H*-pyrazol-3-yl)phenyl)acetamide (87)**

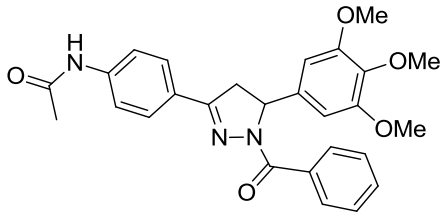

(87)

Mp >230 ^{o}C (EtOAc); **IR** ν_{max}(film)/cm^{-1} 1634, 1602, 1411; **^{1}H NMR** δ_H (500 MHz; $CDCl_3$) 2.17 (3 H, s, CH_3), 3.18 (1 H, dd, *J* 17.5 and 5.0 Hz, pyrazoline CH), 3.75 (1 H, dd, *J* 17.5 and 12.0 Hz, pyrazoline CH), 3.78 (3 H, s, OCH_3), 3.81 (6 H, s, OCH_3), 5.75 (1 H, dd, *J* 12.0 and 5.0 Hz, pyrazoline CH), 6.52 (2 H, s, Ar CH), 7.44-7.50 (3 H, m, Ar CH), 7.56 (2 H, d, *J* 8.0 Hz, Ar CH), 7.65 (2 H, d, *J* 8.0 Hz, Ar CH) and 8.01 (2 H, d, *J* 6.0 Hz, Ar CH); **^{13}C NMR** δ_C (125 MHz; $CDCl_3$) 24.7 (CH_3), 41.7 (CH_2), 56.1 (CH_3), 60.7 (CH_3), 61.4 (CH), 102.3 (CH), 119.4 (CH), 126.9 (Cq), 127.7 (CH), 130.0 (CH), 131.0 (CH), 134.3 (Cq), 137.3 (Cq), 137.6 (Cq), 140.0 (Cq), 153.7 (Cq), 154.3 (Cq), 166.5 (Cq) and 168.3 (Cq); **MS** m/z (ES$^+$) Found 474.2079 (MH^+), $C_{27}H_{28}N_3O_5$ (MH^+) requires 474.2029.

Method R

Following the procedure previously reported,[102] 2-acetylpyridine (1.33 g, 11.0 mmol) and benzaldehyde (1.06 g, 1.02 mL, 10.0 mmol) were added to distilled water (100 mL) cooled to 4 ^{o}C and shaken thoroughly forming a fine emulsion. 10 mL of 10% of NaOH aqueous solution was then added and shaken again for 30 seconds and the reaction left at 4 ^{o}C. After 24 h the solid product was filtered, dried and recrystallised from EtOH to give the chalcone (2.02 g, 97%) as pale green crystals.

(*E*)-3-phenyl-1-(pyridin-2-yl)prop-2-en-1-one (96)

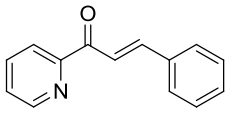

(96)

R_f [PE-EtOAc 4:6] 0.88; **Mp** 72-74 ^{o}C (EtOH); **IR** ν_{max}(film)/cm^{-1} 1667, 1601, 1337 and 1030; **^{1}H NMR** δ_H (500 MHz; $CDCl_3$) 7.40-7.49 (4 H, m, Ph CH), 7.72-7.73 (2 H, m, Ph CH and py CH), 7.85-7.88 (1 H, m, py CH), 7.94 (1 H, d, *J* 16.0 Hz, COC*H*=CH), 8.18-8.19 (1 H, m, py CH), 8.30 (1 H, d, *J* 16.0 Hz, COCH=C*H*) and 8.74-8.76 (1 H, m, py CH); **^{13}C NMR** δ_C (125 MHz; $CDCl_3$) 120.9 (CH), 122.9 (CH), 126.9 (CH), 128.8 (CH), 128.9 (CH), 130.6 (CH), 135.2 (Cq), 137.0 (CH), 144.8 (CH), 148.9 (CH), 154.3 (Cq) and 189.5 (Cq); **MS** m/z (ES$^+$) Found 232.0749 (MNa$^+$), $C_{14}H_{11}N_1NaO$ (MNa$^+$) requires 232.0738.

Method S

Chalcone **(96)** (0.418 g, 2.0 mmol) was dissolved in EtOH (10 mL) and stirred for 10 min at rt until fully dissolved then methylhydrazine (0.368 g, 0.42 mL, 8.0 mmol) was added dropwise and stirred continued at room temperature for 3 h. The solvent was removed under reduced pressure and the resulting yellow oil purified by column chromatography with silica gel using PE:EtOAc 60:40 to afford pyrazoline **(97)** (0.34 g, 72%) as a yellow oil, which solidified upon cooling and was recrystallised from Et_2O to give pale yellow crystals.

2-(1-methyl-5-phenyl-4,5-dihydro-1*H*-pyrazol-3-yl)pyridine (97)

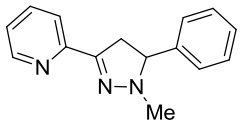

(97)

R_f [PE-EtOAc 4:6] 0.82; **Mp** 52-55 ^{o}C (Et_2O); **IR** ν_{max}(film)/cm^{-1} 2971, 1570, 1456 and 1122; **^{1}H NMR** δ_H (500 MHz; $CDCl_3$) 2.88 (3 H, s, CH_3), 3.08 (1 H, dd, *J* 16.5 and 14.5 Hz, pyrazoline CH), 3.71 (1 H, dd, *J* 16.5 and 10.5 Hz, pyrazoline CH), 4.21 (1 H, dd, *J* 14.5 and 10.5 Hz, pyrazoline CH), 7.18 (1 H, dd, *J* 7.5 and 5.0 Hz, py CH), 7.29-7.34 (1 H, m, Ph CH), 7.35-7.40 (2 H, m, Ph CH), 7.45-7.48 (2 H, m, Ph), 7.66 (1 H, td, *J* 7.5 and 1.0 Hz, py CH), 7.91 (1 H, dt, *J* 8.0 and 1.0 Hz, py CH) and 8.56 (1 H, br.d, *J* 5.0 Hz, py CH); **^{13}C NMR** δ_C (125 MHz; $CDCl_3$) 41.1 (CH_3), 42.6 (CH_2), 73.5 (CH), 120.4 (CH), 122.6 (CH), 127.4 (CH), 127.8 (CH), 128.6 (CH), 136.0 (CH), 140.2 (Cq), 149.1 (CH), 150.4 (Cq) and 152.1 (Cq); **MS** m/z (ES^+) Found 260.1158 (MNa^+), $C_{15}H_{15}N_3Na$ (MNa^+) requires 260.1164; **HPLC** (analytical, system 2) t_R = 18.3 min.

Method T

Following the procedure previously reported for the oxidation of a 1,2,3,4-tetrahydro-β-carboline,[103] pyrazoline **(97)** (0.79 g, 3.4 mmol) was thoroughly ground together with 10 wt. % loading Pd/C (10 mol%, 0.36 g), placed under nitrogen and gradually heated to 200 ^{o}C and kept at 200 ^{o}C for 4 h. After 4 h the flask was cooled to rt and 50 mL of toluene added, heated and vigorously stirred for 10 min., the solution was then filtered through fluted filter paper and cotton wool. The solvent was removed under reduced pressure to give a brown oil which was purified by column chromatography with silica gel using PE:EtOAc 60:40 to afford pyrazole **(98)** (0.63 g, 80%) as a pale yellow solid, which was recrystallised from Et_2O to give pale yellow crystals.

2-(1-methyl-5-phenyl-1*H*-pyrazol-3-yl)pyridine (98)

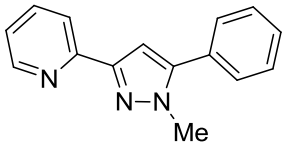

(98)

R_f [PE-EtOAc 4:6] 0.61; **Mp** 108-110 ^{o}C (Et_2O); **IR** ν_{max}(film)/cm^{-1} 1598, 1477 and 1199; **^{1}H NMR** δ_H (500 MHz; $CDCl_3$) 3.97 (3 H, s, CH_3), 6.94 (1 H, s, pyrazole CH), 7.21 (1 H, ddd, *J* 7.5, 4.5 and 1.0 Hz, py CH), 7.42-7.49 (5 H, m, Ph CH), 7.73 (1 H, td, *J* 7.5 and 1.5 Hz, py CH), 7.95 (1 H, dt, *J* 8.0 and 1.0 Hz, py CH) and 8.64 (1 H, ddd, *J* 5.0, 1.5 and 1.0 Hz, py CH); **^{13}C NMR** δ_C (125 MHz; $CDCl_3$) 37.9 (CH_3), 104.6 (CH), 119.9 (CH), 122.4 (CH), 128.6 (CH), 128.7 (2 x CH), 130.5 (Cq), 136.6 (CH), 145.2 (Cq), 149.4 (CH), 150.6 (Cq) and 152.2 (Cq); **MS** m/z (ES^+) Found 236.1194 (MH^+), $C_{15}H_{14}N_3$ (MH^+) requires 236.1188.

1-(5-phenyl-3-(pyridin-2-yl)-4,5-dihydro-1*H*-pyrazol-1-yl)ethanone (100)

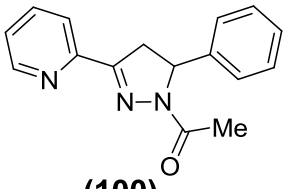

(100)

Following method J, except using 5.0 mmol of chalcone **(96)**, 20.0 mmol hydrazine monohydrate and 10.0 mmol acetyl chloride, pyrazoline **(100)** was obtained as a white solid (0.95 g, 72%).

R_f [PE-EtOAc 4:6] 0.23; **Mp** 120-121 ^{o}C (EtOAc); **IR** ν_{max}(film)/cm^{-1} 1655, 1580, 1413 and 1335; **^{1}H NMR** δ_H (500 MHz; $CDCl_3$) 2.43 (3 H, s, CH_3), 3.38 (1 H, dd, *J* 18.5 and 5.0 Hz, pyrazoline CH), 3.84 (1 H, dd, *J* 18.5 and 12.0 Hz, pyrazoline CH), 5.60 (1 H, dd, *J* 12.0 and 5.0 Hz, pyrazoline CH), 7.21-7.31 (6 H, m, Ph CH and py CH), 7.71-7.75 (1 H, td, *J* 8.0 and 2.0 Hz, py CH), 8.08 (1 H, d, *J* 8.0 Hz, py CH) and 8.58 (1 H, d, *J* 5.0 Hz, py CH); **^{13}C NMR** δ_C (125 MHz; $CDCl_3$) 21.8 (CH_3), 42.0 (CH_2), 60.1 (CH), 121.1 (CH), 124.2 (CH), 125.5 (CH), 127.5 (CH), 128.7 (CH), 136.2 (CH), 141.6 (CH), 149.3 (Cq), 150.6 (Cq), 155.3 (Cq) and 168.9 (Cq); **MS** m/z (ES^+) Found 288.1166 (MNa^+), $C_{16}H_{15}N_3ONa$ (MNa^+) requires 288.1113; **HPLC** (analytical, system 2) t_R = 6.1 min.

2,2,2-trifluoro-1-(5-phenyl-3-(pyridin-2-yl)-4,5-dihydro-1*H*-pyrazol-1-yl)ethanone (101)

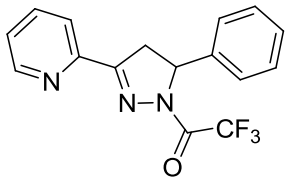

(101)

Following method J, except using 2.5 mmol of chalcone **(96)**, 10.0 mmol hydrazine monohydrate and 7.5 mmol trifluoroacetic anhydride, pyrazoline **(101)** was obtained as a pale green solid (0.52 g, 65%).

R_f [PE-EtOAc 4:6] 0.87; **Mp** 143-145 ^{o}C (EtOH); **IR** ν_{max}(film)/cm^{-1} 1701, 1587, 1463 and 1171; **^{1}H NMR** δ_H (500 MHz; $CDCl_3$) 3.50 (1 H, dd, *J* 19.0 and 5.0 Hz, pyrazoline CH),

3.92 (1 H, dd, *J* 19.0 and 11.5 Hz, pyrazoline CH), 5.64 (1 H, dd, *J* 11.5 and 4.5 Hz, pyrazoline CH), 7.24-7.38 (6 H, m, Ph CH and py CH), 7.80 (1 H, td, *J* 7.5 and 2.0 Hz, py CH), 8.19 (1 H, d, *J* 7.0 Hz, py CH) and 8.62 (1 H, d, *J* 6.0 Hz, py CH); **^{13}C NMR** δ_C (125 MHz; $CDCl_3$) 41.7 (CH_2), 61.8 (CH), 122.0 (CH), 125.1 (CH), 125.7 (CH), 128.4 (CH), 129.1 (CH), 136.5 (CH), 139.5 (Cq), 149.5 (Cq), 149.7 (CH), 154.0 (Cq), 154.3 (Cq) and 159.6 (Cq); **MS** m/z (ES^+) Found 320.1066 (MH^+) and 342.0888 (MNa^+), $C_{16}H_{13}F_3N_3O$ (MH^+) requires 320.1011 and $C_{16}H_{12}F_3N_3ONa$ (MNa^+) requires 342.0831; **HPLC** (analytical, system 2) t_R = 16.4 min.

Method U

Following the procedure reported, chalcone **(96)** (5.0 mmol) and thiosemicarbazide (7.5 mmol) were added to EtOH (50 mL) followed by a solution of sodium hydroxide (5.0 mmol, 0.28 g) in water (10 mL) and refluxed for 6 h. The solvent was then concentrated and the product crystallised from ethanol to give yellow crystals (0.94 g, 67%).

5-phenyl-3-(pyridin-2-yl)-4,5-dihydro-1*H*-pyrazole-1-carbothioamide (102)

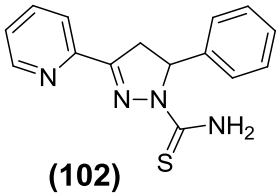

(102)

R_f [PE-EtOAc 4:6] 0.55; **Mp** 185-189 ^oC (EtOH); **IR** ν_{max}(film)/cm^{-1} 3523, 3395, 1569, 1349 and 1195; **^{1}H NMR** δ_H (400 MHz; $CDCl_3$) 3.45 (1 H, dd, *J* 20.0 and 4.0 Hz, pyrazoline CH), 3.96 (1 H, dd, *J* 20.0 and 12.0 Hz, pyrazoline CH), 6.10 (1 H, dd, *J* 12.0 and 4.0 Hz, pyrazoline CH), 6.30 (1 H, broad s, NH), 7.17 (1 H, broad S, NH), 7.26-7.35 (6 H, m, Ph CH and py CH), 7.78 (1 H, td, *J* 8.0 and 4.0 Hz, py CH), 8.07 (1 H, d, *J* 8.0 Hz, CH) and 8.64 (1 H, d, *J* 8.0 Hz, py CH); **^{13}C NMR** δ_C (100 MHz; $CDCl_3$) 39.8 (CH_2), 63.1 (CH), 121.5 (Py CH), 124.8 (Ar CH), 125.2 (Ar CH), 126.9 (Ar CH), 128.5 (Py CH), 136.7

(Py CH), 149.5 (Py CH) and 193.0 (C=S); **MS** m/z (ES^+) Found 283.1004 (MH^+) and 305.0824 (MNa^+), $C_{15}H_{15}N_4S$ (MH^+) requires 283.1017 and $C_{15}H_{14}N_4SNa$ (MNa^+) requires 305.0837; **HPLC** (analytical, system 2) t_R = 6.1 min.

Method V

Pyrazoline **(102)** (1.4 mmol) was added to a solution of potassium hydroxide (4.2 mmol) in THF (20 ml) and stirred for 15 min, methyl iodide (4.2 mmol) was then added and stirring continued for 2 h. Water (100 ml) was then added and stirring continued for 2 h resulting in the formation of a precipitate which was collected by filtration and recrystallised from EtOAc to afford pyrazoline **(103)** as yellow crystals (0.37 g, 89%).

***N*-methyl-5-phenyl-3-(pyridin-2-yl)-4,5-dihydro-1*H*-pyrazole-1-carbothioamide (103)**

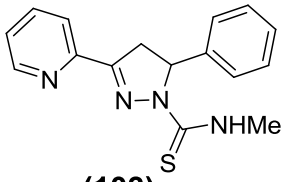

(103)

R_f [PE-EtOAc 4:6] 0.15; **Mp** 157-158 ^oC (EtOH); **IR** ν_{max}(film)/cm^{-1} 1604, 1566, 1320 and 1399; **^{1}H NMR** δ_H (500 MHz; $CDCl_3$) 2.30 (3 H, s, CH_3), 3.34 (1 H, dd, *J* 18.5 and 6.0 Hz, pyrazoline CH), 3.93 (1 H, dd, *J* 18.5 and 12.0 Hz, pyrazoline CH), 5.63 (1 H, dd, *J* 12.0 and 6.0 Hz, pyrazoline CH), 7.24-7.35 (6 H, m, Ph CH and py CH), 7.71 (1 H, td, *J* 7.5 and 1.5 Hz, py CH), 8.12 (1 H, d, *J* 7.5 Hz, py CH) and 8.55 (1 H, d, *J* 7.5 Hz, py CH); **^{13}C NMR** δ_C (125 MHz; $CDCl_3$) 13.1 (CH_3), 42.8 (CH_2), 63.3 (CH), 121.1 (CH), 123.7 (CH), 125.5 (CH), 127.6 (CH), 128.9 (CH), 136.1 (CH), 149.1 (CH), 149.2 (Cq) 151.0 (Cq), 152.3 (Cq) and 160.0 (Cq); **MS** m/z (ES^+) Found 297.1182 (MH^+), $C_{16}H_{17}N_4S$ (MH^+) requires 297.1174; **HPLC** (analytical, system 2) t_R = 5.6 min.

Phenyl(5-phenyl-3-(pyridin-2-yl)-4,5-dihydro-1*H*-pyrazol-1-yl)methanone (104)

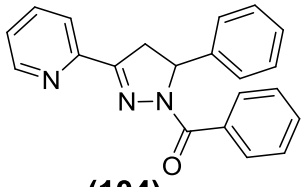

(104)

Following method J, except using 5.0 mmol of chalcone **(96)**, 20.0 mmol hydrazine monohydrate and 10.0 mmol of benzoyl chloride, pyrazoline **(104)** was obtained as a white solid (1.24 g, 76%).

R_f [PE-EtOAc 4:6] 0.76; **Mp** 139-140 ^{o}C (EtOAc); **IR** ν_{max}(film)/cm^{-1} 1641, 1577, 1413 and 1338; **^{1}H NMR** δ_H (500 MHz; $CDCl_3$) 3.44 (1 H, dd, *J* 18.5 and 5.0 Hz, pyrazoline CH), 3.91 (1 H, dd, *J* 18.5 and 12.0 Hz, pyrazoline CH) 5.85 (1 H, dd, *J* 12.0 and 5.0 Hz, pyrazoline CH), 7.27-7.35 (6 H, m, Ph CH and py CH), 7.43-7.50 (3 H, m, Ar CH), 7.70 (1 H, td, *J* 7.5 and 1.5 Hz, py CH), 8.01-8.04 (3 H, m, CH) and 8.59 (1 H, d, *J* 7.5 Hz, py CH); **^{13}C NMR** δ_C (125 MHz; $CDCl_3$) 41.4 (CH_2), 61.5 (CH), 121.4 (CH), 124.3 (CH), 125.7 (CH), 127.5 (CH), 127.6 (CH), 128.8 (CH), 129.9 (CH), 130.9 (CH), 134.2 (Cq), 136.2 (CH), 141.6 (Cq), 149.3 (CH), 150.7 (Cq), 156.2 (Cq) and 166.6 (Cq); **MS** m/z (ES^+) Found 350.1282 (MNa^+), $C_{21}H_{17}N_3ONa$ (MNa^+) requires 350.1269; **HPLC** (analytical, system 2) t_R = 11.7 min.

(5-phenyl-3-(pyridin-2-yl)-4,5-dihydro-1*H*-pyrazol-1-yl)(3,4,5-trimethoxyphenyl)methanone (105))

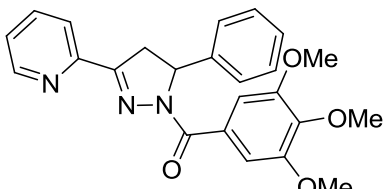

(105)

Following method J, except using 5.0 mmol of chalcone **(96)**, 20.0 mmol hydrazine monohydrate and 10.0 mmol of 3,4,5-trimethoxybenzoyl chloride, pyrazoline **(105)** was obtained as a white solid (1.56 g, 75%).

R_f [PE-EtOAc 4:6] 0.55; **Mp** 173-175 ^{o}C (EtOAc); **IR** ν_{max}(film)/cm^{-1} 1643, 1579, 1412 and 1341; **^{1}H NMR** δ_H (500 MHz; $CDCl_3$) 3.44 (1 H, dd, *J* 18.5 and 5.0 Hz, pyrazoline CH), 3.88-3.94 (10 H, m, OCH_3 and CH), 5.82 (1 H, dd, *J* 12.0 and 5.0 Hz, pyrazoline CH), 7.25-7.33 (6 H, m, Ph CH and py CH), 7.404 (2 H, s, Ar CH), 7.74 (1 H, td, *J* 8.0 and 2.0 Hz, py CH), 8.05 (1 H, d, *J* 8.0 Hz, py CH) and 8.61 (1 H, d, *J* 7.5 Hz, py CH); **^{13}C NMR** δ_C (125 MHz; $CDCl_3$) 41.2 (CH_2), 56.2 (CH), 60.9 (OCH_3), 62.0 (OCH_3), 108.0 (CH), 121.0 (CH), 124.4 (CH), 125.7 (CH), 127.6 (CH), 128.9 (CH), 136.2 (CH), 140.7 (Cq), 141.6 (Cq), 149.5 (CH), 150.8 (Cq), 152.3 (Cq),156.0 (Cq), 156.5 (Cq) and 165.6 (Cq); **MS** m/z (ES^+) Found 418.1776 (MH^+) and 440.1587 (MNa^+), $C_{24}H_{24}N_3O_4$ (MH^+) requires 418.1767 and $C_{24}H_{23}N_3O_4Na$ (MNa^+) requires 440.1586; **Elemental Analysis** Found C (69.15%) H (5.37%) N (9.92%) requires C (69.05%) H (5.55%) N (10.07%); **HPLC** (analytical, system 2) t_R = 9.3 min.

(3-(pyridin-2-yl)-5-(3,4,5-trimethoxyphenyl)-4,5-dihydro-1*H*-pyrazol-1-yl)(3,4,5-trimethoxyphenyl)methanone (106)

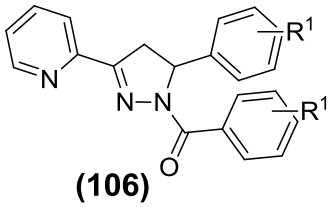

(106)

R^1; 3,4,5 OMe

Following method J, except using 2.0 mmol of chalcone **(64)**, 8.0 mmol hydrazine monohydrate and 4.0 mmol 3,4,5-trimethoxybenzoyl chloride, pyrazoline **(106)** was obtained as a white solid (0.85 g, 84%).

R_f [PE-EtOAc 4:6] 0.41; **Mp** 174-175 ^{o}C (EtOH); **IR** ν_{max}(film)/cm^{-1} 1641, 1580, 1416 and 1128; **^{1}H NMR** δ_H (500 MHz; $CDCl_3$) 3.42 (1 H, dd, *J* 19.0 and 5.0 Hz, pyrazoline CH),

3.81 (3 H, s, OCH_3), 3.82 (6 H, s, OCH_3), 3.85-3.93 (10 H, m, OCH_3 and pyrazoline CH), 5.75 (1 H, dd, *J* 12.0 and 5.0 Hz, pyrazoline CH), 6.52 (2 H, s, Ar CH), 7.32 (1 H, td, *J* 5.0 and 1.0 Hz, py CH), 7.40 (2 H, s, Ar CH), 7.74 (1 H, dt, *J* 7.5 and 1.5 Hz, py CH), 8.04 (1 H, d, *J* 8.0 Hz, py CH) and 8.61 (1 H, d, *J* 5.5 Hz, py CH); **^{13}C NMR** δ_C (125 MHz; $CDCl_3$) 41.4 (CH_2), 56.1 (OCH_3), 56.2 (OCH_3), 56.3 (OCH_3) 60.7 (OCH_3), 62.2 (Ar CH), 102.5 (Ar CH), 108.0 (Ar CH), 121.1 (Ar CH), 124.5 (Ar CH), 128.9 (Ar CH), 136.3 (Ar CH), 137.4 (Cq), 137.5 (Cq), 140.9 (Cq), 149.6 (Cq), 150.7 (Cq), 152.5 (Cq), 153.6 (Cq), 156.7 (Cq) and 165.8 (C=O); **MS** m/z (ES^+) Found 508.2078 (MH^+) and 530.1898 (MNa^+), $C_{27}H_{30}N_3O_7$ (MH^+) requires 508.2084 and $C_{27}H_{29}N_3O_7Na$ (MNa^+) requires 530.1903; **HPLC** (analytical, system 2) t_R = 5.4 min.

1-(3-(pyridin-2-yl)-5-(3,4,5-trimethoxyphenyl)-4,5-dihydro-1*H*-pyrazol-1-yl)ethanone (107)

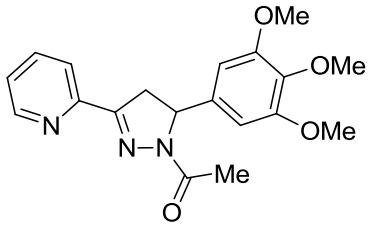

(107)

Following method J, except using 4.0 mmol of chalcone **(64)**, 8.0 mmol hydrazine monohydrate and 8.0 mmol of acetyl chloride, pyrazoline **(107)** was obtained as a yellow solid (1.14 g, 80%).

R_f [PE-EtOAc 4:6] 0.24; **Mp** 173-174 ^oC (EtOH); **IR** ν_{max}(film)/cm^{-1} 1662, 1594, 1416, 1327 and 1132; **^{1}H NMR** δ_H (500 MHz; $CDCl_3$) 2.43 (3 H, s, OCH_3), 3.34 (1 H, dd, *J* 18.5 and 5.0 Hz, pyrazoline CH), 3.77 (3 H, s, OCH_3), 3.79-3.87 (7 H, m, CH_3 and pyrazoline CH), 5.51 (1 H, dd, *J* 12.0 and 5.0 Hz, pyrazoline CH), 6.40 (2 H, s, Ar CH), 7.26-7.30 (1 H, m, py CH), 7.73(1 H, td, *J* 7.5 and 1.5 Hz, py CH), 8.06 (1 H, d, *J* 8.0 Hz, py CH) and 8.57 (1 H, d, *J* 4.5 Hz, py CH); **^{13}C NMR** δ_C (125 MHz; $CDCl_3$) 21.8 (OCH_3), 42.2 (CH_2), 56.0 (CH), 60.3 (OCH_3), 60.6 (CH_3), 102.3 (CH), 121.1 (CH), 124.3 (CH), 136.2 (CH),

137.2 (Cq), 137.4 (Cq), 149.4 (CH), 150.5 (Cq), 153.4 (Cq), 155.4 (Cq) and 169.1 (Cq); **MS** m/z (ES^+) Found 378.1481 (MNa^+), $C_{19}H_{21}N_3O_4Na$ (MNa^+) requires 378.1430; **HPLC** (analytical, system 2) t_R = 4.2 min.

2-(1-phenyl-5-(3,4,5-trimethoxyphenyl)-4,5-dihydro-1*H*-pyrazol-3-yl)pyridine (108)

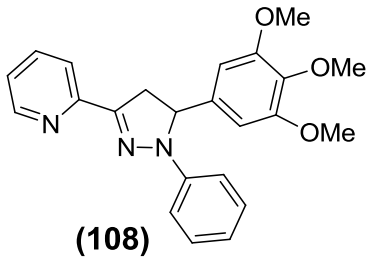

(108)

Following method L, except using 2.5 mmol of chalcone **(64)** and 5.0 mmol of phenyl hydrazine, pyrazoline **(108)** was obtained as a yellow solid (0.33 g, 34%).

R_f [PE-EtOAc 4:6] 0.70; **Mp** 75-77 ^oC (EtOAc); **IR** ν_{max}(film)/cm^{-1} 1601, 1502, 1214 and 1128; **^{1}H NMR** δ_H (500 MHz; $CDCl_3$) 3.33 (1 H, dd, *J* 18.0 and 7.5 Hz, pyrazoline CH), 3.79 (6 H, s, OCH_3), 3.82 (3 H, s, OCH_3), 3.98 (1 H, dd, *J* 18.0 and 12.5 Hz, pyrazoline CH), 5.24 (1 H, dd, *J* 12.5 and 7.5 Hz, pyrazoline CH), 6.51 (2 H, s, Ar CH), 6.85 (1 H, td, *J* 7.0 and 1.0 Hz, py CH), 7.12 (2 H, d, *J* 8.5 Hz, Ar CH), 7.20-7.24 (3 H, m, Ar CH), 7.71 (1 H, td, *J* 7.5 and 1.5 Hz, py CH), 8.14 (1 H, d, *J* 8.0 Hz, Ar CH) and 8.54-8.55 (1 H, d, *J* 7.5 Hz, py CH); **^{13}C NMR** δ_C (125 MHz; $CDCl_3$) 43.3 (CH_2), 56.1 (CH), 60.8 (CH), 65.2 (CH), 102.4 (CH), 113.7 (CH), 119.8 (CH), 120.7 (CH), 122.7 (CH), 128.9 (CH), 130.0 (Cq), 137.1 (Cq), 138.1 (Cq),140.3 (Cq) 144.6 (Cq) and 153.8 (Cq); **MS** m/z (ES^+) Found

390.1882 (MH^+) and 412.1649 (MNa^+), $C_{23}H_{24}N_3O_3$ (MH^+) requires 390.1818 and $C_{23}H_{23}N_3O_3Na$ (MNa^+) requires 412.1637; **HPLC** (analytical, system 2) t_R = 14.6 min.

Method W

Following the procedure reported,[115] to a stirred solution of maltol **(92)** (17.8 g, 0.14 mol) in MeOH (180 mL) was added sodium hydroxide (6 g, 0.15 mol) in water (20 mL) followed by benzyl chloride (20.9 g, 0.16 mol), and the mixture was heated to reflux for 12 h. The solvent was reduced under reduced pressure to afford orange oil which was taken up in CH_2Cl_2 (80 mL) and washed with 5% (w/v) aqueous sodium hydroxide (5 x 30 mL) and water (2 x 50 mL). The organic fraction was dried over anhydrous sodium sulfate and filtered. The solvent was removed by rotary evaporation to give product **(114)** as a pale yellow oil (26.3 g, 87%).

Synthesis of 3-(benzyloxy)-2-methyl-4*H*-pyran-4-one (114)

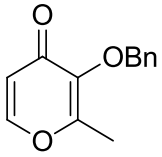

(114)

R_f [PE-EtOAc 4:6] 0.65; **IR** ν_{max}(film)/cm^{-1} 1633, 1431 and 1173; **^{1}H NMR** δ_H (500 MHz; $CDCl_3$) 2.09 (3 H, s, CH_3), 5.16 (2 H, s, Bn CH_2), 6.36 (1 H, d, *J* 5.0 Hz, COC*H*=CH), 7.33-7.39 (5 H, m, Ph CH) and 7.59 (1 H, d, *J* 5.0, COCH=C*H*); **^{13}C NMR** δ_C (125 MHz; $CDCl_3$);

14.8 (CH_3), 73.6 (CH_2), 117.2 (CH), 128.3 (CH), 128.4 (CH), 129.0 (CH), 136.9 (Cq), 143.8 (Cq), 153.4 (Cq), 159.7 (CH) and 175.1 (Cq); **MS** m/z (ES^+) Found 217.0861 (MH^+), $C_{13}H_{13}O_3$ (MH^+) requires 217.0865.

Method X

Following the procedure reported,[115] to a stirred solution of benzylated maltol **(114)** (8.5 g, 39.4 mmol) in EtOH (100 mL) and water (100 mL) was added β-alanine (8.7 g, 97.8 mmol) followed by 10 M sodium hydroxide solution until pH 13 was attained. After heating under reflux for 18 h, the solvent was reduced in volume under reduced pressure and water was added followed by hydrochloric acid to adjust to pH 4. The yellow precipitate was filtered and dried to afford product **(115)** as a pale yellow solid (7.9 g, 70%).

Synthesis of 3-(3-(benzyloxy)-2-methyl-4-oxopyridin-1(4*H*)-yl)propanoic acid (115)

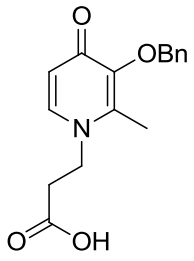

(115)

R_f [CH_2Cl_2-MeOH 9:1] 0.21; **Mp** 172-173 ^oC (EtOH); **IR** ν_{max}(film)/cm^{-1} 1729, 1625 and 1550; **^{1}H NMR** δ_H (500 MHz; DMSO) 2.21 (3 H, s, CH_3), 2.66 (2 H, t, *J* 7.0 Hz, NCH_2CH_2), 4.11 (2 H, t, *J* 7.0 Hz, NCH_2CH_2), 5.00 (2 H, s, Bn CH_2), 6.20 (1 H, d, *J* 7.5 Hz, COC*H*=CH), 7.32-7.41 (5 H, m, Ph CH) and 7.66 (1 H, d, *J* 7.5 Hz, COCH=C*H*); **^{13}C NMR** δ_C (125 MHz; $CDCl_3$); 12.0 (CH_3), 34.5 (CH_2), 48.6 (CH_2), 72.0 (CH_2), 115.9 (CH), 122.1 (Cq), 127.9

(CH), 128.3 (CH), 128.4 (CH), 137.7 (Cq), 139.8 (CH), 145.0 (Cq), 171.9 (Cq) and 172.0 (Cq); **MS** m/z (ES^+) Found 288.1238 (MH^+) and 310.1055 (MNa^+), $C_{16}H_{18}N_1O_4$ (MH^+) requires 288.1236 and $C_{16}H_{17}N_1O_4Na$ (MNa^+) requires 310.1055.

Method Y

Following an adapted literature procedure,[115] to a stirred solution of maltol carboxylic acid **(115)** (5.5 g, 19.1 mmol) in CH_2Cl_2 (60 mL) at rt was added N-hydroxysuccinimide (2.2 g, 19.1 mmol) dissolved in CH_2Cl_2 (60 mL) followed by N,N'-dicyclohexylcarbodiimide (3.9 g, 19.1 mmol) dissolved in CH_2Cl_2 (60 mL) and stirring continued at rt for 18 h. After 18 h the white precipitate was filtered and the solvent concentrated under reduced pressure to afford a pale yellow solid. Recrysalisation from CH_2Cl_2 and Et_2O afforded a white crystalline solid which was collected and dried to give the product **(116)** (5.1 g, 70%).

Synthesis of 2,5-dioxopyrrolidin-1-yl 3-(3-(benzyloxy)-2-methyl-4-oxopyridin-1(4*H*)-yl)propanoate (116)

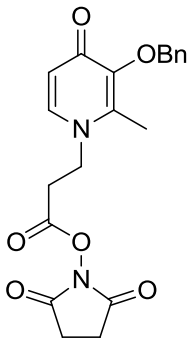

(116)

Mp 72-74 ^oC (CH_2Cl_2/Et_2O); **IR** ν_{max}(film)/cm^{-1} 1782, 1725 and 1633; **^{1}H NMR** δ_H (500 MHz; DMSO) 2.22 (3 H, s, CH_3), 2.82 (4 H, s, 2 x CH_2), 3.19 (2 H, t, *J* 7.0 Hz, NCH_2CH_2), 4.24 (2 H, t, *J* 7.0 Hz, NCH_2CH_2), 5.00 (2 H, s, Bn CH_2), 6.14 (1 H, d, *J* 7.5 Hz, COCH=CH), 7.32-7.42 (5 H, m, Ph CH) and 7.66 (1 H, d, *J* 7.5 Hz, COCH=CH); **^{13}C NMR** δ_C (125 MHz;

DMSO); 11.9 (CH_3), 25.5 (CH_2), 31.2 (CH_2), 47.5 (CH_2), 71.9 (CH_2), 116.1 (CH), 127.8 (CH), 128.2 (CH), 128.4 (CH), 137.8 (Cq), 139.6 (CH), 140.8 (Cq), 145.2 (Cq), 166.8 (Cq), 170.1 (Cq) and 172.0 (Cq); **MS** m/z (ES^+) Found 385.1423 (MH^+), $C_{20}H_{21}N_2O_6$ (MH^+) requires 385.1400.

Method Z

Maltol activated ester **(116)** (1.44 g, 3.8 mmol) was dissolved in DMF (5 mL) and added dropwise to a stirred solution of ethylenediamine (0.09 g, 1.5 mmol) in DMF (2 mL) at rt and stirring continued for 72 h. After 72 h a white precipitate formed which was filtered off and the solvent removed under removed pressure to afford a pale yellow oil which was purified by column chromatography with silica gel using CH_2Cl_2:MeOH 8:2 to afford the desired benzylated maltol dimer **(117)** as a white solid (0.59 g, 65%).

***N*,*N*'-(ethane-1,2-diyl)bis(3-(3-(benzyloxy)-2-methyl-4-oxopyridin-1(4*H*)-yl)propanamide) (117)**

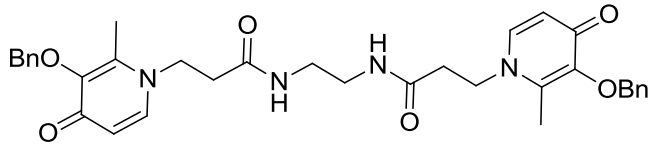

(117)

R_f [CH_2Cl_2-MeOH 9:1] 0.08; **^{1}H NMR** δ_H (500 MHz; $CDCl_3$) 2.12 (6 H, s, CH_3), 2.42 (4 H, t, *J* 6.5 Hz, 2 x CH_2), 3.23 (4 H, br s, CH_2), 4.07 (4 H, t, *J* 6.5 Hz, 2 x CH_2), 5.01 (4 H, s, Bn CH_2), 6.28 (4 H, d, *J* 7.5 Hz, COC*H*=CH), 7.28-7.34 (10 H, m, Ar CH), 7.37 (2 H, d, *J* 7.5 Hz, COCH=C*H*) and 7.89 (2 H, br s, NH); **^{13}C NMR** δ_C (125 MHz; $CDCl_3$); 12.4 (CH_3), 36.5 (CH_2), 39.3 (CH_2), 50.0 (CH_2) 73.2 (CH_2), 116.6 (CH), 128.3 (CH), 128.4 (CH), 128.7 (CH), 136.9 (Cq), 139.4 (CH), 142.1 (Cq), 145.8 (Cq), 169.3 (Cq) and 172.9 (Cq); **MS** m/z (ES^+) Found 621.2686 (MNa^+), $C_{34}H_{38}N_4O_6Na$ (MNa^+) requires 621.2689.

Method AA

Benzylated maltol dimer **(117)** (0.4 g, 0.67 mmol) was added to a stirred solution of 10wt% Pd/C (40 mg) in MeOH (10 mL) under 1 atm of H_2 and stirring continued at rt for 20 h. The solution was filtered through filter paper and the solvent removed under reduced pressure affording maltol dimer **(111)** as a brown solid (0.21 g, 75%).

***N*,*N*'-(ethane-1,2-diyl)bis(3-(3-hydroxy-2-methyl-4-oxopyridin-1(4*H*)-yl)propanamide) (111)**

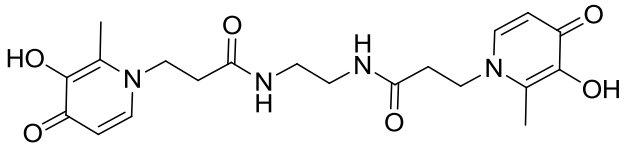

(111)

R_f [CH_2Cl_2-MeOH 8:2] 0.1; **^{1}H NMR** δ_H (500 MHz; DMSO) 2.29 (6 H, s, CH_3), 2.49 (4 H, t, *J* 7.5 Hz, 2 x CH_2), 3.01 (4 H, br s, CH_2), 4.13 (4 H, t, *J* 7.0 Hz, 2 x CH_2), 6.08 (2 H, d, *J* 7.0 Hz, COC*H*=CH), 7.47 (2 H, d, *J* 7.0 Hz, COCH=C*H*) and 8.02 (2 H, br s, NH); **^{13}C NMR** δ_C (125 MHz; DMSO) 11.3 (CH_3), 36.2 (CH_2), 38.1 (CH_2), 49.1 (CH_2), 110.5 (CH), 128.4 (Cq), 137.6 (CH), 145.4 (Cq), 168.9 (Cq) and 169.1 (Cq); **MS** m/z (ES^+) Found 419.1951 (MH^+) and 441.1759 (MNa^+), $C_{20}H_{27}N_4O_6$ (MH^+) requires 419.1931 and $C_{20}H_{26}N_4O_6Na$ (MNa^+) requires 441.1750.

Method AB

Maltol activated ester **(116)** (1.92 g, 5.0 mmol) was dissolved in DMF (5 mL) and added dropwise to a stirred solution of tris(2-aminoethyl)amine (0.15 g, 1.0 mmol) in DMF (5 mL) at rt and stirring continued for 72 h. After 72 h a white precipitate formed which was filtered off and the solvent removed under removed pressure to afford a pale yellow oil which was purified by column chromatography with silica gel using

CH_2Cl_2:MeOH 7:3 to afford the desired benzylated maltol trimer **(118)** as a white solid (0.59 g, 62%).

***N*,*N*',*N*''-(nitrilotris(ethane-2,1-diyl))tris(3-(3-(benzyloxy)-2-methyl-4-oxopyridin-1(4*H*)-yl)propanamide) (118)**

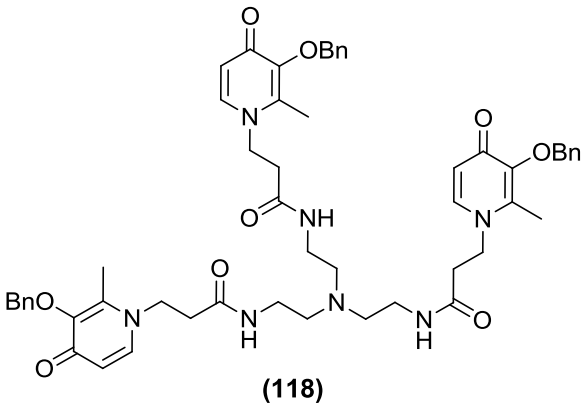

(118)

R_f [CH_2Cl_2-MeOH 8:2] 0.08; **^{1}H NMR** δ_H (500 MHz; $CDCl_3$) 2.14 (9 H, s, CH_3), 2.89 (6 H, t, *J* 6.0 Hz, 3 x CH_2), 2.54 (6 H, t, *J* 6.0 Hz, 3 x CH_2), 3.04 (6 H, t, *J* 6.0 Hz, 3 x CH_2), 4.04 (6 H, t, *J* 6.5 Hz, 3 x CH_2), 5.05 (6 H, s, Bn CH_2), 6.20 (3 H, d, *J* 7.5 Hz, COC*H*=CH), 7.26-7.36 (18 H, m, COCH=C*H* and Ph CH) and 8.00 (3 H, br s, NH); **^{13}C NMR** δ_C (125 MHz; $CDCl_3$) 12.3 (CH_3), 36.5 (CH_2), 37.8 (CH_2), 49.9 (CH_2), 54.2 (CH_2), 72.9 (CH_2), 116.8 (CH), 128.2 (CH), 128.4 (CH), 128.7 (CH), 137.2 (Cq), 139.2 (CH), 141.5 (Cq), 146.0 (Cq), 169.2 (Cq) and 173.2 (Cq); **MS** m/z (ES^+) Found 976.4614 (MNa^+), $C_{54}H_{63}N_7O_9Na$ (MNa^+) requires 976.4585.

Method AC

Benzylated maltol trimer **(118)** (0.34 g, 0.36 mmol) was added to a stirred solution of 10wt% Pd/C (34 mg) in MeOH (10 mL) under 1 atm of H_2 and stirring continued at rt for 72 h. The solution was filtered through filter paper and the solvent removed under reduced pressure affording a mixture of partially deprotected maltol trimer **(112)** and unreacted benzylated maltol trimer **(118)** (0.116 g, 34%).

Method AD

Acetyl chloride (0.23 g, 3.0 mmol) was added dropwise to a stirred solution of MeOH (5.0 mL) on ice, the solution was then allowed to warm to rt. Maltol carboxylic acid **(115)** (0.57 g, 2.0 mmol) was dissolved in MeOH (5 mL) and added dropwise to the solution and the reaction heated to 70 ^{o}C for 1 h. After 1 h the solvent was removed under reduced pressure to afford methyl ester maltol **(119)** as a white solid (0.59 g, 98%).

Synthesis of methyl 3-(3-(benzyloxy)-2-methyl-4-oxopyridin-1(4*H*)-yl)propanoate (119)

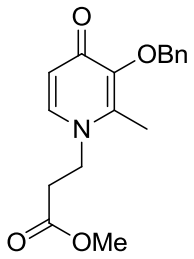

(119)

R_f [CH_2Cl_2-MeOH 9:1] 0.61; **Mp** 144-145 ^{o}C (MeOH); **IR** ν_{max}(film)/cm^{-1} 1742, 1633, 1186; **^{1}H NMR** δ_H (500 MHz; $CDCl_3$); 2.09 (3 H, s, CH_3), 2.63 (2 H, t, *J* 7.0 Hz, NCH_2CH_2), 3.70 (3 H, s, OCH_3), 4.08 (2 H, t, *J* 7.0 Hz, NCH_2CH_2), 5.21 (2 H, s, Bn CH_2), 6.42 (1 H, d, *J* 7.5 Hz, COC*H*=CH) and 7.27-7.40 (6 H, m, Ph CH and COCH=C*H*); **^{13}C NMR** δ_C (125 MHz; $CDCl_3$); 12.4 (CH_3), 34.8 (CH_2), 48.9 (CH_2), 52.3 (OCH_3), 73.0 (CH_2), 117.5 (CH), 128.0 (CH), 128.2 (CH), 129.1 (CH), 137.5 (Cq), 138.4 (CH), 140.2 (Cq), 146.2 (Cq), 170.3 (Cq) and 173.4 (Cq); **MS** m/z (ES^{+}) Found 324.1201 (MNa^{+}), $C_{17}H_{19}N_1O_4Na$ (MNa^{+}) requires 324.1212.

Method AE

Hydrazine monohydrate (0.64 g, 20.0 mmol) was added to a stirred solution of methyl ester maltol **(119)** (1.5 g, 5.0 mmol) in MeOH (10 mL) and rt and heated to 70 ^{o}C for 18 h. After 18 h the solvent was removed under reduced pressure and the residue purified by column chromatography with silica gel using CH_2Cl_2:MeOH 2:8 solvent system to afford the product **(120)** as a pale yellow solid (0.93 g, 62%).

Synthesis of 3-(3-(benzyloxy)-2-methyl-4-oxopyridin-1(4*H*)-yl)propanehydrazide (120)

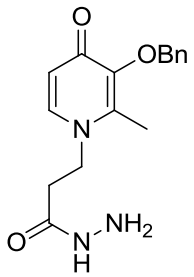

(120)

R_f [CH_2Cl_2-MeOH 9:1] 0.09; **M.p** 76-78 ^{o}C (MeOH); **IR** ν_{max}(film)/cm^{-1} 1664, 1629 and 1127; ^{1}**H NMR** δ_H (400 MHz; DMSO); 2.27 (3 H, s, CH_3), 2.48 (2 H, t, *J* 7.0 Hz, NCH_2CH_2), 4.15 (2 H, t, *J* 7.0 Hz, NCH_2CH_2), 4.38 (1 H, br s, NH), 5.07 (2 H, s, Bn CH_2), 6.18 (1 H, d, *J* 7.5 Hz, COC*H*=CH), 7.37-7.48 (5 H, m, Ph CH), 7.57 (1 H, d, *J* 7.5 Hz, COCH=C*H*) and 9.16 (1 H, s, NH); ^{13}**C NMR** δ_C (125 MHz; DMSO); 11.9 (CH_3), 34.3 (CH_2), 49.2 (CH_2), 71.9 (CH_2), 116.0 (CH), 116.1 (CH), 127.9 (CH), 128.3 (CH), 137.8 (Cq), 139.6 (CH), 140.7 (Cq), 140.8 (Cq), 145.3 (Cq), 168.2 (Cq) and 171.8 (Cq); **MS** m/z (ES$^+$) Found 302.1480 (MH^+) and 324.1310 (MNa^+), $C_{16}H_{20}N_3O_3$ (MH^+) requires 302.1505 and $C_{16}H_{19}N_3O_3Na$ (MNa^+) requires 324.1324.

Method AF

Benzyl protected maltol hydrazide **(120)** (0.93 g, 3.1 mmol) was added to a stirred solution of 20 mol% Pd/C (0.62 mg) in MeOH (10 mL) under 1.0 atm of H_2 and stirring continued at rt for 24 h. The solution was filtered through filter paper and the solvent removed under reduced pressure to give maltol hydrazide **(121)** as a beige coloured solid (0.55g, 82%).

Synthesis of 3-(3-hydroxy-2-methyl-4-oxopyridin-1(4*H*)-yl)propanehydrazide (121)

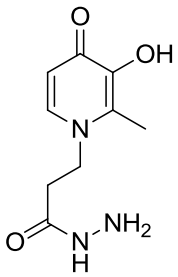

(121)

R_f [CH_2Cl_2-MeOH 9:1] 0.06; **Mp** 102-104^{o}C (MeOH); **IR** ν_{max}(film)/cm^{-1} 3616, 1668 and 1626; **^{1}H NMR** δ_H (500 MHz; DMSO); 2.35 (3H, s, CH_3), 2.56 (2 H, t, *J* 7.0 Hz, NC*H*$_2$CH$_2$), 4.26 (2 H, t, *J* 7.0 Hz, NCH$_2$C*H*$_2$), 6.38 (1 H, d, *J* 7.0 Hz, COC*H*=CH), 7.65 (1 H, d, *J* 7.0 Hz, COCH=C*H*) and 9.71 (1 H, br s, OH); **^{13}C NMR** δ_c (125 MHz; DMSO); 11.6 (CH_3), 34.1 (CH_2), 49.8 (CH_2), 110.7 (CH), 131.8 (Cq), 137.9 (CH), 144.8 (Cq), 166.6 (Cq) and 168.2 (Cq); **MS** m/z (ES$^+$) Found 212.1033 (MH$^+$) and 234.0838 (MNa$^+$), $C_9H_{14}N_3O_3$ (MH$^+$) requires 212.1035 and $C_9H_{13}N_3O_3Na$ (MNa$^+$) requires 234.0855.

MTS Assays

Chalcone (40)

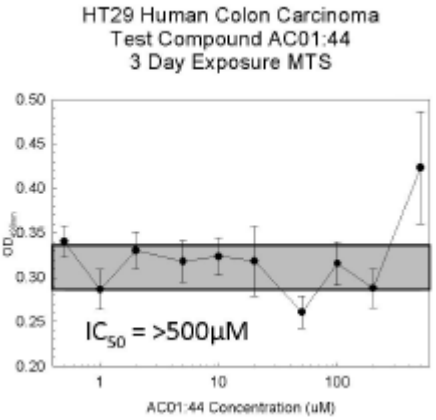

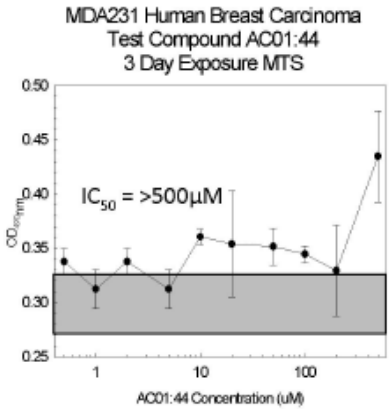

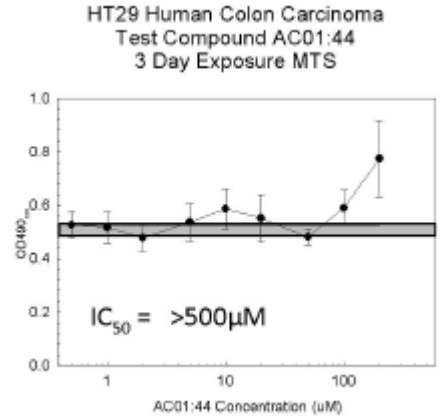

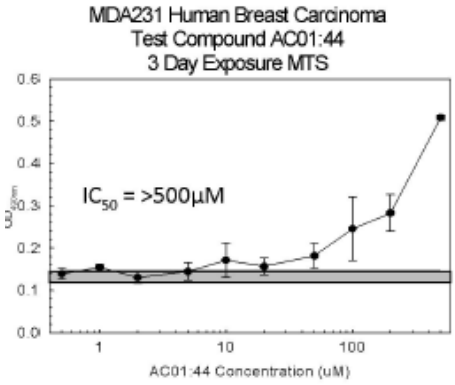

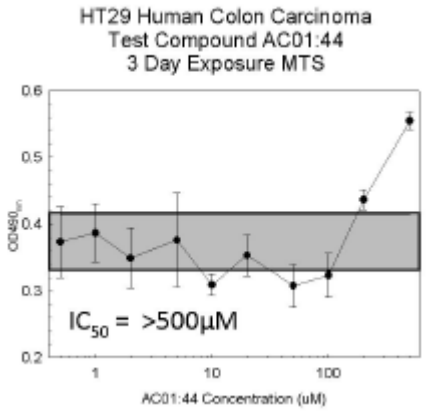

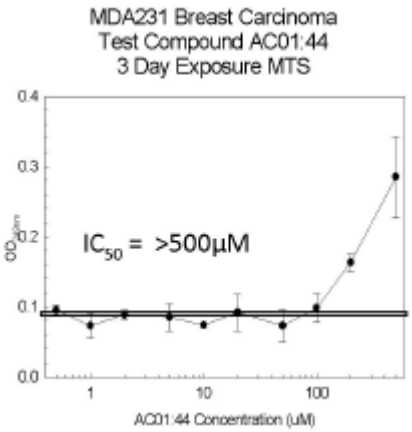

1% DMSO only
Points are means ± s.d
n = 4

Chalcone (40)

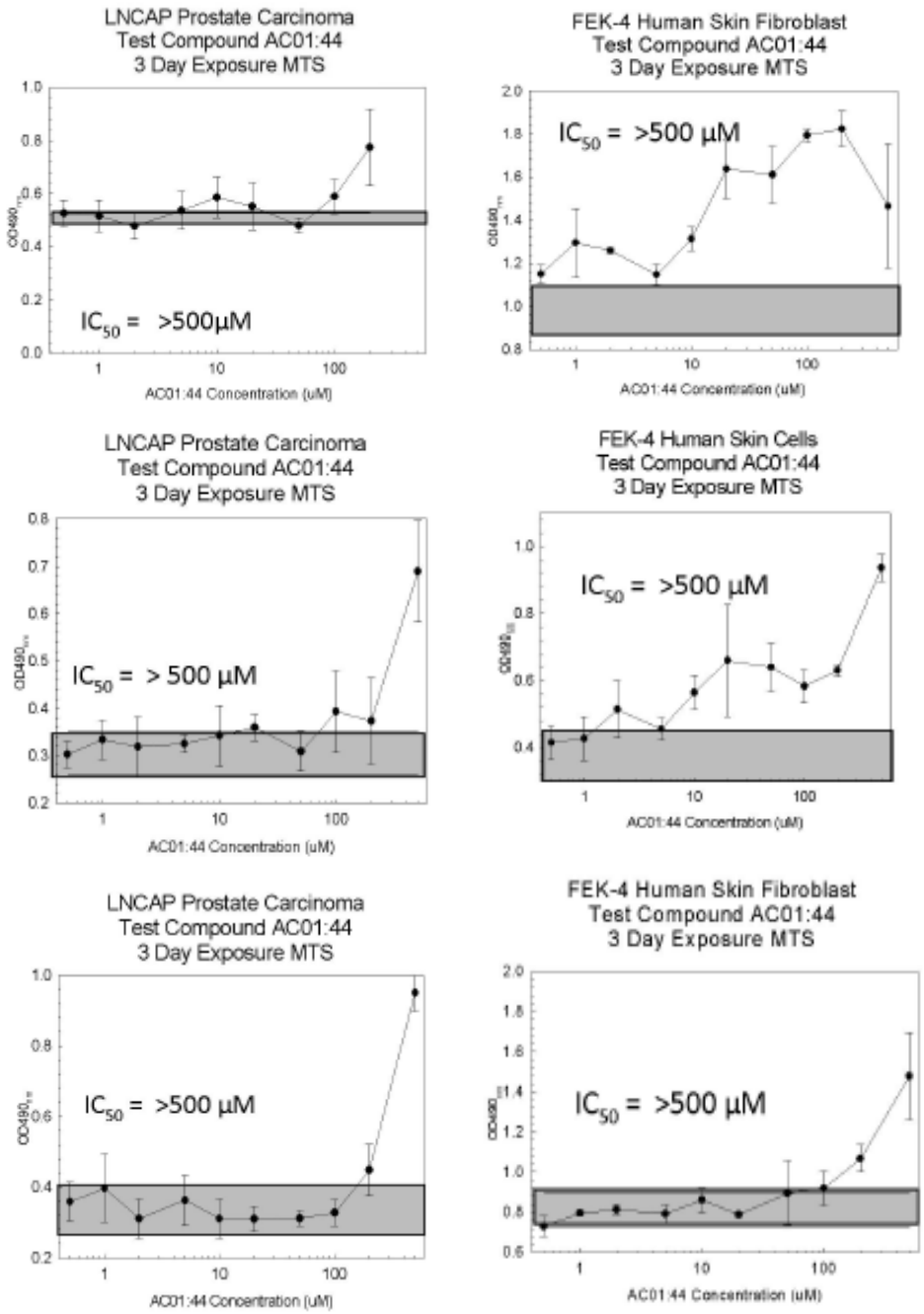

Chalcone (41)

LNCaP Human Prostate Carcinoma

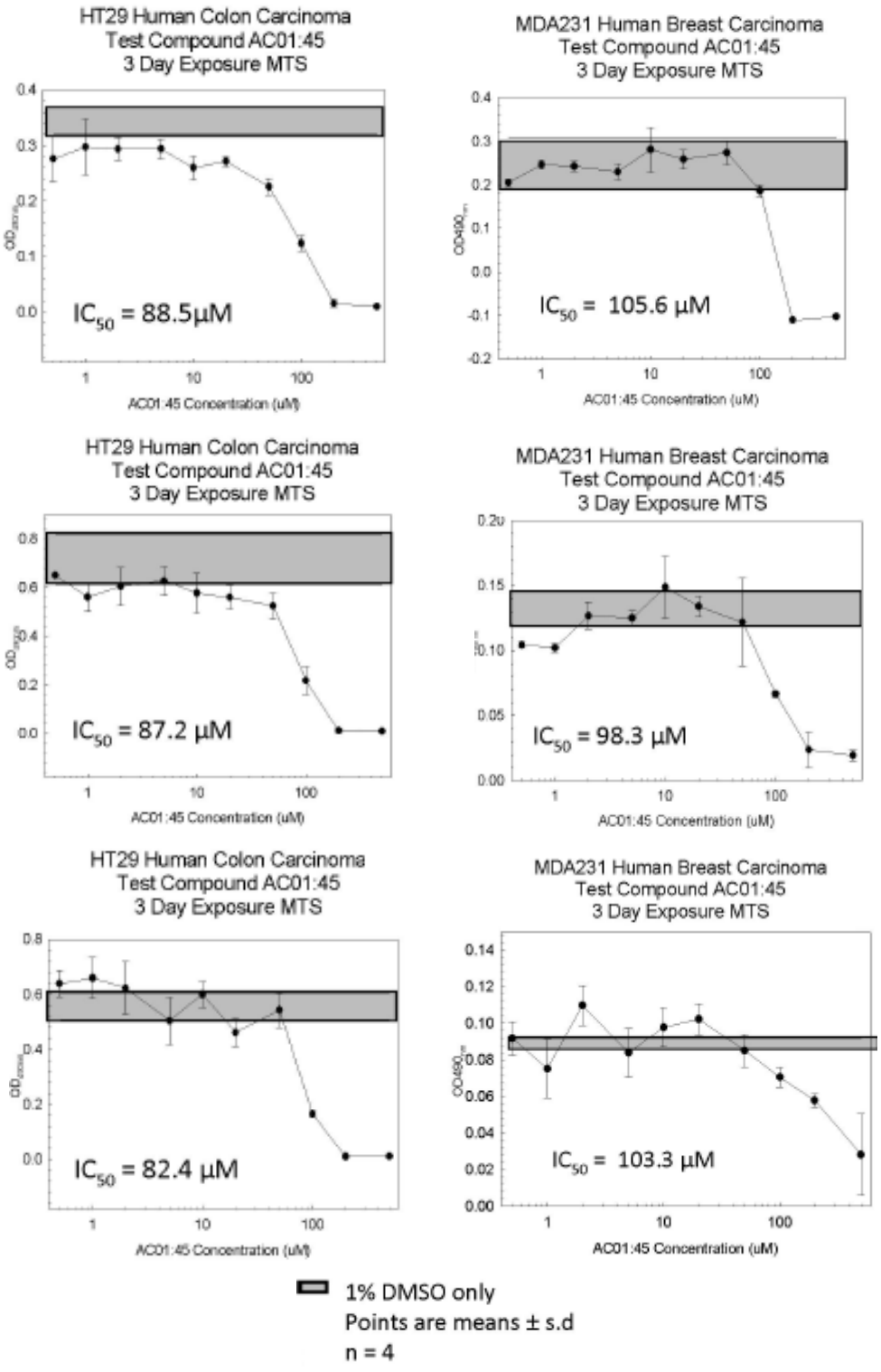
HT29 Human Colon Carcinoma
Test Compound AC01:45
3 Day Exposure MTS
IC50 = 88.5µM
AC01:45 Concentration (uM)
MDA231 Human Breast Carcinoma
Test Compound AC01:45
3 Day Exposure MTS
IC50 = 105.6 µM
AC01:45 Concentration (uM)
HT29 Human Colon Carcinoma
Test Compound AC01:45
3 Day Exposure MTS
IC50 = 87.2 µM
AC01:45 Concentration (uM)
MDA231 Human Breast Carcinoma
Test Compound AC01:45
3 Day Exposure MTS
IC50 = 98.3 µM
AC01:45 Concentration (uM)
HT29 Human Colon Carcinoma
Test Compound AC01:45
3 Day Exposure MTS
IC50 = 82.4 µM
AC01:45 Concentration (uM)
MDA231 Human Breast Carcinoma
Test Compound AC01:45
3 Day Exposure MTS
IC50 = 103.3 µM
AC01:45 Concentration (uM)
1% DMSO only
Points are means ± s.d
n = 4

Chalcone (41)

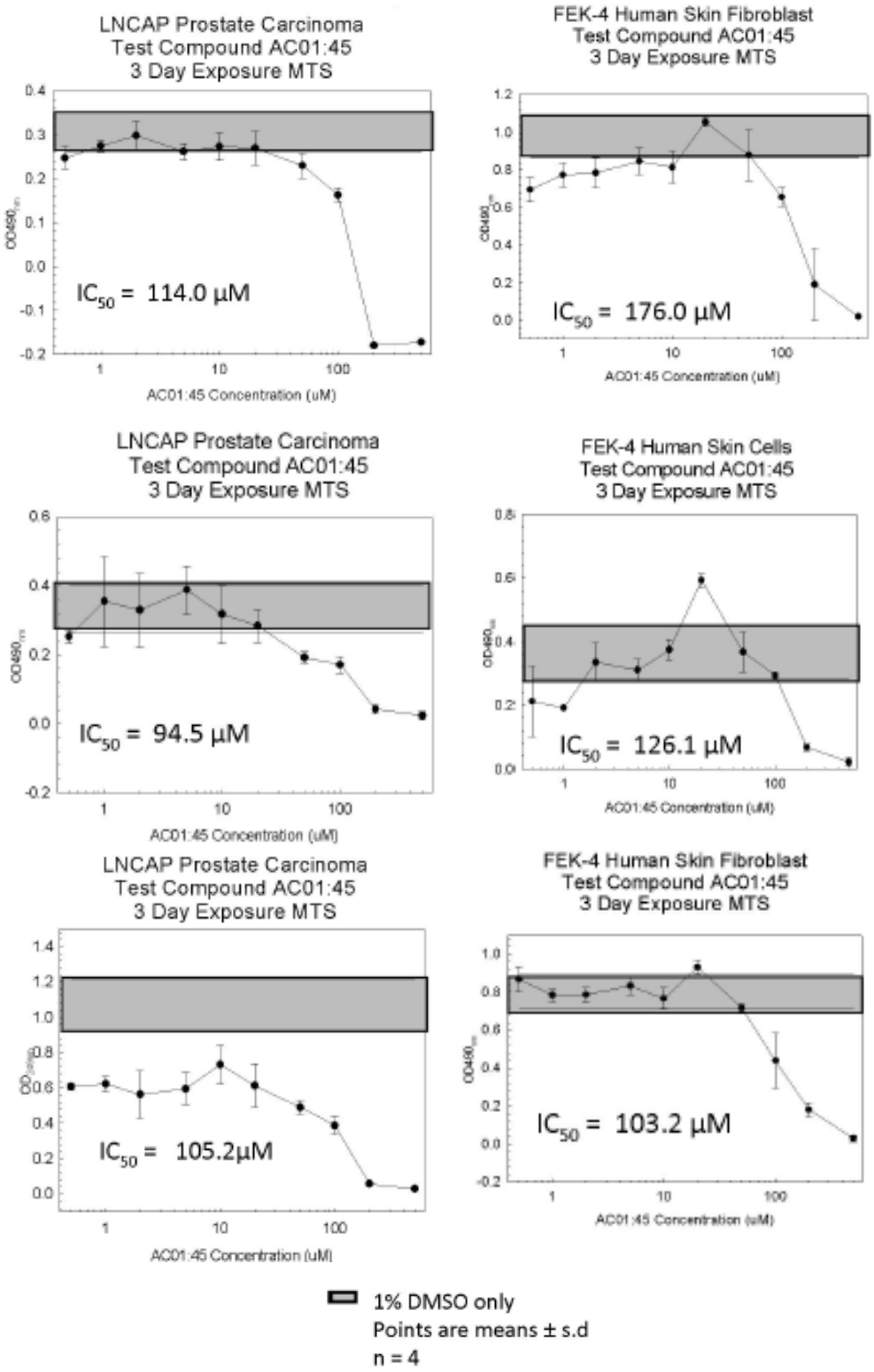
LNCAP Prostate Carcinoma
Test Compound AC01:45
3 Day Exposure MTS
IC50 = 114.0 µM
AC01:45 Concentration (uM)
FEK-4 Human Skin Fibroblast
Test Compound AC01:45
3 Day Exposure MTS
IC50 = 176.0 µM
AC01:45 Concentration (uM)
LNCAP Prostate Carcinoma
Test Compound AC01:45
3 Day Exposure MTS
IC50 = 94.5 µM
AC01:45 Concentration (uM)
FEK-4 Human Skin Cells
Test Compound AC01:45
3 Day Exposure MTS
IC50 = 126.1 µM
AC01:45 Concentration (uM)
LNCAP Prostate Carcinoma
Test Compound AC01:45
3 Day Exposure MTS
IC50 = 105.2µM
AC01:45 Concentration (uM)
FEK-4 Human Skin Fibroblast
Test Compound AC01:45
3 Day Exposure MTS
IC50 = 103.2 µM
AC01:45 Concentration (uM)
1% DMSO only
Points are means ± s.d
n = 4

Chalcone (42)

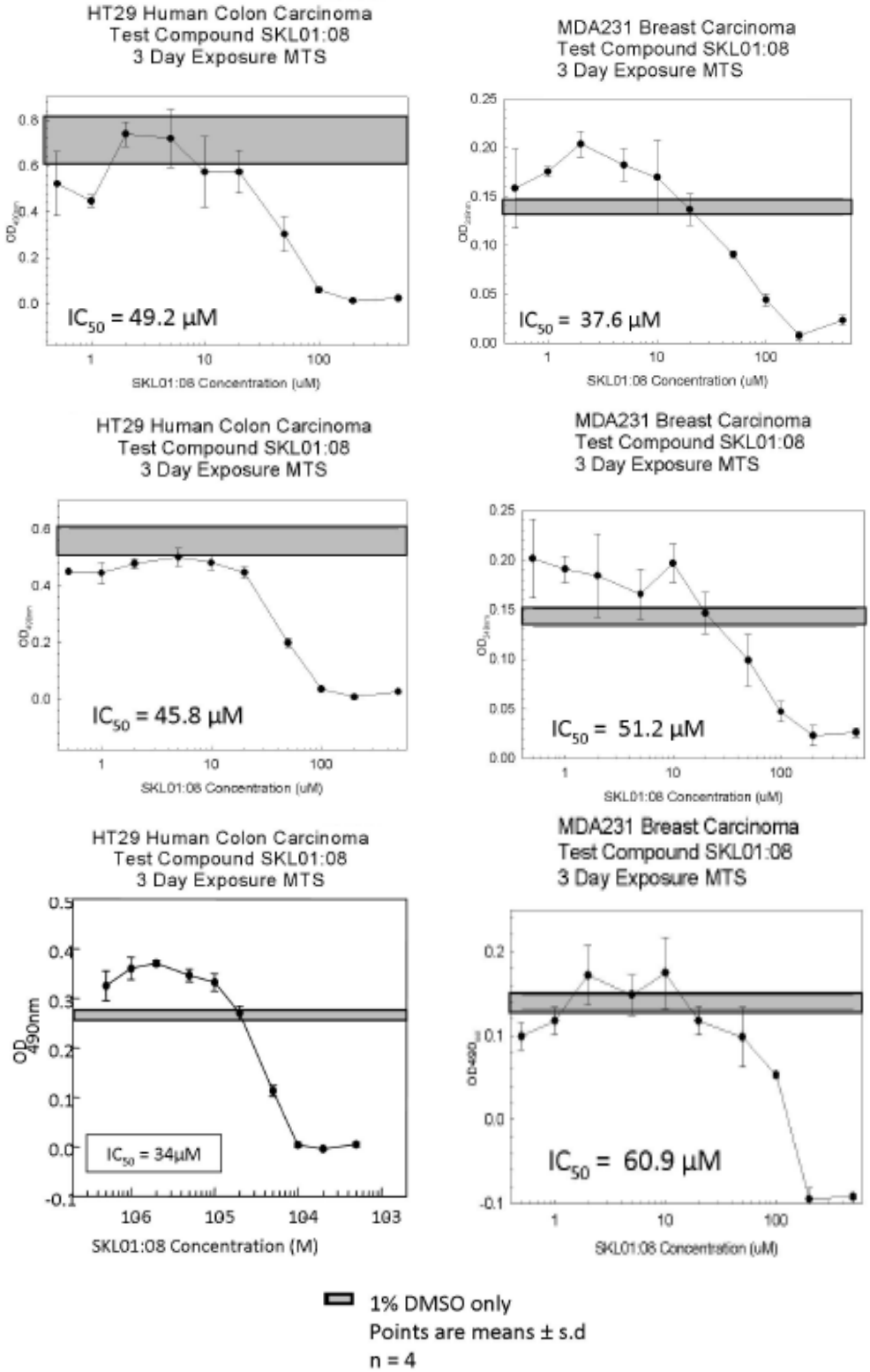
HT29 Human Colon Carcinoma
Test Compound SKL01:08
3 Day Exposure MTS
IC50 = 49.2 µM
SKL01:08 Concentration (uM)
MDA231 Breast Carcinoma
Test Compound SKL01:08
3 Day Exposure MTS
IC50 = 37.6 µM
SKL01:08 Concentration (uM)
HT29 Human Colon Carcinoma
Test Compound SKL01:08
3 Day Exposure MTS
IC50 = 45.8 µM
SKL01:08 Concentration (uM)
MDA231 Breast Carcinoma
Test Compound SKL01:08
3 Day Exposure MTS
IC50 = 51.2 µM
SKL01:08 Concentration (uM)
HT29 Human Colon Carcinoma
Test Compound SKL01:08
3 Day Exposure MTS
OD490nm
IC50 = 34µM
SKL01:08 Concentration (M)
MDA231 Breast Carcinoma
Test Compound SKL01:08
3 Day Exposure MTS
IC50 = 60.9 µM
SKL01:08 Concentration (uM)
1% DMSO only
Points are means ± s.d
n = 4

Chalcone (42)

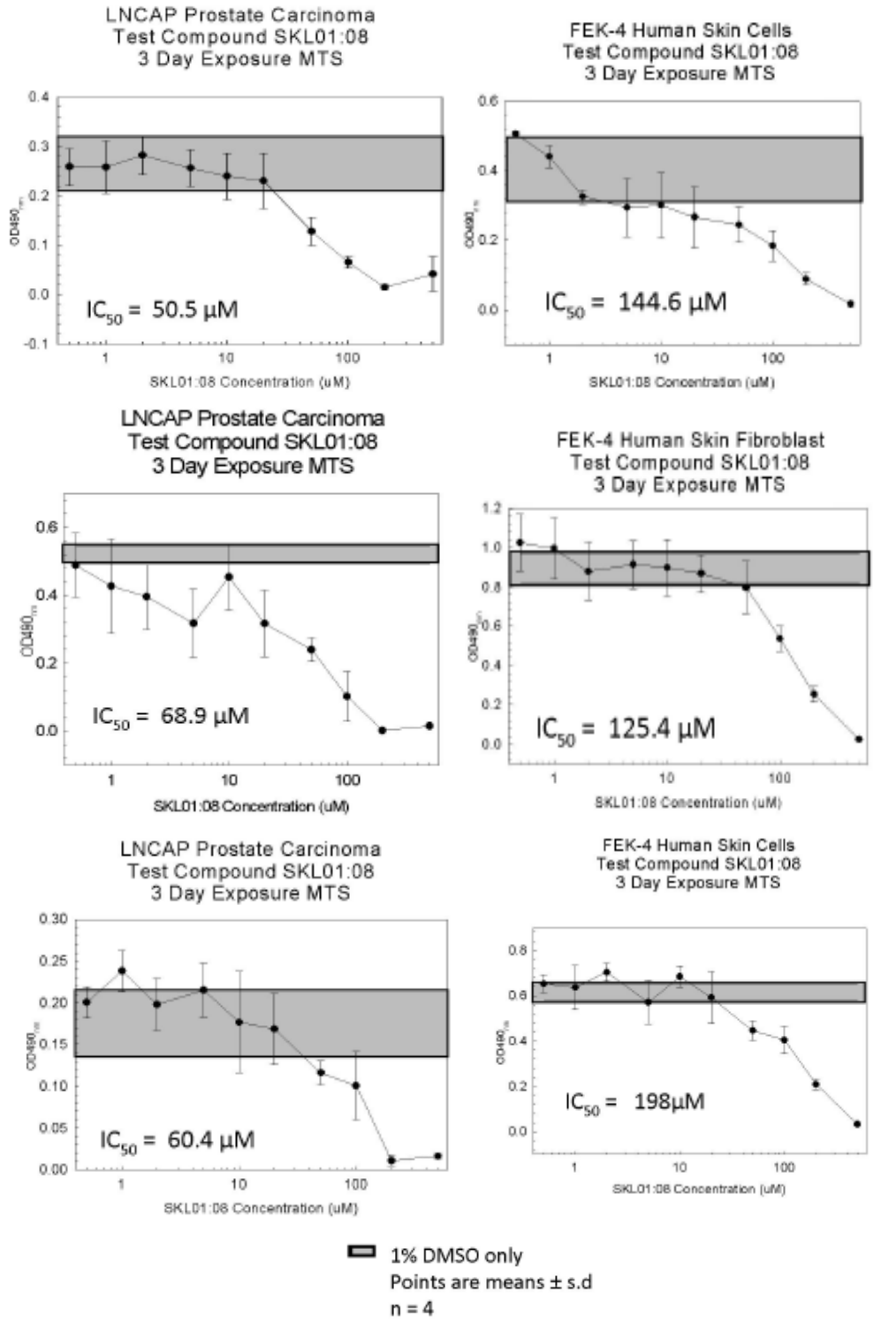
LNCAP Prostate Carcinoma
Test Compound SKL01:08
3 Day Exposure MTS
IC50 = 50.5 µM
SKL01:08 Concentration (uM)
FEK-4 Human Skin Cells
Test Compound SKL01:08
3 Day Exposure MTS
IC50 = 144.6 µM
SKL01:08 Concentration (uM)
LNCAP Prostate Carcinoma
Test Compound SKL01:08
3 Day Exposure MTS
IC50 = 68.9 µM
SKL01:08 Concentration (uM)
FEK-4 Human Skin Fibroblast
Test Compound SKL01:08
3 Day Exposure MTS
IC50 = 125.4 µM
SKL01:08 Concentration (uM)
LNCAP Prostate Carcinoma
Test Compound SKL01:08
3 Day Exposure MTS
IC50 = 60.4 µM
SKL01:08 Concentration (uM)
FEK-4 Human Skin Cells
Test Compound SKL01:08
3 Day Exposure MTS
IC50 = 198µM
SKL01:08 Concentration (uM)
1% DMSO only
Points are means ± s.d
n = 4

Chalcone (43)

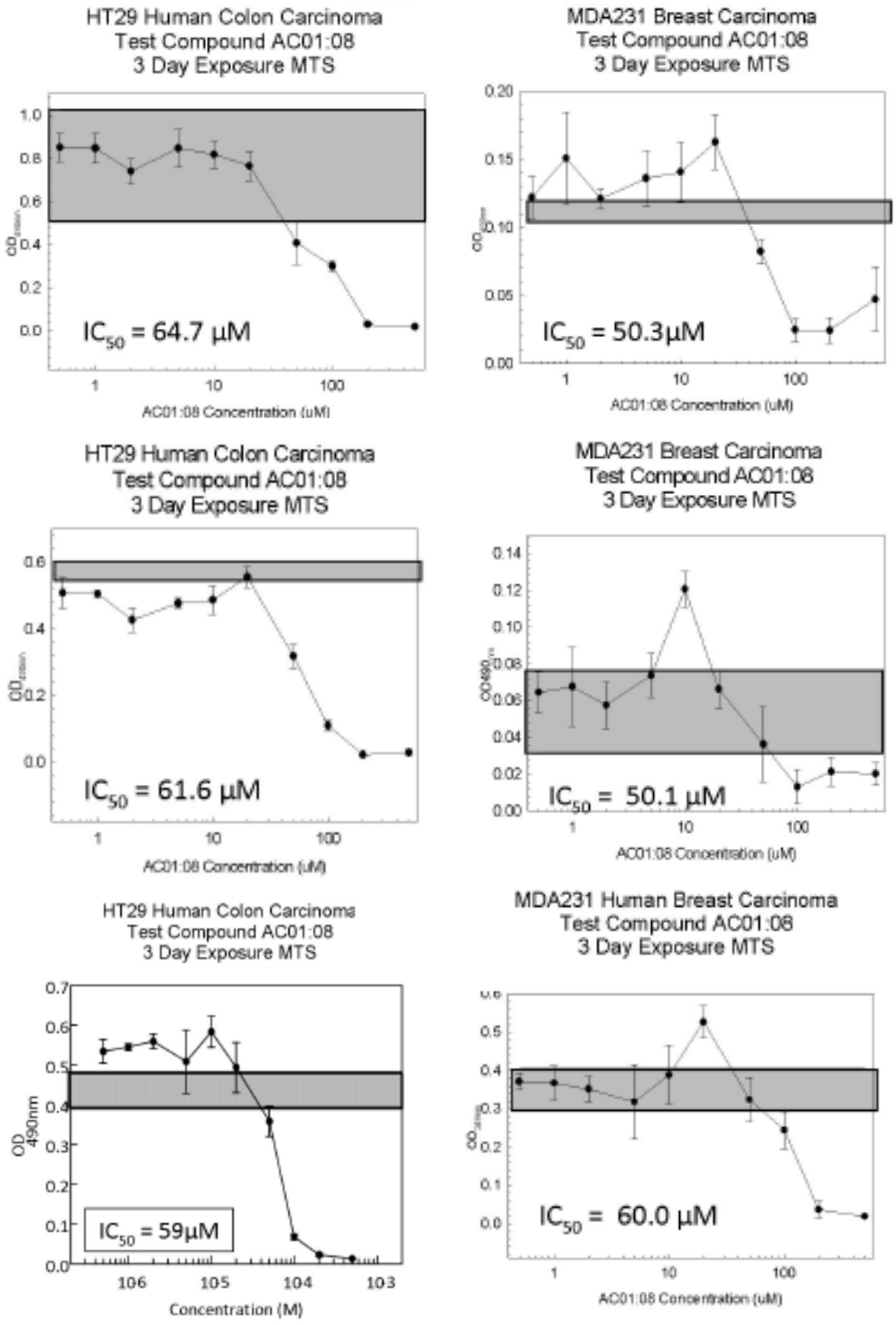
HT29 Human Colon Carcinoma
Test Compound AC01:08
3 Day Exposure MTS
IC50 = 64.7 µM
AC01:08 Concentration (uM)
MDA231 Breast Carcinoma
Test Compound AC01:08
3 Day Exposure MTS
IC50 = 50.3µM
AC01:08 Concentration (uM)
HT29 Human Colon Carcinoma
Test Compound AC01:08
3 Day Exposure MTS
IC50 = 61.6 µM
AC01:08 Concentration (uM)
MDA231 Breast Carcinoma
Test Compound AC01:08
3 Day Exposure MTS
IC50 = 50.1 µM
AC01:08 Concentration (uM)
HT29 Human Colon Carcinoma
Test Compound AC01:08
3 Day Exposure MTS
IC50 = 59µM
OD 490nm
Concentration (M)
MDA231 Human Breast Carcinoma
Test Compound AC01:08
3 Day Exposure MTS
IC50 = 60.0 µM
AC01:08 Concentration (uM)
1% DMSO only
Points are means ± s.d
n = 4

Chalcone (43)

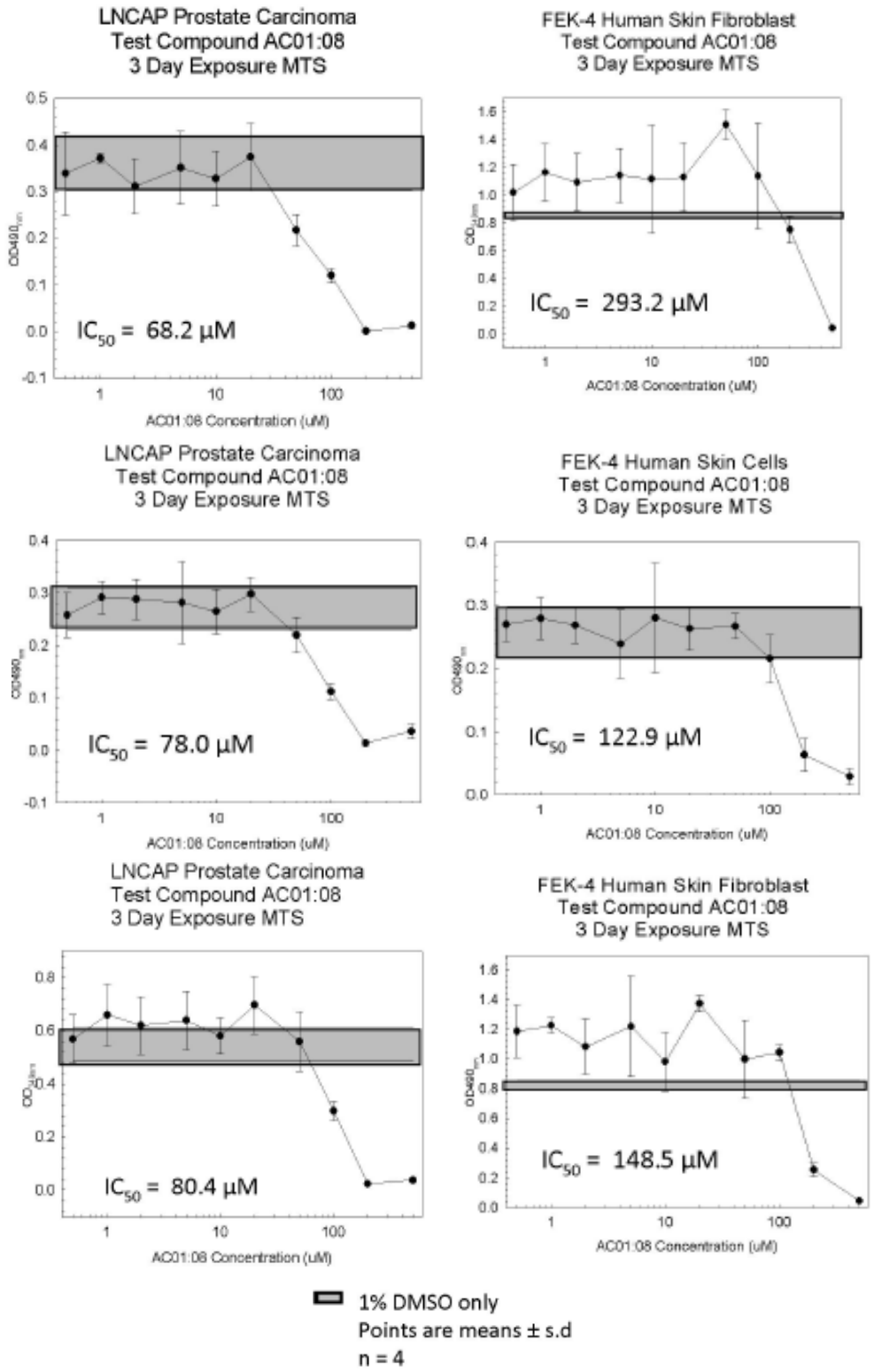
LNCAP Prostate Carcinoma
Test Compound AC01:08
3 Day Exposure MTS
IC50 = 68.2 µM
AC01:08 Concentration (uM)
FEK-4 Human Skin Fibroblast
Test Compound AC01:08
3 Day Exposure MTS
IC50 = 293.2 µM
AC01:08 Concentration (uM)
LNCAP Prostate Carcinoma
Test Compound AC01:08
3 Day Exposure MTS
IC50 = 78.0 µM
AC01:08 Concentration (uM)
FEK-4 Human Skin Cells
Test Compound AC01:08
3 Day Exposure MTS
IC50 = 122.9 µM
AC01:08 Concentration (uM)
LNCAP Prostate Carcinoma
Test Compound AC01:08
3 Day Exposure MTS
IC50 = 80.4 µM
AC01:08 Concentration (uM)
FEK-4 Human Skin Fibroblast
Test Compound AC01:08
3 Day Exposure MTS
IC50 = 148.5 µM
AC01:08 Concentration (uM)
1% DMSO only
Points are means ± s.d
n = 4

Chalcone (44)

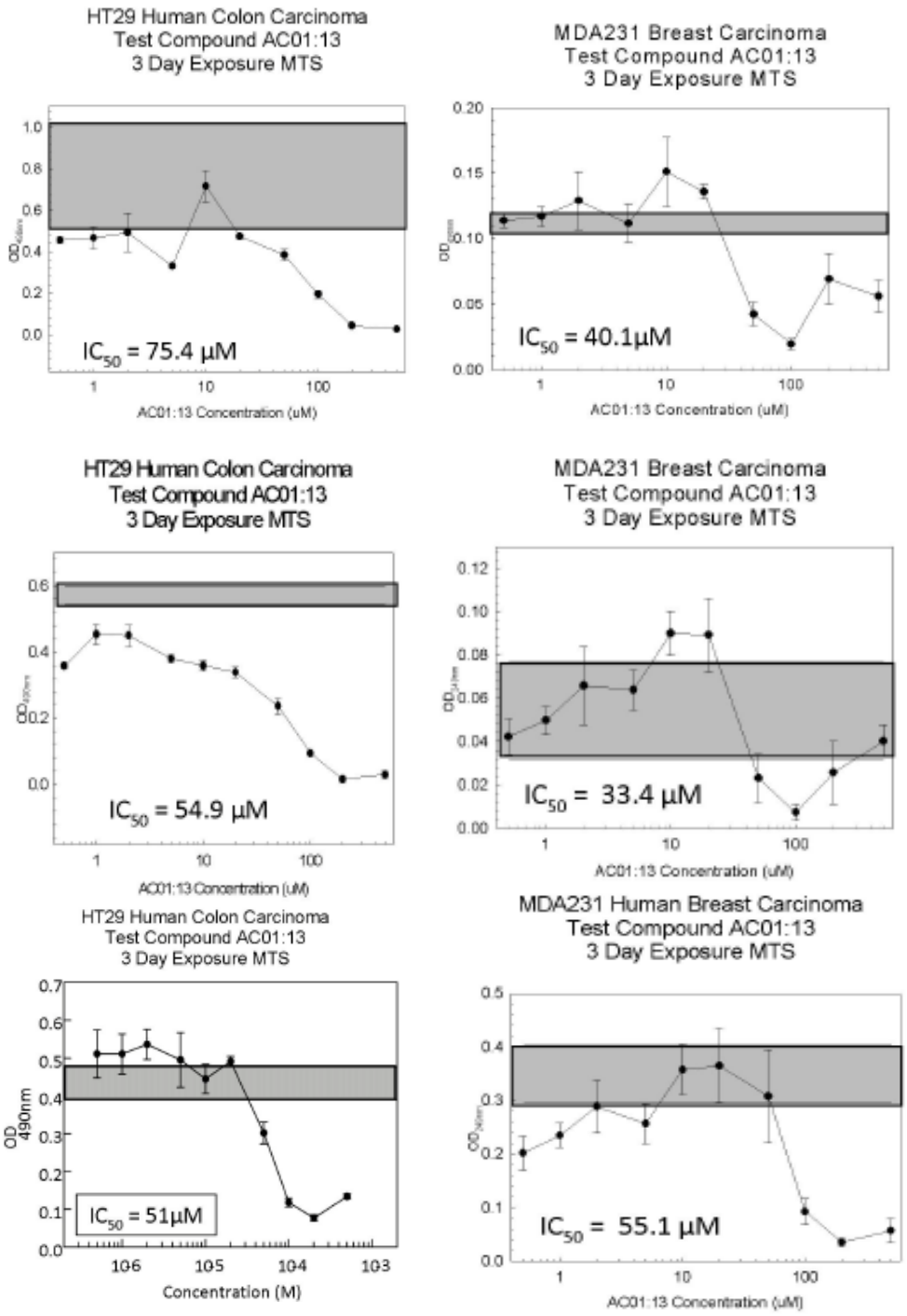
HT29 Human Colon Carcinoma
Test Compound AC01:13
3 Day Exposure MTS
IC50 = 75.4 µM
AC01:13 Concentration (uM)
MDA231 Breast Carcinoma
Test Compound AC01:13
3 Day Exposure MTS
IC50 = 40.1µM
AC01:13 Concentration (uM)
HT29 Human Colon Carcinoma
Test Compound AC01:13
3 Day Exposure MTS
IC50 = 54.9 µM
AC01:13 Concentration (uM)
MDA231 Breast Carcinoma
Test Compound AC01:13
3 Day Exposure MTS
IC50 = 33.4 µM
AC01:13 Concentration (uM)
HT29 Human Colon Carcinoma
Test Compound AC01:13
3 Day Exposure MTS
OD 490nm
IC50 = 51µM
Concentration (M)
MDA231 Human Breast Carcinoma
Test Compound AC01:13
3 Day Exposure MTS
IC50 = 55.1 µM
AC01:13 Concentration (uM)
1% DMSO only
Points are means ± s.d
n = 4

Chalcone (44)

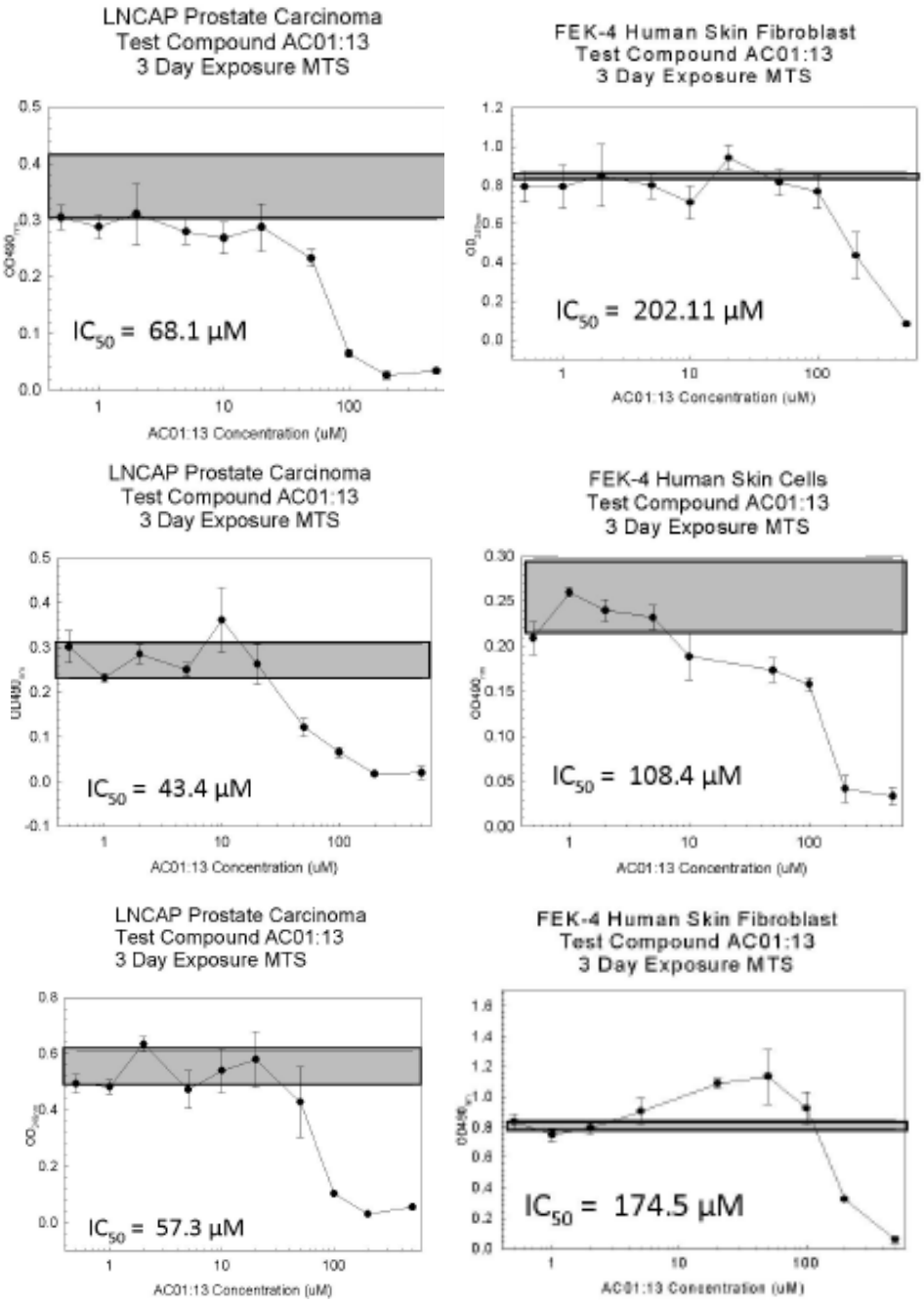
LNCAP Prostate Carcinoma
Test Compound AC01:13
3 Day Exposure MTS
IC50 = 68.1 µM
AC01:13 Concentration (uM)
FEK-4 Human Skin Fibroblast
Test Compound AC01:13
3 Day Exposure MTS
IC50 = 202.11 µM
AC01:13 Concentration (uM)
LNCAP Prostate Carcinoma
Test Compound AC01:13
3 Day Exposure MTS
IC50 = 43.4 µM
AC01:13 Concentration (uM)
FEK-4 Human Skin Cells
Test Compound AC01:13
3 Day Exposure MTS
IC50 = 108.4 µM
AC01:13 Concentration (uM)
LNCAP Prostate Carcinoma
Test Compound AC01:13
3 Day Exposure MTS
IC50 = 57.3 µM
AC01:13 Concentration (uM)
FEK-4 Human Skin Fibroblast
Test Compound AC01:13
3 Day Exposure MTS
IC50 = 174.5 µM
AC01:13 Concentration (uM)
1% DMSO only
Points are means ± s.d
n = 4

Chalcone (45)

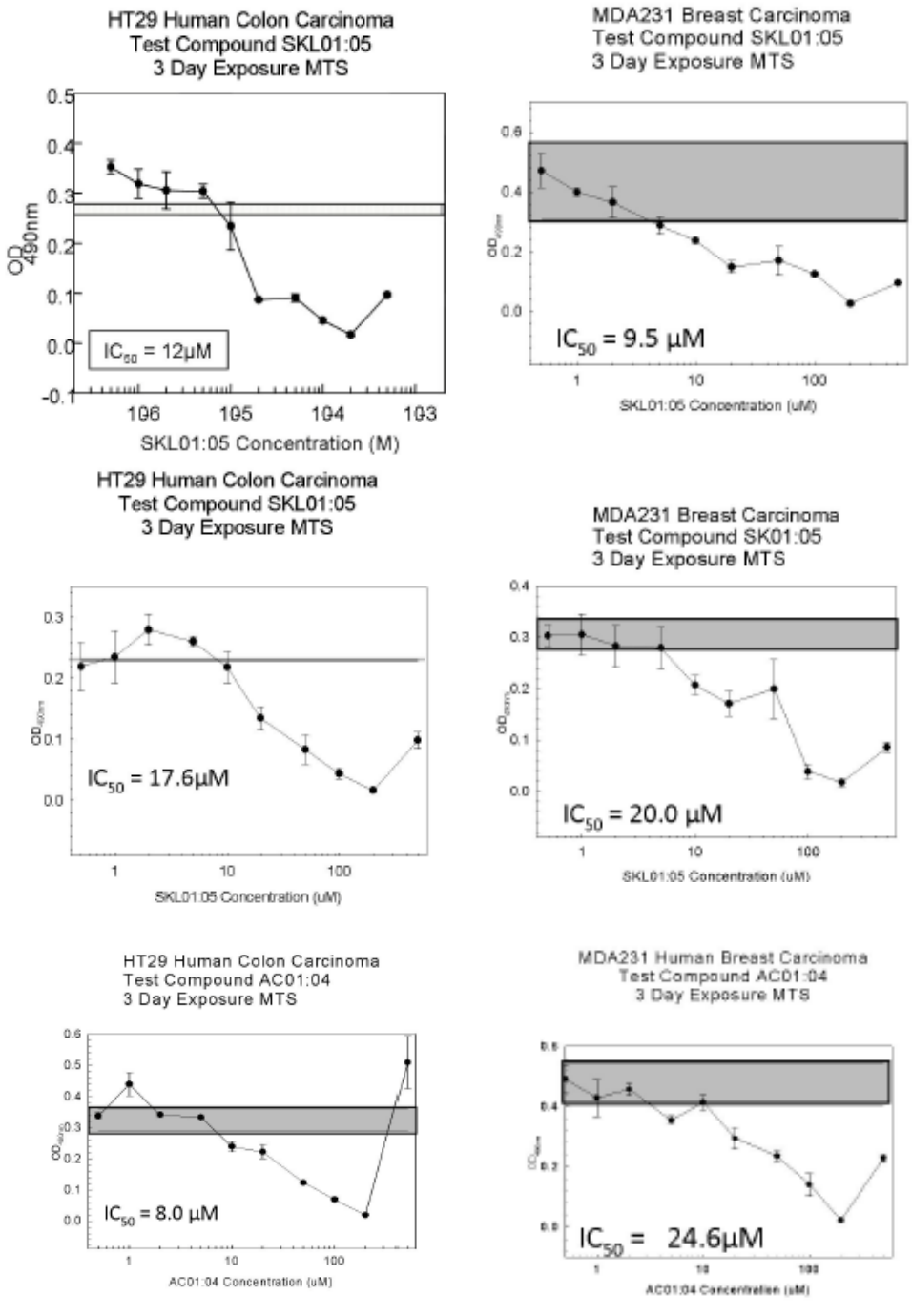
HT29 Human Colon Carcinoma
Test Compound SKL01:05
3 Day Exposure MTS
OD 490nm
IC50 = 12µM
SKL01:05 Concentration (M)
MDA231 Breast Carcinoma
Test Compound SKL01:05
3 Day Exposure MTS
IC50 = 9.5 µM
SKL01:05 Concentration (uM)
HT29 Human Colon Carcinoma
Test Compound SKL01:05
3 Day Exposure MTS
IC50 = 17.6µM
SKL01:05 Concentration (uM)
MDA231 Breast Carcinoma
Test Compound SK01:05
3 Day Exposure MTS
IC50 = 20.0 µM
SKL01:05 Concentration (uM)
HT29 Human Colon Carcinoma
Test Compound AC01:04
3 Day Exposure MTS
IC50 = 8.0 µM
AC01:04 Concentration (uM)
MDA231 Human Breast Carcinoma
Test Compound AC01:04
3 Day Exposure MTS
IC50 = 24.6µM
AC01:04 Concentration (uM)
1% DMSO only
Points are means ± s.d
n = 4

Chalcone (45)

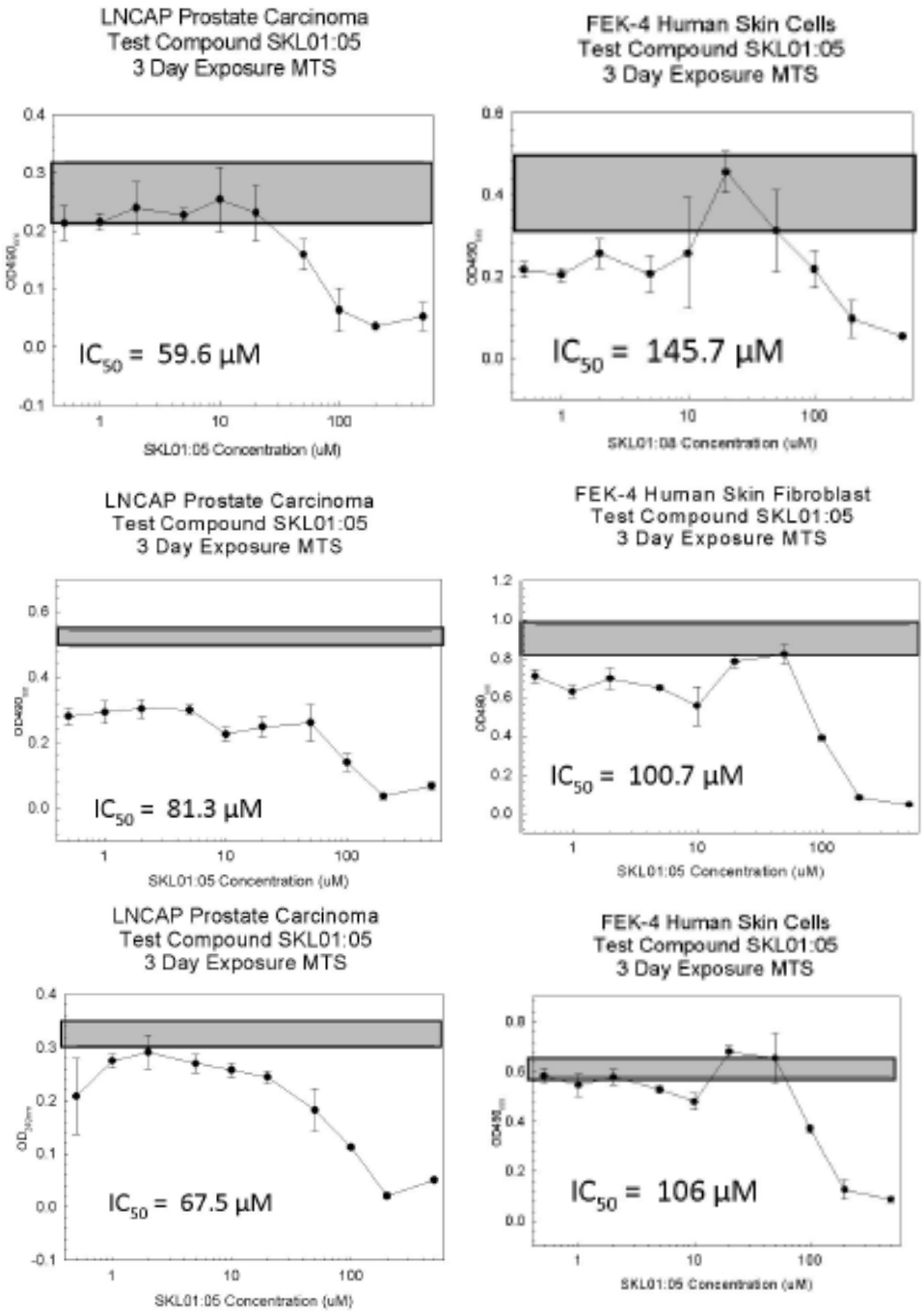
LNCAP Prostate Carcinoma
Test Compound SKL01:05
3 Day Exposure MTS
IC50 = 59.6 µM
SKL01:05 Concentration (uM)
FEK-4 Human Skin Cells
Test Compound SKL01:05
3 Day Exposure MTS
IC50 = 145.7 µM
SKL01:08 Concentration (uM)
LNCAP Prostate Carcinoma
Test Compound SKL01:05
3 Day Exposure MTS
IC50 = 81.3 µM
SKL01:05 Concentration (uM)
FEK-4 Human Skin Fibroblast
Test Compound SKL01:05
3 Day Exposure MTS
IC50 = 100.7 µM
SKL01:05 Concentration (uM)
LNCAP Prostate Carcinoma
Test Compound SKL01:05
3 Day Exposure MTS
IC50 = 67.5 µM
SKL01:05 Concentration (uM)
FEK-4 Human Skin Cells
Test Compound SKL01:05
3 Day Exposure MTS
IC50 = 106 µM
SKL01:05 Concentration (uM)
1% DMSO only
Points are means ± s.d
n = 4

Chalcone (46)

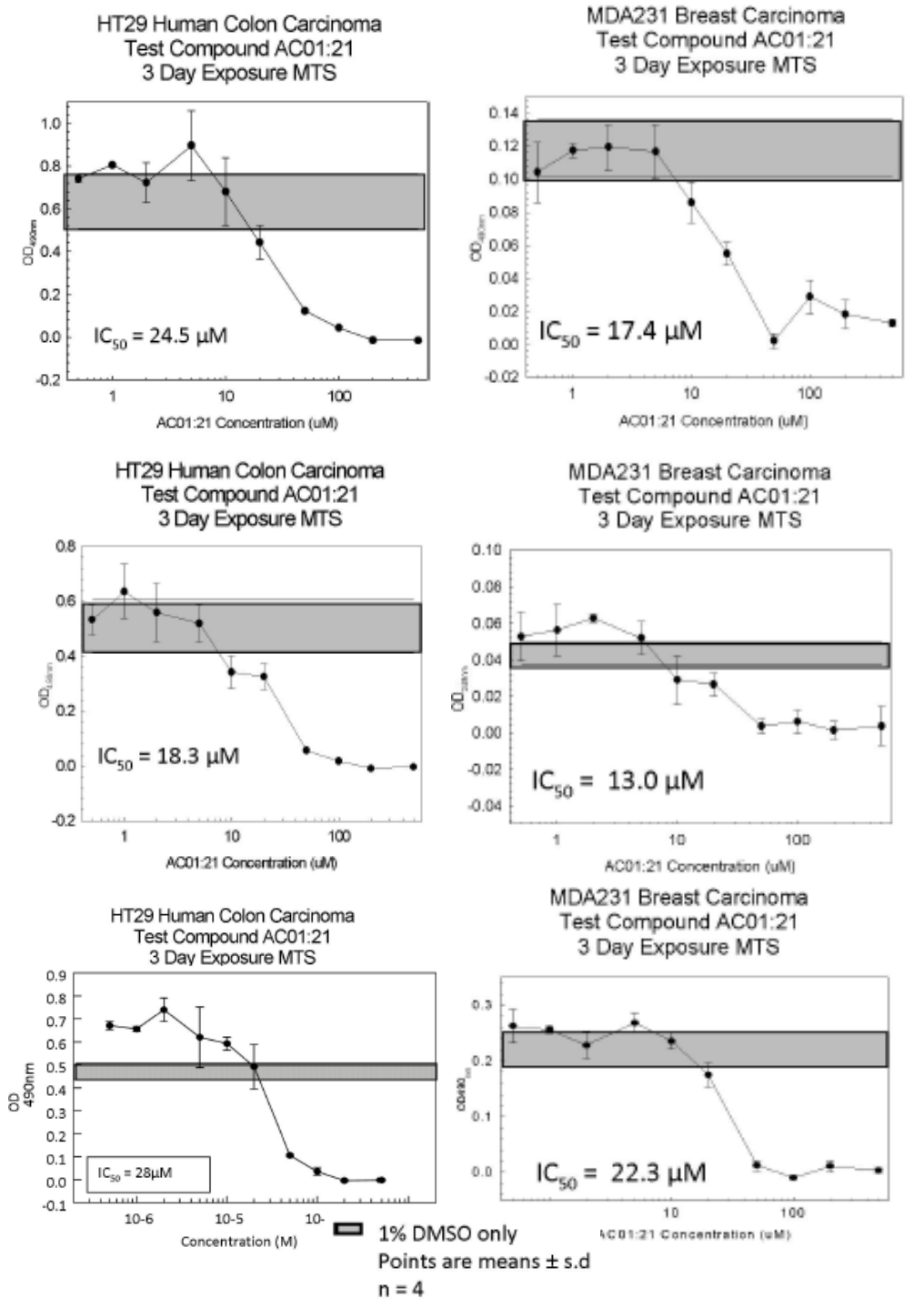
HT29 Human Colon Carcinoma
Test Compound AC01:21
3 Day Exposure MTS
IC50 = 24.5 µM
AC01:21 Concentration (uM)
MDA231 Breast Carcinoma
Test Compound AC01:21
3 Day Exposure MTS
IC50 = 17.4 µM
AC01:21 Concentration (uM)
HT29 Human Colon Carcinoma
Test Compound AC01:21
3 Day Exposure MTS
IC50 = 18.3 µM
AC01:21 Concentration (uM)
MDA231 Breast Carcinoma
Test Compound AC01:21
3 Day Exposure MTS
IC50 = 13.0 µM
AC01:21 Concentration (uM)
HT29 Human Colon Carcinoma
Test Compound AC01:21
3 Day Exposure MTS
OD 490nm
IC50 = 28µM
Concentration (M)
MDA231 Breast Carcinoma
Test Compound AC01:21
3 Day Exposure MTS
IC50 = 22.3 µM
1% DMSO only
Points are means ± s.d
n = 4

Chalcone (46)

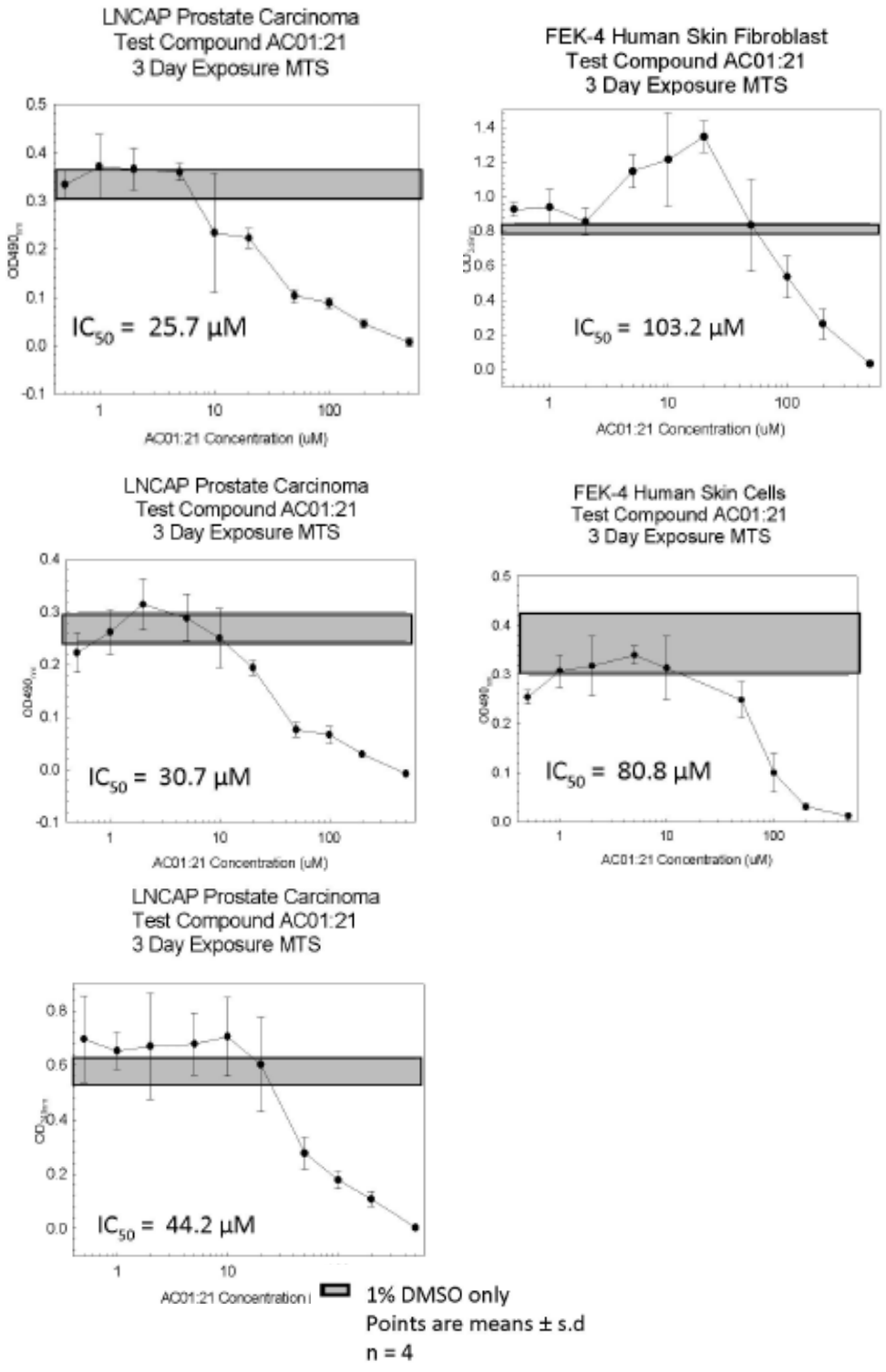
LNCAP Prostate Carcinoma
Test Compound AC01:21
3 Day Exposure MTS
IC50 = 25.7 µM
AC01:21 Concentration (uM)
FEK-4 Human Skin Fibroblast
Test Compound AC01:21
3 Day Exposure MTS
IC50 = 103.2 µM
AC01:21 Concentration (uM)
LNCAP Prostate Carcinoma
Test Compound AC01:21
3 Day Exposure MTS
IC50 = 30.7 µM
AC01:21 Concentration (uM)
FEK-4 Human Skin Cells
Test Compound AC01:21
3 Day Exposure MTS
IC50 = 80.8 µM
AC01:21 Concentration (uM)
LNCAP Prostate Carcinoma
Test Compound AC01:21
3 Day Exposure MTS
IC50 = 44.2 µM
AC01:21 Concentration (uM)
1% DMSO only
Points are means ± s.d
n = 4

Chalcone (47)

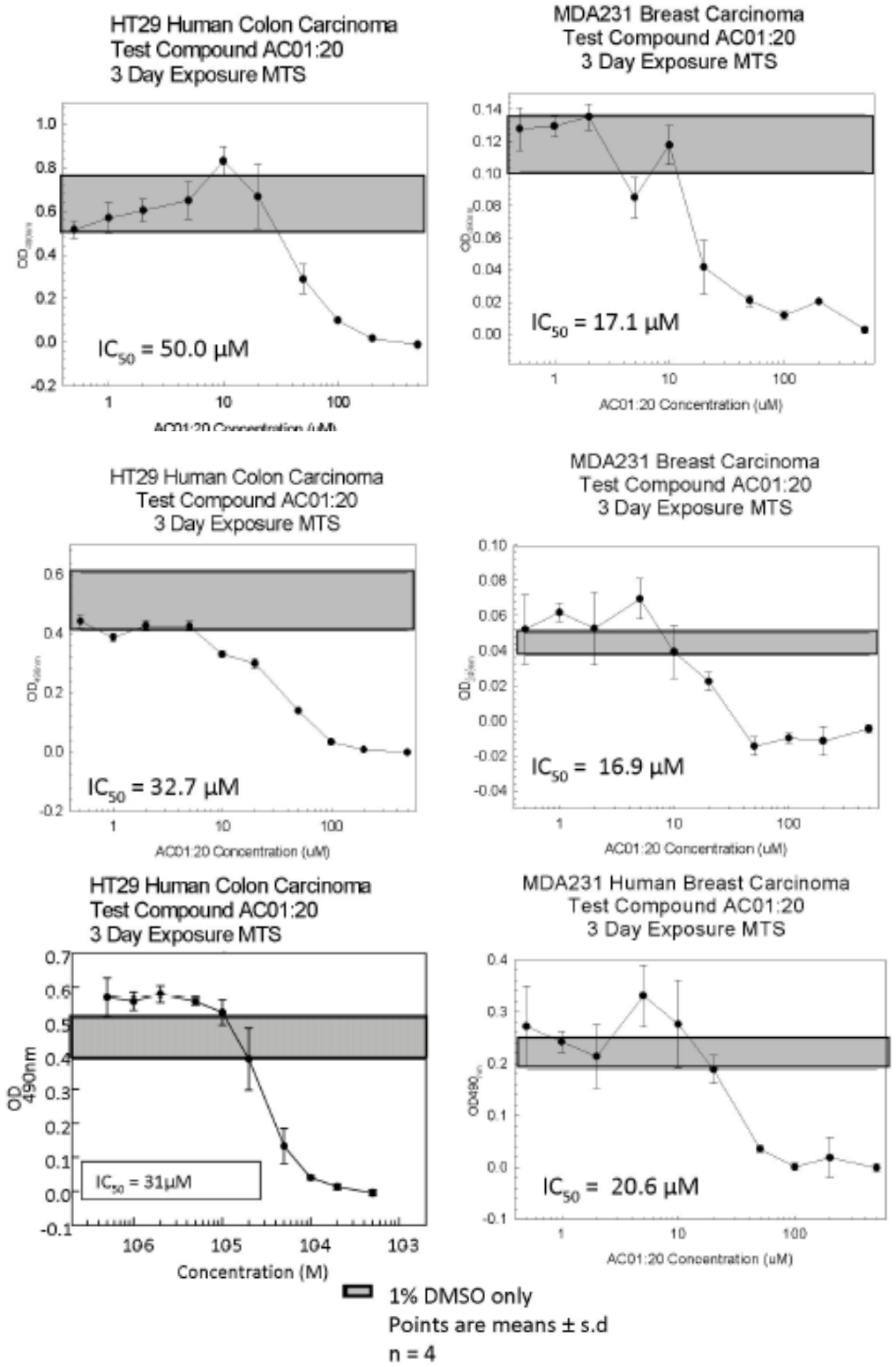
HT29 Human Colon Carcinoma
Test Compound AC01:20
3 Day Exposure MTS
IC50 = 50.0 µM
MDA231 Breast Carcinoma
Test Compound AC01:20
3 Day Exposure MTS
IC50 = 17.1 µM
AC01:20 Concentration (uM)
HT29 Human Colon Carcinoma
Test Compound AC01:20
3 Day Exposure MTS
IC50 = 32.7 µM
AC01:20 Concentration (uM)
MDA231 Breast Carcinoma
Test Compound AC01:20
3 Day Exposure MTS
IC50 = 16.9 µM
AC01:20 Concentration (uM)
HT29 Human Colon Carcinoma
Test Compound AC01:20
3 Day Exposure MTS
IC50 = 31µM
OD 490nm
Concentration (M)
MDA231 Human Breast Carcinoma
Test Compound AC01:20
3 Day Exposure MTS
IC50 = 20.6 µM
AC01:20 Concentration (uM)
1% DMSO only
Points are means ± s.d
n = 4

Chalcone (47)

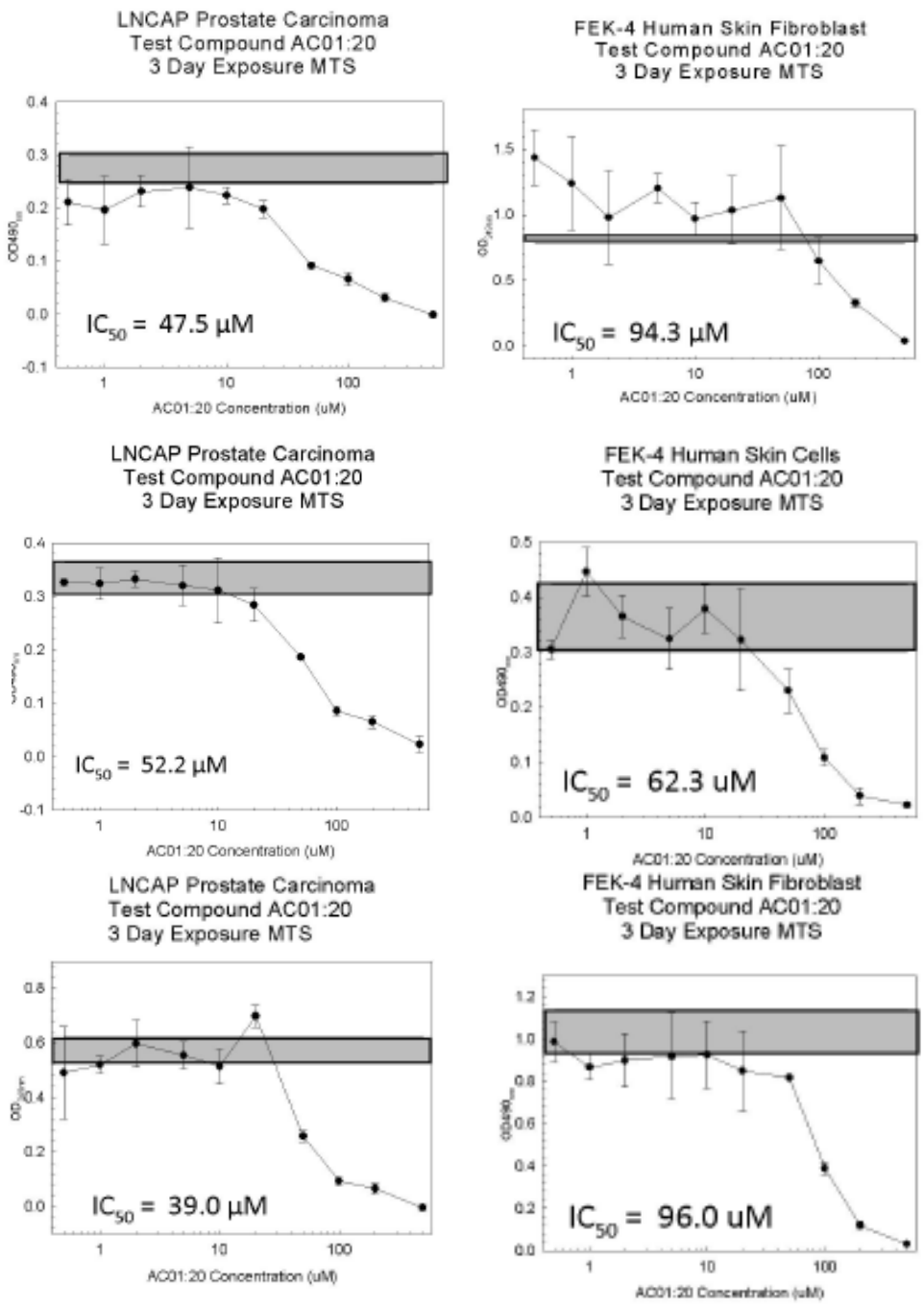
LNCAP Prostate Carcinoma
Test Compound AC01:20
3 Day Exposure MTS
IC50 = 47.5 µM
AC01:20 Concentration (uM)
FEK-4 Human Skin Fibroblast
Test Compound AC01:20
3 Day Exposure MTS
IC50 = 94.3 µM
AC01:20 Concentration (uM)
LNCAP Prostate Carcinoma
Test Compound AC01:20
3 Day Exposure MTS
IC50 = 52.2 µM
AC01:20 Concentration (uM)
FEK-4 Human Skin Cells
Test Compound AC01:20
3 Day Exposure MTS
IC50 = 62.3 uM
AC01:20 Concentration (uM)
LNCAP Prostate Carcinoma
Test Compound AC01:20
3 Day Exposure MTS
IC50 = 39.0 µM
AC01:20 Concentration (uM)
FEK-4 Human Skin Fibroblast
Test Compound AC01:20
3 Day Exposure MTS
IC50 = 96.0 uM
AC01:20 Concentration (uM)
1% DMSO only
Points are means ± s.d
n = 4

Chalcone (48)

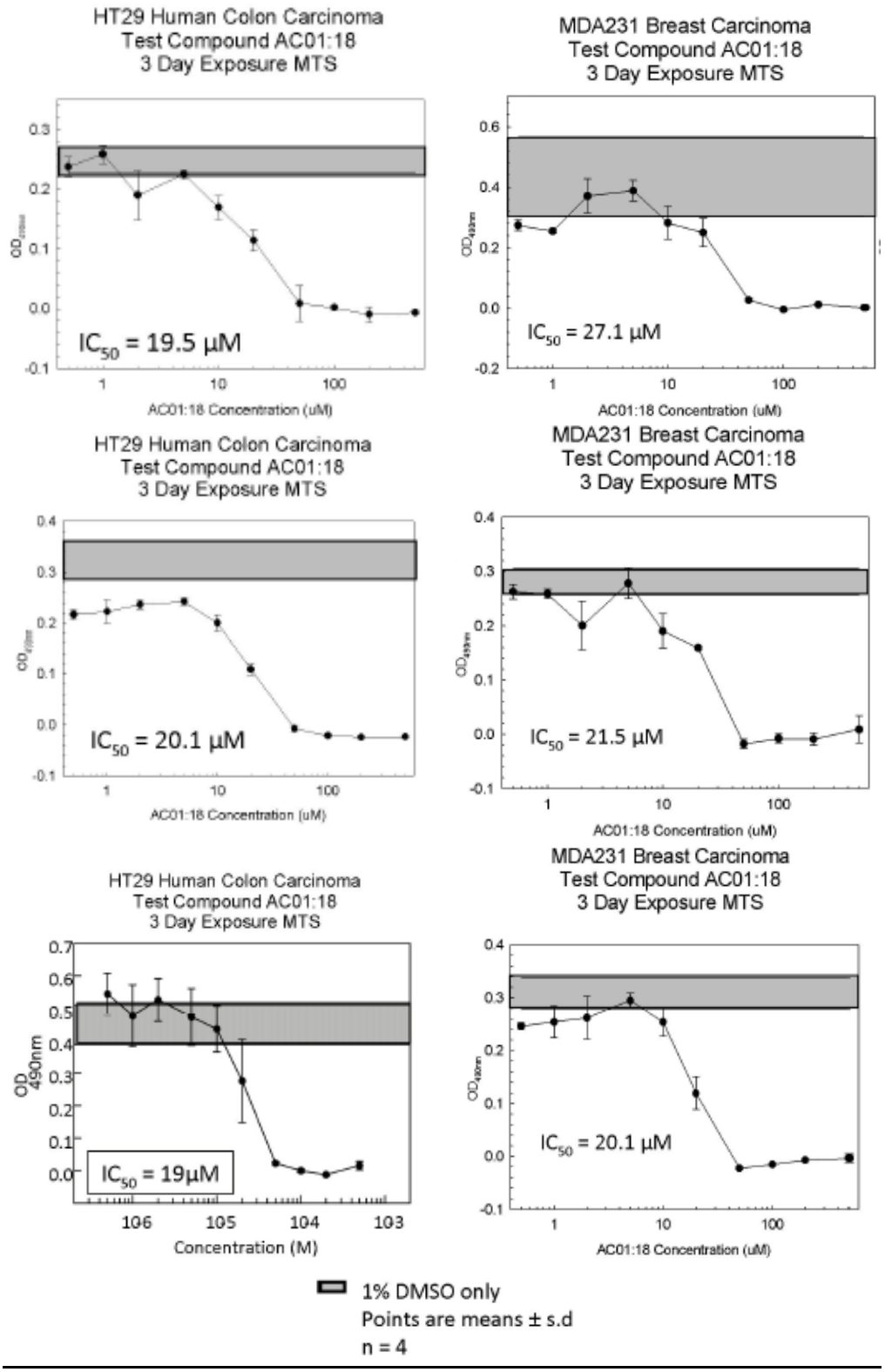
HT29 Human Colon Carcinoma
Test Compound AC01:18
3 Day Exposure MTS
IC50 = 19.5 µM
AC01:18 Concentration (uM)
MDA231 Breast Carcinoma
Test Compound AC01:18
3 Day Exposure MTS
IC50 = 27.1 µM
AC01:18 Concentration (uM)
HT29 Human Colon Carcinoma
Test Compound AC01:18
3 Day Exposure MTS
IC50 = 20.1 µM
AC01:18 Concentration (uM)
MDA231 Breast Carcinoma
Test Compound AC01:18
3 Day Exposure MTS
IC50 = 21.5 µM
AC01:18 Concentration (uM)
HT29 Human Colon Carcinoma
Test Compound AC01:18
3 Day Exposure MTS
OD 490nm
IC50 = 19µM
Concentration (M)
MDA231 Breast Carcinoma
Test Compound AC01:18
3 Day Exposure MTS
IC50 = 20.1 µM
AC01:18 Concentration (uM)
1% DMSO only
Points are means ± s.d
n = 4

Chalcone (48)

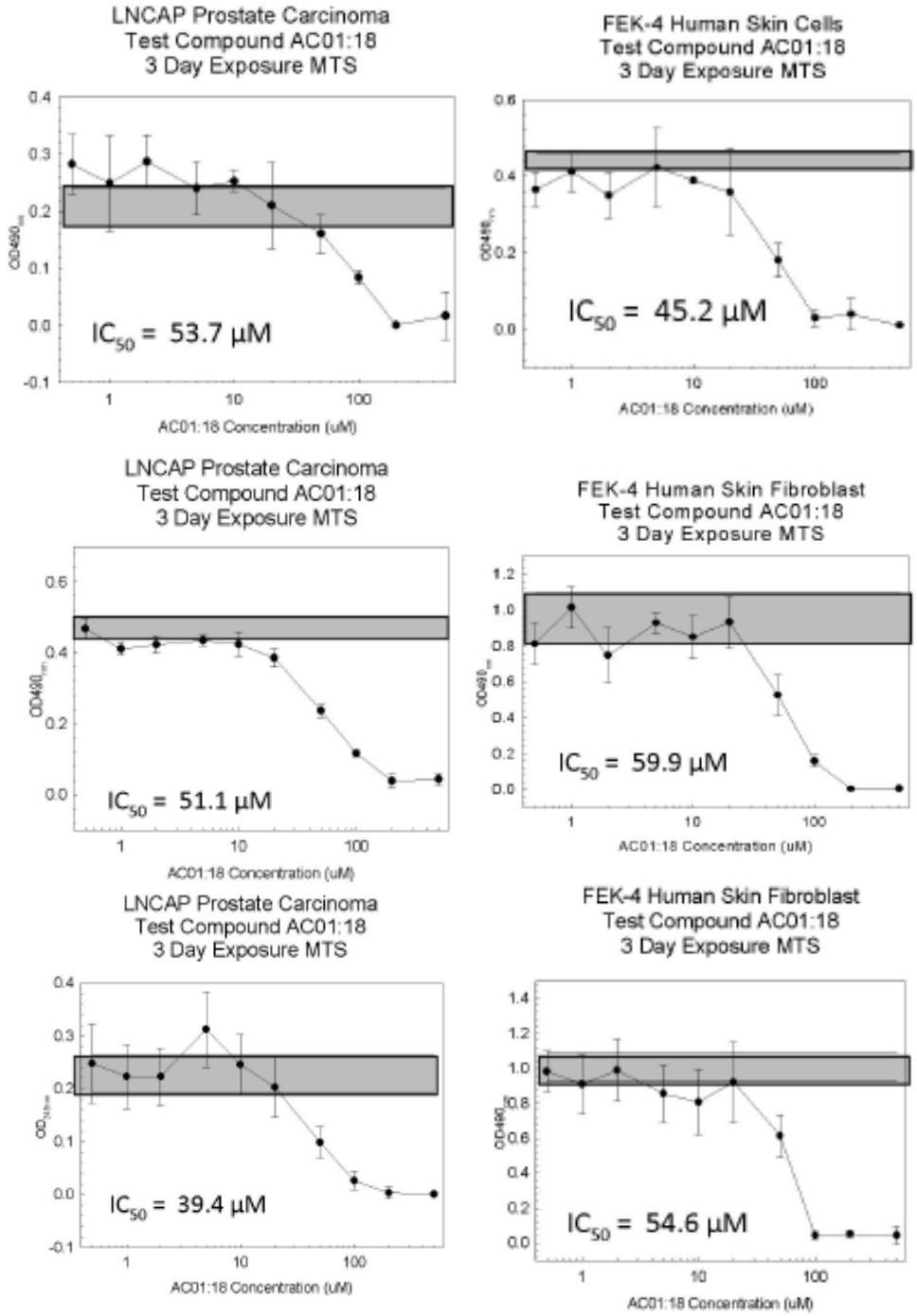
LNCAP Prostate Carcinoma
Test Compound AC01:18
3 Day Exposure MTS
IC50 = 53.7 µM
AC01:18 Concentration (uM)
FEK-4 Human Skin Cells
Test Compound AC01:18
3 Day Exposure MTS
IC50 = 45.2 µM
AC01:18 Concentration (uM)
LNCAP Prostate Carcinoma
Test Compound AC01:18
3 Day Exposure MTS
IC50 = 51.1 µM
AC01:18 Concentration (uM)
FEK-4 Human Skin Fibroblast
Test Compound AC01:18
3 Day Exposure MTS
IC50 = 59.9 µM
AC01:18 Concentration (uM)
LNCAP Prostate Carcinoma
Test Compound AC01:18
3 Day Exposure MTS
IC50 = 39.4 µM
AC01:18 Concentration (uM)
FEK-4 Human Skin Fibroblast
Test Compound AC01:18
3 Day Exposure MTS
IC50 = 54.6 µM
AC01:18 Concentration (uM)
1% DMSO only
Points are means ± s.d
n = 4

Chalcone (49)

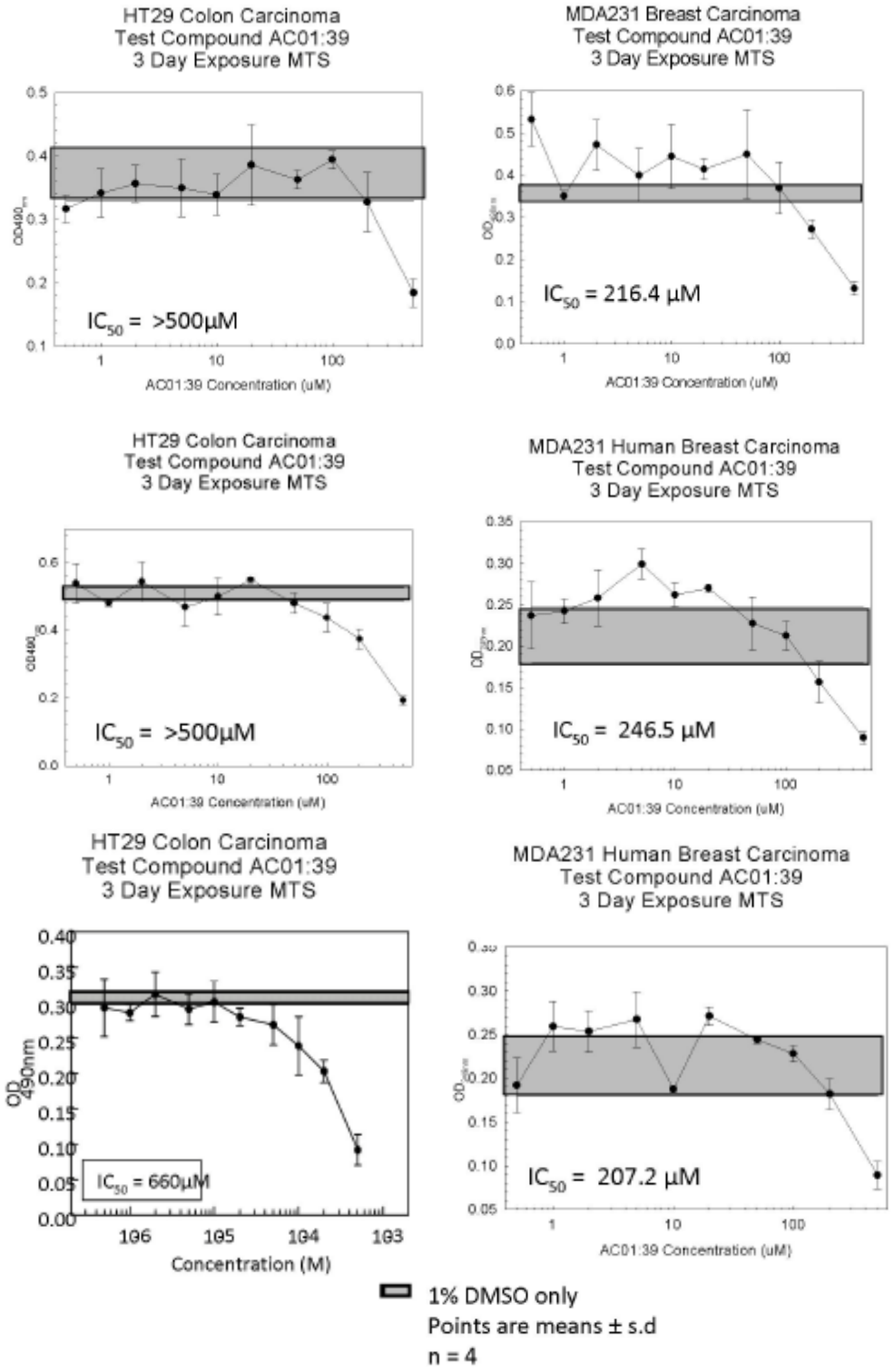
HT29 Colon Carcinoma
Test Compound AC01:39
3 Day Exposure MTS
IC50 = >500µM
AC01:39 Concentration (uM)
MDA231 Breast Carcinoma
Test Compound AC01:39
3 Day Exposure MTS
IC50 = 216.4 µM
AC01:39 Concentration (uM)
HT29 Colon Carcinoma
Test Compound AC01:39
3 Day Exposure MTS
IC50 = >500µM
AC01:39 Concentration (uM)
MDA231 Human Breast Carcinoma
Test Compound AC01:39
3 Day Exposure MTS
IC50 = 246.5 µM
AC01:39 Concentration (uM)
HT29 Colon Carcinoma
Test Compound AC01:39
3 Day Exposure MTS
IC50 = 660µM
OD 490nm
Concentration (M)
MDA231 Human Breast Carcinoma
Test Compound AC01:39
3 Day Exposure MTS
IC50 = 207.2 µM
AC01:39 Concentration (uM)
1% DMSO only
Points are means ± s.d
n = 4

Chalcone (49)

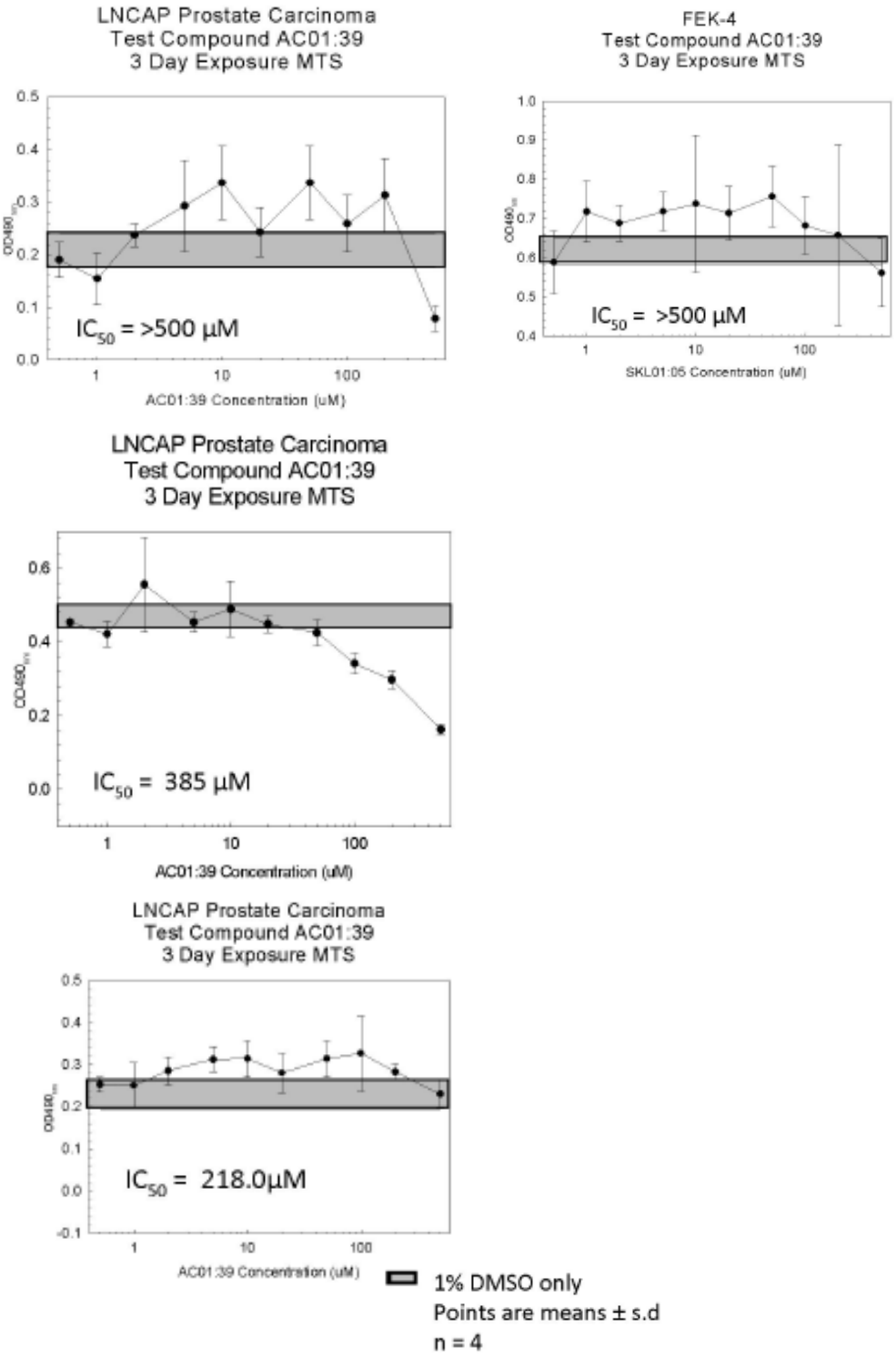
LNCAP Prostate Carcinoma
Test Compound AC01:39
3 Day Exposure MTS
IC50 = >500 µM
AC01:39 Concentration (uM)
FEK-4
Test Compound AC01:39
3 Day Exposure MTS
IC50 = >500 µM
SKL01:05 Concentration (uM)
LNCAP Prostate Carcinoma
Test Compound AC01:39
3 Day Exposure MTS
IC50 = 385 µM
AC01:39 Concentration (uM)
LNCAP Prostate Carcinoma
Test Compound AC01:39
3 Day Exposure MTS
IC50 = 218.0µM
AC01:39 Concentration (uM)
1% DMSO only
Points are means ± s.d
n = 4

Chalcone (50)

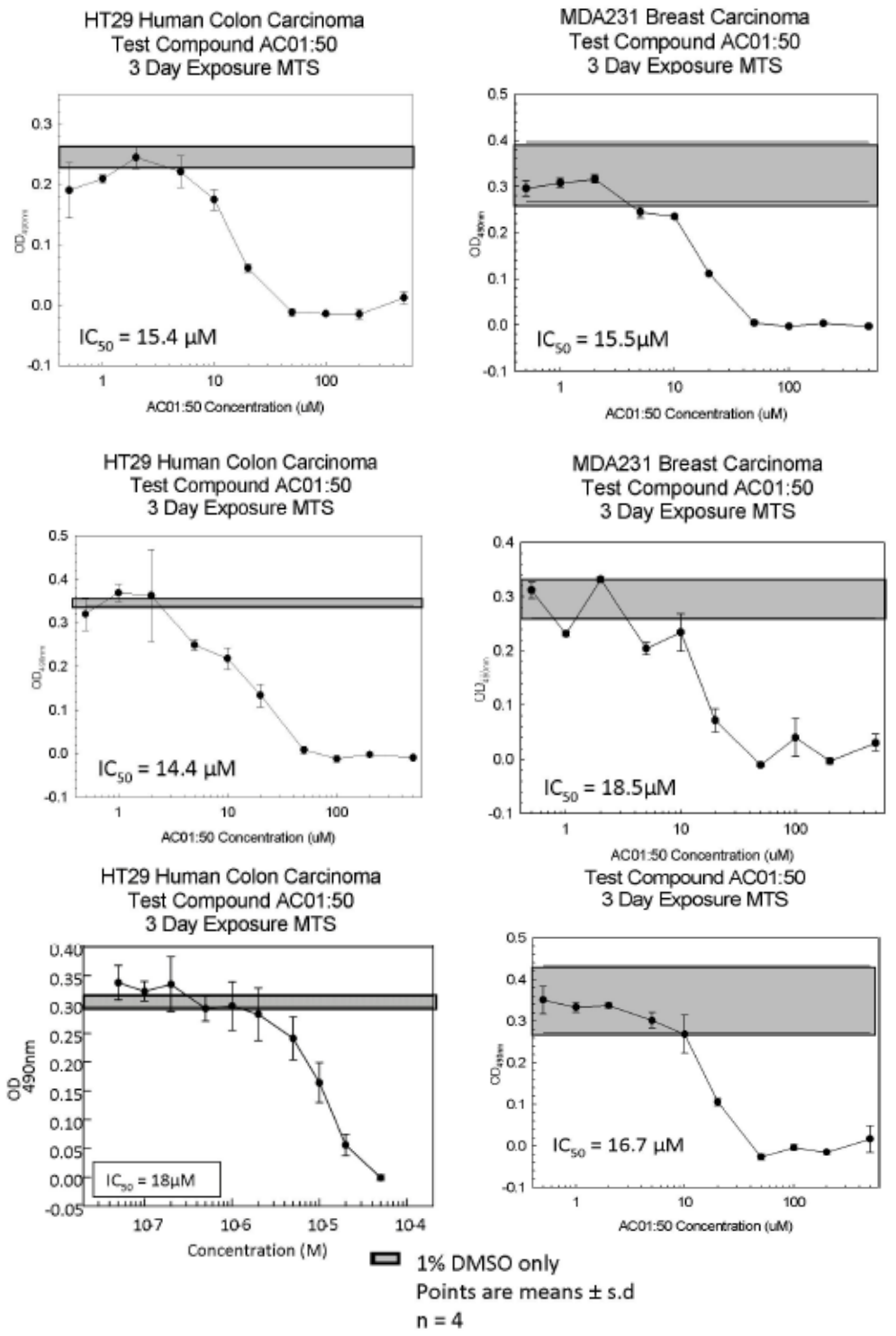
HT29 Human Colon Carcinoma
Test Compound AC01:50
3 Day Exposure MTS
IC50 = 15.4 µM
AC01:50 Concentration (uM)
MDA231 Breast Carcinoma
Test Compound AC01:50
3 Day Exposure MTS
IC50 = 15.5µM
AC01:50 Concentration (uM)
HT29 Human Colon Carcinoma
Test Compound AC01:50
3 Day Exposure MTS
IC50 = 14.4 µM
AC01:50 Concentration (uM)
MDA231 Breast Carcinoma
Test Compound AC01:50
3 Day Exposure MTS
IC50 = 18.5µM
AC01:50 Concentration (uM)
HT29 Human Colon Carcinoma
Test Compound AC01:50
3 Day Exposure MTS
OD 490nm
IC50 = 18µM
Concentration (M)
Test Compound AC01:50
3 Day Exposure MTS
IC50 = 16.7 µM
AC01:50 Concentration (uM)
1% DMSO only
Points are means ± s.d
n = 4

Chalcone (50)

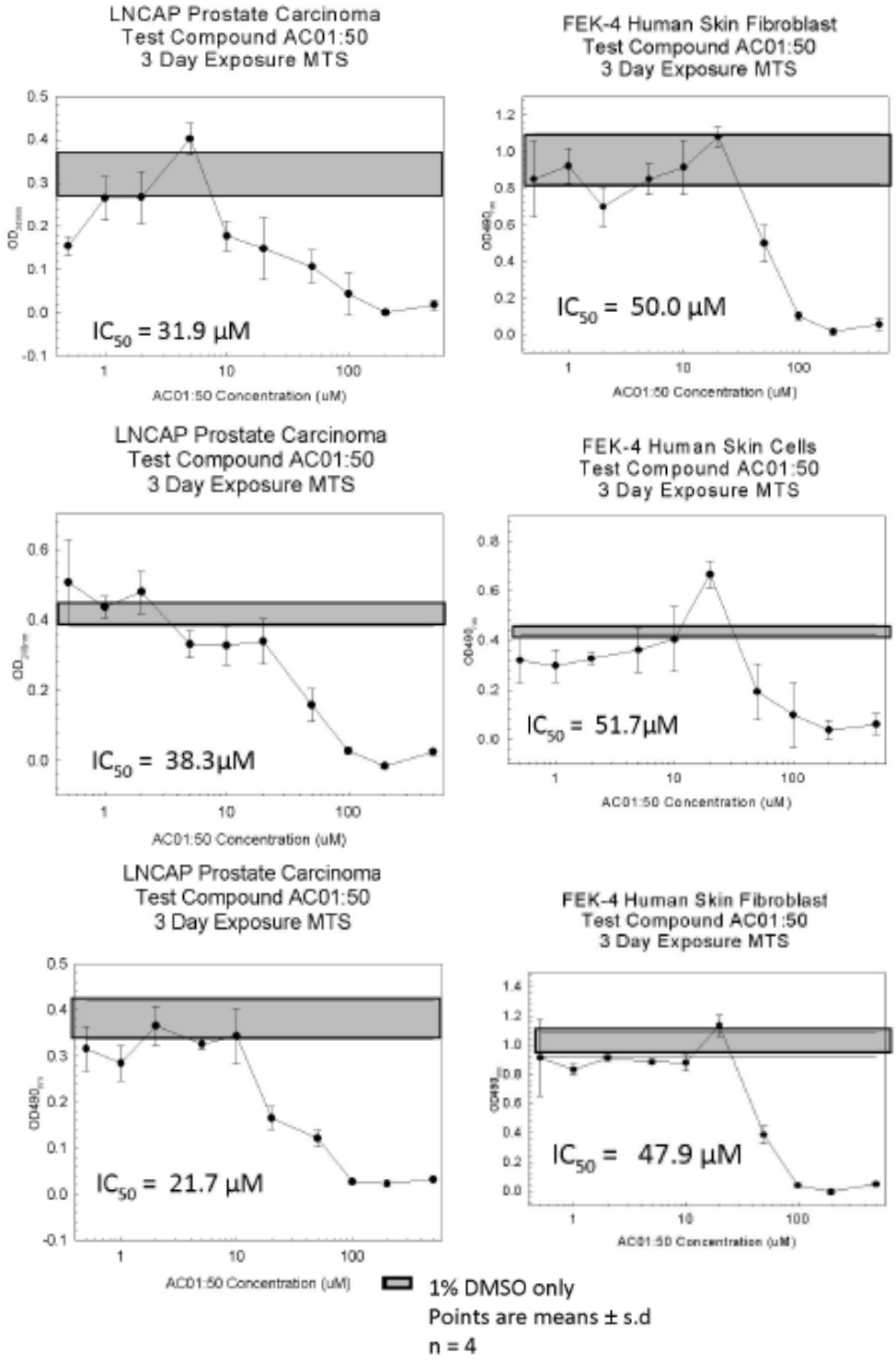
LNCAP Prostate Carcinoma
Test Compound AC01:50
3 Day Exposure MTS
IC50 = 31.9 µM
AC01:50 Concentration (uM)
FEK-4 Human Skin Fibroblast
Test Compound AC01:50
3 Day Exposure MTS
IC50 = 50.0 µM
AC01:50 Concentration (uM)
LNCAP Prostate Carcinoma
Test Compound AC01:50
3 Day Exposure MTS
IC50 = 38.3µM
AC01:50 Concentration (uM)
FEK-4 Human Skin Cells
Test Compound AC01:50
3 Day Exposure MTS
IC50 = 51.7µM
AC01:50 Concentration (uM)
LNCAP Prostate Carcinoma
Test Compound AC01:50
3 Day Exposure MTS
IC50 = 21.7 µM
AC01:50 Concentration (uM)
FEK-4 Human Skin Fibroblast
Test Compound AC01:50
3 Day Exposure MTS
IC50 = 47.9 µM
AC01:50 Concentration (uM)
1% DMSO only
Points are means ± s.d
n = 4

Chalcone (51)

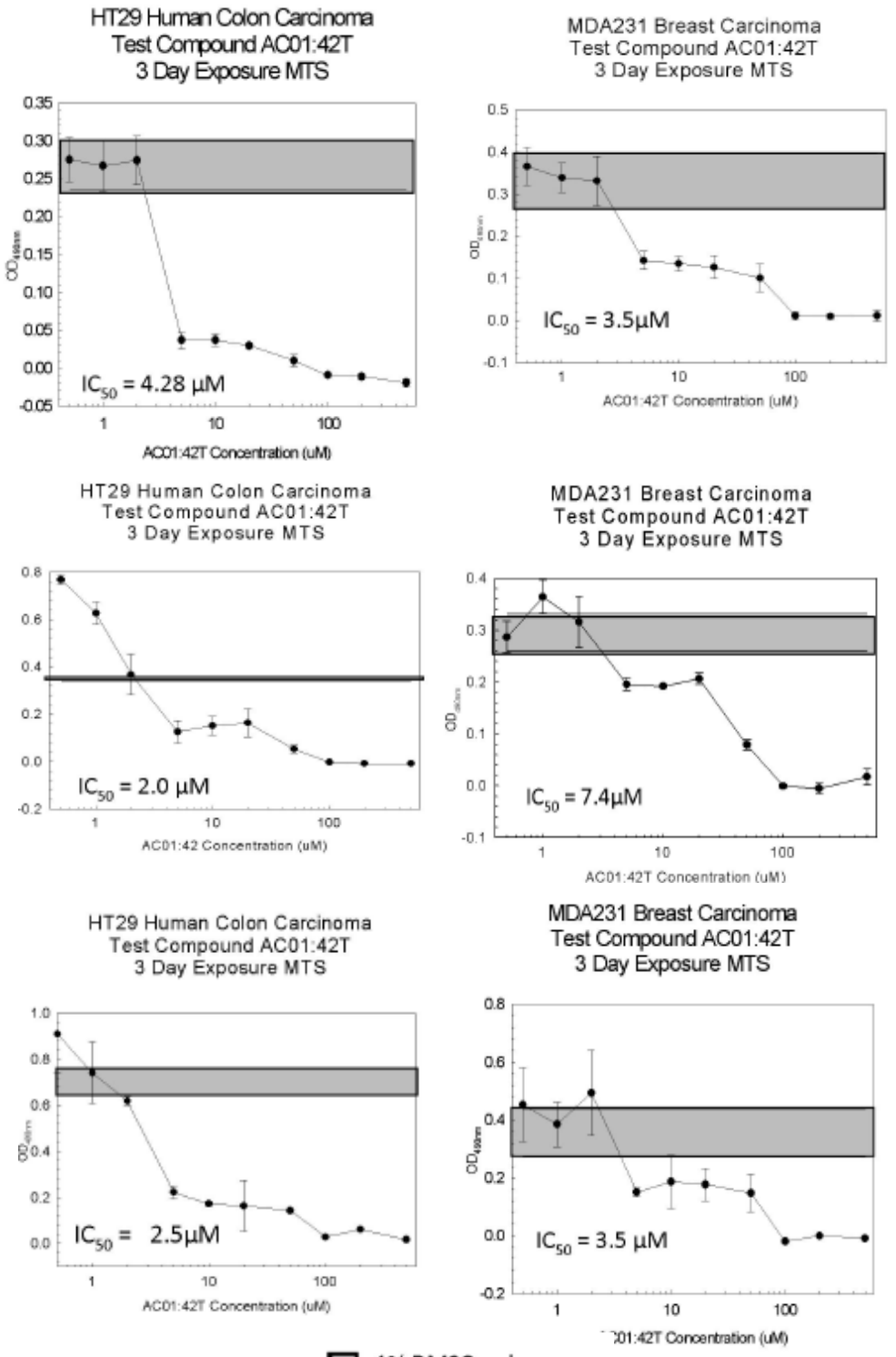
HT29 Human Colon Carcinoma
Test Compound AC01:42T
3 Day Exposure MTS
IC50 = 4.28 µM
AC01:42T Concentration (uM)
MDA231 Breast Carcinoma
Test Compound AC01:42T
3 Day Exposure MTS
IC50 = 3.5µM
AC01:42T Concentration (uM)
HT29 Human Colon Carcinoma
Test Compound AC01:42T
3 Day Exposure MTS
IC50 = 2.0 µM
AC01:42 Concentration (uM)
MDA231 Breast Carcinoma
Test Compound AC01:42T
3 Day Exposure MTS
IC50 = 7.4µM
AC01:42T Concentration (uM)
HT29 Human Colon Carcinoma
Test Compound AC01:42T
3 Day Exposure MTS
IC50 = 2.5µM
AC01:42T Concentration (uM)
MDA231 Breast Carcinoma
Test Compound AC01:42T
3 Day Exposure MTS
IC50 = 3.5 µM
1% DMSO only
Points are means ± s.d
n = 4

Chalcone (51)

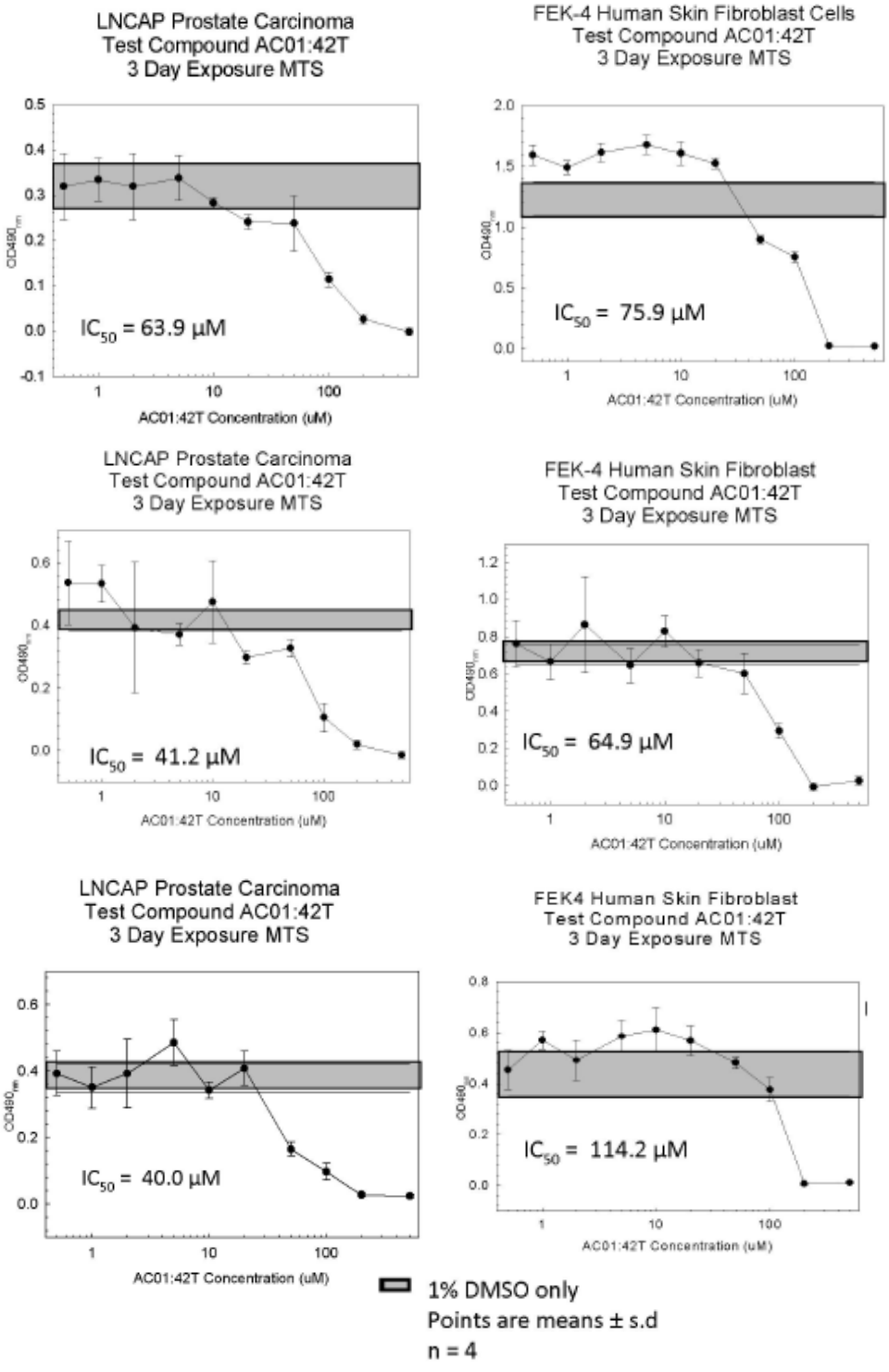
LNCAP Prostate Carcinoma
Test Compound AC01:42T
3 Day Exposure MTS
IC50 = 63.9 µM
AC01:42T Concentration (uM)
FEK-4 Human Skin Fibroblast Cells
Test Compound AC01:42T
3 Day Exposure MTS
IC50 = 75.9 µM
AC01:42T Concentration (uM)
LNCAP Prostate Carcinoma
Test Compound AC01:42T
3 Day Exposure MTS
IC50 = 41.2 µM
AC01:42T Concentration (uM)
FEK-4 Human Skin Fibroblast
Test Compound AC01:42T
3 Day Exposure MTS
IC50 = 64.9 µM
AC01:42T Concentration (uM)
LNCAP Prostate Carcinoma
Test Compound AC01:42T
3 Day Exposure MTS
IC50 = 40.0 µM
AC01:42T Concentration (uM)
FEK4 Human Skin Fibroblast
Test Compound AC01:42T
3 Day Exposure MTS
IC50 = 114.2 µM
AC01:42T Concentration (uM)
1% DMSO only
Points are means ± s.d
n = 4

Chalcone (52)

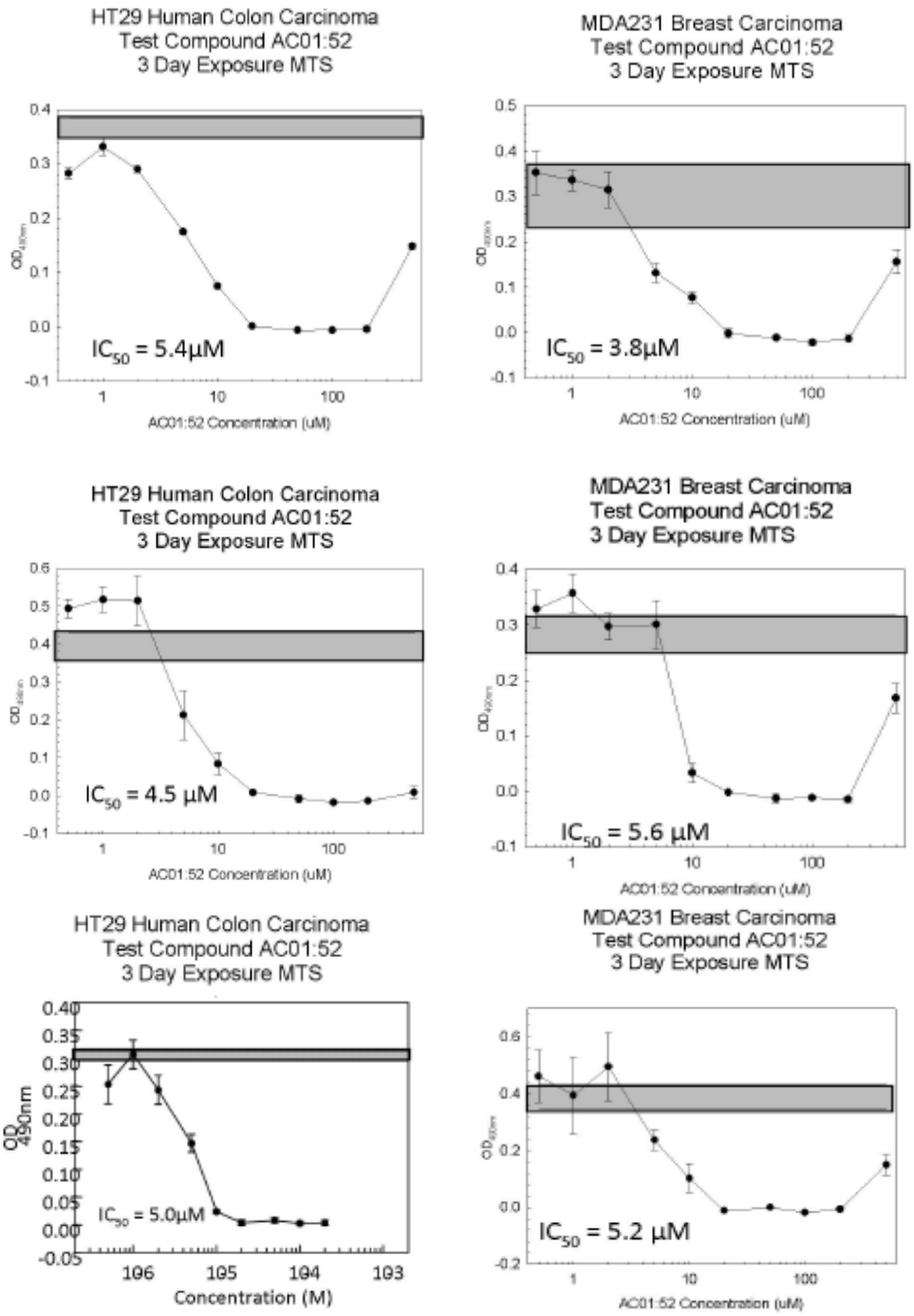
HT29 Human Colon Carcinoma
Test Compound AC01:52
3 Day Exposure MTS
IC50 = 5.4µM
AC01:52 Concentration (uM)
MDA231 Breast Carcinoma
Test Compound AC01:52
3 Day Exposure MTS
IC50 = 3.8µM
AC01:52 Concentration (uM)
HT29 Human Colon Carcinoma
Test Compound AC01:52
3 Day Exposure MTS
IC50 = 4.5 µM
AC01:52 Concentration (uM)
MDA231 Breast Carcinoma
Test Compound AC01:52
3 Day Exposure MTS
IC50 = 5.6 µM
AC01:52 Concentration (uM)
HT29 Human Colon Carcinoma
Test Compound AC01:52
3 Day Exposure MTS
OD 490nm
IC50 = 5.0µM
Concentration (M)
MDA231 Breast Carcinoma
Test Compound AC01:52
3 Day Exposure MTS
IC50 = 5.2 µM
AC01:52 Concentration (uM)
1% DMSO only
Points are means ± s.d
n = 4

Chalcone (52)

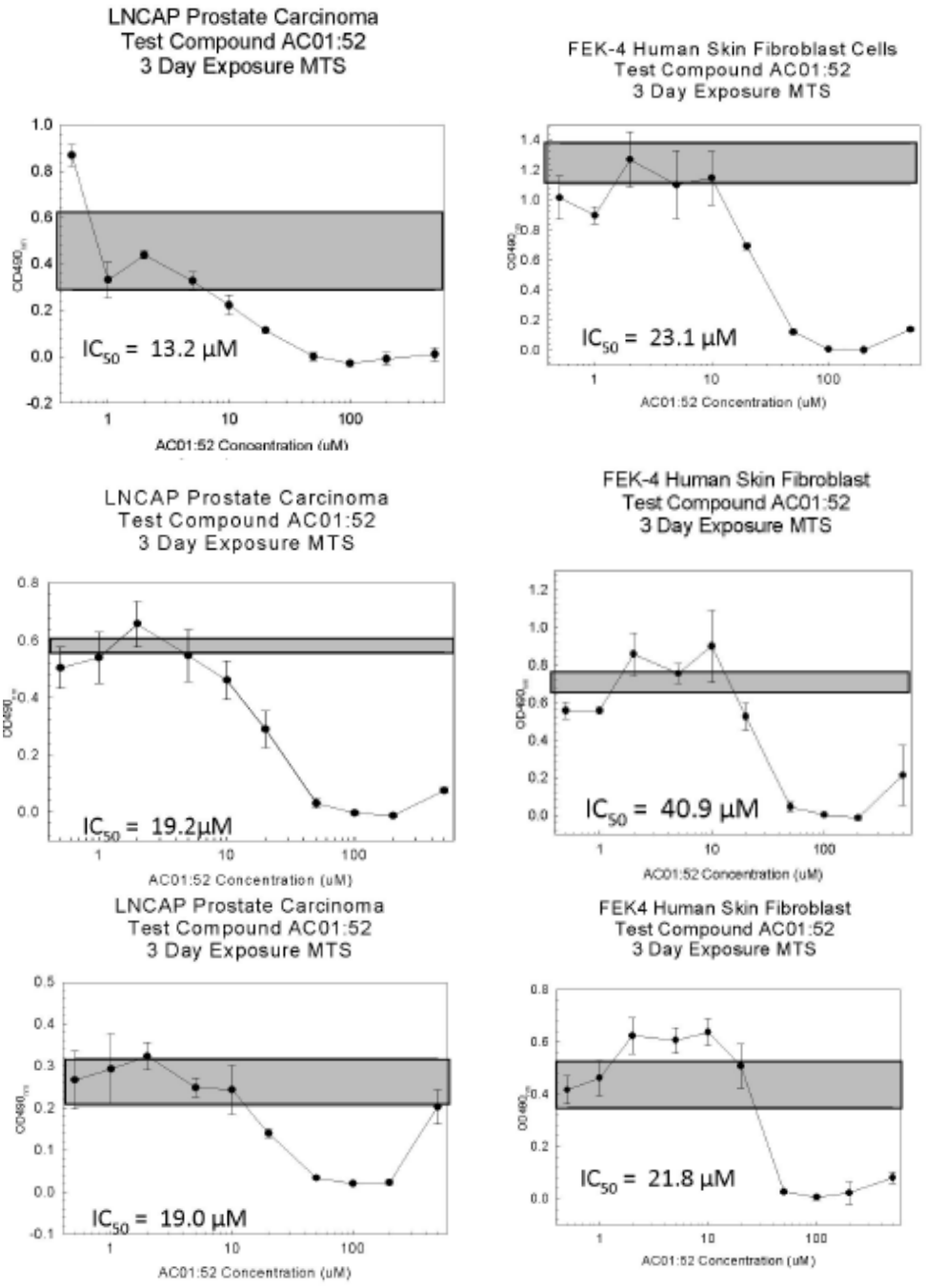
LNCAP Prostate Carcinoma
Test Compound AC01:52
3 Day Exposure MTS
IC50 = 13.2 µM
AC01:52 Concentration (uM)
FEK-4 Human Skin Fibroblast Cells
Test Compound AC01:52
3 Day Exposure MTS
IC50 = 23.1 µM
AC01:52 Concentration (uM)
LNCAP Prostate Carcinoma
Test Compound AC01:52
3 Day Exposure MTS
IC50 = 19.2µM
AC01:52 Concentration (uM)
FEK-4 Human Skin Fibroblast
Test Compound AC01:52
3 Day Exposure MTS
IC50 = 40.9 µM
AC01:52 Concentration (uM)
LNCAP Prostate Carcinoma
Test Compound AC01:52
3 Day Exposure MTS
IC50 = 19.0 µM
AC01:52 Concentration (uM)
FEK4 Human Skin Fibroblast
Test Compound AC01:52
3 Day Exposure MTS
IC50 = 21.8 µM
AC01:52 Concentration (uM)
1% DMSO only
Points are means ± s.d
n = 4

Chalcone (53)

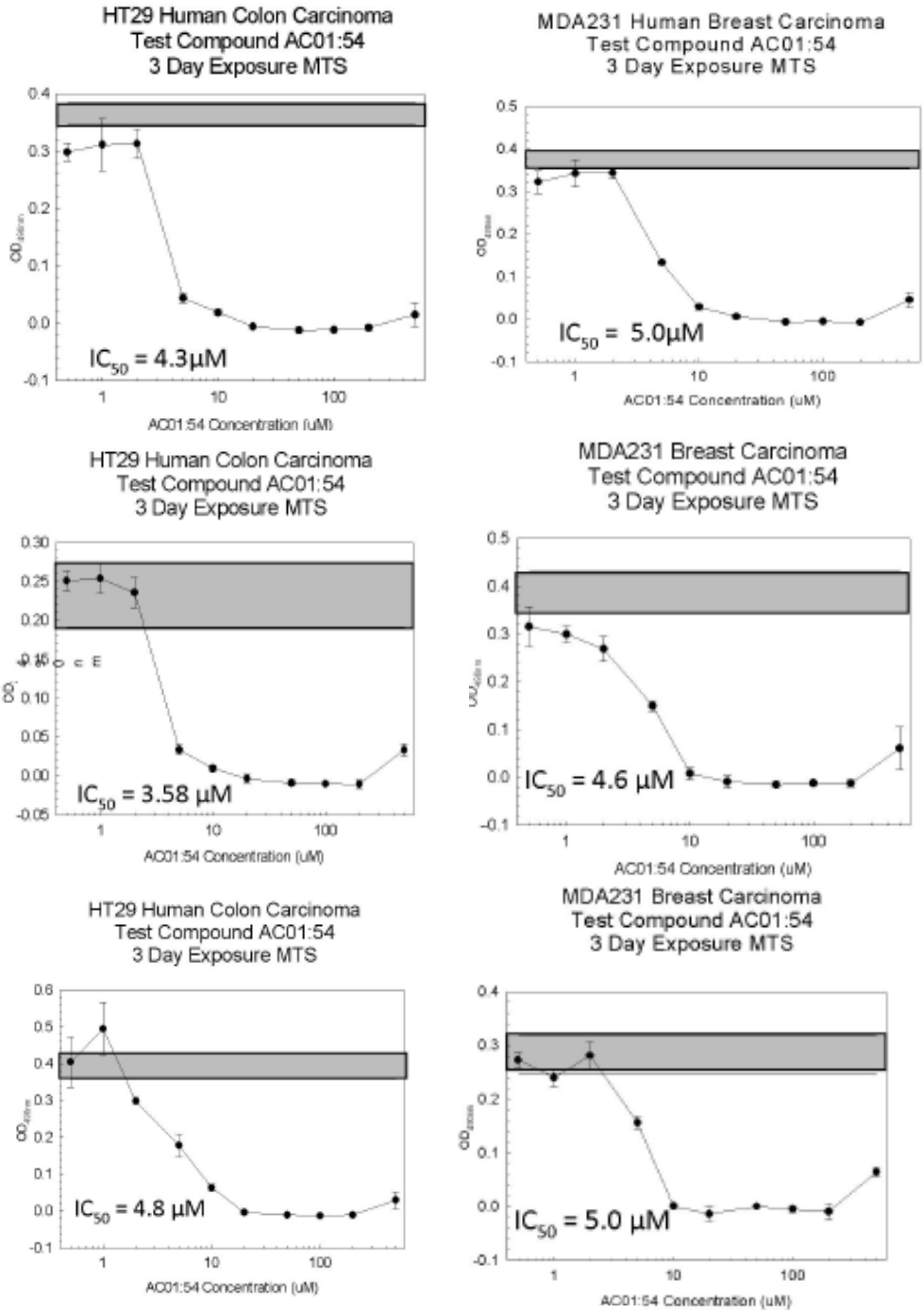
HT29 Human Colon Carcinoma
Test Compound AC01:54
3 Day Exposure MTS
IC50 = 4.3µM
AC01:54 Concentration (uM)
MDA231 Human Breast Carcinoma
Test Compound AC01:54
3 Day Exposure MTS
IC50 = 5.0µM
AC01:54 Concentration (uM)
HT29 Human Colon Carcinoma
Test Compound AC01:54
3 Day Exposure MTS
IC50 = 3.58 µM
AC01:54 Concentration (uM)
MDA231 Breast Carcinoma
Test Compound AC01:54
3 Day Exposure MTS
IC50 = 4.6 µM
AC01:54 Concentration (uM)
HT29 Human Colon Carcinoma
Test Compound AC01:54
3 Day Exposure MTS
IC50 = 4.8 µM
AC01:54 Concentration (uM)
MDA231 Breast Carcinoma
Test Compound AC01:54
3 Day Exposure MTS
IC50 = 5.0 µM
AC01:54 Concentration (uM)
1% DMSO only
Points are means ± s.d
n = 4

Chalcone (53)

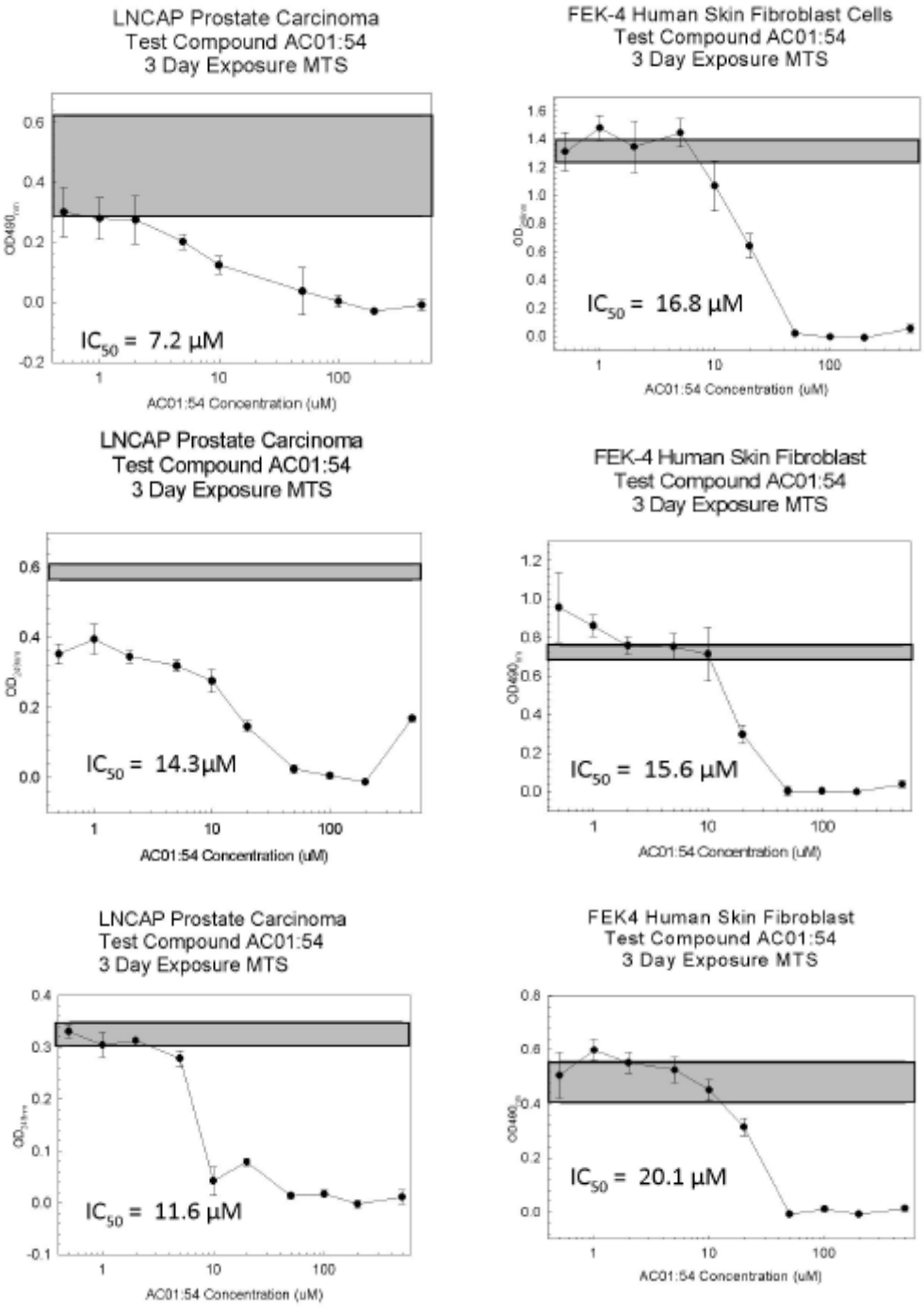
LNCAP Prostate Carcinoma
Test Compound AC01:54
3 Day Exposure MTS
IC50 = 7.2 µM
AC01:54 Concentration (uM)
FEK-4 Human Skin Fibroblast Cells
Test Compound AC01:54
3 Day Exposure MTS
IC50 = 16.8 µM
AC01:54 Concentration (uM)
LNCAP Prostate Carcinoma
Test Compound AC01:54
3 Day Exposure MTS
IC50 = 14.3µM
AC01:54 Concentration (uM)
FEK-4 Human Skin Fibroblast
Test Compound AC01:54
3 Day Exposure MTS
IC50 = 15.6 µM
AC01:54 Concentration (uM)
LNCAP Prostate Carcinoma
Test Compound AC01:54
3 Day Exposure MTS
IC50 = 11.6 µM
AC01:54 Concentration (uM)
FEK4 Human Skin Fibroblast
Test Compound AC01:54
3 Day Exposure MTS
IC50 = 20.1 µM
AC01:54 Concentration (uM)
1% DMSO only
Points are means ± s.d
n = 4

Chalcone (58)

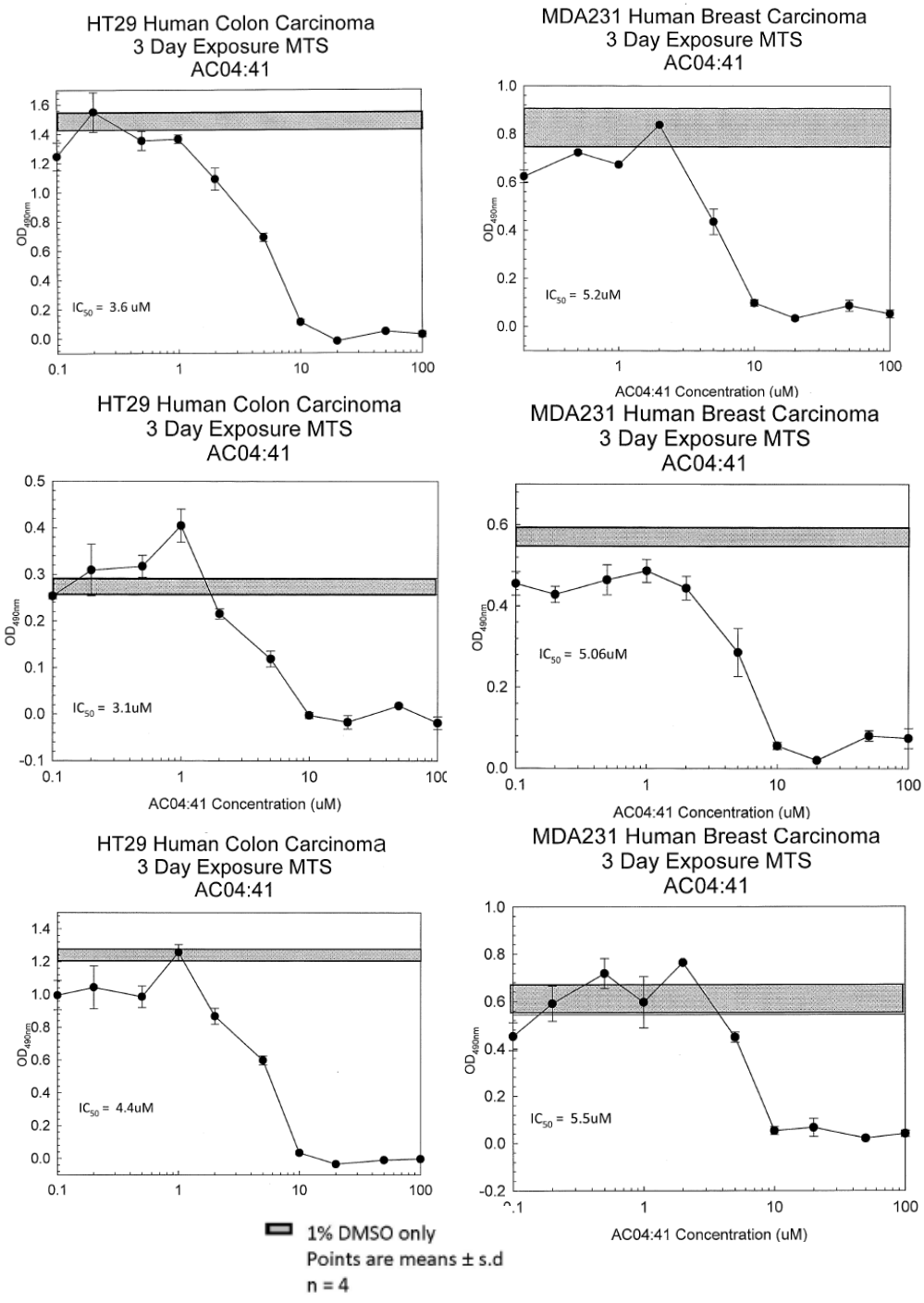
HT29 Human Colon Carcinoma
3 Day Exposure MTS
AC04:41
IC50 = 3.6 uM
MDA231 Human Breast Carcinoma
3 Day Exposure MTS
AC04:41
IC50 = 5.2uM
AC04:41 Concentration (uM)
HT29 Human Colon Carcinoma
3 Day Exposure MTS
AC04:41
IC50 = 3.1uM
AC04:41 Concentration (uM)
MDA231 Human Breast Carcinoma
3 Day Exposure MTS
AC04:41
IC50 = 5.06uM
AC04:41 Concentration (uM)
HT29 Human Colon Carcinoma
3 Day Exposure MTS
AC04:41
IC50 = 4.4uM
MDA231 Human Breast Carcinoma
3 Day Exposure MTS
AC04:41
IC50 = 5.5uM
AC04:41 Concentration (uM)
1% DMSO only
Points are means ± s.d
n = 4

Chalcone (59)

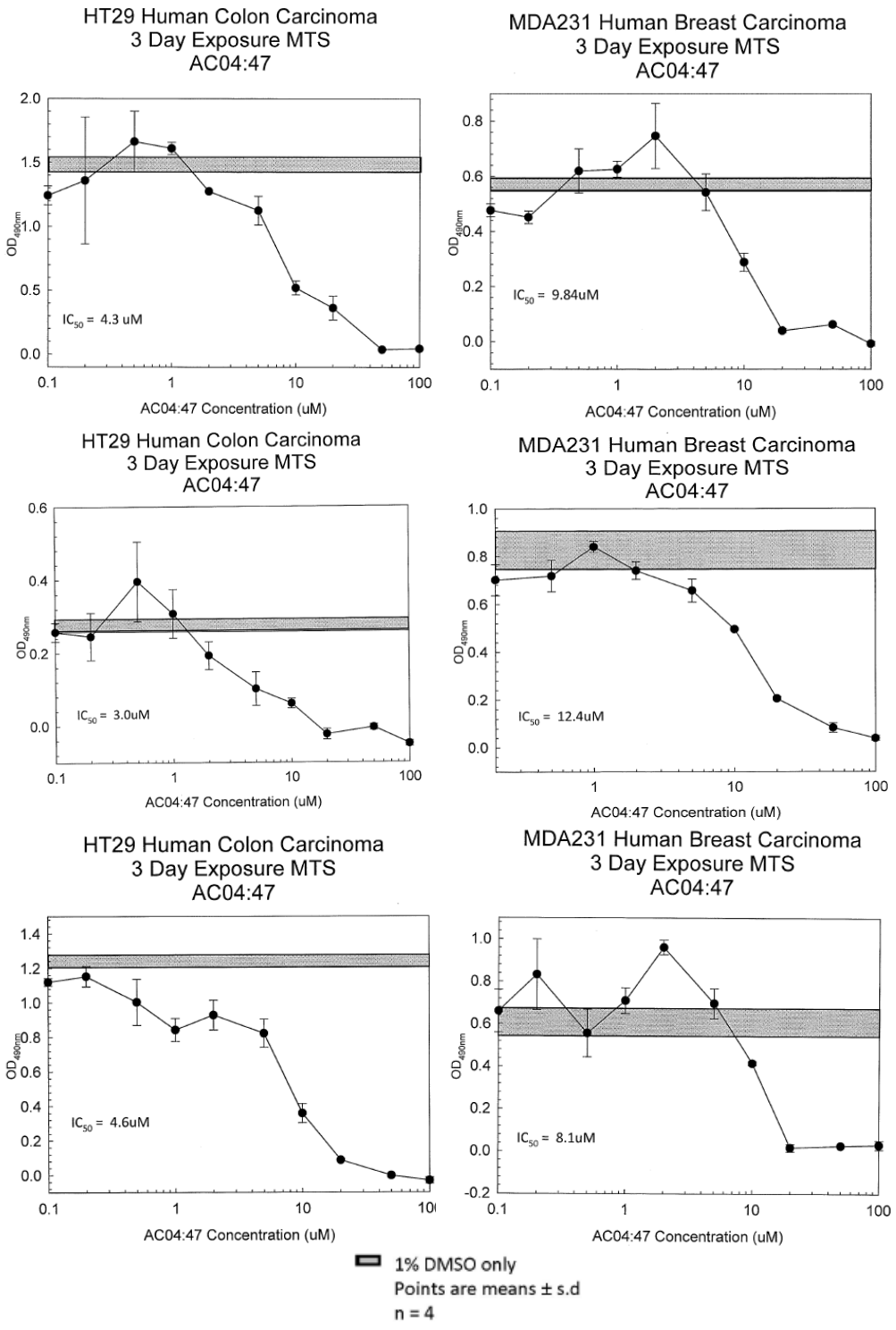
HT29 Human Colon Carcinoma
3 Day Exposure MTS
AC04:47
MDA231 Human Breast Carcinoma
3 Day Exposure MTS
AC04:47
OD490nm
AC04:47 Concentration (uM)
IC50 = 4.3 uM
IC50 = 9.84uM
IC50 = 3.0uM
IC50 = 12.4uM
IC50 = 4.6uM
IC50 = 8.1uM
1% DMSO only
Points are means ± s.d
n = 4

Chalcone (60)

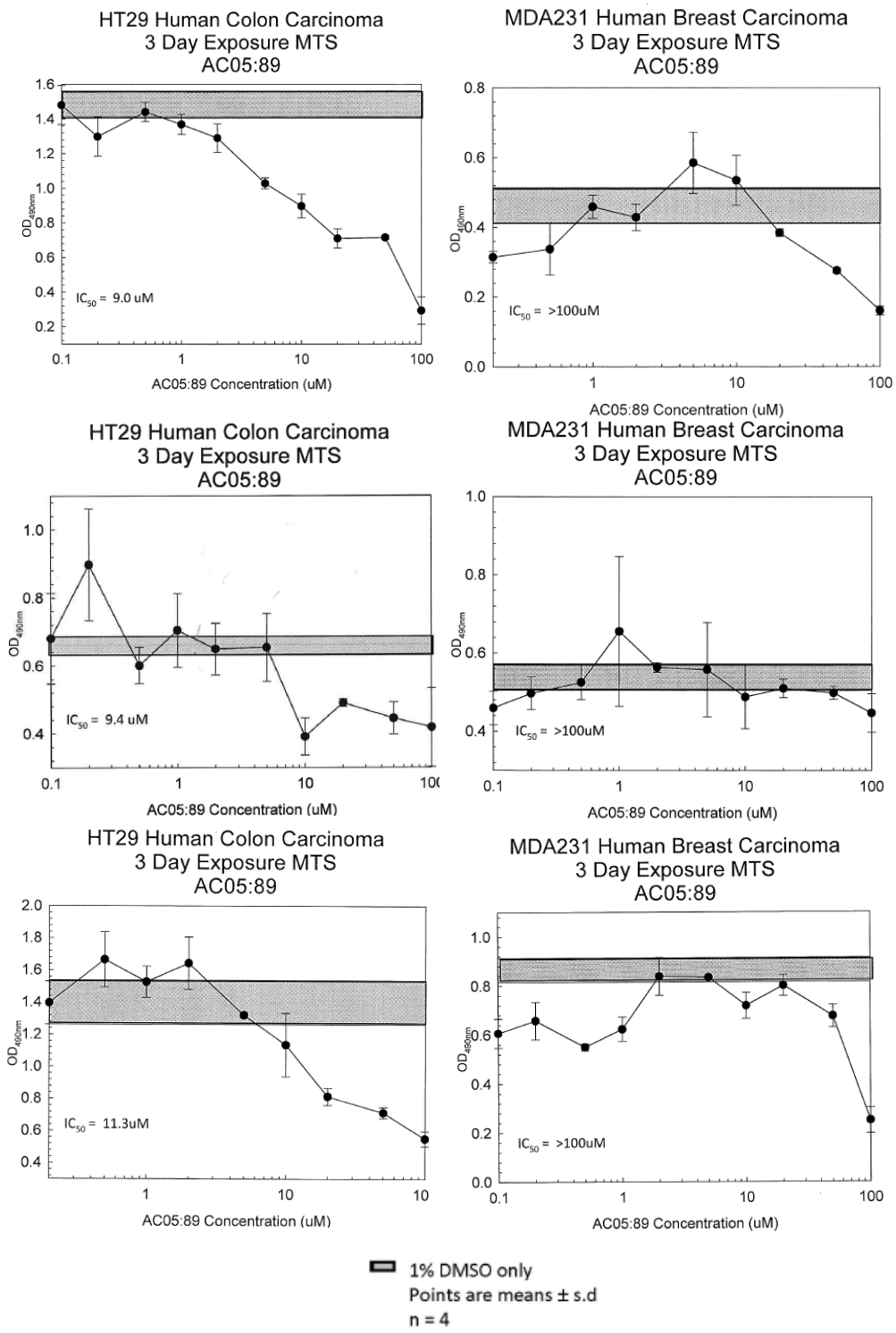
HT29 Human Colon Carcinoma
3 Day Exposure MTS
AC05:89
OD490nm
IC50 = 9.0 uM
AC05:89 Concentration (uM)
MDA231 Human Breast Carcinoma
3 Day Exposure MTS
AC05:89
OD490nm
IC50 = >100uM
AC05:89 Concentration (uM)
HT29 Human Colon Carcinoma
3 Day Exposure MTS
AC05:89
OD490nm
IC50 = 9.4 uM
AC05:89 Concentration (uM)
MDA231 Human Breast Carcinoma
3 Day Exposure MTS
AC05:89
OD490nm
IC50 = >100uM
AC05:89 Concentration (uM)
HT29 Human Colon Carcinoma
3 Day Exposure MTS
AC05:89
OD490nm
IC50 = 11.3uM
AC05:89 Concentration (uM)
MDA231 Human Breast Carcinoma
3 Day Exposure MTS
AC05:89
OD490nm
IC50 = >100uM
AC05:89 Concentration (uM)
1% DMSO only
Points are means ± s.d
n = 4

Chalcone (61)

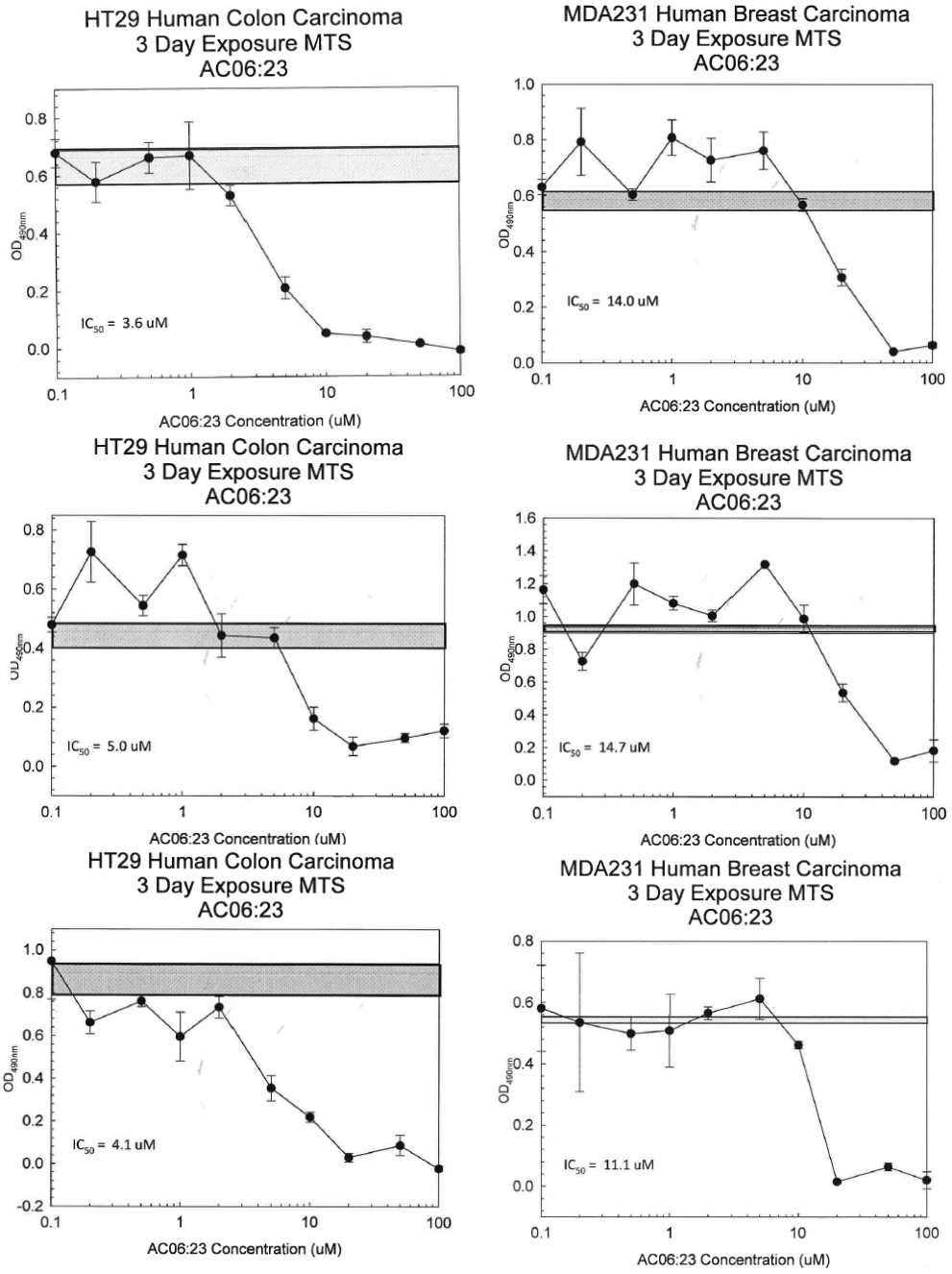
HT29 Human Colon Carcinoma
3 Day Exposure MTS
AC06:23
IC50 = 3.6 uM
AC06:23 Concentration (uM)
MDA231 Human Breast Carcinoma
3 Day Exposure MTS
AC06:23
IC50 = 14.0 uM
AC06:23 Concentration (uM)
HT29 Human Colon Carcinoma
3 Day Exposure MTS
AC06:23
IC50 = 5.0 uM
AC06:23 Concentration (uM)
MDA231 Human Breast Carcinoma
3 Day Exposure MTS
AC06:23
IC50 = 14.7 uM
AC06:23 Concentration (uM)
HT29 Human Colon Carcinoma
3 Day Exposure MTS
AC06:23
IC50 = 4.1 uM
AC06:23 Concentration (uM)
MDA231 Human Breast Carcinoma
3 Day Exposure MTS
AC06:23
IC50 = 11.1 uM
AC06:23 Concentration (uM)
1% DMSO only
Points are means ± s.d
n = 4

Chalcone (62)

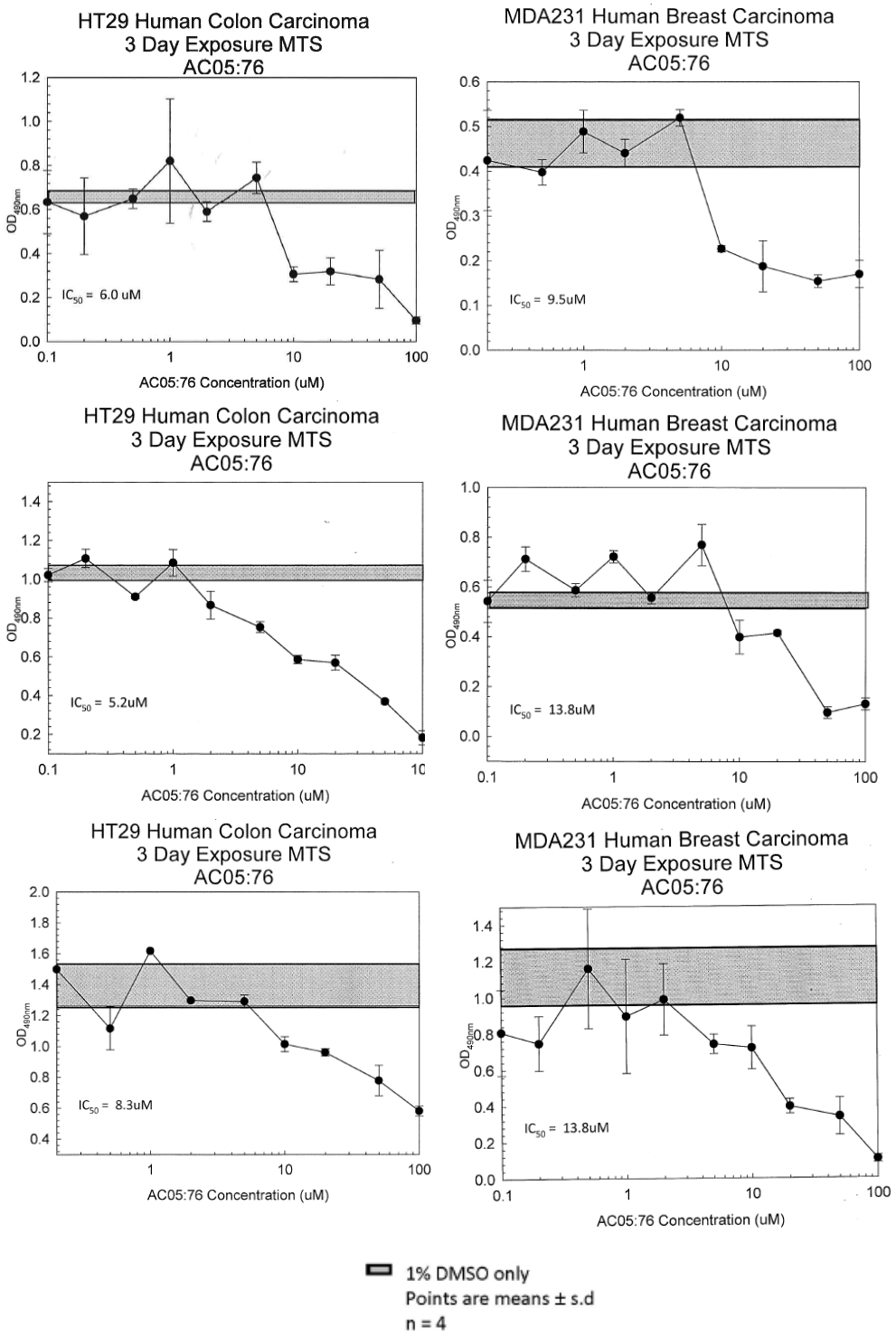
HT29 Human Colon Carcinoma
3 Day Exposure MTS
AC05:76
IC50 = 6.0 uM
AC05:76 Concentration (uM)
MDA231 Human Breast Carcinoma
3 Day Exposure MTS
AC05:76
IC50 = 9.5uM
AC05:76 Concentration (uM)
HT29 Human Colon Carcinoma
3 Day Exposure MTS
AC05:76
IC50 = 5.2uM
AC05:76 Concentration (uM)
MDA231 Human Breast Carcinoma
3 Day Exposure MTS
AC05:76
IC50 = 13.8uM
AC05:76 Concentration (uM)
HT29 Human Colon Carcinoma
3 Day Exposure MTS
AC05:76
IC50 = 8.3uM
AC05:76 Concentration (uM)
MDA231 Human Breast Carcinoma
3 Day Exposure MTS
AC05:76
IC50 = 13.8uM
AC05:76 Concentration (uM)
1% DMSO only
Points are means ± s.d
n = 4

Chalcone (63)

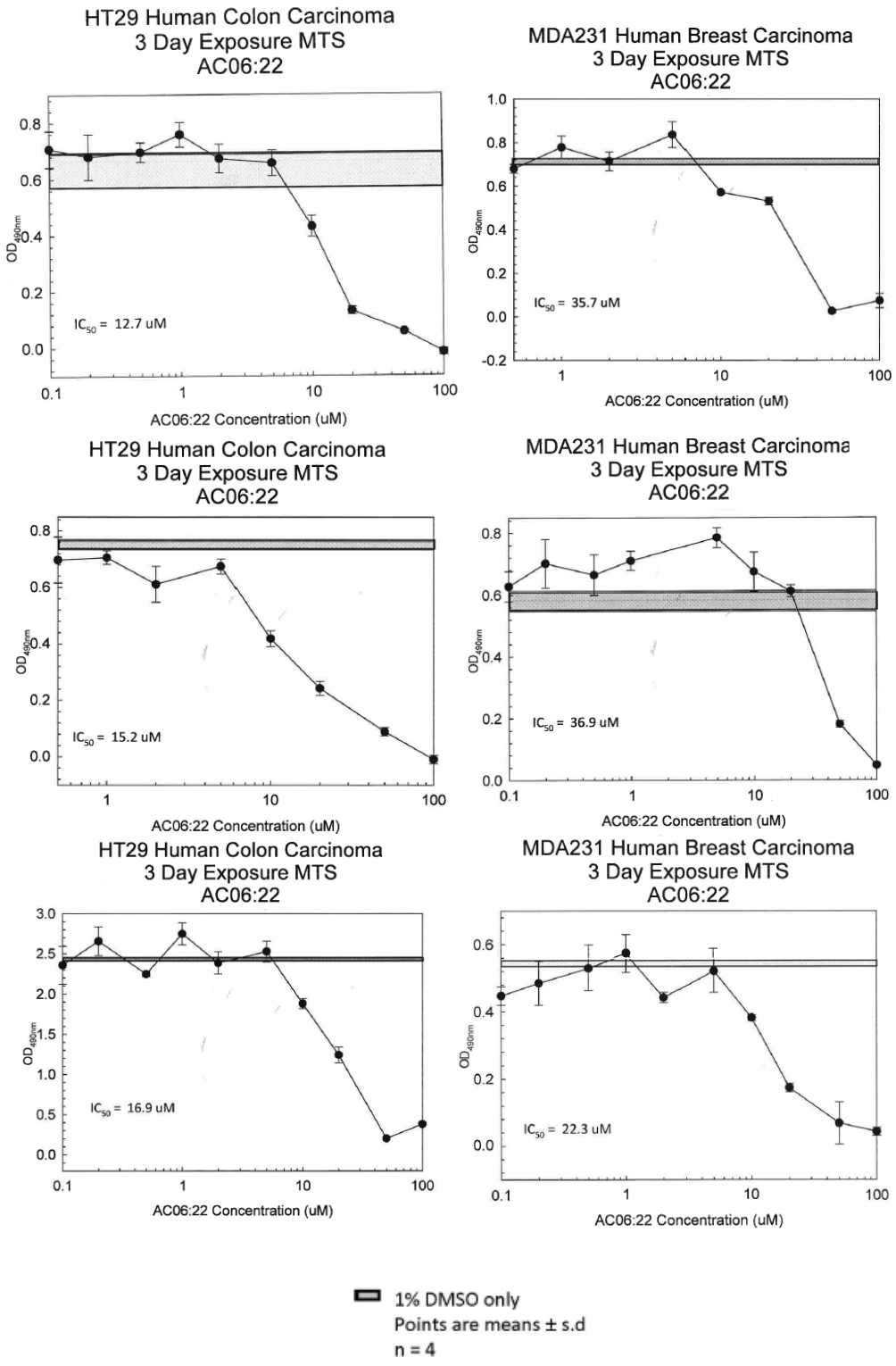
HT29 Human Colon Carcinoma
3 Day Exposure MTS
AC06:22
IC50 = 12.7 uM
AC06:22 Concentration (uM)
MDA231 Human Breast Carcinoma
3 Day Exposure MTS
AC06:22
IC50 = 35.7 uM
AC06:22 Concentration (uM)
HT29 Human Colon Carcinoma
3 Day Exposure MTS
AC06:22
IC50 = 15.2 uM
AC06:22 Concentration (uM)
MDA231 Human Breast Carcinoma
3 Day Exposure MTS
AC06:22
IC50 = 36.9 uM
AC06:22 Concentration (uM)
HT29 Human Colon Carcinoma
3 Day Exposure MTS
AC06:22
IC50 = 16.9 uM
AC06:22 Concentration (uM)
MDA231 Human Breast Carcinoma
3 Day Exposure MTS
AC06:22
IC50 = 22.3 uM
AC06:22 Concentration (uM)
1% DMSO only
Points are means ± s.d
n = 4

Chalcone (64)

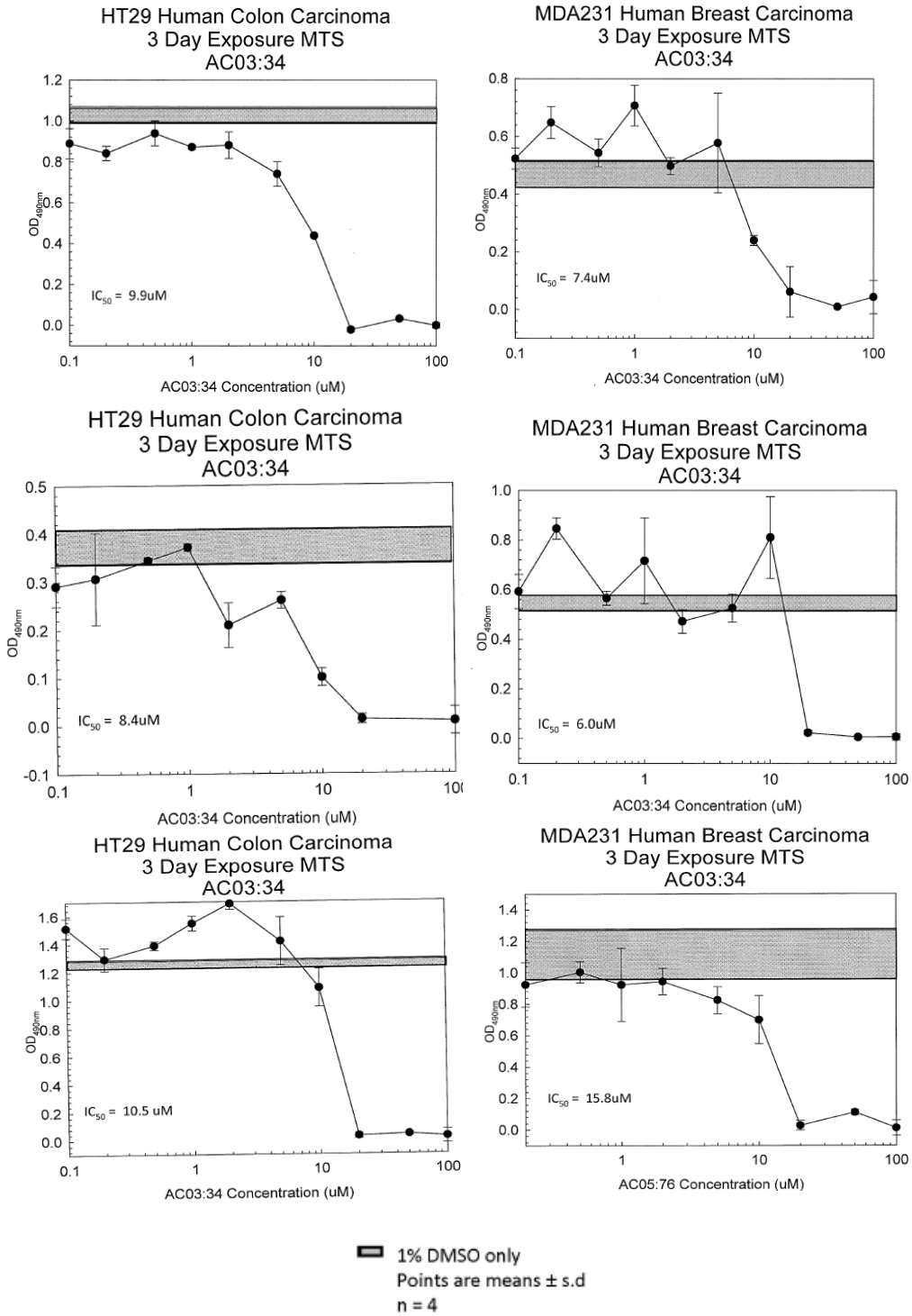
HT29 Human Colon Carcinoma
3 Day Exposure MTS
AC03:34
OD490nm
IC50 = 9.9uM
AC03:34 Concentration (uM)
MDA231 Human Breast Carcinoma
3 Day Exposure MTS
AC03:34
OD490nm
IC50 = 7.4uM
AC03:34 Concentration (uM)
HT29 Human Colon Carcinoma
3 Day Exposure MTS
AC03:34
OD490nm
IC50 = 8.4uM
AC03:34 Concentration (uM)
MDA231 Human Breast Carcinoma
3 Day Exposure MTS
AC03:34
OD490nm
IC50 = 6.0uM
AC03:34 Concentration (uM)
HT29 Human Colon Carcinoma
3 Day Exposure MTS
AC03:34
OD490nm
IC50 = 10.5 uM
AC03:34 Concentration (uM)
MDA231 Human Breast Carcinoma
3 Day Exposure MTS
AC03:34
OD490nm
IC50 = 15.8uM
AC05:76 Concentration (uM)
1% DMSO only
Points are means ± s.d
n = 4

Chalcone (65)

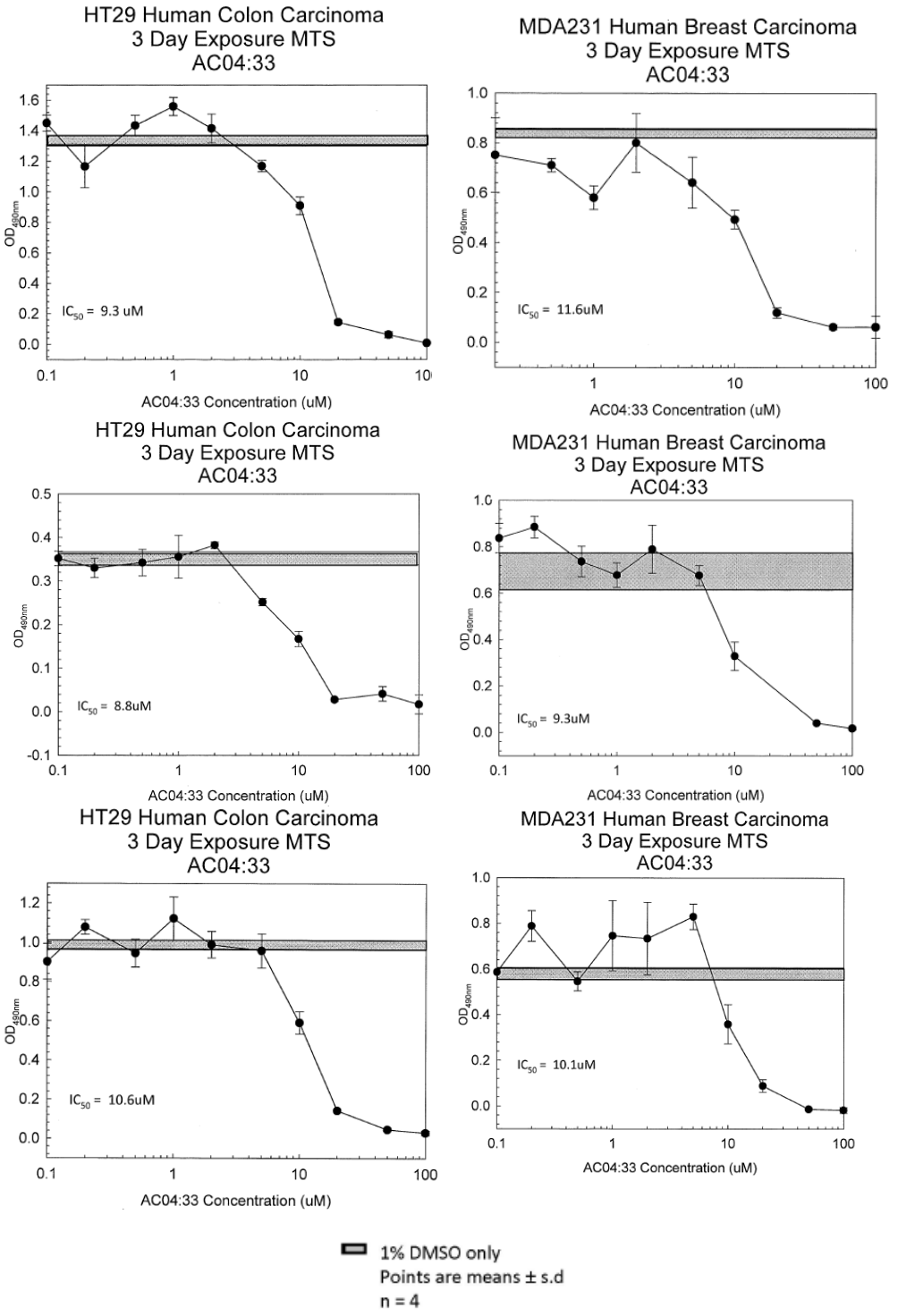
HT29 Human Colon Carcinoma
3 Day Exposure MTS
AC04:33
IC50 = 9.3 uM
AC04:33 Concentration (uM)
MDA231 Human Breast Carcinoma
3 Day Exposure MTS
AC04:33
IC50 = 11.6uM
AC04:33 Concentration (uM)
HT29 Human Colon Carcinoma
3 Day Exposure MTS
AC04:33
IC50 = 8.8uM
AC04:33 Concentration (uM)
MDA231 Human Breast Carcinoma
3 Day Exposure MTS
AC04:33
IC50 = 9.3uM
AC04:33 Concentration (uM)
HT29 Human Colon Carcinoma
3 Day Exposure MTS
AC04:33
IC50 = 10.6uM
AC04:33 Concentration (uM)
MDA231 Human Breast Carcinoma
3 Day Exposure MTS
AC04:33
IC50 = 10.1uM
AC04:33 Concentration (uM)
1% DMSO only
Points are means ± s.d
n = 4

Chalcone (66)

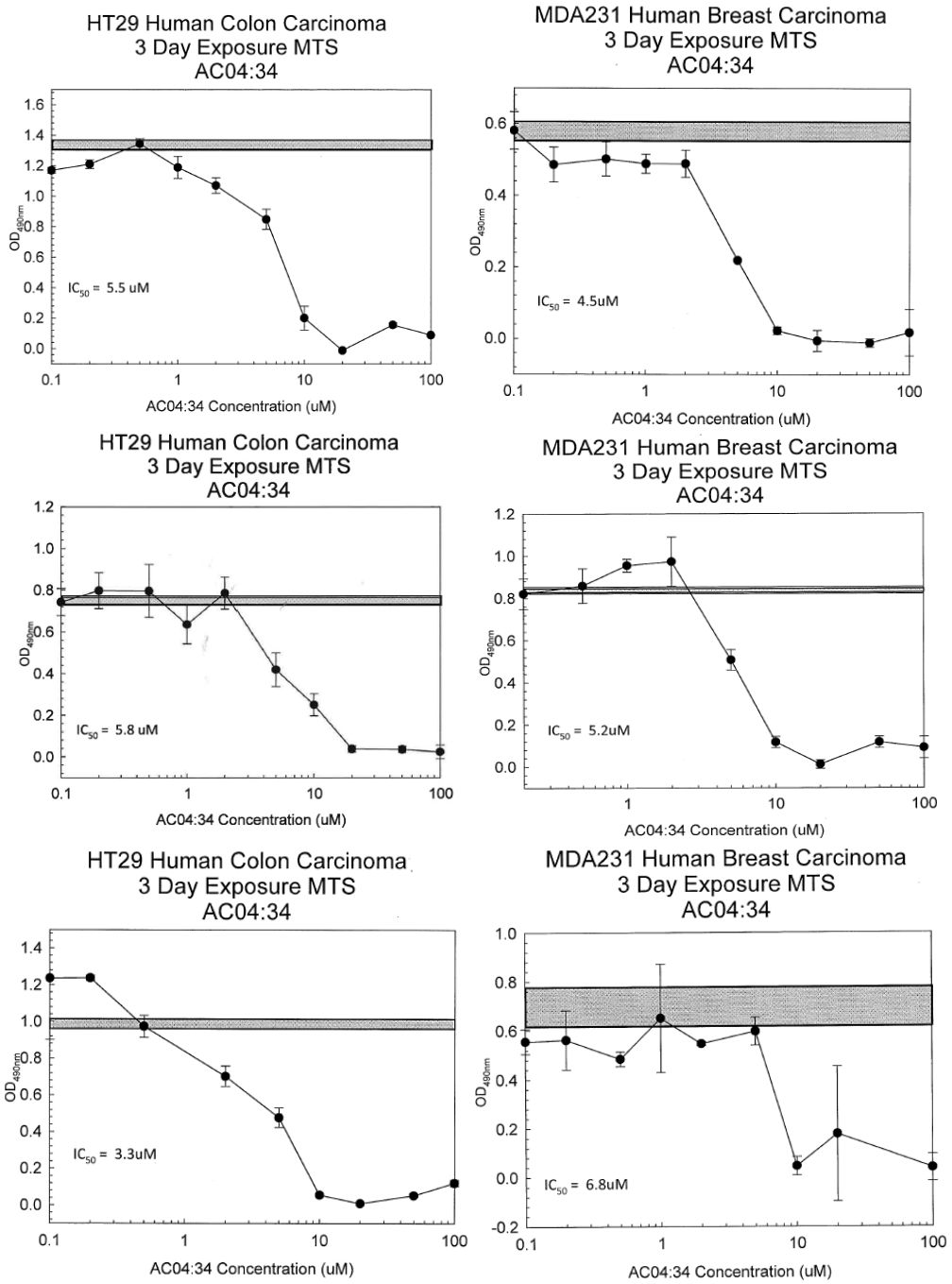
HT29 Human Colon Carcinoma
3 Day Exposure MTS
AC04:34
IC50 = 5.5 uM
AC04:34 Concentration (uM)
MDA231 Human Breast Carcinoma
3 Day Exposure MTS
AC04:34
IC50 = 4.5uM
AC04:34 Concentration (uM)
HT29 Human Colon Carcinoma
3 Day Exposure MTS
AC04:34
IC50 = 5.8 uM
AC04:34 Concentration (uM)
MDA231 Human Breast Carcinoma
3 Day Exposure MTS
AC04:34
IC50 = 5.2uM
AC04:34 Concentration (uM)
HT29 Human Colon Carcinoma
3 Day Exposure MTS
AC04:34
IC50 = 3.3uM
AC04:34 Concentration (uM)
MDA231 Human Breast Carcinoma
3 Day Exposure MTS
AC04:34
IC50 = 6.8uM
AC04:34 Concentration (uM)
1% DMSO only
Points are means ± s.d
n = 4

Chalcone (67)

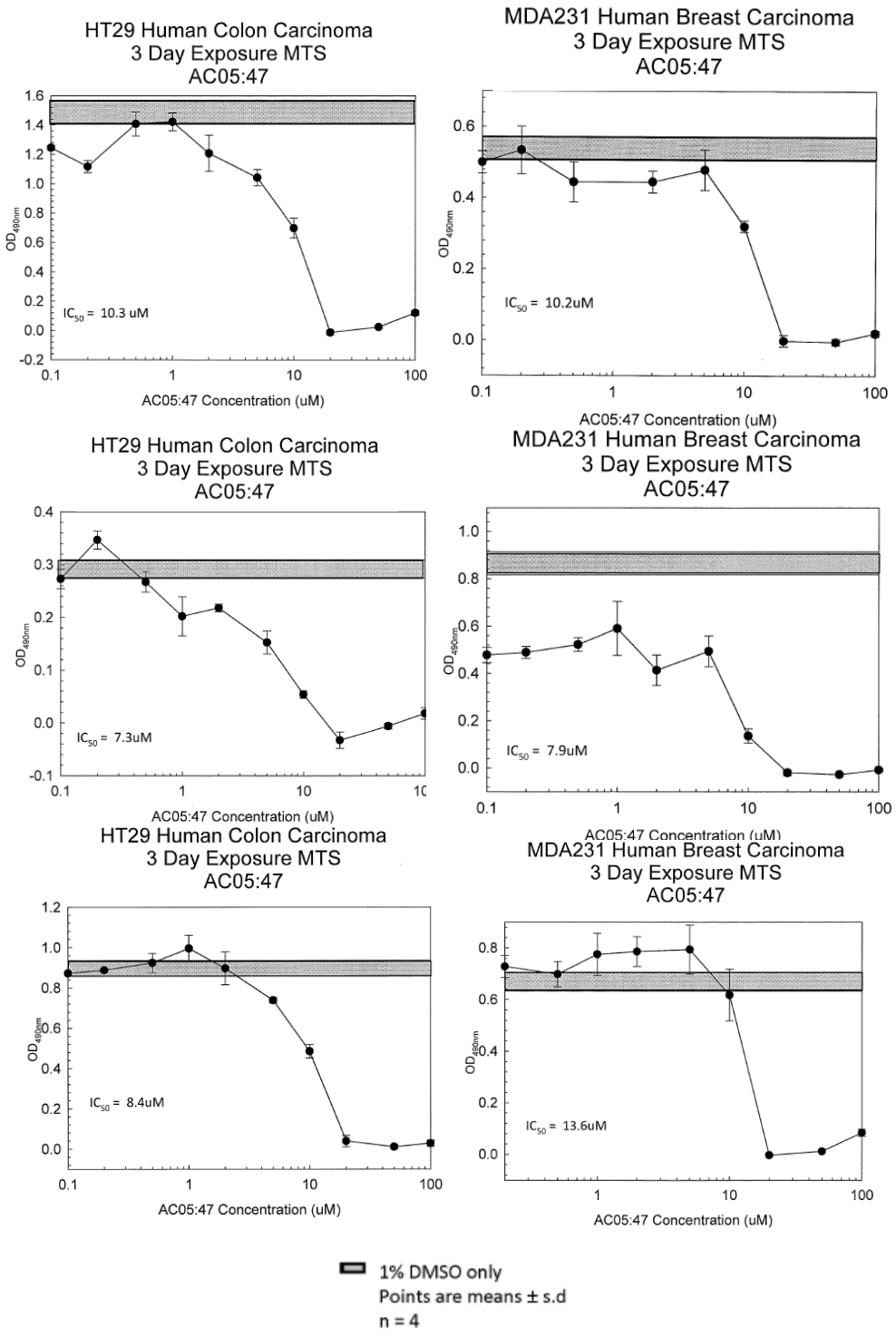
HT29 Human Colon Carcinoma
3 Day Exposure MTS
AC05:47
IC50 = 10.3 uM
AC05:47 Concentration (uM)
MDA231 Human Breast Carcinoma
3 Day Exposure MTS
AC05:47
IC50 = 10.2uM
AC05:47 Concentration (uM)
HT29 Human Colon Carcinoma
3 Day Exposure MTS
AC05:47
IC50 = 7.3uM
AC05:47 Concentration (uM)
MDA231 Human Breast Carcinoma
3 Day Exposure MTS
AC05:47
IC50 = 7.9uM
AC05:47 Concentration (uM)
HT29 Human Colon Carcinoma
3 Day Exposure MTS
AC05:47
IC50 = 8.4uM
AC05:47 Concentration (uM)
MDA231 Human Breast Carcinoma
3 Day Exposure MTS
AC05:47
IC50 = 13.6uM
AC05:47 Concentration (uM)
1% DMSO only
Points are means ± s.d
n = 4

Colchicine

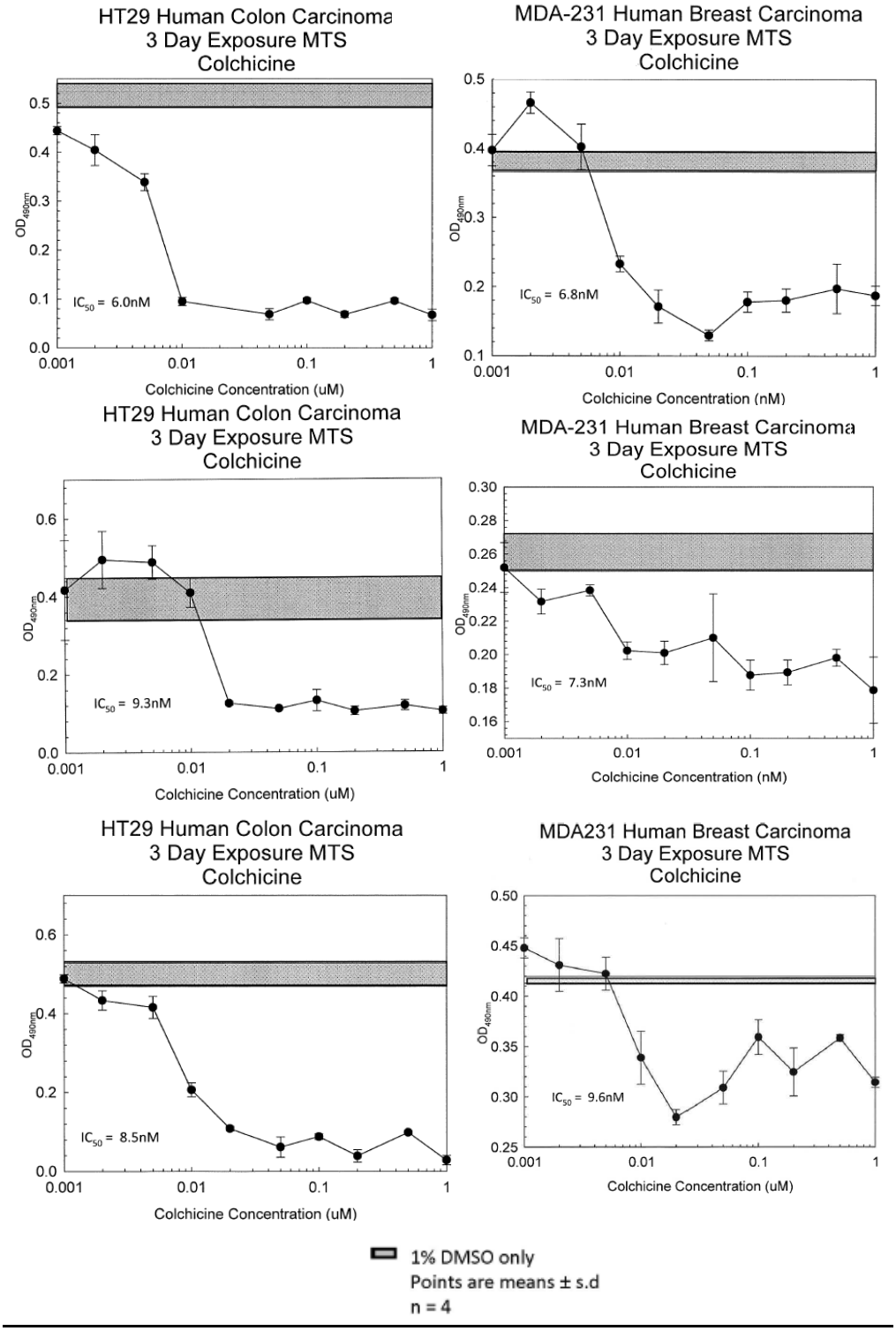
HT29 Human Colon Carcinoma
3 Day Exposure MTS
Colchicine
OD490nm
IC50 = 6.0nM
Colchicine Concentration (uM)
MDA-231 Human Breast Carcinoma
3 Day Exposure MTS
Colchicine
IC50 = 6.8nM
Colchicine Concentration (nM)
HT29 Human Colon Carcinoma
3 Day Exposure MTS
Colchicine
IC50 = 9.3nM
Colchicine Concentration (uM)
MDA-231 Human Breast Carcinoma
3 Day Exposure MTS
Colchicine
IC50 = 7.3nM
Colchicine Concentration (nM)
HT29 Human Colon Carcinoma
3 Day Exposure MTS
Colchicine
IC50 = 8.5nM
Colchicine Concentration (uM)
MDA231 Human Breast Carcinoma
3 Day Exposure MTS
Colchicine
IC50 = 9.6nM
Colchicine Concentration (uM)
1% DMSO only
Points are means ± s.d
n = 4

Colchicine

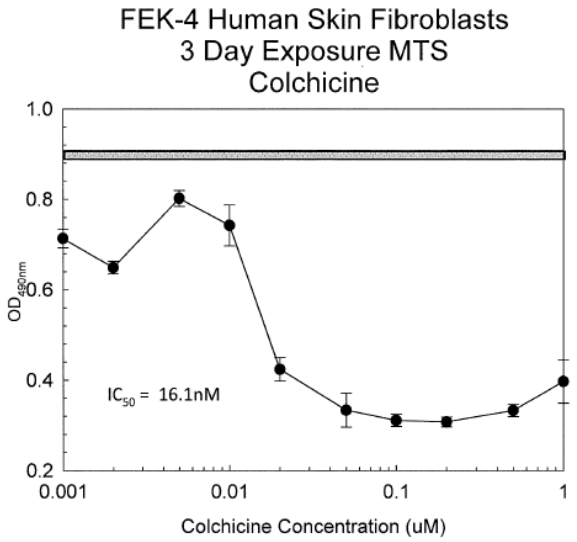

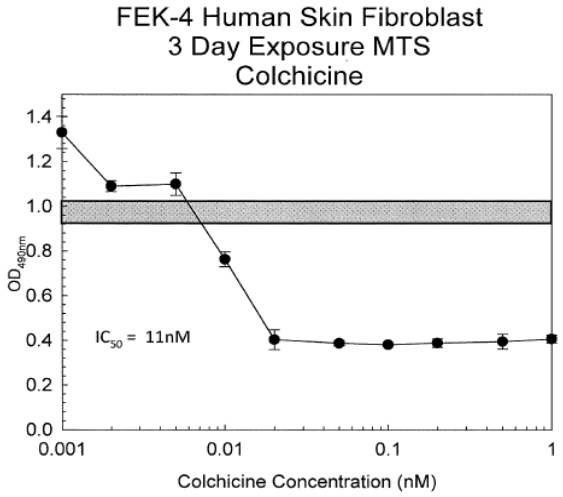

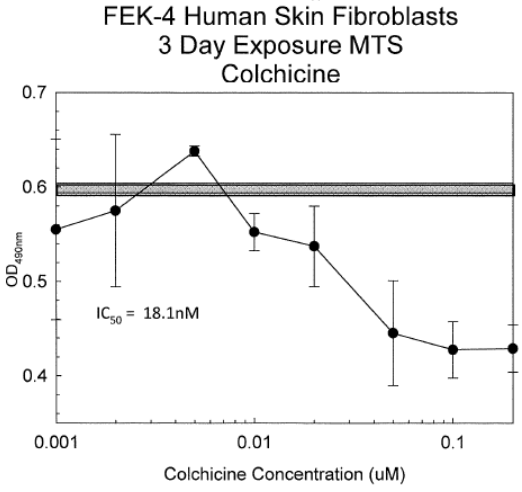

1% DMSO only
Points are means ± s.d
n = 4

Pyrazoline (68)

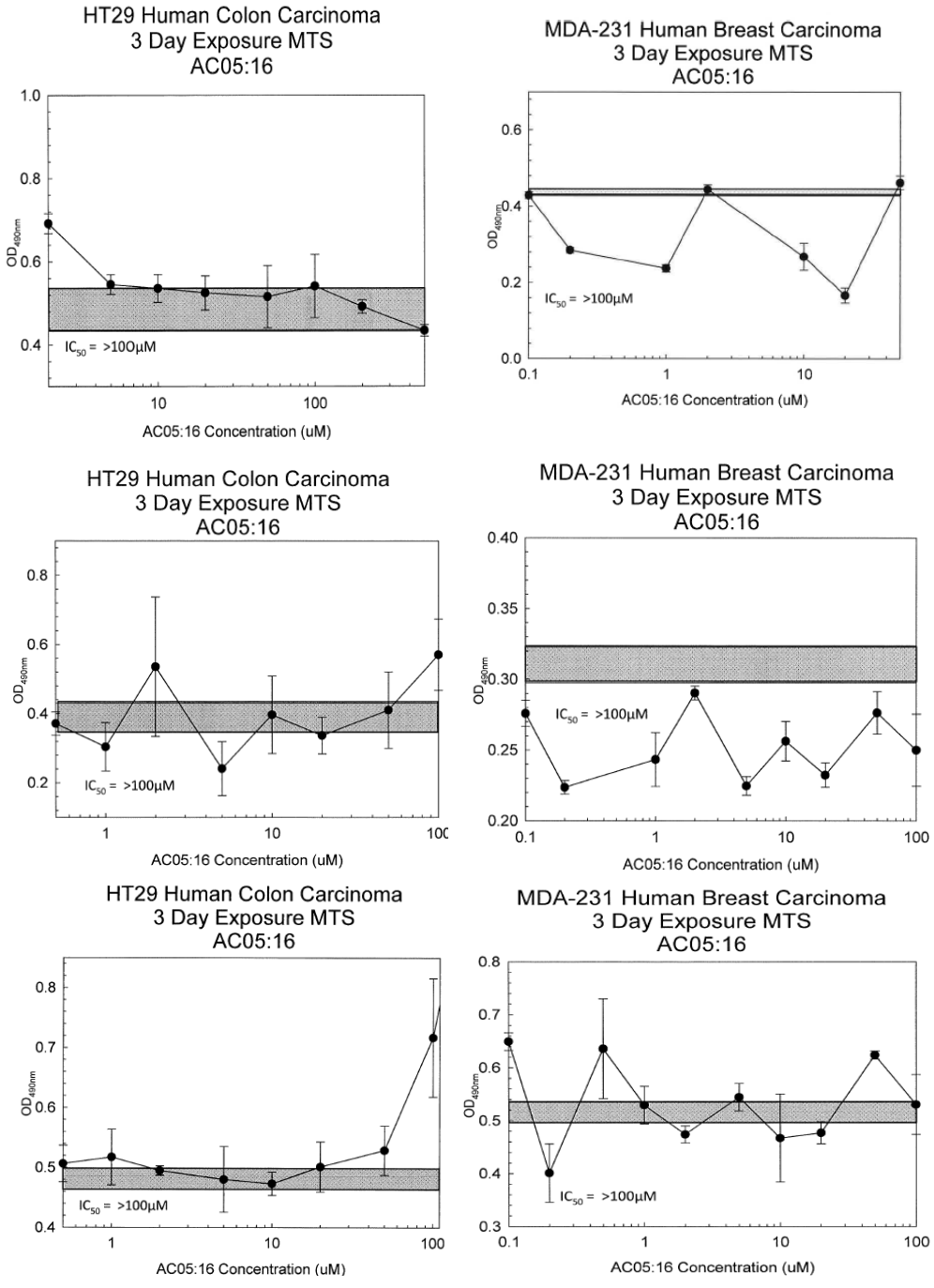

Pyrazoline (69)

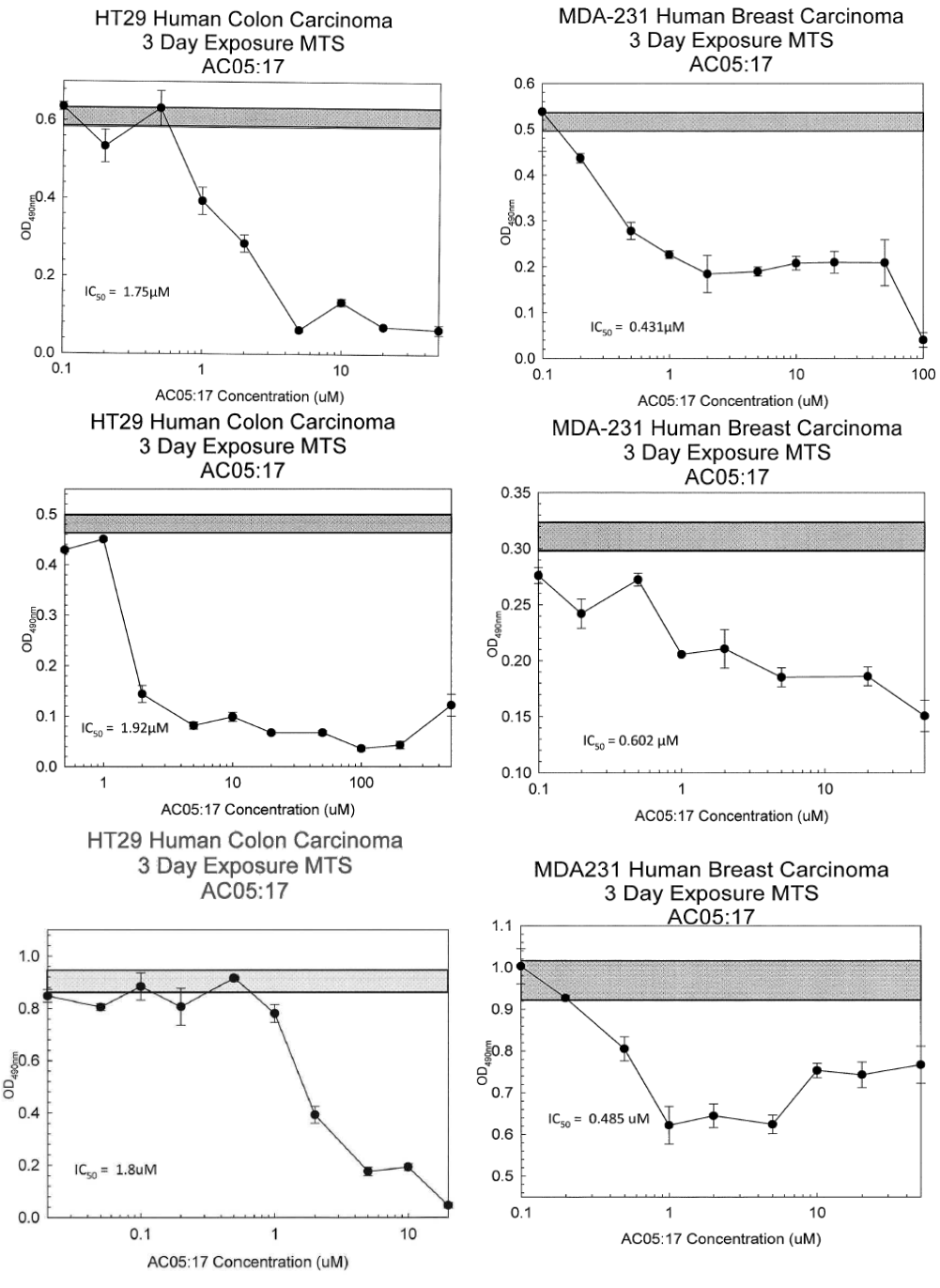

Pyrazoline (70)

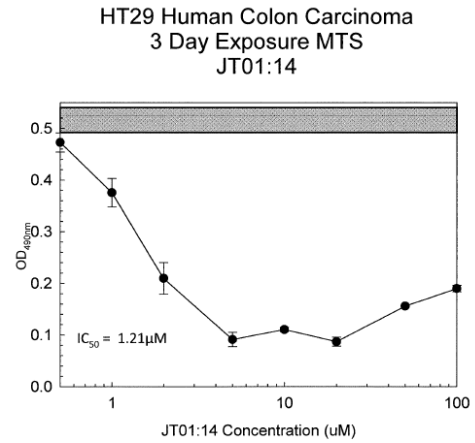

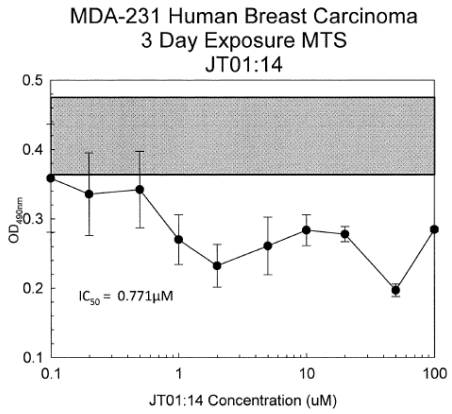

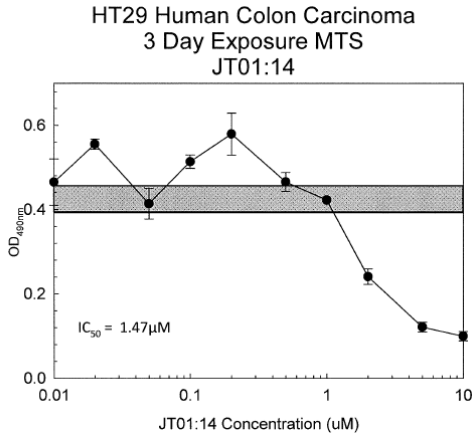

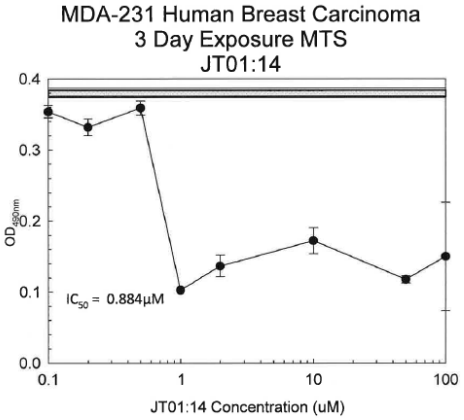

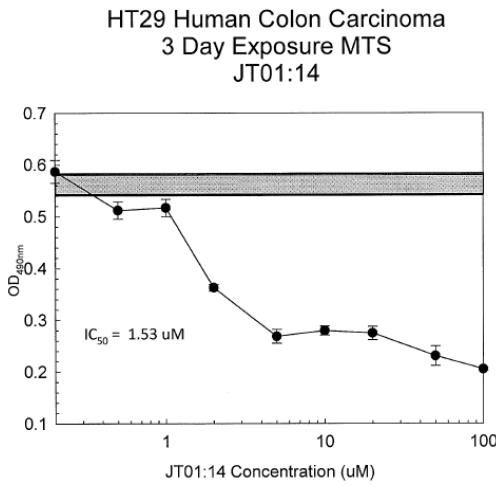

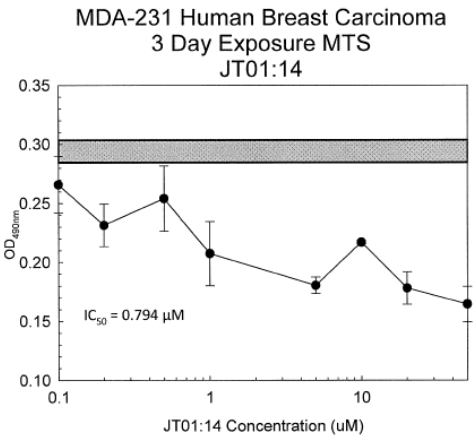

1% DMSO only
Points are means ± s.d
n = 4

Pyrazoline (71)

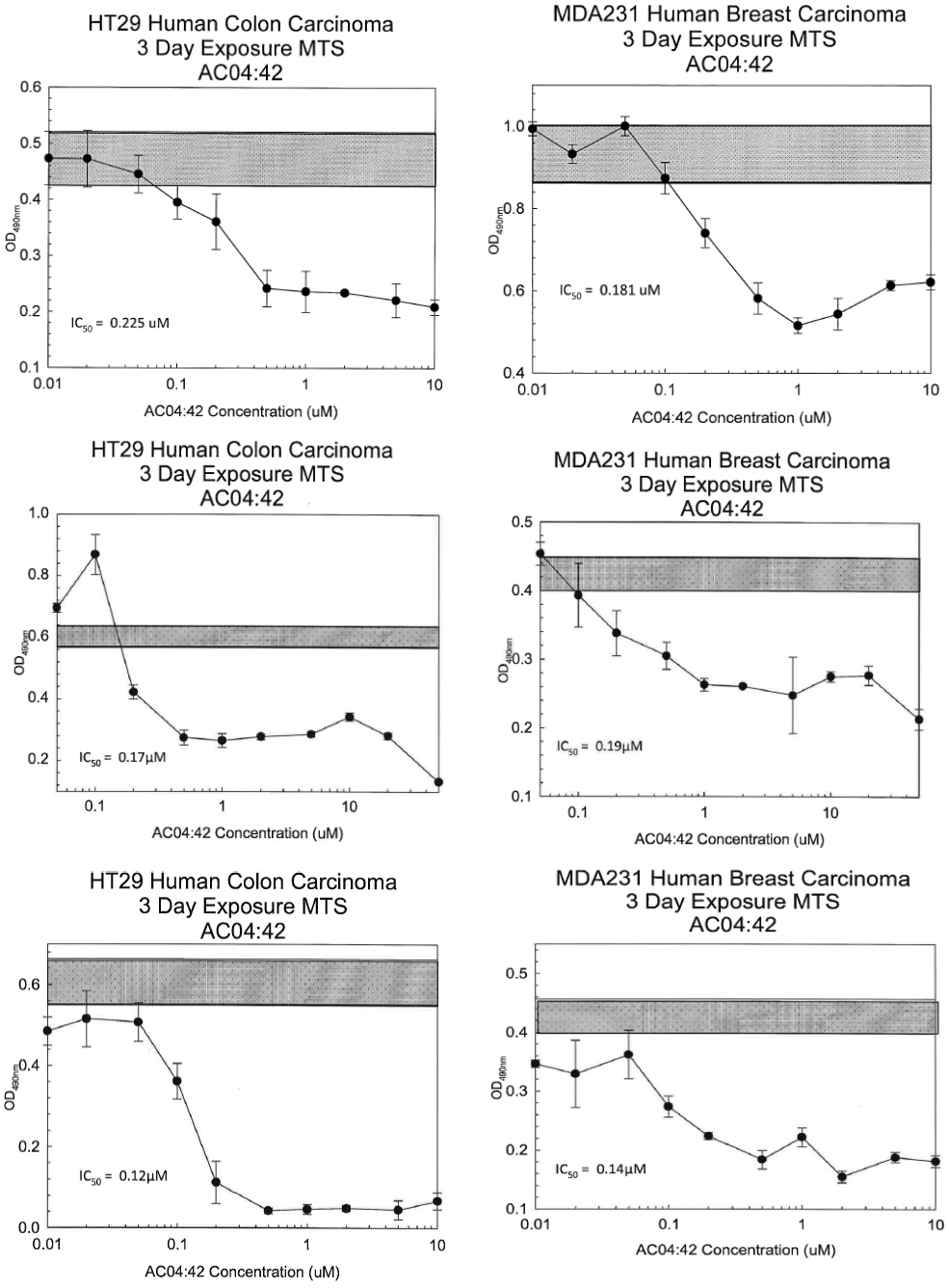

Pyrazoline (71)

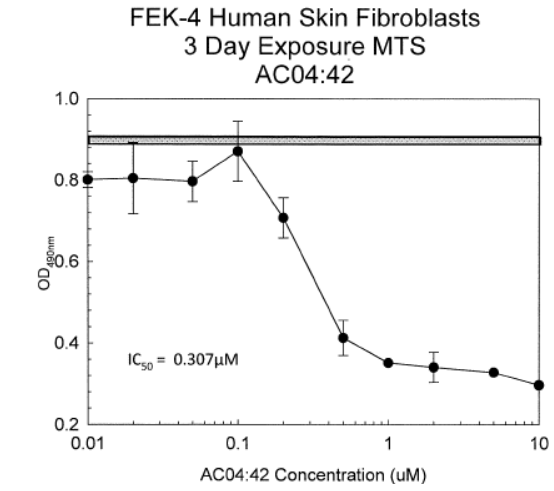

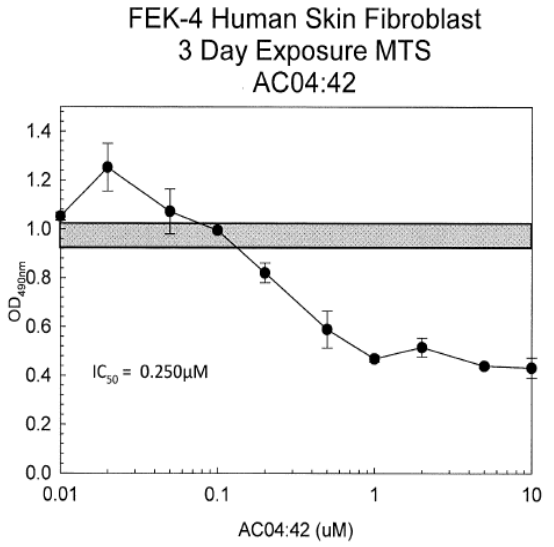

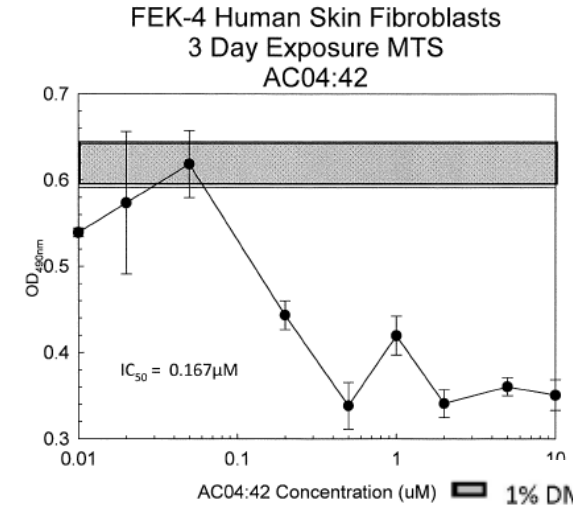

Pyrazoline (71-)

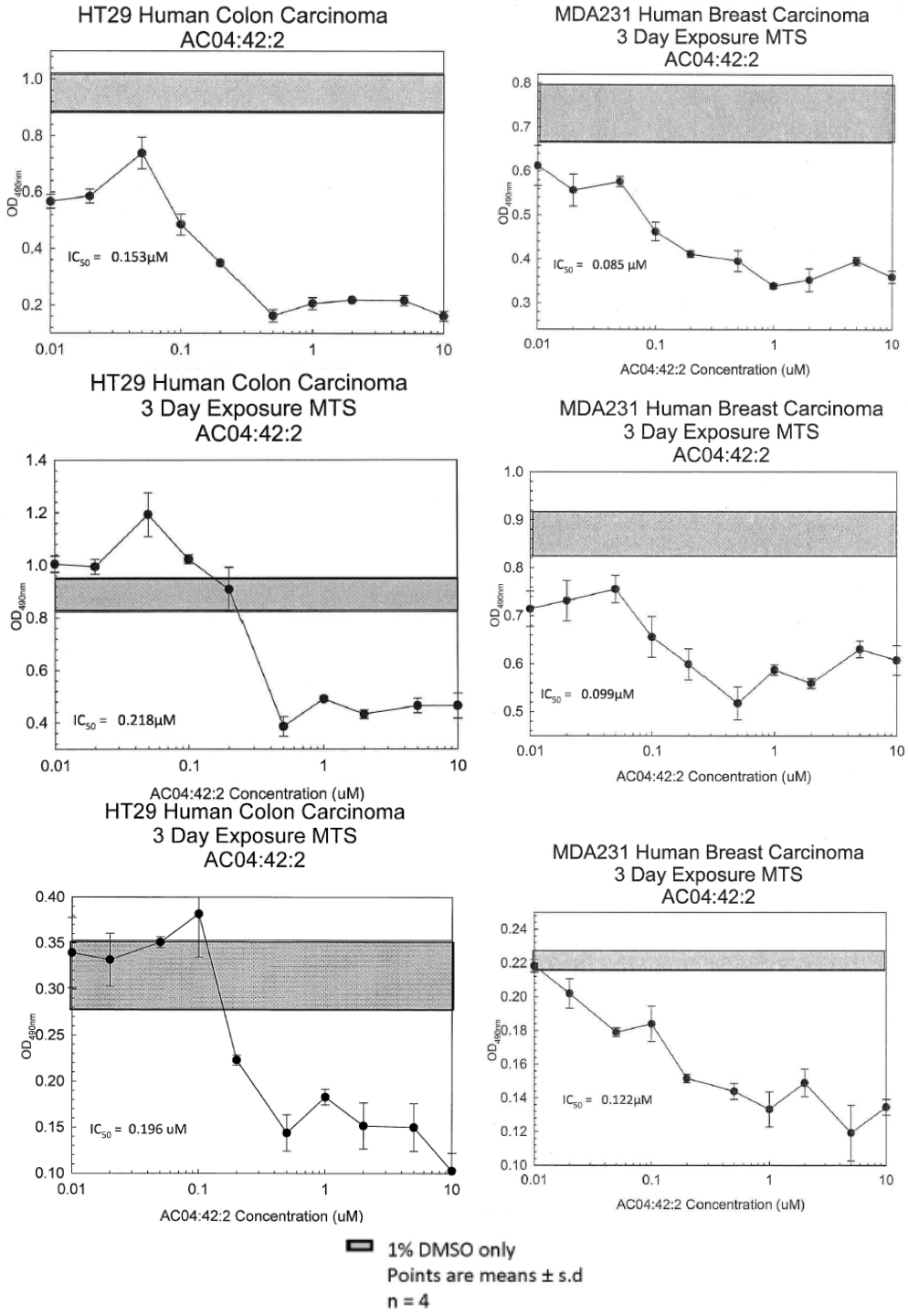

Pyrazoline (71-)

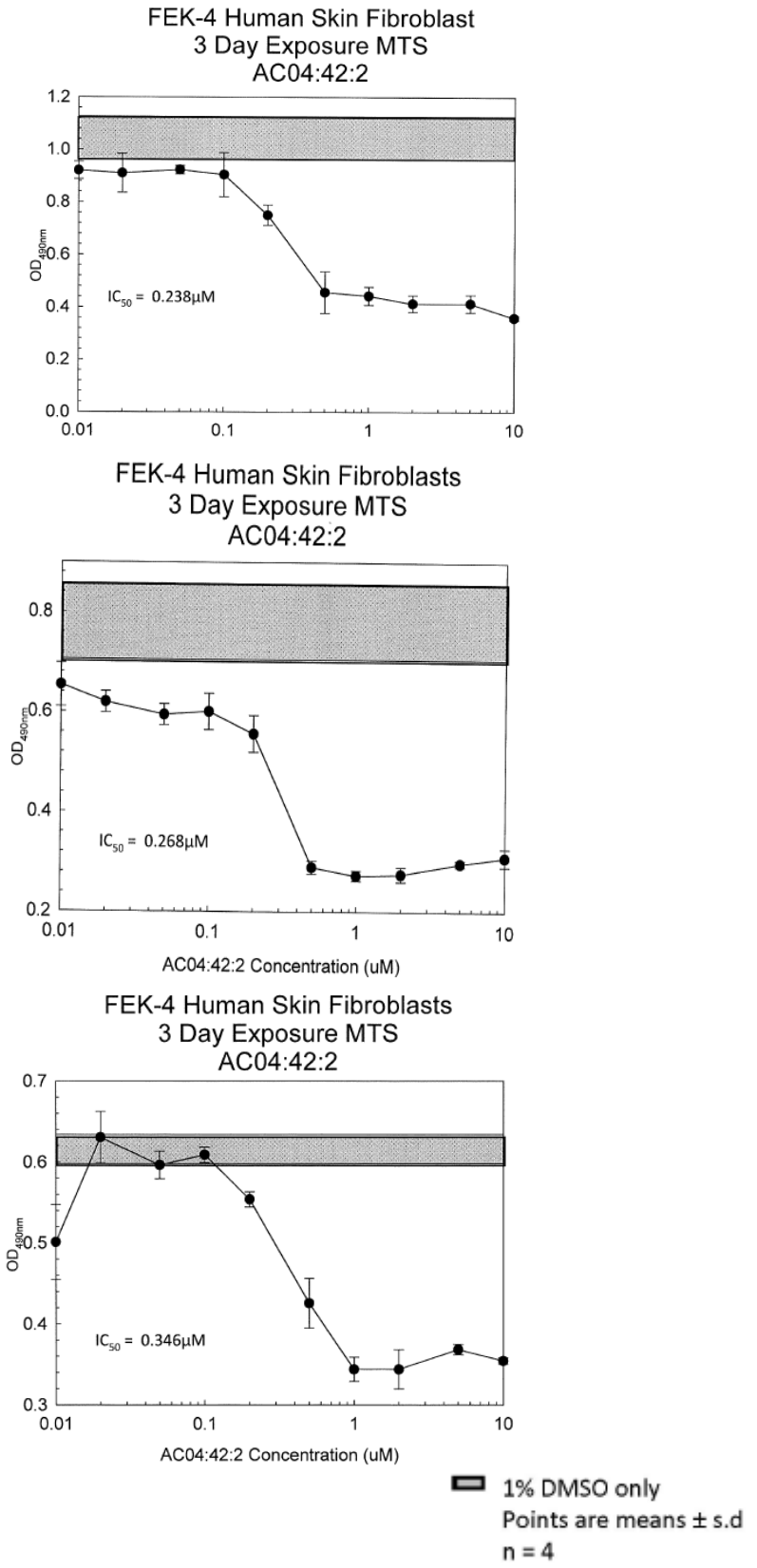

Pyrazoline (71+)

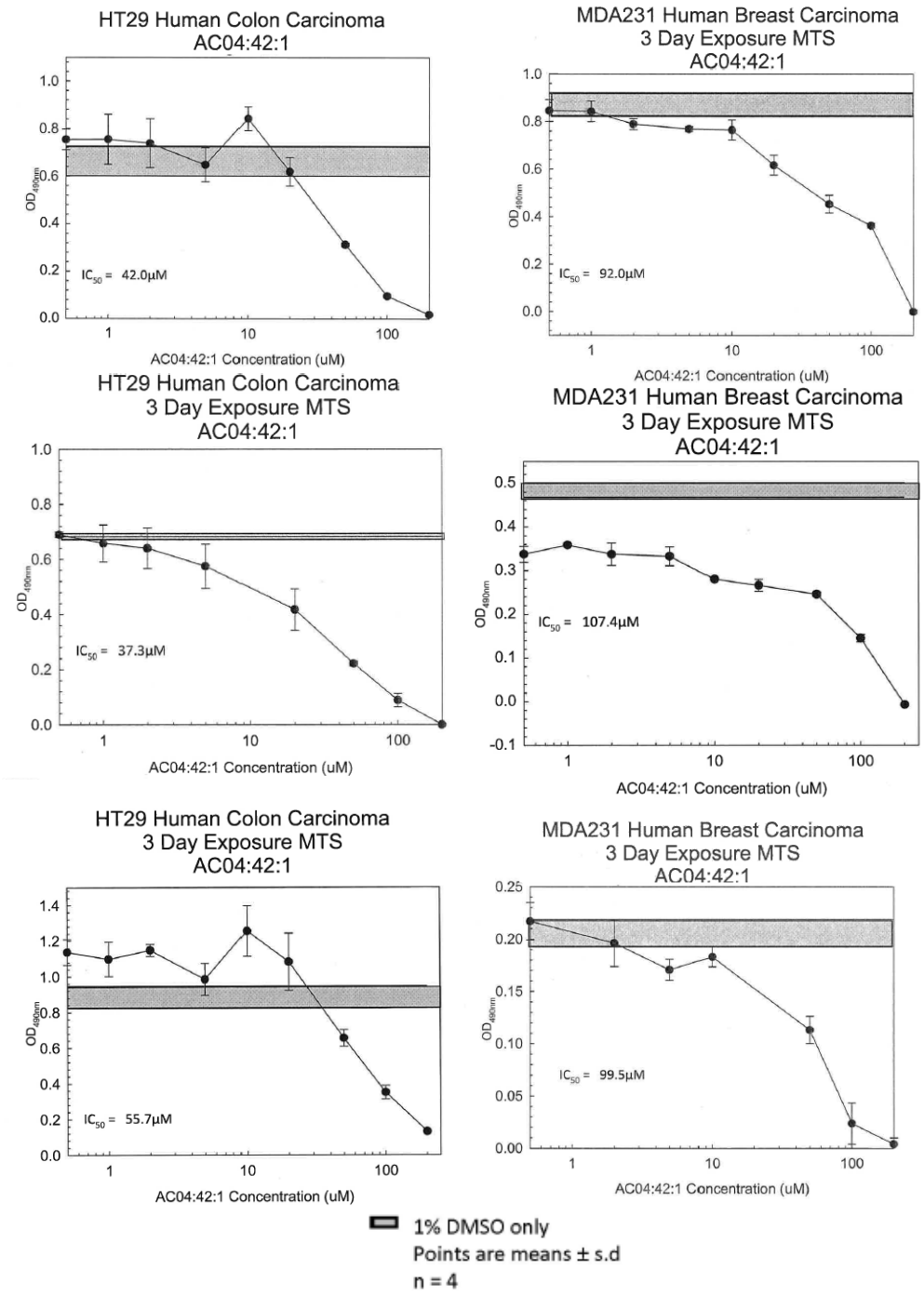

Pyrazoline (71+)

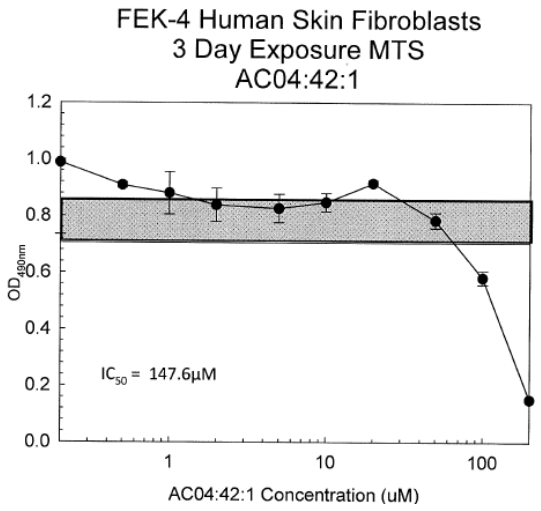

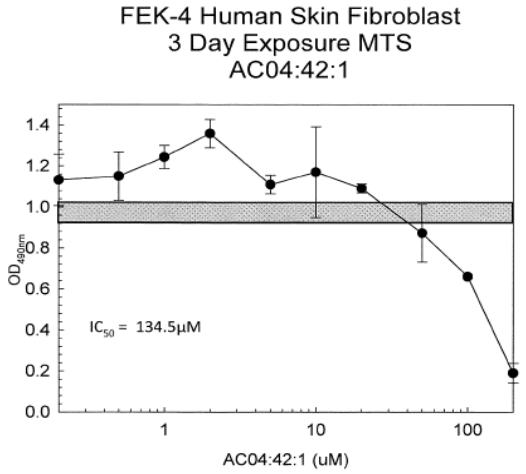

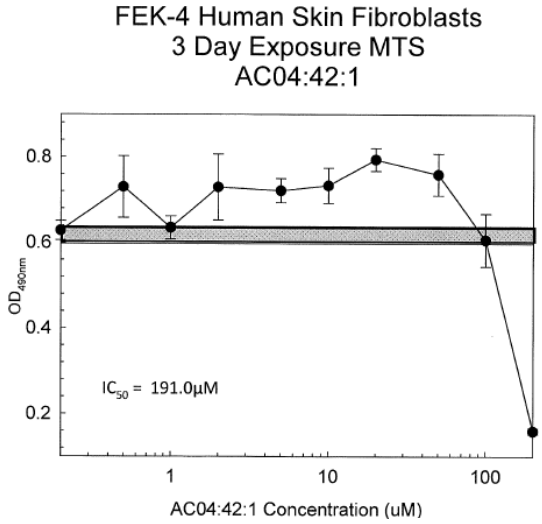

1% DMSO only
Points are means ± s.d
n = 4

Pyrazoline (72)

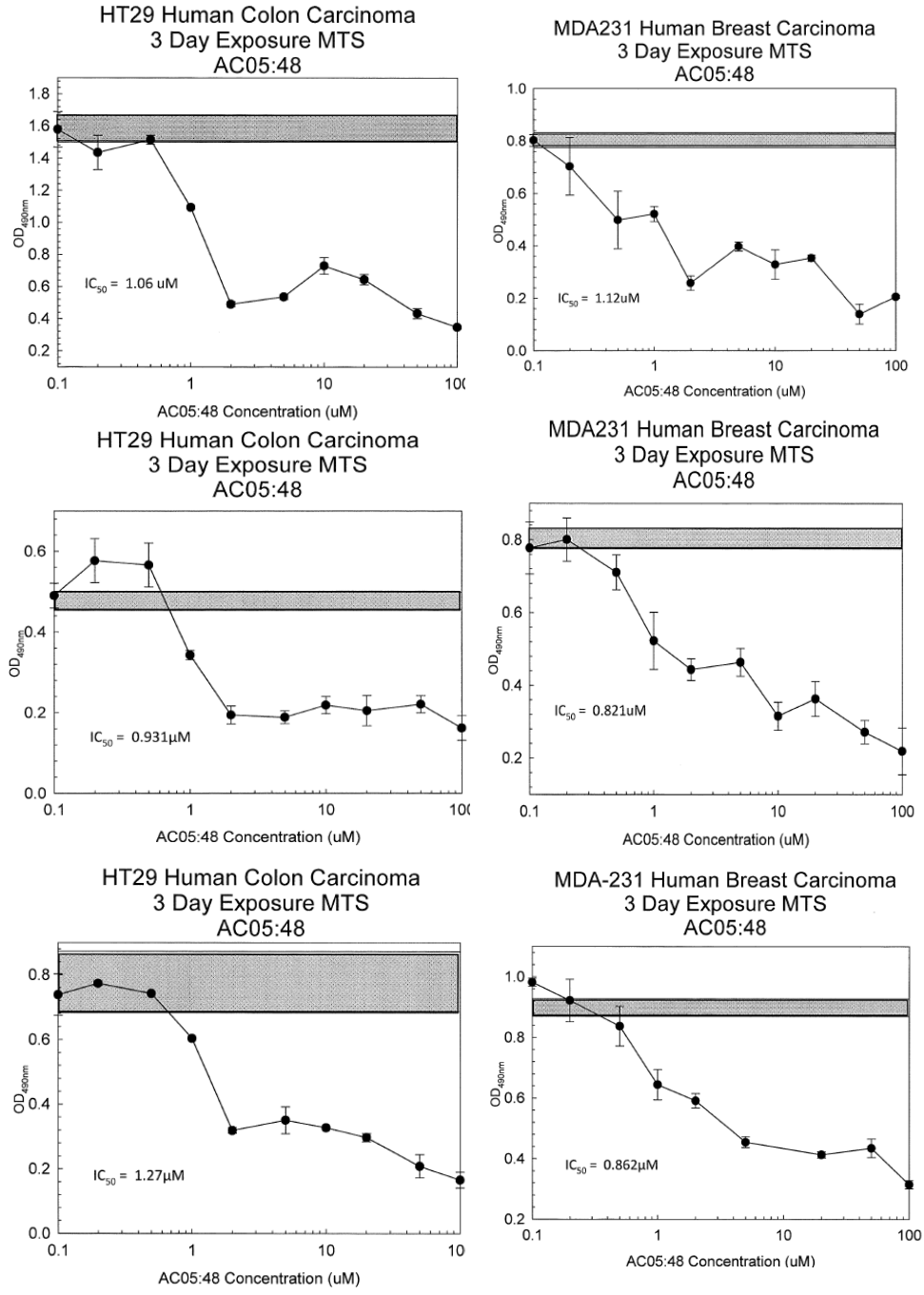

Pyrazoline (73)

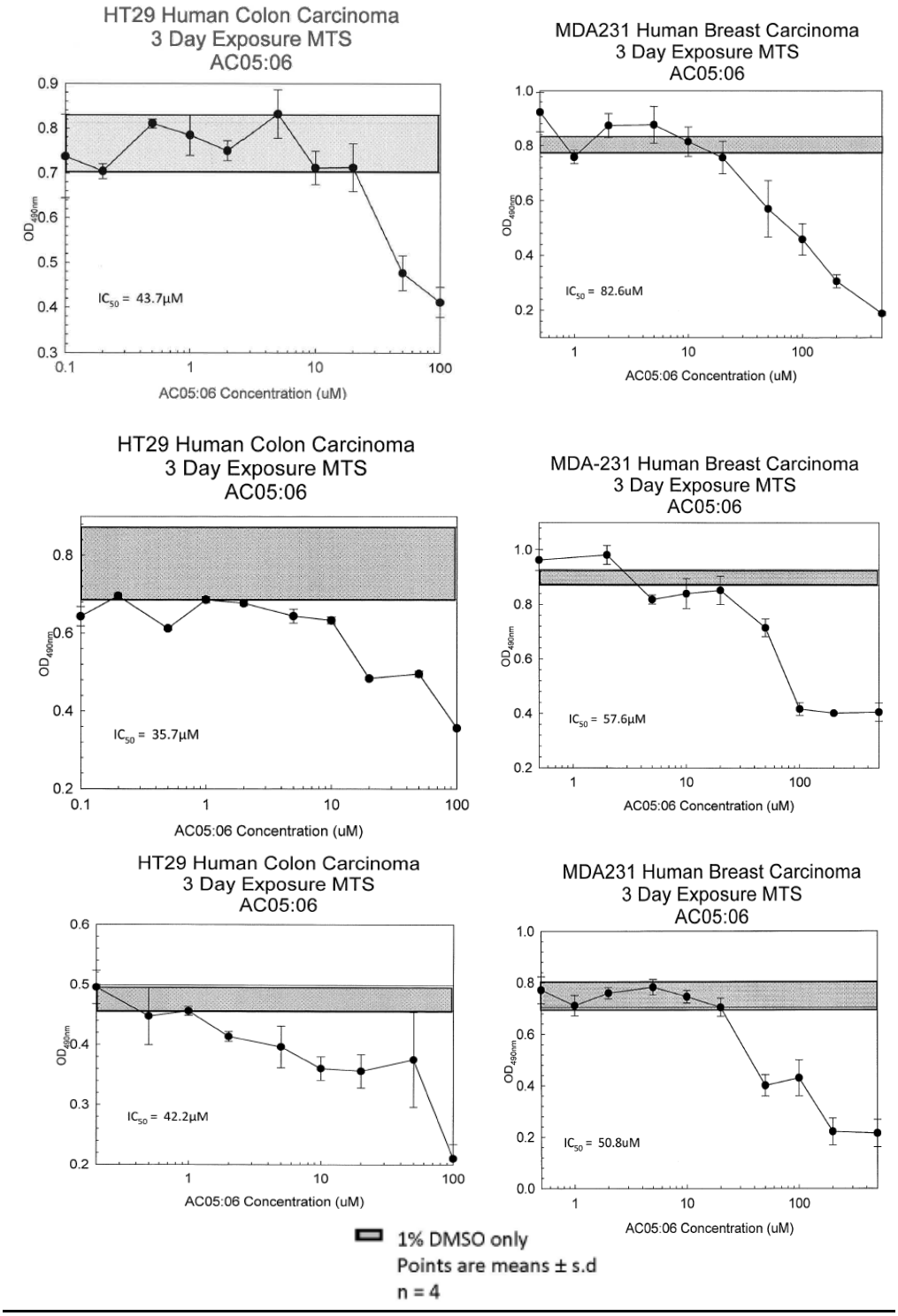

Pyrazoline (74)

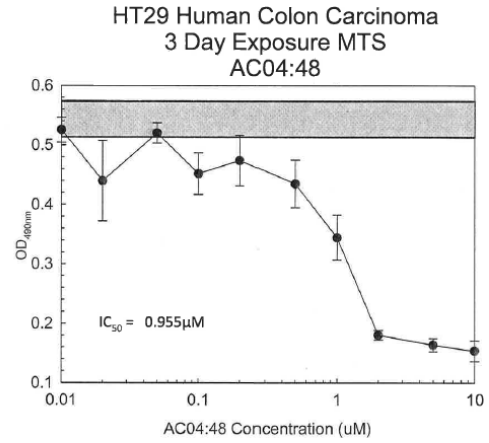

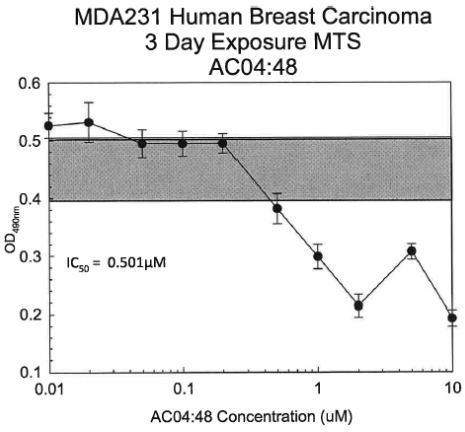

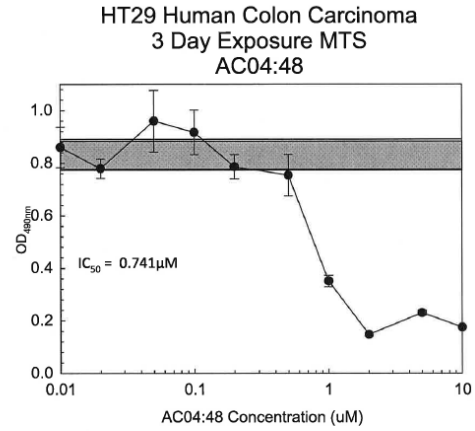

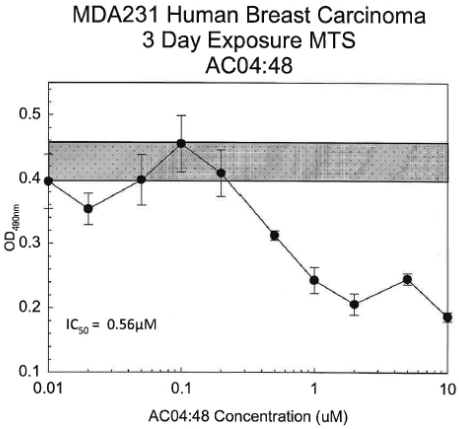

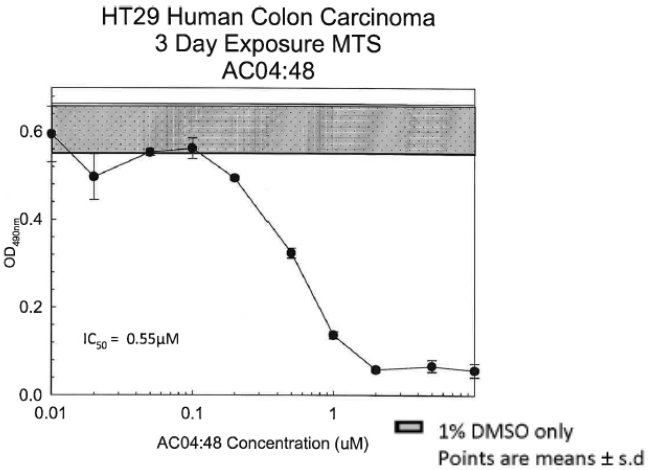

Pyrazoline (74-)

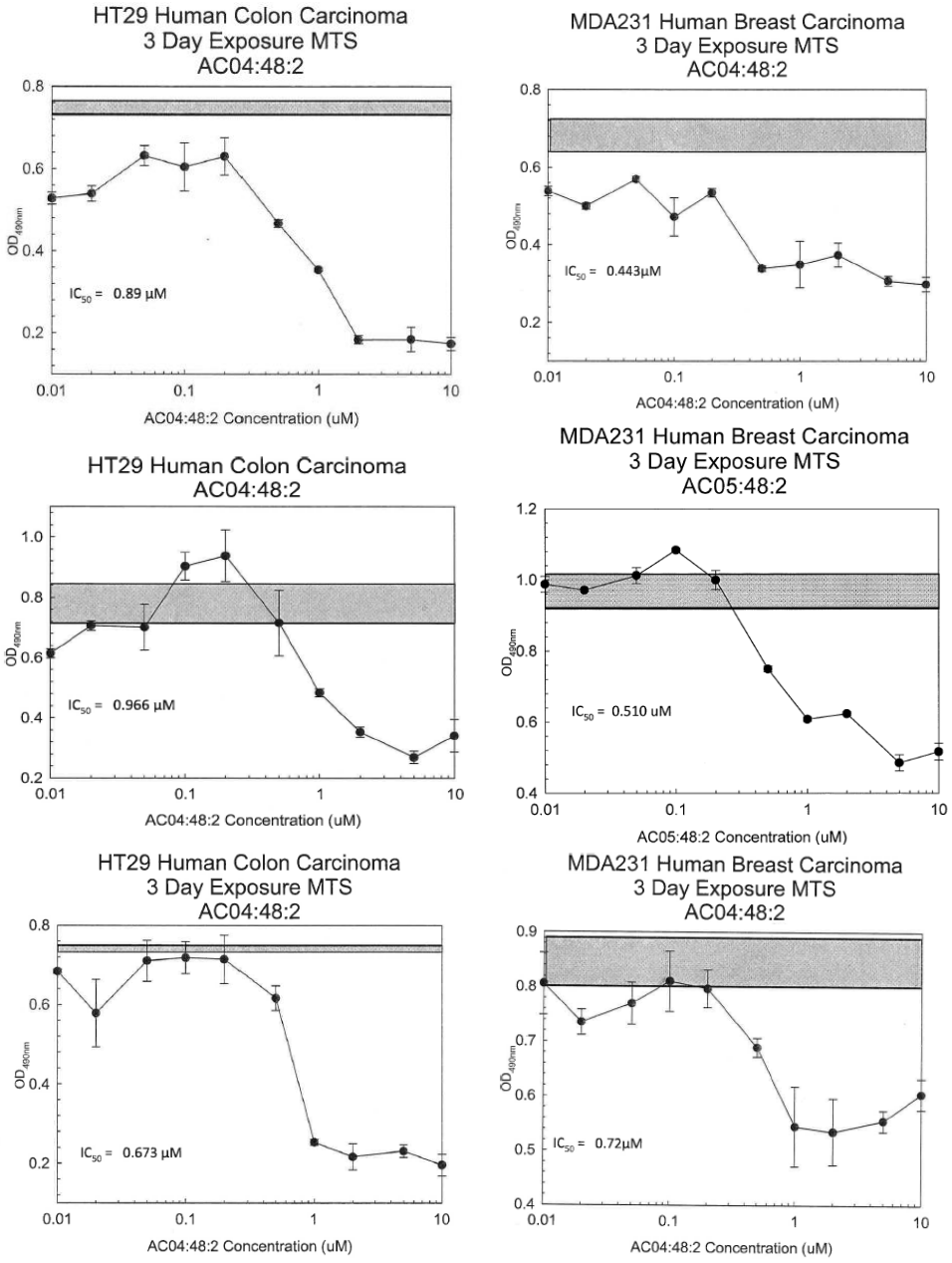

Pyrazoline (74+)

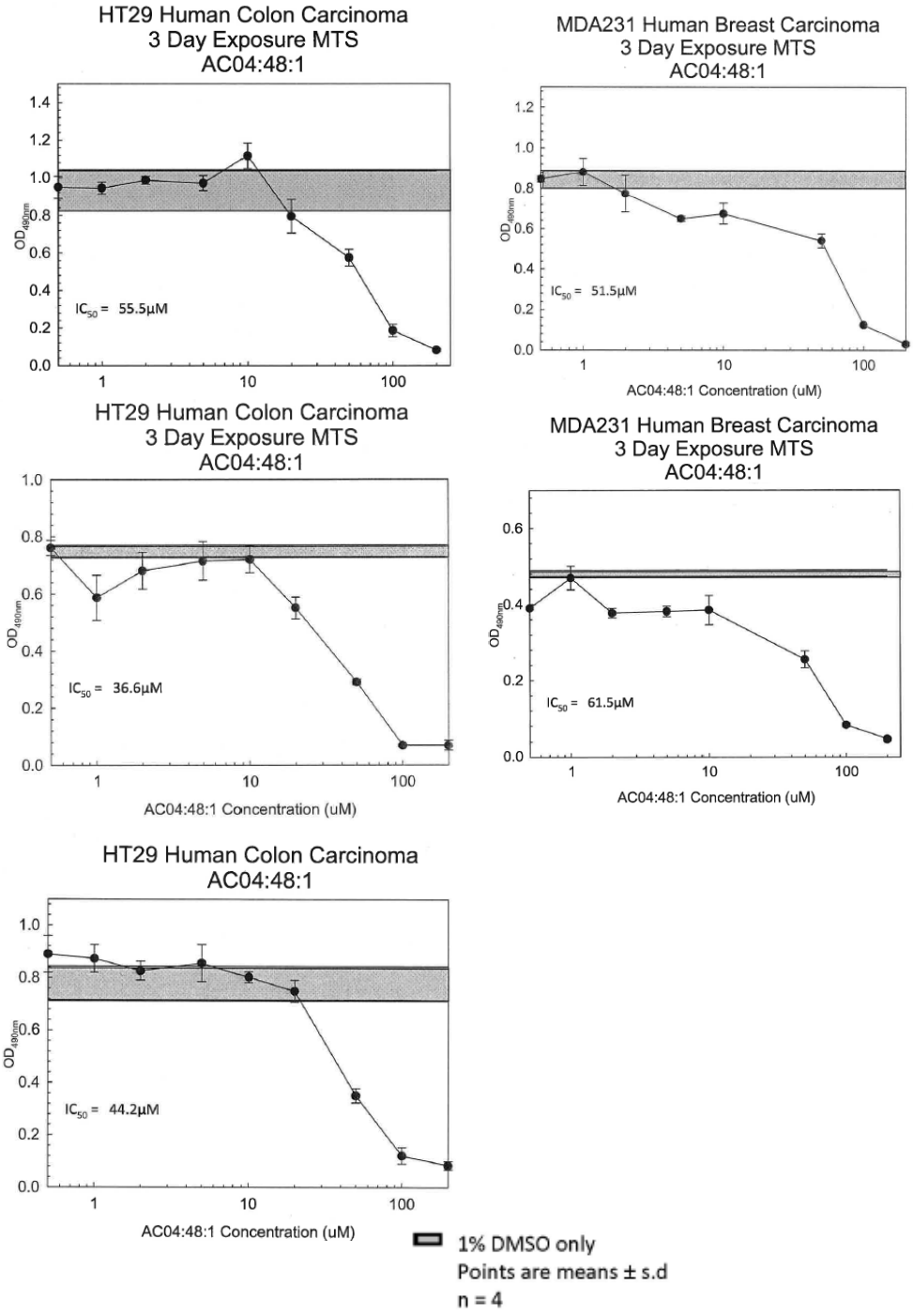

Pyrazoline (75)

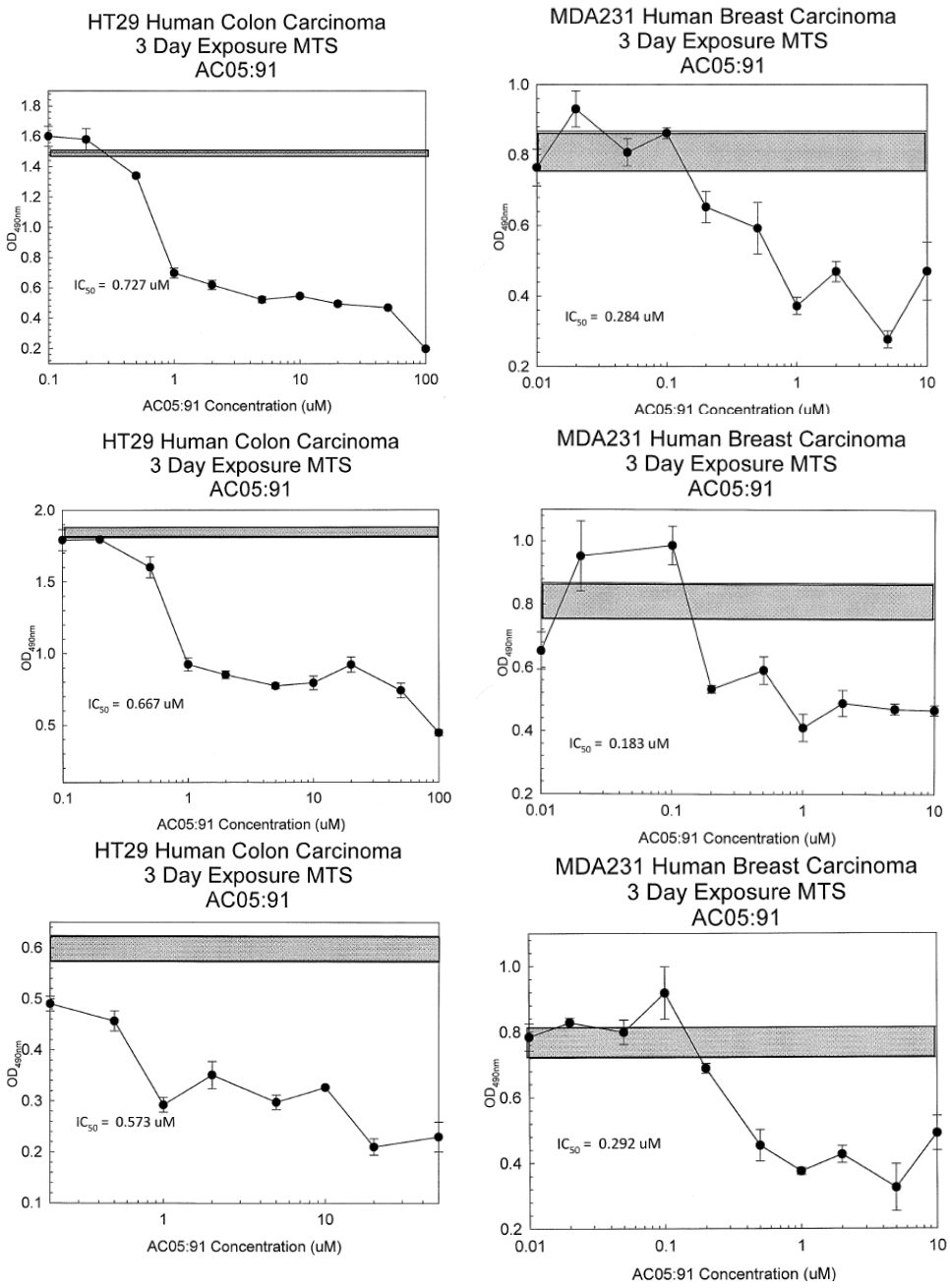

Pyrazoline (76)

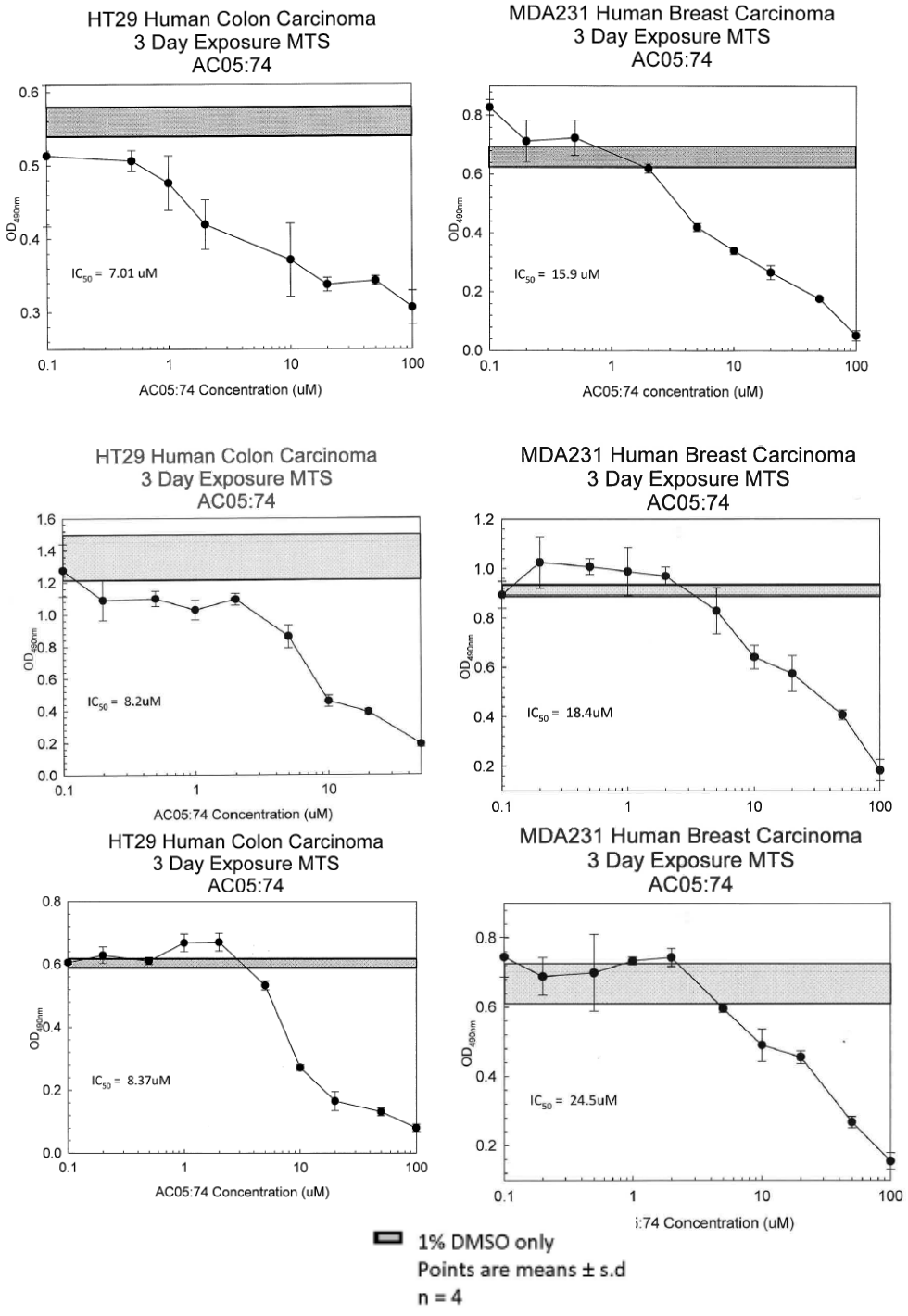

Pyrazoline (77)

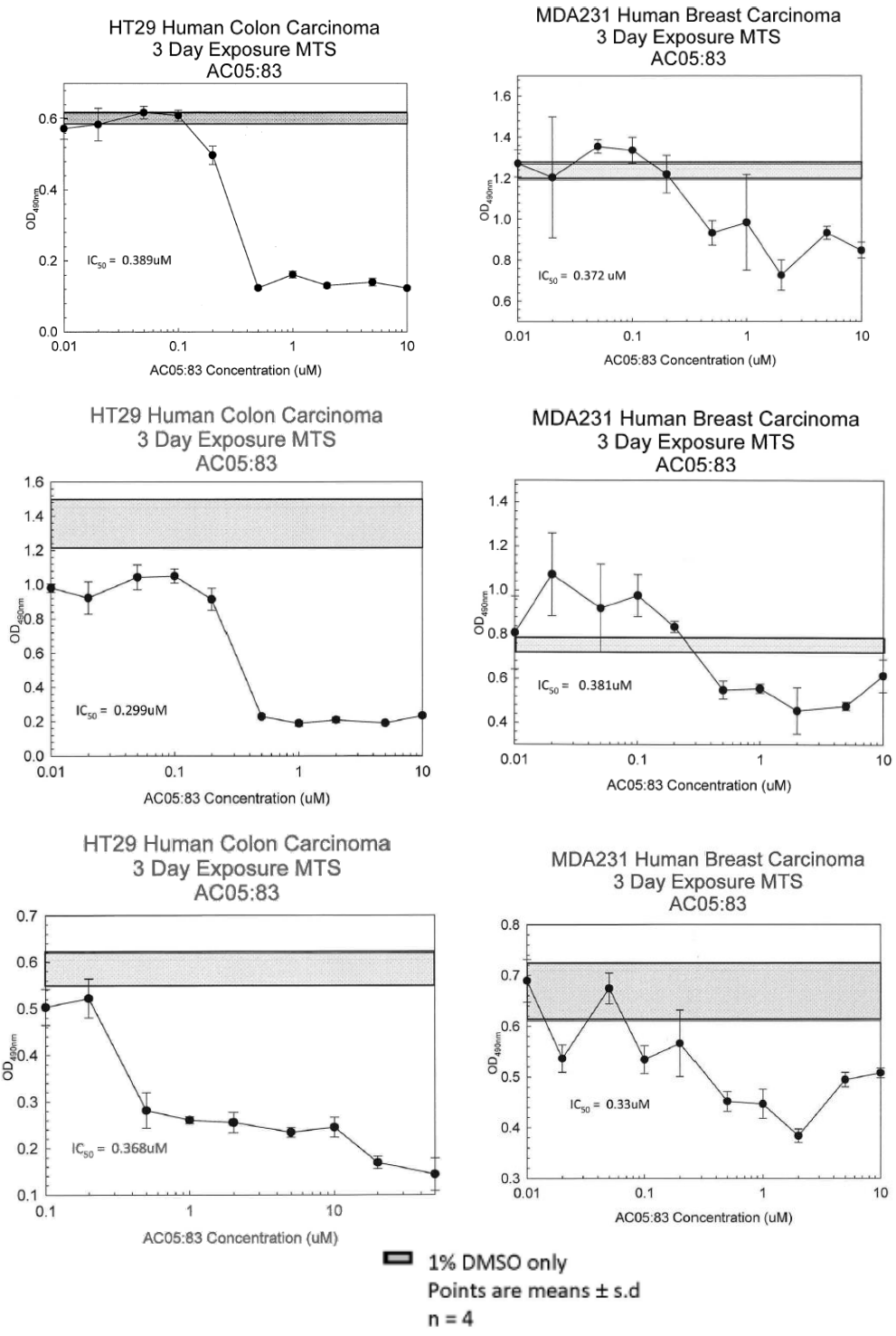

Pyrazoline (78)

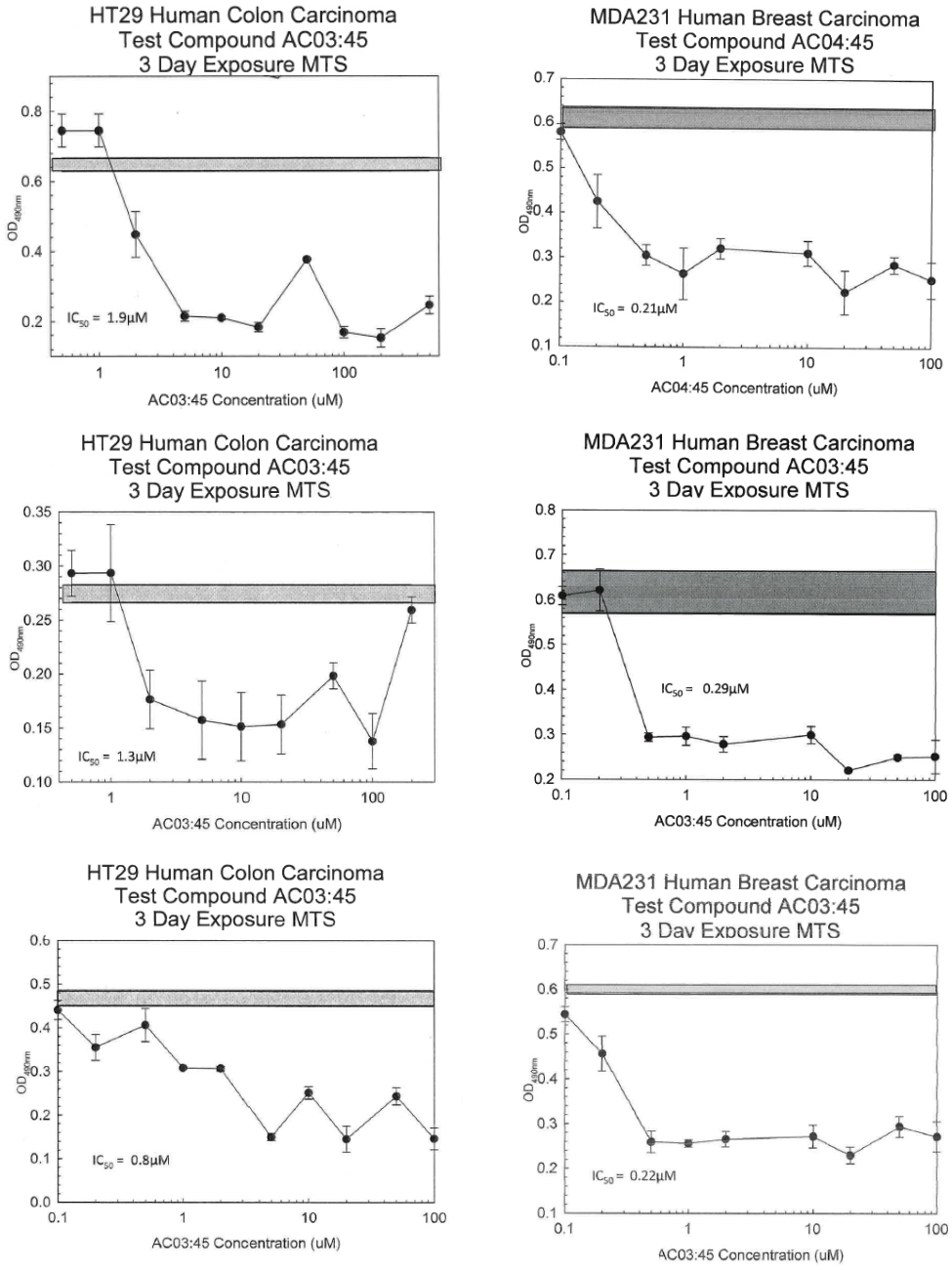

Pyrazoline (78-)

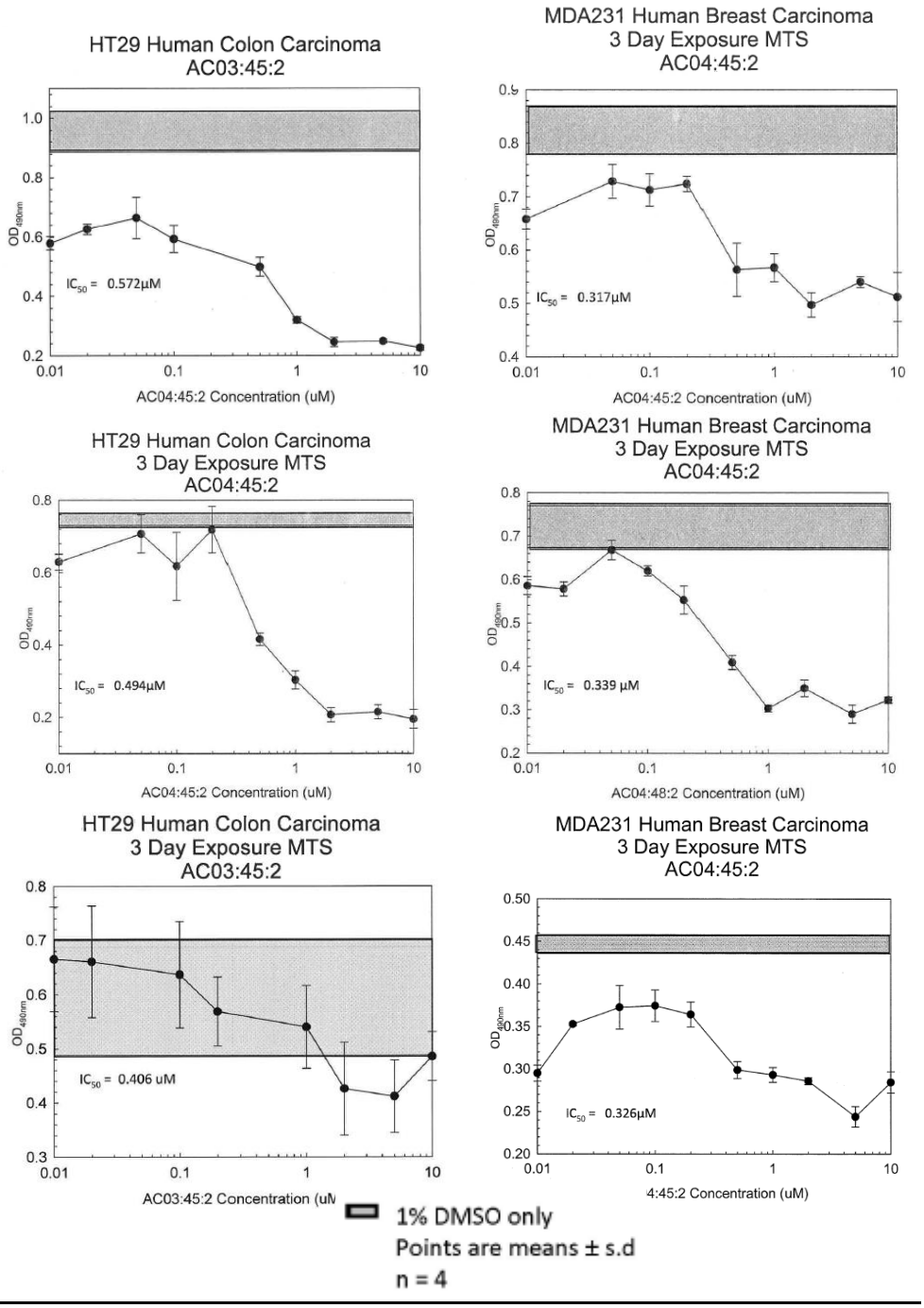

Pyrazoline (78+)

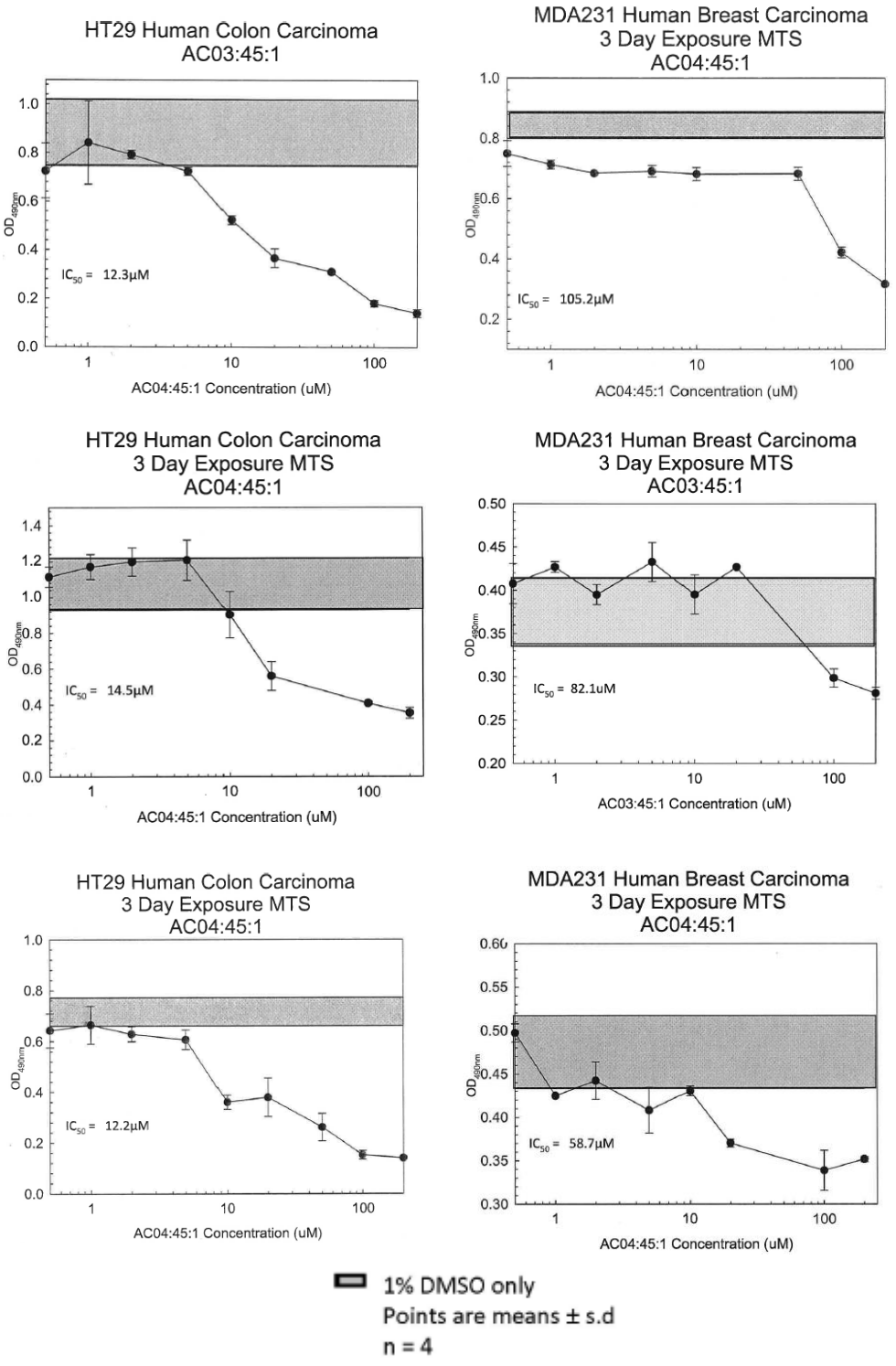

Pyrazoline (79)

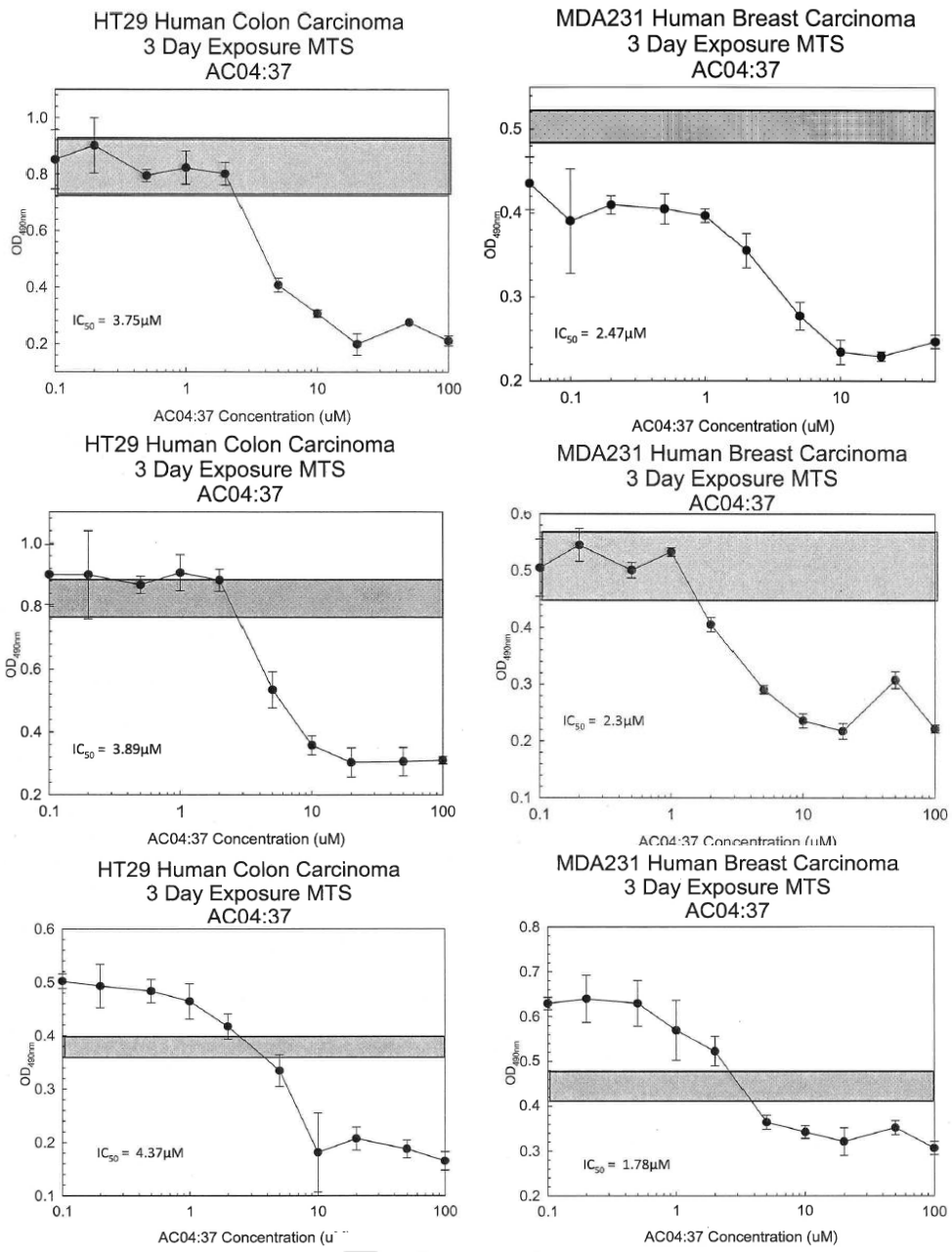

Pyrazoline (80)

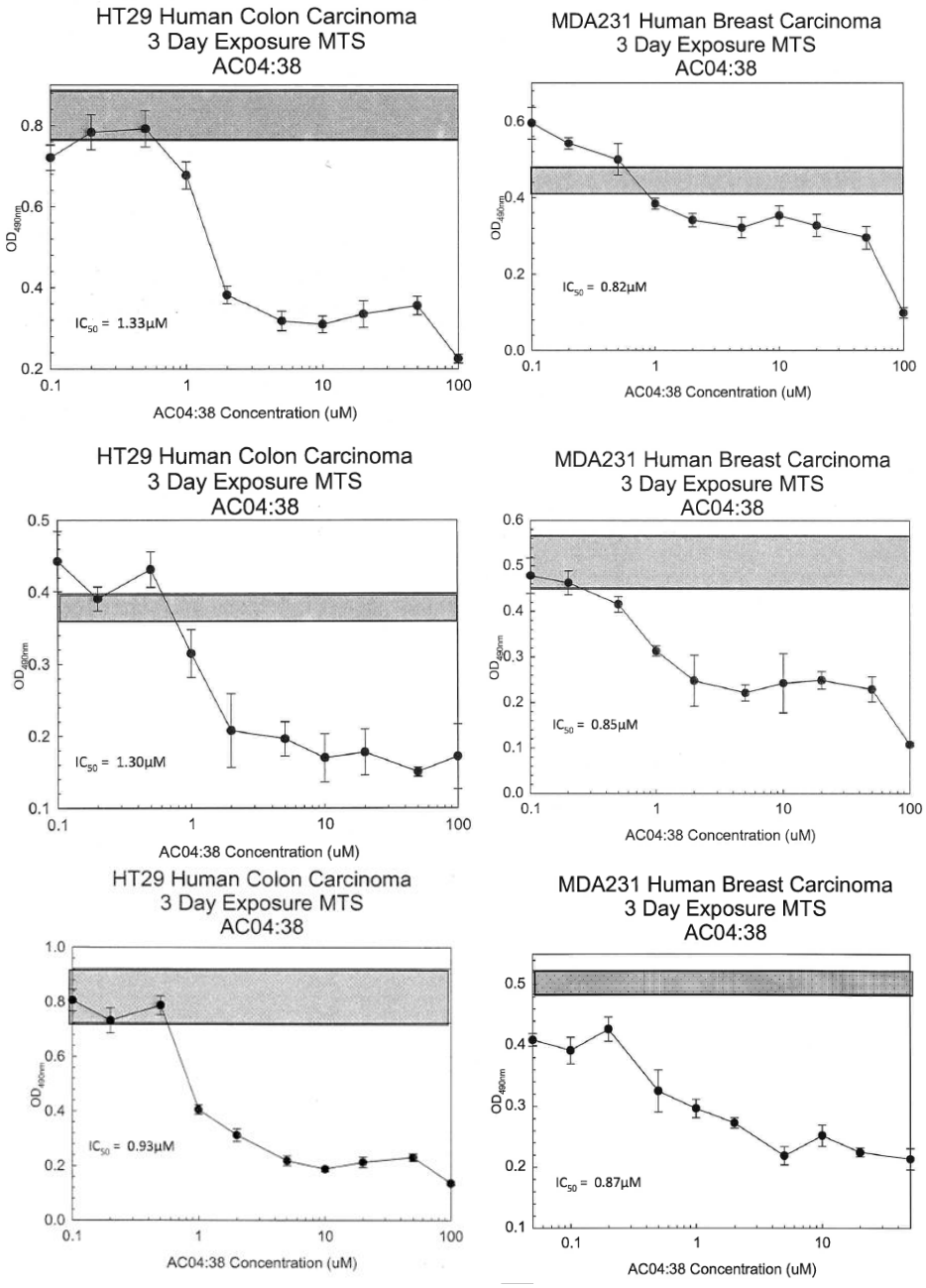

Pyrazoline (81)

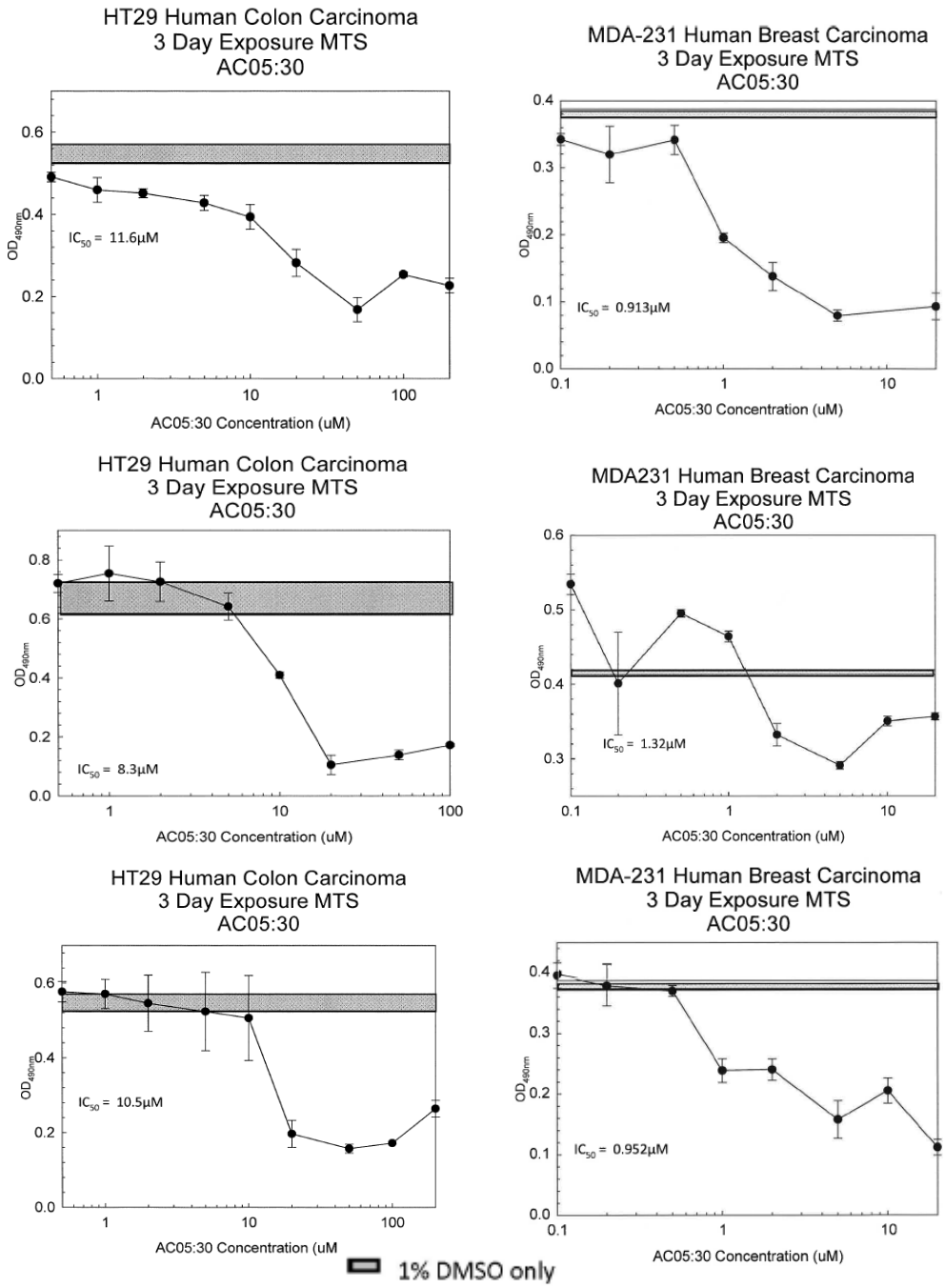

Pyrazoline (85 and 85A)

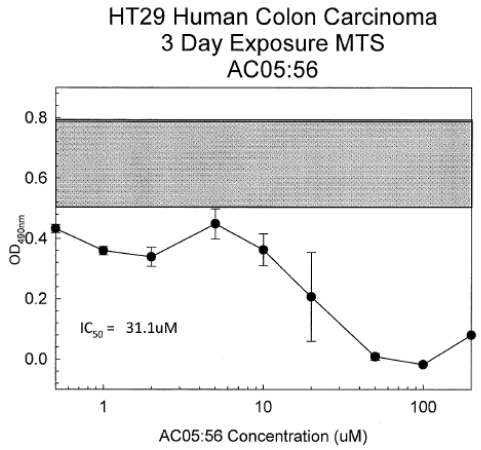

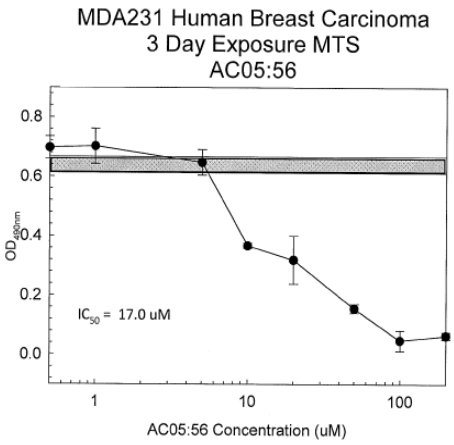

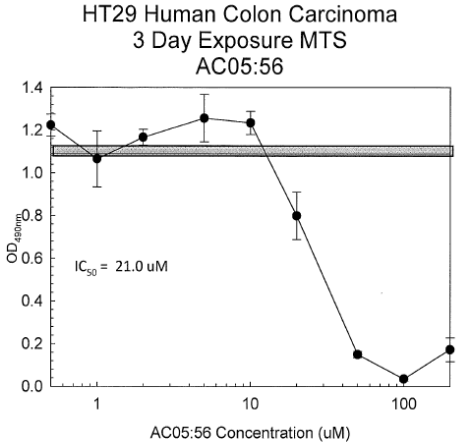

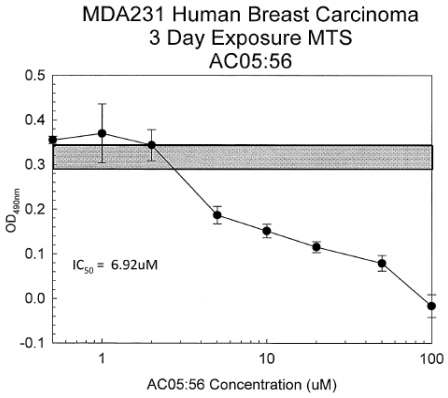

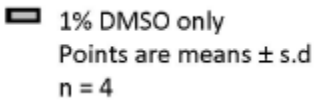

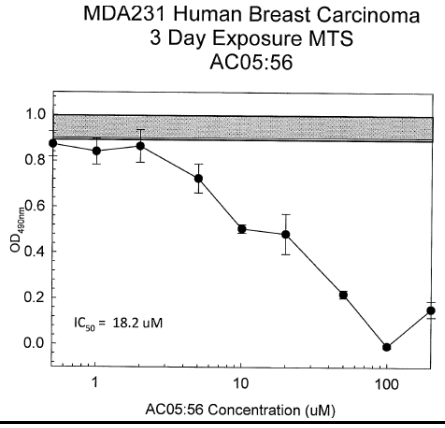

Pyrazoline (86)

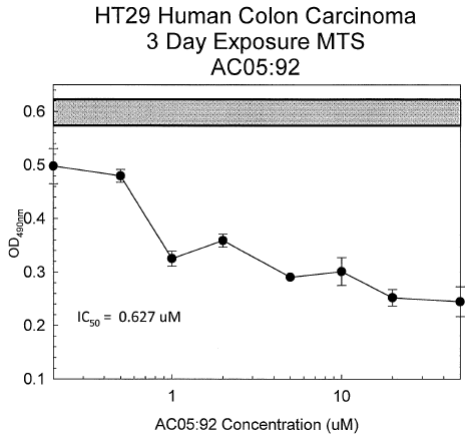

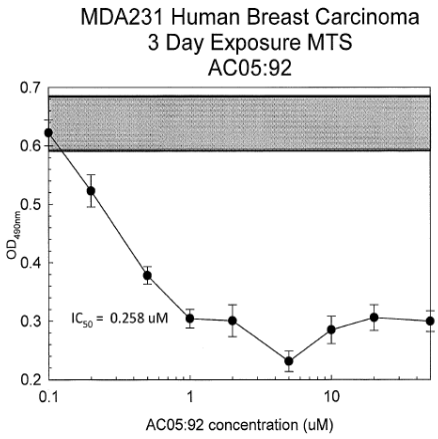

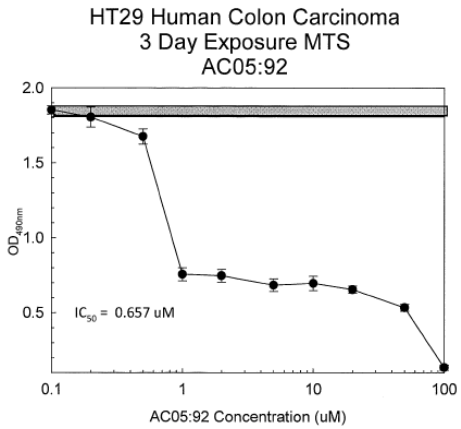

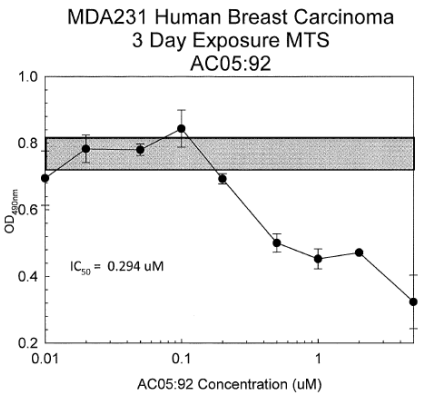

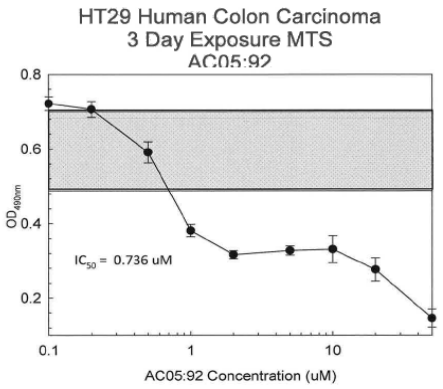

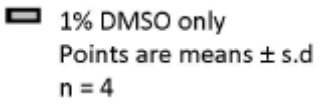

Pyrazoline (87)

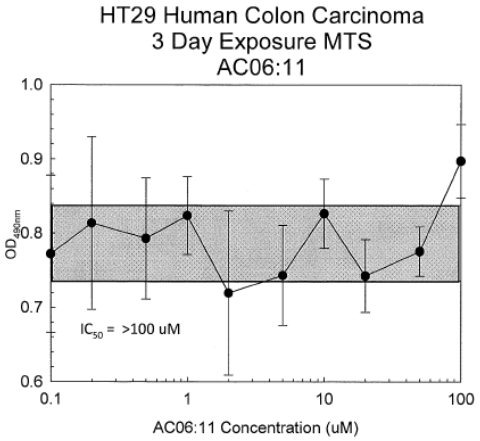

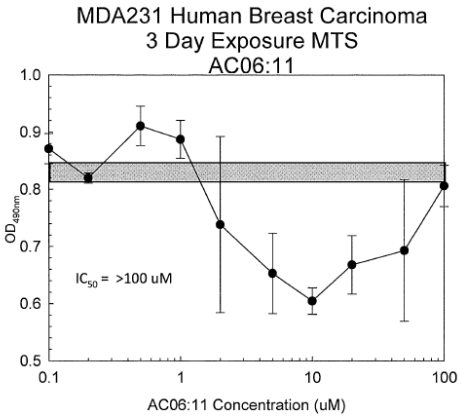

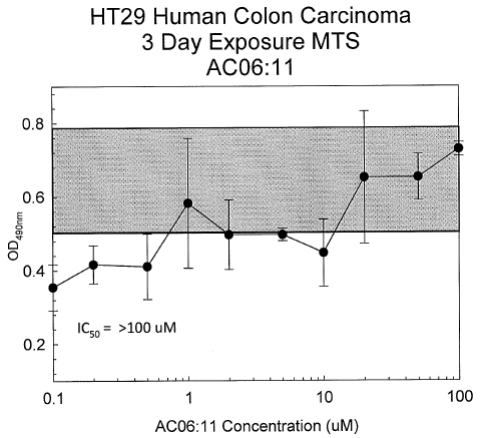

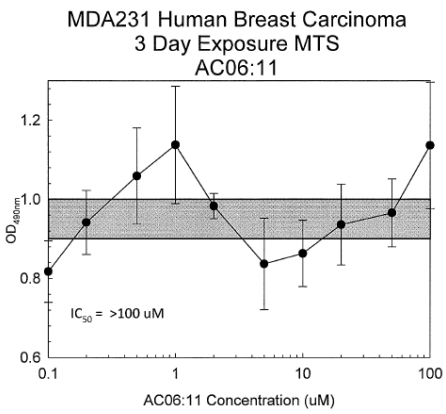

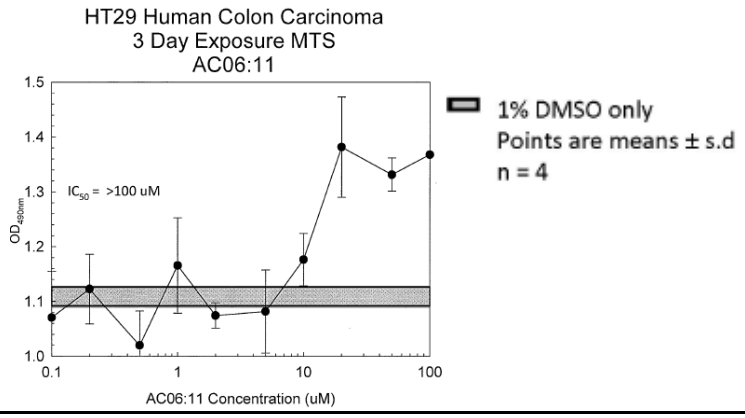

Pyrazoline (97)

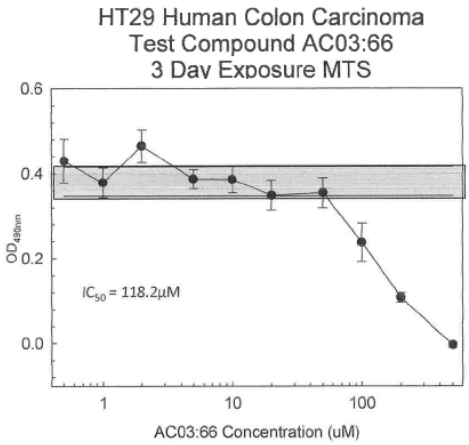

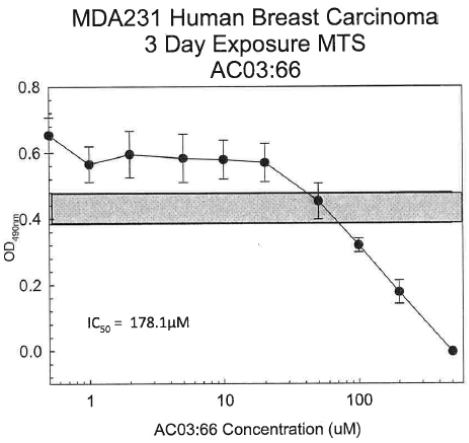

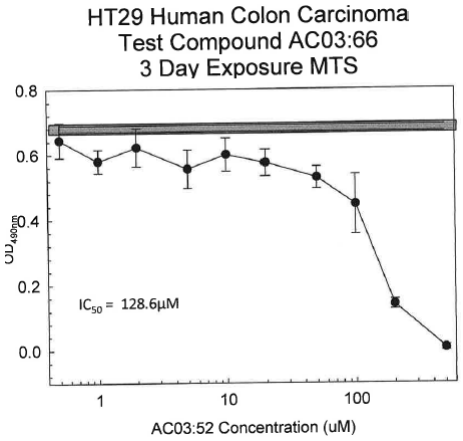

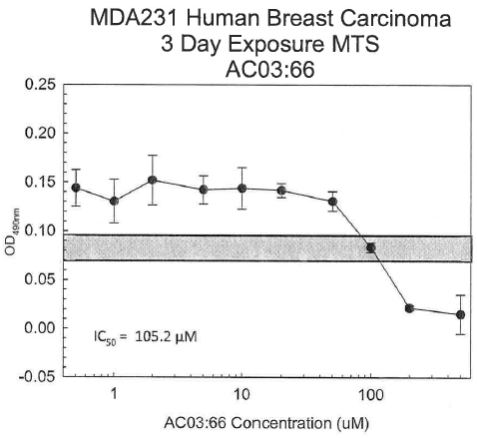

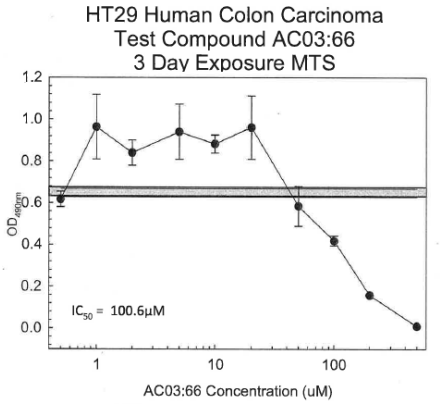

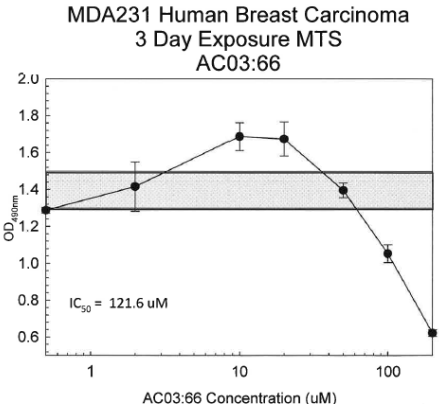

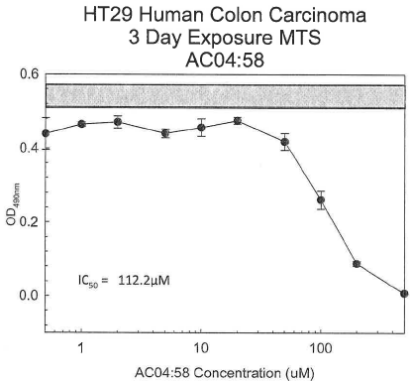

1% DMSO only
Points are means ± s.d
n = 4

Pyrazoline (100)

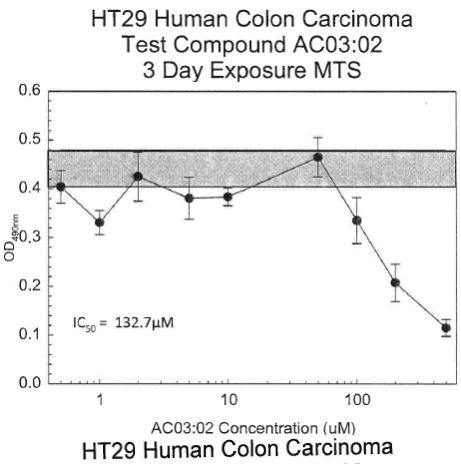

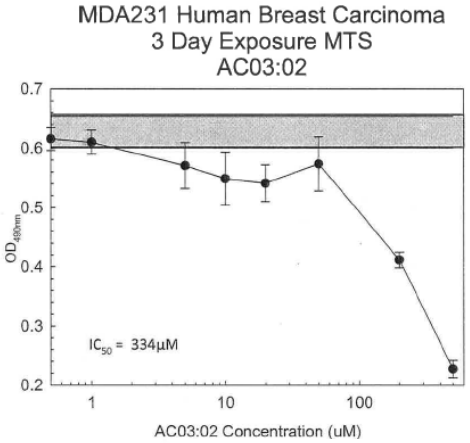

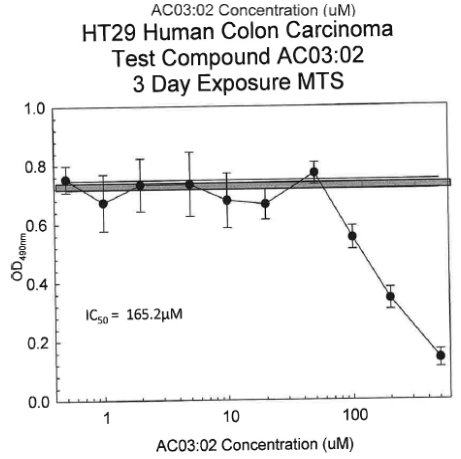

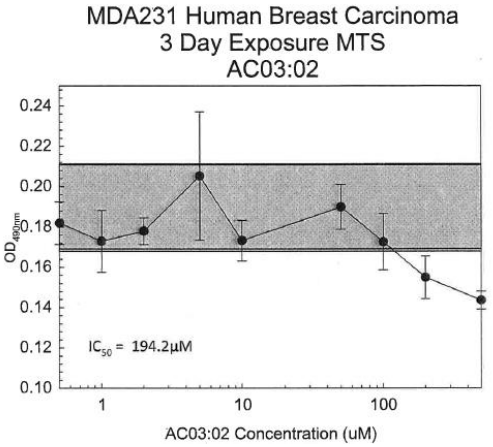

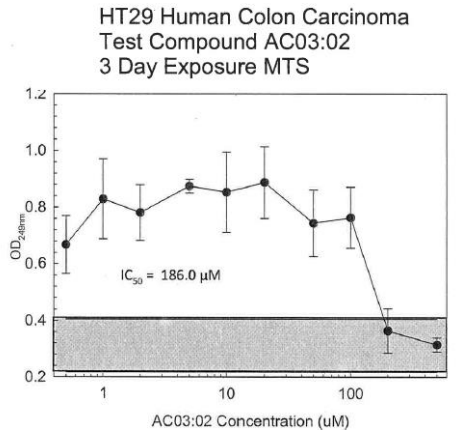

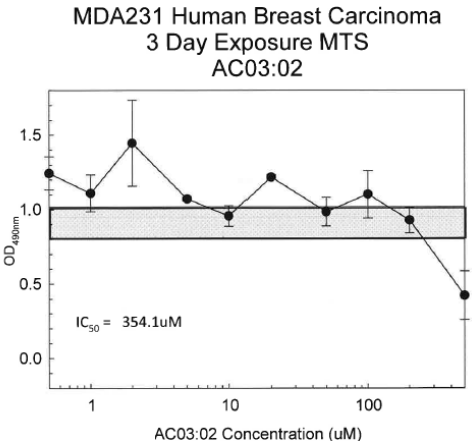

1% DMSO only
Points are means ± s.d
n = 4

Pyrazoline (101)

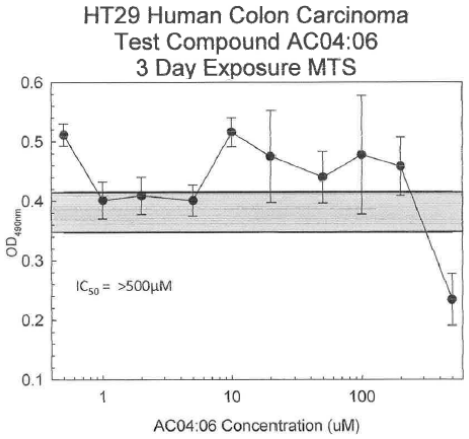

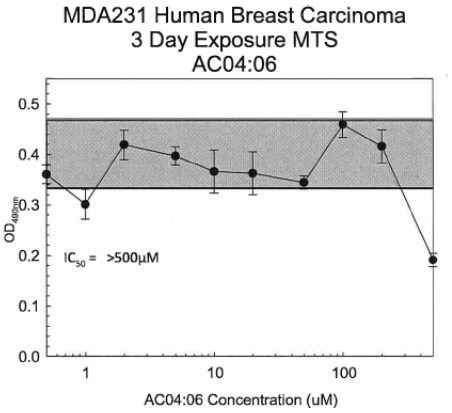

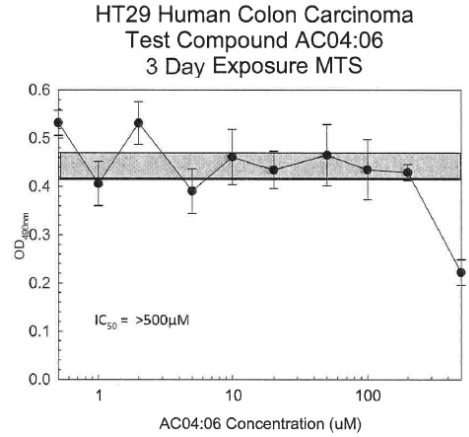

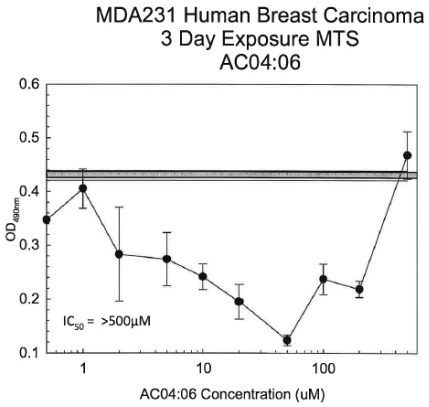

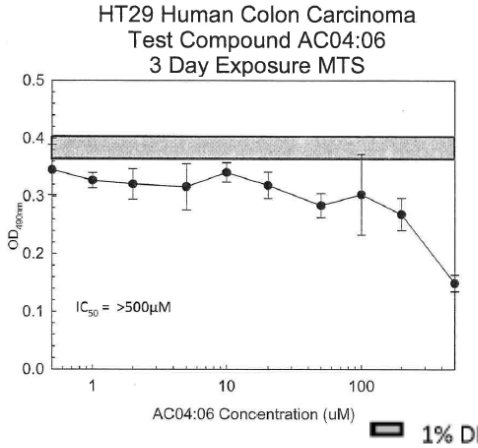

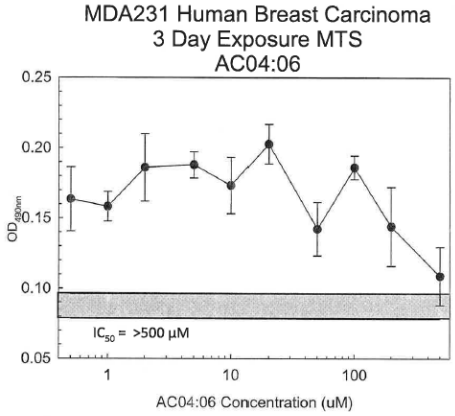

1% DMSO only
Points are means ± s.d
n = 4

Pyrazoline (102)

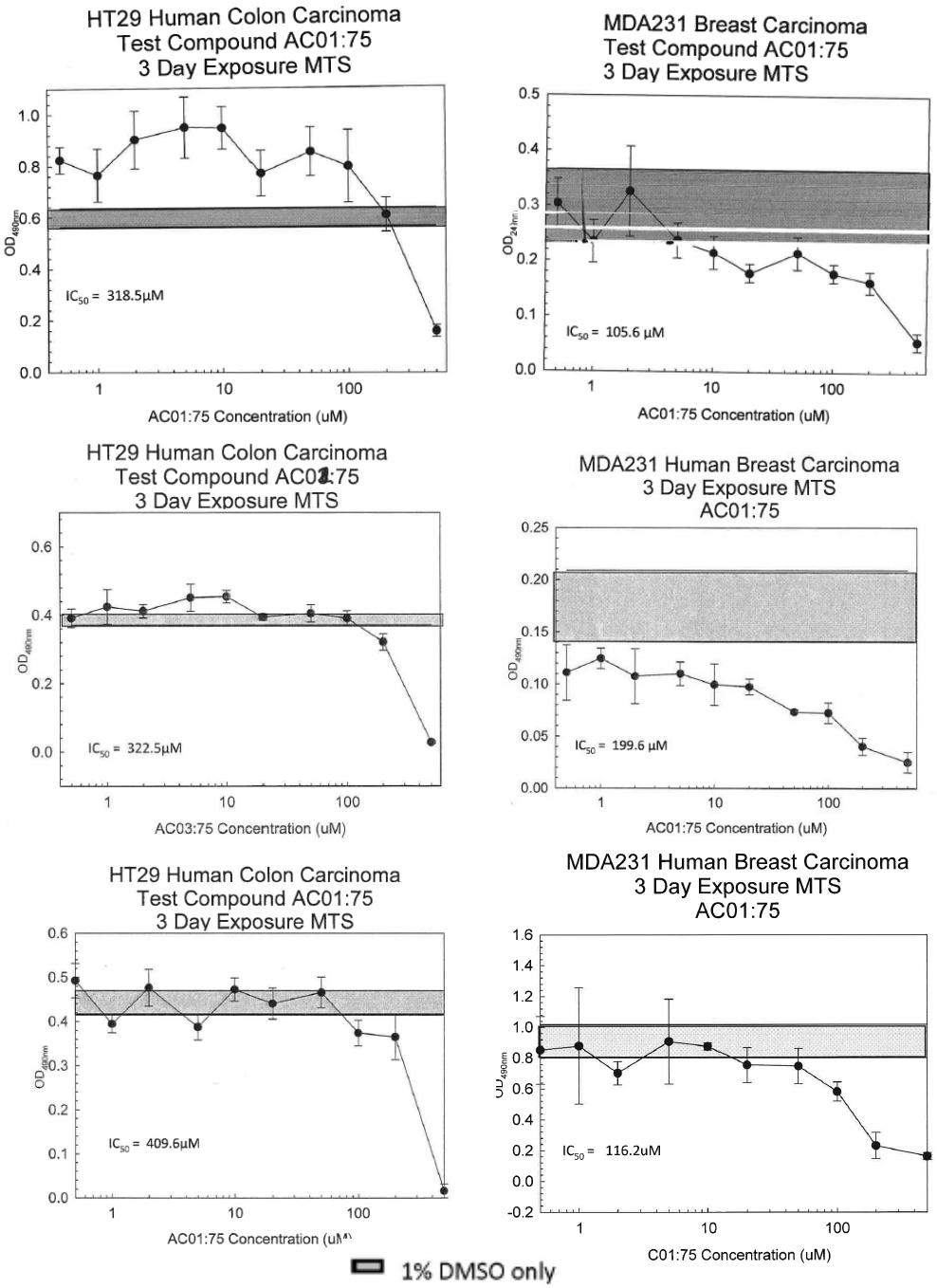

Pyrazoline (103)

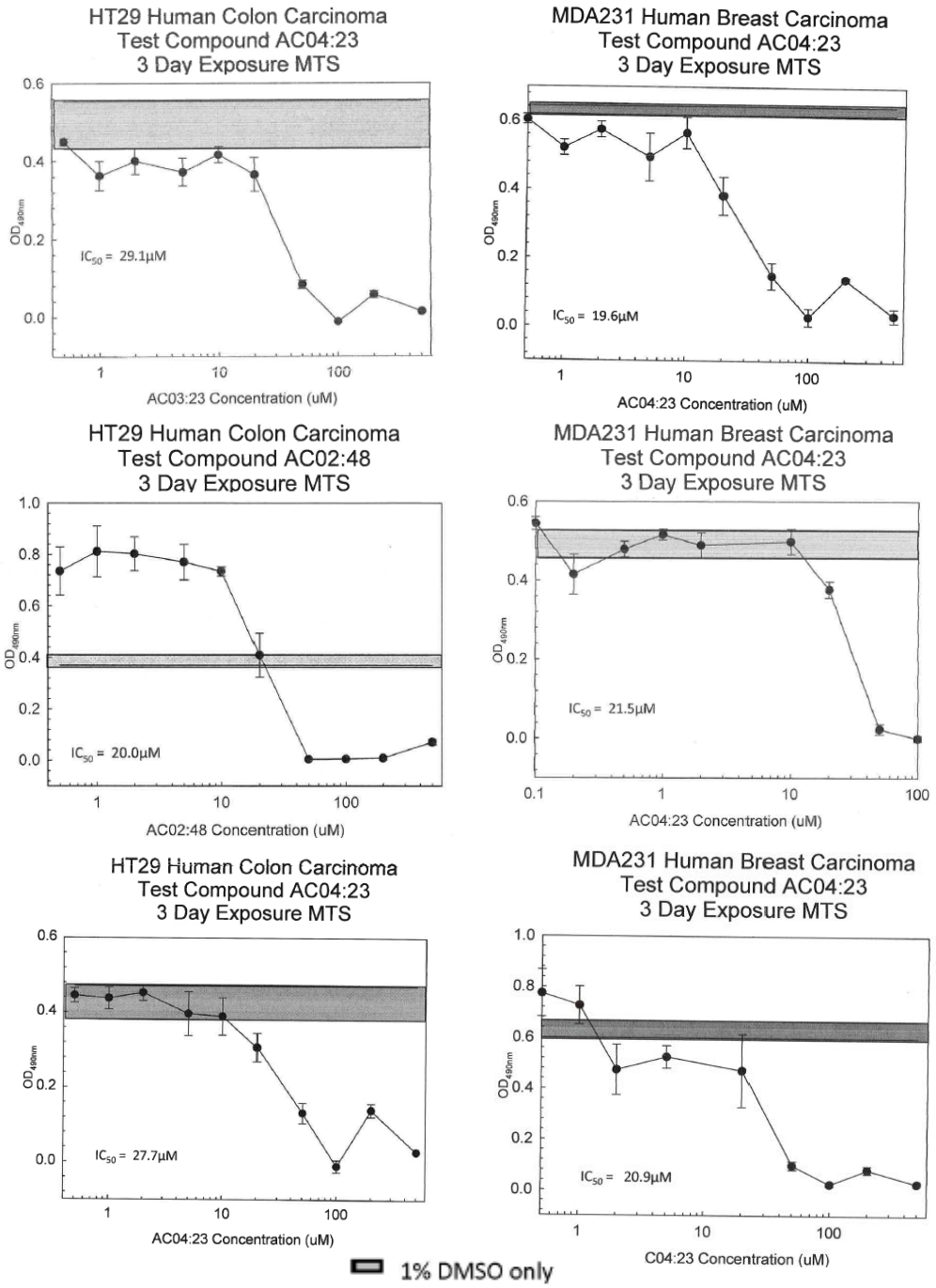

Pyrazoline (104)

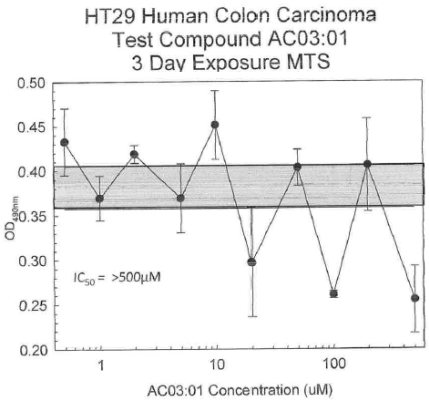

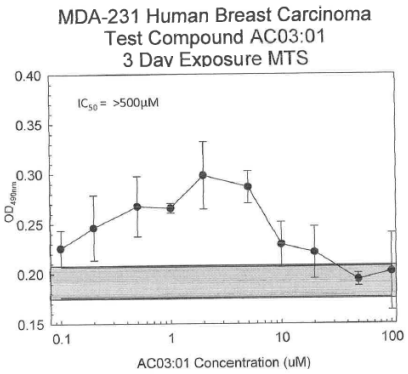

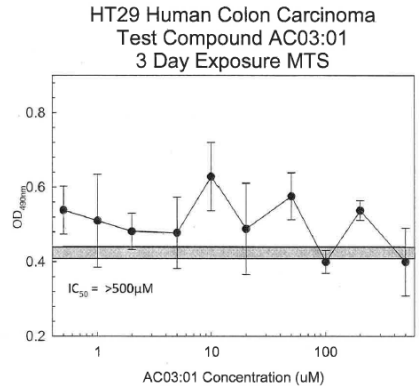

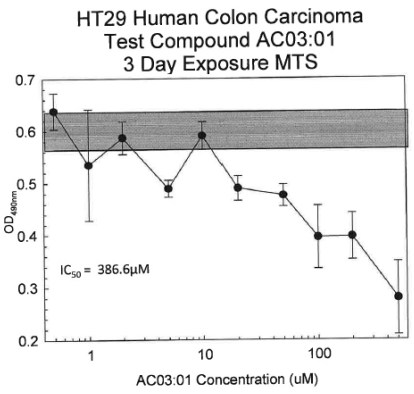

1% DMSO only
Points are means ± s.d
n = 4

Pyrazoline (105)

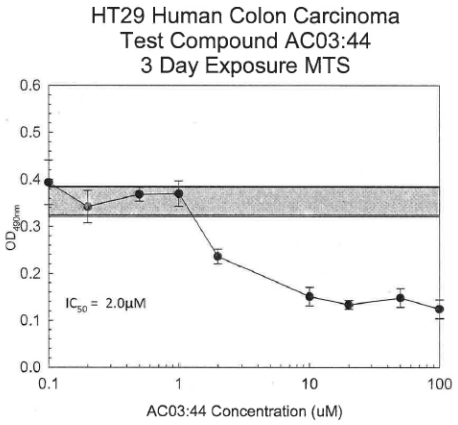

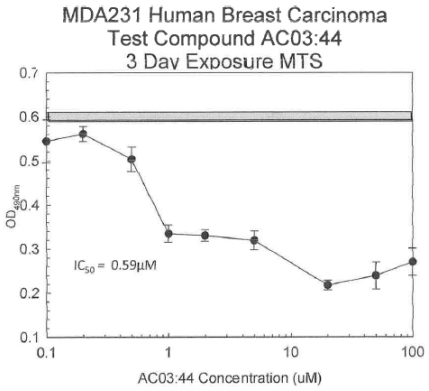

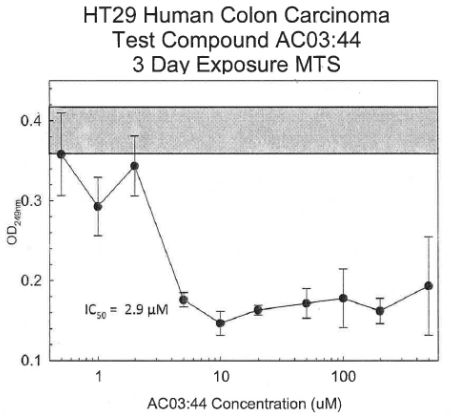

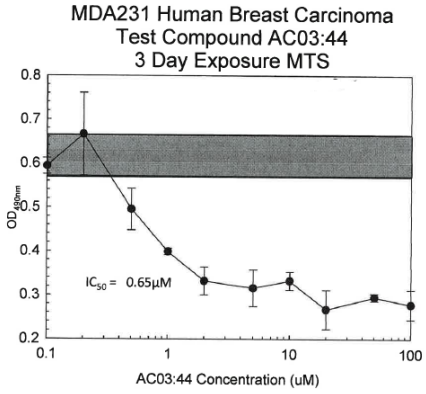

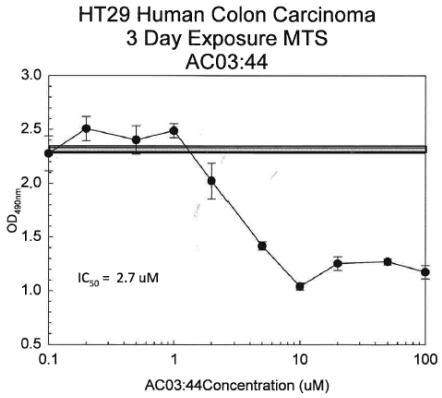

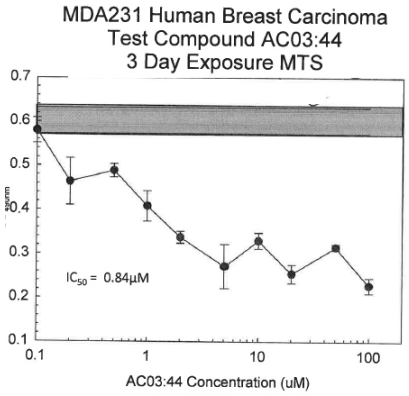

1% DMSO only
Points are means ± s.d
n = 4

Pyrazoline (106)

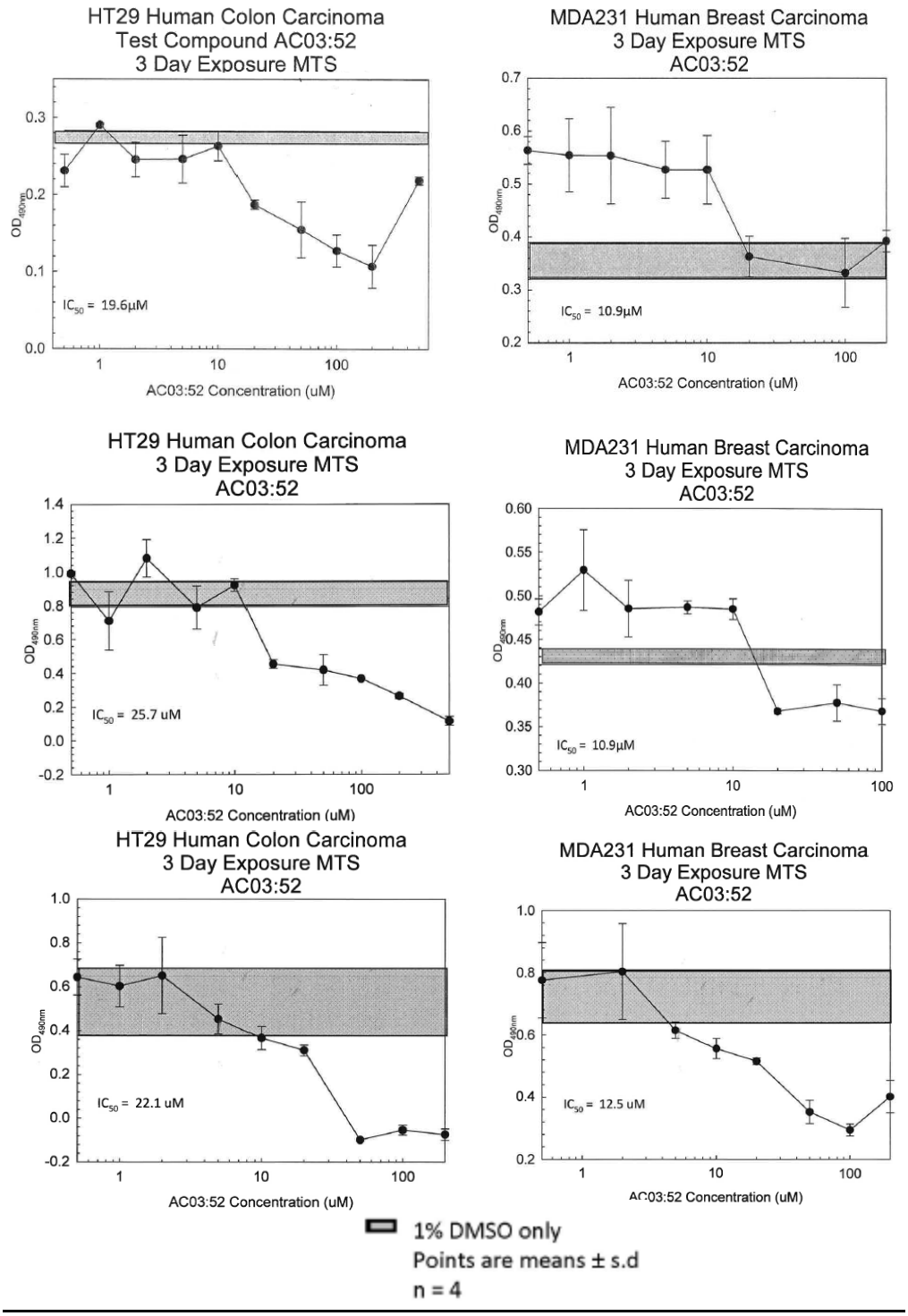

Pyrazoline (107)

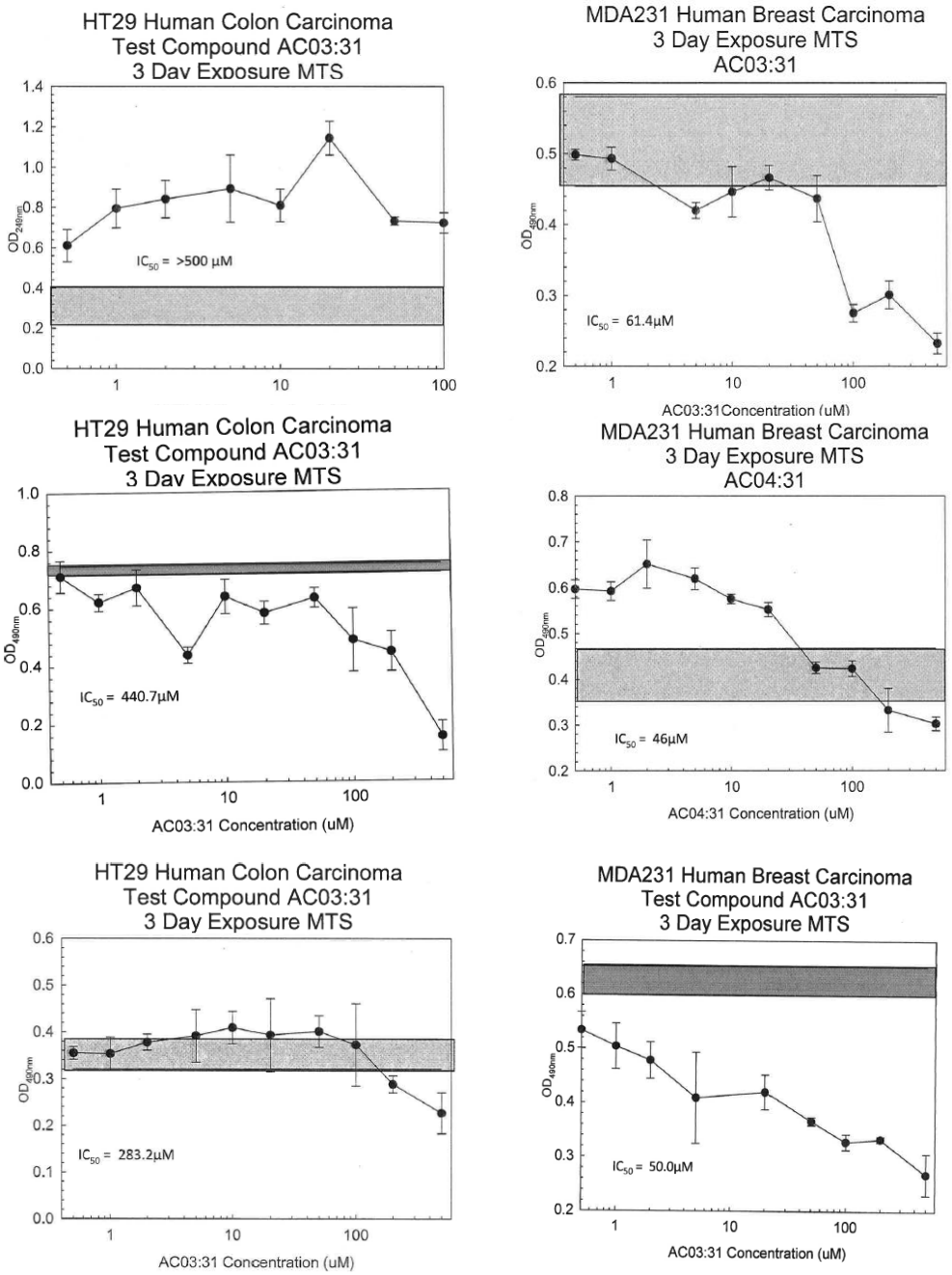

Pyrazoline (108)

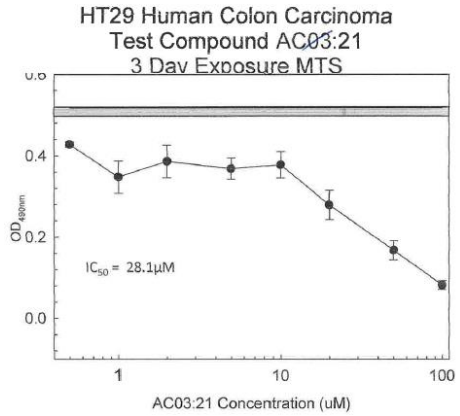

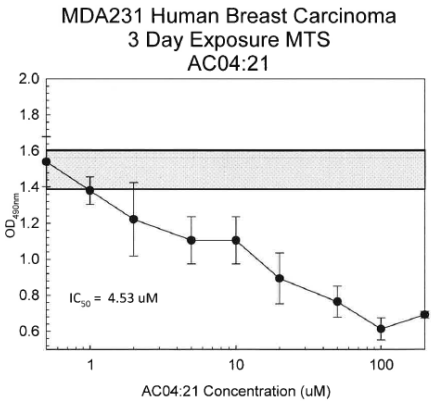

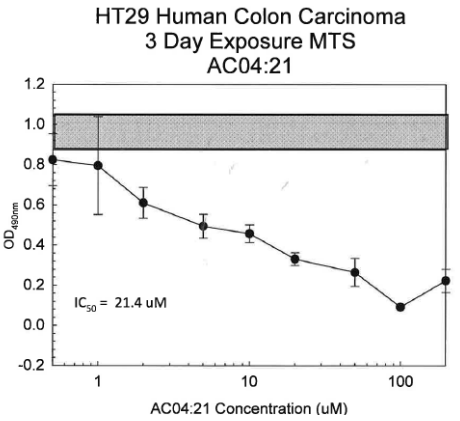

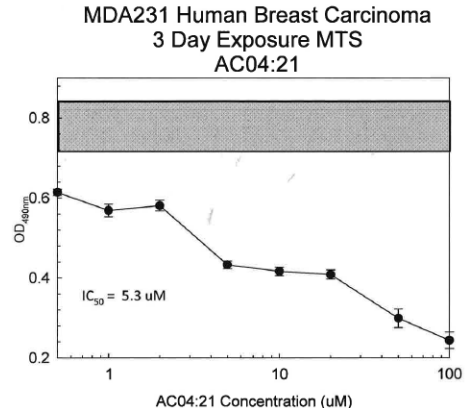

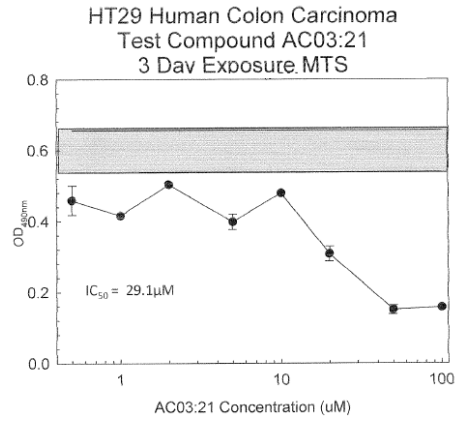

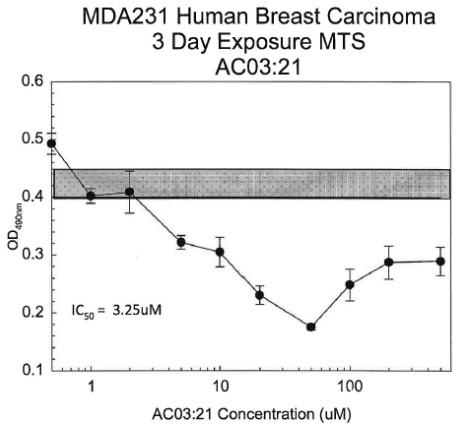

1% DMSO only
Points are means ± s.d
n = 4

Appendix A: NCI Data

Chalcone (45) – Single Dose

Developmental Therapeutics Program
One Dose Mean Graph

NSC: D-761251 / 1	Conc: 1.00E-5 Molar	Test Date: Aug 22, 2011
Experiment ID: 1108OS12		Report Date: Sep 12, 2011

Panel/Cell Line	Growth Percent
Leukemia	
CCRF-CEM	97.85
HL-60(TB)	81.29
K-562	82.20
MOLT-4	92.58
RPMI-8226	83.94
SR	62.24
Non-Small Cell Lung Cancer	
A549/ATCC	95.89
EKVX	102.29
HOP-62	110.23
HOP-92	103.20
NCI-H226	106.05
NCI-H23	101.67
NCI-H322M	108.37
NCI-H460	120.40
NCI-H522	69.41
Colon Cancer	
COLO 205	140.01
HCC-2998	99.83
HCT-116	98.46
HCT-15	93.25
HT29	100.99
KM12	89.04
SW-620	112.71
CNS Cancer	
SF-268	104.64
SF-295	102.17
SF-539	89.69
SNB-19	108.98
SNB-75	63.00
U251	94.52
Melanoma	
LOX IMVI	106.59
MALME-3M	93.58
M14	97.81
MDA-MB-435	85.85
SK-MEL-2	78.26
SK-MEL-28	114.95
SK-MEL-5	102.34
UACC-257	105.35
UACC-62	111.40
Ovarian Cancer	
IGROV1	100.55
OVCAR-3	103.15
OVCAR-4	94.38
OVCAR-5	95.98
OVCAR-8	107.30
NCI/ADR-RES	91.45
SK-OV-3	117.58
Renal Cancer	
786-0	91.03
A498	103.45
ACHN	96.51
CAKI-1	100.27
RXF 393	107.00
SN12C	102.93
TK-10	96.15
UO-31	81.33
Prostate Cancer	
PC-3	105.18
DU-145	107.76
Breast Cancer	
MCF7	89.26
MDA-MB-231/ATCC	112.50
HS 578T	115.93
BT-549	86.77
T-47D	93.08
MDA-MB-468	100.72
Mean	98.52
Delta	36.28
Range	77.77

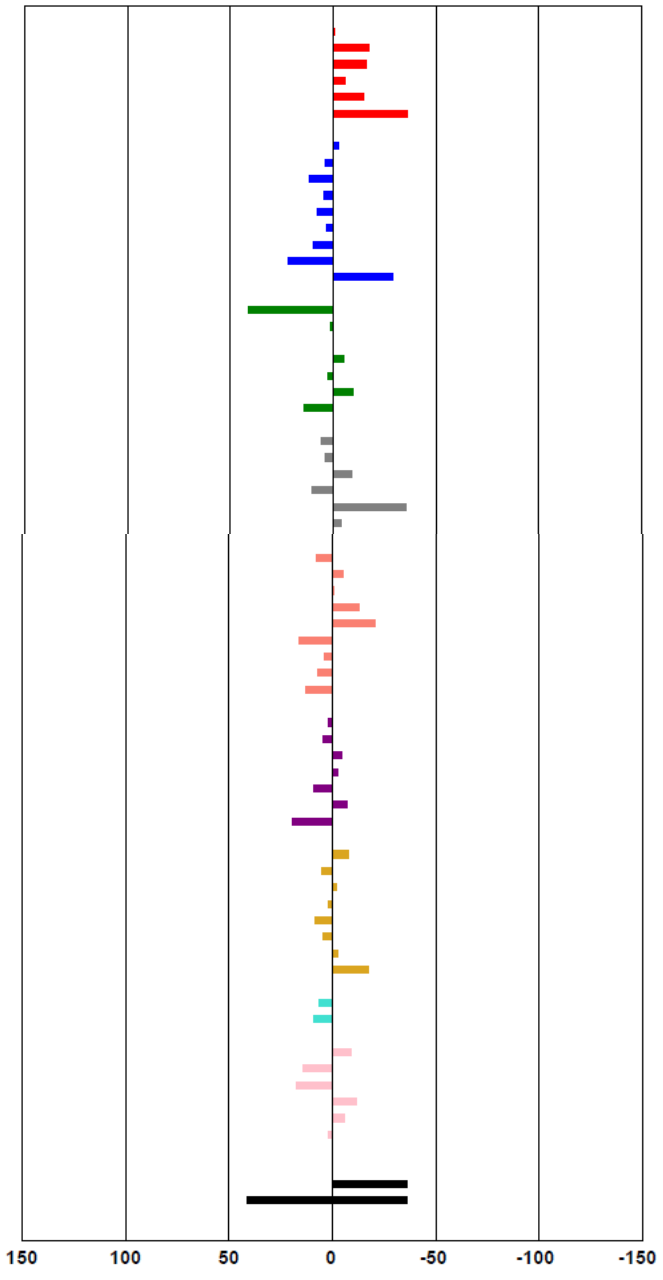

Chalcone (48) – Single Dose

Developmental Therapeutics Program
One Dose Mean Graph

NSC: D-761252 / 1	Conc: 1.00E-5 Molar	Test Date: Aug 22, 2011
Experiment ID: 1108OS12		Report Date: Sep 12, 2011

Panel/Cell Line	Growth Percent
Leukemia	
CCRF-CEM	94.64
HL-60(TB)	81.11
K-562	111.60
MOLT-4	103.22
RPMI-8226	92.28
SR	80.64
Non-Small Cell Lung Cancer	
A549/ATCC	89.80
EKVX	86.09
HOP-62	94.74
HOP-92	77.68
NCI-H226	91.36
NCI-H23	90.80
NCI-H322M	95.86
NCI-H460	113.92
NCI-H522	67.36
Colon Cancer	
COLO 205	106.81
HCC-2998	99.79
HCT-116	93.41
HCT-15	96.24
HT29	94.36
KM12	96.57
SW-620	110.40
CNS Cancer	
SF-268	108.73
SF-295	94.12
SF-539	93.83
SNB-19	89.02
U251	96.71
Melanoma	
LOX IMVI	98.73
MALME-3M	95.56
M14	99.81
MDA-MB-435	89.22
SK-MEL-2	95.53
SK-MEL-28	108.73
SK-MEL-5	104.40
UACC-257	97.57
UACC-62	95.41
Ovarian Cancer	
IGROV1	103.88
OVCAR-3	121.38
OVCAR-5	102.52
OVCAR-8	99.75
NCI/ADR-RES	96.86
SK-OV-3	97.19
Renal Cancer	
786-0	94.67
A498	91.57
ACHN	105.74
CAKI-1	85.81
RXF 393	107.71
SN12C	93.07
TK-10	96.09
UO-31	91.33
Prostate Cancer	
PC-3	94.58
DU-145	113.73
Breast Cancer	
MCF7	90.63
MDA-MB-231/ATCC	90.26
HS 578T	115.31
BT-549	106.00
T-47D	81.45
MDA-MB-468	95.41
Mean	96.74
Delta	29.38
Range	54.02

Mean Growth Percent - Growth Percent

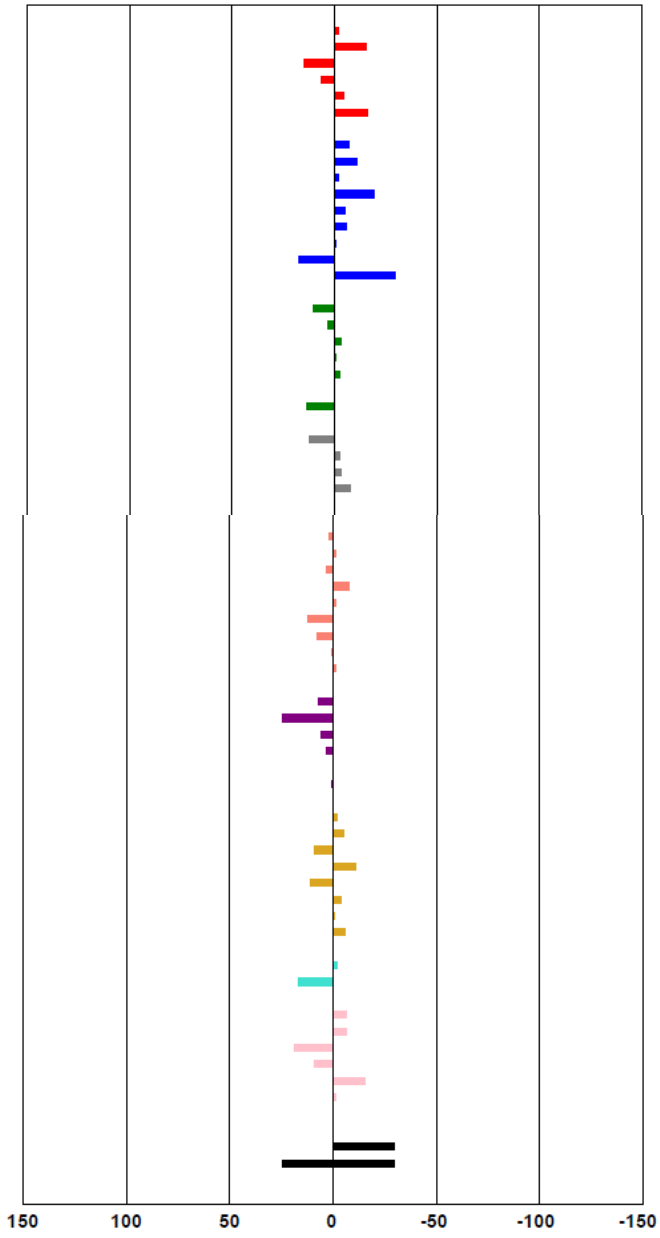

Chalcone (50) – Single Dose

Developmental Therapeutics Program
One Dose Mean Graph

NSC: D-761253 / 1	Conc: 1.00E-5 Molar	Test Date: Aug 22, 2011
Experiment ID: 1108OS12		Report Date: Sep 12, 2011

Panel/Cell Line	Growth Percent
Leukemia	
CCRF-CEM	89.64
HL-60(TB)	74.58
K-562	89.90
MOLT-4	100.43
RPMI-8226	79.25
SR	56.19
Non-Small Cell Lung Cancer	
A549/ATCC	90.98
EKVX	90.22
HOP-62	104.52
HOP-92	84.72
NCI-H226	92.09
NCI-H23	94.96
NCI-H322M	90.50
NCI-H460	112.92
NCI-H522	63.78
Colon Cancer	
COLO 205	115.96
HCC-2998	100.71
HCT-116	81.27
HCT-15	82.27
HT29	97.40
KM12	91.79
SW-620	110.51
CNS Cancer	
SF-268	99.78
SF-295	91.45
SF-539	89.93
SNB-19	92.73
U251	88.42
Melanoma	
LOX IMVI	91.43
MALME-3M	95.62
M14	93.85
MDA-MB-435	83.73
SK-MEL-2	92.11
SK-MEL-28	97.71
SK-MEL-5	106.39
UACC-257	98.24
UACC-62	102.19
Ovarian Cancer	
IGROV1	93.45
OVCAR-3	114.57
OVCAR-5	93.35
OVCAR-8	89.83
NCI/ADR-RES	97.16
SK-OV-3	102.11
Renal Cancer	
786-0	98.58
A498	93.24
ACHN	94.82
CAKI-1	97.11
RXF 393	99.87
SN12C	93.74
TK-10	106.87
UO-31	79.03
Prostate Cancer	
PC-3	96.94
DU-145	103.90
Breast Cancer	
MCF7	68.56
MDA-MB-231/ATCC	92.22
HS 578T	104.84
BT-549	91.72
T-47D	76.21
MDA-MB-468	96.77
Mean	93.16
Delta	36.97
Range	59.77

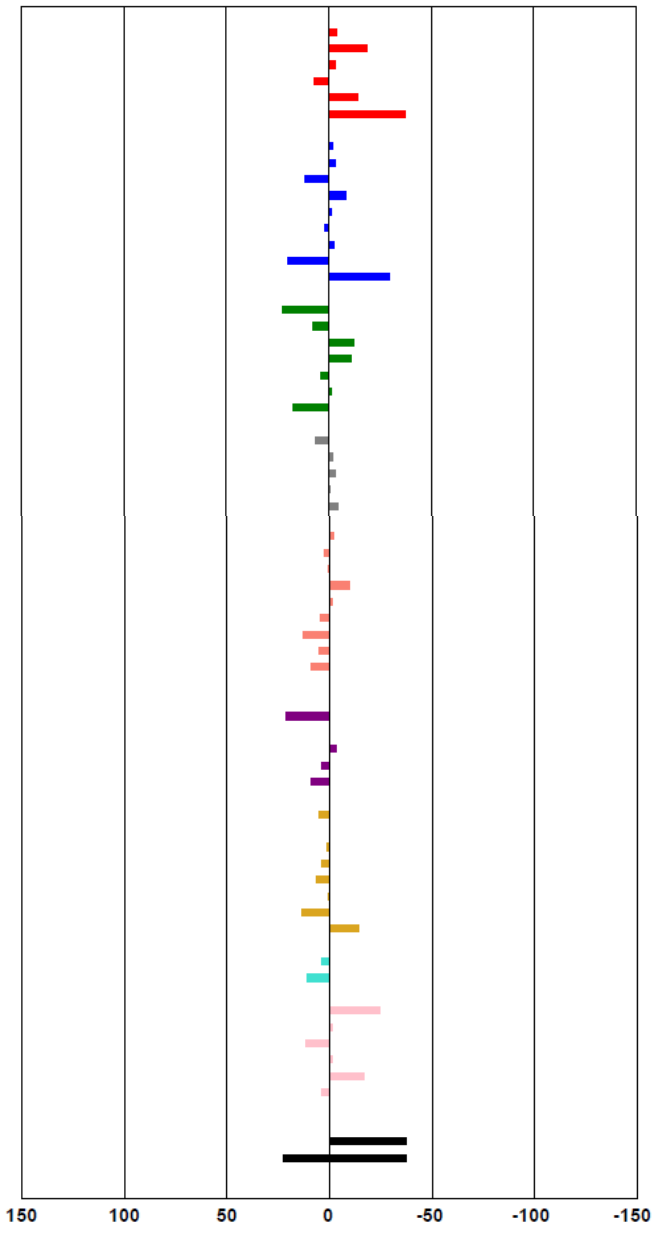

Chalcone (51) – Single Dose

Developmental Therapeutics Program
One Dose Mean Graph

NSC: D-761254 / 1	Conc: 1.00E-5 Molar	Test Date: Aug 22, 2011
Experiment ID: 1108OS12		Report Date: Sep 12, 2011

Panel/Cell Line	Growth Percent
Leukemia	
CCRF-CEM	75.26
HL-60(TB)	49.20
K-562	19.61
MOLT-4	75.01
RPMI-8226	79.27
SR	11.37
Non-Small Cell Lung Cancer	
A549/ATCC	54.69
EKVX	86.78
HOP-62	72.97
HOP-92	73.46
NCI-H226	82.65
NCI-H23	77.31
NCI-H322M	91.15
NCI-H460	54.24
NCI-H522	48.18
Colon Cancer	
COLO 205	50.92
HCT-116	43.07
HCT-15	36.95
HT29	12.86
KM12	28.62
SW-620	32.64
CNS Cancer	
SF-268	90.19
SF-295	64.84
SF-539	69.75
SNB-19	64.84
U251	72.68
Melanoma	
LOX IMVI	67.47
MALME-3M	67.59
M14	58.00
MDA-MB-435	-29.12
SK-MEL-2	83.76
SK-MEL-28	80.63
SK-MEL-5	57.41
UACC-257	77.22
UACC-62	59.72
Ovarian Cancer	
IGROV1	68.78
OVCAR-3	47.51
OVCAR-5	81.41
OVCAR-8	84.25
NCI/ADR-RES	39.50
SK-OV-3	79.79
Renal Cancer	
786-0	81.42
A498	91.58
ACHN	89.61
CAKI-1	56.72
RXF 393	78.59
SN12C	83.26
TK-10	78.12
UO-31	80.78
Prostate Cancer	
PC-3	71.38
DU-145	97.88
Breast Cancer	
MCF7	41.06
MDA-MB-231/ATCC	58.03
HS 578T	93.89
BT-549	73.03
T-47D	47.83
MDA-MB-468	36.40
Mean	63.19
Delta	92.31
Range	127.00

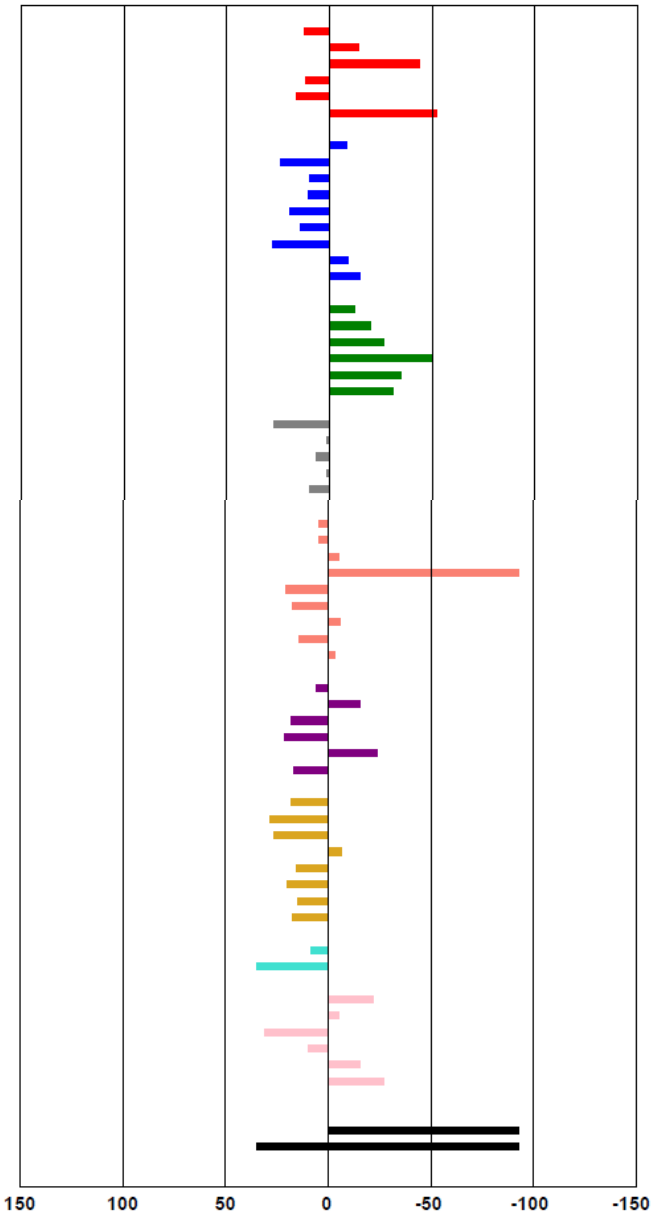

Chalcone (52) – Single Dose

Developmental Therapeutics Program
One Dose Mean Graph

NSC: D-761255 / 1	Conc: 1.00E-5 Molar	Test Date: Aug 22, 2011
Experiment ID: 1108OS12		Report Date: Sep 12, 2011

Panel/Cell Line	Growth Percent
Leukemia	
CCRF-CEM	58.52
HL-60(TB)	51.23
K-562	48.31
MOLT-4	75.79
RPMI-8226	50.47
SR	11.71
Non-Small Cell Lung Cancer	
A549/ATCC	85.06
EKVX	76.60
HOP-62	106.91
HOP-92	62.77
NCI-H226	79.17
NCI-H23	72.95
NCI-H322M	93.04
NCI-H460	72.94
NCI-H522	29.01
Colon Cancer	
COLO 205	95.56
HCT-116	52.00
HCT-15	58.22
HT29	68.54
KM12	73.98
SW-620	82.67
CNS Cancer	
SF-268	96.42
SF-295	94.70
SF-539	80.49
SNB-19	66.43
SNB-75	58.24
U251	74.18
Melanoma	
LOX IMVI	64.18
MALME-3M	82.15
M14	80.85
MDA-MB-435	66.19
SK-MEL-2	62.18
SK-MEL-28	75.45
SK-MEL-5	73.21
UACC-257	83.01
UACC-62	94.58
Ovarian Cancer	
IGROV1	75.63
OVCAR-3	68.83
OVCAR-5	96.14
OVCAR-8	83.21
NCI/ADR-RES	93.57
SK-OV-3	99.66
Renal Cancer	
786-0	82.47
A498	79.84
ACHN	81.40
CAKI-1	52.93
RXF 393	38.30
SN12C	76.65
TK-10	70.80
UO-31	-32.26
Prostate Cancer	
PC-3	99.68
DU-145	37.19
Breast Cancer	
MCF7	30.76
MDA-MB-231/ATCC	76.92
HS 578T	102.64
BT-549	83.16
T-47D	45.59
MDA-MB-468	30.84
Mean	69.51
Delta	101.77
Range	139.17

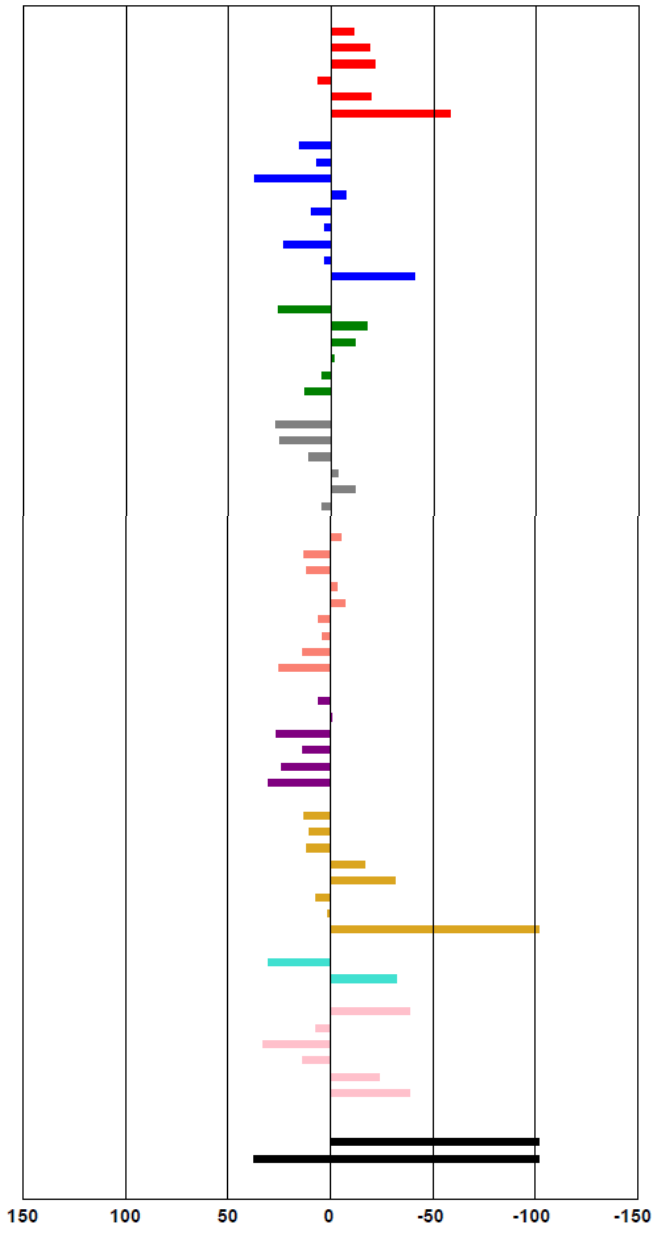

Chalcone (53) – Single Dose

Developmental Therapeutics Program
One Dose Mean Graph

NSC: D-761256 / 1	Conc: 1.00E-5 Molar	Test Date: Aug 22, 2011
Experiment ID: 1108OS12		Report Date: Sep 12, 2011

Panel/Cell Line	Growth Percent
Leukemia	
CCRF-CEM	62.32
HL-60(TB)	48.00
K-562	60.70
MOLT-4	86.49
RPMI-8226	47.49
SR	17.72
Non-Small Cell Lung Cancer	
A549/ATCC	85.08
EKVX	77.88
HOP-62	110.90
HOP-92	51.68
NCI-H226	88.45
NCI-H23	85.30
NCI-H322M	87.77
NCI-H460	63.09
NCI-H522	33.57
Colon Cancer	
COLO 205	96.62
HCC-2998	77.24
HCT-116	53.02
HCT-15	63.16
HT29	82.43
KM12	75.61
SW-620	89.62
CNS Cancer	
SF-268	94.68
SF-295	86.44
SF-539	66.36
SNB-19	78.10
SNB-75	58.13
U251	74.25
Melanoma	
LOX IMVI	63.00
MALME-3M	80.30
M14	90.04
MDA-MB-435	70.27
SK-MEL-2	80.40
SK-MEL-28	92.54
SK-MEL-5	87.51
UACC-257	84.85
UACC-62	91.56
Ovarian Cancer	
IGROV1	76.46
OVCAR-3	81.33
OVCAR-4	52.75
OVCAR-5	83.06
OVCAR-8	78.19
NCI/ADR-RES	79.78
SK-OV-3	96.35
Renal Cancer	
786-0	86.17
A498	89.21
ACHN	84.92
CAKI-1	55.65
RXF 393	46.03
SN12C	73.94
TK-10	87.24
UO-31	77.53
Prostate Cancer	
PC-3	97.56
DU-145	34.49
Breast Cancer	
MCF7	36.13
MDA-MB-231/ATCC	70.50
HS 578T	94.68
BT-549	90.05
T-47D	54.97
MDA-MB-468	45.78
Mean	73.59
Delta	55.87
Range	93.18

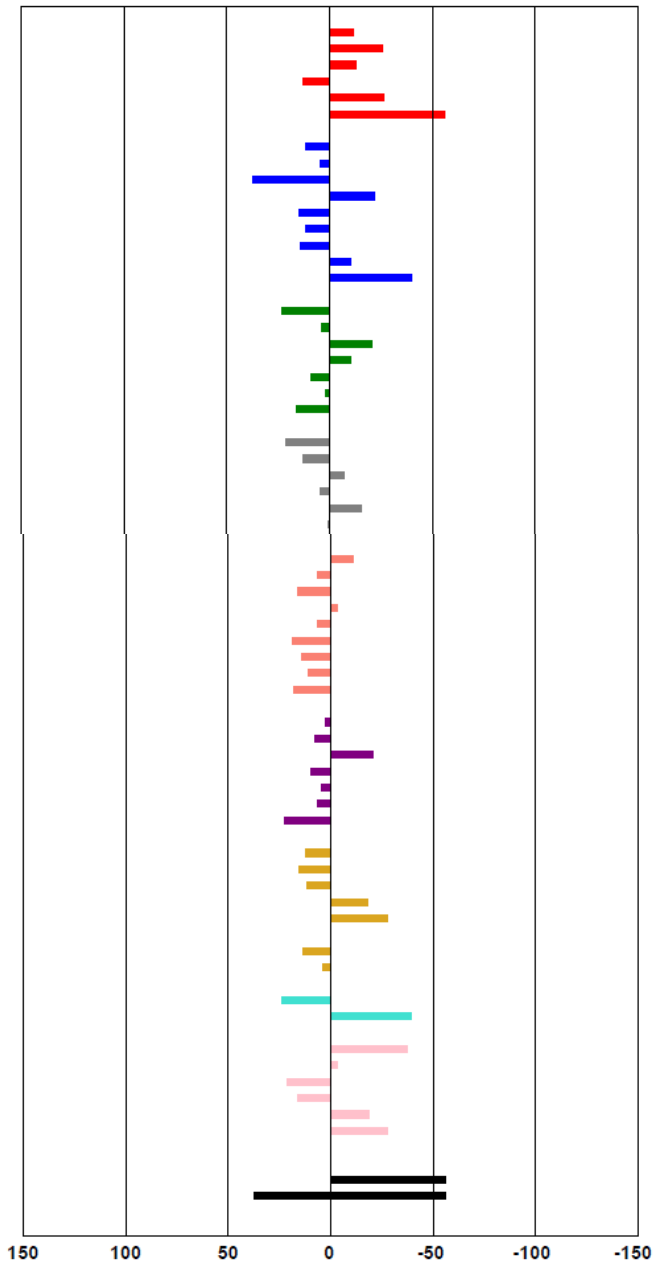

Pyrazoline (71) – Single Dose

Developmental Therapeutics Program
One Dose Mean Graph

NSC: D-761261 / 1	Conc: 1.00E-5 Molar	Test Date: Aug 22, 2011
Experiment ID: 1108OS12		Report Date: Sep 12, 2011

Panel/Cell Line	Growth Percent
Leukemia	
CCRF-CEM	14.73
HL-60(TB)	-26.37
K-562	10.64
MOLT-4	13.50
RPMI-8226	26.90
SR	4.53
Non-Small Cell Lung Cancer	
A549/ATCC	22.15
EKVX	62.73
HOP-62	31.29
HOP-92	30.42
NCI-H226	-11.98
NCI-H23	27.68
NCI-H322M	44.83
NCI-H460	7.14
NCI-H522	-35.66
Colon Cancer	
COLO 205	-44.60
HCC-2998	9.19
HCT-116	9.57
HCT-15	14.03
HT29	0.21
KM12	14.07
SW-620	25.75
CNS Cancer	
SF-268	45.39
SF-295	9.25
SF-539	0.95
SNB-19	15.26
U251	27.09
Melanoma	
LOX IMVI	29.79
MALME-3M	50.13
M14	8.75
MDA-MB-435	-21.30
SK-MEL-2	7.08
SK-MEL-28	48.32
SK-MEL-5	-15.43
UACC-257	67.65
UACC-62	48.03
Ovarian Cancer	
IGROV1	22.07
OVCAR-3	-43.94
OVCAR-5	40.98
OVCAR-8	15.06
NCI/ADR-RES	-6.44
SK-OV-3	-7.31
Renal Cancer	
786-0	34.39
A498	37.32
ACHN	37.03
CAKI-1	52.92
RXF 393	-13.59
SN12C	35.14
TK-10	53.62
UO-31	53.79
Prostate Cancer	
PC-3	20.07
DU-145	13.11
Breast Cancer	
MCF7	10.55
MDA-MB-231/ATCC	45.65
HS 578T	34.57
BT-549	16.40
T-47D	73.86
MDA-MB-468	-18.94
Mean	18.59
Delta	63.19
Range	118.46

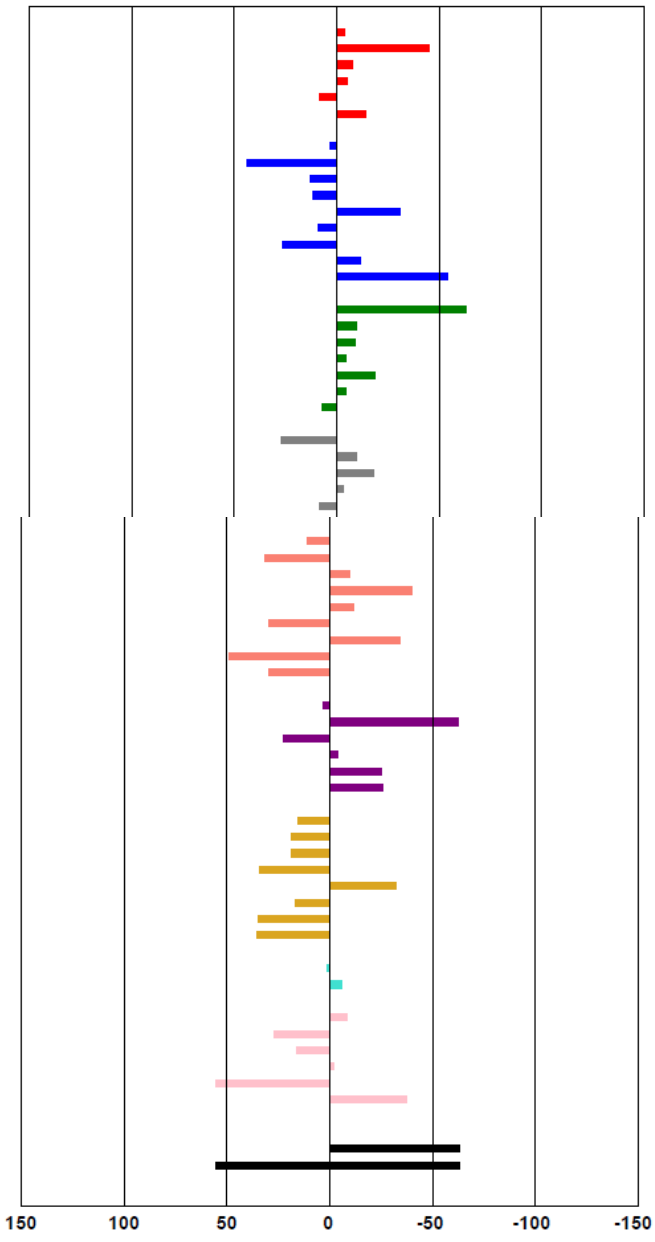

Pyrazoline (71–) – Single Dose

Developmental Therapeutics Program
One Dose Mean Graph

NSC: D-761467 / 1	Conc: 1.00E-5 Molar	Test Date: Sep 12, 2011
Experiment ID: 1109OS23		Report Date: Sep 30, 2011

Panel/Cell Line	Growth Percent
Leukemia	
CCRF-CEM	11.01
HL-60(TB)	-26.17
MOLT-4	9.87
RPMI-8226	17.73
SR	9.06
Non-Small Cell Lung Cancer	
A549/ATCC	15.62
EKVX	40.33
HOP-62	25.71
HOP-92	45.40
NCI-H226	-24.68
NCI-H23	20.44
NCI-H322M	44.67
NCI-H460	7.51
NCI-H522	-33.69
Colon Cancer	
COLO 205	-71.39
HCC-2998	8.10
HCT-116	3.51
HCT-15	19.47
HT29	0.21
KM12	5.75
SW-620	29.50
CNS Cancer	
SF-268	45.62
SF-539	7.27
SNB-19	35.89
SNB-75	14.66
U251	3.48
Melanoma	
LOX IMVI	24.47
MALME-3M	46.75
M14	-9.74
MDA-MB-435	-23.93
SK-MEL-2	-1.81
SK-MEL-28	51.10
SK-MEL-5	-2.29
UACC-257	41.30
UACC-62	38.94
Ovarian Cancer	
IGROV1	29.88
OVCAR-3	-4.84
OVCAR-4	39.72
OVCAR-5	33.14
OVCAR-8	2.78
NCI/ADR-RES	-1.88
SK-OV-3	-7.88
Renal Cancer	
786-0	34.13
A498	50.54
ACHN	34.14
CAKI-1	20.23
RXF 393	6.37
SN12C	30.86
TK-10	57.86
UO-31	34.88
Prostate Cancer	
PC-3	25.79
DU-145	14.55
Breast Cancer	
MCF7	14.14
MDA-MB-231/ATCC	45.71
HS 578T	68.22
BT-549	5.55
T-47D	73.95
MDA-MB-468	6.68
Mean	18.00
Delta	89.39
Range	145.34

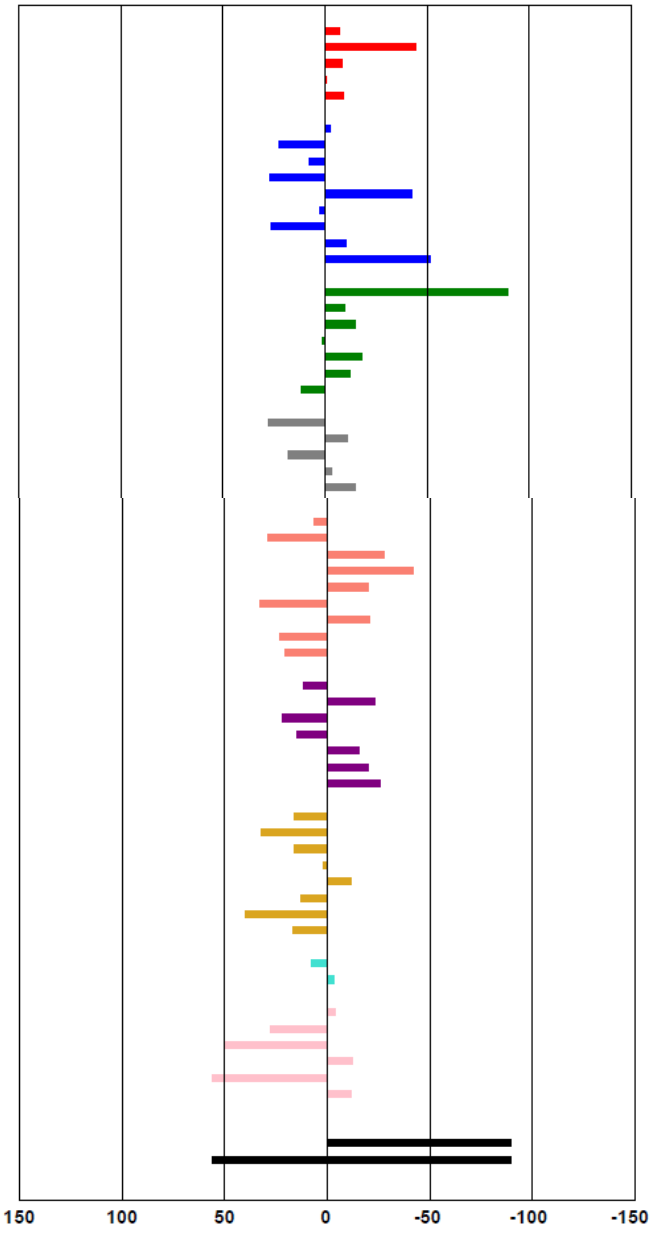

Pyrazoline (71+) – Single Dose

Developmental Therapeutics Program
One Dose Mean Graph

NSC: D-761464 / 1	Conc: 1.00E-5 Molar	Test Date: Sep 12, 2011
Experiment ID: 1109OS23		Report Date: Sep 30, 2011

Panel/Cell Line	Growth Percent
Leukemia	
CCRF-CEM	25.77
HL-60(TB)	-13.20
MOLT-4	36.37
RPMI-8226	33.90
SR	16.39
Non-Small Cell Lung Cancer	
A549/ATCC	35.16
EKVX	53.76
HOP-62	20.98
HOP-92	57.29
NCI-H226	28.76
NCI-H23	41.84
NCI-H322M	35.85
NCI-H460	17.56
NCI-H522	-24.34
Colon Cancer	
COLO 205	0.57
HCC-2998	54.80
HCT-116	28.40
HCT-15	40.55
HT29	6.74
KM12	36.83
SW-620	29.35
CNS Cancer	
SF-268	41.01
SF-539	14.92
SNB-19	51.91
SNB-75	0.54
U251	30.53
Melanoma	
LOX IMVI	39.98
MALME-3M	39.22
M14	28.91
MDA-MB-435	-32.71
SK-MEL-2	-3.01
SK-MEL-28	48.94
SK-MEL-5	15.60
UACC-257	33.39
UACC-62	41.88
Ovarian Cancer	
IGROV1	55.30
OVCAR-3	23.78
OVCAR-4	54.44
OVCAR-5	59.77
OVCAR-8	41.31
NCI/ADR-RES	10.49
SK-OV-3	17.58
Renal Cancer	
786-0	28.95
A498	62.29
ACHN	52.90
CAKI-1	16.65
RXF 393	3.40
SN12C	44.96
TK-10	54.64
UO-31	39.72
Prostate Cancer	
PC-3	27.59
DU-145	32.12
Breast Cancer	
MCF7	18.36
MDA-MB-231/ATCC	61.13
HS 578T	61.42
BT-549	49.04
T-47D	27.15
MDA-MB-468	4.42
Mean	30.38
Delta	63.09
Range	95.00

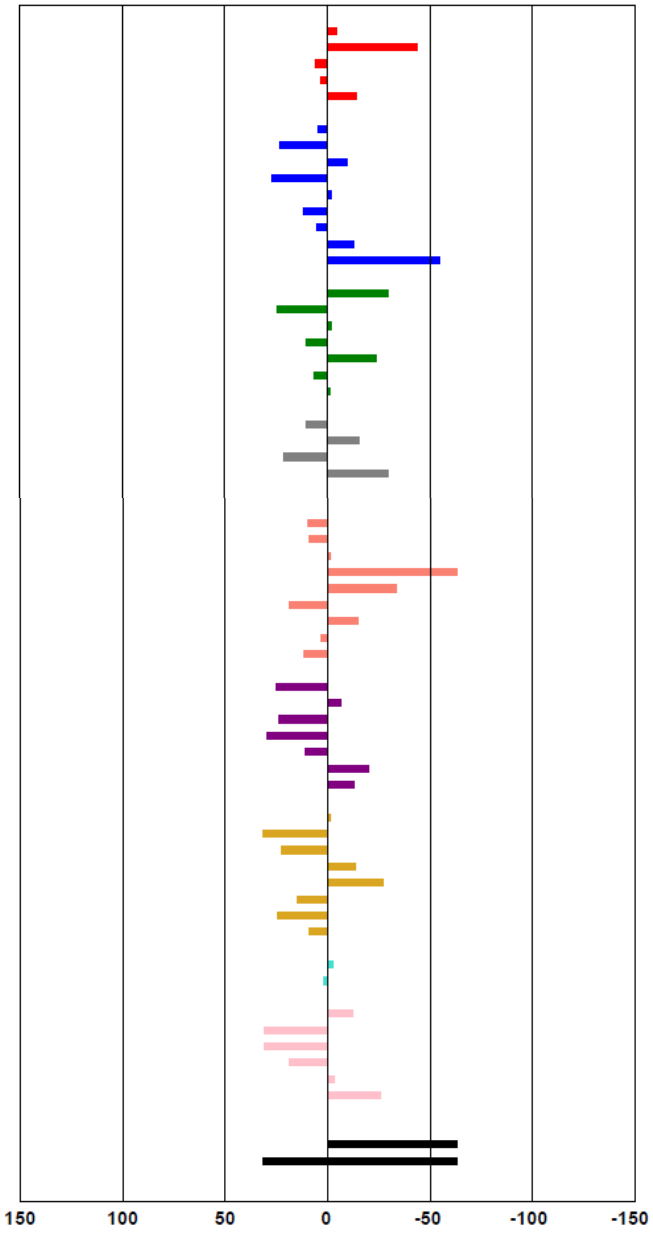

Pyrazoline (74) – Single Dose

Developmental Therapeutics Program
One Dose Mean Graph

NSC: D-761262 / 1	Conc: 1.00E-5 Molar	Test Date: Aug 22, 2011
Experiment ID: 1108OS12		Report Date: Sep 12, 2011

Panel/Cell Line	Growth Percent
Leukemia	
CCRF-CEM	14.69
HL-60(TB)	-27.99
K-562	9.50
MOLT-4	13.39
RPMI-8226	24.99
SR	6.03
Non-Small Cell Lung Cancer	
A549/ATCC	19.58
EKVX	47.24
HOP-62	39.40
HOP-92	61.35
NCI-H226	17.31
NCI-H23	42.21
NCI-H322M	54.52
NCI-H460	12.70
NCI-H522	-53.39
Colon Cancer	
COLO 205	-3.73
HCT-116	19.95
HCT-15	18.58
HT29	4.37
KM12	19.97
SW-620	28.36
CNS Cancer	
SF-268	48.16
SF-295	6.50
SF-539	-11.99
SNB-19	18.06
U251	23.28
Melanoma	
LOX IMVI	50.12
MALME-3M	44.28
M14	2.03
MDA-MB-435	-56.59
SK-MEL-2	-11.45
SK-MEL-28	37.35
SK-MEL-5	8.84
UACC-257	53.16
UACC-62	41.86
Ovarian Cancer	
IGROV1	37.24
OVCAR-3	-41.07
OVCAR-5	42.08
OVCAR-8	20.86
NCI/ADR-RES	14.02
SK-OV-3	-1.46
Renal Cancer	
786-0	30.16
A498	48.60
ACHN	56.61
CAKI-1	43.53
RXF 393	-27.33
SN12C	39.06
TK-10	44.01
UO-31	47.64
Prostate Cancer	
PC-3	17.62
DU-145	7.80
Breast Cancer	
MCF7	12.15
MDA-MB-231/ATCC	47.89
HS 578T	30.53
BT-549	49.19
T-47D	34.32
MDA-MB-468	-7.80
Mean	20.50
Delta	77.09
Range	117.94

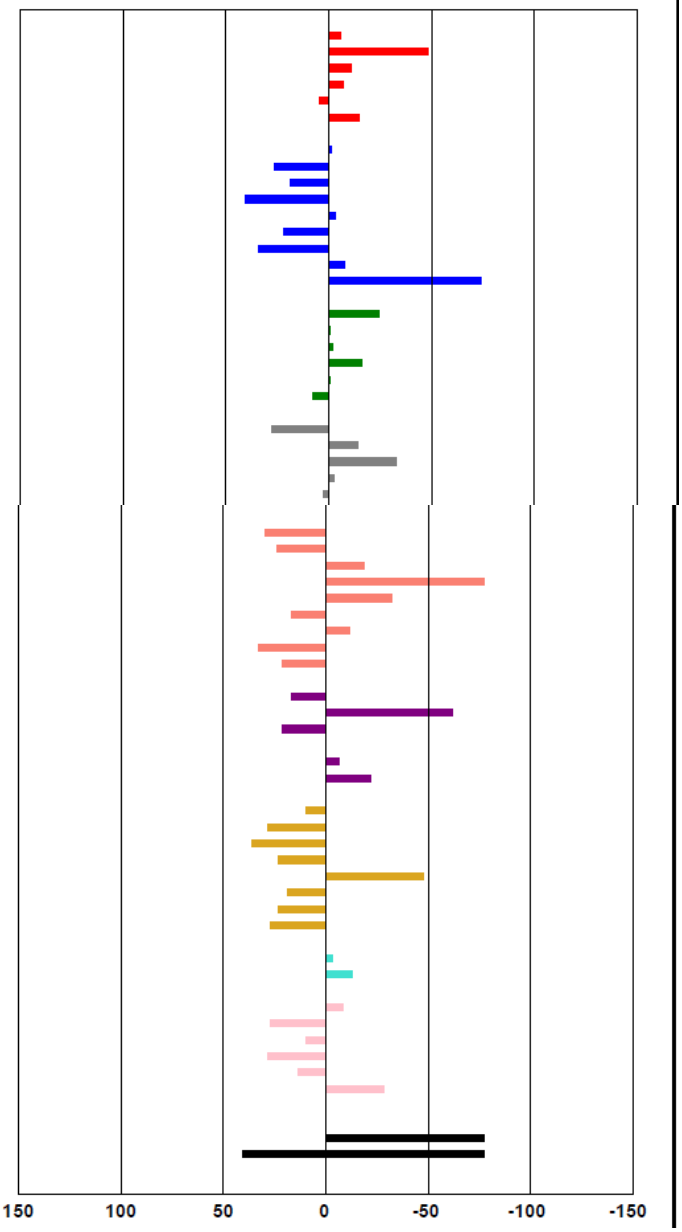

Pyrazoline (74–) – Single Dose

Developmental Therapeutics Program
One Dose Mean Graph

NSC: D-761466 / 1	Conc: 1.00E-5 Molar	Test Date: Sep 12, 2011
Experiment ID: 1109OS23		Report Date: Sep 30, 2011

Panel/Cell Line	Growth Percent
Leukemia	
CCRF-CEM	15.19
HL-60(TB)	-19.08
MOLT-4	28.55
RPMI-8226	24.45
SR	12.37
Non-Small Cell Lung Cancer	
A549/ATCC	17.97
EKVX	37.59
HOP-62	17.20
HOP-92	54.28
NCI-H226	21.96
NCI-H23	28.16
NCI-H322M	41.64
NCI-H460	13.49
NCI-H522	-7.35
Colon Cancer	
COLO 205	-42.90
HCC-2998	28.84
HCT-116	20.37
HCT-15	41.05
HT29	7.20
KM12	19.63
SW-620	24.79
CNS Cancer	
SF-268	51.67
SF-539	4.71
SNB-19	49.67
SNB-75	-7.20
U251	18.89
Melanoma	
LOX IMVI	47.81
MALME-3M	36.13
M14	3.00
MDA-MB-435	-42.04
SK-MEL-2	17.40
SK-MEL-28	45.98
SK-MEL-5	6.96
UACC-257	59.99
UACC-62	46.29
Ovarian Cancer	
IGROV1	42.11
OVCAR-3	28.16
OVCAR-4	57.16
OVCAR-5	40.98
OVCAR-8	31.09
NCI/ADR-RES	-7.03
SK-OV-3	4.79
Renal Cancer	
786-0	22.13
A498	48.66
ACHN	61.31
CAKI-1	28.34
RXF 393	-15.29
SN12C	43.86
TK-10	55.68
UO-31	41.41
Prostate Cancer	
PC-3	19.03
DU-145	22.03
Breast Cancer	
MCF7	16.49
MDA-MB-231/ATCC	62.76
HS 578T	58.38
BT-549	48.66
T-47D	42.45
MDA-MB-468	-18.50
Mean	25.16
Delta	68.06
Range	105.66

Mean Growth Percent - Growth Percent

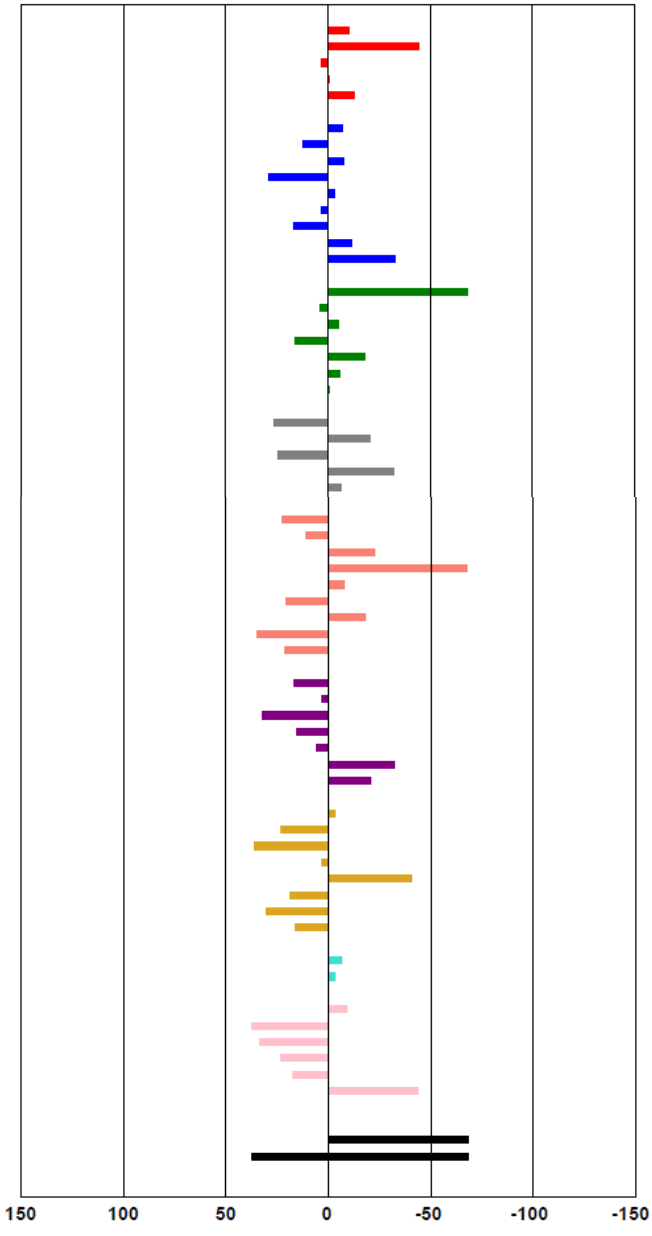

Pyrazoline (74–) – Single Dose

Developmental Therapeutics Program
One Dose Mean Graph

NSC: D-761468 / 1	Conc: 1.00E-5 Molar	Test Date: Sep 12, 2011
Experiment ID: 1109OS23		Report Date: Sep 30, 2011

Panel/Cell Line	Growth Percent
Leukemia	
CCRF-CEM	12.12
HL-60(TB)	-14.55
MOLT-4	13.85
RPMI-8226	22.22
SR	10.69
Non-Small Cell Lung Cancer	
A549/ATCC	21.97
EKVX	40.41
HOP-62	33.15
HOP-92	69.25
NCI-H226	12.26
NCI-H23	30.27
NCI-H322M	48.24
NCI-H460	11.13
NCI-H522	-11.36
Colon Cancer	
COLO 205	-32.26
HCC-2998	8.31
HCT-116	15.16
HCT-15	31.32
HT29	6.10
KM12	19.79
SW-620	30.15
CNS Cancer	
SF-268	53.47
SF-539	2.53
SNB-19	47.50
SNB-75	3.50
U251	15.90
Melanoma	
LOX IMVI	44.70
MALME-3M	46.70
M14	-1.30
MDA-MB-435	-28.52
SK-MEL-2	-6.65
SK-MEL-28	42.03
SK-MEL-5	16.37
UACC-257	54.29
UACC-62	44.49
Ovarian Cancer	
IGROV1	46.16
OVCAR-3	0.48
OVCAR-4	55.86
OVCAR-5	39.38
OVCAR-8	21.82
NCI/ADR-RES	-7.33
SK-OV-3	0.20
Renal Cancer	
786-0	33.00
A498	55.46
ACHN	51.01
CAKI-1	35.66
RXF 393	-17.93
SN12C	44.90
TK-10	60.24
UO-31	40.58
Prostate Cancer	
PC-3	24.37
DU-145	24.55
Breast Cancer	
MCF7	17.13
MDA-MB-231/ATCC	63.75
HS 578T	62.48
BT-549	28.78
T-47D	73.12
MDA-MB-468	7.27
Mean	25.42
Delta	57.68
Range	105.38

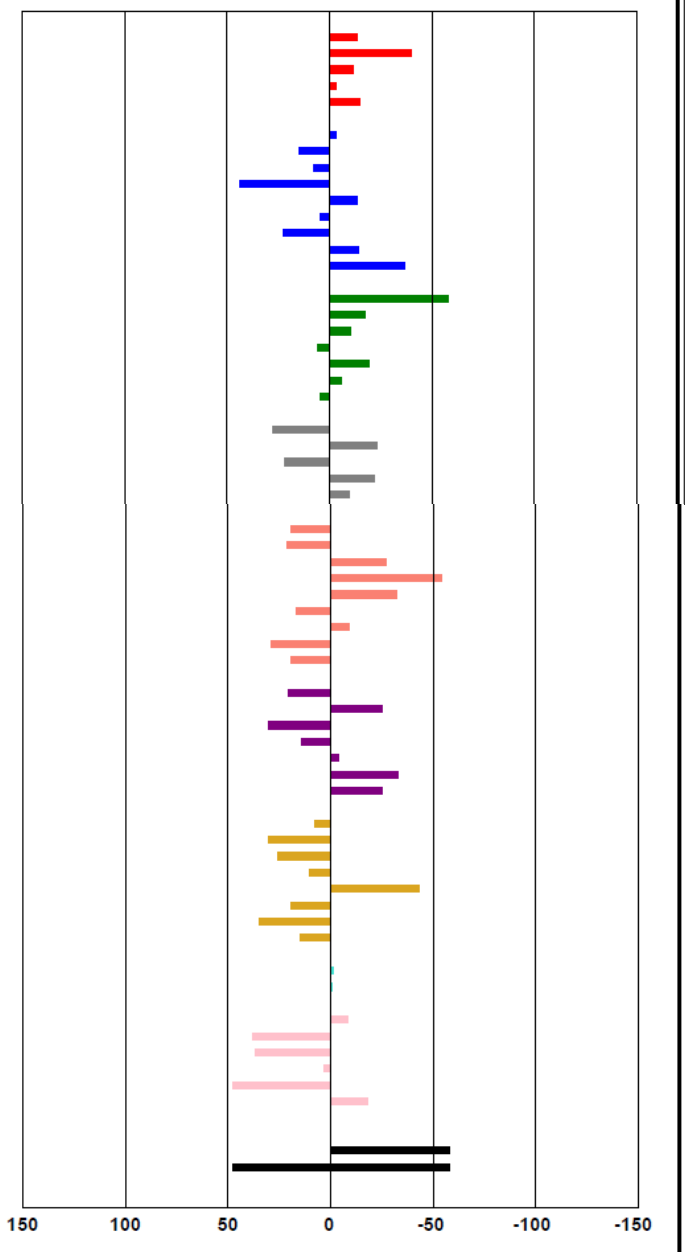

Pyrazoline (74+) – Single Dose

Developmental Therapeutics Program
One Dose Mean Graph

NSC: D-761465 / 1	Conc: 1.00E-5 Molar	Test Date: Sep 12, 2011
Experiment ID: 1109OS23		Report Date: Sep 30, 2011

Panel/Cell Line	Growth Percent
Leukemia	
CCRF-CEM	75.74
HL-60(TB)	71.80
MOLT-4	68.35
RPMI-8226	86.11
SR	20.01
Non-Small Cell Lung Cancer	
A549/ATCC	85.14
EKVX	97.78
HOP-62	78.50
HOP-92	94.41
NCI-H226	90.45
NCI-H23	90.79
NCI-H322M	91.13
NCI-H460	112.66
NCI-H522	63.30
Colon Cancer	
COLO 205	75.84
HCC-2998	89.22
HCT-116	86.77
HCT-15	80.94
HT29	61.54
KM12	52.67
SW-620	75.42
CNS Cancer	
SF-268	74.00
SF-539	93.29
SNB-19	91.17
SNB-75	64.67
U251	87.35
Melanoma	
LOX IMVI	86.33
MALME-3M	83.77
M14	76.12
MDA-MB-435	14.62
SK-MEL-2	71.83
SK-MEL-28	97.83
SK-MEL-5	73.88
UACC-257	85.60
UACC-62	78.04
Ovarian Cancer	
IGROV1	92.64
OVCAR-4	102.96
OVCAR-5	95.84
OVCAR-8	98.65
NCI/ADR-RES	61.11
SK-OV-3	92.31
Renal Cancer	
786-0	90.36
A498	101.65
ACHN	103.64
CAKI-1	72.62
RXF 393	111.45
SN12C	98.26
TK-10	99.12
UO-31	82.72
Prostate Cancer	
PC-3	82.90
DU-145	92.78
Breast Cancer	
MCF7	67.75
MDA-MB-231/ATCC	90.96
HS 578T	100.01
BT-549	99.65
T-47D	86.30
MDA-MB-468	76.17
Mean	82.93
Delta	68.31
Range	98.04

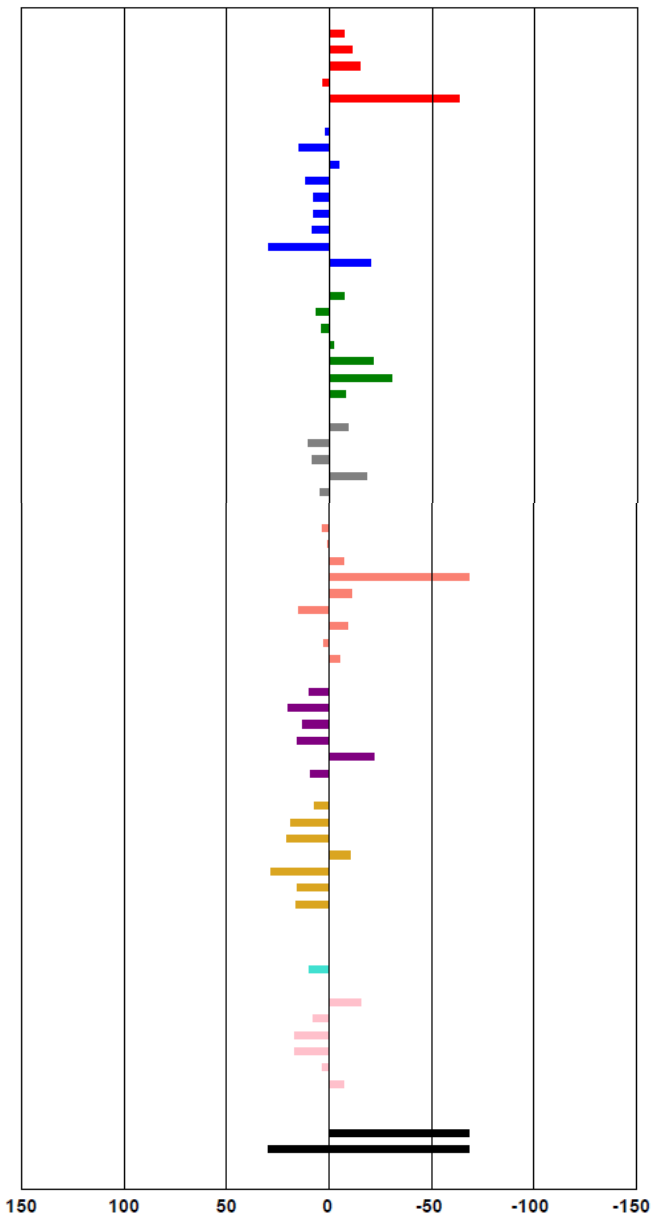

Pyrazoline (78) – Single Dose

Developmental Therapeutics Program One Dose Mean Graph	NSC: D-761257 / 1	Conc: 1.00E-5 Molar	Test Date: Aug 22, 2011
	Experiment ID: 1108OS12		Report Date: Sep 12, 2011

Panel/Cell Line	Growth Percent
Leukemia	
CCRF-CEM	14.15
HL-60(TB)	-31.78
K-562	12.33
MOLT-4	20.19
RPMI-8226	33.37
SR	11.28
Non-Small Cell Lung Cancer	
A549/ATCC	29.40
EKVX	46.51
HOP-62	25.89
HOP-92	39.80
NCI-H226	24.57
NCI-H23	37.96
NCI-H322M	36.84
NCI-H460	13.41
NCI-H522	-36.94
Colon Cancer	
COLO 205	-11.23
HCC-2998	45.94
HCT-116	25.17
HCT-15	30.29
HT29	4.84
KM12	22.02
SW-620	25.78
CNS Cancer	
SF-268	51.90
SF-295	9.65
SF-539	2.72
SNB-19	40.44
SNB-75	23.63
U251	38.03
Melanoma	
LOX IMVI	41.36
MALME-3M	30.33
M14	23.30
MDA-MB-435	-47.11
SK-MEL-2	15.41
SK-MEL-28	40.32
SK-MEL-5	-0.99
UACC-257	68.73
UACC-62	53.74
Ovarian Cancer	
IGROV1	32.57
OVCAR-3	-2.64
OVCAR-4	65.98
OVCAR-5	47.02
OVCAR-8	31.69
NCI/ADR-RES	4.57
SK-OV-3	15.02
Renal Cancer	
786-0	34.59
A498	27.87
ACHN	60.71
CAKI-1	34.59
RXF 393	-20.58
SN12C	44.83
TK-10	43.18
UO-31	44.55
Prostate Cancer	
PC-3	19.84
DU-145	7.79
Breast Cancer	
MCF7	14.77
MDA-MB-231/ATCC	53.90
HS 578T	24.51
BT-549	55.19
T-47D	26.72
MDA-MB-468	-9.60
Mean	24.47
Delta	71.58
Range	115.84

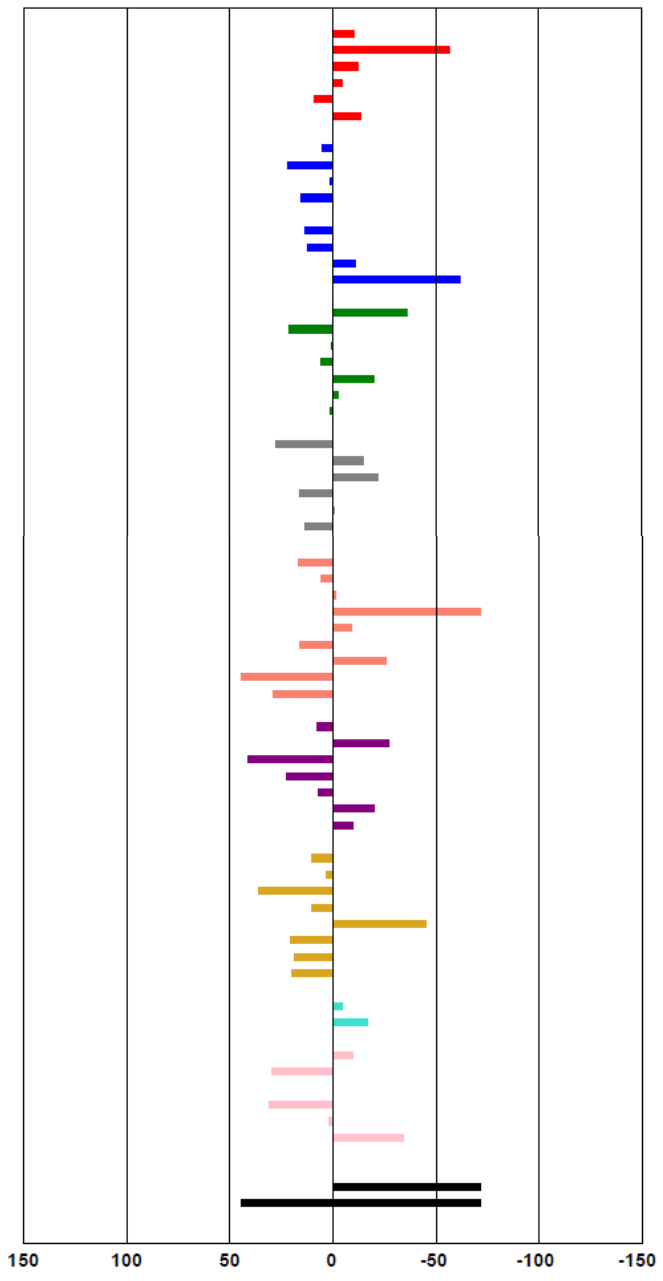

Pyrazoline (78+) – Single Dose

Developmental Therapeutics Program
One Dose Mean Graph

NSC: D-761463 / 1	Conc: 1.00E-5 Molar	Test Date: Sep 12, 2011
Experiment ID: 1109OS23		Report Date: Sep 30, 2011

Panel/Cell Line	Growth Percent
Leukemia	
CCRF-CEM	70.70
HL-60(TB)	43.73
MOLT-4	67.50
RPMI-8226	87.52
SR	19.43
Non-Small Cell Lung Cancer	
A549/ATCC	52.72
EKVX	96.48
HOP-62	61.04
HOP-92	85.06
NCI-H226	84.93
NCI-H23	79.50
NCI-H322M	90.28
NCI-H460	48.50
NCI-H522	33.14
Colon Cancer	
COLO 205	45.84
HCC-2998	79.84
HCT-116	42.24
HCT-15	58.38
HT29	13.20
KM12	46.42
SW-620	45.85
CNS Cancer	
SF-268	81.70
SF-539	77.30
SNB-19	80.01
SNB-75	42.15
U251	65.17
Melanoma	
LOX IMVI	67.08
MALME-3M	69.06
M14	49.11
MDA-MB-435	-3.83
SK-MEL-2	36.45
SK-MEL-28	74.82
SK-MEL-5	49.41
UACC-257	77.31
UACC-62	55.95
Ovarian Cancer	
IGROV1	63.14
OVCAR-3	56.88
OVCAR-4	91.84
OVCAR-5	83.27
OVCAR-8	85.85
NCI/ADR-RES	36.02
SK-OV-3	68.00
Renal Cancer	
786-0	77.77
A498	83.39
ACHN	88.12
CAKI-1	49.33
RXF 393	98.73
SN12C	84.12
TK-10	84.42
UO-31	91.15
Prostate Cancer	
PC-3	74.90
DU-145	82.74
Breast Cancer	
MCF7	32.46
MDA-MB-231/ATCC	67.34
HS 578T	97.18
BT-549	69.09
T-47D	66.45
MDA-MB-468	57.04
Mean	64.88
Delta	68.71
Range	102.56

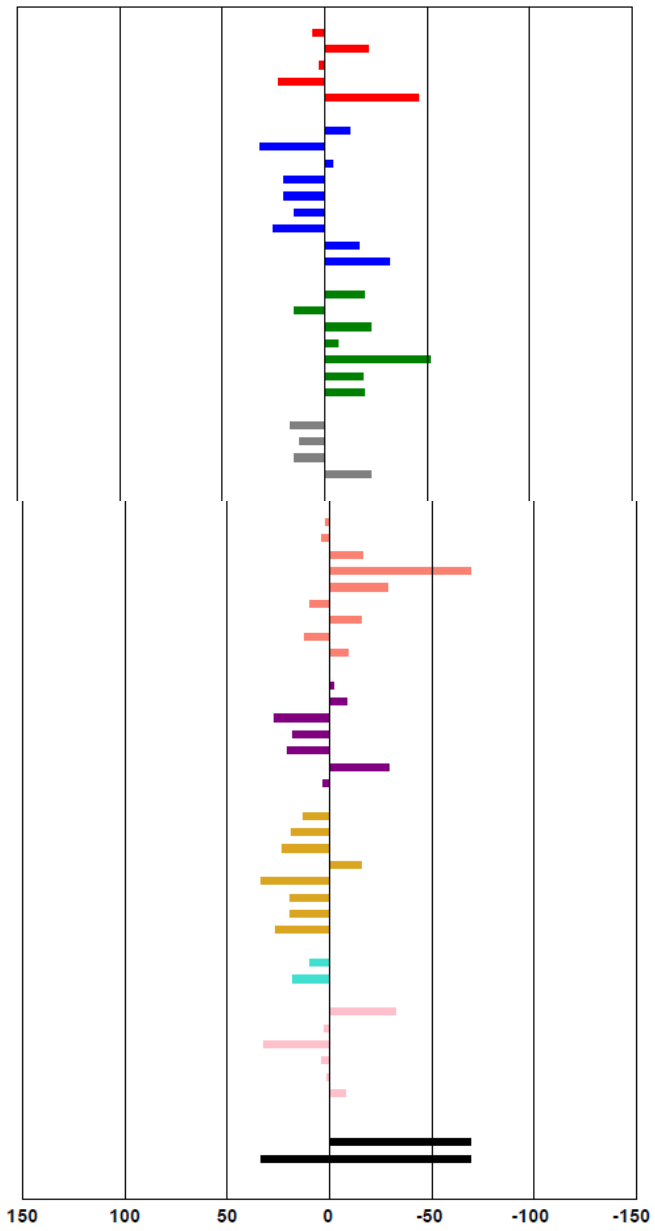

Pyrazoline (79) – Single Dose

Developmental Therapeutics Program One Dose Mean Graph	NSC: D-761259 / 1	Conc: 1.00E-5 Molar	Test Date: Aug 22, 2011
	Experiment ID: 1108OS12		Report Date: Sep 12, 2011

Panel/Cell Line	Growth Percent
Leukemia	
CCRF-CEM	60.52
HL-60(TB)	17.66
K-562	19.92
MOLT-4	54.47
RPMI-8226	73.54
SR	10.32
Non-Small Cell Lung Cancer	
A549/ATCC	47.35
EKVX	80.28
HOP-62	56.84
HOP-92	66.28
NCI-H226	76.42
NCI-H23	70.02
NCI-H322M	70.61
NCI-H460	24.57
NCI-H522	-11.16
Colon Cancer	
COLO 205	37.73
HCC-2998	68.94
HCT-116	27.26
HCT-15	42.10
HT29	9.09
KM12	23.75
SW-620	35.52
CNS Cancer	
SF-268	78.50
SF-295	31.19
SF-539	47.89
SNB-19	53.82
SNB-75	-8.53
U251	57.65
Melanoma	
LOX IMVI	54.57
MALME-3M	40.80
M14	32.46
MDA-MB-435	0.61
SK-MEL-2	0.44
SK-MEL-28	61.25
SK-MEL-5	26.35
UACC-257	74.81
UACC-62	51.24
Ovarian Cancer	
IGROV1	32.95
OVCAR-3	-14.69
OVCAR-4	69.60
OVCAR-5	76.55
OVCAR-8	74.84
NCI/ADR-RES	29.06
SK-OV-3	60.51
Renal Cancer	
786-0	62.81
A498	55.02
ACHN	65.07
CAKI-1	51.56
RXF 393	57.24
SN12C	76.50
TK-10	70.02
UO-31	67.17
Prostate Cancer	
PC-3	50.83
DU-145	78.17
Breast Cancer	
MCF7	20.37
MDA-MB-231/ATCC	68.16
HS 578T	75.99
BT-549	52.73
T-47D	39.81
MDA-MB-468	15.09
Mean	46.67
Delta	61.36
Range	94.97

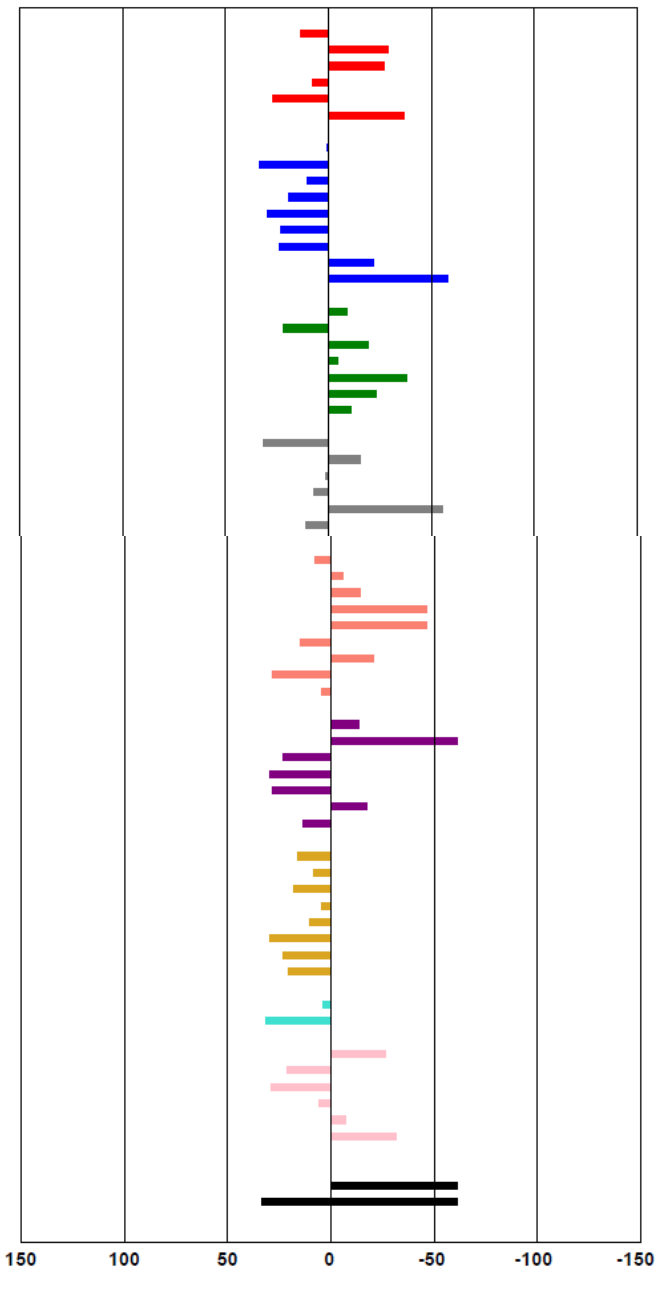

Pyrazoline (80) – Single Dose

Developmental Therapeutics Program
One Dose Mean Graph

NSC: D-761260 / 1	Conc: 1.00E-5 Molar	Test Date: Aug 22, 2011
Experiment ID: 1108OS12		Report Date: Sep 12, 2011

Panel/Cell Line	Growth Percent
Leukemia	
CCRF-CEM	19.89
HL-60(TB)	-5.83
K-562	19.29
MOLT-4	35.55
RPMI-8226	27.38
SR	14.28
Non-Small Cell Lung Cancer	
A549/ATCC	36.65
EKVX	54.14
HOP-62	20.90
HOP-92	42.17
NCI-H226	24.09
NCI-H23	40.11
NCI-H322M	42.76
NCI-H460	13.38
NCI-H522	-26.11
Colon Cancer	
COLO 205	-7.49
HCC-2998	51.90
HCT-116	24.73
HCT-15	32.84
HT29	5.11
KM12	29.12
SW-620	25.72
CNS Cancer	
SF-268	55.45
SF-295	11.46
SF-539	-0.38
SNB-19	33.26
U251	38.59
Melanoma	
LOX IMVI	44.42
MALME-3M	34.27
M14	29.26
MDA-MB-435	-37.79
SK-MEL-2	10.01
SK-MEL-28	44.83
SK-MEL-5	-6.16
UACC-257	60.61
UACC-62	46.15
Ovarian Cancer	
IGROV1	28.34
OVCAR-3	-30.23
OVCAR-5	62.54
OVCAR-8	36.92
NCI/ADR-RES	10.20
SK-OV-3	12.22
Renal Cancer	
786-0	33.55
A498	41.93
ACHN	60.43
CAKI-1	33.82
RXF 393	-20.95
SN12C	45.28
TK-10	48.78
UO-31	55.41
Prostate Cancer	
PC-3	21.92
DU-145	22.51
Breast Cancer	
MCF7	12.28
MDA-MB-231/ATCC	55.84
HS 578T	22.31
BT-549	56.07
T-47D	24.55
MDA-MB-468	-16.09
Mean	25.90
Delta	63.69
Range	100.33

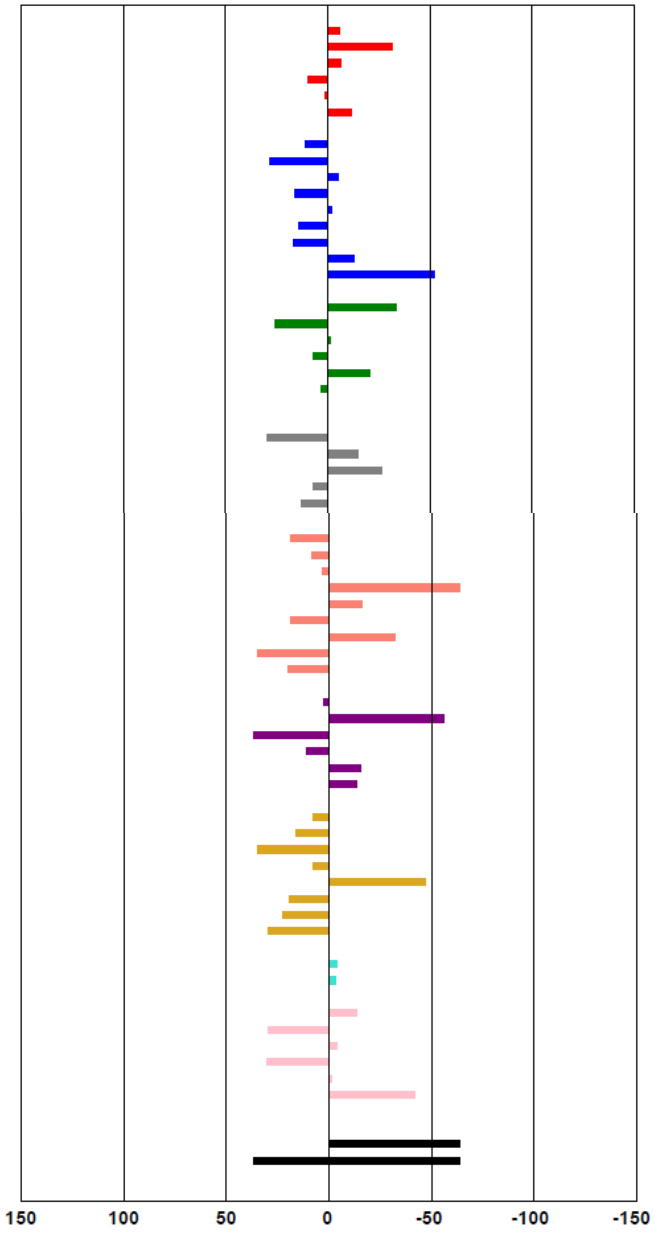

Pyrazoline (105) – Single Dose

Developmental Therapeutics Program
One Dose Mean Graph

NSC: D-761258 / 1	Conc: 1.00E-5 Molar	Test Date: Aug 22, 2011
Experiment ID: 1108OS12		Report Date: Sep 12, 2011

Panel/Cell Line	Growth Percent
Leukemia	
CCRF-CEM	15.28
HL-60(TB)	-19.74
K-562	13.92
MOLT-4	27.77
RPMI-8226	35.40
SR	14.19
Non-Small Cell Lung Cancer	
A549/ATCC	22.14
EKVX	44.62
HOP-62	29.96
HOP-92	5.44
NCI-H226	27.06
NCI-H23	37.40
NCI-H322M	39.12
NCI-H460	11.46
NCI-H522	-43.64
Colon Cancer	
COLO 205	-1.56
HCC-2998	38.08
HCT-116	22.61
HCT-15	28.98
HT29	5.17
KM12	20.19
SW-620	29.02
CNS Cancer	
SF-268	50.59
SF-295	5.51
SF-539	-20.52
SNB-19	25.23
U251	29.87
Melanoma	
LOX IMVI	40.94
MALME-3M	28.74
M14	4.20
MDA-MB-435	-50.29
SK-MEL-2	-2.85
SK-MEL-28	42.61
SK-MEL-5	6.98
UACC-257	76.69
UACC-62	53.39
Ovarian Cancer	
IGROV1	29.81
OVCAR-3	-40.78
OVCAR-5	37.71
OVCAR-8	31.28
NCI/ADR-RES	0.62
SK-OV-3	5.62
Renal Cancer	
786-0	32.68
A498	21.66
ACHN	53.41
CAKI-1	27.53
RXF 393	-24.74
SN12C	37.15
TK-10	34.84
UO-31	34.80
Prostate Cancer	
PC-3	19.36
DU-145	-12.00
Breast Cancer	
MCF7	20.41
MDA-MB-231/ATCC	51.03
HS 578T	20.94
BT-549	51.91
T-47D	31.13
MDA-MB-468	-7.41
Mean	19.84
Delta	70.13
Range	126.98

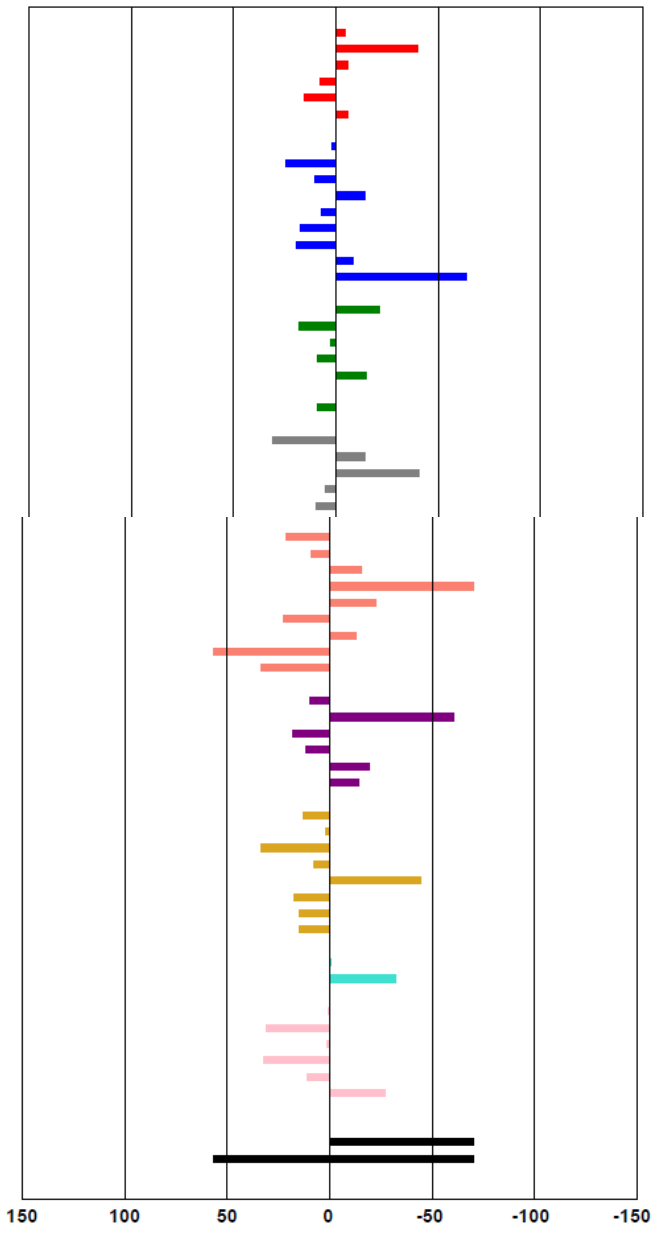

Chalcone (51) – Five Dose

National Cancer Institute Developmental Therapeutics Program
In-Vitro Testing Results

NSC : D - 761254 / 1	Experiment ID : 1109NS21	Test Type : 08	Units : Molar
Report Date : October 26, 2011	Test Date : September 12, 2011	QNS :	MC :
COMI : MCC-C5 (108808)	Stain Reagent : SRB Dual-Pass Related	SSPL : 0Y8X	

			Log10 Concentration											
	Time		Mean Optical Densities					Percent Growth						
Panel/Cell Line	Zero	Ctrl	-8.0	-7.0	-6.0	-5.0	-4.0	-8.0	-7.0	-6.0	-5.0	-4.0	GI50	TGI	LC50
Leukemia															
CCRF-CEM	0.380	1.718	1.632	1.578	1.558	0.974	0.496	94	89	88	44	9	7.44E-6	> 1.00E-4	> 1.00E-4
HL-60(TB)	0.695	2.356	2.403	2.544	2.372	1.314	0.799	103	111	101	37	6	6.31E-6	> 1.00E-4	> 1.00E-4
MOLT-4	0.518	2.220	2.363	2.380	2.460	1.500	0.948	108	109	114	58	25	1.73E-5	> 1.00E-4	> 1.00E-4
RPMI-8226	0.673	2.169	2.188	2.139	2.106	1.330	0.856	101	98	96	44	12	7.63E-6	> 1.00E-4	> 1.00E-4
SR	0.449	2.391	2.336	2.378	1.549	0.776	0.669	97	99	57	17	11	1.47E-6	> 1.00E-4	> 1.00E-4
Non-Small Cell Lung Cancer															
A549/ATCC	0.410	2.026	1.954	1.931	1.987	1.059	0.649	96	94	98	40	15	6.74E-6	> 1.00E-4	> 1.00E-4
EKVX	0.836	2.037	1.948	1.951	1.923	1.786	1.273	93	93	90	79	36	4.79E-5	> 1.00E-4	> 1.00E-4
HOP-62	0.407	1.037	1.030	1.039	1.026	0.668	0.369	99	100	98	41	-9	7.07E-6	6.52E-5	> 1.00E-4
HOP-92	0.903	1.663	1.614	1.604	1.576	1.559	1.314	94	92	89	86	54	> 1.00E-4	> 1.00E-4	> 1.00E-4
NCI-H226	0.668	1.606	1.549	1.497	1.515	1.125	0.643	94	88	90	49	-4	9.32E-6	8.46E-5	> 1.00E-4
NCI-H23	0.445	1.409	1.372	1.310	1.317	0.868	0.627	96	90	90	44	19	7.37E-6	> 1.00E-4	> 1.00E-4
NCI-H322M	0.717	1.567	1.587	1.561	1.563	1.182	0.735	102	99	100	55	2	1.23E-5	> 1.00E-4	> 1.00E-4
NCI-H460	0.172	1.979	2.004	1.977	1.941	0.405	0.141	101	100	98	13	-18	3.66E-6	2.61E-5	> 1.00E-4
NCI-H522	0.798	1.893	1.876	1.913	1.851	1.185	0.911	98	102	96	35	10	5.74E-6	> 1.00E-4	> 1.00E-4
Colon Cancer															
COLO 205	0.315	1.221	1.322	1.321	1.258	0.465	0.100	111	111	104	17	-68	4.15E-6	1.57E-5	6.09E-5
HCC-2998	0.424	1.457	1.438	1.379	1.370	0.939	0.293	98	92	92	50	-31	9.89E-6	4.14E-5	> 1.00E-4
HCT-116	0.194	1.470	1.485	1.469	1.446	0.399	0.247	101	100	98	16	4	3.86E-6	> 1.00E-4	> 1.00E-4
HCT-15	0.395	2.025	1.894	1.971	1.978	0.857	0.579	92	97	97	28	11	4.84E-6	> 1.00E-4	> 1.00E-4
HT29	0.216	1.381	1.424	1.432	1.368	0.328	0.266	104	104	99	10	4	3.52E-6	> 1.00E-4	> 1.00E-4
KM12	0.322	2.286	2.315	2.333	1.916	0.824	0.548	101	102	81	26	11	3.63E-6	> 1.00E-4	> 1.00E-4
SW-620	0.196	1.781	1.763	1.711	1.593	0.491	0.349	99	96	88	19	10	3.53E-6	> 1.00E-4	> 1.00E-4
CNS Cancer															
SF-268	0.280	1.679	1.704	1.658	1.716	0.986	0.546	102	98	103	50	19	1.03E-5	> 1.00E-4	> 1.00E-4
SF-539	0.713	1.972	1.978	2.021	2.039	1.363	0.551	100	104	105	52	-23	1.05E-5	4.95E-5	> 1.00E-4
SNB-19	0.476	1.573	1.569	1.527	1.512	0.968	0.744	100	96	94	45	24	7.86E-6	> 1.00E-4	> 1.00E-4
SNB-75	0.863	1.521	1.389	1.397	1.352	0.820	0.796	80	81	74	-5	-8	2.02E-6	8.64E-6	> 1.00E-4
U251	0.365	1.683	1.655	1.620	1.594	0.815	0.386	98	95	93	34	2	5.39E-6	> 1.00E-4	> 1.00E-4
Melanoma															
LOX IMVI	0.247	1.591	1.567	1.538	1.508	0.796	0.373	98	96	94	41	9	6.70E-6	> 1.00E-4	> 1.00E-4
MALME-3M	0.602	1.299	1.294	1.286	1.321	0.923	0.677	99	98	103	46	11	8.51E-6	> 1.00E-4	> 1.00E-4
M14	0.317	1.157	1.168	1.151	1.132	0.364	0.340	101	99	97	6	3	3.27E-6	> 1.00E-4	> 1.00E-4
MDA-MB-435	0.551	2.492	2.441	2.413	1.822	0.380	0.430	97	96	65	-31	-22	1.45E-6	4.76E-6	> 1.00E-4
SK-MEL-2	0.821	1.704	1.756	1.742	1.766	1.136	0.875	106	104	107	36	6	6.28E-6	> 1.00E-4	> 1.00E-4
SK-MEL-28	0.533	1.364	1.380	1.330	1.344	0.941	0.586	102	96	98	49	6	9.55E-6	> 1.00E-4	> 1.00E-4
SK-MEL-5	0.497	2.255	2.195	2.165	2.182	0.826	0.203	97	95	96	19	-59	3.93E-6	1.74E-5	7.63E-5
UACC-257	0.874	1.941	1.901	1.866	1.868	1.615	1.244	96	93	93	69	35	3.62E-5	> 1.00E-4	> 1.00E-4
UACC-62	0.563	1.802	1.789	1.741	1.629	0.880	0.670	99	95	86	26	9	3.95E-6	> 1.00E-4	> 1.00E-4
Ovarian Cancer															
IGROV1	0.570	1.468	1.534	1.571	1.580	0.969	0.573	107	112	113	44	.	8.28E-6	> 1.00E-4	> 1.00E-4
OVCAR-3	0.235	1.532	1.417	1.502	1.415	0.664	0.539	91	98	91	33	23	5.10E-6	> 1.00E-4	> 1.00E-4
OVCAR-4	0.580	1.179	1.203	1.110	1.100	1.014	0.698	104	88	87	72	20	2.65E-5	> 1.00E-4	> 1.00E-4
OVCAR-5	0.521	1.453	1.455	1.452	1.429	1.033	0.352	100	100	97	55	-32	1.14E-5	4.25E-5	> 1.00E-4
OVCAR-8	0.498	2.241	2.238	2.106	2.228	1.579	0.824	100	92	99	62	19	1.89E-5	> 1.00E-4	> 1.00E-4
NCI/ADR-RES	0.500	1.548	1.533	1.507	1.447	0.551	0.646	99	96	90	5	14	2.96E-6	> 1.00E-4	> 1.00E-4
SK-OV-3	0.563	1.245	1.278	1.264	1.277	0.859	0.468	105	103	105	43	-17	7.79E-6	5.23E-5	> 1.00E-4
Renal Cancer															
786-0	0.661	2.217	2.221	2.205	2.198	1.372	0.727	100	99	99	46	4	8.30E-6	> 1.00E-4	> 1.00E-4
A498	0.701	1.842	1.611	1.590	1.643	1.426	0.873	80	78	83	64	15	1.90E-5	> 1.00E-4	> 1.00E-4
ACHN	0.346	1.408	1.503	1.437	1.458	0.958	0.584	109	103	105	58	22	1.65E-5	> 1.00E-4	> 1.00E-4
CAKI-1	0.638	2.311	2.274	2.170	2.129	1.374	0.853	98	92	89	44	13	7.35E-6	> 1.00E-4	> 1.00E-4
RXF 393	0.511	1.130	1.105	1.086	1.088	0.771	0.483	96	93	93	42	-6	6.99E-6	7.84E-5	> 1.00E-4
SN12C	0.473	1.807	1.757	1.698	1.673	1.124	0.646	96	92	90	49	13	9.34E-6	> 1.00E-4	> 1.00E-4
TK-10	0.909	1.854	1.866	1.918	1.907	1.724	1.285	101	107	106	86	40	6.04E-5	> 1.00E-4	> 1.00E-4
UO-31	0.370	1.262	1.223	1.215	1.199	0.870	0.534	96	95	93	56	18	1.45E-5	> 1.00E-4	> 1.00E-4
Prostate Cancer															
PC-3	0.364	1.238	1.159	1.136	1.163	1.025	0.737	91	88	91	76	43	5.97E-5	> 1.00E-4	> 1.00E-4
DU-145	0.173	1.468	1.447	1.403	1.425	0.813	0.281	98	95	97	49	8	9.70E-6	> 1.00E-4	> 1.00E-4
Breast Cancer															
MCF7	0.280	1.437	1.340	1.329	1.298	0.404	0.370	92	91	88	11	8	3.10E-6	> 1.00E-4	> 1.00E-4
MDA-MB-231/ATCC	0.638	1.650	1.655	1.620	1.597	1.101	0.699	101	97	95	46	6	8.20E-6	> 1.00E-4	> 1.00E-4
HS 578T	0.449	1.835	1.796	1.714	1.739	1.453	0.997	97	91	93	72	40	4.81E-5	> 1.00E-4	> 1.00E-4
BT-549	0.868	1.832	1.876	1.879	1.907	1.298	1.025	105	105	108	45	16	8.22E-6	> 1.00E-4	> 1.00E-4
T-47D	0.549	1.243	1.251	1.227	1.261	0.805	0.583	101	98	103	37	5	6.30E-6	> 1.00E-4	> 1.00E-4
MDA-MB-468	0.579	1.202	1.176	1.112	1.102	0.603	0.515	96	86	84	4	-11	2.65E-6	1.79E-5	> 1.00E-4

Pyrazoline (71) – Five Dose

National Cancer Institute Developmental Therapeutics Program
In-Vitro Testing Results

NSC : D - 761261 / 1	Experiment ID : 1109NS21	Test Type : 08	Units : Molar
Report Date : October 26, 2011	Test Date : September 12, 2011	QNS :	MC :
COMI : AC04:42 (109729)	Stain Reagent : SRB Dual-Pass Related	SSPL : 0Y8X	

			Log10 Concentration											
	Time		Mean Optical Densities					Percent Growth						
Panel/Cell Line	Zero	Ctrl	-8.0	-7.0	-6.0	-5.0	-4.0	-8.0	-7.0	-6.0	-5.0	-4.0	GI50	TGI	LC50
Leukemia															
CCRF-CEM	0.380	1.696	1.756	1.645	0.576	0.576	0.470	105	96	15	15	7	3.70E-7	> 1.00E-4	> 1.00E-4
HL-60(TB)	0.695	2.368	2.554	2.541	0.759	0.664	0.528	111	110	4	-4	-24	3.68E-7	2.89E-6	> 1.00E-4
MOLT-4	0.518	2.283	2.437	2.515	1.162	0.864	0.661	109	113	36	20	8	6.66E-7	> 1.00E-4	> 1.00E-4
RPMI-8226	0.673	2.268	2.284	2.241	1.254	1.136	0.700	101	98	36	29	2	6.03E-7	> 1.00E-4	> 1.00E-4
SR	0.449	2.436	2.478	1.325	0.781	0.662	0.469	102	44	17	11	1	7.91E-8	> 1.00E-4	> 1.00E-4
Non-Small Cell Lung Cancer															
A549/ATCC	0.410	2.001	1.925	1.688	0.801	0.821	0.584	95	80	25	26	11	3.50E-7	> 1.00E-4	> 1.00E-4
EKVX	0.836	2.055	1.996	1.905	1.553	1.587	1.218	95	88	59	62	31	2.42E-5	> 1.00E-4	> 1.00E-4
HOP-62	0.407	1.012	0.997	0.855	0.547	0.578	0.440	97	74	23	28	5	2.96E-7	> 1.00E-4	> 1.00E-4
HOP-92	0.903	1.805	1.739	1.596	1.592	1.484	1.186	93	77	76	64	31	2.73E-5	> 1.00E-4	> 1.00E-4
NCI-H226	0.668	1.619	1.565	1.388	0.773	0.513	0.523	94	76	11	-23	-22	2.49E-7	2.09E-6	> 1.00E-4
NCI-H23	0.445	1.460	1.452	1.258	0.829	0.752	0.605	99	80	38	30	16	5.14E-7	> 1.00E-4	> 1.00E-4
NCI-H322M	0.717	1.621	1.638	1.600	1.164	1.140	1.087	102	98	49	47	41	9.71E-7	> 1.00E-4	> 1.00E-4
NCI-H460	0.172	1.996	2.121	1.807	0.376	0.263	0.135	107	90	11	5	-22	3.20E-7	1.54E-5	> 1.00E-4
NCI-H522	0.798	1.940	1.896	1.526	1.007	0.880	0.622	96	64	18	7	-22	2.01E-7	1.76E-5	> 1.00E-4
Colon Cancer															
COLO 205	0.315	1.239	1.279	1.151	0.243	0.106	0.028	104	90	-23	-66	-91	2.27E-7	6.27E-7	4.19E-6
HCC-2998	0.424	1.533	1.518	1.370	0.501	0.509	0.345	99	85	7	8	-19	2.82E-7	1.96E-5	> 1.00E-4
HCT-116	0.194	1.568	1.607	1.347	0.438	0.260	0.216	103	84	18	5	2	3.26E-7	> 1.00E-4	> 1.00E-4
HCT-15	0.395	2.018	1.951	1.755	0.791	0.605	0.505	96	84	24	13	7	3.71E-7	> 1.00E-4	> 1.00E-4
HT29	0.216	1.475	1.440	1.351	0.334	0.310	0.189	97	90	9	7	-13	3.14E-7	2.37E-5	> 1.00E-4
KM12	0.322	2.395	2.563	1.828	0.943	0.795	0.550	108	73	30	23	11	3.39E-7	> 1.00E-4	> 1.00E-4
SW-620	0.196	1.747	1.725	1.385	0.597	0.531	0.466	99	77	26	22	17	3.35E-7	> 1.00E-4	> 1.00E-4
CNS Cancer															
SF-268	0.280	1.601	1.587	1.373	0.911	0.708	0.439	99	83	48	32	12	8.62E-7	> 1.00E-4	> 1.00E-4
SF-539	0.713	1.976	1.938	1.891	0.706	0.748	0.480	97	93	-1	3	-33	2.88E-7	.	> 1.00E-4
SNB-19	0.476	1.604	1.542	1.432	0.760	0.791	0.645	95	85	25	28	15	3.83E-7	> 1.00E-4	> 1.00E-4
SNB-75	0.863	1.559	1.415	1.135	0.784	0.976	0.808	79	39	-9	16	-6	5.34E-8	.	> 1.00E-4
U251	0.365	1.691	1.680	1.630	0.674	0.587	0.414	99	95	23	17	4	4.26E-7	> 1.00E-4	> 1.00E-4
Melanoma															
LOX IMVI	0.247	1.602	1.548	1.216	0.817	0.503	0.253	96	71	42	19	.	5.37E-7	> 1.00E-4	> 1.00E-4
MALME-3M	0.602	1.328	1.334	1.137	0.913	0.958	0.489	101	74	43	49	-19	5.87E-7	5.28E-5	> 1.00E-4
M14	0.317	1.205	1.228	0.995	0.373	0.354	0.193	103	76	6	4	-39	2.38E-7	1.25E-5	> 1.00E-4
MDA-MB-435	0.551	2.558	2.477	0.865	0.376	0.403	0.353	96	16	-32	-27	-36	3.73E-8	2.14E-7	> 1.00E-4
SK-MEL-2	0.821	1.683	1.701	1.544	1.133	1.163	0.554	102	84	36	40	-33	5.12E-7	3.54E-5	> 1.00E-4
SK-MEL-28	0.533	1.353	1.366	0.981	0.781	0.874	0.459	101	55	30	42	-14	1.55E-7	5.62E-5	> 1.00E-4
SK-MEL-5	0.497	2.316	2.212	1.448	0.883	0.454	0.024	94	52	21	-9	-95	1.18E-7	5.13E-6	3.01E-5
UACC-257	0.874	1.952	1.888	1.674	1.654	1.723	0.970	94	74	72	79	9	2.58E-5	> 1.00E-4	> 1.00E-4
UACC-62	0.563	1.867	1.753	1.038	0.931	0.774	0.400	91	36	28	16	-29	5.65E-8	2.28E-5	> 1.00E-4
Ovarian Cancer															
IGROV1	0.570	1.624	1.692	1.292	0.965	0.731	0.571	106	69	37	15	.	3.94E-7	> 1.00E-4	> 1.00E-4
OVCAR-3	0.235	1.670	1.704	1.361	0.666	0.679	0.421	102	78	30	31	13	3.86E-7	> 1.00E-4	> 1.00E-4
OVCAR-4	0.580	1.179	1.132	1.013	0.815	0.724	0.590	92	72	39	24	2	4.72E-7	> 1.00E-4	> 1.00E-4
OVCAR-5	0.521	1.389	1.387	1.386	0.777	0.742	0.666	100	100	30	25	17	5.10E-7	> 1.00E-4	> 1.00E-4
OVCAR-8	0.498	2.234	2.194	2.139	1.174	0.922	0.645	98	95	39	24	8	6.32E-7	> 1.00E-4	> 1.00E-4
NCI/ADR-RES	0.500	1.577	1.528	1.003	0.383	0.459	0.482	95	47	-23	-8	-4	8.55E-8	4.63E-7	> 1.00E-4
SK-OV-3	0.563	1.245	1.249	1.039	0.561	0.521	0.385	101	70	.	-7	-32	1.91E-7	9.86E-7	> 1.00E-4
Renal Cancer															
786-0	0.661	2.226	2.193	2.073	1.010	1.154	0.581	98	90	22	32	-12	3.91E-7	5.28E-5	> 1.00E-4
A498	0.701	1.924	1.746	1.482	1.251	1.190	0.523	85	64	45	40	-25	5.40E-7	4.08E-5	> 1.00E-4
ACHN	0.346	1.413	1.427	1.246	0.896	0.634	0.347	101	84	51	27	.	1.15E-6	> 1.00E-4	> 1.00E-4
CAKI-1	0.638	2.415	2.333	1.725	1.615	1.380	0.974	95	61	55	42	19	2.38E-6	> 1.00E-4	> 1.00E-4
RXF 393	0.511	1.141	1.136	0.970	0.456	0.604	0.593	99	73	-11	15	13	1.88E-7	.	> 1.00E-4
SN12C	0.473	1.819	1.731	1.632	0.948	0.772	0.395	93	86	35	22	-16	5.14E-7	3.75E-5	> 1.00E-4
TK-10	0.909	1.927	1.943	1.904	1.701	1.741	1.044	101	98	78	82	13	2.90E-5	> 1.00E-4	> 1.00E-4
UO-31	0.370	1.243	1.186	1.095	0.806	0.732	0.460	94	83	50	41	10	9.98E-7	> 1.00E-4	> 1.00E-4
Prostate Cancer															
PC-3	0.364	1.281	1.237	1.067	0.742	0.776	0.595	95	77	41	45	25	5.66E-7	> 1.00E-4	> 1.00E-4
DU-145	0.173	1.397	1.399	1.360	0.512	0.406	0.273	100	97	28	19	8	4.77E-7	> 1.00E-4	> 1.00E-4
Breast Cancer															
MCF7	0.280	1.506	1.415	0.705	0.444	0.404	0.277	93	35	13	10	-1	5.43E-8	8.02E-5	> 1.00E-4
MDA-MB-231/ATCC	0.638	1.663	1.639	1.640	1.127	1.086	0.797	98	98	48	44	15	8.98E-7	> 1.00E-4	> 1.00E-4
HS 578T	0.449	1.794	1.738	1.572	1.123	1.145	1.057	96	83	50	52	45	1.86E-5	> 1.00E-4	> 1.00E-4
BT-549	0.868	1.852	1.905	1.742	1.357	0.810	0.398	105	89	50	-7	-54	9.83E-7	7.61E-6	8.16E-5
T-47D	0.549	1.223	1.201	1.155	0.862	1.030	0.612	97	90	46	71	9	.	> 1.00E-4	> 1.00E-4
MDA-MB-468	0.579	1.226	1.151	1.032	0.622	0.598	0.444	88	70	7	3	-23	2.07E-7	1.29E-5	> 1.00E-4

Pyrazoline (71) – Five Dose Repeat

National Cancer Institute Developmental Therapeutics Program
In-Vitro Testing Results

NSC : D - 761261 / 1	Experiment ID : 1111RS58	Test Type : 08	Units : Molar
Report Date : January 05, 2012	Test Date : November 14, 2011	QNS :	MC :
COMI : AC04:42 (109729)	Stain Reagent : SRB Dual-Pass Related	SSPL : 0Y8X	

			Log10 Concentration												
	Time		Mean Optical Densities					Percent Growth							
Panel/Cell Line	Zero	Ctrl	-8.0	-7.0	-6.0	-5.0	-4.0	-8.0	-7.0	-6.0	-5.0	-4.0	GI50	TGI	LC50
Leukemia															
CCRF-CEM	0.526	1.391	1.413	1.399	0.435	0.632	0.452	103	101	-17	12	-14	2.69E-7	.	> 1.00E-4
HL-60(TB)	0.974	2.264	2.174	2.358	0.787	0.671	0.477	93	107	-19	-31	-51	2.84E-7	7.05E-7	8.88E-5
K-562	0.181	1.110	1.215	0.644	0.238	0.247	0.177	111	50	6	7	-2	9.94E-8	5.49E-5	> 1.00E-4
MOLT-4	0.769	2.107	2.264	2.269	1.105	0.739	0.531	112	112	25	-4	-31	5.17E-7	7.33E-6	> 1.00E-4
RPMI-8226	1.047	2.316	2.253	2.215	1.041	1.259	0.582	95	92	-1	17	-44	2.84E-7	.	> 1.00E-4
SR	0.184	0.780	0.712	0.354	0.220	0.219	0.151	88	29	6	6	-18	4.38E-8	1.74E-5	> 1.00E-4
Non-Small Cell Lung Cancer															
A549/ATCC	0.398	1.495	1.452	1.088	0.522	0.516	0.353	96	63	11	11	-11	1.77E-7	3.06E-5	> 1.00E-4
EKVX	0.769	2.033	1.993	1.887	1.332	1.406	1.110	97	88	45	50	27	.	> 1.00E-4	> 1.00E-4
HOP-62	0.414	1.132	1.137	0.961	0.601	0.589	0.473	101	76	26	24	8	3.32E-7	> 1.00E-4	> 1.00E-4
NCI-H23	0.575	1.608	1.611	1.180	0.729	0.675	0.602	100	59	15	10	3	1.57E-7	> 1.00E-4	> 1.00E-4
NCI-H322M	0.694	1.644	1.686	1.678	1.250	1.218	1.199	104	104	59	55	53	> 1.00E-4	> 1.00E-4	> 1.00E-4
NCI-H460	0.251	2.316	2.313	1.755	0.432	0.361	0.163	100	73	9	5	-35	2.27E-7	1.35E-5	> 1.00E-4
NCI-H522	0.550	1.255	1.228	0.603	0.283	0.304	0.285	96	8	-49	-45	-48	3.32E-8	1.36E-7	> 1.00E-4
Colon Cancer															
COLO 205	0.391	1.578	1.695	1.197	0.293	0.063	0.023	110	68	-25	-84	-94	1.56E-7	5.36E-7	2.65E-6
HCC-2998	0.553	1.795	1.747	1.508	0.491	0.439	0.350	96	77	-11	-21	-37	2.02E-7	7.44E-7	> 1.00E-4
HCT-116	0.239	1.374	1.354	1.181	0.390	0.235	0.191	98	83	13	-2	-20	2.97E-7	7.73E-6	> 1.00E-4
HCT-15	0.363	2.219	2.128	1.654	0.833	0.641	0.511	95	70	25	15	8	2.76E-7	> 1.00E-4	> 1.00E-4
HT29	0.243	1.044	1.076	0.686	0.236	0.205	0.127	104	55	-3	-16	-48	1.23E-7	8.85E-7	> 1.00E-4
KM12	0.557	2.364	2.396	1.319	0.879	0.667	0.525	102	42	18	6	-6	7.38E-8	3.26E-5	> 1.00E-4
SW-620	0.276	1.691	1.664	1.121	0.584	0.588	0.491	98	60	22	22	15	1.80E-7	> 1.00E-4	> 1.00E-4
CNS Cancer															
SF-268	0.557	1.610	1.573	1.365	1.038	0.768	0.423	97	77	46	20	-24	7.27E-7	2.85E-5	> 1.00E-4
SF-295	0.764	2.683	2.530	1.304	0.861	1.007	0.791	92	28	5	13	1	4.55E-8	> 1.00E-4	> 1.00E-4
SF-539	0.687	1.992	2.137	1.766	0.708	0.731	0.515	111	83	2	3	-25	2.53E-7	1.31E-5	> 1.00E-4
SNB-19	0.548	1.856	1.829	1.644	1.066	1.073	0.963	98	84	40	40	32	5.81E-7	> 1.00E-4	> 1.00E-4
SNB-75	0.637	1.212	1.167	0.998	0.666	0.725	0.633	92	63	5	15	-1	1.66E-7	9.03E-5	> 1.00E-4
U251	0.343	1.480	1.465	1.175	0.416	0.375	0.163	99	73	6	3	-52	2.22E-7	1.12E-5	9.02E-5
Melanoma															
LOX IMVI	0.668	2.835	2.711	2.245	1.779	1.345	0.709	94	73	51	31	2	1.15E-6	> 1.00E-4	> 1.00E-4
MALME-3M	0.661	1.267	1.266	1.013	0.945	0.955	0.580	100	58	47	48	-12	5.17E-7	6.28E-5	> 1.00E-4
M14	0.386	1.098	1.092	0.936	0.288	0.349	0.162	99	77	-26	-10	-58	1.84E-7	5.64E-7	6.79E-5
MDA-MB-435	0.413	1.831	1.750	0.498	0.245	0.278	0.323	94	6	-41	-33	-22	3.17E-8	1.34E-7	> 1.00E-4
SK-MEL-28	0.394	1.040	1.024	0.752	0.634	0.716	0.400	98	55	37	50	1	1.97E-7	> 1.00E-4	> 1.00E-4
SK-MEL-5	0.594	2.690	2.396	1.464	0.780	0.466	0.042	86	42	9	-22	-93	6.44E-8	1.95E-6	2.50E-5
UACC-257	0.811	1.476	1.423	1.135	1.072	0.971	0.467	92	49	39	24	-42	9.33E-8	2.30E-5	> 1.00E-4
UACC-62	0.659	2.269	2.252	1.384	1.212	0.968	0.444	99	45	34	19	-33	8.08E-8	2.34E-5	> 1.00E-4
Ovarian Cancer															
IGROV1	0.431	1.322	1.373	1.055	0.825	0.653	0.528	106	70	44	25	11	5.97E-7	> 1.00E-4	> 1.00E-4
OVCAR-3	0.401	1.055	1.094	0.591	0.213	0.215	0.195	106	29	-47	-47	-51	5.34E-8	2.41E-7	5.01E-5
OVCAR-4	0.440	1.176	1.176	0.970	0.787	0.666	0.531	100	72	47	31	12	7.67E-7	> 1.00E-4	> 1.00E-4
OVCAR-5	0.493	1.416	1.415	1.326	0.829	0.843	0.703	100	90	36	38	23	5.59E-7	> 1.00E-4	> 1.00E-4
OVCAR-8	0.344	1.227	1.240	1.080	0.475	0.350	0.267	101	83	15	1	-22	3.06E-7	1.06E-5	> 1.00E-4
NCI/ADR-RES	0.244	0.816	0.776	0.567	0.268	0.280	0.252	93	56	4	6	1	1.33E-7	> 1.00E-4	> 1.00E-4
SK-OV-3	0.570	1.088	1.143	0.940	0.600	0.494	0.438	111	71	6	-13	-23	2.12E-7	1.99E-6	> 1.00E-4
Renal Cancer															
786-0	0.665	1.919	1.965	1.776	0.809	0.711	0.333	104	89	11	4	-50	3.17E-7	1.17E-5	> 1.00E-4
A498	1.322	2.172	2.040	1.629	1.319	1.212	0.865	85	36	.	-8	-35	5.16E-8	9.83E-7	> 1.00E-4
ACHN	0.324	1.406	1.471	1.051	0.897	0.669	0.377	106	67	53	32	5	1.38E-6	> 1.00E-4	> 1.00E-4
CAKI-1	0.681	1.942	1.767	1.293	1.235	1.165	0.818	86	49	44	38	11	9.12E-8	> 1.00E-4	> 1.00E-4
RXF 393	0.680	1.343	1.189	1.092	0.537	0.680	0.628	77	62	-21	.	-8	1.40E-7	5.59E-7	> 1.00E-4
SN12C	0.517	2.161	2.074	1.934	1.143	0.991	0.612	95	86	38	29	6	5.65E-7	> 1.00E-4	> 1.00E-4
TK-10	0.544	1.086	1.060	0.924	0.741	0.740	0.465	95	70	36	36	-15	3.93E-7	5.16E-5	> 1.00E-4
UO-31	0.721	1.789	1.649	1.309	1.183	1.136	0.742	87	55	43	39	2	2.68E-7	> 1.00E-4	> 1.00E-4
Prostate Cancer															
PC-3	0.582	1.508	1.526	1.137	0.668	0.662	0.509	102	60	9	9	-13	1.57E-7	2.55E-5	> 1.00E-4
DU-145	0.421	1.220	1.268	1.202	0.397	0.287	0.249	106	98	-6	-32	-41	2.89E-7	8.81E-7	> 1.00E-4
Breast Cancer															
MCF7	0.199	1.087	1.033	0.446	0.354	0.305	0.178	94	28	17	12	-11	4.62E-8	3.35E-5	> 1.00E-4
MDA-MB-231/ATCC	0.513	1.248	1.252	1.224	0.778	0.609	0.496	100	97	36	13	-3	5.88E-7	6.21E-5	> 1.00E-4
HS 578T	0.962	1.679	1.632	1.473	1.139	1.120	1.016	93	71	25	22	7	2.86E-7	> 1.00E-4	> 1.00E-4
T-47D	0.432	1.002	1.027	0.930	0.745	0.849	0.448	104	87	55	73	3	2.13E-5	> 1.00E-4	> 1.00E-4
MDA-MB-468	0.672	1.582	1.371	1.246	0.652	0.647	0.481	77	63	-3	-4	-28	1.58E-7	9.01E-7	> 1.00E-4

Pyrazoline (71–) – Five Dose

National Cancer Institute Developmental Therapeutics Program
In-Vitro Testing Results

NSC : D - 761467 / 1	Experiment ID : 1110NS32	Test Type : 08	Units : Molar
Report Date : November 28, 2011	Test Date : October 03, 2011	QNS :	MC :
COMI : AC04:42.2 (110258)	Stain Reagent : SRB Dual-Pass Related	SSPL : 0Y8X	

		Log10 Concentration												
	Time	Mean Optical Densities					Percent Growth							
Panel/Cell Line	Zero	Ctrl	-8.0	-7.0	-6.0	-5.0	-4.0	-8.0	-7.0	-6.0	-5.0	-4.0	GI50	TGI	LC50
Leukemia															
CCRF-CEM	0.249	1.778	1.765	1.438	0.468	0.399	0.391	99	78	14	10	9	2.74E-7	> 1.00E-4	> 1.00E-4
HL-60(TB)	0.702	2.202	2.116	1.456	0.486	0.427	0.364	94	50	-31	-39	-48	1.01E-7	4.17E-7	> 1.00E-4
K-562	0.180	1.309	1.223	0.411	0.318	0.264	0.183	92	20	12	7	.	3.88E-8	> 1.00E-4	> 1.00E-4
MOLT-4	0.541	1.792	1.742	1.689	0.773	0.558	0.554	96	92	19	1	1	3.72E-7	> 1.00E-4	> 1.00E-4
RPMI-8226	0.492	2.022	1.914	1.731	0.924	0.798	0.402	93	81	28	20	-18	3.87E-7	3.33E-5	> 1.00E-4
SR	0.206	0.718	0.601	0.264	0.257	0.232	0.200	77	11	10	5	-3	2.58E-8	4.09E-5	> 1.00E-4
Non-Small Cell Lung Cancer															
A549/ATCC	0.472	1.702	1.677	1.036	0.644	0.598	0.354	98	46	14	10	-25	8.31E-8	1.95E-5	> 1.00E-4
EKVX	0.775	1.766	1.743	1.514	1.333	1.208	0.790	98	75	56	44	2	3.14E-6	> 1.00E-4	> 1.00E-4
HOP-62	0.360	0.951	0.955	0.619	0.555	0.494	0.239	101	44	33	23	-34	7.76E-8	2.53E-5	> 1.00E-4
NCI-H226	0.639	1.623	1.518	0.999	0.691	0.439	0.475	89	37	5	-31	-26	5.56E-8	1.39E-6	> 1.00E-4
NCI-H23	0.630	1.503	1.480	1.088	0.833	0.675	0.535	97	52	23	5	-15	1.21E-7	1.79E-5	> 1.00E-4
NCI-H322M	0.626	1.523	1.491	1.370	1.142	1.017	0.955	96	83	57	44	37	3.44E-6	> 1.00E-4	> 1.00E-4
NCI-H460	0.254	2.345	2.389	0.706	0.379	0.278	0.134	102	22	6	1	-47	4.44E-8	1.05E-5	> 1.00E-4
NCI-H522	1.202	1.916	1.837	1.103	0.929	0.638	0.437	89	-8	-23	-47	-64	2.51E-8	8.22E-8	1.52E-5
Colon Cancer															
COLO 205	0.234	1.066	1.105	0.513	0.234	0.088	0.029	105	34	.	-62	-88	5.86E-8	9.86E-7	6.32E-6
HCC-2998	0.549	1.563	1.558	1.175	0.399	0.387	0.231	99	62	-27	-30	-58	1.35E-7	4.93E-7	5.26E-5
HCT-116	0.295	1.595	1.591	0.728	0.461	0.260	0.225	100	33	13	-12	-24	5.60E-8	3.27E-6	> 1.00E-4
HCT-15	0.358	2.085	2.076	1.251	0.828	0.580	0.430	99	52	27	13	4	1.17E-7	> 1.00E-4	> 1.00E-4
HT29	0.261	1.240	1.266	0.468	0.245	0.223	0.144	103	21	-6	-15	-45	4.43E-8	5.89E-7	> 1.00E-4
KM12	0.202	0.975	0.902	0.349	0.308	0.158	0.069	91	19	14	-22	-66	3.69E-8	2.41E-6	4.31E-5
SW-620	0.175	1.155	1.091	0.488	0.376	0.368	0.247	93	32	21	20	7	5.08E-8	> 1.00E-4	> 1.00E-4
CNS Cancer															
SF-268	0.512	1.519	1.435	1.099	0.933	0.609	0.218	92	58	42	10	-57	3.18E-7	1.39E-5	7.75E-5
SF-295	0.620	2.397	2.372	1.103	0.843	0.726	0.487	99	27	13	6	-21	4.79E-8	1.65E-5	> 1.00E-4
SF-539	0.694	1.953	1.920	1.146	0.798	0.763	0.318	97	36	8	5	-54	5.89E-8	1.24E-5	8.49E-5
SNB-19	0.511	1.645	1.616	1.138	0.903	0.902	0.675	97	55	35	34	14	1.80E-7	> 1.00E-4	> 1.00E-4
SNB-75	0.566	1.092	1.030	0.671	0.611	0.635	0.467	88	20	8	13	-17	3.63E-8	2.67E-5	> 1.00E-4
U251	0.369	1.490	1.519	0.791	0.501	0.408	0.224	103	38	12	3	-39	6.45E-8	1.20E-5	> 1.00E-4
Melanoma															
LOX IMVI	0.349	2.032	1.936	1.099	1.030	0.653	0.260	94	45	40	18	-26	7.77E-8	2.60E-5	> 1.00E-4
MALME-3M	0.617	1.381	1.373	1.009	1.022	1.006	0.513	99	51	53	51	-17	1.03E-5	5.63E-5	> 1.00E-4
M14	0.425	1.254	1.208	0.756	0.415	0.308	0.210	94	40	-2	-28	-51	6.53E-8	8.74E-7	9.43E-5
MDA-MB-435	0.333	1.573	1.450	0.300	0.247	0.260	0.237	90	-10	-26	-22	-29	2.51E-8	7.93E-8	> 1.00E-4
SK-MEL-2	1.042	1.702	1.677	1.141	1.002	0.913	0.374	96	15	-4	-12	-64	3.70E-8	6.24E-7	5.33E-5
SK-MEL-28	0.387	1.167	1.152	0.694	0.671	0.722	0.195	98	39	36	43	-50	6.59E-8	2.91E-5	> 1.00E-4
SK-MEL-5	0.456	2.390	2.404	0.946	0.686	0.309	0.021	101	25	12	-32	-96	4.71E-8	1.86E-6	1.90E-5
UACC-257	0.736	1.261	1.219	0.927	1.007	0.897	0.528	92	36	52	31	-28	.	3.31E-5	> 1.00E-4
UACC-62	0.778	2.385	2.308	1.481	1.418	1.036	0.304	95	44	40	16	-61	7.56E-8	1.62E-5	7.20E-5
Ovarian Cancer															
IGROV1	0.475	1.513	1.572	1.041	0.892	0.692	0.496	106	54	40	21	2	2.05E-7	> 1.00E-4	> 1.00E-4
OVCAR-3	0.498	1.311	1.277	0.392	0.249	0.249	0.208	96	-21	-50	-50	-58	2.46E-8	6.57E-8	9.92E-7
OVCAR-4	0.455	0.906	0.898	0.770	0.678	0.605	0.412	98	70	49	33	-9	9.33E-7	6.00E-5	> 1.00E-4
OVCAR-5	0.507	1.674	1.597	1.469	0.976	0.891	0.755	93	82	40	33	21	5.85E-7	> 1.00E-4	> 1.00E-4
OVCAR-8	0.438	1.565	1.549	1.178	0.669	0.481	0.339	99	66	20	4	-23	2.22E-7	1.39E-5	> 1.00E-4
NCI/ADR-RES	0.558	1.514	1.488	0.653	0.449	0.425	0.400	97	10	-20	-24	-28	3.47E-8	2.17E-7	> 1.00E-4
SK-OV-3	0.425	1.129	1.118	0.538	0.457	0.436	0.283	98	16	5	2	-34	3.87E-8	1.11E-5	> 1.00E-4
Renal Cancer															
786-0	0.755	2.067	1.988	1.320	1.114	0.889	0.558	94	43	27	10	-26	7.30E-8	1.91E-5	> 1.00E-4
A498	1.148	1.814	1.698	1.277	1.072	0.948	0.688	83	19	-7	-17	-40	3.27E-8	5.55E-7	> 1.00E-4
ACHN	0.337	1.409	1.398	0.836	0.928	0.662	0.283	99	47	55	30	-16	.	4.49E-5	> 1.00E-4
CAKI-1	0.639	2.273	2.194	1.193	1.402	1.061	0.628	95	34	47	26	-2	5.46E-8	8.61E-5	> 1.00E-4
RXF 393	0.517	1.042	1.042	0.655	0.452	0.574	0.537	100	26	-13	11	4	4.76E-8	.	> 1.00E-4
SN12C	0.531	1.901	1.881	1.666	1.159	0.978	0.408	99	83	46	33	-23	7.70E-7	3.84E-5	> 1.00E-4
TK-10	0.885	1.518	1.553	1.253	1.179	1.078	0.659	106	58	46	30	-26	4.97E-7	3.50E-5	> 1.00E-4
UO-31	0.333	1.050	0.980	0.733	0.733	0.663	0.384	90	56	56	46	7	3.85E-6	> 1.00E-4	> 1.00E-4
Prostate Cancer															
PC-3	0.411	1.272	1.227	0.772	0.619	0.633	0.442	95	42	24	26	4	7.02E-8	> 1.00E-4	> 1.00E-4
DU-145	0.386	1.463	1.504	0.851	0.431	0.255	0.226	104	43	4	-34	-42	7.72E-8	1.28E-6	> 1.00E-4
Breast Cancer															
MCF7	0.239	1.321	1.283	0.385	0.441	0.324	0.135	96	13	19	8	-44	3.63E-8	1.42E-5	> 1.00E-4
MDA-MB-231/ATCC	0.639	1.819	1.946	1.768	1.254	1.066	0.565	111	96	52	36	-12	1.36E-6	5.72E-5	> 1.00E-4
HS 578T	0.897	1.625	1.559	1.177	0.975	0.972	0.925	91	38	11	10	4	6.02E-8	> 1.00E-4	> 1.00E-4
BT-549	1.107	1.798	1.761	1.439	1.282	0.837	0.411	95	48	25	-24	-63	9.05E-8	3.23E-6	4.62E-5
T-47D	0.499	1.292	1.289	0.927	0.972	0.974	0.526	100	54	60	60	3	1.50E-5	> 1.00E-4	> 1.00E-4
MDA-MB-468	0.572	1.227	1.182	0.808	0.660	0.623	0.477	93	36	13	8	-17	5.69E-8	2.07E-5	> 1.00E-4

Pyrazoline (71–) – Five Dose Repeat

National Cancer Institute Developmental Therapeutics Program
In-Vitro Testing Results

NSC : D - 761467 / 1	Experiment ID : 1112RS69	Test Type : 08	Units : Molar
Report Date : February 17, 2012	Test Date : December 05, 2011	QNS :	MC :
COMI : AC04:42.2 (110258)	Stain Reagent : SRB Dual-Pass Related	SSPL : 0Y8X	

		Log10 Concentration												
	Time	Mean Optical Densities					Percent Growth							
Panel/Cell Line	Zero	Ctrl	-8.0	-7.0	-6.0	-5.0	-4.0	-8.0	-7.0	-6.0	-5.0	-4.0	GI50	TGI	LC50
Non-Small Cell Lung Cancer															
A549/ATCC	0.296	1.617	1.588	0.915	0.584	0.526	0.361	98	47	22	17	5	8.67E-8	> 1.00E-4	> 1.00E-4
EKVX	0.426	1.258	1.296	1.039	0.643	0.658	0.521	105	74	26	28	11	3.14E-7	> 1.00E-4	> 1.00E-4
HOP-62	0.454	1.287	1.256	0.831	0.709	0.630	0.394	96	45	31	21	-13	8.06E-8	4.12E-5	> 1.00E-4
NCI-H226	0.526	1.105	1.037	0.741	0.689	0.522	0.383	88	37	28	-1	-27	5.59E-8	9.41E-6	> 1.00E-4
NCI-H23	0.648	2.184	2.168	1.062	0.660	0.611	0.698	99	27	1	-6	3	4.78E-8	.	> 1.00E-4
NCI-H322M	0.746	1.657	1.690	1.571	1.311	1.125	1.028	104	91	62	42	31	3.86E-6	> 1.00E-4	> 1.00E-4
NCI-H460	0.309	2.476	2.465	1.451	0.520	0.416	0.169	99	53	10	5	-45	1.16E-7	1.25E-5	> 1.00E-4
NCI-H522	0.682	1.526	1.447	0.618	0.583	0.519	0.413	91	-9	-15	-24	-39	2.55E-8	8.06E-8	> 1.00E-4
Colon Cancer															
COLO 205	0.316	1.163	1.167	0.537	0.253	0.076	0.054	100	26	-20	-76	-83	4.76E-8	3.67E-7	3.43E-6
HCC-2998	0.382	1.254	1.217	1.027	0.476	0.506	0.336	96	74	11	14	-12	2.39E-7	3.48E-5	> 1.00E-4
HCT-116	0.236	1.603	1.595	0.667	0.458	0.252	0.244	99	32	16	1	1	5.34E-8	> 1.00E-4	> 1.00E-4
HCT-15	0.426	2.299	2.226	1.290	0.840	0.626	0.512	96	46	22	11	5	8.37E-8	> 1.00E-4	> 1.00E-4
HT29	0.249	1.376	1.401	0.769	0.347	0.307	0.178	102	46	9	5	-29	8.54E-8	1.42E-5	> 1.00E-4
KM12	0.625	2.529	2.472	1.299	1.141	1.008	0.672	97	35	27	20	2	5.79E-8	> 1.00E-4	> 1.00E-4
SW-620	0.264	1.650	1.633	0.871	0.602	0.548	0.397	99	44	24	20	10	7.71E-8	> 1.00E-4	> 1.00E-4
CNS Cancer															
SF-268	0.528	1.701	1.652	1.318	1.237	0.997	0.422	96	67	60	40	-20	3.24E-6	4.62E-5	> 1.00E-4
SF-295	0.834	2.577	2.493	1.193	0.870	0.869	0.627	95	21	2	2	-25	4.03E-8	1.19E-5	> 1.00E-4
SNB-19	0.551	1.775	1.676	1.108	0.924	0.906	0.738	92	46	30	29	15	8.01E-8	> 1.00E-4	> 1.00E-4
SNB-75	0.716	1.204	1.154	0.758	0.826	0.835	0.572	90	9	22	24	-20	3.09E-8	3.52E-5	> 1.00E-4
U251	0.365	1.834	1.846	1.068	0.464	0.398	0.116	101	48	7	2	-68	9.11E-8	1.07E-5	5.49E-5
Melanoma															
LOX IMVI	0.286	1.941	2.061	1.156	0.994	0.777	0.351	107	53	43	30	4	1.82E-7	> 1.00E-4	> 1.00E-4
MALME-3M	0.749	1.491	1.465	1.160	1.087	1.115	0.646	97	55	46	49	-14	3.53E-7	6.05E-5	> 1.00E-4
M14	0.429	1.429	1.393	0.906	0.495	0.390	0.216	96	48	7	-9	-50	8.96E-8	2.62E-6	> 1.00E-4
MDA-MB-435	0.561	2.362	2.301	0.627	0.451	0.434	0.352	97	4	-20	-23	-37	3.17E-8	1.43E-7	> 1.00E-4
SK-MEL-2	0.914	1.621	1.595	1.268	1.207	1.138	0.477	96	50	41	32	-48	1.00E-7	2.50E-5	> 1.00E-4
SK-MEL-28	0.333	0.974	0.959	0.651	0.570	0.574	0.147	98	50	37	38	-56	9.83E-8	2.52E-5	8.63E-5
SK-MEL-5	0.584	2.534	2.313	0.510	0.444	0.243	0.006	89	-13	-24	-58	-99	2.41E-8	7.49E-8	5.70E-6
UACC-257	0.593	1.313	1.276	0.910	1.059	1.018	0.544	95	44	65	59	-8	.	7.54E-5	> 1.00E-4
UACC-62	0.632	2.094	2.120	1.153	1.020	0.830	0.208	102	36	27	14	-67	6.06E-8	1.47E-5	6.14E-5
Ovarian Cancer															
IGROV1	0.402	1.343	1.396	0.878	0.686	0.489	0.338	106	51	30	9	-16	1.07E-7	2.32E-5	> 1.00E-4
OVCAR-3	0.491	1.490	1.462	0.809	0.774	0.678	0.395	97	32	28	19	-20	5.28E-8	3.08E-5	> 1.00E-4
OVCAR-4	0.565	1.140	1.104	0.888	0.770	0.684	0.535	94	56	36	21	-5	1.99E-7	6.25E-5	> 1.00E-4
OVCAR-5	0.596	1.444	1.295	1.022	0.849	0.770	0.655	82	50	30	20	7	1.02E-7	> 1.00E-4	> 1.00E-4
NCI/ADR-RES	0.456	1.623	1.634	0.839	0.513	0.528	0.485	101	33	5	6	2	5.59E-8	> 1.00E-4	> 1.00E-4
SK-OV-3	0.592	1.396	1.385	0.812	0.687	0.532	0.485	99	27	12	-10	-18	4.81E-8	3.44E-6	> 1.00E-4
Renal Cancer															
786-0	0.581	1.899	1.917	1.499	0.939	0.766	0.433	101	70	27	14	-26	2.90E-7	2.26E-5	> 1.00E-4
A498	1.385	2.014	2.006	1.506	1.373	1.158	0.598	99	19	-1	-16	-57	4.10E-8	9.06E-7	6.77E-5
ACHN	0.398	1.604	1.569	0.930	0.929	0.641	0.364	97	44	44	20	-9	7.73E-8	5.00E-5	> 1.00E-4
CAKI-1	0.744	1.915	1.849	1.297	1.372	1.106	0.602	94	47	54	31	-19	.	4.14E-5	> 1.00E-4
RXF 393	0.627	1.068	1.037	0.644	0.484	0.604	0.500	93	4	-23	-4	-20	3.04E-8	1.39E-7	> 1.00E-4
SN12C	0.596	2.210	2.165	1.666	1.159	0.951	0.554	97	66	35	22	-7	3.30E-7	5.69E-5	> 1.00E-4
TK-10	0.591	1.201	1.170	1.055	0.882	0.903	0.607	95	76	48	51	3	.	> 1.00E-4	> 1.00E-4
UO-31	0.572	1.623	1.444	1.054	1.010	0.976	0.459	83	46	42	38	-20	7.73E-8	4.57E-5	> 1.00E-4
Prostate Cancer															
PC-3	0.381	1.744	1.739	1.135	0.627	0.601	0.471	100	55	18	16	7	1.39E-7	> 1.00E-4	> 1.00E-4
DU-145	0.556	1.758	1.787	1.511	0.924	0.778	0.539	102	79	31	18	-3	4.00E-7	7.21E-5	> 1.00E-4
Breast Cancer															
MCF7	0.299	1.689	1.575	0.432	0.443	0.339	0.235	92	10	10	3	-22	3.22E-8	1.31E-5	> 1.00E-4
MDA-MB-231/ATCC	0.504	1.088	1.128	0.989	0.636	0.411	0.376	107	83	23	-19	-25	3.51E-7	3.54E-6	> 1.00E-4
HS 578T	0.966	1.788	1.739	1.452	1.035	1.130	0.926	94	59	8	20	-4	1.51E-7	6.72E-5	> 1.00E-4
BT-549	0.873	1.609	1.614	1.410	1.371	1.000	0.403	101	73	68	17	-54	2.24E-6	1.75E-5	8.83E-5
T-47D	0.585	1.624	1.586	0.926	1.213	1.220	0.645	96	33	60	61	6	.	> 1.00E-4	> 1.00E-4
MDA-MB-468	0.583	1.219	1.143	0.538	0.514	0.507	0.420	88	-8	-12	-13	-28	2.49E-8	8.29E-8	> 1.00E-4

Pyrazoline (71–) – Five Dose Third Repeat

National Cancer Institute Developmental Therapeutics Program
In-Vitro Testing Results

NSC : D - 761467 / 1	Experiment ID : 1206RS81	Test Type : 08	Units : Molar
Report Date : August 01, 2012	Test Date : June 04, 2012	QNS :	MC :
COMI : AC04:42.2 (110258)	Stain Reagent : SRB Dual-Pass Related	SSPL : 0Y8X	

		Log10 Concentration												
	Time	Mean Optical Densities					Percent Growth							
Panel/Cell Line	Zero	Ctrl	-8.0	-7.0	-6.0	-5.0	-4.0	-8.0	-7.0	-6.0	-5.0	-4.0	GI50	TGI	LC50
Leukemia															
CCRF-CEM	0.337	1.463	1.470	1.129	0.466	0.416	0.366	101	70	11	7	3	2.21E-7	> 1.00E-4	> 1.00E-4
HL-60(TB)	0.916	3.107	3.004	1.463	0.795	0.743	0.617	95	25	-13	-19	-33	4.41E-8	4.51E-7	> 1.00E-4
K-562	0.237	1.870	1.844	0.651	0.373	0.335	0.258	98	25	8	6	1	4.60E-8	> 1.00E-4	> 1.00E-4
MOLT-4	0.501	1.662	1.669	1.583	0.585	0.448	0.504	101	93	7	-11	.	3.18E-7	.	> 1.00E-4
RPMI-8226	0.793	2.136	2.144	1.713	0.940	0.817	0.522	101	68	11	2	-34	2.09E-7	1.12E-5	> 1.00E-4
Non-Small Cell Lung Cancer															
A549/ATCC	0.415	2.024	2.004	1.212	0.709	0.641	0.443	99	50	18	14	2	9.77E-8	> 1.00E-4	> 1.00E-4
HOP-62	0.352	1.010	0.954	0.652	0.575	0.528	0.289	92	46	34	27	-18	8.00E-8	3.97E-5	> 1.00E-4
HOP-92	1.090	1.638	1.585	1.471	1.522	1.368	0.947	90	70	79	51	-13	1.02E-5	6.22E-5	> 1.00E-4
NCI-H226	0.678	1.551	1.452	1.306	1.348	1.027	0.526	89	72	77	40	-22	5.33E-6	4.37E-5	> 1.00E-4
NCI-H23	0.394	1.302	1.256	0.983	0.532	0.435	0.334	95	65	15	4	-15	1.99E-7	1.68E-5	> 1.00E-4
NCI-H322M	0.673	1.582	1.456	1.377	0.985	0.891	0.772	86	77	34	24	11	4.32E-7	> 1.00E-4	> 1.00E-4
NCI-H460	0.296	2.582	2.549	1.023	0.397	0.282	0.153	99	32	4	-5	-48	5.34E-8	3.04E-6	> 1.00E-4
NCI-H522	0.814	2.269	2.211	0.976	0.659	0.644	0.637	96	11	-19	-21	-22	3.48E-8	2.34E-7	> 1.00E-4
Colon Cancer															
COLO 205	0.329	1.397	1.391	0.657	0.179	0.058	0.012	99	31	-46	-83	-97	5.23E-8	2.52E-7	1.32E-6
HCC-2998	0.834	2.868	2.828	2.363	0.680	0.674	0.317	98	75	-19	-19	-62	1.86E-7	6.34E-7	5.23E-5
HCT-116	0.100	1.317	1.310	0.539	0.267	0.153	0.148	99	36	14	4	4	6.02E-8	> 1.00E-4	> 1.00E-4
HCT-15	0.233	1.577	1.532	0.834	0.457	0.314	0.301	97	45	17	6	5	7.90E-8	> 1.00E-4	> 1.00E-4
HT29	0.236	1.616	1.689	0.805	0.365	0.298	0.214	105	41	9	4	-10	7.30E-8	2.09E-5	> 1.00E-4
KM12	0.458	2.186	2.072	0.884	0.707	0.421	0.279	93	25	14	-8	-39	4.28E-8	4.34E-6	> 1.00E-4
SW-620	0.272	1.882	1.795	0.883	0.585	0.543	0.367	95	38	19	17	6	6.13E-8	> 1.00E-4	> 1.00E-4
CNS Cancer															
SF-268	0.632	1.637	1.587	1.255	1.158	0.792	0.303	95	62	52	16	-52	1.15E-6	1.71E-5	9.30E-5
SF-295	0.821	2.555	2.478	1.073	0.803	0.797	0.370	96	15	-2	-3	-55	3.65E-8	7.34E-7	8.02E-5
SF-539	0.792	2.263	2.191	1.157	0.680	0.688	0.418	95	25	-14	-13	-47	4.38E-8	4.32E-7	> 1.00E-4
SNB-19	0.528	1.495	1.433	1.200	0.883	0.870	0.655	94	69	37	35	13	3.93E-7	> 1.00E-4	> 1.00E-4
SNB-75	0.768	1.407	1.234	0.751	0.823	0.848	0.581	73	-2	9	12	-24	2.02E-8	.	> 1.00E-4
U251	0.428	1.704	1.668	1.311	0.607	0.490	0.263	97	69	14	5	-39	2.22E-7	1.29E-5	> 1.00E-4
Melanoma															
LOX IMVI	0.158	1.297	1.236	0.518	0.296	0.171	0.102	95	32	12	1	-36	5.11E-8	1.07E-5	> 1.00E-4
MALME-3M	0.538	0.979	0.894	0.761	0.771	0.770	0.435	81	51	53	52	-19	1.08E-5	5.40E-5	> 1.00E-4
M14	0.339	1.541	1.493	0.886	0.366	0.355	0.264	96	46	2	1	-22	8.15E-8	1.14E-5	> 1.00E-4
MDA-MB-435	0.404	2.005	1.924	0.369	0.307	0.292	0.220	95	-9	-24	-28	-46	2.72E-8	8.25E-8	> 1.00E-4
SK-MEL-2	0.504	1.091	1.123	0.840	0.771	0.733	0.413	105	57	45	39	-18	4.06E-7	4.81E-5	> 1.00E-4
SK-MEL-28	0.490	1.394	1.358	0.964	0.892	0.906	0.286	96	52	44	46	-42	1.99E-7	3.35E-5	> 1.00E-4
SK-MEL-5	0.455	2.306	2.192	0.564	0.536	0.286	0.044	94	6	4	-37	-90	3.15E-8	1.27E-6	1.74E-5
UACC-257	0.873	2.020	1.952	1.370	1.341	1.247	0.613	94	43	41	33	-30	7.40E-8	3.33E-5	> 1.00E-4
UACC-62	0.595	1.631	1.584	0.905	0.840	0.637	0.152	95	30	24	4	-75	4.93E-8	1.12E-5	4.87E-5
Ovarian Cancer															
IGROV1	0.641	1.776	1.728	1.264	1.070	0.840	0.599	96	55	38	17	-7	1.92E-7	5.34E-5	> 1.00E-4
OVCAR-3	0.575	1.502	1.535	0.504	0.309	0.270	0.181	104	-12	-46	-53	-69	2.89E-8	7.81E-8	3.56E-6
OVCAR-4	0.673	1.440	1.396	1.197	1.003	0.866	0.608	94	68	43	25	-10	5.27E-7	5.27E-5	> 1.00E-4
OVCAR-5	0.445	1.375	1.302	1.141	0.759	0.701	0.550	92	75	34	27	11	4.02E-7	> 1.00E-4	> 1.00E-4
OVCAR-8	0.519	2.115	2.114	1.751	0.804	0.570	0.372	100	77	18	3	-28	2.87E-7	1.26E-5	> 1.00E-4
NCI/ADR-RES	0.524	1.852	1.842	0.782	0.390	0.390	0.379	99	19	-26	-26	-28	4.14E-8	2.69E-7	> 1.00E-4
SK-OV-3	0.478	1.082	1.082	0.683	0.460	0.401	0.340	100	34	-4	-16	-29	5.71E-8	7.94E-7	> 1.00E-4
Renal Cancer															
786-0	0.606	2.203	2.191	1.612	1.378	0.994	0.593	99	63	48	24	-2	7.71E-7	8.24E-5	> 1.00E-4
A498	1.326	1.917	1.930	1.391	1.221	1.082	0.535	102	11	-8	-18	-60	3.74E-8	3.82E-7	5.83E-5
ACHN	0.313	1.222	1.212	0.653	0.677	0.513	0.255	99	37	40	22	-19	6.23E-8	3.47E-5	> 1.00E-4
CAKI-1	0.634	2.588	2.501	1.226	1.310	1.042	0.638	96	30	35	21	.	4.99E-8	> 1.00E-4	> 1.00E-4
RXF 393	0.552	1.041	0.989	0.623	0.559	0.569	0.457	89	15	1	3	-17	3.36E-8	1.46E-5	> 1.00E-4
SN12C	0.507	1.850	1.800	1.642	0.963	0.759	0.295	96	85	34	19	-42	4.81E-7	2.04E-5	> 1.00E-4
UO-31	0.575	1.508	1.453	1.084	1.032	0.912	0.456	94	55	49	36	-21	6.58E-7	4.32E-5	> 1.00E-4
Prostate Cancer															
PC-3	0.578	2.271	2.240	1.470	0.976	0.943	0.615	98	53	23	22	2	1.24E-7	> 1.00E-4	> 1.00E-4
DU-145	0.466	1.547	1.571	1.179	0.498	0.310	0.235	102	66	3	-33	-50	1.79E-7	1.21E-6	> 1.00E-4
Breast Cancer															
MCF7	0.357	1.859	1.688	0.584	0.573	0.473	0.332	89	15	14	8	-7	3.35E-8	3.30E-5	> 1.00E-4
MDA-MB-231/ATCC	0.553	1.337	1.354	1.212	0.826	0.562	0.340	102	84	35	1	-39	4.91E-7	1.06E-5	> 1.00E-4
HS 578T	0.953	1.480	1.402	1.228	1.123	1.103	0.931	85	52	32	28	-2	1.29E-7	8.41E-5	> 1.00E-4
BT-549	0.726	1.972	1.984	1.507	1.068	0.736	0.441	101	63	27	1	-39	2.29E-7	1.04E-5	> 1.00E-4
T-47D	0.618	1.442	1.369	0.854	1.023	1.110	0.599	91	29	49	60	-3	.	8.91E-5	> 1.00E-4
MDA-MB-468	0.594	1.136	1.083	0.550	0.579	0.532	0.423	90	-7	-3	-11	-29	2.58E-8	8.40E-8	> 1.00E-4

Pyrazoline (71+) – Five Dose

National Cancer Institute Developmental Therapeutics Program
In-Vitro Testing Results

NSC : D - 761464 / 1	Experiment ID : 1110NS32	Test Type : 08	Units : Molar
Report Date : November 28, 2011	Test Date : October 03, 2011	QNS :	MC :
COMI : AC04:42.1 (110257)	Stain Reagent : SRB Dual-Pass Related	SSPL : 0Y8X	

Log10 Concentration

	Time	Mean Optical Densities						Percent Growth							
Panel/Cell Line	Zero	Ctrl	-8.0	-7.0	-6.0	-5.0	-4.0	-8.0	-7.0	-6.0	-5.0	-4.0	GI50	TGI	LC50
Leukemia															
CCRF-CEM	0.249	1.975	1.928	1.946	1.891	0.594	0.447	97	98	95	20	11	3.98E-6	> 1.00E-4	> 1.00E-4
HL-60(TB)	0.702	2.148	2.010	1.975	2.082	0.501	0.330	90	88	95	-29	-53	2.32E-6	5.88E-6	7.54E-5
K-562	0.180	1.195	1.209	1.170	0.923	0.216	0.134	101	98	73	3	-26	2.15E-6	1.32E-5	> 1.00E-4
MOLT-4	0.541	1.605	1.634	1.560	1.627	0.819	0.425	103	96	102	26	-21	4.84E-6	3.54E-5	> 1.00E-4
RPMI-8226	0.492	2.005	1.943	1.941	1.927	0.816	0.445	96	96	95	21	-10	4.08E-6	4.89E-5	> 1.00E-4
SR	0.206	0.637	0.493	0.490	0.345	0.189	0.160	67	66	32	-8	-23	2.97E-7	6.19E-6	> 1.00E-4
Non-Small Cell Lung Cancer															
A549/ATCC	0.472	1.777	1.738	1.720	1.710	0.704	0.330	97	96	95	18	-30	3.82E-6	2.35E-5	> 1.00E-4
EKVX	0.775	1.847	1.839	1.841	1.700	1.224	0.937	99	99	86	42	15	6.56E-6	> 1.00E-4	> 1.00E-4
HOP-62	0.360	0.856	0.818	0.778	0.830	0.453	0.341	92	84	95	19	-5	3.88E-6	5.97E-5	> 1.00E-4
NCI-H226	0.639	1.576	1.518	1.515	1.447	0.785	0.502	94	93	86	16	-21	3.25E-6	2.63E-5	> 1.00E-4
NCI-H23	0.630	1.424	1.435	1.423	1.267	0.774	0.541	101	100	80	18	-14	3.06E-6	3.64E-5	> 1.00E-4
NCI-H322M	0.626	1.479	1.439	1.449	1.458	0.987	0.975	95	97	98	42	41	7.25E-6	> 1.00E-4	> 1.00E-4
NCI-H460	0.254	2.191	2.251	2.224	2.101	0.386	0.118	103	102	95	7	-54	3.25E-6	1.30E-5	8.67E-5
NCI-H522	1.202	1.827	1.772	1.743	1.620	0.814	0.521	91	87	67	-32	-57	1.48E-6	4.72E-6	5.33E-5
Colon Cancer															
COLO 205	0.234	0.955	1.048	0.958	1.016	0.246	0.087	113	100	109	2	-63	3.53E-6	1.06E-5	6.33E-5
HCC-2998	0.549	1.470	1.453	1.454	1.347	0.683	0.264	98	98	87	15	-52	3.22E-6	1.65E-5	9.33E-5
HCT-116	0.295	1.501	1.518	1.510	1.528	0.531	0.205	101	101	102	20	-31	4.28E-6	2.46E-5	> 1.00E-4
HCT-15	0.358	1.804	1.703	1.771	1.701	0.727	0.370	93	98	93	26	1	4.33E-6	> 1.00E-4	> 1.00E-4
HT29	0.261	1.155	1.146	1.188	1.187	0.212	0.140	99	104	104	-19	-47	2.74E-6	7.02E-6	> 1.00E-4
KM12	0.202	0.951	0.908	0.944	0.780	0.321	0.145	94	99	77	16	-28	2.77E-6	2.29E-5	> 1.00E-4
SW-620	0.175	1.098	1.058	1.039	0.920	0.320	0.234	96	94	81	16	6	2.97E-6	> 1.00E-4	> 1.00E-4
CNS Cancer															
SF-268	0.512	1.492	1.461	1.420	1.385	0.939	0.523	97	93	89	44	1	7.23E-6	> 1.00E-4	> 1.00E-4
SF-295	0.620	2.296	2.198	2.251	2.001	0.830	0.490	94	97	82	13	-21	2.91E-6	2.36E-5	> 1.00E-4
SF-539	0.694	1.782	1.696	1.705	1.668	0.648	0.476	92	93	90	-7	-31	2.58E-6	8.52E-6	> 1.00E-4
SNB-19	0.511	1.717	1.712	1.529	1.487	0.826	0.686	100	84	81	26	15	3.66E-6	> 1.00E-4	> 1.00E-4
SNB-75	0.566	1.024	0.983	0.941	0.916	0.482	0.426	91	82	76	-15	-25	1.95E-6	6.87E-6	> 1.00E-4
U251	0.369	1.516	1.475	1.477	1.382	0.504	0.242	96	97	88	12	-34	3.16E-6	1.80E-5	> 1.00E-4
Melanoma															
LOX IMVI	0.349	1.835	1.775	1.740	1.613	0.879	0.379	96	94	85	36	2	5.12E-6	> 1.00E-4	> 1.00E-4
MALME-3M	0.617	1.331	1.282	1.300	1.259	0.877	0.521	93	96	90	36	-16	5.57E-6	5.01E-5	> 1.00E-4
M14	0.425	1.185	1.178	1.173	1.120	0.347	0.259	99	98	91	-18	-39	2.38E-6	6.79E-6	> 1.00E-4
MDA-MB-435	0.333	1.427	1.404	1.390	0.726	0.160	0.308	98	97	36	-52	-8	5.85E-7	2.56E-6	
SK-MEL-2	1.042	1.549	1.544	1.561	1.536	0.779	0.595	99	102	97	-25	-43	2.43E-6	6.22E-6	> 1.00E-4
SK-MEL-28	0.387	1.096	1.097	1.098	0.947	0.585	0.436	100	100	79	28	7	3.69E-6	> 1.00E-4	> 1.00E-4
SK-MEL-5	0.456	2.333	2.301	2.186	1.848	0.712	0.057	98	92	74	14	-88	2.51E-6	1.36E-5	4.25E-5
UACC-257	0.736	1.210	1.208	1.218	1.129	0.858	0.509	100	102	83	26	-31	3.76E-6	2.84E-5	> 1.00E-4
UACC-62	0.778	2.291	2.299	2.296	1.960	1.334	0.697	101	100	78	37	-10	4.78E-6	6.00E-5	> 1.00E-4
Ovarian Cancer															
IGROV1	0.475	1.484	1.525	1.530	1.326	0.913	0.582	104	105	84	43	11	6.91E-6	> 1.00E-4	> 1.00E-4
OVCAR-3	0.498	1.293	1.289	1.275	1.223	0.314	0.255	100	98	91	-37	-49	2.10E-6	5.15E-6	> 1.00E-4
OVCAR-4	0.455	0.837	0.799	0.824	0.736	0.604	0.416	90	97	73	39	-9	4.76E-6	6.60E-5	> 1.00E-4
OVCAR-5	0.507	1.508	1.545	1.502	1.507	0.828	0.643	104	99	100	32	14	5.43E-6	> 1.00E-4	> 1.00E-4
OVCAR-8	0.438	1.473	1.471	1.497	1.501	0.618	0.369	100	102	103	17	-16	4.14E-6	3.33E-5	> 1.00E-4
NCI/ADR-RES	0.558	1.400	1.422	1.371	1.144	0.424	0.416	103	97	70	-24	-26	1.62E-6	5.53E-6	> 1.00E-4
SK-OV-3	0.425	1.062	1.068	1.015	1.017	0.408	0.279	101	93	93	-4	-34	2.77E-6	9.07E-6	> 1.00E-4
Renal Cancer															
786-0	0.755	2.134	2.055	2.035	2.050	1.146	0.760	94	93	94	28	.	4.68E-6	> 1.00E-4	> 1.00E-4
A498	1.148	1.686	1.517	1.553	1.432	0.944	0.751	69	75	53	-18	-35	1.09E-6	5.59E-6	> 1.00E-4
ACHN	0.337	1.201	1.222	1.215	1.231	0.761	0.329	102	102	103	49	-2	9.59E-6	8.99E-5	> 1.00E-4
CAKI-1	0.639	2.304	2.272	2.282	1.896	1.218	0.852	98	99	75	35	13	4.22E-6	> 1.00E-4	> 1.00E-4
RXF 393	0.517	1.079	1.031	1.051	0.957	0.412	0.370	91	95	78	-20	-29	1.94E-6	6.22E-6	> 1.00E-4
SN12C	0.531	1.798	1.747	1.742	1.724	1.049	0.594	96	96	94	41	5	6.74E-6	> 1.00E-4	> 1.00E-4
TK-10	0.885	1.467	1.507	1.513	1.520	1.110	0.662	107	108	109	39	-25	6.89E-6	4.03E-5	> 1.00E-4
UO-31	0.333	1.039	0.970	0.969	0.937	0.689	0.403	90	90	85	50	10	1.02E-5	> 1.00E-4	> 1.00E-4
Prostate Cancer															
PC-3	0.411	1.196	1.203	1.196	1.060	0.612	0.386	101	100	83	26	-6	3.74E-6	6.43E-5	> 1.00E-4
DU-145	0.386	1.394	1.413	1.395	1.363	0.304	0.300	102	100	97	-21	-22	2.49E-6	6.61E-6	> 1.00E-4
Breast Cancer															
MCF7	0.239	1.328	1.274	1.262	1.043	0.393	0.180	95	94	74	14	-25	2.51E-6	2.30E-5	> 1.00E-4
MDA-MB-231/ATCC	0.639	1.719	1.749	1.753	1.685	1.176	0.881	103	103	97	50	22	9.86E-6	> 1.00E-4	> 1.00E-4
HS 578T	0.897	1.654	1.600	1.580	1.496	0.935	0.821	93	90	79	5	-9	2.47E-6	2.33E-5	> 1.00E-4
BT-549	1.107	1.926	1.917	1.937	1.901	1.620	0.784	99	101	97	63	-29	1.37E-5	4.81E-5	> 1.00E-4
T-47D	0.499	1.261	1.227	1.198	1.222	0.862	0.532	96	92	95	48	4	8.90E-6	> 1.00E-4	> 1.00E-4
MDA-MB-468	0.572	1.208	1.171	1.178	1.078	0.538	0.426	94	95	80	-6	-26	2.21E-6	8.50E-6	> 1.00E-4

Pyrazoline (74) – Five Dose

National Cancer Institute Developmental Therapeutics Program
In-Vitro Testing Results

NSC : D - 761262 / 1	Experiment ID : 1109NS21	Test Type : 08	Units : Molar
Report Date : October 26, 2011	Test Date : September 12, 2011	QNS :	MC :
COMI : AC04:48 (109730)	Stain Reagent : SRB Dual-Pass Related	SSPL : 0Y8X	

			Log10 Concentration											
	Time		Mean Optical Densities					Percent Growth						
Panel/Cell Line	Zero	Ctrl	-8.0	-7.0	-6.0	-5.0	-4.0	-8.0	-7.0	-6.0	-5.0	-4.0	GI50	TGI	LC50
Leukemia															
CCRF-CEM	0.380	1.539	1.611	1.588	0.630	0.420	0.427	106	104	22	3	4	4.53E-7	> 1.00E-4	> 1.00E-4
HL-60(TB)	0.695	2.367	2.182	2.234	0.808	0.560	0.444	89	92	7	-19	-36	3.11E-7	1.81E-6	> 1.00E-4
MOLT-4	0.518	2.190	2.093	2.156	1.287	0.714	0.502	94	98	46	12	-3	8.37E-7	6.19E-5	> 1.00E-4
RPMI-8226	0.673	2.422	2.414	2.265	1.360	0.964	0.565	100	91	39	17	-16	6.20E-7	3.23E-5	> 1.00E-4
SR	0.449	2.303	2.172	1.919	0.760	0.590	0.368	93	79	17	8	-18	2.94E-7	1.97E-5	> 1.00E-4
Non-Small Cell Lung Cancer															
A549/ATCC	0.410	1.997	1.942	1.909	0.981	0.752	0.526	97	94	36	22	7	5.76E-7	> 1.00E-4	> 1.00E-4
EKVX	0.836	2.019	1.973	1.926	1.645	1.520	1.177	96	92	68	58	29	1.86E-5	> 1.00E-4	> 1.00E-4
HOP-62	0.407	1.030	0.991	0.961	0.592	0.610	0.493	94	89	30	33	14	4.55E-7	> 1.00E-4	> 1.00E-4
HOP-92	0.903	2.106	2.039	1.893	1.431	1.426	1.067	94	82	44	43	14	6.93E-7	> 1.00E-4	> 1.00E-4
NCI-H226	0.668	1.555	1.491	1.475	0.792	0.580	0.409	93	91	14	-13	-39	3.41E-7	3.26E-6	> 1.00E-4
NCI-H23	0.445	1.309	1.224	1.199	0.818	0.585	0.448	90	87	43	16	.	6.97E-7	> 1.00E-4	> 1.00E-4
NCI-H322M	0.717	1.613	1.581	1.527	1.143	1.044	0.936	96	90	48	36	24	8.76E-7	> 1.00E-4	> 1.00E-4
NCI-H460	0.172	1.997	1.962	2.005	0.398	0.269	0.068	98	100	12	5	-60	3.74E-7	1.20E-5	6.93E-5
NCI-H522	0.798	1.818	1.740	1.723	0.865	0.759	0.691	92	91	7	-5	-13	3.04E-7	3.73E-6	> 1.00E-4
Colon Cancer															
COLO 205	0.315	1.214	1.288	1.322	0.400	0.200	0.081	108	112	9	-37	-74	4.02E-7	1.60E-6	2.25E-5
HCC-2998	0.424	1.383	1.383	1.329	0.879	0.451	0.319	100	94	47	3	-25	8.81E-7	1.26E-5	> 1.00E-4
HCT-116	0.194	1.464	1.384	1.345	0.489	0.331	0.163	94	91	23	11	-16	4.00E-7	2.50E-5	> 1.00E-4
HCT-15	0.395	1.951	1.898	1.823	0.920	0.654	0.439	97	92	34	17	3	5.24E-7	> 1.00E-4	> 1.00E-4
HT29	0.216	1.383	1.355	1.352	0.318	0.273	0.187	99	99	9	5	-13	3.50E-7	1.86E-5	> 1.00E-4
KM12	0.322	2.266	2.350	2.077	0.851	0.706	0.482	104	90	27	20	8	4.35E-7	> 1.00E-4	> 1.00E-4
SW-620	0.196	1.717	1.665	1.632	0.486	0.567	0.452	97	94	19	24	17	3.88E-7	> 1.00E-4	> 1.00E-4
CNS Cancer															
SF-268	0.280	1.538	1.593	1.373	0.848	0.704	0.577	104	87	45	34	24	7.64E-7	> 1.00E-4	> 1.00E-4
SF-539	0.713	2.023	1.978	1.903	0.895	0.742	0.615	97	91	14	2	-14	3.40E-7	1.37E-5	> 1.00E-4
SNB-19	0.476	1.634	1.580	1.545	0.904	0.747	0.667	95	92	37	23	16	5.82E-7	> 1.00E-4	> 1.00E-4
SNB-75	0.863	1.588	1.393	1.369	0.601	0.843	0.825	73	70	-30	-2	-4	1.58E-7	4.98E-7	> 1.00E-4
U251	0.365	1.666	1.620	1.567	0.730	0.588	0.367	96	92	28	17	.	4.56E-7	> 1.00E-4	> 1.00E-4
Melanoma															
LOX IMVI	0.247	1.511	1.466	1.437	0.669	0.639	0.237	96	94	33	31	-4	5.33E-7	7.57E-5	> 1.00E-4
MALME-3M	0.602	1.316	1.277	1.202	0.770	0.905	0.735	95	84	23	42	19	3.64E-7	> 1.00E-4	> 1.00E-4
M14	0.317	1.127	1.097	1.038	0.579	0.355	0.190	96	89	32	5	-40	4.87E-7	1.27E-5	> 1.00E-4
MDA-MB-435	0.551	2.486	2.460	2.017	0.281	0.261	0.309	99	76	-49	-53	-44	1.61E-7	4.05E-7	.
SK-MEL-2	0.821	1.689	1.659	1.646	1.044	1.019	0.769	97	95	26	23	-6	4.48E-7	6.04E-5	> 1.00E-4
SK-MEL-28	0.533	1.365	1.375	1.313	0.903	0.810	0.665	101	94	44	33	16	7.71E-7	> 1.00E-4	> 1.00E-4
SK-MEL-5	0.497	2.185	2.159	1.999	0.628	0.597	0.064	98	89	8	6	-87	3.02E-7	1.16E-5	3.99E-5
UACC-257	0.874	1.934	1.852	1.832	1.259	1.459	0.970	92	90	36	55	9	.	> 1.00E-4	> 1.00E-4
UACC-62	0.563	1.891	1.908	1.713	1.047	0.904	0.668	101	87	36	26	8	5.37E-7	> 1.00E-4	> 1.00E-4
Ovarian Cancer															
IGROV1	0.570	1.669	1.696	1.595	0.959	0.757	0.555	102	93	35	17	-3	5.59E-7	7.28E-5	> 1.00E-4
OVCAR-3	0.235	1.649	1.895	1.549	0.669	0.590	0.372	117	93	31	25	10	4.89E-7	> 1.00E-4	> 1.00E-4
OVCAR-4	0.580	1.219	1.177	1.185	0.865	0.778	0.595	93	95	45	31	2	7.78E-7	> 1.00E-4	> 1.00E-4
OVCAR-5	0.521	1.442	1.414	1.370	1.138	0.815	0.773	97	92	67	32	27	3.05E-6	> 1.00E-4	> 1.00E-4
OVCAR-8	0.498	2.206	2.190	2.163	1.415	1.010	0.646	99	97	54	30	9	1.43E-6	> 1.00E-4	> 1.00E-4
NCI/ADR-RES	0.500	1.507	1.513	1.431	0.644	0.498	0.479	101	92	14	.	-4	3.49E-7	9.39E-6	> 1.00E-4
SK-OV-3	0.563	1.265	1.287	1.247	0.655	0.559	0.479	103	97	13	-1	-15	3.65E-7	8.76E-6	> 1.00E-4
Renal Cancer															
786-0	0.661	2.130	2.057	1.953	1.084	1.025	0.678	95	88	29	25	1	4.38E-7	> 1.00E-4	> 1.00E-4
A498	0.701	1.885	1.752	1.753	1.223	1.181	0.834	89	89	44	41	11	7.39E-7	> 1.00E-4	> 1.00E-4
ACHN	0.346	1.373	1.458	1.379	0.870	0.771	0.432	108	101	51	41	8	1.27E-6	> 1.00E-4	> 1.00E-4
CAKI-1	0.638	2.165	2.067	1.996	1.087	1.330	0.882	94	89	29	45	16	4.51E-7	> 1.00E-4	> 1.00E-4
RXF 393	0.511	1.079	1.075	1.043	0.468	0.342	0.432	99	94	-8	-33	-15	2.67E-7	8.27E-7	> 1.00E-4
SN12C	0.473	1.806	1.773	1.795	1.040	0.834	0.470	98	99	42	27	-1	7.37E-7	9.41E-5	> 1.00E-4
TK-10	0.909	1.854	1.808	1.811	1.588	1.580	1.102	95	95	72	71	20	2.60E-5	> 1.00E-4	> 1.00E-4
UO-31	0.370	1.287	1.179	1.130	0.693	0.646	0.415	88	83	35	30	5	4.89E-7	> 1.00E-4	> 1.00E-4
Prostate Cancer															
PC-3	0.364	1.507	1.442	1.344	0.778	0.689	0.509	94	86	36	28	13	5.27E-7	> 1.00E-4	> 1.00E-4
DU-145	0.173	1.339	1.437	1.380	0.651	0.427	0.309	108	103	41	22	12	7.18E-7	> 1.00E-4	> 1.00E-4
Breast Cancer															
MCF7	0.280	1.465	1.350	1.351	0.375	0.390	0.219	90	90	8	9	-22	3.09E-7	1.99E-5	> 1.00E-4
MDA-MB-231/ATCC	0.638	1.733	1.775	1.808	1.356	1.191	0.959	104	107	66	51	29	1.06E-5	> 1.00E-4	> 1.00E-4
HS 578T	0.449	1.798	1.760	1.740	1.107	1.048	0.923	97	96	49	44	35	9.41E-7	> 1.00E-4	> 1.00E-4
BT-549	0.868	1.805	1.776	1.730	1.318	1.001	0.433	97	92	48	14	-50	9.01E-7	1.66E-5	9.94E-5
T-47D	0.549	1.240	1.189	1.186	0.791	0.927	0.621	93	92	35	55	10	.	> 1.00E-4	> 1.00E-4
MDA-MB-468	0.579	1.170	1.121	1.083	0.522	0.535	0.452	92	85	-10	-8	-22	2.35E-7	7.86E-7	> 1.00E-4

Pyrazoline (74) – Five Dose Repeat

National Cancer Institute Developmental Therapeutics Program
In-Vitro Testing Results

NSC : D - 761262 / 1	Experiment ID : 1111RS58	Test Type : 08	Units : Molar
Report Date : January 05, 2012	Test Date : November 14, 2011	QNS :	MC :
COMI : AC04:48 (109730)	Stain Reagent : SRB Dual-Pass Related	SSPL : 0Y8X	

Log10 Concentration

	Time	Mean Optical Densities						Percent Growth							
Panel/Cell Line	Zero	Ctrl	-8.0	-7.0	-6.0	-5.0	-4.0	-8.0	-7.0	-6.0	-5.0	-4.0	GI50	TGI	LC50
Leukemia															
CCRF-CEM	0.526	1.416	1.377	1.414	0.525	0.423	0.459	96	100	.	-20	-13	3.15E-7	9.96E-7	> 1.00E-4
HL-60(TB)	0.974	2.676	2.588	2.367	0.828	0.665	0.566	95	82	-15	-32	-42	2.13E-7	7.00E-7	> 1.00E-4
K-562	0.181	1.129	1.074	0.989	0.319	0.231	0.162	94	85	15	5	-10	3.15E-7	2.15E-5	> 1.00E-4
MOLT-4	0.769	2.135	2.124	2.161	1.238	0.815	0.545	99	102	34	3	-29	5.87E-7	1.27E-5	> 1.00E-4
RPMI-8226	1.047	2.409	2.411	2.429	1.728	1.241	0.712	100	101	50	14	-32	9.98E-7	2.03E-5	> 1.00E-4
SR	0.184	0.703	0.697	0.647	0.227	0.203	0.189	99	89	8	4	1	3.05E-7	> 1.00E-4	> 1.00E-4
Non-Small Cell Lung Cancer															
A549/ATCC	0.398	1.595	1.543	1.571	0.731	0.581	0.381	96	98	28	15	-4	4.83E-7	6.05E-5	> 1.00E-4
EKVX	0.769	2.028	2.030	2.051	1.564	1.455	1.086	100	102	63	54	25	1.42E-5	> 1.00E-4	> 1.00E-4
HOP-62	0.414	1.194	1.209	1.178	0.748	0.724	0.527	102	98	43	40	14	7.39E-7	> 1.00E-4	> 1.00E-4
NCI-H23	0.575	1.692	1.646	1.636	0.798	0.725	0.549	96	95	20	13	-5	3.98E-7	5.55E-5	> 1.00E-4
NCI-H322M	0.694	1.559	1.537	1.543	1.130	1.102	1.070	97	98	50	47	43	1.29E-6	> 1.00E-4	> 1.00E-4
NCI-H460	0.251	2.319	2.421	2.410	0.529	0.351	0.137	105	104	13	5	-45	3.96E-7	1.25E-5	> 1.00E-4
NCI-H522	0.550	1.275	1.184	1.172	0.391	0.393	0.420	87	86	-29	-29	-24	2.05E-7	5.60E-7	> 1.00E-4
Colon Cancer															
COLO 205	0.391	1.588	1.691	1.687	0.598	0.247	0.062	109	108	17	-37	-84	4.37E-7	2.08E-6	1.89E-5
HCC-2998	0.553	1.922	1.873	1.925	1.106	0.487	0.307	96	100	40	-12	-44	6.91E-7	5.91E-6	> 1.00E-4
HCT-116	0.239	1.399	1.431	1.379	0.475	0.339	0.167	103	98	20	9	-30	4.17E-7	1.67E-5	> 1.00E-4
HCT-15	0.363	2.122	2.006	1.983	0.966	0.665	0.467	93	92	34	17	6	5.35E-7	> 1.00E-4	> 1.00E-4
HT29	0.243	0.979	1.050	1.038	0.256	0.226	0.141	110	108	2	-7	-42	3.52E-7	1.57E-6	> 1.00E-4
KM12	0.557	2.271	2.292	2.193	0.966	0.846	0.514	101	95	24	17	-8	4.31E-7	4.82E-5	> 1.00E-4
SW-620	0.276	1.711	1.708	1.633	0.515	0.593	0.494	100	95	17	22	15	3.73E-7	> 1.00E-4	> 1.00E-4
CNS Cancer															
SF-268	0.557	1.593	1.554	1.494	0.947	0.873	0.562	96	90	38	31	.	5.83E-7	> 1.00E-4	> 1.00E-4
SF-295	0.764	2.595	2.385	2.364	1.144	1.104	0.862	89	87	21	19	5	3.64E-7	> 1.00E-4	> 1.00E-4
SF-539	0.687	2.053	2.018	1.956	0.992	0.709	0.586	97	93	22	2	-15	4.06E-7	1.26E-5	> 1.00E-4
SNB-19	0.548	1.785	1.718	1.684	1.100	0.966	0.817	95	92	45	34	22	7.68E-7	> 1.00E-4	> 1.00E-4
SNB-75	0.637	1.183	1.107	1.128	0.611	0.677	0.569	86	90	-4	7	-11	2.66E-7	.	> 1.00E-4
U251	0.343	1.493	1.452	1.458	0.626	0.457	0.267	96	97	25	10	-22	4.45E-7	2.03E-5	> 1.00E-4
Melanoma															
LOX IMVI	0.668	2.921	2.871	2.826	1.775	1.678	0.790	98	96	49	45	5	9.58E-7	> 1.00E-4	> 1.00E-4
MALME-3M	0.661	1.275	1.252	1.192	0.857	0.940	0.805	96	87	32	45	23	4.67E-7	> 1.00E-4	> 1.00E-4
M14	0.386	1.146	1.122	1.119	0.605	0.320	0.255	97	96	29	-17	-34	4.86E-7	4.22E-6	> 1.00E-4
MDA-MB-435	0.413	1.809	1.754	1.499	0.289	0.234	0.288	96	78	-30	-43	-30	1.81E-7	5.26E-7	> 1.00E-4
SK-MEL-28	0.394	1.040	1.087	1.022	0.730	0.726	0.536	107	97	52	51	22	1.11E-5	> 1.00E-4	> 1.00E-4
SK-MEL-5	0.594	2.727	2.678	2.441	0.793	0.824	0.223	98	87	9	11	-63	2.98E-7	1.40E-5	6.74E-5
UACC-257	0.811	1.480	1.480	1.448	0.998	1.084	0.652	100	95	28	41	-20	4.69E-7	4.73E-5	> 1.00E-4
UACC-62	0.659	2.265	2.218	2.075	1.233	1.115	0.659	97	88	36	28	.	5.34E-7	> 1.00E-4	> 1.00E-4
Ovarian Cancer															
IGROV1	0.431	1.244	1.254	1.256	0.873	0.761	0.552	101	101	54	41	15	2.09E-6	> 1.00E-4	> 1.00E-4
OVCAR-3	0.401	1.054	1.131	1.089	0.278	0.237	0.224	112	105	-31	-41	-44	2.55E-7	5.94E-7	> 1.00E-4
OVCAR-4	0.440	1.212	1.176	1.128	0.817	0.680	0.533	95	89	49	31	12	9.37E-7	> 1.00E-4	> 1.00E-4
OVCAR-5	0.493	1.384	1.297	1.289	1.077	0.816	0.725	90	89	66	36	26	3.40E-6	> 1.00E-4	> 1.00E-4
OVCAR-8	0.344	1.282	1.273	1.283	0.728	0.500	0.365	99	100	41	17	2	7.03E-7	> 1.00E-4	> 1.00E-4
NCI/ADR-RES	0.244	0.873	0.903	0.839	0.334	0.285	0.261	105	95	14	6	3	3.59E-7	> 1.00E-4	> 1.00E-4
SK-OV-3	0.570	1.199	1.197	1.206	0.805	0.679	0.567	100	101	37	17	-1	6.33E-7	9.24E-5	> 1.00E-4
Renal Cancer															
786-0	0.665	1.945	1.954	1.950	0.978	0.776	0.548	101	100	24	9	-18	4.61E-7	2.13E-5	> 1.00E-4
A498	1.322	2.093	2.039	2.004	1.324	1.178	0.967	93	88	.	-11	-27	2.73E-7	1.05E-6	> 1.00E-4
ACHN	0.324	1.360	1.381	1.378	0.803	0.729	0.446	102	102	46	39	12	8.56E-7	> 1.00E-4	> 1.00E-4
CAKI-1	0.681	1.883	1.804	1.736	1.180	1.329	0.887	93	88	42	54	17	.	> 1.00E-4	> 1.00E-4
RXF 393	0.680	1.343	1.302	1.167	0.751	0.508	0.547	94	73	11	-25	-20	2.36E-7	1.98E-6	> 1.00E-4
SN12C	0.517	2.130	1.992	2.047	1.288	1.002	0.662	91	95	48	30	9	8.98E-7	> 1.00E-4	> 1.00E-4
TK-10	0.544	1.104	1.100	1.083	0.774	0.724	0.435	99	96	41	32	-20	6.89E-7	4.13E-5	> 1.00E-4
UO-31	0.721	1.757	1.577	1.527	1.101	0.987	0.701	83	78	37	26	-3	4.75E-7	7.99E-5	> 1.00E-4
Prostate Cancer															
PC-3	0.582	1.516	1.482	1.432	0.659	0.661	0.497	96	91	8	8	-15	3.13E-7	2.32E-5	> 1.00E-4
DU-145	0.421	1.189	1.247	1.225	0.550	0.387	0.274	108	105	17	-8	-35	4.19E-7	4.73E-6	> 1.00E-4
Breast Cancer															
MCF7	0.199	1.119	1.085	1.066	0.354	0.344	0.186	96	94	17	16	-7	3.72E-7	5.00E-5	> 1.00E-4
MDA-MB-231/ATCC	0.513	1.221	1.250	1.268	1.044	0.705	0.597	104	107	75	27	12	3.32E-6	> 1.00E-4	> 1.00E-4
HS 578T	0.962	1.669	1.631	1.616	1.124	0.987	0.922	95	92	23	3	-4	4.07E-7	2.85E-5	> 1.00E-4
T-47D	0.432	1.077	1.053	1.026	0.703	0.781	0.536	96	92	42	54	16	.	> 1.00E-4	> 1.00E-4
MDA-MB-468	0.672	1.583	1.536	1.381	0.667	0.632	0.430	95	78	-1	-6	-36	2.26E-7	9.76E-7	> 1.00E-4

Pyrazoline (74–) – Five Dose

National Cancer Institute Developmental Therapeutics Program
In-Vitro Testing Results

NSC : D - 761468 / 1	Experiment ID : 1110NS32	Test Type : 08	Units : Molar
Report Date : November 28, 2011	Test Date : October 03, 2011	QNS :	MC :
COMI : AC04:48.2 (110260)	Stain Reagent : SRB Dual-Pass Related	SSPL : 0Y8X	

			Log10 Concentration											
	Time		Mean Optical Densities					Percent Growth						
Panel/Cell Line	Zero	Ctrl	-8.0	-7.0	-6.0	-5.0	-4.0	-8.0	-7.0	-6.0	-5.0	-4.0	GI50	TGI	LC50
Leukemia															
CCRF-CEM	0.249	1.723	1.663	1.581	0.626	0.406	0.370	96	90	26	11	8	4.20E-7	> 1.00E-4	> 1.00E-4
HL-60(TB)	0.702	2.211	2.006	2.012	0.475	0.453	0.383	86	87	-32	-35	-45	2.04E-7	5.35E-7	> 1.00E-4
K-562	0.180	1.251	1.180	0.910	0.286	0.224	0.135	93	68	10	4	-25	2.05E-7	1.38E-5	> 1.00E-4
MOLT-4	0.541	1.725	1.726	1.698	0.864	0.557	0.463	100	98	27	1	-15	4.76E-7	1.22E-5	> 1.00E-4
RPMI-8226	0.492	1.864	1.798	1.761	0.877	0.769	0.462	95	92	28	20	-6	4.56E-7	5.82E-5	> 1.00E-4
SR	0.206	0.617	0.541	0.350	0.233	0.213	0.186	81	35	7	2	-10	4.75E-8	1.41E-5	> 1.00E-4
Non-Small Cell Lung Cancer															
A549/ATCC	0.472	1.704	1.700	1.735	0.885	0.699	0.394	100	102	34	18	-17	5.77E-7	3.35E-5	> 1.00E-4
EKVX	0.775	1.825	1.834	1.772	1.319	1.232	0.913	101	95	52	44	13	1.66E-6	> 1.00E-4	> 1.00E-4
HOP-62	0.360	0.831	0.873	0.808	0.497	0.474	0.217	109	95	29	24	-40	4.81E-7	2.39E-5	> 1.00E-4
NCI-H226	0.639	1.513	1.477	1.434	0.761	0.554	0.329	96	91	14	-13	-49	3.40E-7	3.23E-6	> 1.00E-4
NCI-H23	0.630	1.470	1.495	1.426	0.832	0.691	0.494	103	95	24	7	-22	4.30E-7	1.79E-5	> 1.00E-4
NCI-H322M	0.626	1.425	1.430	1.422	1.032	1.010	0.828	101	100	51	48	25	1.97E-6	> 1.00E-4	> 1.00E-4
NCI-H460	0.254	2.330	2.376	2.322	0.476	0.380	0.167	102	100	11	6	-34	3.61E-7	1.41E-5	> 1.00E-4
NCI-H522	1.202	1.894	1.842	1.722	1.142	0.900	0.448	92	75	-5	-25	-63	2.06E-7	8.66E-7	4.58E-5
Colon Cancer															
COLO 205	0.234	0.978	0.990	0.948	0.311	0.195	0.090	102	96	10	-17	-62	3.44E-7	2.40E-6	5.47E-5
HCC-2998	0.549	1.508	1.574	1.541	0.945	0.415	0.259	107	103	41	-24	-53	7.23E-7	4.24E-6	7.95E-5
HCT-116	0.295	1.675	1.578	1.555	0.649	0.411	0.116	93	91	26	8	-61	4.25E-7	1.32E-5	6.97E-5
HCT-15	0.358	2.156	2.168	1.986	0.933	0.679	0.385	101	91	32	18	1	4.92E-7	> 1.00E-4	> 1.00E-4
HT29	0.261	1.243	1.257	1.274	0.306	0.269	0.145	101	103	5	1	-44	3.46E-7	1.04E-5	> 1.00E-4
KM12	0.202	0.898	0.990	0.876	0.385	0.259	0.095	113	97	26	8	-53	4.61E-7	1.36E-5	8.86E-5
SW-620	0.175	1.120	1.095	1.023	0.319	0.381	0.295	97	90	15	22	13	3.41E-7	> 1.00E-4	> 1.00E-4
CNS Cancer															
SF-268	0.512	1.521	1.499	1.434	0.992	0.800	0.373	98	91	48	28	-27	8.77E-7	3.25E-5	> 1.00E-4
SF-295	0.620	2.343	2.224	1.920	1.009	0.786	0.472	93	75	23	10	-24	3.02E-7	1.94E-5	> 1.00E-4
SF-539	0.694	1.914	1.882	1.857	0.867	0.735	0.423	97	95	14	3	-39	3.62E-7	1.20E-5	> 1.00E-4
SNB-19	0.511	1.634	1.587	1.517	1.019	0.842	0.631	96	90	45	29	11	7.79E-7	> 1.00E-4	> 1.00E-4
SNB-75	0.566	0.998	0.933	0.900	0.469	0.489	0.308	85	77	-17	-14	-46	1.94E-7	6.57E-7	> 1.00E-4
U251	0.369	1.533	1.509	1.502	0.669	0.515	0.262	98	97	26	13	-29	4.59E-7	2.00E-5	> 1.00E-4
Melanoma															
LOX IMVI	0.349	2.023	1.983	1.819	0.996	0.857	0.282	98	88	39	30	-19	5.87E-7	4.08E-5	> 1.00E-4
MALME-3M	0.617	1.344	1.358	1.218	0.891	0.918	0.667	102	83	38	41	7	5.30E-7	> 1.00E-4	> 1.00E-4
M14	0.425	1.266	1.192	1.131	0.534	0.319	0.154	91	84	13	-25	-64	3.00E-7	2.19E-6	4.40E-5
MDA-MB-435	0.333	1.533	1.514	0.832	0.218	0.241	0.284	98	42	-35	-28	-15	7.11E-8	3.52E-7	> 1.00E-4
SK-MEL-2	1.042	1.710	1.726	1.590	1.052	1.148	0.667	102	82	1	16	-36	2.50E-7	2.02E-5	> 1.00E-4
SK-MEL-28	0.387	1.062	1.093	0.926	0.637	0.622	0.362	105	80	37	35	-7	4.97E-7	6.93E-5	> 1.00E-4
SK-MEL-5	0.456	2.114	2.140	1.660	0.486	0.503	0.135	102	73	2	3	-70	2.09E-7	1.09E-5	5.27E-5
UACC-257	0.736	1.275	1.257	1.195	0.899	0.975	0.621	97	85	30	44	-16	4.36E-7	5.48E-5	> 1.00E-4
UACC-62	0.778	2.485	2.487	2.173	1.458	1.210	0.465	100	82	40	25	-40	5.71E-7	2.43E-5	> 1.00E-4
Ovarian Cancer															
IGROV1	0.475	1.453	1.485	1.358	0.969	0.774	0.431	103	90	51	31	-9	1.06E-6	5.83E-5	> 1.00E-4
OVCAR-3	0.498	1.338	1.321	1.274	0.438	0.342	0.196	98	92	-12	-31	-61	2.54E-7	7.65E-7	4.32E-5
OVCAR-4	0.455	0.770	0.756	0.739	0.627	0.566	0.321	96	90	55	35	-29	1.73E-6	3.51E-5	> 1.00E-4
OVCAR-5	0.507	1.563	1.518	1.553	1.091	0.836	0.636	96	99	55	31	12	1.66E-6	> 1.00E-4	> 1.00E-4
OVCAR-8	0.438	1.543	1.499	1.476	0.733	0.576	0.350	96	94	27	12	-20	4.50E-7	2.42E-5	> 1.00E-4
NCI/ADR-RES	0.558	1.542	1.540	1.330	0.572	0.483	0.407	100	78	1	-14	-27	2.34E-7	1.24E-6	> 1.00E-4
SK-OV-3	0.425	1.008	1.007	0.951	0.503	0.409	0.196	100	90	13	4	-54	3.33E-7	6.02E-6	8.37E-5
Renal Cancer															
786-0	0.755	2.128	2.052	1.918	1.179	1.154	0.627	94	85	31	29	-17	4.41E-7	4.28E-5	> 1.00E-4
A498	1.148	1.747	1.642	1.596	1.143	0.978	0.848	82	75	.	-15	-26	2.14E-7	9.85E-7	> 1.00E-4
ACHN	0.337	1.240	1.226	1.185	0.821	0.692	0.307	98	94	54	39	-9	1.78E-6	6.50E-5	> 1.00E-4
CAKI-1	0.639	2.332	2.268	2.035	1.106	1.263	0.684	96	82	28	37	3	3.90E-7	> 1.00E-4	> 1.00E-4
RXF 393	0.517	1.010	1.016	0.966	0.417	0.430	0.282	101	91	-19	-17	-46	2.36E-7	6.68E-7	> 1.00E-4
SN12C	0.531	1.916	1.879	1.871	1.173	1.042	0.451	97	97	46	37	-15	8.47E-7	5.11E-5	> 1.00E-4
TK-10	0.885	1.569	1.611	1.581	1.189	1.127	0.630	106	102	44	35	-29	8.00E-7	3.55E-5	> 1.00E-4
UO-31	0.333	1.023	0.948	0.920	0.712	0.630	0.264	89	85	55	43	-21	2.59E-6	4.72E-5	> 1.00E-4
Prostate Cancer															
PC-3	0.411	1.272	1.219	1.157	0.616	0.623	0.378	94	87	24	25	-8	3.82E-7	5.68E-5	> 1.00E-4
DU-145	0.386	1.449	1.480	1.401	0.487	0.422	0.202	103	96	10	3	-48	3.38E-7	1.17E-5	> 1.00E-4
Breast Cancer															
MCF7	0.239	1.173	1.150	1.033	0.383	0.324	0.103	98	85	15	9	-57	3.18E-7	1.37E-5	7.81E-5
MDA-MB-231/ATCC	0.639	1.819	1.922	1.897	1.408	1.196	0.763	109	107	65	47	11	6.97E-6	> 1.00E-4	> 1.00E-4
HS 578T	0.897	1.712	1.667	1.602	0.994	0.978	0.877	94	87	12	10	-2	3.08E-7	6.50E-5	> 1.00E-4
BT-549	1.107	1.802	1.795	1.688	1.402	1.071	0.458	99	84	42	-3	-59	6.52E-7	8.47E-6	6.97E-5
T-47D	0.499	1.070	1.078	1.052	0.718	0.815	0.494	101	97	38	55	-1	.	9.60E-5	> 1.00E-4
MDA-MB-468	0.572	1.160	1.129	1.066	0.577	0.594	0.423	95	84	1	4	-26	2.56E-7	1.33E-5	> 1.00E-4

Pyrazoline (74+) – Five Dose

National Cancer Institute Developmental Therapeutics Program
In-Vitro Testing Results

NSC : D - 761468 / 1	Experiment ID : 1112RS69	Test Type : 08	Units : Molar
Report Date : February 17, 2012	Test Date : December 05, 2011	QNS :	MC :
COMI : AC04:48.2 (110260)	Stain Reagent : SRB Dual-Pass Related	SSPL : 0Y8X	

		Log10 Concentration												
	Time	Mean Optical Densities						Percent Growth						
Panel/Cell Line	Zero	Ctrl	-8.0	-7.0	-6.0	-5.0	-4.0	-8.0	-7.0	-6.0	-5.0	-4.0	GI50	TGI	LC50
Non-Small Cell Lung Cancer															
A549/ATCC	0.296	1.532	1.497	1.417	0.655	0.530	0.350	97	91	29	19	4	4.56E-7	> 1.00E-4	> 1.00E-4
EKVX	0.426	1.303	1.322	1.243	0.769	0.706	0.567	102	93	39	32	16	6.28E-7	> 1.00E-4	> 1.00E-4
HOP-62	0.454	1.329	1.348	1.297	0.687	0.806	0.612	102	96	27	40	18	4.62E-7	> 1.00E-4	> 1.00E-4
NCI-H226	0.526	1.106	0.965	1.015	0.772	0.631	0.449	76	84	42	18	-15	6.57E-7	3.56E-5	> 1.00E-4
NCI-H23	0.648	2.150	2.079	1.764	0.759	0.708	0.608	95	74	7	4	-6	2.31E-7	2.45E-5	> 1.00E-4
NCI-H322M	0.746	1.725	1.768	1.760	1.217	1.287	1.044	104	104	48	55	30	.	> 1.00E-4	> 1.00E-4
NCI-H460	0.309	2.468	2.489	2.421	0.567	0.498	0.254	101	98	12	9	-18	3.61E-7	2.14E-5	> 1.00E-4
NCI-H522	0.682	1.477	1.434	1.347	0.620	0.588	0.461	95	84	-9	-14	-32	2.31E-7	7.97E-7	> 1.00E-4
Colon Cancer															
COLO 205	0.316	1.167	1.184	1.210	0.358	0.236	0.056	102	105	5	-25	-82	3.55E-7	1.46E-6	2.70E-5
HCC-2998	0.382	1.274	1.262	1.160	0.796	0.520	0.398	99	87	46	15	2	8.17E-7	> 1.00E-4	> 1.00E-4
HCT-116	0.236	1.652	1.690	1.658	1.518	0.408	0.189	103	100	91	12	-20	3.29E-6	2.38E-5	> 1.00E-4
HCT-15	0.426	2.255	2.252	2.055	0.956	0.687	0.439	100	89	29	14	1	4.47E-7	> 1.00E-4	> 1.00E-4
HT29	0.249	1.323	1.402	1.441	0.343	0.305	0.151	107	111	9	5	-39	3.95E-7	1.31E-5	> 1.00E-4
KM12	0.625	2.512	2.606	2.245	1.278	1.124	0.657	105	86	35	26	2	5.01E-7	> 1.00E-4	> 1.00E-4
SW-620	0.264	1.675	1.566	1.428	0.533	0.651	0.475	92	83	19	27	15	3.26E-7	> 1.00E-4	> 1.00E-4
CNS Cancer															
SF-268	0.528	1.651	1.674	1.551	1.196	1.011	0.610	102	91	60	43	7	3.78E-6	> 1.00E-4	> 1.00E-4
SF-295	0.834	2.614	2.554	2.219	0.966	0.983	0.740	97	78	7	8	-11	2.48E-7	2.66E-5	> 1.00E-4
SNB-19	0.551	1.786	1.755	1.609	1.061	0.982	0.755	97	86	41	35	16	6.37E-7	> 1.00E-4	> 1.00E-4
SNB-75	0.716	1.182	1.094	1.022	0.652	0.779	0.661	81	66	-9	14	-8	1.62E-7	.	> 1.00E-4
U251	0.365	1.786	1.733	1.644	0.582	0.503	0.239	96	90	15	10	-35	3.43E-7	1.66E-5	> 1.00E-4
Melanoma															
LOX IMVI	0.286	2.088	2.054	1.826	1.057	0.907	0.321	98	85	43	34	2	6.77E-7	> 1.00E-4	> 1.00E-4
MALME-3M	0.749	1.539	1.563	1.527	1.172	1.291	0.906	103	98	54	69	20	2.41E-5	> 1.00E-4	> 1.00E-4
M14	0.429	1.507	1.516	1.440	0.689	0.452	0.279	101	94	24	2	-35	4.25E-7	1.14E-5	> 1.00E-4
MDA-MB-435	0.561	2.303	2.270	1.458	0.376	0.447	0.411	98	51	-33	-20	-27	1.04E-7	4.07E-7	> 1.00E-4
SK-MEL-2	0.914	1.572	1.641	1.541	1.157	1.236	0.654	110	95	37	49	-29	5.95E-7	4.28E-5	> 1.00E-4
SK-MEL-28	0.333	0.936	0.927	0.757	0.568	0.608	0.387	99	70	39	46	9	4.45E-7	> 1.00E-4	> 1.00E-4
SK-MEL-5	0.584	2.279	2.059	1.830	0.645	0.518	0.142	87	74	4	-11	-76	2.17E-7	1.74E-6	3.99E-5
UACC-257	0.593	1.276	1.273	1.151	0.952	1.017	0.641	99	82	52	62	7	1.66E-5	> 1.00E-4	> 1.00E-4
UACC-62	0.632	2.148	2.114	1.735	1.091	0.991	0.393	98	73	30	24	-38	3.43E-7	2.43E-5	> 1.00E-4
Ovarian Cancer															
IGROV1	0.402	1.309	1.357	1.335	0.841	0.644	0.394	105	103	48	27	-2	9.35E-7	8.52E-5	> 1.00E-4
OVCAR-3	0.491	1.458	1.456	1.457	0.624	0.497	0.267	100	100	14	1	-46	3.79E-7	1.03E-5	> 1.00E-4
OVCAR-4	0.565	1.115	1.091	1.022	0.888	0.785	0.633	96	83	59	40	12	2.91E-6	> 1.00E-4	> 1.00E-4
OVCAR-5	0.596	1.408	1.456	1.413	0.908	0.797	0.638	106	101	38	25	5	6.51E-7	> 1.00E-4	> 1.00E-4
NCI/ADR-RES	0.456	1.678	1.653	1.376	0.600	0.526	0.502	98	75	12	6	4	2.50E-7	> 1.00E-4	> 1.00E-4
SK-OV-3	0.592	1.428	1.472	1.395	0.810	0.736	0.585	105	96	26	17	-1	4.55E-7	8.62E-5	> 1.00E-4
Renal Cancer															
786-0	0.581	1.946	1.993	1.957	1.066	0.919	0.595	103	101	36	25	1	6.00E-7	> 1.00E-4	> 1.00E-4
A498	1.385	2.046	1.968	1.866	1.275	1.229	0.932	88	73	-8	-11	-33	1.92E-7	7.97E-7	> 1.00E-4
ACHN	0.398	1.489	1.598	1.483	0.928	0.771	0.401	110	99	49	34	.	9.36E-7	> 1.00E-4	> 1.00E-4
CAKI-1	0.744	1.970	1.756	1.624	1.155	1.273	0.676	83	72	33	43	-9	3.71E-7	6.67E-5	> 1.00E-4
RXF 393	0.627	1.050	0.968	0.992	0.494	0.531	0.499	80	86	-21	-15	-20	2.17E-7	6.34E-7	> 1.00E-4
SN12C	0.596	2.236	2.219	2.082	1.139	1.013	0.562	99	91	33	25	-6	5.08E-7	6.56E-5	> 1.00E-4
TK-10	0.591	1.210	1.221	1.210	0.918	0.956	0.575	102	100	53	59	-3	1.40E-5	9.04E-5	> 1.00E-4
UO-31	0.572	1.615	1.352	1.378	1.068	1.007	0.499	75	77	48	42	-13	8.26E-7	5.82E-5	> 1.00E-4
Prostate Cancer															
PC-3	0.381	1.769	1.692	1.578	0.665	0.636	0.467	94	86	20	18	6	3.56E-7	> 1.00E-4	> 1.00E-4
DU-145	0.556	1.774	1.882	1.842	0.843	0.853	0.592	109	106	24	24	3	4.76E-7	> 1.00E-4	> 1.00E-4
Breast Cancer															
MCF7	0.299	1.623	1.498	1.254	0.457	0.415	0.257	91	72	12	9	-14	2.33E-7	2.41E-5	> 1.00E-4
MDA-MB-231/ATCC	0.504	1.057	1.148	1.008	0.733	0.526	0.361	117	91	41	4	-28	6.70E-7	1.33E-5	> 1.00E-4
HS 578T	0.966	1.792	1.710	1.633	1.060	1.178	1.033	90	81	11	26	8	2.77E-7	> 1.00E-4	> 1.00E-4
BT-549	0.873	1.634	1.640	1.601	1.337	1.071	0.534	101	96	61	26	-39	2.06E-6	2.52E-5	> 1.00E-4
T-47D	0.585	1.612	1.625	1.582	0.868	1.178	0.813	101	97	28	58	22	.	> 1.00E-4	> 1.00E-4
MDA-MB-468	0.583	1.203	1.237	1.070	0.491	0.476	0.404	105	78	-16	-18	-31	2.01E-7	6.80E-7	> 1.00E-4

Pyrazoline (78) – Five Dose

National Cancer Institute Developmental Therapeutics Program
In-Vitro Testing Results

NSC : D - 761257 / 1	Experiment ID : 1109NS21	Test Type : 08	Units : Molar
Report Date : October 26, 2011	Test Date : September 12, 2011	QNS :	MC :
COMI : AC03:45 (109725)	Stain Reagent : SRB Dual-Pass Related	SSPL : 0Y8X	

			Log10 Concentration												
	Time		Mean Optical Densities					Percent Growth							
Panel/Cell Line	Zero	Ctrl	-8.0	-7.0	-6.0	-5.0	-4.0	-8.0	-7.0	-6.0	-5.0	-4.0	GI50	TGI	LC50
Leukemia															
CCRF-CEM	0.380	1.644	1.627	1.592	1.052	0.557	0.567	99	96	53	14	15	1.20E-6	> 1.00E-4	> 1.00E-4
HL-60(TB)	0.695	2.424	2.385	2.415	1.253	0.702	0.669	98	99	32	.	-4	5.45E-7	1.25E-5	> 1.00E-4
MOLT-4	0.518	2.348	2.343	2.353	1.720	1.169	0.883	100	100	66	36	20	3.32E-6	> 1.00E-4	> 1.00E-4
RPMI-8226	0.673	2.632	2.592	2.656	2.359	1.701	1.748	98	101	86	52	55	> 1.00E-4	> 1.00E-4	> 1.00E-4
SR	0.449	2.410	2.308	2.019	0.892	0.709	0.664	95	80	23	13	11	3.33E-7	> 1.00E-4	> 1.00E-4
Non-Small Cell Lung Cancer															
A549/ATCC	0.410	1.844	1.828	1.785	1.069	0.742	0.667	99	96	46	23	18	8.30E-7	> 1.00E-4	> 1.00E-4
EKVX	0.836	2.041	1.992	1.994	1.745	1.458	1.421	96	96	75	52	49	3.26E-5	> 1.00E-4	> 1.00E-4
HOP-62	0.407	1.042	1.031	0.980	0.642	0.515	0.295	98	90	37	17	-28	5.71E-7	2.41E-5	> 1.00E-4
HOP-92	0.903	2.203	2.167	2.171	2.014	1.911	1.793	97	97	85	77	68	> 1.00E-4	> 1.00E-4	> 1.00E-4
NCI-H226	0.668	1.606	1.576	1.510	1.018	0.799	0.673	97	90	37	14	.	5.72E-7	> 1.00E-4	> 1.00E-4
NCI-H23	0.445	1.402	1.343	1.320	0.988	0.710	0.541	94	91	57	28	10	1.70E-6	> 1.00E-4	> 1.00E-4
NCI-H322M	0.717	1.919	1.857	1.827	1.586	1.244	1.265	95	92	72	44	46	6.06E-6	> 1.00E-4	> 1.00E-4
NCI-H460	0.172	1.991	2.024	2.029	0.470	0.364	0.241	102	102	16	11	4	4.05E-7	> 1.00E-4	> 1.00E-4
NCI-H522	0.798	1.713	1.692	1.617	0.947	0.652	0.636	98	90	16	-18	-20	3.46E-7	2.95E-6	> 1.00E-4
Colon Cancer															
COLO 205	0.315	1.241	1.258	1.266	0.452	0.213	0.129	102	103	15	-32	-59	3.97E-7	2.05E-6	4.54E-5
HCC-2998	0.424	1.711	1.679	1.656	1.223	0.752	0.497	97	96	62	25	6	2.14E-6	> 1.00E-4	> 1.00E-4
HCT-116	0.194	1.504	1.475	1.513	0.605	0.487	0.305	98	101	31	22	8	5.38E-7	> 1.00E-4	> 1.00E-4
HCT-15	0.395	1.905	1.823	1.753	1.059	0.828	0.685	95	90	44	29	19	7.39E-7	> 1.00E-4	> 1.00E-4
HT29	0.216	1.256	1.310	1.273	0.316	0.262	0.257	105	102	10	4	4	3.64E-7	> 1.00E-4	> 1.00E-4
KM12	0.322	2.445	2.489	2.367	1.069	0.925	0.727	102	96	35	28	19	5.72E-7	> 1.00E-4	> 1.00E-4
SW-620	0.196	1.788	1.790	1.712	0.649	0.538	0.522	100	95	28	21	20	4.76E-7	> 1.00E-4	> 1.00E-4
CNS Cancer															
SF-268	0.280	1.747	1.589	1.662	1.147	1.111	0.806	89	94	59	57	36	2.08E-5	> 1.00E-4	> 1.00E-4
SF-539	0.713	1.970	1.920	1.891	1.207	0.676	0.513	96	94	39	-5	-28	6.36E-7	7.62E-6	> 1.00E-4
SNB-19	0.476	1.593	1.561	1.534	0.987	0.767	0.640	97	95	46	26	15	8.19E-7	> 1.00E-4	> 1.00E-4
SNB-75	0.863	1.553	1.468	1.400	0.757	0.696	0.666	88	78	-12	-19	-23	2.03E-7	7.30E-7	> 1.00E-4
U251	0.365	1.638	1.620	1.644	0.912	0.647	0.395	99	100	43	22	2	7.54E-7	> 1.00E-4	> 1.00E-4
Melanoma															
LOX IMVI	0.247	1.585	1.547	1.515	0.836	0.843	0.649	97	95	44	45	30	7.63E-7	> 1.00E-4	> 1.00E-4
MALME-3M	0.602	1.465	1.416	1.412	1.016	0.915	0.957	94	94	48	36	41	9.04E-7	> 1.00E-4	> 1.00E-4
M14	0.317	1.167	1.132	1.133	0.726	0.389	0.318	96	96	48	8	.	9.13E-7	> 1.00E-4	> 1.00E-4
MDA-MB-435	0.551	2.497	2.492	2.160	0.632	0.299	0.215	100	83	4	-46	-61	2.61E-7	1.21E-6	1.88E-5
SK-MEL-2	0.821	1.506	1.518	1.548	0.916	0.822	0.606	102	106	14	.	-26	4.06E-7	1.01E-5	> 1.00E-4
SK-MEL-28	0.533	1.401	1.400	1.356	0.992	0.761	0.644	100	95	53	26	13	1.29E-6	> 1.00E-4	> 1.00E-4
SK-MEL-5	0.497	2.284	2.165	2.130	0.892	0.629	0.783	93	91	22	7	16	3.96E-7	> 1.00E-4	> 1.00E-4
UACC-257	0.874	1.786	1.759	1.708	1.390	1.416	1.447	97	91	57	59	63	> 1.00E-4	> 1.00E-4	> 1.00E-4
UACC-62	0.563	1.932	1.918	1.826	1.034	1.002	0.861	99	92	34	32	22	5.38E-7	> 1.00E-4	> 1.00E-4
Ovarian Cancer															
IGROV1	0.570	1.803	1.905	1.774	1.256	1.046	0.881	108	98	56	39	25	2.15E-6	> 1.00E-4	> 1.00E-4
OVCAR-3	0.235	1.764	1.684	1.733	0.647	0.535	0.202	95	98	27	20	-14	4.73E-7	3.79E-5	> 1.00E-4
OVCAR-4	0.580	1.192	1.170	1.167	0.896	0.876	0.741	96	96	52	48	26	3.12E-6	> 1.00E-4	> 1.00E-4
OVCAR-5	0.521	1.401	1.405	1.366	1.211	0.798	0.670	100	96	78	31	17	4.02E-6	> 1.00E-4	> 1.00E-4
OVCAR-8	0.498	1.977	1.939	1.962	1.578	0.912	0.848	97	99	73	28	24	3.24E-6	> 1.00E-4	> 1.00E-4
NCI/ADR-RES	0.500	1.581	1.571	1.532	0.736	0.426	0.401	99	95	22	-15	-20	4.14E-7	3.93E-6	> 1.00E-4
SK-OV-3	0.563	1.262	1.267	1.256	0.721	0.535	0.408	101	99	23	-5	-28	4.39E-7	6.60E-6	> 1.00E-4
Renal Cancer															
786-0	0.661	2.219	2.104	2.082	1.316	1.003	0.655	93	91	42	22	-1	6.88E-7	9.06E-5	> 1.00E-4
A498	0.701	1.890	1.762	1.692	1.317	1.199	0.871	89	83	52	42	14	1.52E-6	> 1.00E-4	> 1.00E-4
ACHN	0.346	1.359	1.375	1.392	0.914	0.875	0.628	102	103	56	52	28	1.23E-5	> 1.00E-4	> 1.00E-4
CAKI-1	0.638	2.038	1.997	1.927	1.052	0.996	1.039	97	92	30	26	29	4.71E-7	> 1.00E-4	> 1.00E-4
RXF 393	0.511	1.095	1.085	1.087	0.704	0.316	0.186	98	99	33	-38	-64	5.51E-7	2.90E-6	2.89E-5
SN12C	0.473	1.790	1.768	1.799	1.372	0.944	0.916	98	101	68	36	34	3.65E-6	> 1.00E-4	> 1.00E-4
TK-10	0.909	1.799	1.779	1.767	1.580	1.470	1.252	98	96	75	63	39	3.41E-5	> 1.00E-4	> 1.00E-4
UO-31	0.370	1.389	1.281	1.278	0.977	0.836	0.713	89	89	60	46	34	4.92E-6	> 1.00E-4	> 1.00E-4
Prostate Cancer															
PC-3	0.364	1.552	1.523	1.473	1.123	0.944	0.924	98	93	64	49	47	8.38E-6	> 1.00E-4	> 1.00E-4
DU-145	0.173	1.526	1.495	1.583	1.001	0.529	0.425	98	104	61	26	19	2.09E-6	> 1.00E-4	> 1.00E-4
Breast Cancer															
MCF7	0.280	1.531	1.417	1.391	0.404	0.427	0.417	91	89	10	12	11	3.10E-7	> 1.00E-4	> 1.00E-4
MDA-MB-231/ATCC	0.638	1.692	1.689	1.707	1.270	1.080	0.988	100	101	60	42	33	3.55E-6	> 1.00E-4	> 1.00E-4
HS 578T	0.449	1.874	1.869	1.823	1.415	1.105	0.942	100	96	68	46	35	6.56E-6	> 1.00E-4	> 1.00E-4
BT-549	0.868	1.836	1.821	1.797	1.298	1.330	1.087	98	96	44	48	23	7.80E-7	> 1.00E-4	> 1.00E-4
T-47D	0.549	1.229	1.211	1.176	0.839	0.829	0.756	97	92	43	41	30	7.09E-7	> 1.00E-4	> 1.00E-4
MDA-MB-468	0.579	1.175	1.148	1.139	0.594	0.468	0.479	95	94	3	-19	-17	3.02E-7	1.31E-6	> 1.00E-4

Pyrazoline (78–) – Five Dose

National Cancer Institute Developmental Therapeutics Program
In-Vitro Testing Results

NSC : D - 761466 / 1	Experiment ID : 1110NS32	Test Type : 08	Units : Molar
Report Date : November 28, 2011	Test Date : October 03, 2011	QNS :	MC :
COMI : AC03:45.2 (110256)	Stain Reagent : SRB Dual-Pass Related	SSPL : 0Y8X	

Log10 Concentration

	Time	Mean Optical Densities						Percent Growth						
Panel/Cell Line	Zero	Ctrl	-8.0	-7.0	-6.0	-5.0	-4.0	-8.0	-7.0	-6.0	-5.0	-4.0	GI50	TGI	LC50
Leukemia															
CCRF-CEM	0.249	1.993	2.060	1.960	0.836	0.650	0.523	104	98	34	23	16	5.58E-7	> 1.00E-4	> 1.00E-4
HL-60(TB)	0.702	1.924	2.092	2.143	0.839	0.703	0.536	114	118	11	.	-24	4.33E-7	1.00E-5	> 1.00E-4
K-562	0.180	1.396	1.431	1.354	0.417	0.316	0.269	103	97	19	11	7	4.02E-7	> 1.00E-4	> 1.00E-4
MOLT-4	0.541	1.758	2.025	2.062	1.270	0.877	0.628	122	125	60	28	7	2.02E-6	> 1.00E-4	> 1.00E-4
RPMI-8226	0.492	1.960	2.062	1.979	1.309	1.019	0.856	107	101	56	36	25	1.93E-6	> 1.00E-4	> 1.00E-4
SR	0.206	0.728	0.742	0.568	0.283	0.260	0.178	103	69	15	10	-14	2.25E-7	2.66E-5	> 1.00E-4
Non-Small Cell Lung Cancer															
A549/ATCC	0.472	1.753	1.702	1.717	0.855	0.676	0.399	96	97	30	16	-15	5.02E-7	3.22E-5	> 1.00E-4
EKVX	0.775	1.853	1.799	1.726	1.559	1.422	1.161	95	88	73	60	36	2.59E-5	> 1.00E-4	> 1.00E-4
HOP-62	0.360	0.873	0.908	0.886	0.560	0.467	0.204	107	102	39	21	-43	6.70E-7	2.10E-5	> 1.00E-4
NCI-H226	0.639	1.562	1.513	1.471	0.844	0.778	0.382	95	90	22	15	-40	3.90E-7	1.87E-5	> 1.00E-4
NCI-H23	0.630	1.504	1.476	1.341	0.935	0.807	0.401	97	81	35	20	-36	4.73E-7	2.28E-5	> 1.00E-4
NCI-H322M	0.626	1.477	1.472	1.458	1.061	1.000	0.847	99	98	51	44	26	1.42E-6	> 1.00E-4	> 1.00E-4
NCI-H460	0.254	2.327	2.306	2.231	0.600	0.513	0.262	99	95	17	12	.	3.77E-7	> 1.00E-4	> 1.00E-4
NCI-H522	1.202	1.714	1.802	1.689	1.025	0.958	0.512	117	95	-15	-20	-57	2.58E-7	7.35E-7	6.31E-5
Colon Cancer															
COLO 205	0.234	1.051	1.114	1.064	0.347	0.224	0.199	108	102	14	-4	-15	3.87E-7	5.68E-6	> 1.00E-4
HCC-2998	0.549	1.534	1.507	1.379	0.905	0.498	0.239	97	84	36	-9	-56	5.15E-7	6.24E-6	7.29E-5
HCT-116	0.295	1.491	1.533	1.497	0.548	0.447	0.171	104	101	21	13	-42	4.33E-7	1.70E-5	> 1.00E-4
HCT-15	0.358	1.814	1.814	1.754	0.837	0.651	0.494	100	96	33	20	9	5.34E-7	> 1.00E-4	> 1.00E-4
HT29	0.261	1.174	1.176	1.201	0.288	0.237	0.201	100	103	3	-9	-23	3.38E-7	1.75E-6	> 1.00E-4
KM12	0.202	1.052	1.111	0.996	0.451	0.379	0.246	107	93	29	21	5	4.76E-7	> 1.00E-4	> 1.00E-4
SW-620	0.175	1.173	1.143	1.095	0.418	0.438	0.331	97	92	24	26	16	4.18E-7	> 1.00E-4	> 1.00E-4
CNS Cancer															
SF-268	0.512	1.471	1.489	1.466	1.025	1.006	0.389	102	100	53	51	-24	1.05E-5	4.81E-5	> 1.00E-4
SF-295	0.620	2.269	2.176	2.001	0.956	0.968	0.335	94	84	20	21	-46	3.41E-7	2.06E-5	> 1.00E-4
SF-539	0.694	1.763	1.760	1.788	0.853	0.658	0.261	100	102	15	-5	-62	3.97E-7	5.48E-6	6.07E-5
SNB-19	0.511	1.597	1.574	1.486	0.998	0.867	0.528	98	90	45	33	2	7.66E-7	> 1.00E-4	> 1.00E-4
SNB-75	0.566	1.075	1.021	0.989	0.551	0.536	0.130	89	83	-3	-5	-77	2.43E-7	9.29E-7	4.19E-5
U251	0.369	1.523	1.492	1.428	0.705	0.510	0.157	97	92	29	12	-57	4.64E-7	1.50E-5	7.82E-5
Melanoma															
LOX IMVI	0.349	1.784	1.721	1.646	0.844	0.926	0.426	96	90	34	40	5	5.28E-7	> 1.00E-4	> 1.00E-4
MALME-3M	0.617	1.362	1.374	1.315	0.917	0.918	0.650	102	94	40	40	4	6.56E-7	> 1.00E-4	> 1.00E-4
M14	0.425	1.181	1.195	1.187	0.681	0.346	0.195	102	101	34	-19	-54	5.73E-7	4.42E-6	7.66E-5
MDA-MB-435	0.333	1.553	1.491	0.918	0.293	0.201	0.130	95	48	-12	-40	-61	9.05E-8	6.28E-7	3.04E-5
SK-MEL-2	1.042	1.641	1.709	1.660	1.084	1.164	0.341	111	103	7	20	-67	3.57E-7	1.70E-5	6.35E-5
SK-MEL-28	0.387	1.147	1.128	1.033	0.693	0.630	0.241	97	85	40	32	-38	6.05E-7	2.87E-5	> 1.00E-4
SK-MEL-5	0.456	2.094	2.020	1.746	0.727	0.793	0.090	96	79	17	21	-80	2.90E-7	1.60E-5	5.00E-5
UACC-257	0.736	1.244	1.218	1.139	0.872	0.987	0.528	95	79	27	49	-28	3.61E-7	4.32E-5	> 1.00E-4
UACC-62	0.778	2.300	2.282	2.055	1.365	1.305	0.256	99	84	39	35	-67	5.59E-7	2.19E-5	6.78E-5
Ovarian Cancer															
IGROV1	0.475	1.469	1.538	1.418	1.051	0.852	0.392	107	95	58	38	-18	2.48E-6	4.82E-5	> 1.00E-4
OVCAR-3	0.498	1.327	1.392	1.320	0.571	0.371	0.155	108	99	9	-26	-69	3.50E-7	1.81E-6	3.67E-5
OVCAR-4	0.455	0.868	0.852	0.826	0.726	0.664	0.241	96	90	66	51	-47	1.02E-5	3.30E-5	> 1.00E-4
OVCAR-5	0.507	1.577	1.558	1.546	1.159	0.828	0.666	98	97	61	30	15	2.26E-6	> 1.00E-4	> 1.00E-4
OVCAR-8	0.438	1.462	1.446	1.452	0.902	0.683	0.255	98	99	45	24	-42	8.17E-7	2.31E-5	> 1.00E-4
NCI/ADR-RES	0.558	1.452	1.442	1.324	0.571	0.478	0.319	99	86	1	-14	-43	2.65E-7	1.23E-6	> 1.00E-4
SK-OV-3	0.425	1.062	1.147	1.082	0.545	0.397	0.216	113	103	19	-7	-49	4.27E-7	5.45E-6	> 1.00E-4
Renal Cancer															
786-0	0.755	2.072	2.073	2.097	1.234	1.080	0.504	100	102	36	25	-33	6.19E-7	2.67E-5	> 1.00E-4
A498	1.148	1.679	1.585	1.497	1.205	1.091	0.615	82	66	11	-5	-46	1.93E-7	4.81E-6	> 1.00E-4
ACHN	0.337	1.229	1.278	1.264	0.753	0.810	0.352	105	104	47	53	2	.	> 1.00E-4	> 1.00E-4
CAKI-1	0.639	2.216	2.194	1.998	1.239	1.342	1.030	99	86	38	45	25	5.64E-7	> 1.00E-4	> 1.00E-4
RXF 393	0.517	1.074	1.075	1.011	0.559	0.432	0.145	100	89	7	-16	-72	2.99E-7	2.05E-6	4.02E-5
SN12C	0.531	1.816	1.743	1.694	1.225	1.149	0.642	94	91	54	48	9	4.76E-6	> 1.00E-4	> 1.00E-4
TK-10	0.885	1.484	1.534	1.522	1.227	1.160	0.408	108	106	57	46	-54	4.27E-6	2.88E-5	9.14E-5
UO-31	0.333	1.002	0.967	0.938	0.703	0.716	0.346	95	90	55	57	2	1.35E-5	> 1.00E-4	> 1.00E-4
Prostate Cancer															
PC-3	0.411	1.248	1.199	1.090	0.663	0.648	0.458	94	81	30	28	6	4.07E-7	> 1.00E-4	> 1.00E-4
DU-145	0.386	1.420	1.531	1.473	0.714	0.503	0.266	111	105	32	11	-31	5.63E-7	1.85E-5	> 1.00E-4
Breast Cancer															
MCF7	0.239	1.386	1.299	1.146	0.367	0.376	0.151	92	79	11	12	-37	2.68E-7	1.75E-5	> 1.00E-4
MDA-MB-231/ATCC	0.639	1.752	1.732	1.747	1.297	1.143	0.746	98	100	59	45	10	4.55E-6	> 1.00E-4	> 1.00E-4
HS 578T	0.897	1.726	1.646	1.585	1.114	1.094	0.904	90	83	26	24	1	3.80E-7	> 1.00E-4	> 1.00E-4
BT-549	1.107	1.750	1.774	1.763	1.291	1.385	0.543	104	102	29	43	-51	5.11E-7	2.88E-5	9.77E-5
T-47D	0.499	1.189	1.217	1.220	0.848	0.928	0.529	104	105	51	62	4	1.62E-5	> 1.00E-4	> 1.00E-4
MDA-MB-468	0.572	1.162	1.158	1.077	0.552	0.563	0.360	99	86	-3	-2	-37	2.51E-7	9.14E-7	> 1.00E-4

Pyrazoline (78–) – Five Dose Repeat

National Cancer Institute Developmental Therapeutics Program
In-Vitro Testing Results

NSC : D - 761466 / 1	Experiment ID : 1112RS69	Test Type : 08	Units : Molar
Report Date : February 17, 2012	Test Date : December 05, 2011	QNS :	MC :
COMI : AC03:45.2 (110256)	Stain Reagent : SRB Dual-Pass Related	SSPL : 0Y8X	

		Log10 Concentration												
	Time	Mean Optical Densities					Percent Growth							
Panel/Cell Line	Zero	Ctrl	-8.0	-7.0	-6.0	-5.0	-4.0	-8.0	-7.0	-6.0	-5.0	-4.0	GI50	TGI	LC50
Non-Small Cell Lung Cancer															
A549/ATCC	0.296	1.523	1.476	1.433	0.684	0.571	0.269	96	93	32	22	-9	4.99E-7	5.14E-5	> 1.00E-4
EKVX	0.426	1.388	1.369	1.344	0.930	0.736	0.557	98	95	52	32	14	1.31E-6	> 1.00E-4	> 1.00E-4
HOP-62	0.454	1.477	1.492	1.463	0.931	0.864	0.346	101	99	47	40	-24	8.59E-7	4.24E-5	> 1.00E-4
NCI-H226	0.526	1.127	1.000	1.044	0.807	0.734	0.374	79	86	47	35	-29	8.26E-7	3.50E-5	> 1.00E-4
NCI-H23	0.648	2.104	2.103	1.735	0.703	0.571	0.138	100	75	4	-12	-79	2.23E-7	1.73E-6	3.71E-5
NCI-H322M	0.746	1.740	1.822	1.874	1.277	1.298	1.082	108	113	53	56	34	1.79E-5	> 1.00E-4	> 1.00E-4
NCI-H460	0.309	2.604	2.649	2.487	0.605	0.538	0.265	102	95	13	10	-14	3.53E-7	2.57E-5	> 1.00E-4
NCI-H522	0.682	1.426	1.377	1.298	0.625	0.573	0.335	93	83	-8	-16	-51	2.29E-7	8.08E-7	9.43E-5
Colon Cancer															
COLO 205	0.316	1.104	1.090	1.154	0.382	0.207	0.143	98	106	8	-34	-55	3.75E-7	1.56E-6	5.75E-5
HCC-2998	0.382	1.214	1.208	1.087	0.794	0.533	0.286	99	85	49	18	-25	9.66E-7	2.61E-5	> 1.00E-4
HCT-116	0.236	1.834	1.775	1.768	0.660	0.595	0.161	96	96	27	22	-32	4.59E-7	2.60E-5	> 1.00E-4
HCT-15	0.426	2.504	2.463	2.297	1.213	1.066	0.578	98	90	38	31	7	5.86E-7	> 1.00E-4	> 1.00E-4
HT29	0.249	1.350	1.379	1.358	0.359	0.301	0.226	103	101	10	5	-9	3.63E-7	2.17E-5	> 1.00E-4
KM12	0.625	2.486	2.530	2.262	1.201	1.283	0.959	102	88	31	35	18	4.63E-7	> 1.00E-4	> 1.00E-4
SW-620	0.264	1.763	1.715	1.542	0.624	0.625	0.511	97	85	24	24	16	3.76E-7	> 1.00E-4	> 1.00E-4
CNS Cancer															
SF-268	0.528	1.673	1.705	1.640	1.169	1.278	0.519	103	97	56	65	-2	1.70E-5	9.43E-5	> 1.00E-4
SF-295	0.834	2.696	2.617	2.396	1.116	0.994	0.364	96	84	15	9	-56	3.11E-7	1.36E-5	7.98E-5
SNB-19	0.551	1.846	1.762	1.635	1.077	0.974	0.547	94	84	41	33	-1	6.05E-7	9.45E-5	> 1.00E-4
SNB-75	0.716	1.261	1.160	1.130	0.698	0.773	0.239	81	76	-3	10	-67	2.15E-7	.	6.08E-5
U251	0.365	1.748	1.714	1.662	0.724	0.510	0.147	98	94	26	10	-60	4.42E-7	1.41E-5	7.24E-5
Melanoma															
LOX IMVI	0.286	2.095	2.037	1.911	0.962	1.062	0.417	97	90	37	43	7	5.75E-7	> 1.00E-4	> 1.00E-4
MALME-3M	0.749	1.545	1.532	1.512	1.167	1.227	0.749	98	96	52	60	.	1.47E-5	> 1.00E-4	> 1.00E-4
M14	0.429	1.609	1.585	1.559	0.917	0.532	0.270	98	96	41	9	-37	6.93E-7	1.55E-5	> 1.00E-4
MDA-MB-435	0.561	2.400	2.361	1.414	0.624	0.413	0.189	98	46	3	-26	-66	8.51E-8	1.30E-6	3.89E-5
SK-MEL-2	0.914	1.573	1.605	1.596	1.239	1.202	0.442	105	103	49	44	-52	9.68E-7	2.87E-5	9.60E-5
SK-MEL-28	0.333	0.950	0.944	0.822	0.618	0.553	0.131	99	79	46	36	-61	7.67E-7	2.34E-5	7.73E-5
SK-MEL-5	0.584	2.382	2.111	2.034	0.826	0.876	0.051	85	81	13	16	-91	2.86E-7	1.42E-5	4.13E-5
UACC-257	0.593	1.340	1.295	1.222	0.940	1.045	0.576	94	84	46	60	-3	.	9.01E-5	> 1.00E-4
UACC-62	0.632	2.254	2.198	1.880	1.110	1.098	0.097	97	77	29	29	-85	3.69E-7	1.79E-5	4.94E-5
Ovarian Cancer															
IGROV1	0.402	1.377	1.420	1.391	0.889	0.651	0.313	104	101	50	26	-22	9.95E-7	3.42E-5	> 1.00E-4
OVCAR-3	0.491	1.396	1.468	1.449	0.754	0.741	0.310	108	106	29	28	-37	5.34E-7	2.68E-5	> 1.00E-4
OVCAR-4	0.565	1.159	1.186	1.122	0.930	0.890	0.438	104	94	61	55	-22	1.15E-5	5.11E-5	> 1.00E-4
OVCAR-5	0.596	1.668	1.728	1.624	1.359	1.072	0.848	106	96	71	44	24	6.18E-6	> 1.00E-4	> 1.00E-4
NCI/ADR-RES	0.456	1.639	1.572	1.352	0.584	0.447	0.267	94	76	11	-2	-41	2.49E-7	7.01E-6	> 1.00E-4
SK-OV-3	0.592	1.492	1.526	1.531	0.862	0.721	0.433	104	104	30	14	-27	5.38E-7	2.22E-5	> 1.00E-4
Renal Cancer															
786-0	0.581	2.104	2.148	2.119	1.286	1.163	0.438	103	101	46	38	-25	8.55E-7	4.06E-5	> 1.00E-4
A498	1.385	2.065	2.066	1.908	1.468	1.404	0.691	100	77	12	3	-50	2.60E-7	1.13E-5	9.94E-5
ACHN	0.398	1.652	1.626	1.601	0.948	1.059	0.307	98	96	44	53	-23	.	4.97E-5	> 1.00E-4
CAKI-1	0.744	2.078	1.931	1.770	1.243	1.331	0.986	89	77	37	44	18	4.79E-7	> 1.00E-4	> 1.00E-4
RXF 393	0.627	1.111	0.988	1.035	0.708	0.480	0.208	75	84	17	-24	-67	3.22E-7	2.60E-6	4.09E-5
SN12C	0.596	2.311	2.304	2.141	1.277	1.221	0.705	100	90	40	36	6	6.24E-7	> 1.00E-4	> 1.00E-4
TK-10	0.591	1.199	1.215	1.193	0.996	0.963	0.347	103	99	67	61	41	1.28E-5	3.95E-5	> 1.00E-4
UO-31	0.572	1.678	1.519	1.536	1.135	1.082	0.619	86	87	51	46	4	1.53E-6	> 1.00E-4	> 1.00E-4
Prostate Cancer															
PC-3	0.381	1.823	1.777	1.632	0.777	0.684	0.472	97	87	27	21	6	4.16E-7	> 1.00E-4	> 1.00E-4
DU-145	0.556	1.716	1.802	1.815	1.113	0.929	0.605	107	109	48	32	4	9.26E-7	> 1.00E-4	> 1.00E-4
Breast Cancer															
MCF7	0.299	1.650	1.489	1.371	0.421	0.479	0.158	88	79	9	13	-47	2.61E-7	1.66E-5	> 1.00E-4
MDA-MB-231/ATCC	0.504	1.146	1.224	1.045	0.793	0.639	0.355	112	84	45	21	-30	7.47E-7	2.60E-5	> 1.00E-4
HS 578T	0.966	1.913	1.849	1.765	1.256	1.127	0.899	93	84	31	17	-7	4.35E-7	5.12E-5	> 1.00E-4
BT-549	0.873	1.745	1.744	1.756	1.337	1.464	0.592	100	101	53	68	-32	1.50E-5	4.76E-5	> 1.00E-4
T-47D	0.585	1.580	1.618	1.568	0.838	1.120	0.534	104	99	25	54	-9	.	7.23E-5	> 1.00E-4
MDA-MB-468	0.583	1.209	1.088	1.106	0.480	0.415	0.229	81	84	-18	-29	-61	2.14E-7	6.68E-7	4.58E-5

Pyrazoline (79) – Five Dose

National Cancer Institute Developmental Therapeutics Program
In-Vitro Testing Results

NSC : D - 761259 / 1	Experiment ID : 1109NS21	Test Type : 08	Units : Molar
Report Date : October 26, 2011	Test Date : September 12, 2011	QNS :	MC :
COMI : AC04:37 (109727)	Stain Reagent : SRB Dual-Pass Related	SSPL : 0Y8X	

			Log10 Concentration											
	Time		Mean Optical Densities					Percent Growth						
Panel/Cell Line	Zero	Ctrl	-8.0	-7.0	-6.0	-5.0	-4.0	-8.0	-7.0	-6.0	-5.0	-4.0	GI50	TGI	LC50
Leukemia															
CCRF-CEM	0.380	1.532	1.575	1.598	1.434	0.759	0.582	104	106	92	33	18	5.10E-6	> 1.00E-4	> 1.00E-4
HL-60(TB)	0.695	2.687	2.686	2.686	2.511	0.924	0.751	100	100	91	11	3	3.28E-6	> 1.00E-4	> 1.00E-4
MOLT-4	0.518	2.443	2.523	2.560	2.528	1.497	1.066	104	106	104	51	28	1.09E-5	> 1.00E-4	> 1.00E-4
RPMI-8226	0.673	2.529	2.466	2.454	2.476	1.934	1.565	97	96	97	68	48	7.98E-5	> 1.00E-4	> 1.00E-4
SR	0.449	2.345	2.309	2.348	1.285	0.810	0.685	98	100	44	19	12	7.84E-7	> 1.00E-4	> 1.00E-4
Non-Small Cell Lung Cancer															
A549/ATCC	0.410	1.767	1.696	1.705	1.756	0.910	0.793	95	95	99	37	28	6.15E-6	> 1.00E-4	> 1.00E-4
EKVX	0.836	1.969	1.897	1.854	1.844	1.518	1.339	94	90	89	60	44	4.42E-5	> 1.00E-4	> 1.00E-4
HOP-62	0.407	1.005	0.999	1.013	1.011	0.581	0.541	99	101	101	29	22	5.12E-6	> 1.00E-4	> 1.00E-4
HOP-92	0.903	2.123	2.040	1.991	2.016	1.891	1.786	93	89	91	81	72	> 1.00E-4	> 1.00E-4	> 1.00E-4
NCI-H226	0.668	1.598	1.538	1.493	1.479	0.929	0.732	93	89	87	28	7	4.26E-6	> 1.00E-4	> 1.00E-4
NCI-H23	0.445	1.316	1.311	1.245	1.194	0.874	0.770	99	92	86	49	37	9.54E-6	> 1.00E-4	> 1.00E-4
NCI-H322M	0.717	1.899	1.886	1.881	1.893	1.396	1.301	99	98	99	57	49	8.49E-5	> 1.00E-4	> 1.00E-4
NCI-H460	0.172	1.935	1.940	1.927	1.915	0.454	0.340	100	100	99	16	10	3.89E-6	> 1.00E-4	> 1.00E-4
NCI-H522	0.798	1.612	1.587	1.520	1.506	0.792	0.701	97	89	87	-1	-12	2.64E-6	9.79E-6	> 1.00E-4
Colon Cancer															
COLO 205	0.315	1.186	1.294	1.290	1.192	0.337	0.131	112	112	101	2	-58	3.28E-6	1.10E-5	7.27E-5
HCC-2998	0.424	1.623	1.602	1.530	1.453	1.030	0.742	98	92	86	51	26	1.05E-5	> 1.00E-4	> 1.00E-4
HCT-116	0.194	1.461	1.571	1.565	1.435	0.427	0.406	109	108	98	18	17	4.00E-6	> 1.00E-4	> 1.00E-4
HCT-15	0.395	1.884	1.886	1.817	1.779	0.870	0.745	100	96	93	32	23	5.05E-6	> 1.00E-4	> 1.00E-4
HT29	0.216	1.203	1.219	1.222	1.199	0.254	0.235	102	102	100	4	2	3.29E-6	> 1.00E-4	> 1.00E-4
KM12	0.322	2.486	2.541	2.556	2.000	1.010	1.069	103	103	78	32	34	4.00E-6	> 1.00E-4	> 1.00E-4
SW-620	0.196	1.766	1.757	1.677	1.587	0.507	0.487	99	94	89	20	19	3.64E-6	> 1.00E-4	> 1.00E-4
CNS Cancer															
SF-268	0.280	1.747	1.781	1.765	1.737	1.028	1.045	102	101	99	51	52	> 1.00E-4	> 1.00E-4	> 1.00E-4
SF-539	0.713	1.991	2.002	1.964	1.988	1.070	0.588	101	98	100	28	-18	4.92E-6	4.11E-5	> 1.00E-4
SNB-19	0.476	1.592	1.541	1.496	1.430	0.855	0.815	95	91	85	34	30	4.88E-6	> 1.00E-4	> 1.00E-4
SNB-75	0.863	1.564	1.444	1.377	1.388	0.596	0.649	83	73	75	-31	-25	1.72E-6	5.10E-6	> 1.00E-4
U251	0.365	1.561	1.529	1.491	1.493	0.653	0.621	97	94	94	24	21	4.27E-6	> 1.00E-4	> 1.00E-4
Melanoma															
LOX IMVI	0.247	1.608	1.560	1.547	1.439	0.749	0.780	96	96	88	37	39	5.50E-6	> 1.00E-4	> 1.00E-4
MALME-3M	0.602	1.465	1.441	1.486	1.324	0.957	0.953	97	102	84	41	41	6.19E-6	> 1.00E-4	> 1.00E-4
M14	0.317	1.111	1.127	1.165	1.098	0.452	0.424	102	107	98	17	13	3.93E-6	> 1.00E-4	> 1.00E-4
MDA-MB-435	0.551	2.509	2.453	2.292	1.148	0.500	0.241	97	89	30	-9	-56	4.63E-7	5.85E-6	7.36E-5
SK-MEL-2	0.821	1.436	1.518	1.531	1.467	0.849	0.770	113	115	105	4	-6	3.52E-6	2.62E-5	> 1.00E-4
SK-MEL-28	0.533	1.446	1.402	1.386	1.298	0.876	0.841	95	93	84	38	34	5.38E-6	> 1.00E-4	> 1.00E-4
SK-MEL-5	0.497	2.273	2.172	2.137	2.026	0.715	0.680	94	92	86	12	10	3.08E-6	> 1.00E-4	> 1.00E-4
UACC-257	0.874	1.656	1.619	1.573	1.590	1.228	1.334	95	89	91	45	59	.	> 1.00E-4	> 1.00E-4
UACC-62	0.563	1.921	1.866	1.768	1.628	0.917	0.868	96	89	78	26	22	3.49E-6	> 1.00E-4	> 1.00E-4
Ovarian Cancer															
IGROV1	0.570	1.894	1.959	1.971	1.788	1.154	0.994	105	106	92	44	32	7.52E-6	> 1.00E-4	> 1.00E-4
OVCAR-3	0.235	1.807	1.842	1.910	1.815	0.829	0.695	102	107	100	38	29	6.39E-6	> 1.00E-4	> 1.00E-4
OVCAR-4	0.580	1.213	1.188	1.187	1.158	0.909	0.736	96	96	91	52	25	1.17E-5	> 1.00E-4	> 1.00E-4
OVCAR-5	0.521	1.410	1.395	1.407	1.367	0.997	0.806	98	100	95	54	32	1.46E-5	> 1.00E-4	> 1.00E-4
OVCAR-8	0.498	1.884	1.876	1.853	1.833	1.194	0.884	99	98	96	50	28	1.02E-5	> 1.00E-4	> 1.00E-4
NCI/ADR-RES	0.500	1.547	1.542	1.488	1.326	0.602	0.524	99	94	79	10	2	2.61E-6	> 1.00E-4	> 1.00E-4
SK-OV-3	0.563	1.252	1.276	1.284	1.242	0.675	0.444	103	105	99	16	-21	3.89E-6	2.72E-5	> 1.00E-4
Renal Cancer															
786-0	0.661	2.295	2.252	2.281	2.155	1.277	1.207	97	99	91	38	33	5.90E-6	> 1.00E-4	> 1.00E-4
A498	0.701	1.901	1.813	1.670	1.728	1.308	1.177	93	81	86	51	40	1.14E-5	> 1.00E-4	> 1.00E-4
ACHN	0.346	1.330	1.404	1.387	1.413	0.824	0.861	107	106	108	49	52	.	> 1.00E-4	> 1.00E-4
CAKI-1	0.638	1.899	1.826	1.774	1.630	0.803	0.756	94	90	79	13	9	2.73E-6	> 1.00E-4	> 1.00E-4
RXF 393	0.511	1.101	1.071	1.026	1.008	0.626	0.356	95	87	84	19	-30	3.38E-6	2.46E-5	> 1.00E-4
SN12C	0.473	1.778	1.712	1.675	1.642	0.998	0.923	95	92	90	40	34	6.33E-6	> 1.00E-4	> 1.00E-4
TK-10	0.909	1.806	1.775	1.808	1.787	1.578	1.384	97	100	98	75	53	> 1.00E-4	> 1.00E-4	> 1.00E-4
UO-31	0.370	1.399	1.355	1.340	1.365	0.936	0.797	96	94	97	55	41	2.33E-5	> 1.00E-4	> 1.00E-4
Prostate Cancer															
PC-3	0.364	1.501	1.467	1.427	1.371	1.095	0.949	97	94	89	64	51	> 1.00E-4	> 1.00E-4	> 1.00E-4
DU-145	0.173	1.548	1.657	1.590	1.582	0.932	0.443	108	103	103	55	20	1.40E-5	> 1.00E-4	> 1.00E-4
Breast Cancer															
MCF7	0.280	1.495	1.501	1.377	1.265	0.394	0.427	100	90	81	9	12	2.71E-6	> 1.00E-4	> 1.00E-4
MDA-MB-231/ATCC	0.638	1.738	1.690	1.644	1.507	1.178	1.136	96	91	79	49	45	9.30E-6	> 1.00E-4	> 1.00E-4
HS 578T	0.449	1.878	1.858	1.762	1.781	1.269	1.037	99	92	93	57	41	2.86E-5	> 1.00E-4	> 1.00E-4
BT-549	0.868	1.821	1.838	1.924	1.893	1.263	1.177	102	111	107	41	32	7.41E-6	> 1.00E-4	> 1.00E-4
T-47D	0.549	1.223	1.204	1.204	1.191	0.817	0.791	97	97	95	40	36	6.54E-6	> 1.00E-4	> 1.00E-4
MDA-MB-468	0.579	1.169	1.114	1.064	1.019	0.548	0.493	91	82	75	-5	-15	2.03E-6	8.57E-6	> 1.00E-4

Pyrazoline (80) – Five Dose

National Cancer Institute Developmental Therapeutics Program
In-Vitro Testing Results

NSC : D - 761260 / 1	Experiment ID : 1109NS21	Test Type : 08	Units : Molar
Report Date : October 26, 2011	Test Date : September 12, 2011	QNS :	MC :
COMI : AC04:38 (109728)	Stain Reagent : SRB Dual-Pass Related	SSPL : 0Y8X	

			Log10 Concentration											
	Time		Mean Optical Densities					Percent Growth						
Panel/Cell Line	Zero	Ctrl	-8.0	-7.0	-6.0	-5.0	-4.0	-8.0	-7.0	-6.0	-5.0	-4.0	GI50	TGI	LC50
Leukemia															
CCRF-CEM	0.380	1.548	1.625	1.608	0.943	0.588	0.502	107	105	48	18	10	9.30E-7	> 1.00E-4	> 1.00E-4
HL-60(TB)	0.695	2.265	2.349	2.596	0.867	0.693	0.514	105	121	11	.	-26	4.42E-7	9.43E-6	> 1.00E-4
MOLT-4	0.518	2.098	2.267	2.391	1.404	0.917	0.706	111	119	56	25	12	1.57E-6	> 1.00E-4	> 1.00E-4
RPMI-8226	0.673	2.188	2.250	2.198	1.796	1.152	0.792	104	101	74	32	8	3.69E-6	> 1.00E-4	> 1.00E-4
SR	0.449	2.260	2.194	1.899	0.859	0.701	0.460	96	80	23	14	1	3.34E-7	> 1.00E-4	> 1.00E-4
Non-Small Cell Lung Cancer															
A549/ATCC	0.410	1.995	1.893	1.878	1.359	0.836	0.615	94	93	60	27	13	1.99E-6	> 1.00E-4	> 1.00E-4
EKVX	0.836	2.070	1.941	1.904	1.853	1.444	1.199	90	87	82	49	29	9.49E-6	> 1.00E-4	> 1.00E-4
HOP-62	0.407	1.022	1.037	1.061	0.880	0.559	0.530	102	106	77	25	20	3.27E-6	> 1.00E-4	> 1.00E-4
HOP-92	0.903	1.891	1.821	1.753	1.595	1.555	1.282	93	86	70	66	38	3.79E-5	> 1.00E-4	> 1.00E-4
NCI-H226	0.668	1.603	1.550	1.538	1.441	0.802	0.482	94	93	83	14	-28	3.01E-6	2.18E-5	> 1.00E-4
NCI-H23	0.445	1.390	1.363	1.360	1.168	0.754	0.612	97	97	76	33	18	4.03E-6	> 1.00E-4	> 1.00E-4
NCI-H322M	0.717	1.544	1.554	1.516	1.414	1.093	1.134	101	97	84	45	50	.	> 1.00E-4	> 1.00E-4
NCI-H460	0.172	1.929	1.975	1.867	0.480	0.288	0.139	103	96	18	7	-19	3.88E-7	1.79E-5	> 1.00E-4
NCI-H522	0.798	1.869	1.901	1.827	1.389	0.617	0.632	103	96	55	-23	-21	1.17E-6	5.11E-6	> 1.00E-4
Colon Cancer															
COLO 205	0.315	1.139	1.205	1.258	0.747	0.197	0.025	108	114	52	-38	-92	1.06E-6	3.82E-6	1.69E-5
HCC-2998	0.424	1.613	1.557	1.482	1.246	0.714	0.328	95	89	69	24	-23	2.68E-6	3.29E-5	> 1.00E-4
HCT-116	0.194	1.594	1.640	1.662	0.945	0.489	0.212	103	105	54	21	1	1.29E-6	> 1.00E-4	> 1.00E-4
HCT-15	0.395	1.938	1.996	1.987	1.394	0.779	0.497	104	103	65	25	7	2.35E-6	> 1.00E-4	> 1.00E-4
HT29	0.216	1.379	1.384	1.400	0.602	0.267	0.150	100	102	33	4	-31	5.69E-7	1.33E-5	> 1.00E-4
KM12	0.322	2.403	2.478	2.454	1.098	0.906	0.533	104	102	37	28	10	6.38E-7	> 1.00E-4	> 1.00E-4
SW-620	0.196	1.683	1.633	1.597	0.667	0.486	0.413	97	94	32	20	15	5.09E-7	> 1.00E-4	> 1.00E-4
CNS Cancer															
SF-268	0.280	1.674	1.712	1.691	1.169	0.983	0.647	103	101	64	50	26	1.04E-5	> 1.00E-4	> 1.00E-4
SF-539	0.713	2.004	1.980	1.979	1.868	0.690	0.432	98	98	89	-3	-39	2.66E-6	9.21E-6	> 1.00E-4
SNB-19	0.476	1.556	1.497	1.463	1.250	0.790	0.685	95	91	72	29	19	3.22E-6	> 1.00E-4	> 1.00E-4
SNB-75	0.863	1.473	1.384	1.360	1.061	0.624	0.769	85	81	32	-28	-11	4.38E-7	3.46E-6	> 1.00E-4
U251	0.365	1.667	1.689	1.625	1.393	0.705	0.481	102	97	79	26	9	3.53E-6	> 1.00E-4	> 1.00E-4
Melanoma															
LOX IMVI	0.247	1.564	1.512	1.509	1.041	0.822	0.464	96	96	60	44	16	4.15E-6	> 1.00E-4	> 1.00E-4
MALME-3M	0.602	1.325	1.320	1.319	0.948	0.893	0.826	99	99	48	40	31	9.10E-7	> 1.00E-4	> 1.00E-4
M14	0.317	1.265	1.253	1.239	0.918	0.438	0.219	99	97	63	13	-31	1.84E-6	1.96E-5	> 1.00E-4
MDA-MB-435	0.551	2.578	2.505	2.206	0.623	0.223	0.229	96	82	4	-60	-58	2.54E-7	1.14E-6	7.04E-6
SK-MEL-2	0.821	1.489	1.593	1.584	1.182	0.753	0.683	116	114	54	-8	-17	1.16E-6	7.35E-6	> 1.00E-4
SK-MEL-28	0.533	1.343	1.308	1.274	1.031	0.713	0.578	96	91	61	22	6	1.95E-6	> 1.00E-4	> 1.00E-4
SK-MEL-5	0.497	2.302	2.397	2.188	1.402	0.681	0.245	105	94	50	10	-51	1.01E-6	1.47E-5	9.74E-5
UACC-257	0.874	1.954	1.934	1.853	1.775	1.640	1.268	98	91	83	71	36	4.05E-5	> 1.00E-4	> 1.00E-4
UACC-62	0.563	1.840	1.841	1.723	1.224	0.846	0.583	100	91	52	22	2	1.15E-6	> 1.00E-4	> 1.00E-4
Ovarian Cancer															
IGROV1	0.570	1.610	1.760	1.690	1.099	0.787	0.665	114	108	51	21	9	1.07E-6	> 1.00E-4	> 1.00E-4
OVCAR-3	0.235	1.705	1.797	1.793	0.721	0.681	0.511	106	106	33	30	19	5.86E-7	> 1.00E-4	> 1.00E-4
OVCAR-4	0.580	1.146	1.129	1.117	1.060	0.813	0.611	97	95	85	41	5	6.29E-6	> 1.00E-4	> 1.00E-4
OVCAR-5	0.521	1.405	1.370	1.384	1.347	0.776	0.646	96	98	93	29	14	4.70E-6	> 1.00E-4	> 1.00E-4
OVCAR-8	0.498	2.179	2.176	2.164	2.013	1.110	0.898	100	99	90	36	24	5.58E-6	> 1.00E-4	> 1.00E-4
NCI/ADR-RES	0.500	1.569	1.562	1.462	0.902	0.452	0.456	99	90	38	-10	-9	5.80E-7	6.26E-6	> 1.00E-4
SK-OV-3	0.563	1.210	1.229	1.218	0.996	0.545	0.362	103	101	67	-3	-36	1.74E-6	9.00E-6	> 1.00E-4
Renal Cancer															
786-0	0.661	2.187	2.172	2.214	1.964	1.105	0.689	99	102	85	29	2	4.25E-6	> 1.00E-4	> 1.00E-4
A498	0.701	1.933	1.777	1.625	1.332	1.232	1.026	87	75	51	43	26	1.39E-6	> 1.00E-4	> 1.00E-4
ACHN	0.346	1.378	1.433	1.404	1.207	0.874	0.487	105	103	83	51	14	1.07E-5	> 1.00E-4	> 1.00E-4
CAKI-1	0.638	2.371	2.248	2.101	1.440	1.086	0.803	93	84	46	26	10	7.99E-7	> 1.00E-4	> 1.00E-4
RXF 393	0.511	1.110	1.107	1.063	0.992	0.396	0.353	99	92	80	-23	-31	1.97E-6	6.04E-6	> 1.00E-4
SN12C	0.473	1.766	1.681	1.701	1.620	0.964	0.545	93	95	89	38	6	5.78E-6	> 1.00E-4	> 1.00E-4
TK-10	0.909	1.788	1.806	1.786	1.686	1.487	1.261	102	100	88	66	40	4.08E-5	> 1.00E-4	> 1.00E-4
UO-31	0.370	1.262	1.178	1.215	0.875	0.750	0.459	91	95	57	43	10	2.94E-6	> 1.00E-4	> 1.00E-4
Prostate Cancer															
PC-3	0.364	1.339	1.262	1.204	0.852	0.763	0.624	92	86	50	41	27	9.99E-7	> 1.00E-4	> 1.00E-4
DU-145	0.173	1.272	1.375	1.364	0.940	0.460	0.325	109	108	70	26	14	2.83E-6	> 1.00E-4	> 1.00E-4
Breast Cancer															
MCF7	0.280	1.533	1.470	1.371	0.719	0.416	0.292	95	87	35	11	1	5.16E-7	> 1.00E-4	> 1.00E-4
MDA-MB-231/ATCC	0.638	1.621	1.609	1.544	1.504	1.071	0.920	99	92	88	44	29	7.31E-6	> 1.00E-4	> 1.00E-4
HS 578T	0.449	1.831	1.765	1.713	1.559	1.076	0.978	95	91	80	45	38	7.36E-6	> 1.00E-4	> 1.00E-4
BT-549	0.868	1.809	1.864	1.894	1.605	1.380	0.777	106	109	78	54	-11	1.17E-5	6.88E-5	> 1.00E-4
T-47D	0.549	1.217	1.226	1.215	1.179	0.822	0.682	101	100	94	41	20	6.72E-6	> 1.00E-4	> 1.00E-4
MDA-MB-468	0.579	1.218	1.183	1.149	0.999	0.565	0.540	94	89	66	-3	-7	1.70E-6	9.19E-6	> 1.00E-4

Pyrazoline (105) – Five Dose

National Cancer Institute Developmental Therapeutics Program
In-Vitro Testing Results

NSC : D - 761258 / 1	Experiment ID : 1109NS21	Test Type : 08	Units : Molar
Report Date : October 26, 2011	Test Date : September 12, 2011	QNS :	MC :
COMI : AC03:44 (109726)	Stain Reagent : SRB Dual-Pass Related	SSPL : 0Y8X	

			Log10 Concentration											
	Time		Mean Optical Densities					Percent Growth						
Panel/Cell Line	Zero	Ctrl	-8.0	-7.0	-6.0	-5.0	-4.0	-8.0	-7.0	-6.0	-5.0	-4.0	GI50	TGI	LC50
Leukemia															
CCRF-CEM	0.380	1.644	1.659	1.714	1.206	0.596	0.533	101	106	65	17	12	2.08E-6	> 1.00E-4	> 1.00E-4
HL-60(TB)	0.695	2.424	2.467	2.384	1.440	0.703	0.586	102	98	43	.	-16	7.47E-7	1.07E-5	> 1.00E-4
MOLT-4	0.518	2.348	2.443	2.465	2.096	1.075	0.807	105	106	86	30	16	4.46E-6	> 1.00E-4	> 1.00E-4
RPMI-8226	0.673	2.632	2.607	2.555	2.361	1.769	1.627	99	96	86	56	49	6.63E-5	> 1.00E-4	> 1.00E-4
SR	0.449	2.410	2.379	2.292	0.896	0.760	0.707	98	94	23	16	13	4.15E-7	> 1.00E-4	> 1.00E-4
Non-Small Cell Lung Cancer															
A549/ATCC	0.410	1.844	1.794	1.773	1.113	0.772	0.710	96	95	49	25	21	9.52E-7	> 1.00E-4	> 1.00E-4
EKVX	0.836	2.041	1.957	1.925	1.746	1.473	1.440	93	90	75	53	50	> 1.00E-4	> 1.00E-4	> 1.00E-4
HOP-62	0.407	1.042	1.029	1.028	0.772	0.589	0.573	98	98	57	29	26	1.82E-6	> 1.00E-4	> 1.00E-4
HOP-92	0.903	2.203	2.125	2.055	1.855	1.707	1.611	94	89	73	62	54	> 1.00E-4	> 1.00E-4	> 1.00E-4
NCI-H226	0.668	1.606	1.527	1.493	1.195	0.733	0.745	92	88	56	7	8	1.33E-6	> 1.00E-4	> 1.00E-4
NCI-H23	0.445	1.402	1.384	1.354	1.093	0.778	0.719	98	95	68	35	29	3.45E-6	> 1.00E-4	> 1.00E-4
NCI-H322M	0.717	1.919	1.958	1.914	1.766	1.486	1.487	103	100	87	64	64	> 1.00E-4	> 1.00E-4	> 1.00E-4
NCI-H460	0.172	1.991	2.027	1.955	0.714	0.358	0.285	102	98	30	10	6	5.05E-7	> 1.00E-4	> 1.00E-4
NCI-H522	0.798	1.713	1.732	1.709	1.168	0.838	0.801	102	100	40	4	.	6.88E-7	> 1.00E-4	> 1.00E-4
Colon Cancer															
COLO 205	0.315	1.241	1.314	1.333	0.610	0.239	0.254	108	110	32	-24	-20	5.85E-7	3.71E-6	> 1.00E-4
HCC-2998	0.424	1.711	1.699	1.663	1.303	0.658	0.625	99	96	68	18	16	2.32E-6	> 1.00E-4	> 1.00E-4
HCT-116	0.194	1.504	1.597	1.552	0.637	0.445	0.269	107	104	34	19	6	5.86E-7	> 1.00E-4	> 1.00E-4
HCT-15	0.395	1.905	1.888	1.806	1.099	0.696	0.572	99	93	47	20	12	9.48E-7	> 1.00E-4	> 1.00E-4
HT29	0.216	1.256	1.318	1.344	0.386	0.263	0.241	106	108	16	5	2	4.31E-7	> 1.00E-4	> 1.00E-4
KM12	0.322	2.445	2.591	2.570	1.177	0.966	0.792	107	106	40	30	22	7.11E-7	> 1.00E-4	> 1.00E-4
SW-620	0.196	1.788	1.737	1.724	0.753	0.601	0.599	97	96	35	25	25	5.67E-7	> 1.00E-4	> 1.00E-4
CNS Cancer															
SF-268	0.280	1.747	1.814	1.797	1.262	1.114	0.922	105	103	67	57	44	3.34E-5	> 1.00E-4	> 1.00E-4
SF-539	0.713	1.970	2.023	2.122	1.362	0.634	0.663	104	112	52	-11	-7	1.06E-6	6.64E-6	> 1.00E-4
SNB-19	0.476	1.593	1.549	1.497	1.145	0.745	0.804	96	91	60	24	29	1.89E-6	> 1.00E-4	> 1.00E-4
SNB-75	0.863	1.553	1.427	1.423	0.938	0.762	1.041	82	81	11	-12	26	2.77E-7	.	> 1.00E-4
U251	0.365	1.638	1.578	1.544	0.966	0.641	0.568	95	93	47	22	16	8.68E-7	> 1.00E-4	> 1.00E-4
Melanoma															
LOX IMVI	0.247	1.585	1.488	1.476	0.924	0.763	0.505	93	92	51	39	19	1.13E-6	> 1.00E-4	> 1.00E-4
MALME-3M	0.602	1.465	1.451	1.455	1.102	1.034	1.077	98	99	58	50	55	> 1.00E-4	> 1.00E-4	> 1.00E-4
M14	0.317	1.167	1.165	1.170	0.697	0.398	0.480	100	100	45	10	19	8.01E-7	> 1.00E-4	> 1.00E-4
MDA-MB-435	0.551	2.497	2.488	2.250	0.588	0.275	0.304	100	87	2	-50	-45	2.73E-7	1.09E-6	.
SK-MEL-2	0.821	1.506	1.576	1.598	1.083	0.830	0.915	110	114	38	1	14	6.99E-7	> 1.00E-4	> 1.00E-4
SK-MEL-28	0.533	1.401	1.385	1.338	1.002	0.807	0.811	98	93	54	32	32	1.51E-6	> 1.00E-4	> 1.00E-4
SK-MEL-5	0.497	2.284	2.204	2.074	0.999	0.799	0.558	96	88	28	17	3	4.32E-7	> 1.00E-4	> 1.00E-4
UACC-257	0.874	1.786	1.727	1.705	1.433	1.520	1.496	94	91	61	71	68	> 1.00E-4	> 1.00E-4	> 1.00E-4
UACC-62	0.563	1.932	1.835	1.787	1.052	1.070	0.957	93	89	36	37	29	5.41E-7	> 1.00E-4	> 1.00E-4
Ovarian Cancer															
IGROV1	0.570	1.803	1.895	1.933	1.365	1.156	0.918	107	111	64	48	28	7.13E-6	> 1.00E-4	> 1.00E-4
OVCAR-3	0.235	1.764	1.918	1.887	0.851	0.656	0.566	110	108	40	28	22	7.19E-7	> 1.00E-4	> 1.00E-4
OVCAR-4	0.580	1.192	1.178	1.136	0.984	0.858	0.703	98	91	66	45	20	5.95E-6	> 1.00E-4	> 1.00E-4
OVCAR-5	0.521	1.401	1.385	1.404	1.257	0.767	0.758	98	100	84	28	27	4.01E-6	> 1.00E-4	> 1.00E-4
OVCAR-8	0.498	1.977	1.968	1.900	1.564	0.932	0.832	99	95	72	29	23	3.28E-6	> 1.00E-4	> 1.00E-4
NCI/ADR-RES	0.500	1.581	1.559	1.515	0.851	0.480	0.543	98	94	32	-4	4	5.19E-7	.	> 1.00E-4
SK-OV-3	0.563	1.262	1.300	1.279	0.864	0.509	0.495	105	102	43	-10	-12	7.62E-7	6.57E-6	> 1.00E-4
Renal Cancer															
786-0	0.661	2.219	2.186	2.202	1.542	1.001	0.985	98	99	57	22	21	1.54E-6	> 1.00E-4	> 1.00E-4
A498	0.701	1.890	1.702	1.621	1.287	1.154	1.116	84	77	49	38	35	9.43E-7	> 1.00E-4	> 1.00E-4
ACHN	0.346	1.359	1.432	1.386	0.994	0.771	0.596	107	103	64	42	25	4.29E-6	> 1.00E-4	> 1.00E-4
CAKI-1	0.638	2.038	1.947	1.883	1.097	0.962	0.854	94	89	33	23	15	4.93E-7	> 1.00E-4	> 1.00E-4
RXF 393	0.511	1.095	1.073	1.043	0.810	0.364	0.495	96	91	51	-29	-3	1.03E-6	4.36E-6	> 1.00E-4
SN12C	0.473	1.790	1.691	1.660	1.403	0.908	0.755	93	90	71	33	21	3.53E-6	> 1.00E-4	> 1.00E-4
TK-10	0.909	1.799	1.815	1.848	1.645	1.530	1.490	102	106	83	70	65	> 1.00E-4	> 1.00E-4	> 1.00E-4
UO-31	0.370	1.389	1.329	1.352	1.131	0.772	0.642	94	96	75	39	27	5.01E-6	> 1.00E-4	> 1.00E-4
Prostate Cancer															
PC-3	0.364	1.552	1.514	1.432	1.177	0.991	0.988	97	90	68	53	53	> 1.00E-4	> 1.00E-4	> 1.00E-4
DU-145	0.173	1.526	1.659	1.698	1.267	0.603	0.545	110	113	81	32	27	4.26E-6	> 1.00E-4	> 1.00E-4
Breast Cancer															
MCF7	0.280	1.531	1.438	1.357	0.474	0.470	0.444	93	86	15	15	13	3.24E-7	> 1.00E-4	> 1.00E-4
MDA-MB-231/ATCC	0.638	1.692	1.648	1.576	1.163	1.101	0.982	96	89	50	44	33	9.89E-7	> 1.00E-4	> 1.00E-4
HS 578T	0.449	1.874	1.827	1.769	1.518	1.148	1.141	97	93	75	49	49	9.18E-6	> 1.00E-4	> 1.00E-4
BT-549	0.868	1.836	1.862	1.899	1.512	1.287	0.874	103	107	67	43	1	5.13E-6	> 1.00E-4	> 1.00E-4
T-47D	0.549	1.229	1.247	1.241	0.956	0.928	0.908	103	102	60	56	53	> 1.00E-4	> 1.00E-4	> 1.00E-4
MDA-MB-468	0.579	1.175	1.133	1.080	0.753	0.545	0.579	93	84	29	-6	.	4.17E-7	6.80E-6	> 1.00E-4

Appendix B: X-Ray Crystallographic Data

X-ray Structure Determination of Pyrazole (99) Zn^{2+} Complex

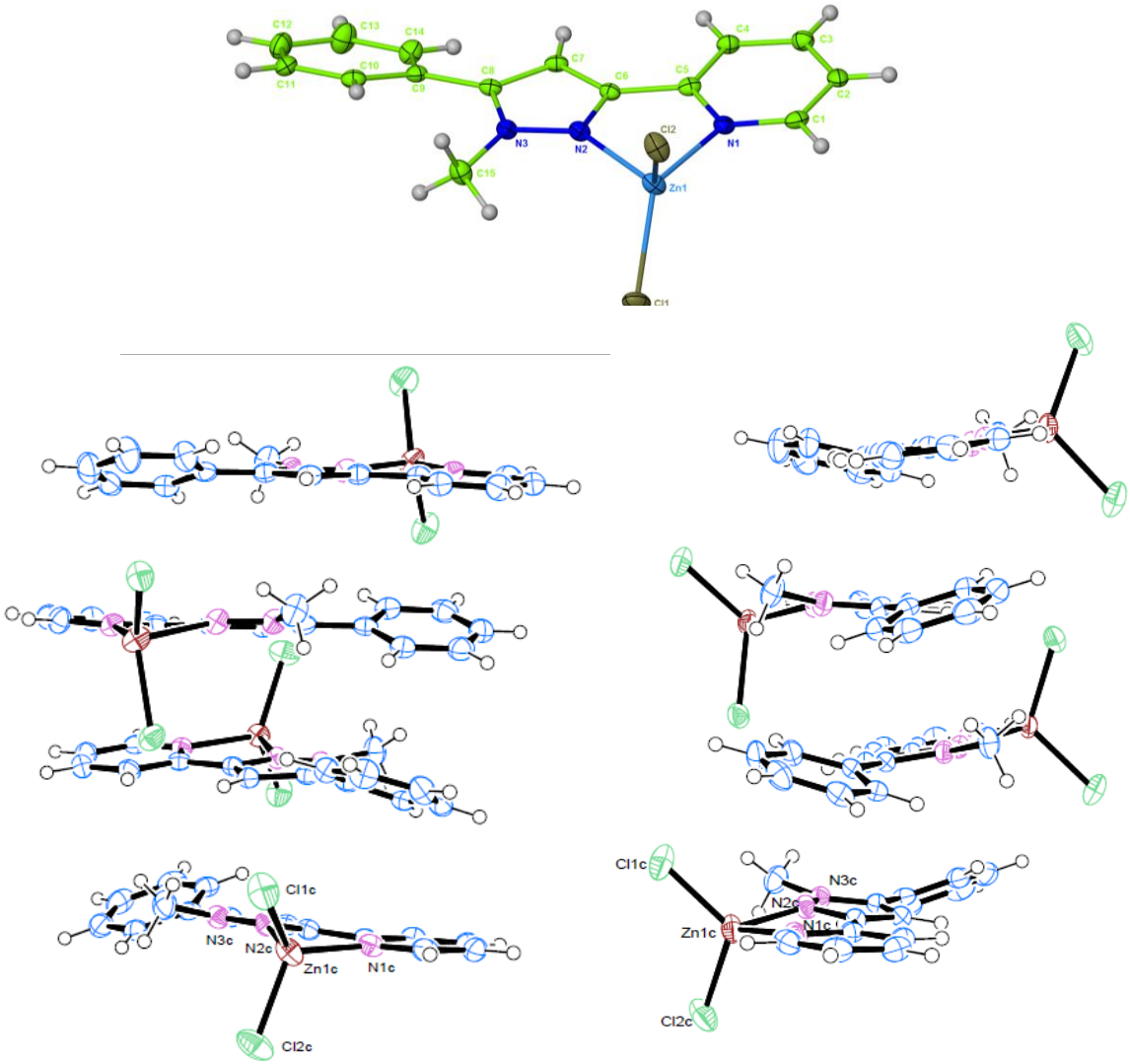

Ortep3 representations, showing the four independent structures. Right – highlighting the alternating positions of the bound metal. All ellipsoids are shown at 50% probability.

Table 1. Crystal data and structure refinement for pyrazole **(99)** Zn^{2+} Complex.

Identification code	k12farm1
Empirical formula	C60 H52 Cl8 N12 Zn4
Formula weight	1486.22
Temperature	150(2) K
Wavelength	0.71073 Å
Crystal system	Monoclinic
Space group	P21/c
Unit cell dimensions	a = 14.2600(2)Å alpha = 90°
	b = 26.1400(4)Å beta = 101.476(1)°
	c = 16.8220(2)Å gamma = 90°
Volume	6145.15(15) $Å^3$
Z	4
Density (calculated)	1.606 Mg/m^3
Absorption coefficient	1.941 mm^{-1}
F(000)	3008
Crystal size	0.40 x 0.25 x 0.14 mm
Theta range for data collection	3.51 to 27.47°
Index ranges	-18<=h<=18; -33<=k<=33; -21<=l<=21
Reflections collected	99814
Independent reflections	14032 [R(int) = 0.0737]
Reflections observed (>2sigma)	9917
Data Completeness	0.997
Absorption correction	Semi-empirical from equivalents
Max. and min. transmission	0.565 and 0.457
Refinement method	Full-matrix least-squares on F^2
Data / restraints / parameters	14032 / 0 / 761
Goodness-of-fit on F^2	1.031
Final R indices [I>2sigma(I)]	R1 = 0.0452 wR2 = 0.1015
R indices (all data)	R1 = 0.0782 wR2 = 0.1156
Largest diff. peak and hole	2.273 and -0.882 $eÅ^{-3}$

Notes:

4 independent molecules in the asymmetric unit. Largest residual peak in difference Fourier electron density map is at a chemically insignificantly distance from Zn1A.

Table 2. Atomic coordinates (x 10^4) and equivalent isotropic displacement parameters ($Å^2$ x 10^3) for 1.U(eq) is defined as one third of the trace of the orthogonalized Uij tensor.

Atom	x	y	z	U(eq)
Zn(1)	1522(1)	3005(1)	4492(1)	34(1)
Cl(1)	184(1)	3211(1)	4892(1)	50(1)
Cl(2)	2821(1)	2998(1)	5450(1)	46(1)
N(1)	1540(2)	2451(1)	3607(1)	29(1)
N(2)	1582(2)	3462(1)	3500(1)	29(1)
N(3)	1565(2)	3963(1)	3307(1)	28(1)
C(1)	1583(2)	1943(1)	3708(2)	33(1)
C(2)	1606(2)	1608(1)	3074(2)	35(1)
C(3)	1577(2)	1804(1)	2309(2)	36(1)
C(4)	1545(2)	2325(1)	2197(2)	31(1)
C(5)	1536(2)	2641(1)	2854(2)	28(1)
C(6)	1536(2)	3202(1)	2806(2)	28(1)
C(7)	1503(2)	3539(1)	2163(2)	28(1)
C(8)	1528(2)	4027(1)	2493(2)	28(1)
C(9)	1500(2)	4522(1)	2074(2)	30(1)
C(10)	1826(2)	4980(1)	2452(2)	33(1)
C(11)	1761(2)	5432(1)	2013(2)	39(1)
C(12)	1394(3)	5430(2)	1191(2)	48(1)
C(13)	1097(3)	4974(2)	808(2)	54(1)
C(14)	1139(3)	4523(1)	1237(2)	40(1)
C(15)	1549(3)	4332(1)	3955(2)	40(1)
Zn(1A)	4005(1)	4683(1)	458(1)	33(1)
Cl(1A)	5541(1)	4459(1)	390(1)	36(1)
Cl(2A)	2798(1)	4447(1)	-528(1)	39(1)
N(1A)	4013(2)	5165(1)	1446(1)	28(1)
N(2A)	3841(2)	4157(1)	1413(1)	30(1)
N(3A)	3807(2)	3645(1)	1534(1)	30(1)
C(1A)	3987(2)	5677(1)	1428(2)	34(1)
C(2A)	4093(2)	5972(1)	2122(2)	35(1)
C(3A)	4237(2)	5729(1)	2866(2)	33(1)
C(4A)	4249(2)	5201(1)	2899(2)	29(1)
C(5A)	4122(2)	4929(1)	2177(2)	26(1)
C(6A)	4063(2)	4369(1)	2148(2)	28(1)
C(7A)	4171(2)	3997(1)	2750(2)	28(1)
C(8A)	4001(2)	3531(1)	2345(2)	28(1)
C(9A)	4034(2)	3014(1)	2690(2)	29(1)
C(10A)	4252(2)	2576(1)	2286(2)	32(1)
C(11A)	4301(2)	2101(1)	2655(2)	38(1)
C(12A)	4148(2)	2052(1)	3440(2)	40(1)
C(13A)	3941(2)	2482(1)	3847(2)	39(1)
C(14A)	3880(2)	2958(1)	3486(2)	34(1)
C(15A)	3457(3)	3320(1)	829(2)	40(1)
Zn(1B)	6478(1)	4369(1)	4600(1)	29(1)
Cl(1B)	5060(1)	4224(1)	4899(1)	43(1)
Cl(2B)	7730(1)	4325(1)	5602(1)	44(1)
N(1B)	6581(2)	4960(1)	3800(1)	26(1)
N(2B)	6571(2)	3955(1)	3576(1)	26(1)
N(3B)	6526(2)	3464(1)	3323(1)	25(1)

C(1B)	6628(2)	5462(1)	3950(2)	30(1)
C(2B)	6702(2)	5825(1)	3373(2)	34(1)
C(3B)	6710(2)	5660(1)	2593(2)	35(1)
C(4B)	6664(2)	5143(1)	2420(2)	29(1)
C(5B)	6613(2)	4800(1)	3037(2)	25(1)
C(6B)	6596(2)	4243(1)	2926(2)	25(1)
C(7B)	6582(2)	3941(1)	2252(2)	25(1)
C(8B)	6531(2)	3440(1)	2513(2)	24(1)
C(9B)	6462(2)	2964(1)	2032(2)	26(1)
C(10B)	6781(2)	2490(1)	2355(2)	27(1)
C(11B)	6654(2)	2060(1)	1863(2)	35(1)
C(12B)	6225(3)	2096(1)	1050(2)	38(1)
C(13B)	5945(3)	2567(1)	724(2)	38(1)
C(14B)	6064(2)	3000(1)	1200(2)	31(1)
C(15B)	6413(3)	3065(1)	3900(2)	37(1)
Zn(1C)	8769(1)	3081(1)	472(1)	34(1)
Cl(1C)	7528(1)	3147(1)	-539(1)	50(1)
Cl(2C)	10158(1)	3263(1)	124(1)	53(1)
N(1C)	8853(2)	2515(1)	1360(2)	30(1)
N(2C)	8725(2)	3519(1)	1490(1)	28(1)
N(3C)	8748(2)	4018(1)	1684(1)	28(1)
C(1C)	8811(2)	2007(1)	1261(2)	34(1)
C(2C)	8945(2)	1666(1)	1908(2)	36(1)
C(3C)	9139(2)	1859(1)	2690(2)	36(1)
C(4C)	9168(2)	2384(1)	2806(2)	30(1)
C(5C)	9014(2)	2701(1)	2128(2)	26(1)
C(6C)	8979(2)	3261(1)	2186(2)	27(1)
C(7C)	9155(2)	3596(1)	2837(2)	27(1)
C(8C)	9009(2)	4081(1)	2507(2)	27(1)
C(9C)	9111(2)	4574(1)	2925(2)	29(1)
C(10C)	9417(2)	5018(1)	2594(2)	33(1)
C(11C)	9545(2)	5470(1)	3039(2)	40(1)
C(12C)	9371(3)	5485(1)	3819(2)	45(1)
C(13C)	9067(2)	5046(1)	4155(2)	40(1)
C(14C)	8936(2)	4597(1)	3715(2)	32(1)
C(15C)	8418(3)	4386(1)	1042(2)	39(1)

Table 3. Bond lengths [Å] and angles [^{o}] for 1.

Zn(1)-N(2)	2.066(2)	Zn(1)-N(1)	2.081(2)
Zn(1)-Cl(2)	2.2012(9)	Zn(1)-Cl(1)	2.2124(10)
N(1)-C(1)	1.338(4)	N(1)-C(5)	1.359(4)
N(2)-C(6)	1.341(4)	N(2)-N(3)	1.349(3)
N(3)-C(8)	1.371(4)	N(3)-C(15)	1.459(4)
C(1)-C(2)	1.387(4)	C(2)-C(3)	1.379(4)
C(3)-C(4)	1.373(4)	C(4)-C(5)	1.384(4)
C(5)-C(6)	1.469(4)	C(6)-C(7)	1.389(4)
C(7)-C(8)	1.388(4)	C(8)-C(9)	1.470(4)
C(9)-C(10)	1.391(4)	C(9)-C(14)	1.399(4)
C(10)-C(11)	1.386(4)	C(11)-C(12)	1.379(5)
C(12)-C(13)	1.381(5)	C(13)-C(14)	1.378(5)
Zn(1A)-N(1A)	2.084(2)	Zn(1A)-N(2A)	2.162(2)
Zn(1A)-Cl(2A)	2.2261(9)	Zn(1A)-Cl(1A)	2.2932(9)
Zn(1A)-Cl(1A)#1	2.8025(9)	Cl(1A)-Zn(1A)#1	2.8026(9)

N(1A)-C(1A)	1.339(4)	N(1A)-C(5A)	1.358(4)
N(2A)-C(6A)	1.335(4)	N(2A)-N(3A)	1.356(3)
N(3A)-C(8A)	1.369(4)	N(3A)-C(15A)	1.465(4)
C(1A)-C(2A)	1.382(4)	C(2A)-C(3A)	1.380(4)
C(3A)-C(4A)	1.382(4)	C(4A)-C(5A)	1.389(4)
C(5A)-C(6A)	1.466(4)	C(6A)-C(7A)	1.390(4)
C(7A)-C(8A)	1.391(4)	C(8A)-C(9A)	1.469(4)
C(9A)-C(10A)	1.397(4)	C(9A)-C(14A)	1.408(4)
C(10A)-C(11A)	1.383(4)	C(11A)-C(12A)	1.386(5)
C(12A)-C(13A)	1.378(5)	C(13A)-C(14A)	1.379(4)
Zn(1B)-N(2B)	2.062(2)	Zn(1B)-N(1B)	2.072(2)
Zn(1B)-Cl(2B)	2.2002(9)	Zn(1B)-Cl(1B)	2.2107(9)
N(1B)-C(1B)	1.337(4)	N(1B)-C(5B)	1.359(3)
N(2B)-C(6B)	1.333(4)	N(2B)-N(3B)	1.349(3)
N(3B)-C(8B)	1.365(3)	N(3B)-C(15B)	1.457(4)
C(1B)-C(2B)	1.375(4)	C(2B)-C(3B)	1.383(4)
C(3B)-C(4B)	1.382(4)	C(4B)-C(5B)	1.384(4)
C(5B)-C(6B)	1.467(4)	C(6B)-C(7B)	1.379(4)
C(7B)-C(8B)	1.387(4)	C(8B)-C(9B)	1.475(4)
C(9B)-C(10B)	1.393(4)	C(9B)-C(14B)	1.406(4)
C(10B)-C(11B)	1.388(4)	C(11B)-C(12B)	1.385(5)
C(12B)-C(13B)	1.375(5)	C(13B)-C(14B)	1.376(4)
Zn(1C)-N(2C)	2.071(2)	Zn(1C)-N(1C)	2.089(3)
Zn(1C)-Cl(1C)	2.2032(9)	Zn(1C)-Cl(2C)	2.2259(10)
N(1C)-C(1C)	1.338(4)	N(1C)-C(5C)	1.355(4)
N(2C)-C(6C)	1.338(4)	N(2C)-N(3C)	1.344(3)
N(3C)-C(8C)	1.370(4)	N(3C)-C(15C)	1.453(4)
C(1C)-C(2C)	1.390(4)	C(2C)-C(3C)	1.385(5)
C(3C)-C(4C)	1.385(4)	C(4C)-C(5C)	1.392(4)
C(5C)-C(6C)	1.469(4)	C(6C)-C(7C)	1.387(4)
C(7C)-C(8C)	1.383(4)	C(8C)-C(9C)	1.463(4)
C(9C)-C(10C)	1.393(4)	C(9C)-C(14C)	1.400(4)
C(10C)-C(11C)	1.393(4)	C(11C)-C(12C)	1.385(5)
C(12C)-C(13C)	1.386(5)	C(13C)-C(14C)	1.379(4)
N(2)-Zn(1)-N(1)	79.45(10)	N(2)-Zn(1)-Cl(2)	115.60(8)
N(1)-Zn(1)-Cl(2)	112.91(7)	N(2)-Zn(1)-Cl(1)	106.41(7)
N(1)-Zn(1)-Cl(1)	121.40(8)	Cl(2)-Zn(1)-Cl(1)	115.48(4)
C(1)-N(1)-C(5)	118.3(3)	C(1)-N(1)-Zn(1)	127.3(2)
C(5)-N(1)-Zn(1)	114.4(2)	C(6)-N(2)-N(3)	106.6(2)
C(6)-N(2)-Zn(1)	114.0(2)	N(3)-N(2)-Zn(1)	138.94(19)
N(2)-N(3)-C(8)	110.7(2)	N(2)-N(3)-C(15)	117.7(2)
C(8)-N(3)-C(15)	131.5(3)	N(1)-C(1)-C(2)	122.5(3)
C(3)-C(2)-C(1)	118.8(3)	C(4)-C(3)-C(2)	119.5(3)
C(3)-C(4)-C(5)	119.2(3)	N(1)-C(5)-C(4)	121.8(3)
N(1)-C(5)-C(6)	114.6(3)	C(4)-C(5)-C(6)	123.6(3)
N(2)-C(6)-C(7)	110.2(3)	N(2)-C(6)-C(5)	117.3(3)
C(7)-C(6)-C(5)	132.5(3)	C(8)-C(7)-C(6)	106.0(3)
N(3)-C(8)-C(7)	106.3(3)	N(3)-C(8)-C(9)	125.3(3)
C(7)-C(8)-C(9)	128.4(3)	C(10)-C(9)-C(14)	118.8(3)
C(10)-C(9)-C(8)	124.3(3)	C(14)-C(9)-C(8)	116.9(3)
C(11)-C(10)-C(9)	120.5(3)	C(12)-C(11)-C(10)	120.3(3)
C(11)-C(12)-C(13)	119.3(3)	C(14)-C(13)-C(12)	121.2(3)
C(13)-C(14)-C(9)	119.8(3)	N(1A)-Zn(1A)-N(2A)	77.08(9)

N(1A)-Zn(1A)-Cl(2A)	130.00(7)	N(2A)-Zn(1A)-Cl(2A)	101.27(7)
N(1A)-Zn(1A)-Cl(1A)	109.91(7)	N(2A)-Zn(1A)-Cl(1A)	96.89(7)
Cl(2A)-Zn(1A)-Cl(1A)	119.76(3)	N(1A)-Zn(1A)-Cl(1A)#1	87.49(7)
N(2A)-Zn(1A)-Cl(1A)#1	163.17(7)	Cl(2A)-Zn(1A)-Cl(1A)#1	93.76(3)
Cl(1A)-Zn(1A)-Cl(1A)#1	81.93(3)	Zn(1A)-Cl(1A)-Zn(1A)#1	98.06(3)
C(1A)-N(1A)-C(5A)	118.3(3)	C(1A)-N(1A)-Zn(1A)	126.2(2)
C(5A)-N(1A)-Zn(1A)	115.3(2)	C(6A)-N(2A)-N(3A)	106.1(2)
C(6A)-N(2A)-Zn(1A)	112.6(2)	N(3A)-N(2A)-Zn(1A)	138.77(18)
N(2A)-N(3A)-C(8A)	111.0(2)	N(2A)-N(3A)-C(15A)	117.9(2)
C(8A)-N(3A)-C(15A)	130.5(3)	N(1A)-C(1A)-C(2A)	122.6(3)
C(3A)-C(2A)-C(1A)	118.8(3)	C(2A)-C(3A)-C(4A)	119.6(3)
C(3A)-C(4A)-C(5A)	118.6(3)	N(1A)-C(5A)-C(4A)	122.0(3)
N(1A)-C(5A)-C(6A)	115.5(2)	C(4A)-C(5A)-C(6A)	122.5(3)
N(2A)-C(6A)-C(7A)	110.9(3)	N(2A)-C(6A)-C(5A)	116.4(3)
C(7A)-C(6A)-C(5A)	132.7(3)	C(6A)-C(7A)-C(8A)	105.8(3)
N(3A)-C(8A)-C(7A)	106.2(3)	N(3A)-C(8A)-C(9A)	125.3(3)
C(7A)-C(8A)-C(9A)	128.6(3)	C(10A)-C(9A)-C(14A)	118.0(3)
C(10A)-C(9A)-C(8A)	123.8(3)	C(14A)-C(9A)-C(8A)	118.2(3)
C(11A)-C(10A)-C(9A)	120.8(3)	C(10A)-C(11A)-C(12A)	120.5(3)
C(13A)-C(12A)-C(11A)	119.3(3)	C(12A)-C(13A)-C(14A)	121.1(3)
C(13A)-C(14A)-C(9A)	120.4(3)	N(2B)-Zn(1B)-N(1B)	79.84(9)
N(2B)-Zn(1B)-Cl(2B)	115.82(7)	N(1B)-Zn(1B)-Cl(2B)	112.65(7)
N(2B)-Zn(1B)-Cl(1B)	108.29(7)	N(1B)-Zn(1B)-Cl(1B)	117.44(7)
Cl(2B)-Zn(1B)-Cl(1B)	117.15(4)	C(1B)-N(1B)-C(5B)	118.0(3)
C(1B)-N(1B)-Zn(1B)	128.2(2)	C(5B)-N(1B)-Zn(1B)	113.86(19)
C(6B)-N(2B)-N(3B)	106.6(2)	C(6B)-N(2B)-Zn(1B)	113.92(19)
N(3B)-N(2B)-Zn(1B)	139.10(18)	N(2B)-N(3B)-C(8B)	110.5(2)
N(2B)-N(3B)-C(15B)	118.4(2)	C(8B)-N(3B)-C(15B)	130.9(2)
N(1B)-C(1B)-C(2B)	123.6(3)	C(1B)-C(2B)-C(3B)	118.1(3)
C(4B)-C(3B)-C(2B)	119.6(3)	C(3B)-C(4B)-C(5B)	118.9(3)
N(1B)-C(5B)-C(4B)	121.7(3)	N(1B)-C(5B)-C(6B)	115.0(2)
C(4B)-C(5B)-C(6B)	123.3(3)	N(2B)-C(6B)-C(7B)	110.6(3)
N(2B)-C(6B)-C(5B)	117.3(2)	C(7B)-C(6B)-C(5B)	132.1(3)
C(6B)-C(7B)-C(8B)	105.9(2)	N(3B)-C(8B)-C(7B)	106.4(2)
N(3B)-C(8B)-C(9B)	125.0(3)	C(7B)-C(8B)-C(9B)	128.6(3)
C(10B)-C(9B)-C(14B)	118.8(3)	C(10B)-C(9B)-C(8B)	123.7(3)
C(14B)-C(9B)-C(8B)	117.4(3)	C(11B)-C(10B)-C(9B)	119.7(3)
C(12B)-C(11B)-C(10B)	120.8(3)	C(13B)-C(12B)-C(11B)	119.5(3)
C(12B)-C(13B)-C(14B)	120.7(3)	C(13B)-C(14B)-C(9B)	120.3(3)
N(2C)-Zn(1C)-N(1C)	78.90(10)	N(2C)-Zn(1C)-Cl(1C)	116.30(8)
N(1C)-Zn(1C)-Cl(1C)	122.03(7)	N(2C)-Zn(1C)-Cl(2C)	105.88(7)
N(1C)-Zn(1C)-Cl(2C)	114.33(8)	Cl(1C)-Zn(1C)-Cl(2C)	113.61(4)
C(1C)-N(1C)-C(5C)	118.0(3)	C(1C)-N(1C)-Zn(1C)	128.3(2)
C(5C)-N(1C)-Zn(1C)	113.7(2)	C(6C)-N(2C)-N(3C)	106.7(2)
C(6C)-N(2C)-Zn(1C)	113.4(2)	N(3C)-N(2C)-Zn(1C)	137.31(19)
N(2C)-N(3C)-C(8C)	110.5(2)	N(2C)-N(3C)-C(15C)	118.2(2)
C(8C)-N(3C)-C(15C)	130.9(3)	N(1C)-C(1C)-C(2C)	122.9(3)
C(3C)-C(2C)-C(1C)	118.7(3)	C(2C)-C(3C)-C(4C)	119.3(3)
C(3C)-C(4C)-C(5C)	118.6(3)	N(1C)-C(5C)-C(4C)	122.4(3)
N(1C)-C(5C)-C(6C)	114.8(3)	C(4C)-C(5C)-C(6C)	122.7(3)
N(2C)-C(6C)-C(7C)	110.4(3)	N(2C)-C(6C)-C(5C)	116.8(3)
C(7C)-C(6C)-C(5C)	132.8(3)	C(8C)-C(7C)-C(6C)	105.8(3)
N(3C)-C(8C)-C(7C)	106.6(3)	N(3C)-C(8C)-C(9C)	124.9(3)
C(7C)-C(8C)-C(9C)	128.5(3)	C(10C)-C(9C)-C(14C)	118.2(3)

C(10C)-C(9C)-C(8C)	123.4(3)	C(14C)-C(9C)-C(8C)	118.3(3)
C(11C)-C(10C)-C(9C)	120.6(3)	C(12C)-C(11C)-C(10C)	120.3(3)
C(11C)-C(12C)-C(13C)	119.5(3)	C(14C)-C(13C)-C(12C)	120.4(3)
C(13C)-C(14C)-C(9C)	121.0(3)		

Symmetry transformations used to generate equivalent atoms:
#1 -x+1,-y+1,-z

Table 4. Anisotropic displacement parameters ($Å^2 \times 10^3$) for 1. The anisotropic displacement factor exponent takes the form: $-2\ gpi^2\ [\ h^2\ a^{*2}\ U11 + ... + 2\ h\ k\ a^*\ b^*\ U$

Atom	U11	U22	U33	U23	U13	U12
Zn(1)	43(1)	39(1)	20(1)	2(1)	6(1)	12(1)
Cl(1)	59(1)	58(1)	40(1)	10(1)	27(1)	15(1)
Cl(2)	61(1)	44(1)	27(1)	-4(1)	-7(1)	11(1)
N(1)	26(1)	34(2)	26(1)	1(1)	5(1)	4(1)
N(2)	32(2)	34(2)	22(1)	0(1)	5(1)	6(1)
N(3)	30(2)	31(1)	23(1)	2(1)	4(1)	5(1)
C(1)	24(2)	42(2)	32(2)	5(1)	6(1)	0(1)
C(2)	31(2)	33(2)	43(2)	1(2)	11(2)	1(1)
C(3)	37(2)	36(2)	36(2)	-8(2)	10(2)	-2(2)
C(4)	31(2)	40(2)	23(2)	0(1)	6(1)	1(1)
C(5)	23(2)	36(2)	23(1)	1(1)	5(1)	1(1)
C(6)	24(2)	35(2)	24(2)	-2(1)	6(1)	1(1)
C(7)	25(2)	40(2)	20(1)	-1(1)	5(1)	2(1)
C(8)	22(2)	37(2)	23(1)	-2(1)	3(1)	2(1)
C(9)	22(2)	41(2)	27(2)	4(1)	7(1)	2(1)
C(10)	27(2)	42(2)	30(2)	-3(1)	6(1)	0(1)
C(11)	35(2)	38(2)	45(2)	1(2)	15(2)	-4(2)
C(12)	58(3)	42(2)	48(2)	10(2)	17(2)	-2(2)
C(13)	72(3)	54(2)	32(2)	11(2)	6(2)	-6(2)
C(14)	50(2)	41(2)	28(2)	3(2)	5(2)	-5(2)
C(15)	57(2)	37(2)	27(2)	-4(1)	8(2)	6(2)
Zn(1A)	35(1)	41(1)	21(1)	-5(1)	2(1)	7(1)
Cl(1A)	40(1)	42(1)	27(1)	8(1)	10(1)	12(1)
Cl(2A)	45(1)	42(1)	25(1)	2(1)	-4(1)	-5(1)
N(1A)	29(1)	35(2)	20(1)	-1(1)	6(1)	4(1)
N(2A)	35(2)	30(2)	23(1)	-2(1)	4(1)	3(1)
N(3A)	33(2)	31(2)	24(1)	-2(1)	2(1)	2(1)
C(1A)	41(2)	34(2)	28(2)	4(1)	9(1)	5(2)
C(2A)	38(2)	34(2)	34(2)	0(1)	10(2)	1(2)
C(3A)	34(2)	36(2)	27(2)	-8(1)	5(1)	-1(1)
C(4A)	28(2)	36(2)	21(1)	1(1)	6(1)	2(1)
C(5A)	22(2)	36(2)	22(1)	-1(1)	5(1)	3(1)
C(6A)	23(2)	37(2)	23(1)	-1(1)	5(1)	1(1)
C(7A)	24(2)	36(2)	23(1)	0(1)	5(1)	3(1)
C(8A)	22(2)	36(2)	26(2)	-1(1)	2(1)	1(1)
C(9A)	18(2)	36(2)	32(2)	-1(1)	0(1)	-2(1)
C(10A)	26(2)	37(2)	32(2)	-2(1)	5(1)	-2(1)
C(11A)	30(2)	39(2)	45(2)	-4(2)	4(2)	0(2)
C(12A)	30(2)	40(2)	49(2)	8(2)	3(2)	-3(2)
C(13A)	31(2)	52(2)	33(2)	7(2)	4(1)	-2(2)
C(14A)	28(2)	41(2)	32(2)	-1(1)	6(1)	2(1)

C(15A)	52(2)	34(2)	30(2)	-7(1)	-6(2)	2(2)
Zn(1B)	33(1)	35(1)	18(1)	0(1)	3(1)	-1(1)
Cl(1B)	41(1)	63(1)	28(1)	-4(1)	13(1)	-6(1)
Cl(2B)	49(1)	47(1)	29(1)	1(1)	-11(1)	1(1)
N(1B)	23(1)	30(1)	23(1)	0(1)	3(1)	-1(1)
N(2B)	28(1)	27(1)	21(1)	2(1)	3(1)	-2(1)
N(3B)	27(1)	28(1)	20(1)	1(1)	4(1)	-1(1)
C(1B)	22(2)	37(2)	30(2)	-4(1)	3(1)	2(1)
C(2B)	32(2)	27(2)	42(2)	-3(1)	6(2)	0(1)
C(3B)	35(2)	30(2)	41(2)	5(1)	11(2)	0(1)
C(4B)	28(2)	35(2)	26(2)	2(1)	8(1)	-1(1)
C(5B)	21(2)	31(2)	23(1)	-3(1)	5(1)	0(1)
C(6B)	22(2)	33(2)	21(1)	3(1)	5(1)	0(1)
C(7B)	24(2)	31(2)	20(1)	2(1)	5(1)	1(1)
C(8B)	21(2)	30(2)	21(1)	0(1)	5(1)	-1(1)
C(9B)	22(2)	35(2)	24(2)	1(1)	10(1)	-2(1)
C(10B)	21(2)	33(2)	28(2)	1(1)	7(1)	-2(1)
C(11B)	34(2)	32(2)	42(2)	1(1)	18(2)	-2(1)
C(12B)	46(2)	34(2)	37(2)	-9(2)	19(2)	-7(2)
C(13B)	47(2)	47(2)	21(2)	-6(1)	8(2)	-1(2)
C(14B)	35(2)	34(2)	25(2)	1(1)	9(1)	1(1)
C(15B)	53(2)	33(2)	26(2)	5(1)	10(2)	-1(2)
Zn(1C)	40(1)	40(1)	23(1)	-4(1)	8(1)	-12(1)
Cl(1C)	60(1)	52(1)	31(1)	1(1)	-5(1)	-12(1)
Cl(2C)	56(1)	66(1)	45(1)	-16(1)	28(1)	-22(1)
N(1C)	27(1)	33(2)	30(1)	-5(1)	9(1)	-5(1)
N(2C)	30(1)	30(1)	26(1)	1(1)	8(1)	-3(1)
N(3C)	28(1)	31(1)	26(1)	2(1)	4(1)	-3(1)
C(1C)	30(2)	37(2)	38(2)	-7(2)	12(1)	-4(1)
C(2C)	31(2)	28(2)	49(2)	-4(2)	9(2)	1(1)
C(3C)	29(2)	35(2)	42(2)	4(2)	4(2)	0(1)
C(4C)	28(2)	35(2)	29(2)	-2(1)	6(1)	-2(1)
C(5C)	21(2)	32(2)	27(2)	-2(1)	6(1)	-4(1)
C(6C)	24(2)	33(2)	25(2)	1(1)	7(1)	-2(1)
C(7C)	24(2)	34(2)	24(2)	-1(1)	7(1)	-1(1)
C(8C)	22(2)	33(2)	26(2)	-1(1)	6(1)	-2(1)
C(9C)	18(2)	32(2)	35(2)	-2(1)	2(1)	2(1)
C(10C)	24(2)	34(2)	40(2)	0(2)	4(1)	2(1)
C(11C)	32(2)	32(2)	55(2)	-1(2)	3(2)	-1(1)
C(12C)	36(2)	34(2)	58(2)	-17(2)	-2(2)	3(2)
C(13C)	33(2)	47(2)	37(2)	-12(2)	1(2)	5(2)
C(14C)	24(2)	36(2)	35(2)	-6(1)	3(1)	0(1)
C(15C)	43(2)	38(2)	33(2)	9(2)	2(2)	0(2)

Table 5. Hydrogen coordinates (x 10^4) and isotropic displacement parameters ($Å^2$ x 10^3) for 1.

Atom	x	y	z	U(eq)
H(1)	1597	1808	4235	39
H(2)	1642	1249	3165	42
H(3)	1578	1582	1863	43
H(4)	1528	2466	1674	38
H(7)	1470	3453	1609	34

H(10)	2096	4983	3016	39
H(11)	1971	5743	2280	46
H(12)	1346	5740	890	58
H(13)	860	4971	239	64
H(14)	922	4214	966	48
H(15A)	1287	4169	4388	61
H(15B)	1147	4624	3738	61
H(15C)	2201	4451	4172	61
H(1A)	3891	5845	917	41
H(2A)	4067	6334	2089	42
H(3A)	4328	5924	3352	39
H(4A)	4342	5028	3406	34
H(7A)	4328	4049	3320	33
H(10A)	4367	2604	1751	38
H(11A)	4440	1807	2369	46
H(12A)	4185	1726	3693	48
H(13A)	3839	2450	4386	47
H(14A)	3733	3249	3776	40
H(15D)	4002	3174	633	60
H(15E)	3069	3525	397	60
H(15F)	3066	3043	984	60
H(1B)	6609	5575	4483	36
H(2B)	6746	6178	3506	41
H(3B)	6747	5901	2178	41
H(4B)	6666	5024	1887	35
H(7B)	6602	4052	1718	30
H(10B)	7085	2462	2910	33
H(11B)	6864	1736	2086	42
H(12B)	6124	1798	721	45
H(13B)	5667	2595	163	46
H(14B)	5876	3324	965	37
H(15G)	7044	2934	4159	55
H(15H)	6028	2785	3615	55
H(15I)	6091	3206	4315	55
H(1C)	8683	1873	725	41
H(2C)	8904	1307	1815	43
H(3C)	9252	1634	3143	43
H(4C)	9290	2524	3337	37
H(7C)	9338	3510	3396	33
H(10C)	9540	5011	2059	40
H(11C)	9753	5770	2805	48
H(12C)	9460	5794	4123	53
H(13C)	8947	5054	4690	48
H(14C)	8725	4300	3951	38
H(15J)	8960	4499	808	58
H(15K)	8135	4681	1265	58
H(15L)	7936	4225	619	58

Table 6. Dihedral angles [°] for 1.

Atom1 - Atom2 - Atom3 - Atom4	Dihedral
N(2) - Zn(1) - N(1) - C(1)	175.1(3)
Cl(2) - Zn(1) - N(1) - C(1)	61.6(3)
Cl(1) - Zn(1) - N(1) - C(1)	-82.1(3)
N(2) - Zn(1) - N(1) - C(5)	-2.8(2)
Cl(2) - Zn(1) - N(1) - C(5)	-116.25(19)
Cl(1) - Zn(1) - N(1) - C(5)	100.1(2)
N(1) - Zn(1) - N(2) - C(6)	4.3(2)
Cl(2) - Zn(1) - N(2) - C(6)	114.8(2)
Cl(1) - Zn(1) - N(2) - C(6)	-115.5(2)
N(1) - Zn(1) - N(2) - N(3)	176.1(3)
Cl(2) - Zn(1) - N(2) - N(3)	-73.4(3)
Cl(1) - Zn(1) - N(2) - N(3)	56.3(3)
C(6) - N(2) - N(3) - C(8)	-1.2(3)
Zn(1) - N(2) - N(3) - C(8)	-173.4(2)
C(6) - N(2) - N(3) - C(15)	176.3(3)
Zn(1) - N(2) - N(3) - C(15)	4.1(4)
C(5) - N(1) - C(1) - C(2)	-1.2(4)
Zn(1) - N(1) - C(1) - C(2)	-178.9(2)
N(1) - C(1) - C(2) - C(3)	-0.5(5)
C(1) - C(2) - C(3) - C(4)	1.3(5)
C(2) - C(3) - C(4) - C(5)	-0.4(5)
C(1) - N(1) - C(5) - C(4)	2.1(4)
Zn(1) - N(1) - C(5) - C(4)	-179.8(2)
C(1) - N(1) - C(5) - C(6)	-177.1(3)
Zn(1) - N(1) - C(5) - C(6)	0.9(3)
C(3) - C(4) - C(5) - N(1)	-1.4(5)
C(3) - C(4) - C(5) - C(6)	177.8(3)
N(3) - N(2) - C(6) - C(7)	0.8(3)
Zn(1) - N(2) - C(6) - C(7)	175.2(2)
N(3) - N(2) - C(6) - C(5)	-179.6(2)
Zn(1) - N(2) - C(6) - C(5)	-5.2(3)
N(1) - C(5) - C(6) - N(2)	2.9(4)
C(4) - C(5) - C(6) - N(2)	-176.4(3)
N(1) - C(5) - C(6) - C(7)	-177.6(3)
C(4) - C(5) - C(6) - C(7)	3.1(5)
N(2) - C(6) - C(7) - C(8)	-0.2(3)
C(5) - C(6) - C(7) - C(8)	-179.7(3)
N(2) - N(3) - C(8) - C(7)	1.1(3)
C(15) - N(3) - C(8) - C(7)	-176.0(3)
N(2) - N(3) - C(8) - C(9)	179.9(3)
C(15) - N(3) - C(8) - C(9)	2.9(5)
C(6) - C(7) - C(8) - N(3)	-0.5(3)
C(6) - C(7) - C(8) - C(9)	-179.3(3)
N(3) - C(8) - C(9) - C(10)	22.9(5)
C(7) - C(8) - C(9) - C(10)	-158.6(3)
N(3) - C(8) - C(9) - C(14)	-158.5(3)
C(7) - C(8) - C(9) - C(14)	20.0(5)
C(14) - C(9) - C(10) - C(11)	2.3(5)
C(8) - C(9) - C(10) - C(11)	-179.1(3)
C(9) - C(10) - C(11) - C(12)	-1.6(5)

C(10) - C(11) - C(12) - C(13)	-0.4(6)
C(11) - C(12) - C(13) - C(14)	1.7(6)
C(12) - C(13) - C(14) - C(9)	-1.0(6)
C(10) - C(9) - C(14) - C(13)	-1.0(5)
C(8) - C(9) - C(14) - C(13)	-179.7(3)
N(1A) - Zn(1A) - Cl(1A) - Zn(1A)#1	-84.35(8)
N(2A) - Zn(1A) - Cl(1A) - Zn(1A)#1	-163.07(7)
Cl(2A) - Zn(1A) - Cl(1A) - Zn(1A)#1	89.73(4)
Cl(1A)#1 - Zn(1A) - Cl(1A) - Zn(1A)#1	0.0
N(2A) - Zn(1A) - N(1A) - C(1A)	-171.5(3)
Cl(2A) - Zn(1A) - N(1A) - C(1A)	-77.5(3)
Cl(1A) - Zn(1A) - N(1A) - C(1A)	95.8(3)
Cl(1A)#1 - Zn(1A) - N(1A) - C(1A)	15.3(3)
N(2A) - Zn(1A) - N(1A) - C(5A)	13.3(2)
Cl(2A) - Zn(1A) - N(1A) - C(5A)	107.2(2)
Cl(1A) - Zn(1A) - N(1A) - C(5A)	-79.5(2)
Cl(1A)#1 - Zn(1A) - N(1A) - C(5A)	-160.0(2)
N(1A) - Zn(1A) - N(2A) - C(6A)	-15.6(2)
Cl(2A) - Zn(1A) - N(2A) - C(6A)	-144.4(2)
Cl(1A) - Zn(1A) - N(2A) - C(6A)	93.3(2)
Cl(1A)#1 - Zn(1A) - N(2A) - C(6A)	8.4(4)
N(1A) - Zn(1A) - N(2A) - N(3A)	-174.4(3)
Cl(2A) - Zn(1A) - N(2A) - N(3A)	56.8(3)
Cl(1A) - Zn(1A) - N(2A) - N(3A)	-65.5(3)
Cl(1A)#1 - Zn(1A) - N(2A) - N(3A)	-150.4(2)
C(6A) - N(2A) - N(3A) - C(8A)	0.3(3)
Zn(1A) - N(2A) - N(3A) - C(8A)	160.0(2)
C(6A) - N(2A) - N(3A) - C(15A)	172.4(3)
Zn(1A) - N(2A) - N(3A) - C(15A)	-27.9(4)
C(5A) - N(1A) - C(1A) - C(2A)	1.9(5)
Zn(1A) - N(1A) - C(1A) - C(2A)	-173.2(2)
N(1A) - C(1A) - C(2A) - C(3A)	0.3(5)
C(1A) - C(2A) - C(3A) - C(4A)	-1.6(5)
C(2A) - C(3A) - C(4A) - C(5A)	0.5(5)
C(1A) - N(1A) - C(5A) - C(4A)	-3.0(4)
Zn(1A) - N(1A) - C(5A) - C(4A)	172.6(2)
C(1A) - N(1A) - C(5A) - C(6A)	175.0(3)
Zn(1A) - N(1A) - C(5A) - C(6A)	-9.4(3)
C(3A) - C(4A) - C(5A) - N(1A)	1.8(4)
C(3A) - C(4A) - C(5A) - C(6A)	-176.0(3)
N(3A) - N(2A) - C(6A) - C(7A)	-0.2(3)
Zn(1A) - N(2A) - C(6A) - C(7A)	-165.8(2)
N(3A) - N(2A) - C(6A) - C(5A)	-178.6(2)
Zn(1A) - N(2A) - C(6A) - C(5A)	15.7(3)
N(1A) - C(5A) - C(6A) - N(2A)	-4.8(4)
C(4A) - C(5A) - C(6A) - N(2A)	173.2(3)
N(1A) - C(5A) - C(6A) - C(7A)	177.2(3)
C(4A) - C(5A) - C(6A) - C(7A)	-4.8(5)
N(2A) - C(6A) - C(7A) - C(8A)	0.0(3)
C(5A) - C(6A) - C(7A) - C(8A)	178.1(3)
N(2A) - N(3A) - C(8A) - C(7A)	-0.4(3)
C(15A) - N(3A) - C(8A) - C(7A)	-171.1(3)
N(2A) - N(3A) - C(8A) - C(9A)	-179.3(3)
C(15A) - N(3A) - C(8A) - C(9A)	10.0(5)

C(6A) - C(7A) - C(8A) - N(3A)	0.2(3)
C(6A) - C(7A) - C(8A) - C(9A)	179.1(3)
N(3A) - C(8A) - C(9A) - C(10A)	26.7(5)
C(7A) - C(8A) - C(9A) - C(10A)	-152.0(3)
N(3A) - C(8A) - C(9A) - C(14A)	-156.3(3)
C(7A) - C(8A) - C(9A) - C(14A)	25.1(5)
C(14A) - C(9A) - C(10A) - C(11A)	0.9(4)
C(8A) - C(9A) - C(10A) - C(11A)	177.9(3)
C(9A) - C(10A) - C(11A) - C(12A)	-0.9(5)
C(10A) - C(11A) - C(12A) - C(13A)	0.3(5)
C(11A) - C(12A) - C(13A) - C(14A)	0.3(5)
C(12A) - C(13A) - C(14A) - C(9A)	-0.3(5)
C(10A) - C(9A) - C(14A) - C(13A)	-0.2(4)
C(8A) - C(9A) - C(14A) - C(13A)	-177.5(3)
N(2B) - Zn(1B) - N(1B) - C(1B)	-176.6(3)
Cl(2B) - Zn(1B) - N(1B) - C(1B)	-62.7(3)
Cl(1B) - Zn(1B) - N(1B) - C(1B)	78.0(2)
N(2B) - Zn(1B) - N(1B) - C(5B)	2.60(19)
Cl(2B) - Zn(1B) - N(1B) - C(5B)	116.47(18)
Cl(1B) - Zn(1B) - N(1B) - C(5B)	-102.84(19)
N(1B) - Zn(1B) - N(2B) - C(6B)	-3.3(2)
Cl(2B) - Zn(1B) - N(2B) - C(6B)	-113.66(19)
Cl(1B) - Zn(1B) - N(2B) - C(6B)	112.41(19)
N(1B) - Zn(1B) - N(2B) - N(3B)	-175.1(3)
Cl(2B) - Zn(1B) - N(2B) - N(3B)	74.5(3)
Cl(1B) - Zn(1B) - N(2B) - N(3B)	-59.4(3)
C(6B) - N(2B) - N(3B) - C(8B)	0.6(3)
Zn(1B) - N(2B) - N(3B) - C(8B)	172.7(2)
C(6B) - N(2B) - N(3B) - C(15B)	-175.2(3)
Zn(1B) - N(2B) - N(3B) - C(15B)	-3.0(4)
C(5B) - N(1B) - C(1B) - C(2B)	0.4(4)
Zn(1B) - N(1B) - C(1B) - C(2B)	179.5(2)
N(1B) - C(1B) - C(2B) - C(3B)	1.2(5)
C(1B) - C(2B) - C(3B) - C(4B)	-1.3(5)
C(2B) - C(3B) - C(4B) - C(5B)	-0.2(5)
C(1B) - N(1B) - C(5B) - C(4B)	-2.0(4)
Zn(1B) - N(1B) - C(5B) - C(4B)	178.7(2)
C(1B) - N(1B) - C(5B) - C(6B)	177.7(3)
Zn(1B) - N(1B) - C(5B) - C(6B)	-1.6(3)
C(3B) - C(4B) - C(5B) - N(1B)	1.9(4)
C(3B) - C(4B) - C(5B) - C(6B)	-177.8(3)
N(3B) - N(2B) - C(6B) - C(7B)	-0.9(3)
Zn(1B) - N(2B) - C(6B) - C(7B)	-175.26(19)
N(3B) - N(2B) - C(6B) - C(5B)	177.9(2)
Zn(1B) - N(2B) - C(6B) - C(5B)	3.5(3)
N(1B) - C(5B) - C(6B) - N(2B)	-1.3(4)
C(4B) - C(5B) - C(6B) - N(2B)	178.4(3)
N(1B) - C(5B) - C(6B) - C(7B)	177.1(3)
C(4B) - C(5B) - C(6B) - C(7B)	-3.2(5)
N(2B) - C(6B) - C(7B) - C(8B)	0.8(3)
C(5B) - C(6B) - C(7B) - C(8B)	-177.7(3)
N(2B) - N(3B) - C(8B) - C(7B)	0.0(3)
C(15B) - N(3B) - C(8B) - C(7B)	175.0(3)
N(2B) - N(3B) - C(8B) - C(9B)	-178.2(3)

C(15B) - N(3B) - C(8B) - C(9B)	-3.1(5)
C(6B) - C(7B) - C(8B) - N(3B)	-0.5(3)
C(6B) - C(7B) - C(8B) - C(9B)	177.6(3)
N(3B) - C(8B) - C(9B) - C(10B)	-28.5(4)
C(7B) - C(8B) - C(9B) - C(10B)	153.8(3)
N(3B) - C(8B) - C(9B) - C(14B)	152.6(3)
C(7B) - C(8B) - C(9B) - C(14B)	-25.1(4)
C(14B) - C(9B) - C(10B) - C(11B)	-3.5(4)
C(8B) - C(9B) - C(10B) - C(11B)	177.6(3)
C(9B) - C(10B) - C(11B) - C(12B)	0.9(5)
C(10B) - C(11B) - C(12B) - C(13B)	1.8(5)
C(11B) - C(12B) - C(13B) - C(14B)	-1.8(5)
C(12B) - C(13B) - C(14B) - C(9B)	-0.9(5)
C(10B) - C(9B) - C(14B) - C(13B)	3.5(5)
C(8B) - C(9B) - C(14B) - C(13B)	-177.5(3)
N(2C) - Zn(1C) - N(1C) - C(1C)	171.8(3)
Cl(1C) - Zn(1C) - N(1C) - C(1C)	57.6(3)
Cl(2C) - Zn(1C) - N(1C) - C(1C)	-85.6(3)
N(2C) - Zn(1C) - N(1C) - C(5C)	-11.3(2)
Cl(1C) - Zn(1C) - N(1C) - C(5C)	-125.54(19)
Cl(2C) - Zn(1C) - N(1C) - C(5C)	91.2(2)
N(1C) - Zn(1C) - N(2C) - C(6C)	14.0(2)
Cl(1C) - Zn(1C) - N(2C) - C(6C)	134.34(19)
Cl(2C) - Zn(1C) - N(2C) - C(6C)	-98.4(2)
N(1C) - Zn(1C) - N(2C) - N(3C)	172.6(3)
Cl(1C) - Zn(1C) - N(2C) - N(3C)	-67.0(3)
Cl(2C) - Zn(1C) - N(2C) - N(3C)	60.2(3)
C(6C) - N(2C) - N(3C) - C(8C)	-0.5(3)
Zn(1C) - N(2C) - N(3C) - C(8C)	-160.0(2)
C(6C) - N(2C) - N(3C) - C(15C)	-174.6(3)
Zn(1C) - N(2C) - N(3C) - C(15C)	25.8(4)
C(5C) - N(1C) - C(1C) - C(2C)	-1.5(5)
Zn(1C) - N(1C) - C(1C) - C(2C)	175.2(2)
N(1C) - C(1C) - C(2C) - C(3C)	-0.5(5)
C(1C) - C(2C) - C(3C) - C(4C)	1.8(5)
C(2C) - C(3C) - C(4C) - C(5C)	-1.0(5)
C(1C) - N(1C) - C(5C) - C(4C)	2.4(4)
Zn(1C) - N(1C) - C(5C) - C(4C)	-174.8(2)
C(1C) - N(1C) - C(5C) - C(6C)	-175.6(3)
Zn(1C) - N(1C) - C(5C) - C(6C)	7.2(3)
C(3C) - C(4C) - C(5C) - N(1C)	-1.1(4)
C(3C) - C(4C) - C(5C) - C(6C)	176.7(3)
N(3C) - N(2C) - C(6C) - C(7C)	0.8(3)
Zn(1C) - N(2C) - C(6C) - C(7C)	165.9(2)
N(3C) - N(2C) - C(6C) - C(5C)	-179.6(2)
Zn(1C) - N(2C) - C(6C) - C(5C)	-14.6(3)
N(1C) - C(5C) - C(6C) - N(2C)	4.9(4)
C(4C) - C(5C) - C(6C) - N(2C)	-173.1(3)
N(1C) - C(5C) - C(6C) - C(7C)	-175.6(3)
C(4C) - C(5C) - C(6C) - C(7C)	6.4(5)
N(2C) - C(6C) - C(7C) - C(8C)	-0.8(3)
C(5C) - C(6C) - C(7C) - C(8C)	179.7(3)
N(2C) - N(3C) - C(8C) - C(7C)	0.0(3)
C(15C) - N(3C) - C(8C) - C(7C)	173.1(3)

N(2C) - N(3C) - C(8C) - C(9C)	179.5(3)
C(15C) - N(3C) - C(8C) - C(9C)	-7.3(5)
C(6C) - C(7C) - C(8C) - N(3C)	0.5(3)
C(6C) - C(7C) - C(8C) - C(9C)	-179.0(3)
N(3C) - C(8C) - C(9C) - C(10C)	-32.7(5)
C(7C) - C(8C) - C(9C) - C(10C)	146.7(3)
N(3C) - C(8C) - C(9C) - C(14C)	150.4(3)
C(7C) - C(8C) - C(9C) - C(14C)	-30.1(5)
C(14C) - C(9C) - C(10C) - C(11C)	0.0(4)
C(8C) - C(9C) - C(10C) - C(11C)	-176.8(3)
C(9C) - C(10C) - C(11C) - C(12C)	0.2(5)
C(10C) - C(11C) - C(12C) - C(13C)	-0.2(5)
C(11C) - C(12C) - C(13C) - C(14C)	0.0(5)
C(12C) - C(13C) - C(14C) - C(9C)	0.2(5)
C(10C) - C(9C) - C(14C) - C(13C)	-0.2(5)
C(8C) - C(9C) - C(14C) - C(13C)	176.8(3)

X-ray Structure Determination of Pyrazoline (102)

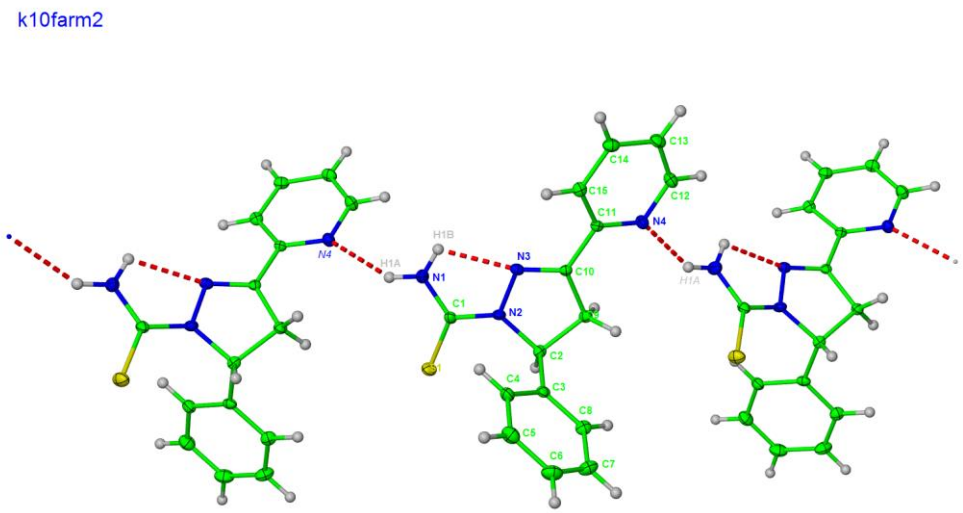

Table 1. Crystal data and structure refinement for pyrazoline (102).

Identification code	k10farm2
Empirical formula	C14 H15 N4 S
Formula weight	271.36
Temperature	150(2) K
Wavelength	0.71073 Å
Crystal system	Monoclinic
Space group	P21/n
Unit cell dimensions	a = 9.7950(2)Å □ = 90°
	b = 14.7280(3)Å □ = 107.768(1)°
	c = 10.0360(2)Å □ = 90°
Volume	1378.74(5) Å^3
Z	4

Density (calculated)	1.307 Mg/m^3
Absorption coefficient	0.227 mm^{-1}
F(000)	572
Crystal size	.35 x .35 x .12 mm
Theta range for data collection	3.52 to 27.52^o
Index ranges	-12<=h<=12; -19<=k<=19; -13<=l<=13
Reflections collected	24456
Independent reflections	3152 [R(int) = 0.0669]
Reflections observed (>2□)	2385
Data Completeness	0.996
Absorption correction	Semi-empirical from equivalents
Max. and min. transmission	0.938 and 0.716
Refinement method	Full-matrix least-squares on F^2
Data / restraints / parameters	3152 / 2 / 190
Goodness-of-fit on F^2	1.025
Final R indices [I>2□(I)]	R1 = 0.0388 wR2 = 0.0882
R indices (all data)	R1 = 0.0604 wR2 = 0.0977
Largest diff. peak and hole	0.260 and -0.235 $eÅ^{-3}$

Notes:

H1A and H1B located and refined at a distance of 0.98Å from N1.

Hydrogen bonding in the lattice.

Hydrogen bonds with H..A < r(A) + 2.000 Angstroms and <DHA > 110 deg.

D-H	d(D-H)	d(H..A)	<DHA	d(D..A)	A
N1-H1A	0.974	2.131	151.06	3.020	N4 [x-1/2, -y+1/2, z+1/2]
N1-H1B	0.973	2.685	153.02	3.579	S1 [x-1/2, -y+1/2, z-1/2]

Table 2. Atomic coordinates (x 10^4) and equivalent isotropic displacement parameters ($Å^2$ x 10^3) for 1.U(eq) is defined as one third of the trace of the orthogonalized Uij tensor.

Atom	x	y	z	U(eq)
S(1)	4628(1)	1778(1)	10745(1)	31(1)
N(1)	2367(2)	2474(1)	8805(2)	29(1)
N(2)	4541(1)	2782(1)	8521(1)	22(1)
N(3)	3811(1)	3255(1)	7308(1)	21(1)
N(4)	4898(1)	3550(1)	4307(1)	24(1)
C(1)	3790(2)	2369(1)	9288(2)	22(1)
C(2)	6091(2)	2733(1)	8703(2)	21(1)
C(3)	6924(2)	3463(1)	9689(2)	21(1)
C(4)	6280(2)	4048(1)	10399(2)	27(1)
C(5)	7078(2)	4704(1)	11299(2)	35(1)
C(6)	8530(2)	4781(1)	11503(2)	39(1)
C(7)	9185(2)	4210(1)	10789(2)	36(1)
C(8)	8388(2)	3558(1)	9887(2)	27(1)
C(9)	6100(2)	2885(1)	7186(2)	22(1)
C(10)	4676(2)	3346(1)	6575(2)	19(1)

C(11)	4195(2)	3800(1)	5208(2)	19(1)
C(12)	4427(2)	3897(1)	3010(2)	28(1)
C(13)	3310(2)	4510(1)	2582(2)	28(1)
C(14)	2626(2)	4782(1)	3531(2)	27(1)
C(15)	3063(2)	4417(1)	4866(2)	24(1)

Table 3. Bond lengths [Å] and angles [^{o}] for 1.

S(1)-C(1)	1.6842(16)	N(1)-C(1)	1.338(2)
N(1)-H(1A)	0.974(5)	N(1)-H(1B)	0.973(5)
N(2)-C(1)	1.359(2)	N(2)-N(3)	1.3960(17)
N(2)-C(2)	1.4748(19)	N(3)-C(10)	1.2870(19)
N(4)-C(12)	1.343(2)	N(4)-C(11)	1.3440(19)
C(2)-C(3)	1.519(2)	C(2)-C(9)	1.541(2)
C(2)-H(2)	1.0000	C(3)-C(4)	1.386(2)
C(3)-C(8)	1.393(2)	C(4)-C(5)	1.390(2)
C(4)-H(4)	0.9500	C(5)-C(6)	1.379(3)
C(5)-H(5)	0.9500	C(6)-C(7)	1.384(3)
C(6)-H(6)	0.9500	C(7)-C(8)	1.385(2)
C(7)-H(7)	0.9500	C(8)-H(8)	0.9500
C(9)-C(10)	1.504(2)	C(9)-H(9A)	0.9900
C(9)-H(9B)	0.9900	C(10)-C(11)	1.468(2)
C(11)-C(15)	1.394(2)	C(12)-C(13)	1.382(2)
C(12)-H(12)	0.9500	C(13)-C(14)	1.380(2)
C(13)-H(13)	0.9500	C(14)-C(15)	1.384(2)
C(14)-H(14)	0.9500	C(15)-H(15)	0.9500
C(1)-N(1)-H(1A)	117.5(13)	C(1)-N(1)-H(1B)	120.9(12)
H(1A)-N(1)-H(1B)	120.4(17)	C(1)-N(2)-N(3)	119.74(12)
C(1)-N(2)-C(2)	128.48(13)	N(3)-N(2)-C(2)	111.48(11)
C(10)-N(3)-N(2)	107.42(12)	C(12)-N(4)-C(11)	116.95(14)
N(1)-C(1)-N(2)	115.28(14)	N(1)-C(1)-S(1)	123.48(12)
N(2)-C(1)-S(1)	121.23(12)	N(2)-C(2)-C(3)	111.95(12)
N(2)-C(2)-C(9)	100.77(11)	C(3)-C(2)-C(9)	112.13(12)
N(2)-C(2)-H(2)	110.5	C(3)-C(2)-H(2)	110.5
C(9)-C(2)-H(2)	110.5	C(4)-C(3)-C(8)	118.34(15)
C(4)-C(3)-C(2)	122.43(14)	C(8)-C(3)-C(2)	119.23(14)
C(3)-C(4)-C(5)	120.80(16)	C(3)-C(4)-H(4)	119.6
C(5)-C(4)-H(4)	119.6	C(6)-C(5)-C(4)	120.29(17)
C(6)-C(5)-H(5)	119.9	C(4)-C(5)-H(5)	119.9
C(5)-C(6)-C(7)	119.55(17)	C(5)-C(6)-H(6)	120.2
C(7)-C(6)-H(6)	120.2	C(6)-C(7)-C(8)	120.13(16)
C(6)-C(7)-H(7)	119.9	C(8)-C(7)-H(7)	119.9
C(7)-C(8)-C(3)	120.87(16)	C(7)-C(8)-H(8)	119.6
C(3)-C(8)-H(8)	119.6	C(10)-C(9)-C(2)	100.62(12)
C(10)-C(9)-H(9A)	111.6	C(2)-C(9)-H(9A)	111.6
C(10)-C(9)-H(9B)	111.6	C(2)-C(9)-H(9B)	111.6
H(9A)-C(9)-H(9B)	109.4	N(3)-C(10)-C(11)	120.13(13)
N(3)-C(10)-C(9)	114.22(13)	C(11)-C(10)-C(9)	125.43(13)
N(4)-C(11)-C(15)	123.04(14)	N(4)-C(11)-C(10)	114.83(13)
C(15)-C(11)-C(10)	122.10(13)	N(4)-C(12)-C(13)	123.74(15)
N(4)-C(12)-H(12)	118.1	C(13)-C(12)-H(12)	118.1
C(14)-C(13)-C(12)	118.66(15)	C(14)-C(13)-H(13)	120.7
C(12)-C(13)-H(13)	120.7	C(13)-C(14)-C(15)	118.95(15)

C(13)-C(14)-H(14)	120.5	C(15)-C(14)-H(14)	120.5
C(14)-C(15)-C(11)	118.61(14)	C(14)-C(15)-H(15)	120.7
C(11)-C(15)-H(15)	120.7		

Table 4. Anisotropic displacement parameters ($Å^2$ x 10^3) for 1. The anisotropic displacement factor exponent takes the form: -2 gpi^2 [h^2 a^{*2} U11 + ... + 2 h k a* b* U

Atom	U11	U22	U33	U23	U13	U12
S(1)	28(1)	36(1)	25(1)	10(1)	4(1)	-5(1)
N(1)	21(1)	42(1)	25(1)	8(1)	8(1)	-4(1)
N(2)	17(1)	28(1)	20(1)	4(1)	5(1)	-1(1)
N(3)	21(1)	23(1)	16(1)	0(1)	4(1)	-2(1)
N(4)	25(1)	28(1)	20(1)	1(1)	11(1)	0(1)
C(1)	22(1)	25(1)	20(1)	-1(1)	7(1)	-5(1)
C(2)	17(1)	23(1)	22(1)	3(1)	6(1)	1(1)
C(3)	22(1)	23(1)	17(1)	6(1)	4(1)	1(1)
C(4)	28(1)	33(1)	21(1)	1(1)	9(1)	-2(1)
C(5)	43(1)	36(1)	26(1)	-7(1)	11(1)	-1(1)
C(6)	40(1)	34(1)	35(1)	-5(1)	-1(1)	-8(1)
C(7)	24(1)	32(1)	44(1)	2(1)	-1(1)	-4(1)
C(8)	24(1)	24(1)	33(1)	3(1)	6(1)	2(1)
C(9)	21(1)	25(1)	21(1)	-2(1)	7(1)	0(1)
C(10)	20(1)	20(1)	18(1)	-3(1)	7(1)	-2(1)
C(11)	19(1)	20(1)	17(1)	-3(1)	7(1)	-5(1)
C(12)	33(1)	34(1)	21(1)	1(1)	13(1)	0(1)
C(13)	31(1)	29(1)	21(1)	7(1)	4(1)	-3(1)
C(14)	23(1)	24(1)	29(1)	2(1)	3(1)	1(1)
C(15)	24(1)	24(1)	25(1)	-3(1)	9(1)	-1(1)

Table 5. Hydrogen coordinates (x 10^4) and isotropic displacement parameters ($Å^2$ x 10^3) for 1.

Atom	x	y	z	U(eq)
H(2)	6473	2117	9040	25
H(4)	5280	3999	10268	32
H(5)	6621	5101	11775	42
H(6)	9078	5224	12130	47
H(7)	10184	4264	10918	43
H(8)	8845	3171	9396	33
H(9A)	6905	3280	7147	27
H(9B)	6150	2303	6708	27
H(12)	4889	3712	2349	34
H(13)	3018	4739	1653	33
H(14)	1868	5212	3272	32
H(15)	2600	4585	5535	28
H(1A)	1791(19)	2159(13)	9300(20)	55(6)
H(1B)	1915(19)	2747(13)	7894(11)	47(6)

Table 6. Dihedral angles [^{o}] for 1.

Atom1 - Atom2 - Atom3 - Atom4	Dihedral
C(1) - N(2) - N(3) - C(10)	-161.42(14)
C(2) - N(2) - N(3) - C(10)	12.75(16)
N(3) - N(2) - C(1) - N(1)	-1.3(2)
C(2) - N(2) - C(1) - N(1)	-174.40(14)
N(3) - N(2) - C(1) - S(1)	179.10(11)
C(2) - N(2) - C(1) - S(1)	6.0(2)
C(1) - N(2) - C(2) - C(3)	-89.28(18)
N(3) - N(2) - C(2) - C(3)	97.19(14)
C(1) - N(2) - C(2) - C(9)	151.37(15)
N(3) - N(2) - C(2) - C(9)	-22.16(15)
N(2) - C(2) - C(3) - C(4)	4.7(2)
C(9) - C(2) - C(3) - C(4)	117.11(16)
N(2) - C(2) - C(3) - C(8)	-174.86(13)
C(9) - C(2) - C(3) - C(8)	-62.44(18)
C(8) - C(3) - C(4) - C(5)	-0.8(2)
C(2) - C(3) - C(4) - C(5)	179.62(15)
C(3) - C(4) - C(5) - C(6)	-0.2(3)
C(4) - C(5) - C(6) - C(7)	1.0(3)
C(5) - C(6) - C(7) - C(8)	-0.7(3)
C(6) - C(7) - C(8) - C(3)	-0.4(3)
C(4) - C(3) - C(8) - C(7)	1.2(2)
C(2) - C(3) - C(8) - C(7)	-179.28(15)
N(2) - C(2) - C(9) - C(10)	21.41(14)
C(3) - C(2) - C(9) - C(10)	-97.81(14)
N(2) - N(3) - C(10) - C(11)	178.38(12)
N(2) - N(3) - C(10) - C(9)	3.41(17)
C(2) - C(9) - C(10) - N(3)	-16.74(16)
C(2) - C(9) - C(10) - C(11)	168.61(13)
C(12) - N(4) - C(11) - C(15)	-2.5(2)
C(12) - N(4) - C(11) - C(10)	175.33(13)
N(3) - C(10) - C(11) - N(4)	-154.21(14)
C(9) - C(10) - C(11) - N(4)	20.1(2)
N(3) - C(10) - C(11) - C(15)	23.7(2)
C(9) - C(10) - C(11) - C(15)	-161.97(14)
C(11) - N(4) - C(12) - C(13)	2.2(2)
N(4) - C(12) - C(13) - C(14)	-0.3(3)
C(12) - C(13) - C(14) - C(15)	-1.4(2)
C(13) - C(14) - C(15) - C(11)	1.0(2)
N(4) - C(11) - C(15) - C(14)	1.0(2)
C(10) - C(11) - C(15) - C(14)	-176.75(14)

X-ray Structure Determination of pyrazoline (105)

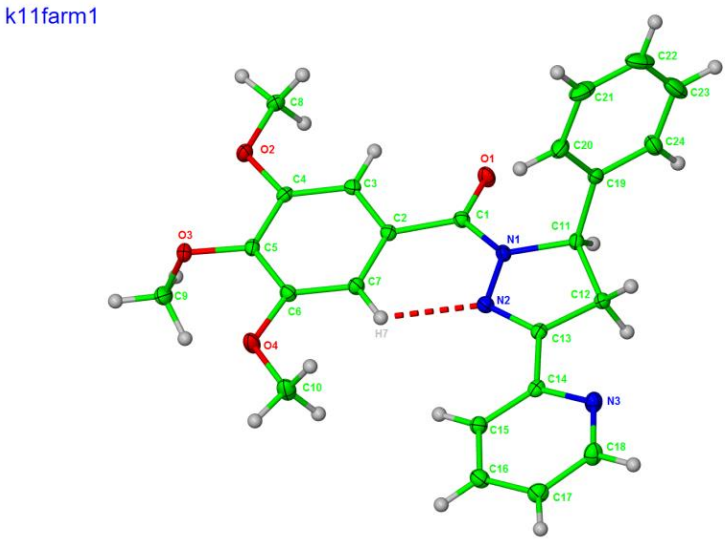

Table 1. Crystal data and structure refinement for pyrazoline **(105)**.

Identification code	k11farm1
Empirical formula	C24 H23 N3 O4
Formula weight	417.45
Temperature	150(2) K
Wavelength	0.71073 Å
Crystal system	Orthorhombic
Space group	Pbca
Unit cell dimensions	a = 6.9770(1)Å □ = 90°
	b = 22.0950(2)Å □ = 90°
	c = 26.6010(3)Å □ = 90°
Volume	4100.73(8) Å^3
Z	8
Density (calculated)	1.352 Mg/m^3
Absorption coefficient	0.093 mm^{-1}
F(000)	1760
Crystal size	0.40 x 0.25 x 0.25 mm
Theta range for data collection	3.54 to 27.47°
Index ranges	-8<=h<=9; -28<=k<=27; -34<=l<=34
Reflections collected	56599
Independent reflections	4679 [R(int) = 0.0645]
Reflections observed (>2□)	3531
Data Completeness	0.997
Absorption correction	Semi-empirical from equivalents
Max. and min. transmission	0.982 and 0.893
Refinement method	Full-matrix least-squares on F^2
Data / restraints / parameters	4679 / 0 / 283
Goodness-of-fit on F^2	1.051
Final R indices [I>2□(I)]	R1 = 0.0422 wR2 = 0.0882
R indices (all data)	R1 = 0.0649 wR2 = 0.0991
Largest diff. peak and hole	0.182 and -0.215 eÅ^{-3}

Table 2. Atomic coordinates (x 10^4) and equivalent isotropic displacement parameters (Å^2 x 10^3) for 1.U(eq) is defined as one third of the trace of the orthogonalized Uij tensor.

Atom	x	y	z	U(eq)
O(1)	8672(2)	1985(1)	7146(1)	34(1)
O(2)	13646(1)	441(1)	6698(1)	32(1)
O(3)	12242(1)	-195(1)	5936(1)	29(1)
O(4)	8769(2)	32(1)	5556(1)	36(1)
N(1)	6394(2)	2016(1)	6564(1)	25(1)
N(2)	5409(2)	1815(1)	6142(1)	25(1)
N(3)	982(2)	2382(1)	5679(1)	31(1)
C(1)	8030(2)	1763(1)	6756(1)	25(1)
C(2)	9030(2)	1235(1)	6514(1)	23(1)
C(3)	10824(2)	1096(1)	6719(1)	24(1)
C(4)	11870(2)	613(1)	6532(1)	23(1)
C(5)	11148(2)	263(1)	6140(1)	24(1)
C(6)	9351(2)	399(1)	5941(1)	26(1)
C(7)	8287(2)	882(1)	6126(1)	26(1)
C(8)	14362(2)	728(1)	7139(1)	32(1)
C(9)	11790(2)	-777(1)	6138(1)	38(1)
C(10)	6969(2)	171(1)	5328(1)	41(1)
C(11)	5385(2)	2514(1)	6834(1)	24(1)
C(12)	3449(2)	2530(1)	6551(1)	26(1)
C(13)	3785(2)	2096(1)	6126(1)	24(1)
C(14)	2400(2)	1975(1)	5720(1)	25(1)
C(15)	2544(2)	1469(1)	5410(1)	29(1)
C(16)	1184(2)	1382(1)	5039(1)	34(1)
C(17)	-269(2)	1802(1)	4988(1)	34(1)
C(18)	-314(2)	2286(1)	5315(1)	35(1)
C(19)	6439(2)	3111(1)	6804(1)	26(1)
C(20)	7541(2)	3265(1)	6388(1)	37(1)
C(21)	8358(2)	3836(1)	6354(1)	51(1)
C(22)	8092(3)	4255(1)	6730(1)	58(1)
C(23)	7013(3)	4104(1)	7147(1)	55(1)
C(24)	6190(2)	3533(1)	7187(1)	38(1)

Table 3. Bond lengths [Å] and angles [^{o}] for 1.

O(1)-C(1)	1.2310(17)	O(2)-C(4)	1.3690(17)
O(2)-C(8)	1.4238(18)	O(3)-C(5)	1.3787(16)
O(3)-C(9)	1.4294(18)	O(4)-C(6)	1.3670(17)
O(4)-C(10)	1.4276(19)	N(1)-C(1)	1.3705(18)
N(1)-N(2)	1.3873(16)	N(1)-C(11)	1.4921(17)
N(2)-C(13)	1.2918(18)	N(3)-C(18)	1.341(2)
N(3)-C(14)	1.3421(18)	C(1)-C(2)	1.5041(19)
C(2)-C(7)	1.393(2)	C(2)-C(3)	1.400(2)
C(3)-C(4)	1.3843(19)	C(3)-H(3)	0.9500

C(4)-C(5)	1.394(2)	C(5)-C(6)	1.394(2)
C(6)-C(7)	1.389(2)	C(7)-H(7)	0.9500
C(8)-H(8A)	0.9800	C(8)-H(8B)	0.9800
C(8)-H(8C)	0.9800	C(9)-H(9A)	0.9800
C(9)-H(9B)	0.9800	C(9)-H(9C)	0.9800
C(10)-H(10A)	0.9800	C(10)-H(10B)	0.9800
C(10)-H(10C)	0.9800	C(11)-C(19)	1.5117(19)
C(11)-C(12)	1.5468(19)	C(11)-H(11)	1.0000
C(12)-C(13)	1.500(2)	C(12)-H(12A)	0.9900
C(12)-H(12B)	0.9900	C(13)-C(14)	1.473(2)
C(14)-C(15)	1.395(2)	C(15)-C(16)	1.381(2)
C(15)-H(15)	0.9500	C(16)-C(17)	1.380(2)
C(16)-H(16)	0.9500	C(17)-C(18)	1.379(2)
C(17)-H(17)	0.9500	C(18)-H(18)	0.9500
C(19)-C(20)	1.389(2)	C(19)-C(24)	1.391(2)
C(20)-C(21)	1.387(2)	C(20)-H(20)	0.9500
C(21)-C(22)	1.375(3)	C(21)-H(21)	0.9500
C(22)-C(23)	1.382(3)	C(22)-H(22)	0.9500
C(23)-C(24)	1.391(3)	C(23)-H(23)	0.9500
C(24)-H(24)	0.9500		
C(4)-O(2)-C(8)	117.34(11)	C(5)-O(3)-C(9)	113.00(11)
C(6)-O(4)-C(10)	116.84(11)	C(1)-N(1)-N(2)	125.76(11)
C(1)-N(1)-C(11)	120.92(11)	N(2)-N(1)-C(11)	113.05(11)
C(13)-N(2)-N(1)	107.96(11)	C(18)-N(3)-C(14)	116.80(13)
O(1)-C(1)-N(1)	117.08(12)	O(1)-C(1)-C(2)	120.08(13)
N(1)-C(1)-C(2)	122.84(12)	C(7)-C(2)-C(3)	119.87(13)
C(7)-C(2)-C(1)	125.41(13)	C(3)-C(2)-C(1)	114.70(12)
C(4)-C(3)-C(2)	120.04(13)	C(4)-C(3)-H(3)	120.0
C(2)-C(3)-H(3)	120.0	O(2)-C(4)-C(3)	125.15(13)
O(2)-C(4)-C(5)	114.44(12)	C(3)-C(4)-C(5)	120.40(13)
O(3)-C(5)-C(4)	120.14(12)	O(3)-C(5)-C(6)	120.46(13)
C(4)-C(5)-C(6)	119.33(12)	O(4)-C(6)-C(7)	124.25(13)
O(4)-C(6)-C(5)	115.03(12)	C(7)-C(6)-C(5)	120.71(13)
C(6)-C(7)-C(2)	119.63(13)	C(6)-C(7)-H(7)	120.2
C(2)-C(7)-H(7)	120.2	O(2)-C(8)-H(8A)	109.5
O(2)-C(8)-H(8B)	109.5	H(8A)-C(8)-H(8B)	109.5
O(2)-C(8)-H(8C)	109.5	H(8A)-C(8)-H(8C)	109.5
H(8B)-C(8)-H(8C)	109.5	O(3)-C(9)-H(9A)	109.5
O(3)-C(9)-H(9B)	109.5	H(9A)-C(9)-H(9B)	109.5
O(3)-C(9)-H(9C)	109.5	H(9A)-C(9)-H(9C)	109.5
H(9B)-C(9)-H(9C)	109.5	O(4)-C(10)-H(10A)	109.5
O(4)-C(10)-H(10B)	109.5	H(10A)-C(10)-H(10B)	109.5
O(4)-C(10)-H(10C)	109.5	H(10A)-C(10)-H(10C)	109.5
H(10B)-C(10)-H(10C)	109.5	N(1)-C(11)-C(19)	112.84(11)
N(1)-C(11)-C(12)	101.14(11)	C(19)-C(11)-C(12)	112.32(11)
N(1)-C(11)-H(11)	110.1	C(19)-C(11)-H(11)	110.1
C(12)-C(11)-H(11)	110.1	C(13)-C(12)-C(11)	102.50(11)
C(13)-C(12)-H(12A)	111.3	C(11)-C(12)-H(12A)	111.3
C(13)-C(12)-H(12B)	111.3	C(11)-C(12)-H(12B)	111.3
H(12A)-C(12)-H(12B)	109.2	N(2)-C(13)-C(14)	120.86(13)
N(2)-C(13)-C(12)	114.72(12)	C(14)-C(13)-C(12)	124.40(12)
N(3)-C(14)-C(15)	122.79(13)	N(3)-C(14)-C(13)	115.03(13)
C(15)-C(14)-C(13)	122.17(13)	C(16)-C(15)-C(14)	118.97(14)

C(16)-C(15)-H(15)	120.5	C(14)-C(15)-H(15)	120.5
C(17)-C(16)-C(15)	118.79(14)	C(17)-C(16)-H(16)	120.6
C(15)-C(16)-H(16)	120.6	C(18)-C(17)-C(16)	118.43(14)
C(18)-C(17)-H(17)	120.8	C(16)-C(17)-H(17)	120.8
N(3)-C(18)-C(17)	124.20(14)	N(3)-C(18)-H(18)	117.9
C(17)-C(18)-H(18)	117.9	C(20)-C(19)-C(24)	119.25(14)
C(20)-C(19)-C(11)	121.66(13)	C(24)-C(19)-C(11)	118.94(14)
C(21)-C(20)-C(19)	120.06(17)	C(21)-C(20)-H(20)	120.0
C(19)-C(20)-H(20)	120.0	C(22)-C(21)-C(20)	120.71(19)
C(22)-C(21)-H(21)	119.6	C(20)-C(21)-H(21)	119.6
C(21)-C(22)-C(23)	119.58(17)	C(21)-C(22)-H(22)	120.2
C(23)-C(22)-H(22)	120.2	C(22)-C(23)-C(24)	120.34(18)
C(22)-C(23)-H(23)	119.8	C(24)-C(23)-H(23)	119.8
C(19)-C(24)-C(23)	120.05(18)	C(19)-C(24)-H(24)	120.0
C(23)-C(24)-H(24)	120.0		

Table 4. Anisotropic displacement parameters ($Å^2$ x 10^3) for 1. The anisotropic displacement factor exponent takes the form: -2 gpi^2 [h^2 a^{*2} U11 + ... + 2 h k a* b* U

Atom	U11	U22	U33	U23	U13	U12
O(1)	36(1)	34(1)	32(1)	-10(1)	-10(1)	9(1)
O(2)	22(1)	35(1)	39(1)	-10(1)	-7(1)	7(1)
O(3)	26(1)	28(1)	33(1)	-4(1)	3(1)	5(1)
O(4)	34(1)	37(1)	37(1)	-15(1)	-14(1)	11(1)
N(1)	24(1)	22(1)	28(1)	-4(1)	-3(1)	3(1)
N(2)	25(1)	24(1)	24(1)	1(1)	-3(1)	1(1)
N(3)	31(1)	33(1)	29(1)	1(1)	-4(1)	9(1)
C(1)	25(1)	22(1)	26(1)	0(1)	-2(1)	1(1)
C(2)	24(1)	21(1)	24(1)	2(1)	0(1)	0(1)
C(3)	23(1)	23(1)	25(1)	0(1)	-1(1)	-2(1)
C(4)	18(1)	25(1)	26(1)	3(1)	0(1)	0(1)
C(5)	23(1)	23(1)	26(1)	0(1)	4(1)	2(1)
C(6)	28(1)	25(1)	25(1)	-2(1)	-2(1)	0(1)
C(7)	25(1)	25(1)	28(1)	-1(1)	-4(1)	4(1)
C(8)	22(1)	36(1)	38(1)	-6(1)	-5(1)	1(1)
C(9)	31(1)	25(1)	59(1)	-3(1)	-1(1)	3(1)
C(10)	38(1)	44(1)	42(1)	-15(1)	-18(1)	11(1)
C(11)	23(1)	23(1)	27(1)	-1(1)	3(1)	3(1)
C(12)	23(1)	22(1)	33(1)	-2(1)	0(1)	0(1)
C(13)	23(1)	21(1)	27(1)	4(1)	2(1)	0(1)
C(14)	23(1)	25(1)	26(1)	6(1)	2(1)	1(1)
C(15)	28(1)	26(1)	35(1)	1(1)	-3(1)	3(1)
C(16)	37(1)	29(1)	36(1)	-2(1)	-5(1)	0(1)
C(17)	32(1)	38(1)	31(1)	2(1)	-9(1)	2(1)
C(18)	34(1)	40(1)	32(1)	1(1)	-6(1)	12(1)
C(19)	20(1)	23(1)	34(1)	-1(1)	-4(1)	3(1)
C(20)	28(1)	32(1)	50(1)	3(1)	8(1)	1(1)
C(21)	28(1)	43(1)	82(2)	19(1)	2(1)	-7(1)
C(22)	43(1)	29(1)	103(2)	7(1)	-26(1)	-11(1)
C(23)	58(1)	30(1)	77(2)	-17(1)	-26(1)	3(1)
C(24)	39(1)	32(1)	43(1)	-11(1)	-7(1)	5(1)

Table 5. Hydrogen coordinates (x 10^4) and isotropic displacement parameters ($Å^2$ x 10^3) for 1.

Atom	x	y	z	U(eq)
H(3)	11325	1333	6987	28
H(7)	7060	970	5990	31
H(8A)	14436	1166	7083	48
H(8B)	15643	571	7215	48
H(8C)	13502	645	7422	48
H(9A)	12140	-789	6495	57
H(9B)	12509	-1089	5956	57
H(9C)	10413	-853	6103	57
H(10A)	5941	115	5575	62
H(10B)	6755	-100	5042	62
H(10C)	6975	591	5212	62
H(11)	5175	2400	7194	29
H(12A)	2385	2393	6769	32
H(12B)	3162	2941	6424	32
H(15)	3561	1187	5452	35
H(16)	1248	1040	4823	40
H(17)	-1215	1758	4734	41
H(18)	-1328	2570	5280	42
H(20)	7736	2978	6126	44
H(21)	9110	3938	6069	61
H(22)	8646	4646	6702	70
H(23)	6833	4391	7408	66
H(24)	5456	3430	7475	46

Table 6. Dihedral angles [^{o}] for 1.

Atom1 - Atom2 - Atom3 - Atom4	Dihedral
C(1) - N(1) - N(2) - C(13)	169.20(13)
C(11) - N(1) - N(2) - C(13)	-4.79(15)
N(2) - N(1) - C(1) - O(1)	-177.09(13)
C(11) - N(1) - C(1) - O(1)	-3.5(2)
N(2) - N(1) - C(1) - C(2)	2.6(2)
C(11) - N(1) - C(1) - C(2)	176.19(12)
O(1) - C(1) - C(2) - C(7)	168.54(14)
N(1) - C(1) - C(2) - C(7)	-11.2(2)
O(1) - C(1) - C(2) - C(3)	-9.42(19)
N(1) - C(1) - C(2) - C(3)	170.87(13)
C(7) - C(2) - C(3) - C(4)	0.9(2)
C(1) - C(2) - C(3) - C(4)	179.01(12)
C(8) - O(2) - C(4) - C(3)	8.8(2)
C(8) - O(2) - C(4) - C(5)	-172.17(12)
C(2) - C(3) - C(4) - O(2)	179.03(13)
C(2) - C(3) - C(4) - C(5)	0.0(2)
C(9) - O(3) - C(5) - C(4)	97.25(16)
C(9) - O(3) - C(5) - C(6)	-85.70(16)
O(2) - C(4) - C(5) - O(3)	-2.82(19)
C(3) - C(4) - C(5) - O(3)	176.28(12)
O(2) - C(4) - C(5) - C(6)	-179.90(12)
C(3) - C(4) - C(5) - C(6)	-0.8(2)
C(10) - O(4) - C(6) - C(7)	1.5(2)

C(10) - O(4) - C(6) - C(5)	-177.62(14)
O(3) - C(5) - C(6) - O(4)	2.7(2)
C(4) - C(5) - C(6) - O(4)	179.79(13)
O(3) - C(5) - C(6) - C(7)	-176.46(13)
C(4) - C(5) - C(6) - C(7)	0.6(2)
O(4) - C(6) - C(7) - C(2)	-178.76(14)
C(5) - C(6) - C(7) - C(2)	0.3(2)
C(3) - C(2) - C(7) - C(6)	-1.1(2)
C(1) - C(2) - C(7) - C(6)	-178.97(13)
C(1) - N(1) - C(11) - C(19)	73.16(16)
N(2) - N(1) - C(11) - C(19)	-112.52(13)
C(1) - N(1) - C(11) - C(12)	-166.64(12)
N(2) - N(1) - C(11) - C(12)	7.68(14)
N(1) - C(11) - C(12) - C(13)	-7.14(13)
C(19) - C(11) - C(12) - C(13)	113.43(13)
N(1) - N(2) - C(13) - C(14)	-179.52(12)
N(1) - N(2) - C(13) - C(12)	-0.65(16)
C(11) - C(12) - C(13) - N(2)	5.34(16)
C(11) - C(12) - C(13) - C(14)	-175.84(12)
C(18) - N(3) - C(14) - C(15)	-0.7(2)
C(18) - N(3) - C(14) - C(13)	-179.71(13)
N(2) - C(13) - C(14) - N(3)	-165.69(13)
C(12) - C(13) - C(14) - N(3)	15.6(2)
N(2) - C(13) - C(14) - C(15)	15.3(2)
C(12) - C(13) - C(14) - C(15)	-163.49(14)
N(3) - C(14) - C(15) - C(16)	0.6(2)
C(13) - C(14) - C(15) - C(16)	179.55(14)
C(14) - C(15) - C(16) - C(17)	0.2(2)
C(15) - C(16) - C(17) - C(18)	-0.8(2)
C(14) - N(3) - C(18) - C(17)	0.0(2)
C(16) - C(17) - C(18) - N(3)	0.8(3)
N(1) - C(11) - C(19) - C(20)	31.53(19)
C(12) - C(11) - C(19) - C(20)	-82.02(17)
N(1) - C(11) - C(19) - C(24)	-153.00(13)
C(12) - C(11) - C(19) - C(24)	93.45(16)
C(24) - C(19) - C(20) - C(21)	-0.8(2)
C(11) - C(19) - C(20) - C(21)	174.63(15)
C(19) - C(20) - C(21) - C(22)	0.0(3)
C(20) - C(21) - C(22) - C(23)	0.6(3)
C(21) - C(22) - C(23) - C(24)	-0.4(3)
C(20) - C(19) - C(24) - C(23)	1.0(2)
C(11) - C(19) - C(24) - C(23)	-174.57(15)
C(22) - C(23) - C(24) - C(19)	-0.4(3)